



**This electronic thesis or dissertation has been
downloaded from Explore Bristol Research,
<http://research-information.bristol.ac.uk>**

Author:
Belbin, Fiona E

Title:
The Interactions Between Circadian Rhythms and Herbicides

General rights

Access to the thesis is subject to the Creative Commons Attribution - NonCommercial-No Derivatives 4.0 International Public License. A copy of this may be found at <https://creativecommons.org/licenses/by-nc-nd/4.0/legalcode>. This license sets out your rights and the restrictions that apply to your access to the thesis so it is important you read this before proceeding.

Take down policy

Some pages of this thesis may have been removed for copyright restrictions prior to having it been deposited in Explore Bristol Research. However, if you have discovered material within the thesis that you consider to be unlawful e.g. breaches of copyright (either yours or that of a third party) or any other law, including but not limited to those relating to patent, trademark, confidentiality, data protection, obscenity, defamation, libel, then please contact collections-metadata@bristol.ac.uk and include the following information in your message:

- Your contact details
- Bibliographic details for the item, including a URL
- An outline nature of the complaint

Your claim will be investigated and, where appropriate, the item in question will be removed from public view as soon as possible.

THE INTERACTIONS BETWEEN CIRCADIAN RHYTHMS AND HERBICIDES

Fiona Elizabeth Belbin



School of Biological Sciences

A dissertation submitted to the University of Bristol in
accordance with the requirements for award of the degree of
Doctor of Philosophy in the Faculty of Life Sciences.

September 2019

Word count: c. 59,000

Abstract

Global food production is required to increase by more than 70% by 2050 in order to feed the growing population, since global population is expected to increase by more than 2 billion. A major constraint on crop yield is weeds; within the field, weeds compete with crops for resources such as light, space, and nutrients. Herbicides are used to control weeds; however, herbicide overuse has led to increased resistance of plants in addition to environmental pollution. Furthermore, over \$11 billion is spent per year on herbicides in the USA alone. As such, it would be beneficial to use herbicides more effectively.

Plants, as sessile organisms, possess a circadian oscillator that is responsible for adapting the timing of processes within the plant to the changing environment, in order to enhance fitness. The circadian oscillator can also restrict responses to stimuli to specific times of day, which is known as circadian gating. Herbicides have previously been observed to have fluctuating efficacy dependent on the time of application. Therefore, it was hypothesised that the circadian oscillator might restrict certain responses to herbicides to specific times of day. The interactions between herbicides and the circadian oscillator were investigated in depth in this thesis.

Three different mode-of-action herbicides were investigated: glyphosate, mesotrione and terbuthylazine. This thesis presents data relating to two overarching findings. (i) The circadian oscillator can regulate signalling or metabolism to produce varying levels of efficacy depending on the time of herbicide application. (ii) Herbicides can alter the emergent properties of the circadian oscillator, potentially causing dissonance between the plant and its environment.

These results led to the proposal of a new concept that we have termed agricultural chronotherapy. In a wider context, this could improve the use of agrochemicals in the future.

Acknowledgements

Throughout my PhD I have received a great deal of support from many people. Firstly, I would like to express my gratitude to my supervisor Dr Antony Dodd, for his support, encouragement and advice over these four years and whose expertise has been invaluable in this work. I would also like to thank Prof Kerry Franklin, in particular for ideas early on in this research.

I'd like to acknowledge Syngenta for funding this project with the BBSRC, and those at Syngenta who have provided useful insight, particularly Carl and Gavin. Aspects of this work would not have been possible without the assistance of others, including Adrian and Bartosz in the Physics Workshop, the Bristol Genomics Facility and Tom Batstone, and the undergraduate students that I have had the pleasure of working with.

I would like to thank members of the Dodd lab, past and present. In particular, Kelly, Noriane and Paige for your support and friendship through some testing times. Thanks to everyone else in Life Sciences over the years who have made my time enjoyable and have provided many entertaining discussions over much needed coffee, particularly Donald, Katie, Ashley, Chiara and James.

To my dear friends, Lucy and Lucy, and all my other girls, no matter where you are in the world, your support and friendship is so special and I appreciate you all.

To my family, Mum, Dad, George, Matt, Noah and Willow, who have no idea what I have been doing for the last four years, I cannot thank you enough for your continued support and advice for any decision I make, for being there whenever I need you, for the happy distractions, and for helping me retain my sanity.

Finally to Calum, my sidekick for life, the Jim to my Pam, for believing in me when I don't believe in myself, for your unwavering support, and the numerous scientific discussions, thank you. This journey hasn't been an easy one but I can't wait for all our future adventures together.

Author's Declaration

I declare that the work in this dissertation was carried out in accordance with the requirements of the University's Regulations and Code of Practice for Research Degree Programmes and that it has not been submitted for any other academic award. Except where indicated by specific reference in the text, the work is the candidate's own work. Work done in collaboration with, or with the assistance of, others, is indicated as such. Any views expressed in the dissertation are those of the author.

SIGNED: DATE:.....

Contents

1	Introduction	1
1.1	The problem of weeds	2
1.2	A background to herbicides	3
1.3	The problems with herbicides	4
1.4	Factors affecting herbicide efficacy	5
1.4.1	Environmental factors affecting herbicide efficacy	5
1.4.2	Physiological factors affecting herbicide efficacy	7
1.5	The circadian oscillator	8
1.5.1	Architecture of the Arabidopsis circadian oscillator	8
1.5.2	Regulatory mechanisms within the circadian oscillator	10
1.5.3	Entrainment of the circadian oscillator	13
1.5.4	Outputs of the circadian oscillator	14
1.5.5	Circadian gating	16
1.6	Glyphosate	17
1.6.1	Glyphosate mode of action	18
1.6.2	Glyphosate movement within the plant	20
1.6.3	Glyphosate metabolism within the plant	22
1.6.4	Glyphosate in the environment	22
1.6.5	Glyphosate concentrations in agriculture	23
1.6.6	Glyphosate time of day effects	24
1.6.7	Glyphosate effects on auxin biosynthesis and signalling	26
1.6.8	IAA biosynthesis	27

1.6.9	Glyphosate conclusions	28
1.7	Mesotrione	29
1.7.1	Mesotrione mode of action	30
1.7.2	Mesotrione uptake, movement and metabolism	32
1.7.3	Environmental mesotrione degradation	33
1.7.4	Mesotrione conclusions	33
1.8	Terbuthylazine	34
1.8.1	Terbuthylazine mode of action	35
1.8.2	Movement of terbuthylazine within the plant	37
1.8.3	Metabolism of terbuthylazine	37
1.8.4	Triazine interactions with circadian regulation	38
1.8.5	Terbuthylazine conclusions	39
1.9	Summary	39
1.10	Aims	40
2	Materials and Methods	41
2.1	Plant material and growth conditions	41
2.2	Application of treatments	43
2.3	Herbicide formulations	44
2.4	Adjuvants	45
2.5	Plant physiology measurements	45
2.5.1	Rosette properties	45
2.5.2	Hypocotyl and coleoptile length	46
2.5.3	Hypocotyl elongation rate	47
2.5.4	Petiole length	47
2.6	Chlorophyll fluorescence measurements	48
2.7	Data meta-analysis	50
2.8	RNA isolation	50
2.9	cDNA synthesis	51
2.10	Quantitative reverse-transcription PCR	51

2.11	Bioluminescence imaging	53
2.11.1	Entrainment assay	54
2.11.2	Effect of herbicides on circadian oscillator promoters	54
2.11.3	Effect of herbicides with supplemental sucrose	55
2.12	GUS staining	55
2.13	Fluorescence microscopy	55
2.14	Electrolyte leakage	56
2.15	Chlorophyll content	56
2.16	RNA-sequencing	58
2.17	Bioinformatics	58
2.18	Statistical analyses	59

3 Using Arabidopsis as a model to investigate the circadian regulation of plant responses to herbicides 61

3.1	Introduction	61
3.2	Physiological effects of herbicides on Arabidopsis	62
3.2.1	Herbicides inhibit growth and cause quantifiable damage in Arabidopsis	63
3.3	Design and construction of a laboratory-sized track sprayer	71
3.4	Herbicides affect photosynthesis in Arabidopsis	74
3.4.1	Greater concentrations of herbicides tested negatively affect chlorophyll fluorescence	76
3.4.2	Each herbicide tested takes different lengths of time to affect chlorophyll fluorescence	82
3.4.3	The time of herbicide application has varying effects on chlorophyll fluorescence	87
3.5	Identification of glyphosate marker genes	93
3.5.1	Glyphosate takes 6 hours to alter transcript abundance	94
3.5.2	Glyphosate alters marker gene transcript abundance in a time-of-day-dependent manner under light-dark cycles	97

3.5.3	The circadian oscillator is involved in the time-of-day sensitivity of glyphosate marker genes	101
3.6	Discussion	105
3.6.1	Herbicides appear to cause small time-of-day-dependent differences to Arabidopsis physiology	105
3.6.2	Herbicides affect photosynthetic measurements with time-of-day-dependent efficacy	108
3.6.3	Circadian gating may lead to time-of-day sensitivity of glyphosate marker genes	112
3.7	Conclusions	114
4	Photoperiodic and circadian regulation of responses to glyphosate	117
4.1	Introduction	117
4.2	Glyphosate-regulated transcripts are rhythmic	119
4.3	Glyphosate-responsive rhythmic transcripts are enriched for auxin signalling	125
4.4	Response to glyphosate has time of day sensitivity under light-dark cycles	127
4.4.1	Hypocotyl length is most sensitive to glyphosate when applied at dawn in wild type Arabidopsis	129
4.4.2	Validation of experimental methods	131
4.4.3	Plants have increased sensitivity to glyphosate pre-dawn and post-dusk	133
4.4.4	Glyphosate reduced hypocotyl elongation rate when applied at dawn but not at dusk	137
4.4.5	Higher glyphosate concentrations are required at dusk than dawn to cause the same inhibition of hypocotyl elongation . . .	139
4.4.6	Seedlings have decreased sensitivity to glyphosate applied at dusk	140
4.5	Sensitivity to glyphosate at dawn is circadian-regulated	141
4.5.1	Glyphosate sensitivity is rhythmic under constant light conditions in wild-type Arabidopsis	141

4.5.2	Plants that have altered circadian oscillators are not sensitive to different concentrations of glyphosate	144
4.6	Cell death markers have circadian responses to glyphosate	145
4.6.1	Glyphosate appears to increase programmed cell death with circadian regulation	145
4.6.2	Glyphosate does not affect electrolyte leakage under our experimental conditions	149
4.6.3	Glyphosate alters pigment composition in a time-of-day-dependent manner	151
4.7	Discussion	152
4.7.1	Circadian regulation in the response to glyphosate could lead to agricultural chronotherapy	152
4.7.2	Glyphosate treatment causes an increase in PCD-promoting transcripts	153
4.7.3	Glyphosate does not increase electrolyte leakage in these experimental conditions	154
4.7.4	Glyphosate increases chlorophyll degradation and causes an increase in ROS toxicity through reduced quenching by carotenoids	155
4.7.5	The interaction between glyphosate, auxin and hypocotyl elongation is regulated by the circadian oscillator	157
4.8	Conclusions	160
5	Circadian regulation of a glyphosate response is potentially due to rhythmic auxin signalling	161
5.1	Introduction	161
5.2	Glyphosate appears to alter hypocotyl elongation through inhibition of auxin signalling	162
5.2.1	Hypocotyls are most sensitive to the auxin biosynthesis inhibitor L-kynurenine at dawn	163
5.2.2	Exogenous auxin overcomes the effect of glyphosate	164

5.2.3	Auxin transport is required for the rhythmic response to glyphosate	166
5.2.4	PhyB mutation does not confer resistance to glyphosate	169
5.3	Glyphosate has variable effects on DR5::GUS	171
5.4	Glyphosate does not alter DR5::VENUS fluorescence or transcript accumulation	172
5.5	Glyphosate has time-of-day-dependent effects on auxin-related transcripts	177
5.6	Discussion	180
5.6.1	Glyphosate is likely to inhibit all auxin biosynthesis pathways .	180
5.6.2	<i>phyB</i> is more susceptible to glyphosate due to its longer hypocotyls	182
5.6.3	Effect of glyphosate on reporters could have been masked by the inhibition of protein synthesis	183
5.6.4	The effect of glyphosate on auxin-related transcript abundance correlates with the function of the genes in auxin biosynthesis and hypocotyl elongation	184
5.7	Conclusion	187
6	Extending findings to older plants and agriculturally-relevant species	189
6.1	Introduction	189
6.2	Glyphosate inhibits petiole elongation	190
6.3	Glyphosate reduces hypocotyl and coleoptile elongation in species additional to <i>Arabidopsis</i>	193
6.4	Discussion	196
6.4.1	Regulation of petiole elongation is determined by growth conditions	196
6.4.2	Multiple factors regulate coleoptile elongation	198
6.5	Conclusion	199
7	RNA-sequencing of <i>Arabidopsis</i> treated with mesotrione and terbutylazine	201

7.1	Introduction	201
7.2	RNA-sequencing data collection	202
7.3	Principal component analysis separates samples into clusters by treatment	203
7.4	Mesotrione, Agridex and TBA treatments cause differential gene expression	205
7.5	Genes representing many metabolic pathways were enriched by herbicide treatment	216
7.6	Three core promoter motifs were enriched in herbicide-treated seedlings	222
7.7	Significant overlaps of herbicide-response genes and nycthemeral and circadian regulated transcript sets	225
7.8	Discussion	228
7.8.1	<i>PDR12</i> is a detoxifying gene highly up-regulated in response to mesotrione and adjuvant	228
7.8.2	<i>WRKY30</i> and <i>MAPKKKs</i> could be components of the same stress-response signalling cascade	229
7.8.3	Herbicide-induced oxidative stress is regulated through <i>ERFs</i> and <i>GSTs</i>	231
7.8.4	CPuORFs regulate translation of downstream genes in response to herbicide treatments	235
7.8.5	G-box motifs could determine circadian regulation of differentially expressed genes	238
7.8.6	Core promoter hexamers could be causing a pathogen-like response after both mesotrione and adjuvant treatment	241
7.9	Conclusion	243
8	Herbicides alter circadian period and phase	245
8.1	Introduction	245
8.2	Bioluminescence data collection and analysis	248
8.3	Some herbicides alter circadian period, depending on the reporter	248

8.4	The adjuvant components of herbicide formulations alter the properties of the circadian oscillator under free-running conditions	261
8.5	Phase can be altered by herbicides under entrained conditions	271
8.6	Exogenous sucrose rescues the effect of mesotrione on entrained phase and circadian period	285
8.7	Discussion	296
8.7.1	Herbicides cause different effects on the circadian oscillator under constant conditions compared to entrainment conditions	297
8.7.2	Photosynthesis-inhibiting herbicides may affect metabolic entrainment of the circadian oscillator	298
8.7.3	Mesotrione has no effect upon circadian period under constant low light	300
8.7.4	Herbicides could be affecting the circadian oscillator through oxidative stress	302
8.7.5	Herbicides may influence de-synchronisation of oscillator components	304
8.7.6	Further observations	307
8.8	Conclusions	308
9	General discussion	311
9.1	Summary of novel findings	311
9.2	Broad implications of these findings for agriculture	314
9.2.1	How do these findings extend to field conditions?	314
9.2.2	What species are these results important for?	316
9.2.3	Can we use these results to reduce agrochemical use?	317
9.3	Application of these findings to new products	318
9.3.1	Have these results provided recommendations for testing new agrochemicals?	318
9.3.2	Could the circadian oscillator be a target for agrochemicals?	319
9.4	Overall conclusions	320

List of Figures

1.5.1	Circadian oscillator architecture	9
1.6.1	Glyphosate structure	17
1.6.2	Glyphosate inhibition	19
1.6.3	IAA biosynthesis	28
1.7.1	Mesotrione structure	29
1.7.2	Mesotrione inhibition	31
1.8.1	TBA structure	35
1.8.2	Terbuthylazine inhibition	36
2.1.1	Example of an imaging plate setup	43
2.6.1	Chlorophyll fluorescence trace	49
3.2.1	Rosette damage caused by treatment of herbicides	64
3.2.2	Mesotrione inhibits growth and causes damage to Arabidopsis rosettes	65
3.2.3	Terbuthylazine inhibits growth and causes damage to Arabidopsis rosettes	67
3.2.4	Glyphosate inhibits growth and causes damage to Arabidopsis rosettes	70
3.3.1	Diagram of the custom-built track sprayer	72
3.3.2	Testing of track sprayer	73
3.3.3	Arabidopsis rosettes sprayed with track sprayer	73
3.4.1	Example of chlorophyll fluorescence imaging plate	77
3.4.2	Increasing concentrations of glyphosate negatively affects photosynthesis	78
3.4.3	Increasing concentrations of mesotrione negatively affects photosynthesis	80

3.4.4	Terbutylazine negatively affects photosynthesis	81
3.4.5	Glyphosate takes more than 8 hours to affect photosynthesis	83
3.4.6	Mesotrione starts to affect photosynthesis after 60 minutes	85
3.4.7	Terbutylazine immediately affects photosynthesis	86
3.4.8	Glyphosate application time determines response of chlorophyll fluorescence	88
3.4.9	Mesotrione application time determines response of chlorophyll fluorescence	90
3.4.10	Terbutylazine application time determines response of chlorophyll fluorescence	92
3.5.1	Time taken for glyphosate to affect marker gene transcripts	96
3.5.2	Glyphosate affects the abundance of marker gene transcripts in a time of day dependent manner in Col-0	98
3.5.3	Glyphosate affects the abundance of marker gene transcripts in a time of day dependent manner in <i>CCA1-ox</i>	100
3.5.4	Response of marker gene transcripts to glyphosate is circadian regulated in Col-0	102
3.5.5	Response of marker gene transcripts to glyphosate is circadian regulated in <i>CCA1-ox</i>	104
4.2.1	Overlap between glyphosate-regulated transcripts and light-dark- or circadian-regulated transcripts	120
4.2.2	Rhythmic glyphosate transcripts analysis	121
4.4.1	Glyphosate causes a shorter hypocotyl length	130
4.4.2	Experimental method controls	132
4.4.3	Effect of hypocotyl measurement time	134
4.4.4	Glyphosate sensitivity under different photoperiods	135
4.4.5	Sensitivity to glyphosate in the dark	136
4.4.6	Effect of glyphosate on the rate of hypocotyl elongation	138
4.4.7	1.5x more glyphosate is required at dusk	139

4.4.8	Long term effect of glyphosate on seedlings	140
4.5.1	Entrainment of seedlings	142
4.5.2	Effect of glyphosate on hypocotyls under constant light	143
4.5.3	The effect of glyphosate is regulated by the circadian oscillator	144
4.6.1	Glyphosate alters PCD transcripts	147
4.6.2	Effect of glyphosate on PCD is circadian regulated	148
4.6.3	Glyphosate does not alter electrolyte leakage	150
4.6.4	Glyphosate alters pigment content	152
5.2.1	L-kynurenine inhibits hypocotyl elongation	164
5.2.2	Exogenous auxin overcomes the effect of glyphosate	165
5.2.3	Glyphosate may have an indirect effect through auxin transport	167
5.2.4	The response to diflufenzopyr is time-of-day-dependent	168
5.2.5	Mutation in phyB does not confer glyphosate resistance	170
5.3.1	Glyphosate had an inconsistent effect on DR5:GUS	172
5.4.1	Glyphosate may reduce DII-VENUS fluorescence	174
5.4.2	Glyphosate did not affect DR5::VENUS	174
5.4.3	Effect of glyphosate in DR5::VENUS hypocotyls	176
5.5.1	Glyphosate changes the transcript abundance of auxin signalling-related genes	178
5.5.2	Glyphosate changes the transcript abundance of auxin-related genes	179
6.2.1	Glyphosate shortens the Arabidopsis petiole	191
6.3.1	Glyphosate significantly reduced hypocotyl length in other species	195
7.3.1	Principal component analysis	205
7.4.1	Mesotrione-treated heat map	207
7.4.2	TBA-treated heat map	208
7.6.1	Mesotrione up-regulated promoter motifs	224
7.6.2	Adjuvant down-regulated promoter motifs	224

7.7.1	Overlap between mesotrione-regulated transcripts and circadian-regulated transcripts	226
7.7.2	Overlap between adjuvant-regulated transcripts and circadian-regulated transcripts	226
7.7.3	Overlap between TBA-regulated transcripts and circadian-regulated transcripts	227
8.3.1	Glyphosate affects <i>CCA1::LUC</i> under constant light	250
8.3.2	Glyphosate has little effect on <i>TOC1::LUC</i> under constant light	252
8.3.3	Mesotrione affects <i>CCA1::LUC</i> under constant light	254
8.3.4	Mesotrione affects <i>TOC1::LUC</i> under constant light	256
8.3.5	TBA affects <i>CCA1::LUC</i> under constant light	258
8.3.6	TBA affects <i>TOC1::LUC</i> under constant light	260
8.4.1	Glyphosate adjuvant affects <i>CCA1::LUC</i>	263
8.4.2	Glyphosate adjuvant affects <i>TOC1::LUC</i>	265
8.4.3	Effect of glyphosate adjuvants on <i>Arabidopsis</i>	266
8.4.4	Agridex affects <i>CCA1::LUC</i>	268
8.4.5	Agridex affects <i>TOC1::LUC</i>	270
8.5.1	Glyphosate affects <i>CCA1::LUC</i> under light-dark cycles	273
8.5.2	Glyphosate affects <i>TOC1::LUC</i> under light-dark cycles	275
8.5.3	Mesotrione affects <i>CCA1::LUC</i> under light-dark cycles	277
8.5.4	Mesotrione affects <i>TOC1::LUC</i> under light-dark cycles	279
8.5.5	TBA affects <i>CCA1::LUC</i> under light-dark cycles	281
8.5.6	TBA affects <i>TOC1::LUC</i> under light-dark cycles	283
8.6.1	Exogenous sucrose inhibits effects of mesotrione on <i>CCA1::LUC</i>	286
8.6.2	Effect of mesotrione in the presence of sorbitol or sucrose	287
8.6.3	Exogenous sucrose inhibits the effect of TBA on <i>CCA1</i>	289
8.6.4	Effect of TBA and Agridex in the presence of sorbitol or sucrose	291
8.6.5	Sucrose inhibits effect of mesotrione on <i>CCA1::LUC</i> under constant light	293

8.6.6	Sucrose inhibits the effect of mesotrione under constant low light . . .	295
9.1.1	Interaction between herbicides and the circadian oscillator	312

List of Tables

2.1.1	Seed genotypes used	42
2.3.1	Herbicides used	44
2.6.1	Chlorophyll fluorescence parameters	49
2.10.1	Primer sequences	52
3.2.1	Scoring system example	63
4.2.1	Rhythmic transcripts induced by glyphosate	122
4.2.2	Rhythmic transcripts repressed by glyphosate	123
4.3.1	Auxin GO terms	125
4.3.2	Glyphosate-, rhythmic- and auxin-regulated genes	127
6.2.1	Leaf morphology after glyphosate treatment	192
7.3.1	RNA-seq summary	204
7.4.1	Summary of differential gene expression in response to mesotrione treatment	209
7.4.2	Summary of differential gene expression in response to adjuvant treatment	209
7.4.3	Summary of differential gene expression in response to TBA treatment	210
7.4.4	Mesotrione up-regulated genes	211
7.4.5	Mesotrione down-regulated genes	212
7.4.6	Adjuvant up-regulated genes	213
7.4.7	Adjuvant down-regulated genes	214

7.4.8	TBA up-regulated genes	215
7.4.9	TBA down-regulated genes	216
7.5.1	Mesotrione up-regulated KEGG pathways	218
7.5.2	Mesotrione down-regulated KEGG pathways	219
7.5.3	Adjuvant up-regulated KEGG pathways	220
7.5.4	Adjuvant down-regulated KEGG pathways	221
7.5.5	TBA down-regulated KEGG pathways	222
8.3.1	Summary of herbicide effects under constant light	261
8.4.1	Summary of adjuvant effects under constant light	271
8.5.1	Summary of herbicide effects under light-dark cycles	284
8.6.1	Summary of herbicide effects with sucrose under light-dark cycles . . .	290
8.6.2	Mesotrione effect with sucrose under constant light	292
8.6.3	Mesotrione effect with sucrose under constant low light	296

Abbreviations

2,4-D	2-4-dichlorophenoxyacetic acid
4-HPP	4-hydroxyphenylpyruvate
ACT2	ACTIN2
AI	active ingredient
AMBA	2-amino-4-(methylsulfonyl) benzoic acid
AMPA	aminomethylphosphonic acid
bHLH	basic helix-loop-helix
BL	blade length
BR	brassinosteroid
BW	blade width
bZIP	basic leucine zipper
C	control
CAB	CHLOROPHYLL A/B-BINDING
CCA1	CIRCADIAN CLOCK ASSOCIATED1
cDNA	complementary DNA
CK	casein kinase
CM	control for mesotrione sample (water)
COP1	CONSTITUTIVELY PHOTOMORPHOGENIC1
CPuORF	conserved peptide upstream open reading frame
CRY	CRYPTOCHROME
CT	control for terbuthylazine sample (adjuvant)
DAD1	DEFENDER AGAINST APOPTOTIC DEATH1
DCMU	3-(3,4-dichlorophenyl)-1, 1-dimethylurea
DFP	diflufenzopyr
DMSO	dimethyl sulfoxide
DNOC	4,6-dinitro-ortho-cresol
DREB	dehydration-responsive element binding
DTX1	DETOXIFICATION1
E4P	erythrose-4-phosphate
EC	evening complex

EE	evening element
ELF3	EARLY FLOWERING3
ELF4	EARLY FLOWERING4
EM-CCD	electron multiplying-charged coupled device
EPSP	5-enolpyruvylshikimate-3-phosphate
EPSPS	5-enolpyruvylshikimate-3-phosphate synthase
ERF	ethylene-responsive element binding factor
EXPA	EXPANSIN
FDR	false discovery rate
FFT-NLLS	fast Fourier transform-nonlinear least-squares
GH3	GRETCHEN HAGEN-3
GI	GIGANTEA
GO	Gene Ontology
GOX	glyphosate oxidoreductase
GSA	gene specific analysis
GST	glutathione S-transferase
GUS	β -glucuronidase
HPPD	4-hydroxyphenylpyruvate dioxygenase
IAA	indole-3-acetic acid
IAM	indole-3-acetamide
IAOx	indole-3-acetaldoxime
IPyA	indole-3-pyruvic acid
IR	infra-red
KEGG	Kyoto Encyclopedia of Genes and Genomes
kyn	L-kynurenine
LHY	LATE ELONGATED HYPOCOTYL
LUC	LUCIFERASE
MAPK	MITOGEN-ACTIVATED PROTEIN KINASE
MC1	METACASPASE1
MNBA	4-methylsulfonyl-2-nitrobenzoic acid
MS	Murashige and Skoog nutrient mix
n.s.	non-significant difference

NAA	1-naphthaleneacetic acid
NPA	1-N-naphthylphthalamic acid
NPQ	non-photochemical quenching
nt	nucleotide
OM66	OUTER MITOCHONDRIAL MEMBRANE PROTEIN OF 66 KDA
OPDA	12-oxo-phytodienoic
PAP	3'-phosphoadenosine 5'-phosphate
PC	principal component
PCA	principal component analysis
PCD	programmed cell death
PDR12	PLEIOTROPIC DRUG RESISTANCE 12
PEP	phosphoenolpyruvate
PHYB	PHYTOCHROME B
PIF4	PHYTOCHROME INTERACTING FACTOR 4
PIN3	PIN-FORMED 3
PL	petiole length
PME5	PECTIN METHYLESTERASE 5
PQ	plastoquinone
PPFD	photosynthetic photon flux density
PRR5	PSEUDO-RESPONSE REGULATOR5
PRR7	PSEUDO-RESPONSE REGULATOR7
PRR9	PSEUDO-RESPONSE REGULATOR9
PSII	photosystem II
qPCR	quantitative reverse-transcription polymerase chain reaction
RAE	relative amplitude error
RNA-seq	RNA-sequencing
ROS	reactive oxygen species
RuBP	ribulose 1,5-bisphosphate
RVE	REVEILLE
S3P	shikimate-3-phosphate
SAS	shade avoidance syndrome
SAUR	SMALL AUXIN UP RNA

SEM	standard error of the mean
SPA	SUPPRESSOR OF PHYA
T	treated
TAA1	TRYPTOPHAN AMINOTRANSFERASE OF ARABIDOPSIS1
TAM	tryptamine
TAR	TRYPTOPHAN AMINOTRANSFERASE RELATED
TBA	terbuthylazine
TF	transcription factor
TFBS	transcription factor binding site
TM	treated mesotrione
TOC1	TIMING OF CAB2 EXPRESSION1
TPM	transcripts per million
TT	treated terbuthylazine
UGT74E2	URIDINE DIPHOSPHATE GLYCOSYLTRANSFERASE 74E2
UTR	untranslated region
X-Gluc	5-bromo-4-chloro-3-indolyl glucuronide salt
YUC	YUCCA
ZTL	ZEITLLEUPE

Chapter 1

Introduction

Global food production needs to increase by at least 70% by 2050 in order to feed the rising population (FAO, 2009). One of the major factors affecting crop production is pests, with weeds in particular having the potential to cause crop losses of up to 34% (Oerke, 2006). Herbicides are utilised in order to mitigate the effect of weeds upon crop production however herbicide resistance, environmental pollution, and a lack of new mode of action herbicides means that existing herbicides need to be used more effectively. Herbicides are also used for harvest management, e.g. to kill potato top-growth or to synchronise cereal head desiccation (Orson and Davies, 2007).

Previous research has identified that the time of day of herbicide application alters the effectiveness of herbicides (Norsworthy et al., 1999; Martinson et al., 2002; Miller et al., 2003; Mohr et al., 2007; Stewart et al., 2009). However, the majority of this research was conducted in the field, and attributes the sensitivity responses to a variety of factors. The plant circadian oscillator is involved in a vast number of plant processes (Greenham and McClung, 2015) and is proposed to restrict such processes to occur at the most appropriate time of day (Hotta et al., 2007). Therefore, we hypothesise that the circadian oscillator could be responsible for such time of day efficacy of herbicides. However, to date, there has been no direct or conclusive evidence to support this.

The aim of this research is to understand the mechanisms behind the time of day

sensitivity to three different mode of action herbicides: glyphosate, mesotrione, and terbuthylazine, and how the circadian oscillator is involved in these responses. This chapter reviews the current knowledge surrounding these herbicides of interest and their known time of day effectiveness.

1.1 The problem of weeds

Cultivation of land in order to produce optimal agricultural growth is frequently seen as an invitation for unwanted plant species. Weeds growing on arable land enforce major constraints on crop agriculture by reducing the quality and yield of harvest. If weeds are not controlled they can outgrow crops and monopolise available space, light, nutrients, water and carbon dioxide, negatively impacting the neighbouring crops (Mazur and Falco, 1989). Weeds can carry diseases and pathogens that may be passed on to the crop species, further reducing crop quantity (Zimdahl, 2013). Furthermore, weeds among crops can make harvest more difficult and less efficient, and can contaminate the produce (Orson and Davies, 2007). Current estimates suggest that 34% of global crop losses are due to around 200 weed species, with a global economic loss of over \$100 billion annually (Oerke, 2006; Hatfield et al., 2014; Swanton et al., 2015). Furthermore, over \$11 billion is spent per year controlling weeds in the USA, and over €12.5 billion in Europe (Hatfield et al., 2014; Plank et al., 2016). Consequently, weeds impact the global issue of food security, at a huge financial cost. Therefore, it is fundamental that weeds are controlled to maximise yields and profit. Aside from being agricultural pests, weeds persist in other locations such as along railways and roadsides obstructing vision, in water supplies restricting water flow, in golf courses and gardens, and in urban amenity areas (Kristoffersen et al., 2008; Borggaard and Gimsing, 2008). Therefore, despite their potential in terms of biodiversity and supporting ecosystems, weeds require control.

1.2 A background to herbicides

Whilst farming is ancient, mechanical and chemical methods for controlling weeds are comparatively recent inventions. In less-developed regions, weed control is still carried out by hand but this is an expensive and relatively ineffective task (Oerke, 2006; Délye et al., 2013). Herbicides, chemical substances toxic to plants, are the most common weed control method used elsewhere.

At the beginning of the twentieth century copper sulphate was the first chemical used for weed control, shortly after, corrosive fertilisers and industrial chemicals were identified as having herbicidal properties (Zimdahl, 2013). In 1932, the first purpose-produced herbicide was developed, 4,6-dinitro-ortho-cresol (DNOC), for control of annual weeds in cereals (Cobb and Reade, 2010). 2,4-Dichlorophenoxyacetic acid (2,4-D) and other synthetic growth hormone-based compounds were later produced, which could successfully control broadleaf weeds (Oerke, 2006). Today, herbicide use has become widespread and is considered the norm in intensive agriculture.

Current herbicides have various modes of action, meaning they act upon different molecular processes in plants to provide weed control (Harding and Raizada, 2015). Herbicides also possess different selectivity: non-selective herbicides kill all plant material in which they come into contact, whereas selective herbicides only kill the weed and not the crop species (Harding and Raizada, 2015). Furthermore, herbicides can be either contact or systemic (LeBaron et al., 2008). Contact herbicides kill parts of the plant that they come into contact with and there is minimal movement of the chemical through the plant. Systemic herbicides are translocated throughout the plant by the roots and the phloem and xylem (Zimdahl, 2013). A problem of systemic herbicides is that if too much is applied to the leaf, it kills the leaf before the chemical can be translocated. With over 25 groups of herbicides with different modes of action, and dozens of commercially available formulations per herbicide type, herbicide use has become so widespread that they have become inefficient in numerous ways.

1.3 The problems with herbicides

Specificity of herbicides has introduced natural selection pressures on weeds, with many herbicide-resistant weeds emerging worldwide (Harding and Raizada, 2015; Délye et al., 2008). Some 256 weed species have become resistant to 23 of the 26 current herbicide modes of action and to at least 167 herbicide formulations (Heap, 2019; Délye et al., 2008). In some cases, development of resistance to a novel herbicide has taken only three years (Duke, 2012). Although new herbicides are reported with different active ingredients, no new mode of action herbicide has been commercially available in the last 25 years. Prior to this, a herbicide with a new mode of action was reported every three years (Duke, 2012). Herbicide development is a complex task; compounds are screened for novel traits against a range of the most common weeds, while avoiding any damage to crops, followed by small scale field trials (Mazur and Falco, 1989). Herbicide-resistant crops may be accelerating this process. When only one type of herbicide is required, resistant weeds have a higher chance of emerging (Duke, 2012).

In the UK strict legislation, some EU-wide, applies to the use and production of herbicides (Kristoffersen et al., 2008). Potential new chemicals need to pass toxicology tests to ensure no harm is caused to crops, animals, and humans, in addition to limited residual soil- and water-mobility and persistence (Mazur and Falco, 1989; Kristoffersen et al., 2008). These factors add difficulty to development of new herbicides but has the benefit of restricting over- and improper use. Many herbicides leach from soil into ground water (Otto et al., 2016) and persist for weeks, making it a complex task to remove such contamination from water prior to consumption. Herbicide run-off is likely to increase with climate change causing more frequent heavy rainfall (Otto et al., 2016). Herbicide removal from water is one of the major financial contributions in water treatment (Kristoffersen et al., 2008).

Due to an increase in herbicide resistance, a lack in the development of new herbicide modes of action, strict environmental regulations and legislation, and the high costs

related to herbicide use, it would be advantageous to use existing herbicides more efficiently (Godar et al., 2015; Beckie and Tardif, 2012). Since global demands for crops will double in the next 35 years (Beltran et al., 2012), more effective herbicide use would improve crop yields while being financially beneficial. To use herbicides more effectively, different strategies could be implemented such as using multiple mode of action herbicides simultaneously, using herbicides in a specific sequence or at more effective times (Godar et al., 2015).

1.4 Factors affecting herbicide efficacy

Many factors determine the efficacy of herbicides. These include both fluctuations in environmental conditions and physiological processes occurring in the plant. It is likely that such factors contribute to the time of day efficacy of herbicides.

1.4.1 Environmental factors affecting herbicide efficacy

Translocation of some herbicides has been shown to be greatly increased under high humidity (Clor et al., 1963; McWhorter and Jordan, 1976). This could be because humid air provides an opportunity for the plant to absorb the herbicide through open stomata and hydrated cuticles. Humidity prevents the herbicide from drying out on the leaf surface, meaning that herbicide uptake is prolonged (Miller et al., 2003). Variation in humidity throughout the day could produce optimal times of herbicide application. However, herbicides do not commonly enter the leaf through the stomata unless specific additives are included within the formulation (Roggenbuck et al., 1990; Field and Bishop, 1988). At night dew can form on leaves under humid conditions. This means further re-wetting of the leaf could increase herbicide uptake, possibly by re-dissolving crystallised herbicides (Monaco et al., 2002). However, it is unclear whether this helps enhance absorption, or whether it means herbicides will run off or become more dilute (Miller et al., 2003). Furthermore, rainfall can cause similar

consequences for herbicide efficacy; depending on the amount of rain and time after application, this could cause the herbicide to wash off the leaf surface.

There is conflicting evidence for the effect of temperature on herbicide efficacy. Increasing temperature has been shown to increase translocation of herbicides within a plant (Dudek et al., 1973; Miller et al., 2003). This could be due to increased activity of physiological processes such as respiration and transpiration rates, and membrane permeability (Miller et al., 2003). However, temperature-dependent effects appear to vary depending on the chemistry of the herbicide and the weed species being controlled, since some herbicides have also been shown to cause greater damage to weeds at lower temperatures (Godar et al., 2015). High temperatures may increase the likelihood of the herbicide evaporating before it can be fully absorbed by the leaf, although some argue that the water evaporates and as such, the active ingredient remains at higher concentration on the leaf surface (Norsworthy et al., 1999).

Light can affect metabolic plant processes; for example, low light may mean that plants are photosynthesising less and consequently reducing translocation of herbicides (Miller et al., 2003). Conversely, high light may increase the efficacy of herbicides if they affect the photosynthetic apparatus. High light could, however, cause photodegradation of the chemicals in the herbicide, and as such, this has been a method investigated for removal of persistent herbicides in water systems (Orellana-García et al., 2014).

Another factor affecting herbicide efficacy in the field is wind. The majority of herbicides are sprayed on large scale farms, and strong winds can mean that little herbicide comes into contact with weeds. Conversely, wind can also lead to the herbicide drying more quickly, similar to high temperatures or low relative humidity (Sellers et al., 2003).

In the field, multiple environmental factors interact, for example when humidity decreases, temperature increases. This makes it difficult to determine which of these

factors has a primary effect on herbicide efficacy at different times of day (Skuterud et al., 1998).

1.4.2 Physiological factors affecting herbicide efficacy

The leaf architecture of some weed species affects the ability of the herbicide to penetrate through the leaf surface. Some weeds have a thick waxy cuticle, while others have many trichomes on the surface. The waxy surface of some leaves means that the high surface tension of the herbicide has difficulty saturating the surface, this can be made more difficult by the thickness of some cuticles (Monaco et al., 2002). Trichomes may contribute to herbicide efficacy because they help prevent herbicide running off the leaf (Martinson et al., 2002). Adjuvants are chemicals that can be added to the herbicide formulation to enhance herbicide permeation and its toxic effect by at least three times (Martinson et al., 2002). Adjuvants can reduce surface tension, or enhance cuticular penetration (McWhorter and Jordan, 1976). Other factors that can enhance permeation include: droplet size, droplet number, and pressure of application (Monaco et al., 2002).

Post-emergence herbicides are best applied when weeds are at a younger stage (one to three leaves) (Jordan et al., 1997). Younger weeds are growing rapidly, therefore the chances of a herbicide being translocated, increasing toxicity, is higher.

Many plant physiological processes follow a diel pattern correlated with environmental changes (Norsworthy et al., 1999). One example in velvetleaf (*Abutilon theophrasti*) is the dramatic alteration of leaf angle throughout the day depending on the availability of light. When the leaf angle deviates from 0° (at a right angle to the stem), herbicide efficiency is reduced by up to 67%, due to reduced available leaf area (Sellers et al., 2003; Mohr et al., 2007).

The factors described above outline possible explanations that lead to variation in the effectiveness of herbicides. Many of these factors alter throughout one day, and consequently may contribute to differences in effectiveness of herbicides during the day.

Many plant processes occur at certain times of day since they are regulated by the plant circadian oscillator (McClung, 2006). The circadian oscillator has the ability to restrict the response to certain factors depending on the timing of the exposure (Hotta et al., 2007). Therefore, it is possible that herbicide effectiveness is also influenced by the circadian oscillator and this must be considered when attempting to elucidate the effectiveness of herbicide applications at different times of day.

1.5 The circadian oscillator

Plants, as sessile organisms, evolved endogenous, self-sustaining circadian rhythms in order to adapt to, and predict, their changing environmental conditions such as the daily fluctuations in light, temperature, and humidity (Harmer, 2009; McClung, 2006). As such, the circadian oscillator is an internal regulator of the responses to the environment, set to an approximate 24-hour cycle (Harmer, 2009). Rhythms persist under constant conditions and are compensated for temperature fluctuations. Correct entrainment of the circadian oscillator to the environment confers a fitness advantage through increased photosynthesis, biomass, and carbon fixation (Dodd et al., 2005). Whilst most of our knowledge of the plant circadian system is derived from experiments with *Arabidopsis thaliana* (*Arabidopsis*), information is emerging in other plant species such as soybean (*Glycine max*) (Watanabe et al., 2011), maize (*Zea mays*) (Khan et al., 2010), rice (*Oryza sativa*) (Sugiyama et al., 2001), and in other land plants such as *Marchantia polymorpha* and *Anthoceros agrestis* (Linde et al., 2017).

1.5.1 Architecture of the *Arabidopsis* circadian oscillator

The *Arabidopsis* circadian oscillator is comprised of three core interconnected transcription-translation feedback loops (McClung, 2006). The core loop consists of three main components: two MYB-like transcription factors CIRCADIAN CLOCK

ASSOCIATED1 (CCA1) and LATE ELONGATED HYPOCOTYL (LHY) that reach peak protein levels in the morning and, by directly binding to an Evening Element (EE) promoter motif, repress *TIMING OF CAB2 EXPRESSION1* (*TOC1*; Fig. 1.5.1) (Alabadí et al., 2001; Adams et al., 2015). Towards the end of the day CCA1 and LHY protein levels decrease allowing *TOC1* to accumulate and subsequently repress the morning components (Gendron et al., 2012; Huang et al., 2012b). The evening loop, or complex, consisting of LUX, EARLY FLOWERING3 (ELF3) and ELF4, down-regulate *TOC1* transcription allowing CCA1 and LHY to be expressed again in the morning (Adams et al., 2015) (Fig. 1.5.1).

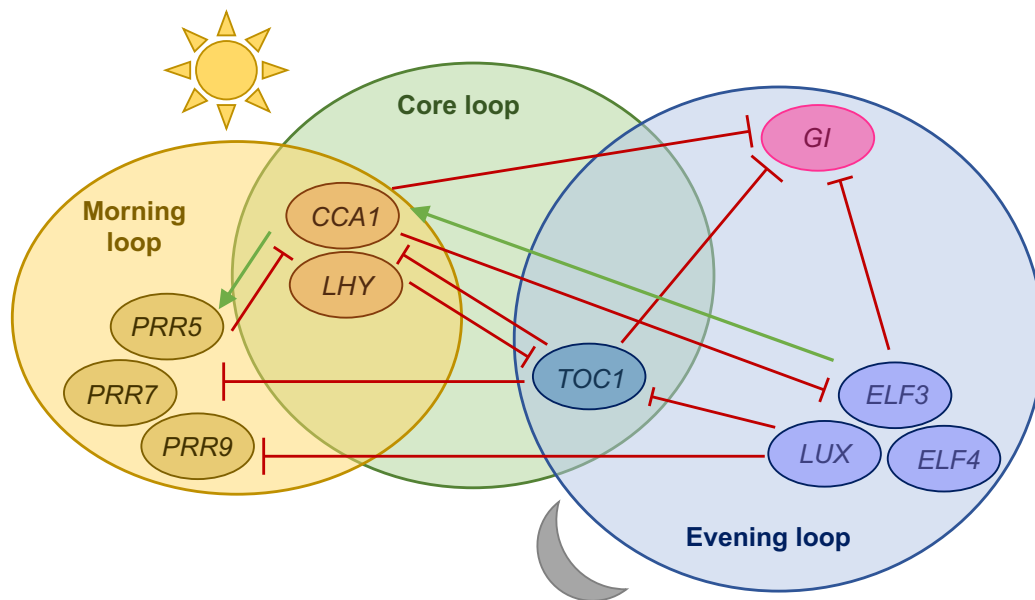


Figure 1.5.1: A simplified overview of the Arabidopsis circadian oscillator. CCA1 and LHY repress *TOC1*, *ELF3* and *ELF4*, and *LUX* transcription in the morning, and activate *PRR5*, *PRR7* and *PRR9*. In the evening, *TOC1* transcription is down-regulated, which allows CCA1 and LHY to be expressed in the morning. The evening complex can bind to *PRR7* and *PRR9*, which repress *CCA1* and *LHY*. Circles indicate phase of gene expression. Red lines indicate negative transcriptional regulation, green arrows indicate positive transcriptional regulation. Diagram synthesised from Harmer (2009) and Greenham and McClung (2015).

The morning loop contains *TOC1* homologs PSEUDO-RESPONSE REGULATOR5 (*PRR5*), *PRR7*, and *PRR9* that also bind to the *CCA1* and *LHY* promoters to repress their activity (Nakamichi et al., 2010) (Fig. 1.5.1); however, CCA1 and LHY

can also activate *PRR* transcripts, explaining why these transcripts peak a few hours after the early morning genes (Farré et al., 2005). Other regulatory mechanisms of the oscillator include CCA1 and LHY directly suppressing the transcription of *ELF4* and *LUX* (Li et al., 2011), and ELF3 and ELF4 repress *PRR7* and *PRR9*, and finally LUX represses *PRR9* (Nakamichi et al., 2010). It has been suggested that CCA1 and LHY can negatively auto-regulate their own and each other's transcripts (Adams et al., 2015), and that LHY can repress all other oscillator components, including the *PRR* genes (Adams et al., 2015). *GIGANTEA* (*GI*) is repressed by CCA1 and LHY, and may form a loop with TOC1 (Greenham and McClung, 2015; Dalchau et al., 2011).

One of the more recently identified components of the Arabidopsis circadian oscillator is that involving the *REVEILLE* (*RVE*) gene family, which are MYB-like homologs of CCA1 and LHY (Rawat et al., 2011). RVE8 protein abundance peaks in the afternoon, later than CCA1 and LHY (Rawat et al., 2011). RVE8 forms a feedback loop with *PRR5*, where RVE8 promotes expression of *PRR5*, and *PRR5* represses expression of *RVE8* (Rawat et al., 2011). Transcriptional activation by RVE8, and two close homologs RVE4 and RVE6, was found to extend to several other genes within the core oscillator that contain an EE, including *TOC1* and *ELF4* (Hsu et al., 2013). This transcriptional activation by RVE4 and RVE8 is understood to occur by direct interaction with two other morning-expressed proteins NIGHT LIGHT-INDUCIBLE AND CLOCK-REGULATED1 (LNK1) and LNK2, which act as co-activators necessary for expression of *TOC1* and *PRR5* (Xie et al., 2014; Xing et al., 2015). These interconnected transcriptional-translational feedback loops are thought to comprise the current model of the Arabidopsis circadian oscillator, however it is likely that there are components that are not yet understood or known.

1.5.2 Regulatory mechanisms within the circadian oscillator

For the transcription-translation feedback loops of circadian oscillator components to

function, more intricate regulatory mechanisms must occur. These include epigenetic regulation of gene expression through chromatin remodelling and post-translational modifications, such as phosphorylation, of the core oscillator proteins (Nohales and Kay, 2016).

Since transcriptional regulation underlies the basis of the core circadian oscillator, and this relies on chromatin status, it is necessary to understand changes in chromatin structure (Chen and Mas, 2019). The extent of chromatin compaction affects transcriptional status, where compact DNA prevents access of transcriptional machinery and an open chromatin structure favours initiation of transcription (Stratmann and Más, 2008). Covalent modification of histones by acetylation and methylation, and DNA methylation determine such chromatin remodelling (Du et al., 2019). For example, histone hyperacetylation is associated with an open, accessible chromatin and transcriptional activation, whereas histone hypoacetylation is associated with a compact chromatin and gene repression (Grunstein, 1997). Within the circadian oscillator, repression of *TOC1* by CCA1 depends on a repressive chromatin environment in the *TOC1* promoter, caused by rhythmic histone deacetylation (Perales and Más, 2007; Malapeira et al., 2012). Conversely, RVE8 causes an increase in acetylation at the *TOC1* promoter, opening the chromatin structure and enhancing *TOC1* expression (Farinas and Más, 2011). Also within the core oscillator, trimethylation of histone 3 lysine 4 (H3K4me3) is rhythmic (Malapeira et al., 2012). Reduced H3K4me3 activity is associated with increased oscillator-repressor binding (such as CCA1) suggesting that methylation is responsible for correct timing of gene activity and consequently precise timing of the oscillator (Malapeira et al., 2012; Chen and Mas, 2019). Similar mechanisms are reported for LHY, PRR9, PRR7, and LUX (Malapeira et al., 2012; Chen and Mas, 2019; Yang et al., 2018). Furthermore, acetylation and methylation appear to occur with different phases, suggesting modification mechanisms are related to timing-specificity (Malapeira et al., 2012). These examples demonstrate that epigenetic regulation is an important factor of circadian oscillator function.

The post-translational modification phosphorylation is an essential component of cell

signalling. Phosphorylation is required for different aspects of circadian regulation including oscillator entrainment, function, and outputs (Kusakina and Dodd, 2012). Furthermore, many kinases and phosphatases are circadian-regulated (Nohales and Kay, 2016). Within the oscillator, phosphorylation can regulate: protein-protein interactions, protein-DNA interactions, and degradation of oscillator components (Kusakina and Dodd, 2012). Casein kinase 2 (CK2) is the best understood kinase involved in circadian regulation in *Arabidopsis* (Nohales and Kay, 2016). CK2 phosphorylates CCA1 and LHY (Sugano et al., 1998, 1999). CCA1 phosphorylation alters protein dimerisation, and DNA-binding activity (Daniel et al., 2004). In turn, this determines the circadian period (Daniel et al., 2004). CK2 phosphorylation of CCA1 is also essential for temperature compensation by the circadian oscillator (Portolés and Más, 2010). PRRs are also phosphorylated (Fujiwara et al., 2008). Greater levels of PRR5 and TOC1 phosphorylation cause increased binding to the F-box protein ZEITLUPE (ZTL), and subsequently enhances proteolysis (Fujiwara et al., 2008). Conversely, phosphorylation of PRR3 and TOC1 is necessary for their protein-protein interaction and protects from degradation by ZTL (Fujiwara et al., 2008). These examples of post-translational modification through phosphorylation regulate the phase-specific protein levels and cyclic activity of oscillator proteins (Fujiwara et al., 2008).

Alternative splicing of oscillator genes including *CCA1*, *LHY*, *RVE8*, and the *PRR* genes is also reported to occur under certain environmental conditions to regulate oscillator performance (Nohales and Kay, 2016). For example, *LHY* and *PRR7* undergo alternative splicing under cold temperatures, which reduces the number of functional transcripts (James et al., 2012). Production of truncated proteins through alternative splicing events is likely to interfere with correct dimerisation of proteins within the oscillator. However, much of the work on alternative splicing and circadian regulation is involved in the downstream response to environmental signals rather than the core oscillator function.

Whilst an enormous amount of research has been conducted to elucidate the architecture and regulatory mechanisms that comprise the circadian oscillator, many aspects

remain to be determined. For example, a somewhat recent discovery was the existence of tissue-specific oscillators (Endo et al., 2014; Takahashi et al., 2015). The coupling and signalling between tissue-specific oscillators is reminiscent of the mammalian circadian system, but how the core oscillator can signal between cell type-specific oscillators remains poorly understood in plants.

1.5.3 Entrainment of the circadian oscillator

Although circadian rhythms are self-sustaining, environmental signals are required to convey timing information to set the phase of the oscillator to the correct time of day (Nohales and Kay, 2016). Environmental signals known to entrain the oscillator are light and temperature (Salomé and McClung, 2005b). Photoreceptors are responsible for integrating light information to the oscillator, where the phytochrome (phy) and cryptochrome (cry) perceive red and blue light (Somers et al., 1998a). Aschoff (1960) identified that under constant light conditions, the activity phase shortens in nocturnal organisms and lengthens in diurnal organisms. Plants are neither diurnal or nocturnal but their circadian oscillator responds as that of diurnal animals. Furthermore, in plants, an increase in light intensity increases the pace of the circadian oscillator, and consequently shortens the circadian period (Aschoff, 1979; Somers et al., 1998a). Increased red light intensity shortens the circadian period, where phyB is the main high-intensity red light photoreceptor and phyA transmits information concerning low-intensity red and blue light (Somers et al., 1998a). Cry1 is the main low blue light photoreceptor where a longer circadian period is reported, and cry2 is the key high blue light photoreceptor (Somers et al., 1998a). UV RESISTANCE LOCUS 8 (UVR8) is a UV-B photoreceptor (Rizzini et al., 2011). Low intensity UV-B entrains the oscillator by interacting with CONSTITUTIVELY PHOTOMORPHOGENIC 1 (COP1) (Fehér et al., 2011; Favory et al., 2009). Little is known about the mechanism for exactly how these photoreceptors relay information to the oscillator. In contrast, the mechanism through which ZTL signals as a blue-light sensor to the oscillator is better understood. ZTL is an E3 ubiquitin ligase that causes degradation of TOC1

and PRR5 and increases the pace of the oscillator (Baudry et al., 2010). However, this only occurs in the dark, since perception of blue light initiates an interaction between ZTL and GI, stabilising ZTL and preventing binding to proteasomal targets (Kim et al., 2007). Metabolic sugars arising from photosynthesis are also able to entrain the circadian oscillator early in the photoperiod by regulating expression of core oscillator components, and this is dependent on PRR7 (Haydon et al., 2013).

Temperature entrainment of the circadian oscillator is less well understood than light entrainment. There has been no identification of an oscillator-specific thermosensor, but other oscillator-related components such as phyB have been reported to convey temperature information (Legris et al., 2016; Gil and Park, 2019). PRR7 and PRR9 are also important for temperature entrainment, since plants that lack these proteins cannot entrain to warm/cold cycles (Salomé and McClung, 2005b).

1.5.4 Outputs of the circadian oscillator

The circadian oscillator regulates many plant responses, termed “outputs”, of the circadian oscillator. Much of the regulation is conducted through transcriptional regulation where 6-89% of the Arabidopsis transcriptome has been reported to have rhythmic expression under at least one type of cyclic condition (Harmer et al., 2000; Edwards et al., 2006; Michael et al., 2008). Rhythmic changes in gene expression coordinate visible changes in plant physiology including hypocotyl elongation (Dowson-Day and Millar, 1999) and cotyledon and leaf movement (Kim et al., 1993). Indeed, it was observations of leaf movements in 1729 that first led to the recognition of possible endogenous rhythms across all kingdoms of life (de Mairan, 1729).

Light-dependent rhythmic hypocotyl elongation requires the transcription factors PHYTOCHROME-INTERACTING FACTOR 4 (PIF4) and PIF5 (Nozue et al., 2007). PIF4 and PIF5 expression correlates with elongation, which peaks at the end of the night (Nozue et al., 2007). PIF degradation depends on PHYB after exposure to light. Furthermore, *PIF4* and *PIF5* are circadian regulated whereby ELF3, of the

evening complex, interacts with PIF4 and inhibits its activity as a transcriptional regulator (Greenham and McClung, 2015). ELF3 has also been reported to be essential in rhythmic leaf growth (Dornbusch et al., 2014). However, maximal leaf growth occurs after dawn, unlike hypocotyl elongation (Dornbusch et al., 2014). Therefore, *PIF4* and *PIF5* are not essential in rhythmic leaf growth and this provides evidence that circadian regulation of physiology works through many pathways. Photoperiodic flowering also relies on rhythmic components driven by the oscillator where light signalling later in the day leads to degradation of flowering repressors including CYCLING DOF FACTORS (CDFs), and activates flowering inducers such as CONSTANS (CO). The oscillator component GI is also involved in this targeted degradation of flowering repressors (Song et al., 2012).

Nutrient elements and ions, such as nitrogen, calcium, iron and magnesium, are essential for physiology and metabolism (Haydon et al., 2015). Nutrient demand follows a rhythmic pattern, indicating that it is under circadian control (Sanchez and Kay, 2016). Many of these nutrients can both affect the function of the oscillator and be rhythmically regulated. For example, nitrogen required for nucleotide and protein biosynthesis can modify *CCA1* expression and induce a phase shift in the oscillator (Gutiérrez et al., 2008). Additionally, *CCA1* regulates genes downstream in N metabolism by binding to gene promoters (Gutiérrez et al., 2008; Sanchez and Kay, 2016). Iron has been shown to be involved in maintaining correct period, since iron-deficiency causes a long period (Chen et al., 2013). *CCA1* and *LHY* are required for signalling iron deficiency (Chen et al., 2013). This suggests reciprocal regulation between the oscillator and iron homeostasis (Chen et al., 2013). Furthermore, in plants there are circadian rhythms in the concentration of cytosolic free calcium ions and such concentrations are able to affect circadian period (Martí Ruiz et al., 2018). Finally, magnesium ions are regulated by the circadian oscillator in *Ostreococcus* to increase during periods of higher energetic demand (Feeney et al., 2016). In turn, the magnesium feeds back to regulate circadian period and phase of oscillator gene expression (Feeney et al., 2016).

The interaction between the core oscillator and the outputs determines the phenotype of the plant. Many outputs of the oscillator also feed back in to the oscillator creating a complex connected loop (Sanchez and Kay, 2016). As such, it can be difficult to elucidate the effect of one factor on the circadian oscillator, and vice versa, since the oscillator is intertwined with so many processes.

1.5.5 Circadian gating

The circadian oscillator provides the plant with the ability to restrict the response to a stimulus to a certain time of day and to alter the magnitude of such response through a concept known as “gating” (Hotta et al., 2007). Circadian gating of a pathway can occur through regulating the levels of signalling intermediates, regulating the activity of signalling molecules, or regulating the availability of metabolites (Hotta et al., 2007). This is thought to allow the plant to respond at a time of day that is more physiologically suitable and to prevent wasting resources (Covington and Harmer, 2007).

An example of circadian gating is that of the cold-induced *C-REPEAT BINDING FACTOR1* (*CBF1*) gene being induced to different extents depending on the time at which a freezing treatment is applied. Maximum *CBF* expression is restricted to 4 hours after subjective dawn, since it depends on *CCA1* binding and acting as a transcription activator (Fowler et al., 2005). The response of plants to vegetational shade has also been shown to be circadian gated (Salter et al., 2003). *PIF3-like 1* (*PIL1*) transcripts encode a protein that interacts with *TOC1* (Salter et al., 2003). *PIL1* is strongly induced by low R:FR ratios at subjective dawn, but induced weakly at subjective dusk (Salter et al., 2003).

There is much still to learn about the advantageous role of circadian gating, and the significance of gating responses in the environment. However, these examples show that the circadian oscillator is not only necessary for correct plant function, but that the plant is capable of restricting the responses, via the circadian oscillator, to

certain times of day. Therefore, it may be possible that there is circadian regulation of responses of plants to herbicides, and that differing magnitudes in response will be observed at different times of day due to circadian regulation.

1.6 Glyphosate

Glyphosate, *N*-(phosphonomethyl)glycine, is a broad-spectrum, non-selective herbicide (Duke and Powles, 2008) that is currently the most widely used herbicide globally (Benbrook, 2016). Glyphosate was discovered in 1950 by Henri Martin at Cilag, a Swiss pharmaceutical company, but no mammalian pharmaceutical activity was ever identified for the compound (Dill et al., 2010). John Franz at Monsanto successfully increased the toxicity of glyphosate and in 1970 Monsanto synthesised and patented glyphosate, which was sold commercially as Roundup in 1974 (Duke and Powles, 2008; Dill et al., 2010).

Glyphosate is an odourless, white crystalline solid that is highly soluble in water (Cañero et al., 2011; Dill et al., 2010). The compound contains an amino group derivative of the naturally occurring amino acid glycine, plus a phosphonate group, from which the name glyphosate originates (Fig. 1.6.1) (Dill et al., 2010).

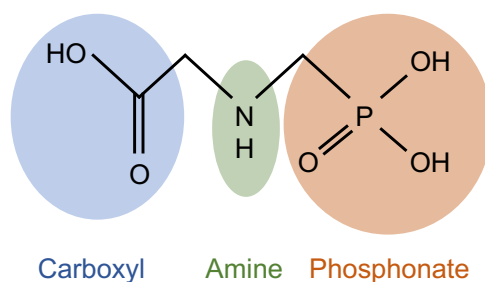


Figure 1.6.1: Chemical structure of glyphosate. Glyphosate, *N*-(phosphonomethyl)glycine, contains a carboxyl group (blue) and an amine group (green), similar to the amino acid glycine, plus a phosphonate group (orange).

1.6.1 Glyphosate mode of action

The mechanism underlying the herbicidal activity of glyphosate was identified soon after glyphosate was available commercially. Jaworski (1972) identified that glyphosate inhibited the aromatic amino acid biosynthesis pathway by rescuing growth inhibition by the addition of L-phenylalanine. Subsequently, Amrhein et al. (1980) discovered that glyphosate inhibited, more specifically, the incorporation of shikimate into the three naturally occurring aromatic amino acids: phenylalanine, tyrosine and tryptophan. They identified that, as chorismate is the common precursor substrate to these amino acids, glyphosate must inhibit chorismate formation, or a preceding step (Amrhein et al., 1980). It was later discovered that the enzyme 5-enolpyruvylshikimate-3-phosphate synthase (EPSPS) was inhibited by glyphosate (Steinrücken and Amrhein, 1980) (Fig. 1.6.2). EPSPS is required for the penultimate stage of the shikimate pathway (Herrmann and Weaver, 1999).

The shikimate pathway is a seven-step metabolic process that begins with phosphoenolpyruvate (PEP) and erythrose-4-phosphate and ultimately leads to chorismate synthesis (Herrmann, 1995). Subsequent to the shikimate pathway, chorismate feeds into the aromatic amino acids and, ultimately, other essential plant metabolites (Herrmann and Weaver, 1999). The shikimate pathway is only present in plants and microorganisms, making EPSPS an effective herbicide target (Steinrücken and Amrhein, 1980). Glyphosate is currently the only herbicide with this mode of action (Duke and Powles, 2008).

EPSPS catalyses the reversible formation of 5-enolpyruvylshikimate-3-phosphate (EPSP), plus an inorganic phosphate, from the transfer of the enolpyruvyl group from a PEP to shikimate-3-phosphate (S3P) via a tetrahedral intermediate complex (EPSPS-S3P-PEP; Fig. 1.6.2) (Herrmann and Weaver, 1999; Schönbrunn et al., 2001; Alibhai and Stallings, 2001). The precise way in which glyphosate blocks EPSPS activity took many years to understand, S3P binds to EPSPS before PEP binds (Majumder et al., 1995). Glyphosate can bind to the EPSPS-S3P complex, mimicking the EPSPS-

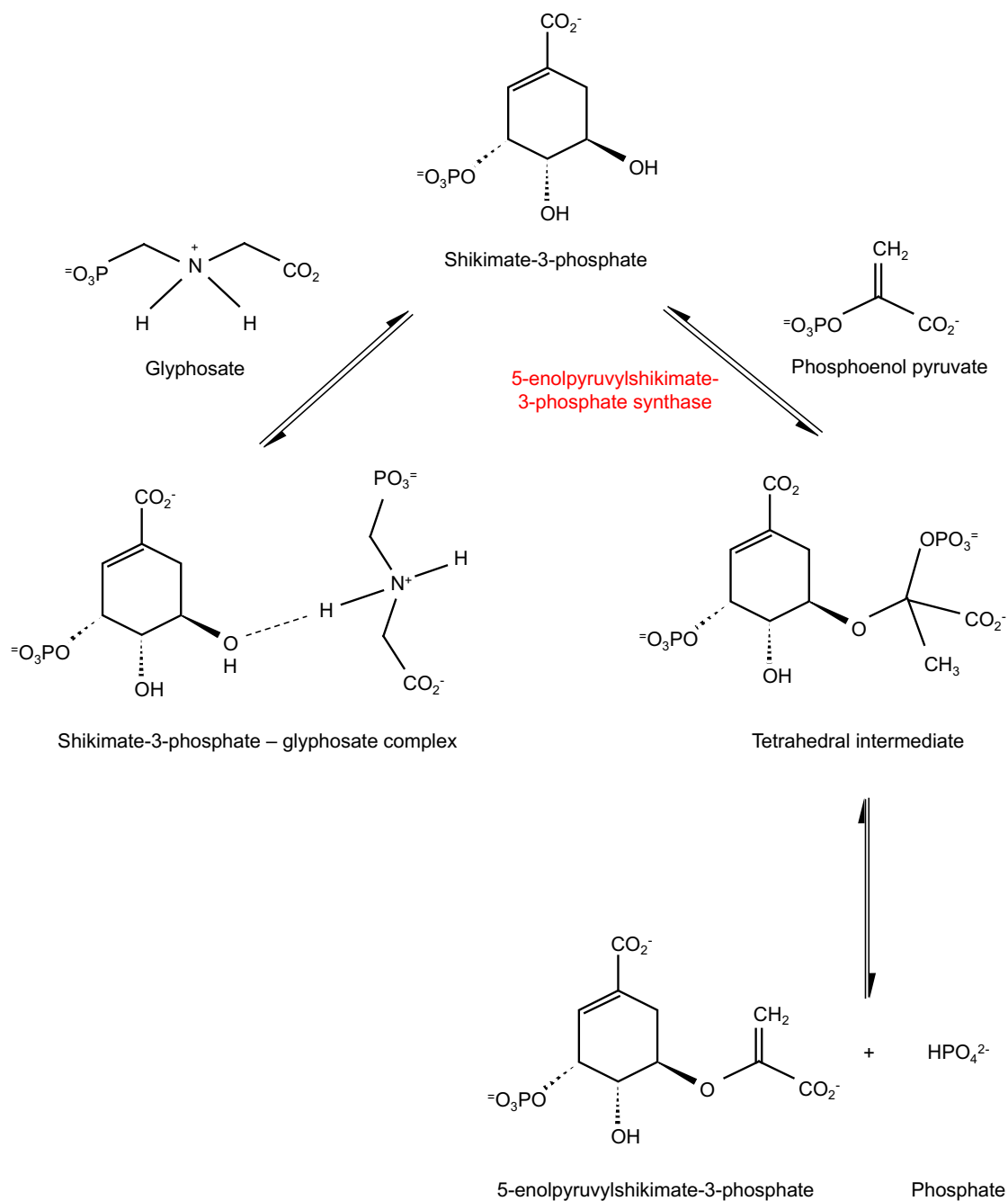


Figure 1.6.2: The inhibition of phosphoenol pyruvate (PEP) and 5-enolpyruvylshikimate-3-phosphate synthase (EPSPS) activity by glyphosate in the shikimate pathway. Glyphosate competes with PEP to bind to shikimate-3-phosphate (S3P), stopping EPSPS (in red) catalysing the transfer of the enolpyruvyl group from PEP to S3P, and consequently preventing the formation of EPSP. Diagram redrawn from Alibhai and Stallings (2001).

S3P-PEP complex, thus preventing PEP binding (Christensen and Schaefer, 1993). Therefore, EPSP cannot be produced by reaction with EPSPS in the presence of glyphosate. When present, glyphosate is a competitive inhibitor of PEP and therefore S3P will preferentially bind to glyphosate over PEP (Alibhai and Stallings, 2001). Glyphosate has high specificity for the PEP binding site on S3P but, interestingly, glyphosate does not inhibit other reactions that use PEP as a substrate (Herrmann and Weaver, 1999).

Inhibition of EPSPS results in a decrease in aromatic amino acid concentrations, inhibits incorporation of shikimate into the aromatic amino acids, and causes several hundredfold accumulation of shikimate within plant tissues by increasing carbon flow to S3P (Steinrücken and Amrhein, 1980). Different species have variations in their sensitivity to glyphosate, one explanation is that some plants have a higher baseline level of metabolic activity of pathways such as the shikimate pathway. This suggests more carbon flow through the pathway and a greater concentration of aromatic amino acids (Westwood and Weller, 1997). Alternatively, a higher level of aromatic amino acids before treatment with glyphosate may mean that a plant can continue with other metabolic processes even though glyphosate will be preventing more from being made (Westwood and Weller, 1997). Another alternative is that the differences in sensitivity are due to differences in inhibition constants between genotypes or species (Herrmann and Weaver, 1999). Finally, higher copy numbers of the *EPSPS* gene have been observed in natural populations that have evolved resistance to glyphosate, and it is this mechanism through which glyphosate-resistant crops are usually produced (Yang et al., 2017).

1.6.2 Glyphosate movement within the plant

EPSPS transcripts are expressed most highly in the meristem and flowers, then in the stem, followed by mature leaves and cotyledons (Weaver and Herrmann, 1997; Hetherington et al., 1999). As such, these tissues are the most sensitive to glyphosate

(Shaner, 2009). EPSPS translocates from the nucleus to the chloroplast where the aromatic amino acids are synthesised. Therefore, in order for glyphosate to be effective, it needs to reach the chloroplast. Glyphosate readily transports around a plant within a few hours of application (Gougler and Geiger, 1981). Translocation occurs via the phloem, where it follows sucrose movement from the source leaves to the sink tissues (Gougler and Geiger, 1981; Shaner, 2009; Gomes et al., 2014). Some transport occurs within the xylem, although it rapidly reloads back into the phloem, resulting in larger accumulation in sink tissue rather than at leaf tips (Preston and Wakelin, 2008; Schrübbers et al., 2016). Initial uptake is rapid in the cuticle, followed by slower uptake through the symplast (Gomes et al., 2014).

There are two glyphosate uptake mechanisms into the cell: an active uptake mechanism working at low concentrations, and a passive mass flow system (Shaner, 2009; Gougler and Geiger, 1981). Efflux experiments suggest that glyphosate predominantly localises to the cell wall and the cytoplasm, with very little accumulating in the vacuole. A study comparing the translocation of glyphosate in susceptible- and resistant-horseweed plants found that in the resistant plants, more than 85% of the glyphosate was in the vacuole, whereas in the susceptible plants, there was only 15% in the vacuole (Ge et al., 2010). Glyphosate enters the cytoplasm at the same rate for both resistant and susceptible plants, but within hours in the resistant plants glyphosate enters the vacuole, which does not occur until much later in the susceptible plants. This suggests a transporter is present, or present with a higher activity in the resistant plants. While glyphosate remains in the cytoplasm, it is available to be transported to sink tissues, whereas when it is in the vacuole it is not able to be transported via the phloem (Ge et al., 2010). There are also reports of glyphosate exiting the plant via the roots into the soil (Gomes et al., 2014).

1.6.3 Glyphosate metabolism within the plant

It was originally thought that glyphosate is metabolised very slowly within plants, if at all (Duke, 2011; Arregui et al., 2003). The main metabolite of glyphosate is aminomethylphosphonic acid (AMPA), which is produced by splitting the C-N bond in glyphosate to also produce glyoxylate (Duke, 2011). This reaction requires a glyphosate oxidoreductase (GOX) enzyme, but this is only found naturally in a few plant species such as soybean (Duke, 2011). Therefore, most plants cannot metabolise glyphosate naturally.

There is data suggesting glyphosate metabolism in some weed species (*Agropyron repens*, *Convolvulus arvensis*, *Ipomoea purpurea*) (Duke, 2011), implying that these species may have a GOX. Other weed species may have lower levels of this enzyme, or in contrast, have an enzyme that is able to further degrade AMPA (Duke, 2011). It is possible that the stage of growth at which the plants are treated has an effect on the ability of the plant to break down glyphosate. Duke (2011) found that plants in full bloom contained much higher levels of glyphosate and AMPA in them compared to those sprayed two weeks earlier. Alternatively, it could appear that levels of glyphosate are decreasing due to a dilution effect of the plant growing (Bernal et al., 2012).

1.6.4 Glyphosate in the environment

Due to the extensive use of glyphosate it is important to understand what happens to the substance in the environment. The persistence and leachability of a herbicide in soil is variable and depends on the ability to attach to soil components (Borggaard and Gimsing, 2008). Glyphosate does not chemically decompose by itself in the environment, instead it is strongly adsorbed by minerals in soil due to its polar functional groups (Sprankle et al., 1975a). Glyphosate sorption varies depending on the components in the soil, and the soil pH. In soils with low organic components (e.g. clay), and higher sand content, less adsorption can occur resulting in a higher level of leaching to water courses (Sprankle et al., 1975a,b; Lupi et al., 2015).

Environmental degradation of glyphosate in soil and water is thought to occur only through the action of microorganisms, with no degradation occurring in sterile conditions (Rueppel et al., 1977). This degradation by microorganisms occurs through two pathways, resulting in different intermediates forming: sarcosine and glycine, or AMPA and glyoxylate by using microbial GOX (Liu et al., 1991). The initial degradation of glyphosate in soil is rapid but the degradation of downstream metabolites is slower (Dill et al., 2010). Reported half-life rates of glyphosate in soil range considerably, although it is suggested that it is around 3 days for glyphosate, but between 100-1000 days for AMPA (Borggaard and Gimsing, 2008; Assalin et al., 2010). Microbial GOX has been transformed into some glyphosate resistant crops, in addition to EPSPS, to cause glyphosate degradation and prevent damage by the herbicide (Duke, 2011). Finally, photo-degradation of glyphosate only occurs under artificial conditions, or by using a catalyst (Shifu and Yunzhang, 2007; Dill et al., 2010). Therefore, in addition to glyphosate having low-toxicity, it does not persist in the environment for very long under the majority of naturally occurring conditions. However, the breakdown product AMPA does persist, and is mildly phytotoxic (Duke, 2011).

1.6.5 Glyphosate concentrations in agriculture

In the field, glyphosate is usually sprayed at a minimum rate of 720 g active ingredient per hectare (g/ha), with 1 hectare receiving a nominal 200 litres spray volume (Waltz et al., 2004; Hilgenfeld et al., 2004). This high dose ensures a lethal effect regardless of species; but lower doses are still lethal. Various factors affect the minimum lethal concentration, such as the species of the plant, and the growth stage at which they are treated (de Carvalho et al., 2013). Some experiments have used very high concentrations such as 2.1 kg/ha, and 0.96-1.68 kg/ha for soybean experiments (Jiang et al., 2013; Arregui et al., 2003). A field experiment for velvet leaf control used 210-840 g/ha, and in controlled growth chamber experiments 840 g/ha (Waltz et al., 2004).

In the few studies using *Arabidopsis*, the concentrations of glyphosate used are generally lower. For example, 10 g/ha is estimated to give a 50% reduction in the dry mass of *Arabidopsis* (Das et al., 2010). Similarly, Brotherton et al. (2007) used 11.5 g/ha. Some research used a concentration of 200 μ M glyphosate, which equates to approximately 6 g/ha glyphosate (Sharkhuu et al., 2014; Faus et al., 2015). These concentrations are unlike field experiments as they are not intended to completely kill all the weed species present; instead, they are designed to detect more subtle effects of glyphosate.

1.6.6 Glyphosate time of day effects

Several studies have shown that the efficacy of the herbicide can depend on the time of day that it is applied. The majority of research has been conducted in the field and concludes that the time of day changes in efficacy of glyphosate are due to environmental factors.

One study of time of day effects of glyphosate application examined four time points: 45 minutes pre-dawn, 4 hours after dawn, 3 hours pre-dusk and 90 minutes after dusk, with four different weed species (Norsworthy et al., 1999). The effects varied between species but regardless of this and glyphosate concentration a similar trend was apparent: glyphosate was least effective pre-dawn and post-dusk (Norsworthy et al., 1999).

Martinson et al. (2002) found that 420 g/ha glyphosate without adjuvant had the greatest effect between 09:00 and 18:00. When adjuvant was added, this increased the length of the efficacy to several hours either side of the original peak time. The lowest times of efficacy were dawn, dusk, and three hours after dusk. Statistically, temperature was the only other factor alongside time that significantly affected glyphosate efficacy, even though these experiments were field experiments with multiple other factors having the potential to affect herbicide efficacy (Martinson et al., 2002). Further research applied glyphosate in the field at two concentrations (half field rate and quarter field rate) every three hours between 06:00 and 24:00, when dawn and dusk

were approximately 05:30 and 21:00, respectively (Miller et al., 2003). Environmental factors present in the field were the main focus and were affecting the outcome of any underlying circadian effects. When the combined data from different field sites and different years was examined, Miller et al. (2003) found that greatest weed control occurred between 09:00 and 18:00. This is quite a wide range of effective times. Another study also found glyphosate provided the most control in the field when treatment was between 09:00 and 18:00 (Stopps et al., 2013). However, this study failed to state the times of dawn and dusk or how long the treatments were before and after the light period.

In field experiments using 840 g/ha glyphosate, velvetleaf control was low when glyphosate was applied before dawn, at about 70% control (Waltz et al., 2004). Glyphosate applied after sunset was even less effective than glyphosate applied before sunrise, at around 30% control, whereas at midday velvetleaf control was around 100% (Waltz et al., 2004). Likewise, in growth chamber experiments, velvetleaf biomass and height were affected more by applications after the onset of light compared to applications before the onset of light (Waltz et al., 2004). In these growth chamber experiments, temperature was kept constant therefore this was not a contributing factor to daily changes in glyphosate efficacy (Waltz et al., 2004). In the field, the most effective glyphosate treatment time was while relative humidity was lowest. In the growth chambers, relative humidity did not fluctuate so could not contribute to changes in glyphosate efficacy (Waltz et al., 2004). In the growth chamber, leaf blades were kept at a horizontal angle in one experiment to control for the variable leaf angles that occur in velvetleaf. This, however, did not have a significant effect on glyphosate treatment and was also not a main contributor to time of day efficacy of glyphosate (Waltz et al., 2004). This suggests that light alone is a major factor in the efficacy of glyphosate. This may be because as photosynthetic photon flux density (PPFD) increases, photosynthesis increases, leading to greater translocation of glyphosate through the plant (Waltz et al., 2004).

Another study found that glyphosate applications of 840 g/ha shortly after dawn

caused the smallest decrease in broadleaf weed biomass, meaning a less effective treatment in comparison to treatments throughout the light period, all of which had similar effects on biomass (Mohr et al., 2007). For grass species, there was little difference in biomass across different times of glyphosate treatment, except in one field site where biomass was significantly higher when glyphosate was applied around dusk or dawn (Mohr et al., 2007). In greenhouse experiments, glyphosate treatments to barnyardgrass (*Echinochloa colona*) and velvetleaf around dusk were less effective (Mohr et al., 2007). Again, when removing the effects of leaf angle in velvetleaf, glyphosate remained less effective when treated near dusk, but time of day effects were still observed in barnyardgrass that lacks leaf movement (Mohr et al., 2007).

The only investigation into time of day variation in the efficacy of glyphosate using *Arabidopsis* to date involved spraying of 200 μM glyphosate every 4 hours between 05:00 and 21:00 (Sharkhuu et al., 2014). Using inflorescence extension as a model, they found that treatments at 05:00 and 09:00 were lethal, whereas treatments later in the day were not lethal but arrested growth to various extents (Sharkhuu et al., 2014). The time of dawn, dusk, and experimental temperature were not explained by the authors.

In conclusion, several studies have found that glyphosate provides the highest levels of control during the daylight hours, with midday being the most effective in field experiments on various weed species. The study conducted on *Arabidopsis* in controlled conditions found that the most effective treatments were early in the day. These variable time of day effects could be due to various metabolic pathways across the species being expressed at different times of day, plus there was variation in environmental factors across the field conditions.

1.6.7 Glyphosate effects on auxin biosynthesis and signalling

Auxin is vital phytohormone related to almost every stage of plant growth and development (Gomes et al., 2014; Covington and Harmer, 2007). The major auxin indole-

3-acetic acid (IAA) is synthesised from tryptophan, a downstream product of the shikimate pathway (Gomes et al., 2014; Jiang et al., 2013). Therefore, inhibition of the shikimate pathway by glyphosate suggests that auxin biosynthesis may decrease and, consequently, reduce plant growth. Several studies support this action. For example, Baur (1979) proposed that basipetal auxin transport is inhibited by multiple concentrations of glyphosate. Application of exogenous IAA in combination with glyphosate had no effect on auxin transport in the hypocotyls of cotton (Baur, 1979). Therefore, the inhibitory effect of glyphosate was overcome by adding auxin. Jiang et al. (2013) found that several auxin-related transcripts in soybean had altered expression after glyphosate treatment, further suggesting the interaction between glyphosate treatment and auxin.

1.6.8 IAA biosynthesis

IAA biosynthesis is a complex process that is not fully elucidated. It is thought that the main pathways are evolutionarily conserved between plant species since IAA is a fundamental plant molecule (Mano and Nemoto, 2012). There are two ways in which IAA is thought to be synthesised: by using tryptophan as a precursor, or by using a tryptophan-independent pathway (Fig. 1.6.3) (Zhao, 2012). Chorismate, the final metabolite from the shikimate pathway, is the starting point for the biosynthesis of tryptophan (Fig. 1.6.3) (Tzin and Galili, 2010). This is the only known way in which tryptophan is synthesised in plants. Tryptophan-dependent IAA biosynthesis can follow one of four proposed pathways in *Arabidopsis* (Mano and Nemoto, 2012). Little is currently known about tryptophan-independent IAA biosynthesis, or what proportion of IAA is made from each pathway (Mano and Nemoto, 2012). Indole-3-glycerol phosphate or indole are suggested precursors for the tryptophan-independent IAA biosynthesis, and these two compounds are also produced using chorismate as a precursor (Mano and Nemoto, 2012). Therefore, any of the IAA biosynthesis pathways could be inhibited by glyphosate application.

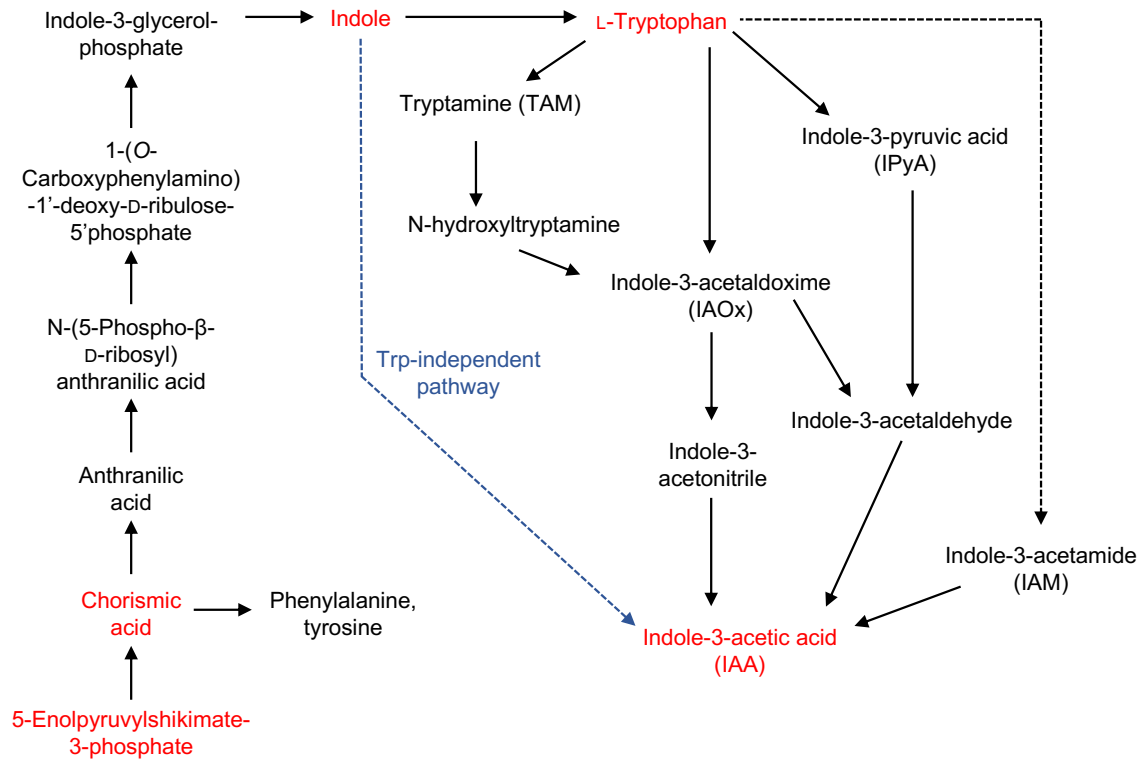


Figure 1.6.3: A simplified diagram of the multiple IAA biosynthesis pathways. Red text indicates key points of the pathway. Blue arrow shows the tryptophan-independent IAA biosynthesis pathway. Partially unknown components drawn using dashed arrows. Diagram re-drawn using information from Soeno et al. (2010).

1.6.9 Glyphosate conclusions

Since glyphosate is the most widely used herbicide, there is an abundance of research on how it functions, its effect on many plant species, and many types of assay have been used to identify the effects of glyphosate. However, there is little information as to why glyphosate has varying efficacy at different times of day, and the circadian regulation of the effect of glyphosate is not known. Based on how glyphosate works and the pathways it affects, we have presented some hypotheses for why glyphosate might be more effective at certain times of day but these need to be investigated.

1.7 Mesotrione

Mesotrione is a triketone herbicide, consisting of a ketone with three carbonyl groups (Fig. 1.7.1), based on the structure of benzoylcyclohexane-1,3-dione (Beaudegnies et al., 2009). The discovery of this class of herbicides occurred in 1977 by chance, when very few plants were growing under a bottlebrush (*Callistemon citrinus*) plant at a Stauffer Chemical research centre (now Syngenta) (Mitchell et al., 2001; Beaudegnies et al., 2009). Analysis of the soil under the shrub determined that the plant was specifically excreting leptospermone. Further analysis identified that leptospermone is a natural herbicide capable of broadleaf and grass control. Both this herbicidal activity and synthetic analogues were patented in 1980 (Mitchell et al., 2001; Beaudegnies et al., 2009).

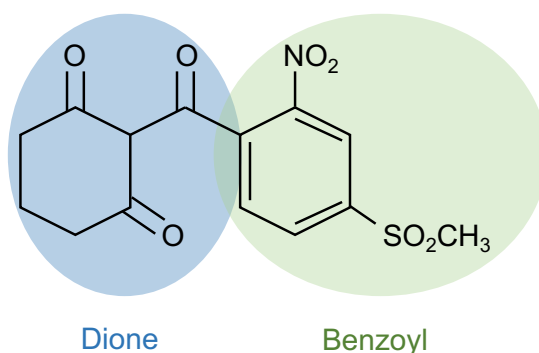


Figure 1.7.1: Chemical structure of Mesotrione. Mesotrione contains two moieties on the benzoyl ring that are critical for herbicidal function. Unlike some benzoylcyclohexanediones, mesotrione does not have any substituents on the dione ring as these cause a loss in maize selectivity.

The original benzoylcyclohexanedione herbicide to be commercialised was sulcotrione in 1993; following that, mesotrione was first sold in 2001 by Zeneca (Mitchell et al., 2001). Mesotrione is now sold in more than 50 countries and generates over \$400 million annual revenue (Carles et al., 2017). Mesotrione is used for pre- and post-emergence control of broad-leaf, and some grass, weeds (Mitchell et al., 2001). One of the reasons this herbicide is so commercially useful is that it does not affect maize

when used at the recommended concentration (Mitchell et al., 2001; Beaudegnies et al., 2009). Soybean, however, is very sensitive to mesotrione when used post-emergence (Mitchell et al., 2001).

The specific structure of the benzoylcyclohexanedione herbicide determines the activity of the chemical with the two moieties, benzoyl and dione, having unique roles (Fig. 1.7.1). For herbicidal activity, the benzoyl moiety requires a substituent at the 2-position of the phenyl ring and another substituent at the 4-position further enhances herbicidal activity (Fig. 1.7.1) (Mitchell et al., 2001). These substituents should be electron-withdrawing and acidic. By adding substituents to the cyclohexanedione ring, sites of metabolism by the plant are blocked and the herbicide has a greater effect as plants cannot detoxify the substance (Mitchell et al., 2001). However, these substituents cause a loss of maize selectivity and prevent the breakdown of the herbicide in soil (Mitchell et al., 2001). Therefore, mesotrione lacks these substituents (Fig. 1.7.1). Mesotrione does not affect maize because of oxidative metabolism of the dione; mesotrione is more potent towards dicotyledonous species and it is taken up more slowly in maize (Mitchell et al., 2001; Beaudegnies et al., 2009).

1.7.1 Mesotrione mode of action

The triketone herbicides including mesotrione inhibit 4-hydroxyphenylpyruvate dioxygenase (HPPD; Fig. 1.7.2). HPPD-dependent tyrosine degradation is present in all aerobic organisms but HPPD-inhibiting herbicides are solely toxic to plants (Beaudegnies et al., 2009). In plants, HPPD is required in the pathway that converts tyrosine to plastoquinone and α -tocopherol via 4-hydroxyphenylpyruvate (4-HPP) and homogentisic acid (Fig. 1.7.2) (Beaudegnies et al., 2009). The role of HPPD is to catalyse the oxidative decarboxylation of the 2-oxoacid side chain of 4-HPP, to form homogentisic acid (Dayan et al., 2007).

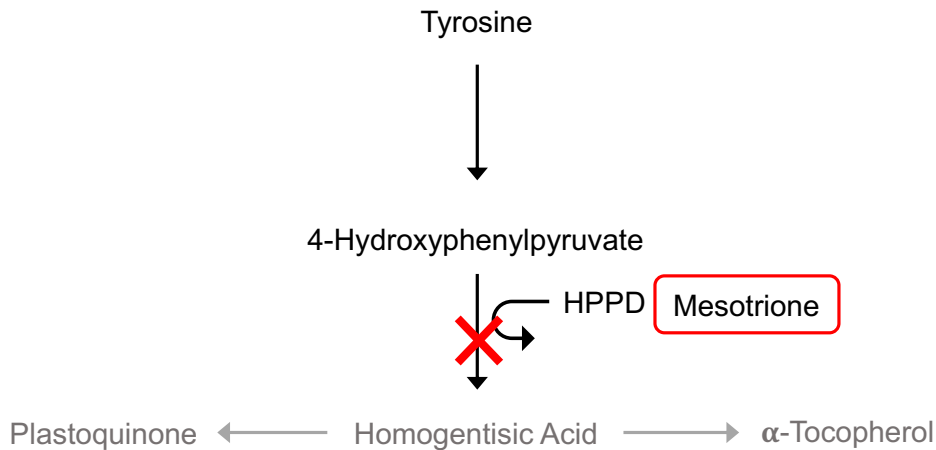


Figure 1.7.2: Mesotrione competitively binds to, and inhibits, 4-hydroxyphenylpyruvate dioxygenase (HPPD). HPPD is required for the degradation of tyrosine to homogentisic acid. Inhibition of HPPD prevents synthesis of plastoquinone and α -tocopherol. Pathway of mesotrione inhibition is indicated by a red cross, components down-regulated after mesotrione inhibition are shown in grey. Figure adapted from Mitchell et al. (2001).

In *Arabidopsis*, HPPD contains an Fe(II) active site to which mesotrione binds rapidly. The initial enzyme-inhibitor complex is weak but slowly forms the final, highly stable enzyme by isomerizing to a chromophore (Beaudegnies et al., 2009). Mesotrione is a strong competitive inhibitor of HPPD and the dissociation is so slow it is considered effectively irreversible (Beaudegnies et al., 2009). It has been suggested that because of high conservation of the sequence of the enzyme active site, any differences in inhibitor specificity between plant species is likely to arise due to differing metabolism of the herbicide (Beaudegnies et al., 2009). *Arabidopsis* HPPD is localised in the cytosol with no known ability to be able to move across the membrane where the downstream biosynthetic pathways of plastoquinone and α -tocopherol are located (Garcia et al., 1999).

The main cause of lethality of mesotrione is due to the lack of plastoquinone synthesis and subsequent inhibition of carotenoid biosynthesis (Mitchell et al., 2001; Hall et al., 2001b). Plastoquinone is required as a cofactor for phytoene desaturase, which is a component of the carotenoid biosynthesis pathway (Norris et al., 1995). The caroten-

oids are needed for the photosynthetic tissue to quench high-energy triplet states of chlorophyll (Knox and Dodge, 1985). Mesotrione carotenoid-depletion causes protein-damaging oxygen singlets in addition to disassembly of the photosynthetic apparatus and release of free chlorophyll (Beaudegnies et al., 2009). This is photodestructive and eventually destroys all leaf pigment (Hall et al., 2001b; Monaco et al., 2002). This suggests that the light intensity will determine the effectiveness of mesotrione, such that a higher fluence rate may be more effective. Plastoquinone is also required for electron transport between photosystem II (PSII) and PSI (Rochaix, 2011). Therefore, in mature tissues, the direct lack of plastoquinone may also contribute to the lethal effect. Triketone herbicides causing a lack in α -tocopherol production may be contributing to D1 protein depletion within PSII (Abendroth et al., 2006). Growth will be inhibited almost immediately after application because without photosynthetic tissue, growth cannot be sustained (Beaudegnies et al., 2009). The lack of carotenoid pigments causes characteristic bleaching in the newly forming tissues, and eventually is seen in older tissue due to pigment turnover; after growth ceases, necrosis begins and death may take up to two weeks (Monaco et al., 2002).

1.7.2 Mesotrione uptake, movement and metabolism

Mesotrione is acidic and water soluble (Monaco et al., 2002), which allows uptake and translocation of the herbicide through the plant (Mitchell et al., 2001). Mesotrione uptake into the weed can be rapid and species-dependent, with 55-90% taken up within 24 hours (Mitchell et al., 2001; Godar et al., 2015). Seven days post-treatment to a single leaf, 48% of the herbicide has been seen to move to other plant tissue (Mitchell et al., 2001). Mesotrione can be absorbed both acropetally and basipetally (Mitchell et al., 2001). However, uptake and efficacy depend on temperature and relative humidity, but with extensive species-specific effects (Johnson and Young, 2002; Godar et al., 2015).

Mesotrione metabolism within the plant is also species-dependent. Mesotrione meta-

bolism in maize is very rapid (Mitchell et al., 2001). Conversely, in broadleaf weeds metabolism is very slow, which contributes to why mesotrione is significantly less effective on maize (Mitchell et al., 2001). This has been shown to depend on temperature, with reduced translocation at low temperatures, and increased translocation at higher temperatures, at least in *Amaranthus palmeri* (Godar et al., 2015). It appears that cytochrome P450 is involved in mesotrione metabolism within the plant (Siminszky, 2006). Species that express more or less P450, may make the plant more or less susceptible to the herbicide, as found in some sweetcorn hybrids (Meyer et al., 2010).

1.7.3 Environmental mesotrione degradation

Mesotrione is very soluble and breaks down rapidly in soils with a half-life of 5-9 days in the light, and 2-18 days in the dark (James et al., 2006; Otto et al., 2016; Barchanska et al., 2016). Soil pH, sunlight and soil microorganisms all have a significant impact in the rate at which mesotrione can break down (Barchanska et al., 2016; Monaco et al., 2002). For example, photolysis to half-life of mesotrione at the field rate occurs after around 2 hours (Lavielle et al., 2009). Mesotrione is broken down into two metabolites 2-amino-4-(methylsulfonyl) benzoic acid (AMBA) and 4-methylsulfonyl-2-nitrobenzoic acid (MNBA) (Barchanska et al., 2016; Durand et al., 2010). AMBA was found to be more toxic than the parent compound, and is more stable in the environment with a half-life up to 46 days (Bonnet et al., 2008; Barchanska et al., 2016). Such rapid soil degradation may require higher concentrations to be used in order for mesotrione to be effective before being degraded, but only when used pre-emergence (James et al., 2006).

1.7.4 Mesotrione conclusions

Little research has been conducted into the effects of mesotrione other than to understand its main mechanism of action and toxicity. This could be because it is a relatively

new herbicide and patents have expired more recently compared to glyphosate. Therefore, there is considerable scope for mesotrione research in the future; for example, there is nothing in the literature on the effects of mesotrione on the transcriptome, or any other metabolic or cellular pathways that may be affected other than the mode of action. Furthermore, there has been no published research regarding any time of day effects or circadian regulation of plant responses to mesotrione.

1.8 Terbutylazine

Terbutylazine, *2-N-tert-butyl-6-chloro-4-N-ethyl-1,3,5-triazine-2,4-diamine* (TBA), is in the triazine family of herbicides (Fig. 1.8.1) (LeBaron et al., 2008). The first triazine was discovered in 1952. Since then, triazines have been essential for improving modern agriculture by reducing weeds growing alongside crops, leading to significantly increased yields (LeBaron et al., 2008). Atrazine was the most popular of the triazine herbicides, one reason being that they are easily mixed with other herbicides for broad-spectrum control (LeBaron et al., 2008). Mixing active ingredients in tank mixtures led to a reduction in the overall concentration of atrazine use in the USA (LeBaron et al., 2008). Atrazine was banned by the EU in 2004 (European Union, 2004) due to groundwater concentrations and concerns regarding the safety of atrazine and atrazine-containing products. Therefore, herbicides with related mechanisms and efficacy, such as TBA, have superseded atrazine.

TBA, first sold in the 1970s, is a selective, broad spectrum herbicide that inhibits photosynthesis (LeBaron et al., 2008; WHO, 2003). TBA was originally used for weed control in potato crops, followed by use in corn to control marigolds. Marigolds give a bad flavour to corn and the herbicide predecessor atrazine did not control marigolds (LeBaron et al., 2008). TBA is used widely throughout Europe, but is only used in the USA in cooling towers for microbe control (LeBaron et al., 2008). There are four different structural classes of the triazine herbicides. TBA is in the chloro-*s*-

triazine class and is characterised by ethylamino and *tert*-butylamino side chains (Fig. 1.8.1).

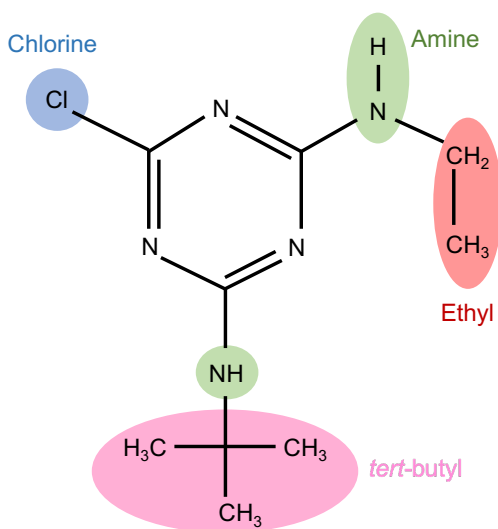


Figure 1.8.1: Chemical structure of terbuthylazine (TBA). TBA is an *s*-triazine that has 3 nitrogens in the triazine ring. TBA is specified by the ethyl (red) and *tert*-butyl (pink) side chains.

1.8.1 Terbuthylazine mode of action

Any organism that has oxygen-evolving photosynthesis will be susceptible to the triazine class of herbicides. In light-dependent, oxygen-evolving photosynthesis, the first protein complex involved in electron transport is PSII, located in the thylakoid membrane (LeBaron et al., 2008). Within PSII, energy from light transfers electrons through a series of coenzymes to reduce a secondary plastoquinone (Fig. 1.8.2) (Lambrev et al., 2014). Plastoquinone is required to accept electrons and transfer them to PSI for successful photosynthesis. This electron transfer occurs via the Q_B binding site on the D1 protein (Fig. 1.8.2). The D1 protein is approximately 32 kDal, which is encoded by the *psbA* gene (Golden and Haselkorn, 1985) and is rapidly turned over in light (Greenberg et al., 1987).

The triazine herbicides function by displacing plastoquinone from the Q_B binding site on D1 in PSII (Fig. 1.8.2) (Gardner, 1981; Pfister et al., 1981; Steinback et al.,

1981). The herbicide inhibits electron transport because it is a non-reducible analogue of plastoquinone (Fuerst and Norman, 1991). This, in turn, causes excited singlet chlorophyll molecules to form triplet chlorophyll that reacts with oxygen to form damaging singlet oxygen (Fuerst and Norman, 1991).

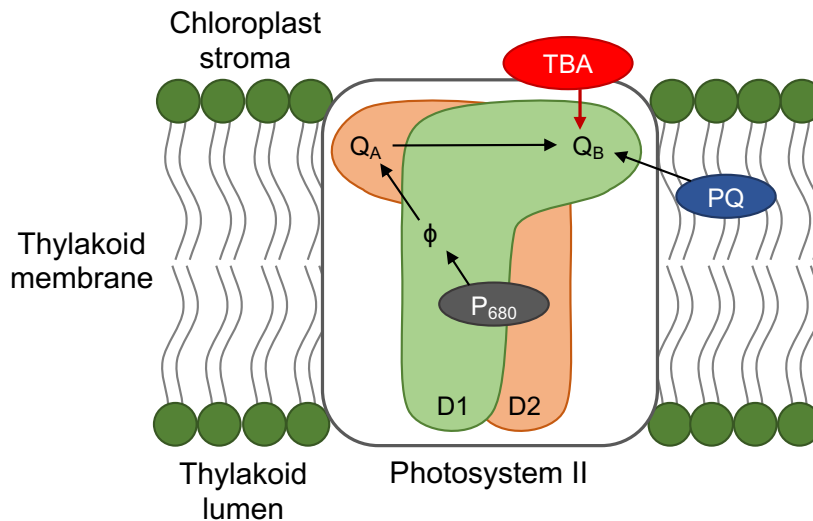


Figure 1.8.2: Inhibition of electron transport in photosystem II by terbuthylazine (TBA). P₆₈₀ passes an electron to pheophytin (Φ), the electron moves to a plastoquinone bound to the Q_A binding site on the D2 protein. Electron flow stops when TBA blocks the Q_B site on the D1 protein by acting as a plastoquinone (PQ) analogue. Adapted from Giardi and Pace (2005).

The singlet oxygen causes lethal photo-oxidation of the photosynthetic membrane. Protective substances, such as carotenoids and α -tocopherol, are usually produced by the plant in small quantities during photosynthesis. The damaging substances are produced so extensively when triazines are present, the plant can no longer protect itself leading to death (Fuerst and Norman, 1991). Furthermore, lipid peroxidation occurs whereby the singlet oxygen can react with the fatty acids in the thylakoid membrane depleting the membrane and causing a loss in cellular compartmentation (Fuerst and Norman, 1991). Therefore, it is not solely the starvation of photosynthesis that is lethal (Rutherford and Krieger-Liszkay, 2001). This mechanism also suggests that light is necessary, because the plant would not be attempting to reduce the

plastoquinone unless light were present; furthermore, the light intensity may have an effect on herbicide efficacy.

1.8.2 Movement of terbuthylazine within the plant

There are few reports on the translocation of TBA within plants, however there is more information about triazines as a herbicide class. The lipophilic nature of the triazine herbicides means that they can rapidly and passively diffuse across the membrane into plant cells (Sterling, 1994). Once in the plant cells it was found that within 4 hours of foliar treatment, up to 90% triazine was absorbed (Aper et al., 2012). However, less than 10% of the herbicide was translocated out of the leaves, and only 1% reached the roots (Aper et al., 2012). Based on the mechanism of the herbicide it may be more important that it remains in the photosynthetic tissue.

Movement of TBA within the plant depends on where the application occurred. If applied to the leaves, TBA remains where it was applied. Conversely, if applied to the roots, TBA moves around the plant quickly (WHO, 2003; Singh et al., 2015). Translocation was originally thought to only occur acropetally, suggesting that movement only occurred via the xylem (Wax and Behrens, 1965). However, more recently, it was found that translocation occurred both acropetally and basipetally, and suggest that transfer of the substance can occur between the xylem and phloem (Aper et al., 2012).

1.8.3 Metabolism of terbuthylazine

Metabolism of TBA (and similarly for other triazine herbicides) within the plant or in the environment occurs through two major pathways: removal of the chlorine group by hydroxylation to form non-phytotoxic hydroxyl-terbuthylazine, and dealkylation of the two amine groups to give either deethyl-terbuthylazine or deisopropyl-atrazine (Gikas et al., 2012). These metabolites were consistent with the wider *s*-triazines in

multiple species identified using a radiochromatogram (Singh et al., 2015). Metabolism appears to be rapid and extensive, with reported metabolism within 3 hours (European Food Safety Authority, 2011; Singh et al., 2015).

In the environment, the speed of TBA metabolism depends on factors including temperature, light, moisture, presence of microorganisms, pH and aeration (WHO, 2003; Sahid and Teoh, 1994). Under aerobic conditions the environmental persistence of TBA was designated moderate to high but it can degrade to metabolites, under anaerobic conditions TBA is stable (European Food Safety Authority, 2011; WHO, 2003). At higher temperatures, TBA half-life is much shorter than at lower temperatures regardless of soil type, suggesting that in certain parts of the world TBA may have different persistency (Sahid and Teoh, 1994). Adsorption to soil occurs within two hours after application, which could decrease TBA metabolism and activity depending on the environment (WHO, 2003).

1.8.4 Triazine interactions with circadian regulation

To date there are no studies regarding the varying efficacy of TBA applied at different times of day. However, one study examined the effect of atrazine applied at different times of day in the field. Application of 1000 g/ha atrazine at different time points throughout the day found that in terms of weed control, 15:00 was the optimal time to apply atrazine (Stewart et al., 2009). However, the study fails to report the time of sunrise and sunset, therefore it is difficult to draw conclusions from this work.

Furthermore, atrazine has been shown to have a direct effect on the circadian oscillator of a cyanobacterium (Qian et al., 2014). Atrazine affected the circadian rhythms of the key central circadian oscillator genes, and photosynthesis genes in *Microcystis aeruginosa*. This suggests that, although cyanobacteria have a different circadian oscillator, there could be similarities in the effects of atrazine and other triazine herbicides, such as TBA, in plants. It would be interesting to determine the extent of these findings to the plant circadian oscillator.

1.8.5 Terbutylazine conclusions

Much of the published work on TBA concerns approaches to reduce environmental contamination, and to remediate polluted water or soil. Experiments using atrazine are much more common, although still limited, and there is limited published work regarding potential circadian regulation of the plant responses to triazine herbicides.

Combining PSII inhibitors such as TBA with HPPD inhibitors such as mesotrione is now a popular method of weed control, as the two herbicide modes of action complement each other and increase lethality (Abendroth et al., 2006). This could be investigated, however it may not be that there is a time of day at which both herbicides would have the same effect.

1.9 Summary

There is evidence to suggest that there could be an interaction between circadian rhythms and herbicides, in particular that the circadian oscillator could restrict the response to the herbicide to particular times of day. While there have been some studies that have linked the two in the past, the mechanisms and nature of such responses remain elusive. In order to use herbicides more efficiently for agricultural purposes, such as by reducing the quantity of chemical used or finding a time that is optimum to spray, it would be beneficial to obtain a greater understanding of any such circadian regulation. Further to this, it is not known how, or whether, herbicides can affect the circadian oscillator.

1.10 Aims

The overarching aims of this research were (i) to investigate the extent of circadian regulation of the responses to three different mode of action herbicides (glyphosate, mesotrione and terbuthylazine) and (ii) to determine the effect of these herbicides on the function of the circadian oscillator.

Chapter 2

Materials and Methods

2.1 Plant material and growth conditions

For all experiments, unless stated otherwise, seeds of *Arabidopsis thaliana* (L.) Heynh. (Table 2.1.1) were surface sterilised with 70% (v/v) EtOH for 1 minute (min), 20% (v/v) domestic bleach for 12 min, followed by two washes with sterile distilled H₂O. Seeds were re-suspended in 0.1% (w/v) agar (Sigma). Petri dishes were prepared with half-strength (2.15 g L⁻¹) Murashige and Skoog (MS) nutrient mix (basal salts without vitamins, pH 6.8; Duchefa Biochimie) and 0.8% (w/v) agar. For experiments with seedlings, sterile plastic rings (Nalgene) were embedded in media (Figure 2.1.1) (Love et al., 2004; Noordally et al., 2013). Approximately 12 seeds were sown per ring. Seeds were stratified for 3 days in the dark at 4 °C before transfer to growth cabinets (19 °C, 100 μmol m⁻² s⁻¹; MLR-352, Panasonic), under either 12 hour (h) light /12 h dark, or 8 h light /16 h dark cycles for the length of the experiment.

Alternatively, for experiments with rosettes where plants required 5-6 true leaves (approximately 17 days old) (Boyes et al., 2001), seeds were sterilised and germinated as above but were sown individually onto agar. After 7 days growth, seedlings were transplanted into a 3:1 mix of sieved compost (Levington Advance F2 Seed & Modular, ICL) and sand (Horticultural Silver Sand, Melcourt) and transferred into a Snijders

Table 2.1.1: Genotypes used in this work and the original publications.

Genotype	Background	Reference
Columbia (Col-0)		
Landsberg <i>erecta</i> (L. <i>er</i>)		
<i>CCA1-ox</i>	Col-0	Wang and Tobin (1998)
<i>TOC1-ox</i>	Col-0	Más et al. (2003)
<i>CAB2::LUCIFERASE</i> (<i>CAB2::LUC</i>)	Wassilewskija (Ws)	Hall et al. (2001a)
<i>cca1-11 lhy-21 toc1-21</i>	<i>CAB2::LUC</i> Ws	Ding et al. (2007)
<i>pin3-3</i>	Col-0	Friml et al. (2002)
<i>phyB</i>	L. <i>er</i>	Koornneef et al. (1980); Reed et al. (1993)
<i>DR5::GUS</i>	Col-0	Ulmasov et al. (1997)
<i>DR5::VENUS</i>	Col-0	Brunoud et al. (2012)
DII-VENUS	Col-0	Brunoud et al. (2012)
<i>CCA1::LUCIFERASE</i> (<i>CCA1::LUC</i>)	Col-4	Kusakina et al. (2014)
<i>TOC1::LUCIFERASE</i> (<i>TOC1::LUC</i>)	Col-4	Kusakina et al. (2014)

Labs Micro Clima-Series growth chamber (12 h light /12 h dark or 8 h light /16 h dark 19 °C, 100 $\mu\text{mol m}^{-2} \text{s}^{-1}$, 70% relative humidity) for the duration of the experiment. Plants grown on compost were watered with approximately 8 mL water per plant three times per week.

For other plant species, non-sterile seeds (rapeseed (*Brassica napus*), wild mustard (*Sinapis arvensis*), proso millet (*Panicum miliaceum*)) were placed onto water-saturated filter paper (Fisher Scientific) in petri dishes for 3 days (*S. arvensis*, *P. miliaceum*) or 5 days (*B. napus*) at room temperature (approximately 19 °C) under constant light. Germinated seeds were then transplanted onto compost as above and placed into growth chambers (8 h light /16 h dark, 19 °C, 100 $\mu\text{mol m}^{-2} \text{s}^{-1}$, 70% relative humidity; Snijders Labs Micro Clima-Series) for the duration of the experiment. Seeds from these species were provided by Syngenta.

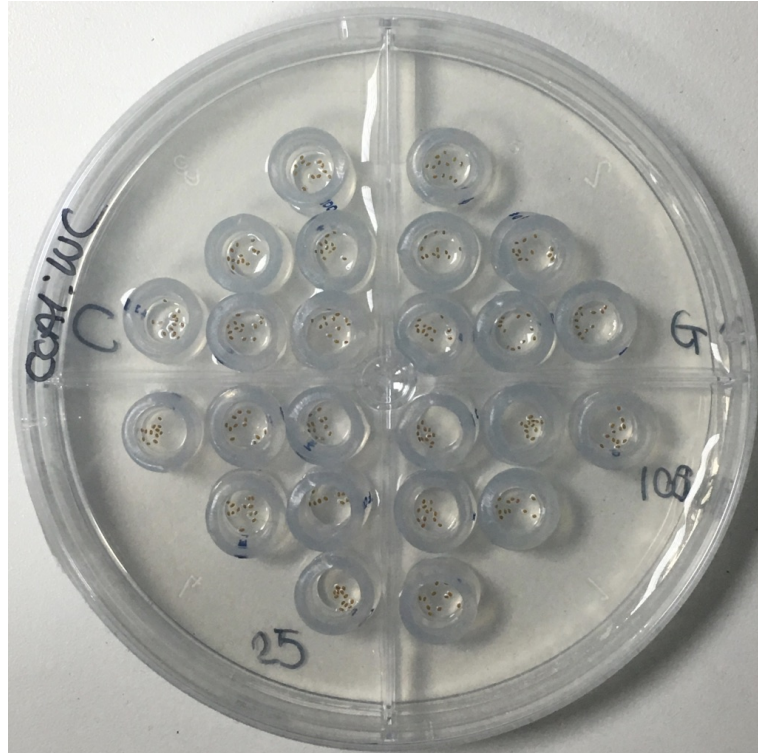


Figure 2.1.1: An example of a 90 mm petri dish with sterile plastic rings embedded into media that 12 seeds were sown into. This is an example of a luciferase imaging plate that has four compartments, each for a different chemical treatment. Seeds have not yet germinated. Six rings of seedlings were used as technical repeats per treatment. Image not to scale.

2.2 Application of treatments

Treatments (herbicides or other chemicals) were applied in one of two ways depending on the age of the plant at the time of treatment. Where experiments were conducted with seedlings, plants were grown in sterile plastic rings embedded within the media to ensure the chemical was dosed equally across the seedlings (Figure 2.1.1). The treatment was applied by pipetting 20 μL (for 3 day old treatments) or 100 μL (for 10 day old treatments) to each ring to saturate the surface of the seedlings. Where multiple chemicals were applied per plate, multiple-compartment petri dishes (Phoenix Biomedical) were used to avoid any transfer of chemical through media (Figure 2.1.1). Treatments were applied in a sterile flow hood and under a dim green safe light for any dark time points.

For the preliminary experiments conducted with *Arabidopsis* rosettes, a hand pump spray bottle was used to apply treatments until the rosette was saturated. For all subsequent experiments conducted with *Arabidopsis* rosettes, or with species other than *Arabidopsis*, a custom-built laboratory size track sprayer was designed and built to simulate spraying in the field. This is described in more detail in Chapter 3.2.1.

2.3 Herbicide formulations

A list of the herbicides used in this work and their common formulations is provided (Table 2.3.1). All herbicides were provided by Syngenta. Throughout this work, herbicides are referred to by their active ingredient (AI).

Table 2.3.1: Herbicide formulations used in this work.

Commercial name	Active ingredient	Product code
Touchdown Total 500SC	Glyphosate	A13013M
Callisto 100SC	Mesotrione	A12739A
Gardoprim 500SC	Terbuthylazine	A5435E

In the agricultural sector, herbicide concentration is commonly expressed as the mass of active ingredient per hectare (g/ha) based on a typical spray volume application rate of 200 litres per hectare; this is the convention used throughout this work. For reference, glyphosate formulations that are used at the typical field rate of 840 g/ha contain 24.8 μM of glyphosate. Terbuthylazine (TBA) formulations sprayed at a field rate of 750 g/ha contain 16.3 μM TBA, and mesotrione formulations sprayed at a field rate of 150 g/ha contain 2.2 μM mesotrione.

2.4 Adjuvants

Herbicide formulations commonly contain adjuvants, or require adjuvants to be added into a sprayer tank mixture. Adjuvants are required to increase herbicide efficiency through increasing uptake and increasing sorption (Crouzet et al., 2013). The Touch-down Total formulation (Table 2.3.1) contains a proprietary adjuvant. This adjuvant component was formulated uniquely by Syngenta as a glyphosate blank adjuvant (product code: A17039F) for this work in order to perform control tests. The mass of this adjuvant equivalent to the mass of glyphosate in a formulation was used for such experiments. Commercial treatments with TBA usually contain 0.2% (v/v) Agridex adjuvant (sample reference: A8383A, Syngenta). Therefore 0.2% Agridex was added to all TBA treatments, and applied alone as a control.

2.5 Plant physiology measurements

2.5.1 Rosette properties

To quantify the effect of herbicides on mature *Arabidopsis*, plants were grown under 12 h light /12 h dark cycles. Once at the six true leaf stage, plants were treated with one of three concentrations per herbicide. Plants were treated at one of five time points throughout the light period of the day: dawn, 3 h, 6 h, 9 h or 12 h after dawn. Plants were photographed 0, 4, 7, 10 and 14 days after treatment (Nikon D80). Rosette area, growth inhibition, leaf number, and rosette damage were quantified using the image processing program ImageJ (imagej.net/; accessed 09/12/18). Three (mesotrione and TBA) or five (glyphosate) plants were used per treatment per time point.

2.5.2 Hypocotyl and coleoptile length

To investigate the effect of glyphosate on elongating hypocotyls, seeds were grown within two plastic rings per 50 mm petri dish, using two petri dishes per treatment, per time point (8 h light /16 h dark, 12 h light /12 h dark, or 16 h light /8 h dark). Treatments (water control, glyphosate or other manipulations) were applied on day three after germination at specified time points and plates were replaced in the growth cabinet. Four days after treatment, 18-25 plants were measured per treatment, per time point by positioning plants on 1% agar for photographing, followed by measuring length using ImageJ.

A range of glyphosate concentrations were tested (50-500 g/ha). The majority of experiments were conducted using a sub-lethal concentration of 100 g/ha glyphosate.

For experiments with L-kynurenine (kyn; Sigma-Aldrich), 150 μM , 200 μM , 300 μM , or 500 μM kyn were applied using 1% (v/v) dimethyl sulfoxide (DMSO) as a carrier control (for the highest volume DMSO). Subsequent experiments used 500 μM kyn.

For experiments with 1-naphthaleneacetic acid (NAA; Sigma-Aldrich), seedlings were treated with 500 μM kyn plus either 1 μM , 5 μM , 10 μM , 50 μM , or 100 μM NAA. The control was 0.7% (v/v) EtOH + 1% (v/v) DMSO. Subsequent experiments used 50 μM NAA.

For experiments with 1-N-naphthylphthalamic acid (NPA; Sigma-Aldrich), 100 μM NPA or a 0.02% (v/v) DMSO carrier control. For experiments with diflufenzopyr (Syngenta), seedlings were treated with 250 g/ha or a 0.25% (v/v) DMSO carrier control.

To investigate the circadian sensitivity of the elongation of hypocotyls to glyphosate treatment, plants were placed under one cycle of 8 h light /16 h dark followed by constant light. Herbicide treatments began after 46 h in constant light. Treatments were at specified time points across 2 days, and hypocotyls were measured 3 and 4

days later, as above. For time points in the subjective night (ZT62, ZT66, ZT86, and ZT90), experiments were conducted in a growth chamber in reverse night /day cycles.

To investigate the effect of glyphosate on the hypocotyls or coleoptiles of species other than *Arabidopsis*, post-germination plants were grown on soil for 3 days. Plants were sprayed (100 g/ha glyphosate or 200 g/ha for *P. miliaceum*) using the custom-built track sprayer at dawn, midday, or dusk. Four days after treatment, plants were imaged, and hypocotyls or coleoptiles were measured, as in previous hypocotyl assays.

2.5.3 Hypocotyl elongation rate

To measure the rate of hypocotyl elongation, seedlings were sown individually onto petri dishes, and plates were germinated vertically (Snijders Labs Micro Clima-Series, 8 h light /16 h dark 19 °C, 100 $\mu\text{mol m}^{-2} \text{s}^{-1}$, 70% relative humidity). Treatments were made at either dawn or dusk on day 3 and imaging began after the treatment was applied. 1.6 μL of either water or 100 g/ha glyphosate were applied to each seedling (equivalent volume to other treatments). Time lapse images were captured with a Nikon D80 DSLR with the infra-red (IR) blocking filter removed, fitted with an IR pass filter ($>850 \text{ nm}$) (Zomei, Jiangsu, China). Plates were back lit with a custom-built IR LED array (880 nm). Images were captured every 30 min following treatment, for 96 h. 10 seedlings were measured per treatment. Images were analysed to measure hypocotyl length using ImageJ.

2.5.4 Petiole length

To quantify the effect of glyphosate on the length of the petiole, *Arabidopsis* rosettes were sprayed with 100 g/ha glyphosate once the fifth leaf had emerged (approximately 26 days after germination, under 8 h light /16 h dark). Treatments were sprayed at one of three time points: dawn, midday or dusk. One week after treatment the fifth

leaf was removed from the rosette at the base of the petiole and placed onto 1% agar and imaged. 13-15 plants were measured per treatment per time point. Petiole length, leaf blade length and leaf blade width were measured using ImageJ. Blade length to blade width ratio and petiole length to blade length ratio were also calculated from these measurements.

2.6 Chlorophyll fluorescence measurements

To investigate the effect of different concentrations of herbicides on photosynthetic parameters, different herbicide treatment lengths, and herbicide treatment time of day, chlorophyll fluorescence measurements were made on day 11 or 12. All plants were dark adapted for at least 30 min prior to measurements. Measurements were made using Imaging-PAM *M-series* MAXI (Walz) modulated chlorophyll fluorimeter running a custom script (saturating pulse, 10 min actinic light ($107 \mu\text{mol m}^{-2} \text{s}^{-1}$), saturating pulse; Fig 2.6.1). Six replicates (rings containing 12 plants) were measured for each treatment. Maximum potential PSII activity from the dark adapted state (F_v/F_m), effective PSII quantum yield ($Y(\text{II})$) and non-photochemical quenching (NPQ) were recorded (Table 2.6.1).

Table 2.6.1: Chlorophyll fluorescence parameters used in this work. Descriptions and equations from Maxwell and Johnson (2000).

Parameter	Definition	Equation
F_o	Yield of fluorescence in the absence of actinic light	
F_m	Maximum fluorescence yield in the dark adapted state	
F_o'	Fluorescence yield in the light	
F_m'	Maximum fluorescence yield in the light	
F_v/F_m	Maximum efficiency of PSII in the dark adapted state	$(F_m - F_o)/F_m$
Y(II)	Efficiency of PSII in actinic light	$(F_m' - F_o')/F_m'$
NPQ	Non-photochemical quenching	$(F_m - F_m')/F_m'$

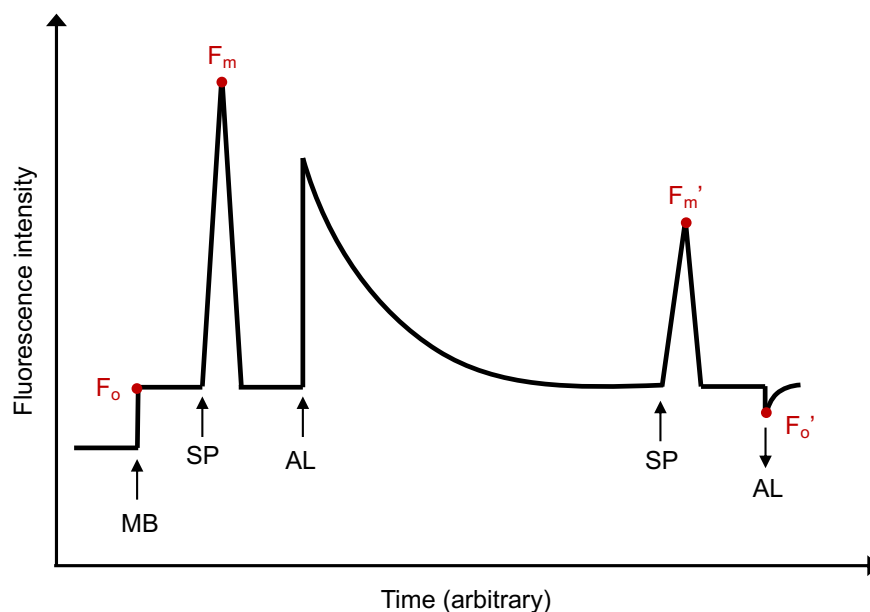


Figure 2.6.1: An example of the chlorophyll fluorescence trace and program used in this work showing the points of obtaining the fluorescence parameters. The measuring light (MB) was switched on (upwards arrow), followed by a saturating pulse (SP). Actinic light (AL) was applied for 10 min, followed by another SP. Actinic light was then turned off (downwards arrow). Red dots indicate the point of measuring each parameter stated in red. Diagram recreated from Maxwell and Johnson (2000).

2.7 Data meta-analysis

To identify genes of interest that may be involved in the time of day sensitivity to glyphosate, six publicly-available datasets were analysed. Lists of transcripts that are either induced or repressed by glyphosate (Faus et al., 2015) were compared to those that are circadian- (Dodd et al., 2007; Edwards et al., 2006; Covington and Harmer, 2007) and nycthemeral-(Bläsing et al., 2005; Smith et al., 2004) regulated. Comparisons were conducted in Excel. Each transcript was then categorised into bins of 4 h by circadian phase (Dodd et al., 2007; Frank et al., 2018). Gene descriptions were obtained using the Bulk Gene Descriptions tool from TAIR (arabidopsis.org/tools/bulk/genes/index.jsp; accessed 24/11/17).

2.8 RNA isolation

Aerial plant tissue was harvested at specified time points after treatments from either 5 day old seedlings or 11 day old seedlings. For samples from 5 day old seedlings, aerial tissue was taken from approximately 40 seedlings; for samples from day 11, tissue was sampled from approximately 20 seedlings. Tissue was sampled from 4-6 rings of seedlings from across two petri dishes. Plant tissue was removed and subsequently blotted on absorbent paper to remove any excess liquid from treatments that could interfere with downstream processing. Samples were flash frozen in liquid nitrogen and stored at -80°C .

Frozen tissue was homogenised with stainless steel beads (Qiagen) using a TissueLyser II (Qiagen). RNA was extracted using NucleoSpin RNA extraction kit (Macherey-Nagel) according to manufacturers instructions; samples were eluted in 30–40 μL RNase-free H_2O . RNA yield was quantified using NanoDrop ND-100 Spectrophotometer (Thermo Fisher Scientific). RNA purity was inferred using the 260/280 and 260/230 ratios where absorbencies of 2 and 2-2.2, respectively were considered pure and could be used in subsequent reactions.

2.9 cDNA synthesis

1.5 µg RNA was used to synthesise cDNA using High Capacity cDNA Reverse Transcription Kit, with RNase Inhibitor (Life Technologies) according to manufacturers instructions. Reactions were carried out using Mastercycler Nexus Gradient (Eppendorf) with the following thermal profile: 25 °C 10 min, 37 °C 120 min and 85 °C 5 min.

2.10 Quantitative reverse-transcription PCR

For experiments with glyphosate marker transcripts, quantitative reverse-transcription polymerase chain reaction (qRT-PCR) analysis was performed using Brilliant III Ultra-Fast SYBR Green qRT-PCR Master Mix (Agilent). Each reaction contained: 5 µL cDNA, 1x Brilliant III Ultra-Fast SYBR Green QPCR master mix, 0.5 µM each forward and reverse primer, 0.03 µM ROX reference dye and nuclease-free water up to 20 µL. The following thermal cycling conditions were used: 3 min at 95 °C, followed by 40 cycles of 5 seconds (s) at 95 °C and 20 s at 60 °C.

For all subsequent qRT-PCR, quantification was performed using HOT FIREPol EvaGreen (Solis BioDyne) due to manufacturer price changes. Each reaction contained: 5 µL cDNA, 1x HOT FIREPol EvaGreen qPCR Mix Plus, 250 nM each forward and reverse primer, 0.03 µM ROX reference dye and nuclease-free water up to 20 µL. The thermal cycling conditions were: 15 min at 95 °C, followed by 40 cycles of 15 s at 95 °C, 20 s at 60 °C, and 20 s at 72 °C. All qRT-PCR was performed using Agilent Mx3005P qRT-PCR instruments.

All primers were tested for efficiency and specificity by running a dissociation curve with a 1:10 serial dilution. Primers were considered acceptable if they had an R^2 value over 0.98 and an efficiency between 90-110%, and a single peak in the dissociation curve. Primers were supplied by Sigma Aldrich and diluted to a concentration of 100 µM with H₂O. For use in qRT-PCR, primers were diluted to 10 µM. Primer

sequences used are listed in Table 2.10.1. Depending on the primer efficiency, cDNA was diluted for qRT-PCR to 1:500 for 11 day old samples or 1:50 for samples from 5 day old seedlings. Three biological replicates and two technical replicates were quantified for each treatment per time point. Threshold Ct values were determined with the MxPro 4.10 software (Agilent). Relative transcript abundance was calculated using the $2^{-\Delta\Delta C_t}$ method (Livak and Schmittgen, 2001) using either *ACTIN2* or *PP2AA3* as a reference transcript.

Table 2.10.1: List of primer sequences used in this work and the original citations.

Gene	Sequence	Reference
<i>Actin2</i>	F: TCAGATGCCCAGAAGTGTTGTTTC R: CCGTACAGATCCTTCCTGATATC	Hayes et al. (2014)
<i>PP2AA3</i>	F: TAACGTGGCCAAAATGATGC R: GTTCTCCACAACCGCTTGGT	Czechowski et al. (2005)
<i>OM66</i>	F: TGCTGAGACCAGGACGTATG R: ACCTTCCTCGATCTTGCTGA	Zhang et al. (2014a)
<i>PME5</i>	F: TTCGATAGCGTCAAGATTCG R: CCACATAACAATGGACCCGTA	This work
<i>UGT7</i>	F: GAATCGTCCTCATACCCGAAT R: GCTTTGGACCCATTTCAACA	Tognetti et al. (2010)
<i>PDR12</i>	F: CACTGTTTACGAGTCCTTGGT R: CAGCTCCATCACTTCCTCTATG	This work
<i>DTX1</i>	F: TTCTCAAGTCACATGGCATAACA R: GACCGAGATGACAGGCAATAA	This work
<i>YUC8</i>	F: ATCAACCCTAAGTTCAACGAGTG R: CTCCCGTAGCCACCACAAG	Hayes et al. (2014)
<i>YUC9</i>	F: GTCCCATTCGTTGTGGTCG R: TTGCCACAGTGACGCTATGC	Hayes et al. (2014)
<i>IAA29</i>	F: ATCACCATCATTGCCCGTAT R: ATTGCCACACCATCCATCTT	Hayes et al. (2014)
<i>GH3.3</i>	F: GGTCGGGAAAGAGTACGAGC R: CTCCTCCGCACAAACTTGA	Hayes et al. (2014)
<i>EXPA8</i>	F: CCGAAGAGTACCATGTATGAAG R: GAGATCAGAACGAGGTTGAAG	Simon et al. (2018)

Continued on next page

Table 2.10.1 – continued

Gene	Sequence	Reference
<i>EPSPS1</i>	F: AGCAGCATCCACGAGCTTAT R: GCCGTGGAAACAGAAGACAT	Sharkhuu et al. (2014)
<i>PHYB</i>	F: CCGTGACATTCCCGAAGAGAT R: ATACTCAGCAGAAACTCAGCCA	Casson and Hetherington (2014)
<i>TPL</i>	F: CTCGAGGCTTTGGATAAGCATG R: ACACTTTCAAATCCTTCACTAGTATATCCAC	Wang et al. (2013)
<i>PIF4</i>	F: GCCAAAACCCGGTACAAAACCA R: CGCCGGTGAACTAAATCTCAACATC	Zhu et al. (2016)
<i>PIN3</i>	F: GAGGGAGAAGGAAGAAAGGGAAA C R: CTTGGCTTGTAATGTTGGCATCAG	Wang et al. (2015)
<i>GUS</i>	F: CCCTTACGCTGAAGAGATGC R: GAGGTAAAGCCGACAGCAG	Hayes et al. (2014)
<i>VENUS</i>	F: TAAACGGCCACAAGTTCAG R: AGATGAGCTTCAGGGTCAG	This work
<i>MC1</i>	F: TGGTACCGTTCTGGATTTAC R: GATGATCCTCCCACACATAC	This work
<i>DAD1</i>	F: AGGAATTCAAGGATTTAGCAC R: CTATCCGAGGAAGTTGATGAT	This work
<i>CCA1</i>	F: GCACTTTCCGCGAGTTCTTG R: TGACTCCTTTCTTACCCTGTTATTCTG	Noordally et al. (2013)
<i>TOC1</i>	F: TCTTCGCAGAATCCCTGTGAT R: GCTGCACCTAGCTTCAAGCA	Noordally et al. (2013)

2.11 Bioluminescence imaging

To investigate the promoter activity of circadian oscillator components, luciferase reporter lines were sown into six sterile plastic rings per treatment (Figure 2.1.1). 24 h before imaging, each ring of seedlings was dosed with 100 μ L 5 mM sterile luciferin

(potassium salt of D-luciferin; Melford Laboratories Ltd). Monochromatic red and blue LEDs were used to expose plants to $25 \mu\text{mol m}^{-2} \text{s}^{-1}$ light of each wavelength, or $5 \mu\text{mol m}^{-2} \text{s}^{-1}$ for low light experiments. Bioluminescence was detected using an Electron Multiplying Charged Coupled Device (EM-CCD; Photek) controlled by Image32 software (Photek). Custom scripts were used to control the day and night light settings, the frequency of image capture (1-2 images per hour), EM gain (2700), and length of image exposure (40 s). Lights were switched off 2 min before each image was captured in order to avoid capturing chlorophyll auto-fluorescence.

Four background readings were taken per plate and the mean value of these at each time point was subtracted from each data point in order to remove any background signal. Analysis of rhythmic features in the data was conducted using the fast Fourier transform-nonlinear least-squares (FFT-NLLS) algorithm within either BRASS software (Southern and Millar, 2005), or BioDare2 (biodare2.ed.ac.uk; accessed 07/12/18) (Zielinski et al., 2014).

2.11.1 Entrainment assay

To investigate how rapidly elongating seedlings became entrained to light/dark cycles, stratified *CCA1::LUC* seeds were placed into 8 h light /16 h dark conditions for either 1 or 2 days in a growth cabinet followed by placing into the EM-CCD under continuous light. Seedlings were imaged for 6 days.

2.11.2 Effect of herbicides on circadian oscillator promoters

To determine the effect of herbicides and their adjuvants on the promoters of circadian oscillator genes, *CCA1::LUC* and *TOC1::LUC* plants were placed into the EM-CCD imaging system on day 11 after germination and imaged every 28 or 58 min for 24 h. On day 12, plants were treated with either herbicide, adjuvant, or control and imaged

for a further 96-120 h. Data were collected under both 12 h light/ 12 h dark cycles and constant light.

2.11.3 Effect of herbicides with supplemental sucrose

For experiments investigating the effect of herbicides and their adjuvants on circadian oscillator components with sucrose, media was supplemented with either 3% sucrose (87.6 mM; Fisher) or 87.6 mM D-sorbitol (Melford) as an osmotic control. *CCA1::LUC* seedlings were treated and imaged as above.

2.12 GUS staining

DR5::GUS seeds were sterilised and grown on petri dishes and treated (100 g/ha glyphosate or water control) on day 12 at either dawn or dusk (8 h light /16 h dark). On day 17, approximately 40 seedlings were immersed in assay buffer (0.1 M NaPO₄ (pH 7.0), 10 mM EDTA, 0.1% Triton X-100, and 2 mM 5-bromo-4-chloro-3-indolyl glucuronide salt (X-Gluc; Thermo Fisher)) and incubated in the dark at 37 °C for 42 h (Hayes et al., 2014). Samples were then washed twice in 80% (v/v) EtOH and suspended in 70% (v/v) EtOH for imaging (Keyence VHX-1000E digital microscope).

2.13 Fluorescence microscopy

To check for VENUS expression in leaves, one intact rosette leaf was submerged in 2 mL of either 100 g/ha glyphosate, water control, 50 µM NAA, or 500 µM kyn for 2 h. Leaves were then removed and visualised. Images were acquired with an 8 min exposure for DII-VENUS, or 30 s exposure for *DR5::VENUS*.

To investigate *DR5::VENUS* fluorescence in the hypocotyl, rings of seedlings were treated with 20 µL water, 100 g/ha glyphosate, 0.7% (v/v) EtOH, 50 µM NAA, 1%

(v/v) DMSO, or 500 μ M kyn at dawn or dusk on day four and hypocotyls were imaged on day six. Five hypocotyls were imaged per treatment, per time point. Images were taken at 2.5x magnification; brightfield images were taken with 118ms exposure and fluorescence images were taken with 1 min 52 s exposure. All fluorescence images were obtained using a Leica Fluo III attached to a Leica MZ16 fluorescence stereomicroscope with a GFP2 filter. *DR5::VENUS* fluorescence images were analysed to quantify fluorescence intensity using ImageJ.

2.14 Electrolyte leakage

Electrolyte leakage was measured from elongating hypocotyls that had been treated with 100 g/ha glyphosate or a water control at either dawn or dusk. Herbicide treatments were 6 h. 0.05 g fresh aerial tissue was initially washed with Milli-Q H₂O (Merck) to remove excess electrolytes and treatments. Tissue was then suspended in Milli-Q H₂O and placed into a shaking incubator (150 rpm, 19 °C; Stuart SI500). Conductivity of the water was measured (PRIMO5 Pocket Conductivity Tester, HANNA Instruments) at specified time points after the start of the assay. After the final measurement time point, 100% electrolyte leakage was determined by placing tissue samples into -80 °C for 1 h to elute all remaining solutes, followed by a further 3 h in the shaking incubator and water conductivity was measured (Hemsley et al., 2014). Electrolyte leakage per time point was calculated as a percentage of the total electrolyte leakage.

2.15 Chlorophyll content

Total chlorophyll was extracted from elongating hypocotyls using buffered 80% aqueous acetone (80% acetone, 2.5 mM sodium phosphate buffer, pH 7.8) (Porra et al., 1989). Extractions were performed under a dim green light to prevent degradation of samples. 0.05 g fresh tissue was sampled from 7 day old seedlings that had been

treated at dawn or dusk on day three, and homogenised in extraction buffer using a micropestle. Extracted chlorophyll was loaded into a quartz cuvette and absorbency was measured at 663, 646 and 470 nm. Chlorophylls *a* and *b* were calculated according to Porra et al. (1989) (Equations (2.1) to (2.3)). Total carotenoids were calculated according to Lichtenthaler and Wellburn (1983) (Equation 2.4), where W = mass of plant tissue (g), and V = Volume of buffered 80% acetone (mL).

$$(2.1) \quad \text{Chl } a \text{ (mg g}^{-1}\text{)} = \frac{V(12.25A^{663} - 2.55A^{646})}{1000W}$$

$$(2.2) \quad \text{Chl } b \text{ (mg g}^{-1}\text{)} = \frac{V(20.31A^{646} - 4.91A^{663})}{1000W}$$

$$(2.3) \quad \text{Total Chl (mg g}^{-1}\text{)} = \frac{V(17.76A^{646} + 7.34A^{663})}{1000W}$$

$$(2.4) \quad \text{Carotenoids (mg g}^{-1}\text{)} = \frac{V((1000A^{470}) - (3.27\text{Chl}a) - (104\text{Chl}b))}{1000W}$$

2.16 RNA-sequencing

Seedlings were sterilised and grown under 12 h light /12 h dark cycles. Seedlings were treated (100 μ L water control, 10 g/ha mesotrione, 0.2% Agridex, or 1 g/ha terbutylazine) at dawn on day 11 and sampled after 4 h. RNA was extracted as in Section 2.8. Three RNA samples were pooled to ensure high yield RNA. Sample libraries were prepared using Stranded mRNA Truseq (Illumina), with PolyA tail capture and strand specificity, then sequenced using Illumina NextSeq with NextSeq 500 Hi-Output Kit v2, using paired-end reads, performed by the Bristol Genomics Facility, University of Bristol. Data were analysed using Partek Flow software (partek.com/partek-flow/; accessed 23/11/17) using the TopHat2 Tuxedo pipeline (Trapnell et al., 2012). RNA fragments were trimmed at each end to remove low quality sequence and Illumina adapter sequences, and reads were mapped to the *Arabidopsis thaliana* reference genome (TAIR10).

2.17 Bioinformatics

To determine whether there were differences between treatments in the RNA-sequencing data, a principal component analysis (PCA) was performed (Partek Flow). Furthermore, differential gene expression lists between control and treated samples were obtained (Partek Flow). A correction for false-discovery rates (FDR) was applied (0.05). For differential gene expression, fold change was constrained to ≤ -2 - and ≥ 2 -fold for output feature lists. These lists of genes were compared to nycthemeral- and circadian-regulated datasets as above (Section 2.7).

Gene lists were entered into the KEGG pathway database (https://www.genome.jp/kegg/tool/map_pathway1.html; accessed 13/10/17) to identify components of metabolic pathways that were represented by the genes within the lists. Hypergeometric tests were conducted to identify significant overlaps between the input gene lists and the pathway identified. A minimum overlap of five genes between the input list and

the pathway list was required, plus a P value of ≤ 0.05 . Pathways common to multiple treatments were identified to find those unique to one treatment.

The MEME-LaB tool (wsbc.warwick.ac.uk/wsbcToolsWebpage; accessed 09/12/18 (Brown et al., 2013)) was used to identify transcription factor binding sites within the promoter region of groups of genes (for both glyphosate microarray datasets (Faus et al., 2015), and RNA-sequencing data). Minimum and maximum motif widths were set to six and 14, respectively. Motifs identified were considered significant if they occurred in $>15\%$ of the sequences in an input cluster and had an E value ≤ 0.05 .

2.18 Statistical analyses

Throughout this thesis, data were plotted and statistical analyses were conducted in SigmaPlot v13 (Systat Software, Inc.) or Microsoft Excel (v16.19).

Chapter 3

Using *Arabidopsis* as a model to investigate the circadian regulation of plant responses to herbicides

3.1 Introduction

Arabidopsis thaliana (*Arabidopsis*) has been recognised as the plant model organism of choice since the 1980s (Meinke et al., 1998). This choice was largely due to the small, and now fully sequenced, genome and establishment of techniques enabling genetic experiments, in addition to the short generation time and small plant size (Meyerowitz, 1989; Koornneef and Meinke, 2010). Consequently, it is informative to use *Arabidopsis*, as opposed to weed or crop species, in this work in order to understand the molecular mechanisms underlying any identified relationships between the circadian oscillator and herbicides. However, relatively little research has been conducted using *Arabidopsis* within this subject area.

A plethora of experimental methods are used to measure plant responses to herbicides. These can involve visual inspection of plant physiology, or more specific methods

dependent on the known mode of action of the herbicide, such as measuring chlorophyll fluorescence for photosystem-inhibiting herbicides.

The primary aim of the work in this chapter was to develop experimental methods that could reveal quantifiable changes in *Arabidopsis* with the application of multiple herbicides, and to further preliminarily test the efficacy of each herbicide when applied at different times of day. This was conducted with the goal of developing methods to study daily or circadian rhythms in herbicide effectiveness. Different types of assay may work more, or less, effectively for each herbicide depending on the mode of action of the herbicide.

Three initial methods were tested here: (i) the visual physiological effects of herbicides on mature *Arabidopsis* rosettes, (ii) the effects of the herbicides on chlorophyll fluorescence in seedlings and (iii) transcriptional responses of herbicide-marker genes. For the first two assay types, multiple concentrations of herbicides were tested to find suitable concentrations that show quantifiable changes in *Arabidopsis*. Herbicide concentration choices were based on advice from both Syngenta and the literature.

3.2 Physiological effects of herbicides on *Arabidopsis*

Visual inspection of plants is frequently used to determine the effectiveness of a herbicide treatment. This is commonly conducted using a scoring system, such as the example in Table 3.2.1 (Dear et al., 2003). Such scoring is often subjective and generalised. The aim of this initial experiment was to accurately quantify damage caused by herbicides applied at different times of day through different physiological measurements.

Table 3.2.1: European Weed Research Council (EWRC) scoring system for measuring herbicide efficacy (adapted from Dear et al. (2003)).

EWRC Score	Efficacy
1	Complete kill
2	Excellent
3	Very good
4	Good-acceptable
5	Moderate but not acceptable
6	Fair
7	Poor
8	Very poor
9	None

Glyphosate, mesotrione and terbuthylazine were applied until saturation on the surface of the rosette using a pump spray bottle. Three concentrations were tested per herbicide, and five time of day treatment points. Plants were sprayed when they were at the six true leaf stage and photographs were taken at specified intervals over 2 weeks for image analysis.

3.2.1 Herbicides inhibit growth and cause quantifiable damage in *Arabidopsis*

All three herbicides began to have visual effects on *Arabidopsis* rosettes four days after treatment. An example of the damage caused by the herbicides to the rosettes can be seen in Figure 3.2.1. Mesotrione caused typical bleaching to newly forming tissue (McCurdy et al., 2009; Abendroth et al., 2006), and TBA and glyphosate caused bleaching and necrosis to older tissue (Blancard, 2017; Lassiter et al., 2007). In addition, growth was either inhibited or the rosette appeared to decrease in size potentially due to dehydration. This damage was quantified and compared to control plants (Figures 3.2.2 to 3.2.4).

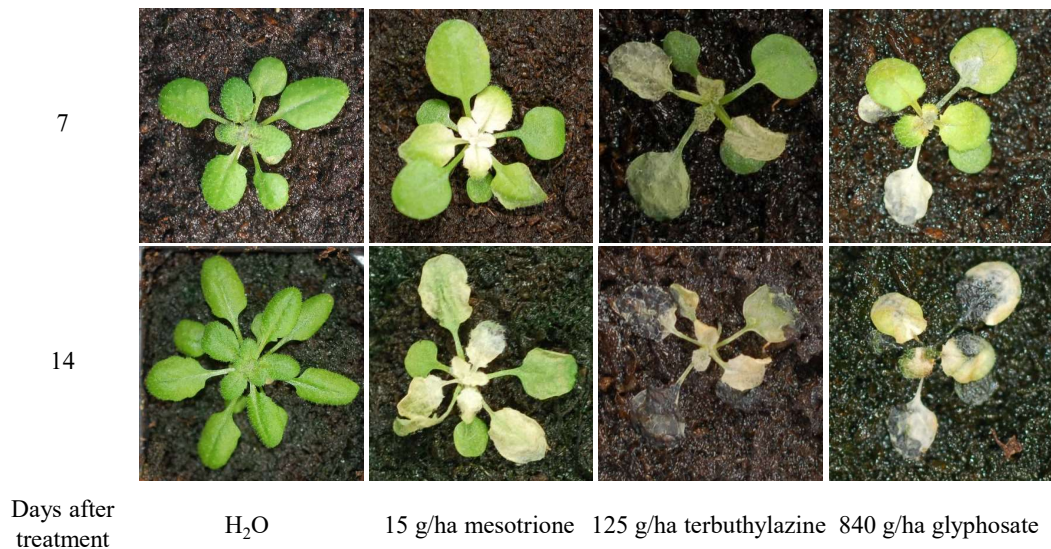


Figure 3.2.1: Example of rosette damage caused by herbicides 7 (top) and 14 (bottom) days after application. Images are of the same plant taken one week apart. These are example images that were used for image analysis. Water-treated control rosette is included for comparison. Images not to scale.

Mesotrione

The plants treated with mesotrione continued to grow for 4 days after treatment, from 63 mm² on day 0 to 126 mm² on day 4 (Fig. 3.2.2a). Rosettes then began to decrease in area because some leaves possibly became dehydrated and so decreased in size. After 14 days the treated rosettes had reduced to a similar size to that on day 0 (70 mm²). Control plants continued to grow for the 14 days that measurements were taken, and increased in area from 53 mm² on day 0 to 670 mm² on day 14 (Fig. 3.2.2a).

The change in area from the day of treatment to 14 days later was also measured (Fig. 3.2.2b). Mesotrione-treated plants resulted in a similar final area, with little change in area since day 0, regardless of mesotrione concentration and treatment time, increasing only around 6 mm² (Fig. 3.2.2b). There were no significant differences in the change in rosette area between treatment times for any of the concentrations tested (one-way ANOVA within each concentration).

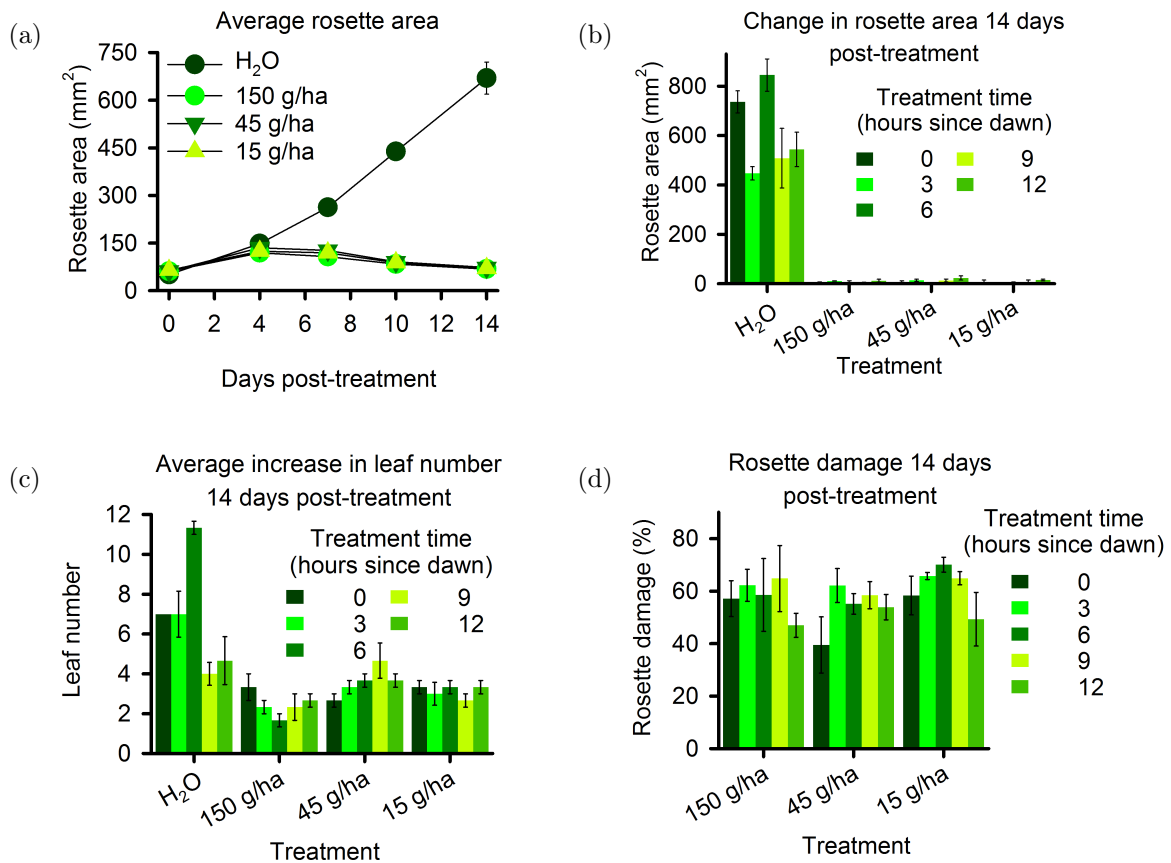


Figure 3.2.2: Mesotrione inhibits growth and causes damage to Arabidopsis rosettes. Plants at the six true leaf stage were treated with one of three concentrations of mesotrione at five time points throughout the day. Images of the rosettes were taken on specified days after treatment and were analysed to quantify the effects of the herbicide. (a) Average rosette area decreases 4 days after mesotrione treatment, whereas control plants continue to increase. (b) Rosette area is smaller after 14 days mesotrione treatment compared to control plants. (c) Leaf number increases after mesotrione treatment, but less than control plants. (d) Mesotrione causes damage to rosettes with a similar level for all three concentrations and treatment times. Data shown are the mean of 3 plants per time point \pm SEM.

There were small, but not statistically significant, differences in the rosette area of control plants that had been sprayed with water at different times of day. Control treatments at 0 and 6 hours after dawn resulted in greater increases in growth with rosettes increasing by approximately 736 mm² and 845 mm², respectively (Fig. 3.2.2b). In comparison, rosettes were approximately 500 mm² larger when treatments occurred 3 h, 9 h, and 12 h after dawn.

Mesotrione-treated plants increased leaf number by 1-6 leaves in the 14 days after

treatment (Fig. 3.2.2c). The 150 g/ha mesotrione treatment had the lowest increase in leaf number when applied at midday, with the greatest increase in leaf number for the plants treated at the start and end of the day (Fig. 3.2.2c). Plants treated with 45 g/ha showed a different pattern, with the earliest time point of the day causing the smallest increase in leaf number. The 15 g/ha treatment caused similar increases in leaf number (2-4) for all treatment time points. There were no statistically significant differences in the increase in leaf number for the different treatment time points for each concentration. Control plants increased in leaf number from 4-11, depending on application time. The control plants for the 6 hour treatment significantly increased in leaf number compared to all other time points (one-way ANOVA).

The percentage of rosette damage was variable for all mesotrione concentrations (Fig. 3.2.2d), and there was a mean of 58% damage overall. The 150 g/ha mesotrione treatments caused very little treatment time-dependent damage (Fig. 3.2.2d). Plants treated with 45 g/ha mesotrione at dawn appeared to be slightly less damaged than plants treated at other time points. For the 15 g/ha mesotrione treatments, the middle of the day appeared to cause the most damage, whereas dawn and dusk may be less effective treatment times, as there was slightly less rosette damage (Fig. 3.2.2d). However, no treatment times for any concentration were statistically different from any other (one-way ANOVA).

There did not appear to be a distinct treatment time point that consistently affected all measurement parameters to a greater or lesser extent than other time points. There was also variability across the control plants for different time points. This could partly be because there were low replicate numbers. There did not appear to be a distinct difference in the effectiveness of the three concentrations of mesotrione, therefore they could all be too high for *Arabidopsis*.

Terbuthylazine

The rosettes of plants that had been treated with TBA did not increase in area after treatment (Fig. 3.2.3a), instead they decreased in size gradually over the two weeks from around 39 mm² to around 28 mm² (Fig. 3.2.3a). Control plants increased in area from 0 to 14 days, by approximately 424 mm², after treatment (Fig. 3.2.3a). There does not appear to be a distinct difference in the average rosette area resulting from treatments with different concentrations of TBA.

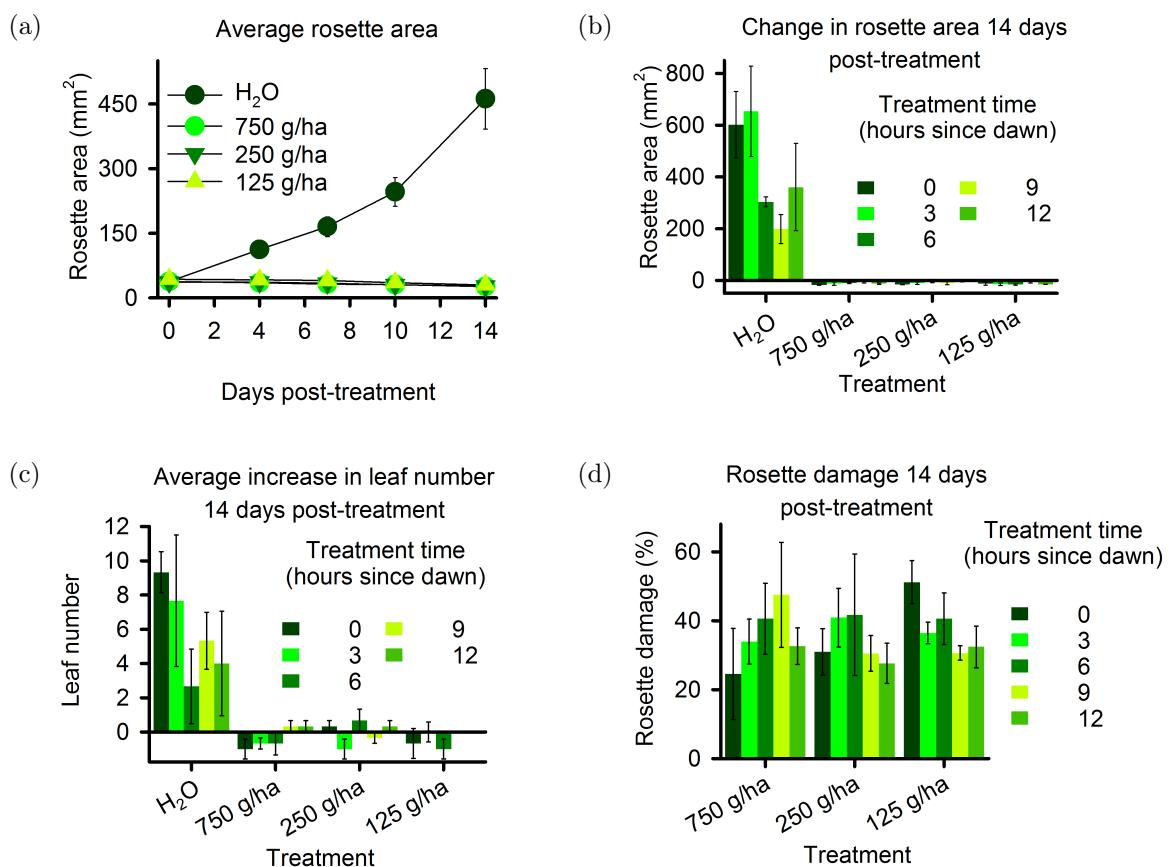


Figure 3.2.3: Terbuthylazine inhibits growth and causes damage to Arabidopsis rosettes. Plants at the six true leaf stage were treated with one of three concentrations of TBA at five time points throughout the day. Images of the rosettes were taken on specified days after treatment and were analysed to quantify the effects of the herbicide. (a) Average rosette area decreases immediately after TBA treatment, whereas control plants continue to increase. (b) Rosette area is smaller after 14 days TBA treatment compared to both control plants and the initial starting rosette area. (c) Leaf number decreases at some time points after TBA treatment. (d) TBA causes damage to rosettes with some treatment time of day differences. Data shown are the mean of 3 plants per time point \pm SEM.

All plants treated with TBA had a reduction in rosette area over the duration of the experiment (Fig. 3.2.3b), meaning that they decreased in size compared to the day of the treatment. Rosettes decreased by a mean of 11 mm². There does not appear to be any obvious time of day differences between the treatment times and the change in rosette area, and no statistically significant differences were detected for different treatment times within each concentration (one-way ANOVA). The control plants had variable change in rosette areas increasing by 198-653 mm² (Fig. 3.2.3b).

TBA treatment largely inhibited new leaves from forming (Fig. 3.2.3c). For 750 g/ha TBA treatments in the first half of the day, a decrease in leaf number was observed after 14 days, whereas treatments later in the day increased in leaf number, but these differences in treatment time were not significant (one-way ANOVA; Fig. 3.2.3c). The decrease in leaf number was probably due to leaves shrivelling or rotting after TBA treatment. This was not consistent across the other concentrations of TBA where the change in leaf number was variable (Fig. 3.2.3c). No data indicate the leaf number stayed the same as the day of treatment. All control plants increased in leaf number from the day of treatment from between 2-11 leaves.

The degree of rosette damage caused by TBA applications was inconsistent across treatment concentrations (Fig. 3.2.3d). For 750 g/ha and 250 g/ha it appeared that dawn and dusk may be slightly less effective treatments as they caused less damage, however this was not seen in the 125 g/ha treatments, where the dawn treatment time point caused the greatest percentage of rosette damage. However, there was no significant difference between the treatment times and the results were noisy.

It does not appear that the higher concentration of TBA had much greater effect than the lower concentrations of TBA, therefore perhaps the concentrations chosen for Arabidopsis were too high.

Glyphosate

Glyphosate-treated plants had around the same area as at the onset of the experiment at approximately 65 mm^2 , until around day 7 (Fig. 3.2.4a). After this point, the rosettes begin to decrease in area. The decrease in area of the 840 g/ha glyphosate treated plants becomes more evident after 14 days (Fig. 3.2.4a). Control plants continued to grow throughout the 14 days of the experiment increasing from around 66 mm^2 to around 485 mm^2 (Fig. 3.2.4a).

Plants treated with 840 g/ha glyphosate all decreased in area (approximately -17 mm^2) compared to the start of the experiment, with no significant difference between time points (one-way ANOVA; Fig. 3.2.4b). Plants treated with 100 g/ha glyphosate had a similar area to the start of the experiment. Plants treated with 25 g/ha glyphosate increased in area slightly, with dawn and midday increasing in area the least, and dusk treatment time increasing the most (42 mm^2) (Fig. 3.2.4b). Control plants had a similar change in rosette area across time points, increasing by a mean of 420 mm^2 .

The majority of glyphosate-treated plants decreased in leaf number compared to the start of the experiment (Fig. 3.2.4c). The only two treatment time points that increased in leaf number were for 25 g/ha at 3 and 12 hours after dawn. All control plants increased in leaf number from the start of the experiment, although there were inconsistencies (Fig. 3.2.4c).

For 840 g/ha glyphosate treatment, the times of treatment that caused the most rosette damage were 0 and 12 hours after dawn (Fig. 3.2.4d), with around 50% of the rosette being damaged. The least effective was 3 h after dawn with only 27% damage. For 100 g/ha and 25 g/ha , the time point that caused the least damage to the rosette, and was therefore less effective, was dawn. However, there were no statistically significant changes between the treatment times within each concentration (one-way ANOVA)

For the 25 g/ha glyphosate treatment, the largest increases in area and leaf number were for treatments 3 h and 12 h after dawn (3.2.4b and 3.2.4c). This suggests that

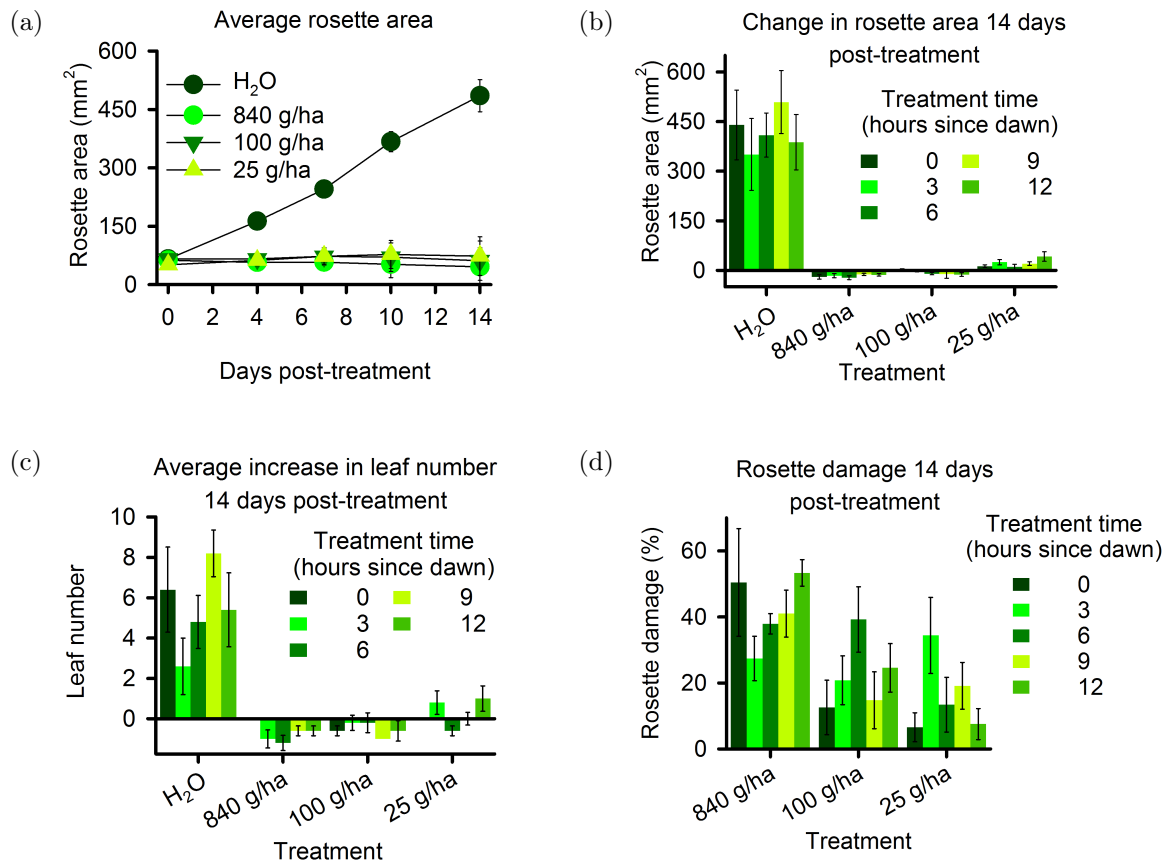


Figure 3.2.4: Glyphosate inhibits growth and causes damage to Arabidopsis rosettes. Plants at the six true leaf stage were treated with one of three concentrations of glyphosate at five time points throughout the day. Images of the rosettes were taken on specified days after treatment and were analysed to quantify the effects of the herbicide. (a) Average rosette area remains relatively constant after glyphosate treatment, except for treatment with 840 g/ha glyphosate where it decreases after 7 days treatment, control plants continue to increase in area. (b) Rosette area is smaller after 14 days treatment for 840 g/ha glyphosate, 100 g/ha glyphosate treatment causes rosettes to stay a similar size to pre-treatment, and 25 g/ha glyphosate treatment allows rosettes to increase in size, control plants increase in rosette area. (c) Leaf number decreases for almost all glyphosate treatments. (d) Glyphosate causes damage to rosettes with treatment time of day differences. Data shown are the mean of 5 plants per time point \pm SEM.

treatments at these time points were less effective. However, the treatment time that caused the most damage for 25 g/ha was also 3 h after dawn, suggesting that is the most effective time point. Only small and non-statistically significant differences were seen between treatments at different times of day for each concentration of glyphosate. Differences were also apparent between glyphosate concentrations, whereby the higher the concentration, the greater the damage and inhibition of growth.

3.3 Design and construction of a laboratory-sized track sprayer

To address the problem of inconsistent manual spraying between experiments, and in order to replicate more closely how plants would be sprayed in the field, a laboratory-sized track sprayer was designed and constructed. The sprayer was designed with the assistance of a spraying technology expert from Syngenta, and was based on previous sprayers of a similar nature. The sprayer was constructed by the University of Bristol Physics Workshop. All parameters were designed to ensure replication of the type of spray plants would receive in the field. This allows for all aspects to be controlled between treatments within and across experiments. Factors designed to be the same were: speed of spray, pressure of spray droplets, size of spray droplets, volume of spray, and height above the plant. Furthermore, the sprayer was designed to fit inside a fume cupboard.

Figure 3.3.1 shows a diagram of the custom-built sprayer produced for this work with the main components and specifications outlined. The sprayer is 748 mm wide and sprays 500 mm above the plant. The nozzle (Teejet 250033) is identical to those used in the field and produces a fan-shaped spray swath. The liquid is contained within a pressurised vessel, controlled by a solenoid switch.

To test the sprayer, water sensitive paper (Syngenta) was placed beneath the swath of the sprayer and one test run was conducted. The aim is to obtain a spray with an even dispersal at an intersection of the spray path. The initial test run of this sprayer (Fig. 3.3.2a) found that the nozzle was not spraying correctly. The spray was not dispersed evenly; there was a very narrow spray with no defined droplets. The droplets to each side of the main spray area are droplets that were splashed back onto the paper. A new spray nozzle (of the identical type) was obtained and a test spray was run (Fig. 3.3.2b). For this test, the pressure was set to 2 bar which gave a spray volume of 110 mL min^{-1} and the speed of nozzle movement was set to 0.6 m s^{-1} . These

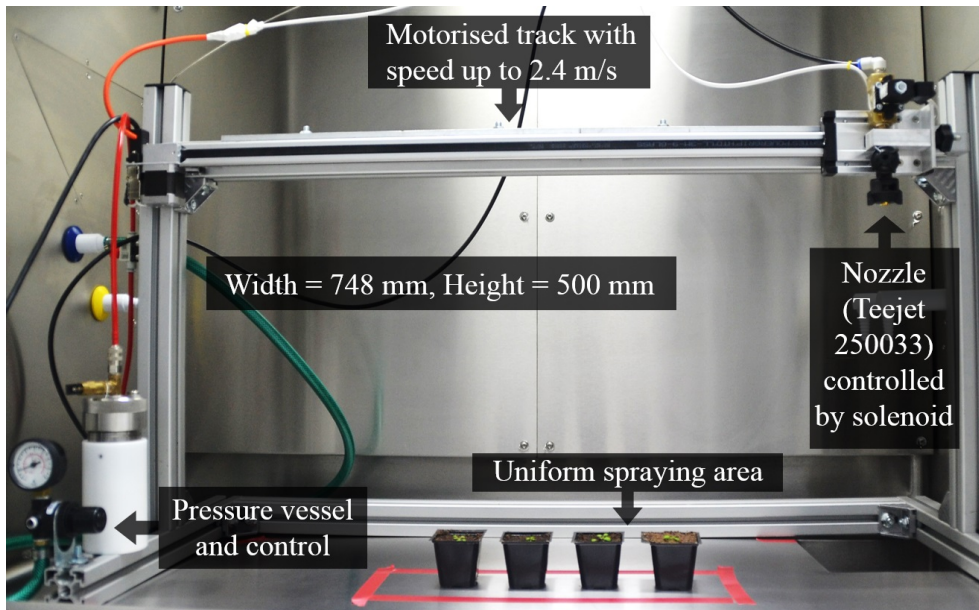


Figure 3.3.1: The bespoke track sprayer designed and built for this work.

conditions caused a dense spray with a higher concentration of droplets in the centre. The pressure was reduced to 1.75 bar, which reduced the spray volume to 95 mL min^{-1} at a speed of 0.6 m s^{-1} . These settings created a more evenly dispersed spray (Fig. 3.3.2c), as expected based on advice from Syngenta. Figure 3.3.2d shows a test spray along the length of the track, conducted to test the length of the even spray dispersal. This test found that the spray is evenly dispersed for the length of the test strip, 50 cm. This is enough to fit at least six plants in one sprayer run. Once the sprayer had been optimised, test sprays were conducted with *Arabidopsis* plants to ensure the spray remained evenly dispersed on the surface of plants. Figure 3.3.3 shows two rosettes that were sprayed with the settings tested above (Fig. 3.3.2c). The plants were sprayed with an even distribution across the rosette and spray droplets were even in size. This optimisation meant that future experiments could be conducted using this equipment knowing that there would be consistency in spraying across plants within and across experiments.

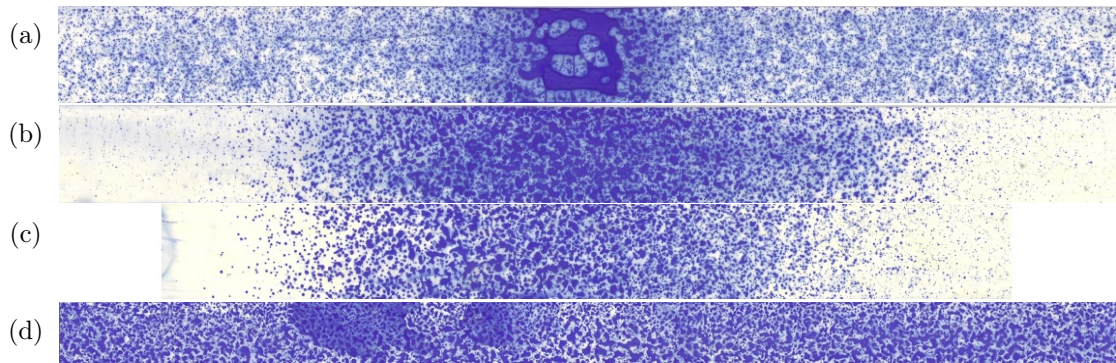


Figure 3.3.2: The track sprayer was tested and adjusted until an evenly distributed spray was produced. These are images of water-sensitive paper where the paper becomes coloured when wet. Tests were conducted by running the sprayer over water-sensitive paper strips (provided by Syngenta). (a) The first test identified that the nozzle was not working correctly and was probably blocked. There was no distribution of droplets in the centre of the strip. (b) Sprayer pressure set to 2 bar caused a dense spray in the centre of the test strip. (c) Pressure was reduced to 1.75 bar causing an even distribution of droplets from the centre of the spray. (d) A test spray along the length of the track found that there was an even distribution for at least 50 cm in length. Images not to scale, actual height of a strip = 2.5 cm.



Figure 3.3.3: Example images of Arabidopsis rosettes that were sprayed using the custom-built track sprayer. Water droplets on the leaves of the Arabidopsis rosettes can be seen to be even in size and distribution across the two plants. Plants are to the same scale.

3.4 Herbicides affect photosynthesis in Arabidopsis

Mesotrione and TBA have a direct effect on the photosynthetic apparatus (Mitchell et al., 2001; LeBaron et al., 2008), whereas glyphosate does not. However, glyphosate could have an indirect effect on photosynthesis. Damage to photosystem II (PSII) is one of the first indicators of stress in a leaf (Maxwell and Johnson, 2000) and it is likely that glyphosate treatment would cause a quantifiable response in photosynthesis. Therefore, it was of interest to see whether the effects of the three herbicides could be measured by chlorophyll fluorescence in Arabidopsis.

Chlorophyll fluorescence can measure the efficiency of PSII photochemistry, which is usually correlated well to carbon assimilation by photosynthesis (Maxwell and Johnson, 2000). Therefore, chlorophyll fluorescence measurements can suggest a proxy for photosynthesis, although some decoupling of the two can occur (Maxwell and Johnson, 2000). Light energy absorbed by chlorophyll is subject to three competing fates: light can be used in photochemistry to drive photosynthesis, excess energy can be dissipated as heat, or light can be re-emitted as fluorescence. This re-emitted fluorescence can be measured and the other relative processes can be quantified (Maxwell and Johnson, 2000). If this assay detected an effect of the herbicides, then it would be a rapid, non-invasive method to potentially determine time of day effects.

Chlorophyll fluorescence parameters of interest here were F_v/F_m , $Y(II)$, and non-photochemical quenching (NPQ). F_v/F_m is the maximum efficiency of PSII when all available reaction centres are open, in the dark adapted state (Ni et al., 2014). Measuring F_v/F_m allows the maximum amount of light to take the fluorescence pathway (Maxwell and Johnson, 2000). The minimum fluorescence is measured in the dark-adapted state by using a non-actinic light source (Fig. 2.6.1). At this point PSII reaction centres are open and can accept electrons to pass through the electron transport chain. Minimum fluorescence is compared to the maximum fluorescence after a saturating light pulse (Fig. 2.6.1). The saturating light pulse closes all reaction centres, which means they cannot be reduced, and light is re-emitted as fluorescence.

If a plant is stressed, fewer open reaction centres are available, lowering Fv/Fm. In the context of the experiments with these herbicides, a decrease in Fv/Fm would suggest the herbicide is effective at reducing the ability of the plant to use light energy since fewer reaction centres would be open.

Y(II) measures the proportion of the light absorbed by chlorophyll associated with PSII that is used in photochemistry since it is measured when plants are under light conditions that are able to drive photosynthesis (Maxwell and Johnson, 2000). Fluorescence minimum for Y(II) is taken whilst plants are exposed to actinic light and fluorescence maximum is consequently taken after a saturating pulse (Fig. 2.6.1). As such, Y(II) can give a measure of the rate of linear electron transport and an indication of overall photosynthesis (Maxwell and Johnson, 2000). A decrease in Y(II) would suggest the herbicide is affecting the ability of the plant to use light energy to drive PSII photosynthesis.

Light energy can also be de-excited through thermal dissipation, termed NPQ (Maxwell and Johnson, 2000). Non-photochemical quenching is measured by comparing the maximum fluorescence point at which thermal dissipation is at a minimum to the maximum fluorescence after exposure to actinic light (Fig. 2.6.1) (Maxwell and Johnson, 2000). NPQ is particularly important when the number of excited chlorophyll increases, and the capacity for photosynthesis is saturated. Increased quenching avoids damage to cells by singlet oxygen that evolves through decaying triplet chlorophyll. A herbicide causing an increase in NPQ would suggest that more energy is being released as heat rather than being used to drive photosynthesis (Maxwell and Johnson, 2000).

Considering the known link between the mode of action of these herbicides and photosynthesis, there has been little published on the subject, in particular using Arabidopsis or identifying any time of day application effects. Before testing the effect of the herbicides at different times of day, initial experiments were required to determine a concentration that has a measurable, non-lethal effect on photosynthesis in Arabidop-

sis and the length of time the herbicide is needed to be in contact with the plant to have an effect. Therefore, the first experiment was to determine what concentration of each herbicide could have an effect on photosynthesis.

3.4.1 Greater concentrations of herbicides tested negatively affect chlorophyll fluorescence

To determine the effects of the herbicides on photosynthetic parameters in seedlings, a range of herbicide concentrations were tested. Treatments were applied at dawn on day 10 after germination and fluorescence parameters were measured 24 h later, following a 12 hour dark adaptation (overnight). At least the three highest concentrations tested of each herbicide had an effect on photosynthesis after 24 h. The aim was to determine the minimum concentration to have a significant effect on these parameters, so that subtle time of day differences could be identified.

An example of the Fv/Fm chlorophyll fluorescence data collection is shown in Figure 3.4.1. Three concentrations of TBA were tested on one imaging plate. The software uses false colours to show the difference in Fv/Fm values. The cooler colours (blue) show a higher Fv/Fm as seen for the control plants (0 g/ha). Colours that appear warmer (red) are a lower Fv/Fm, which can be seen for the higher concentrations of TBA.

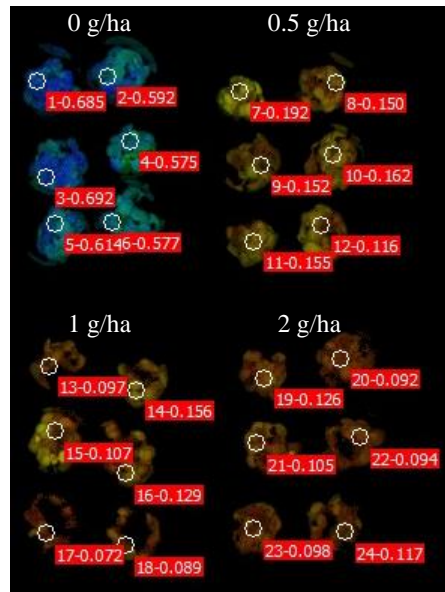


Figure 3.4.1: An example of chlorophyll fluorescence data collection. Six rings of plants per treatment are shown, and each ring of plants contains one circular area of interest from which the data is collected. Images are false coloured, where cooler colours are a higher F_v/F_m and warmer colours are a lower F_v/F_m . This plate shows the effect of three TBA dilutions (0.5 g/ha, 1 g/ha, and 2 g/ha) plus water treated controls. The F_v/F_m for each area of interest is displayed in the red highlighted text. Each of the six areas of interest were then averaged.

Glyphosate

The minimum concentration of glyphosate required to reduce F_v/F_m was 100 g/ha (Fig. 3.4.2a). This reduced F_v/F_m from 0.7 to 0.6. The highest concentration of glyphosate tested, 840 g/ha, did not reduce F_v/F_m more than the lower concentrations. Similarly, 100 g/ha was the minimum concentration of glyphosate to give a reduction in $Y(II)$ (Fig. 3.4.2b). 100 g/ha glyphosate reduced $Y(II)$ from 0.4 in control plants to 0.27. The three higher concentrations tested decreased $Y(II)$ further, to 0.19. A higher concentration, 200 g/ha glyphosate, was required to increase NPQ (Fig. 3.4.2c). In control plants, NPQ was 0.21 but concentrations of glyphosate \geq 200 g/ha increased NPQ to 0.28-0.35. This shows that glyphosate can alter photosynthetic parameters when used at a minimum concentration of 100 g/ha. Therefore, this is the concentration that was selected to be used in future experiments.

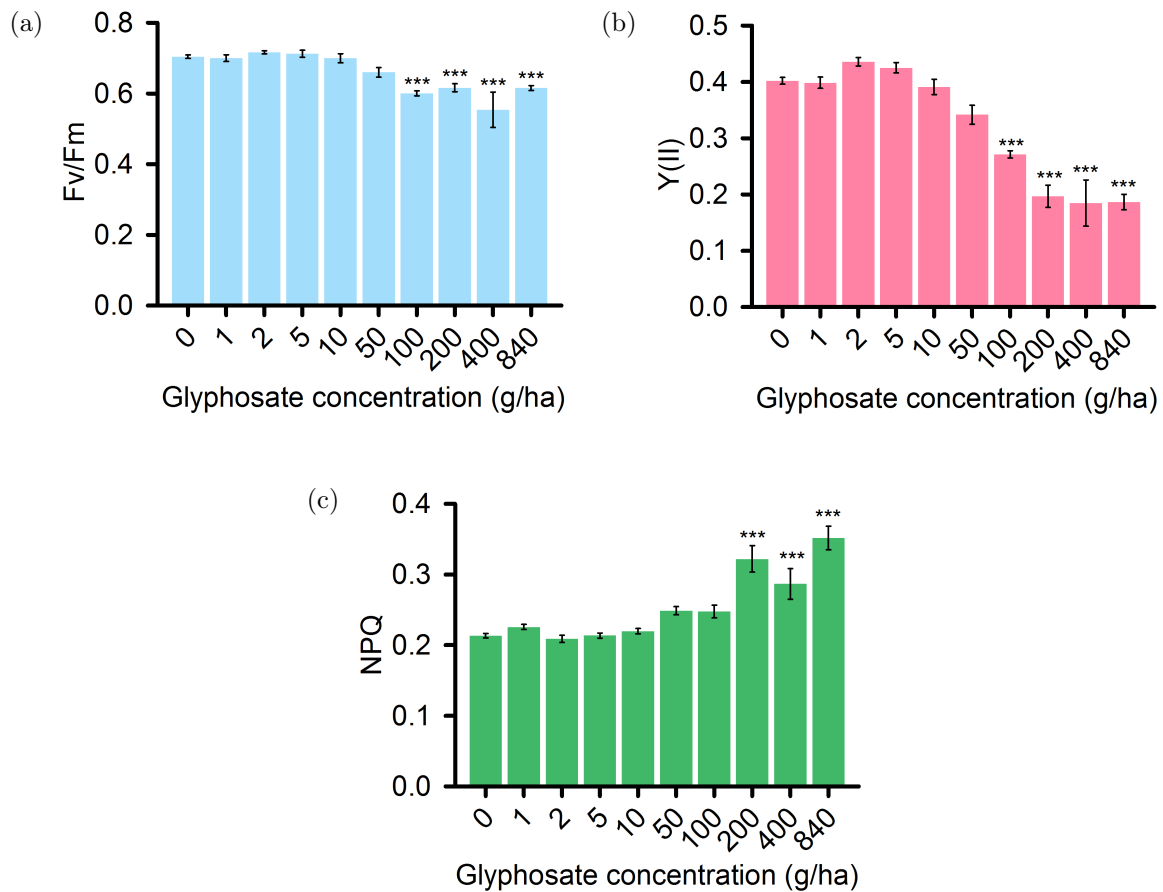


Figure 3.4.2: Increasing concentrations of glyphosate negatively affects photosynthetic parameters measured by chlorophyll fluorescence. 10 day old seedlings were treated at dawn with a dilution series of glyphosate. 24 hours later chlorophyll fluorescence was measured using a custom script. (a) 100 g/ha glyphosate and higher decreases Fv/Fm. Significance determined by one-way ANOVA ($F(9, 62) = 12.9, P \leq 0.001$). (b) 100 g/ha glyphosate and higher decreases Y(II). Significance determined by one-way ANOVA ($F(9, 62) = 43.2, P \leq 0.001$). (c) 200 g/ha glyphosate and higher increases NPQ. Significance determined by one-way ANOVA ($F(9, 62) = 25.2, P \leq 0.001$). Values shown are the mean of six rings of 12 plants \pm SEM. *** = $P \leq 0.001$, relative to control determined by Tukey's post hoc test. No asterisk indicates a non-significant difference.

Mesotrione

10 g/ha mesotrione was required to reduce Fv/Fm significantly compared to the control (Fig. 3.4.3a). This decreased Fv/Fm from 0.73 to 0.6. Higher concentrations of mesotrione further decreased Fv/Fm. 30 g/ha reduced Fv/Fm to more than half of the control plants (0.34), whereas 80 g/ha and 150 g/ha mesotrione completely inhibited Fv/Fm. 5 g/ha was the minimum concentration of mesotrione required to have a significant effect on Y(II) (Fig. 3.4.3b). This decreased Y(II) from 0.43 to 0.32. 10 g/ha mesotrione reduced this 50% more and a further 50% reduction for 30 g/ha. Again, 80 g/ha and 150 g/ha mesotrione completely inhibited Y(II). 5 g/ha mesotrione significantly increased NPQ compared to the control (0.23 to 0.32) (Fig. 3.4.3c). 10 g/ha and 30 g/ha increased NPQ further, up to 0.41. 80 g/ha reduced NPQ to 0.02 and 150 g/ha mesotrione inhibited NPQ. From these results, 10 g/ha mesotrione was selected as the concentration to use in future experiments.

Terbuthylazine

0.5 g/ha TBA, the lowest concentration tested, reduced Fv/Fm from 0.62 in control plants to 0.15 after 24 hours (Fig. 3.4.4a). With increasing concentrations, the effect of TBA on Fv/Fm also increased to the point where the highest concentration (750 g/ha TBA) inhibited Fv/Fm. All concentrations of TBA inhibited Y(II) completely (Fig. 3.4.4b). 0.5 g/ha TBA appeared to increase NPQ slightly, although this was not a significant increase (Fig. 3.4.4c). Concentrations of TBA of 1 g/ha and higher reduced NPQ significantly from 0.29 in control plants to 0.23 to 0.12. It did not appear to be a linear decrease in NPQ as concentration was increased. Due to the severity of the effects of TBA at the lowest concentration after 24 h treatment, three concentrations (1 g/ha, 10 g/ha and 200 g/ha) were chosen to take forward into the next experiment with the aim of further elucidating the optimal concentration to use to observe subtle effects.

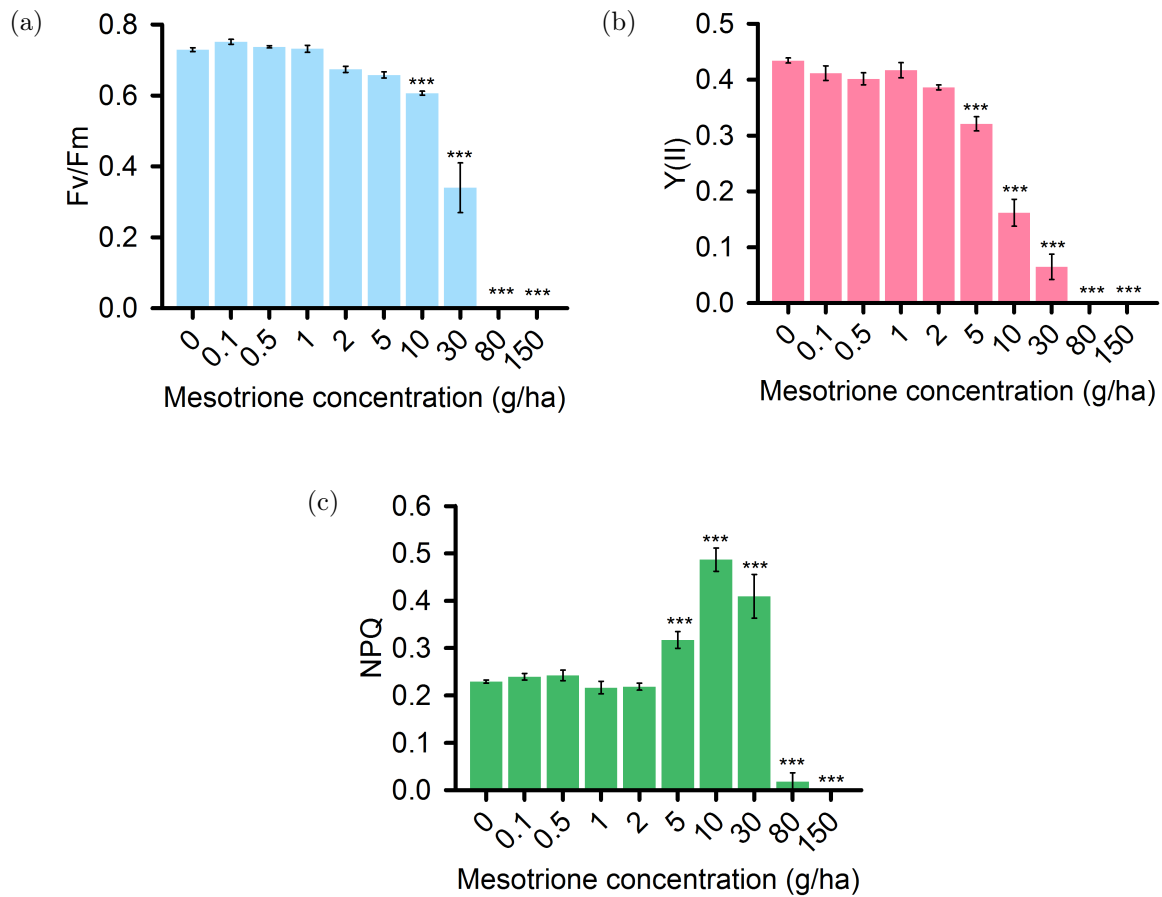


Figure 3.4.3: Increasing concentrations of mesotrione negatively affects photosynthetic parameters measured by chlorophyll fluorescence. 10 day old seedlings were treated at dawn with a dilution series of mesotrione. 24 hours later chlorophyll fluorescence was measured using a custom script. (a) 10 g/ha mesotrione and higher decreases Fv/Fm. Significance determined by one-way ANOVA ($F(9, 62) = 218, P \leq 0.001$). (b) 5 g/ha mesotrione and higher decreases Y(II). Significance determined by one-way ANOVA ($F(9, 62) = 249, P \leq 0.001$). (c) 5 - 30 g/ha mesotrione increases NPQ whereas higher concentrations reduce NPQ, compared to the control. Significance determined by one-way ANOVA ($F(9, 62) = 72.2, P \leq 0.001$). Values shown are the mean of six rings of 12 plants \pm SEM. *** = $P \leq 0.001$, relative to control determined by Tukey's post hoc test. No asterisk indicates a non-significant difference.

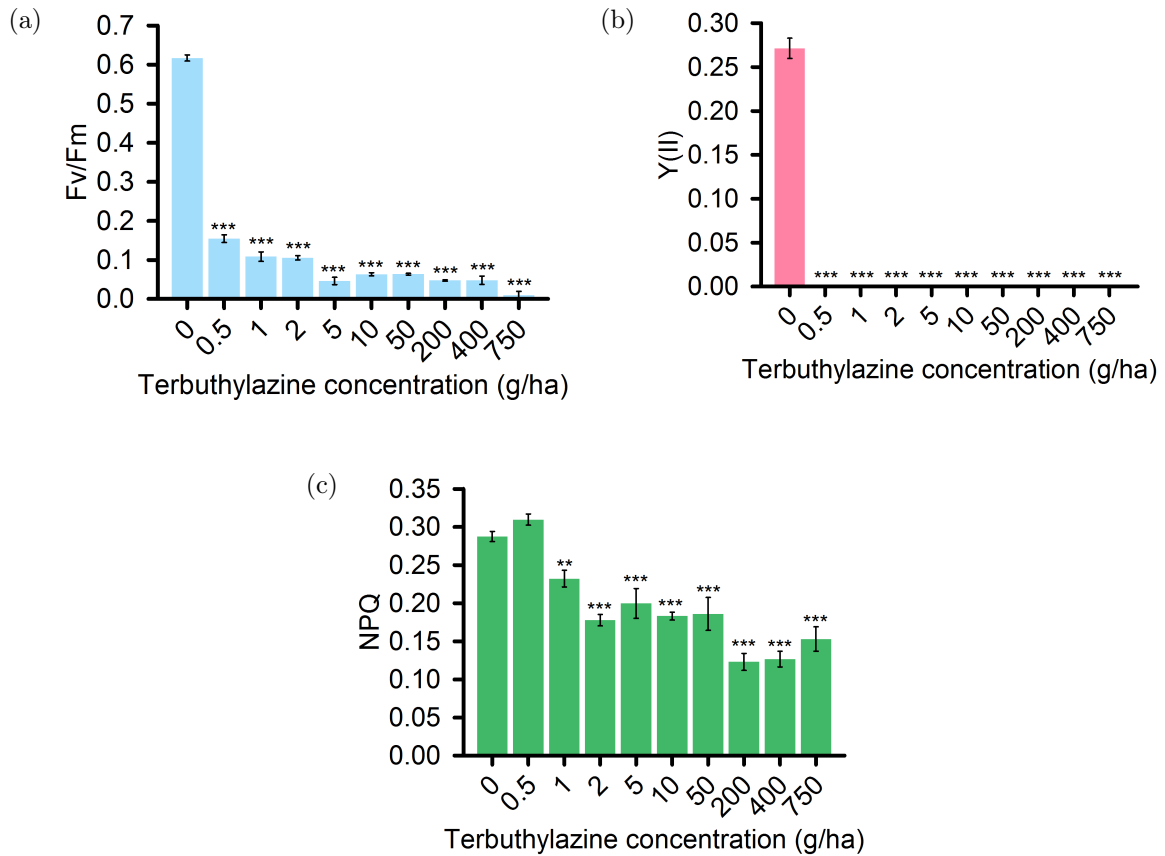


Figure 3.4.4: The nine concentrations of terbuthylazine tested negatively affect photosynthetic parameters measured by chlorophyll fluorescence. 10 day old seedlings were treated at dawn with a dilution series of TBA. 24 hours later chlorophyll fluorescence was measured using a custom script. (a) Concentrations of TBA above 0.5 g/ha reduce Fv/Fm. Significance determined by one-way ANOVA ($F(9, 62) = 769.8, P \leq 0.001$). (b) TBA treatments completely inhibit Y(II). Significance determined by one-way ANOVA ($F(9, 62) = 32.6, P \leq 0.001$). (c) 1 g/ha TBA and higher decrease NPQ. Significance determined by one-way ANOVA ($F(9, 62) = 176.8, P \leq 0.001$). Values shown are the mean of six rings of 12 plants \pm SEM. *** = $P \leq 0.001$, relative to control determined by Tukey's post hoc test. No asterisk indicates a non-significant difference.

3.4.2 Each herbicide tested takes different lengths of time to affect chlorophyll fluorescence

To provide a basis for time of day studies, the time taken by each herbicide to affect chlorophyll fluorescence was investigated. Plants were treated at dawn on day 11 after germination with the chosen concentration for each herbicide (Section 3.4.1). Measurements were made at specified time points after treatment (0 min, 10 min, 30 min, 1 h, 2 h, 3 h, 6 h, or 8 h). Plates were dark adapted after treatment for the length of the experiment. The time for the herbicide to have an effect was dependent on the individual herbicide (Figures 3.4.5 to 3.4.7).

Glyphosate

100 g/ha glyphosate did not alter Fv/Fm significantly after 480 min (Fig. 3.4.5a). In contrast, in the previous experiment (Fig. 3.4.2a) 100 g/ha glyphosate did have an effect on Fv/Fm after 24 hours. Unexpectedly, the Fv/Fm value was lower than the anticipated value of 0.7 (Fig. 3.4.5a). 100 g/ha glyphosate also did not significantly alter Y(II) after 480 minutes (Fig. 3.4.5b). However, at the 480 min time point glyphosate might have started to alter Y(II) because Y(II) was slightly lower in the treated plants, even though it was not statistically significant. 100 g/ha had no significant effect on NPQ after 480 minutes (Fig. 3.4.5c). It appears that glyphosate may be starting to have an effect on NPQ 480 min after treatment because NPQ was higher than the control, but again this difference is not statistically significant. Overall, it is concluded that glyphosate treatments need to be longer than 8 hours to have a great enough effect on photosynthesis to detect differences in time of day responses.

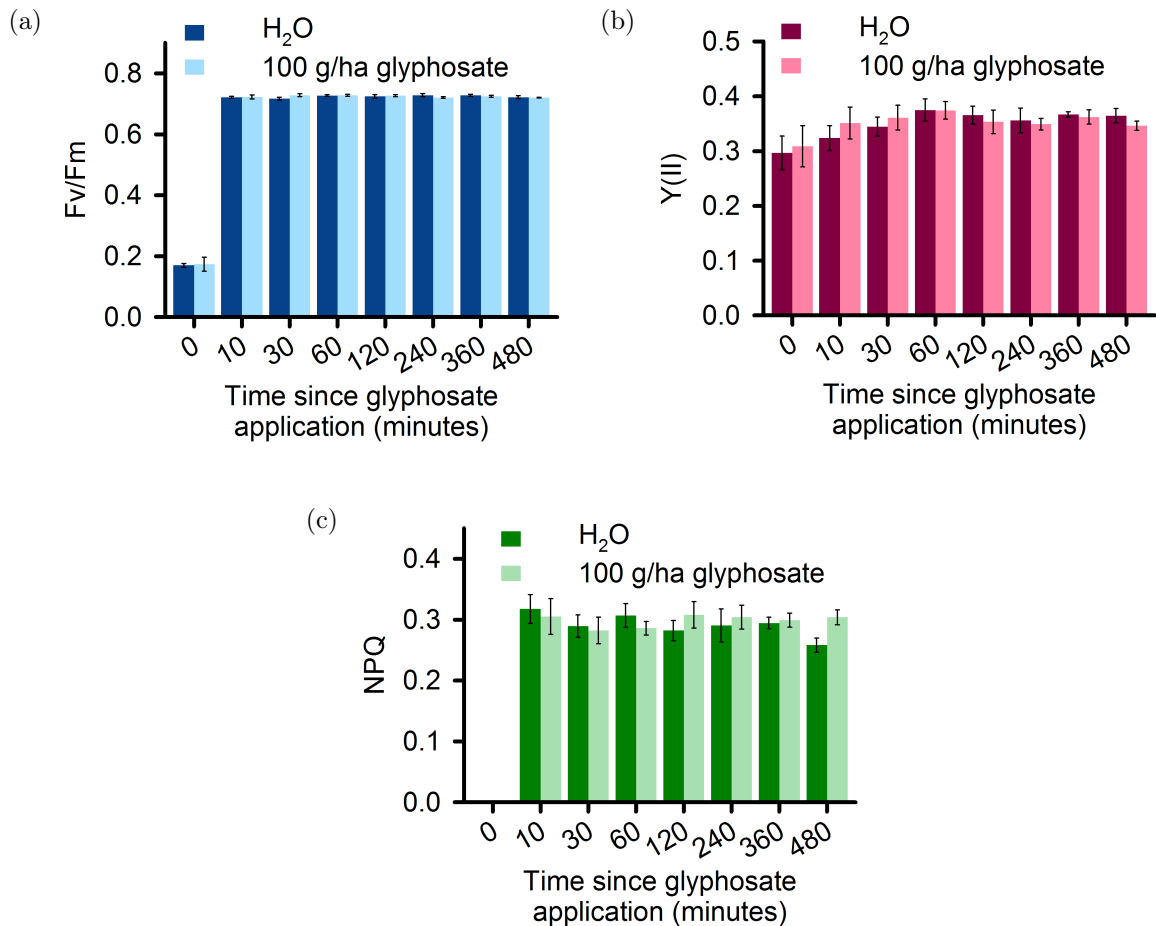


Figure 3.4.5: Glyphosate takes more than 8 hours to affect photosynthesis. 11 day old plants were treated with either 100 g/ha glyphosate or a water control and chlorophyll fluorescence was measured after specified time points. (a) 100 g/ha glyphosate has no effect on Fv/Fm after 480 minutes. (b) 100 g/ha glyphosate has no effect on Y(II) after 480 minutes. (c) 100 g/ha glyphosate has no effect on NPQ after 480 minutes. Values shown are the mean of six rings of 12 plants \pm SEM. Asterisks indicate statistically significant difference between control and treated plants determined by *t*-test at each time point where: * = $P \leq 0.05$, ** = $P \leq 0.01$, *** = $P \leq 0.001$. No asterisk indicates a non-significant difference.

Mesotrione

10 g/ha mesotrione began to alter Fv/Fm relative to the control after 60 minutes (Fig. 3.4.6a). The effect of mesotrione on Fv/Fm became more pronounced with time, with a reduction in Fv/Fm to 0.66 after 480 minutes. 10 g/ha mesotrione took 120 minutes to have a significant effect on Y(II) (Fig. 3.4.6b). Longer mesotrione exposure enhanced its effect on Y(II), but after 480 minutes, Y(II) was not completely abolished. 10 g/ha mesotrione increased NPQ after 120 minutes (Fig. 3.4.6c), and continued to increase NPQ with time. This indicated that two hours is a sufficient treatment length for 10 g/ha mesotrione to reduce photosynthesis.

Terbuthylazine

To identify TBA exposure times that might allow detection of rhythmic responses, three concentrations of TBA (1 g/ha, 10 g/ha, 200 g/ha) were tested because in the previous experiment with TBA, all treatments were so effective (Fig. 3.4.7). Measuring chlorophyll fluorescence immediately after application of the three concentrations of TBA resulted in a significant reduction in Fv/Fm (Fig. 3.4.7a). As expected, longer treatments and higher concentrations of TBA increased the effect on Fv/Fm. 10 g/ha and 200 g/ha TBA abolished Y(II) after treatment lengths ≥ 10 minutes (Fig. 3.4.7b). 1 g/ha TBA measured immediately reduced Y(II) by 65%. All concentrations of TBA tested reduced NPQ (Fig. 3.4.7c), with the higher concentrations reducing NPQ the most. There was little difference in the level of reduction in NPQ across time points, whereby the average NPQ of treated plants was 0.19 and the control NPQ is 0.37. The optimal time to measure chlorophyll fluorescence after TBA treatment was straight after application, and using the lowest concentration of 1 g/ha.

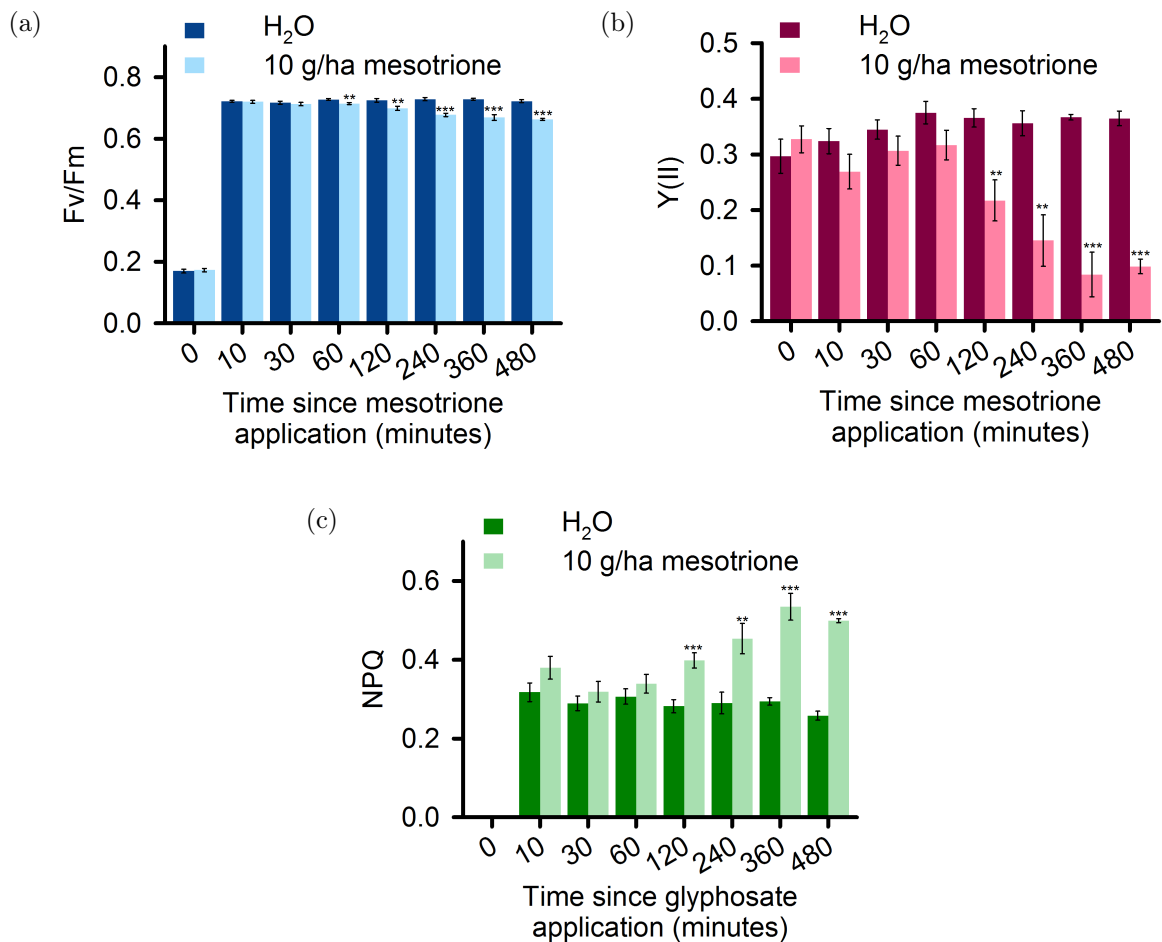


Figure 3.4.6: Mesotrione alters photosynthetic parameters from 60 minutes after application. 11 day old plants were treated with either 10 g/ha mesotrione or a water control and chlorophyll fluorescence was measured after specified time points. (a) 60 minutes after application, 10 g/ha mesotrione reduced Fv/Fm. (b) 120 minutes after application, 10 g/ha mesotrione reduces Y(II). (c) 120 minutes after application 10 g/ha mesotrione increases NPQ. Values shown are the mean of six rings of 12 plants \pm SEM. Asterisks indicate statistically significant difference between control and treated plants determined by *t*-test at each time point where: * = $P \leq 0.05$, ** = $P \leq 0.01$, *** = $P \leq 0.001$. No asterisk indicates a non-significant difference.

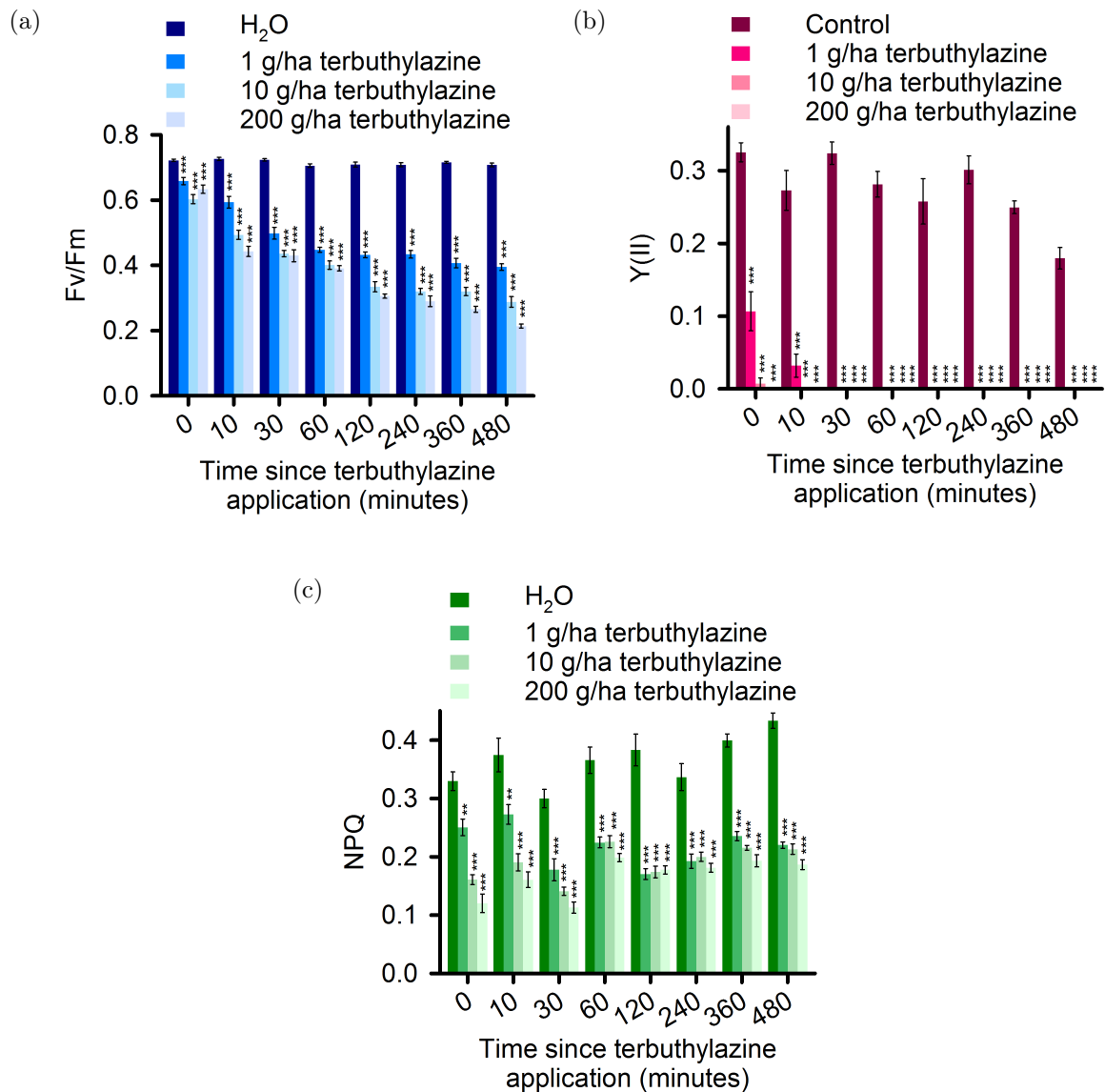


Figure 3.4.7: Application of terbuthylazine has an immediate effect on photosynthetic parameters. Three concentrations of TBA (1 g/ha, 10 g/ha or 200 g/ha) were applied to 11 day old plants and chlorophyll fluorescence was measured at specified time points after application. (a) All three concentrations of TBA immediately reduced Fv/Fm. (b) 30 minutes after application, all concentrations of TBA abolished Y(II). (c) NPQ was reduced after TBA treatment for all concentrations at all time points measured. Values shown are the mean of six rings of 12 plants \pm SEM. Asterisks indicate statistically significant difference between control and treated plants determined by *t*-test at each time point where: * = $P \leq 0.05$, ** = $P \leq 0.01$, *** = $P \leq 0.001$. No asterisk indicates a non-significant difference.

3.4.3 The time of herbicide application has varying effects on chlorophyll fluorescence

Using the information obtained from Sections 3.4.1 and 3.4.2, an experiment was designed to measure whether the effect of herbicide treatment upon chlorophyll fluorescence depended on the treatment time. Plants were treated at one of five time points throughout the light period of the day (under 8 h light /16 h dark cycles). Chlorophyll fluorescence was measured after the time period identified in the previous experiment (Section 3.4.2). Plants were dark-adapted 30 min before measuring. For this experiment, *CCA1-ox* seedlings were also used. *CCA1-ox* constitutively expresses one of the key components of the circadian oscillator, *CCA1*, meaning that *CCA1-ox* plants are arrhythmic under constant conditions (Wang and Tobin, 1998). *CCA1-ox* plants still retain the ability to respond to changes in light/dark cycles, but are unable to anticipate dawn (Green et al., 2002). Therefore, there are changes to the circadian oscillator function in these plants under diurnal conditions. Differences in the time of day responses to the herbicides between Col-0 and *CCA1-ox* might be interpreted as indicating that the circadian timing affects these herbicide responses. The treatment time of day effectiveness was specific to each herbicide (Figures 3.4.8 to 3.4.10).

Glyphosate

Only glyphosate treatments at dawn had a significant effect on Fv/Fm (Fig. 3.4.8a). Treatments 2 h and 4 h after dawn also appeared to reduce Fv/Fm, but were not statistically significant. The response of Fv/Fm to glyphosate appeared to be greatest at dawn with lower sensitivity later in the day. Similarly in *CCA1-ox*, dawn was the only treatment time to give a significant reduction in Fv/Fm after glyphosate treatment (Fig. 3.4.8b). However, treatment at other times also appeared to have no effect on Fv/Fm.

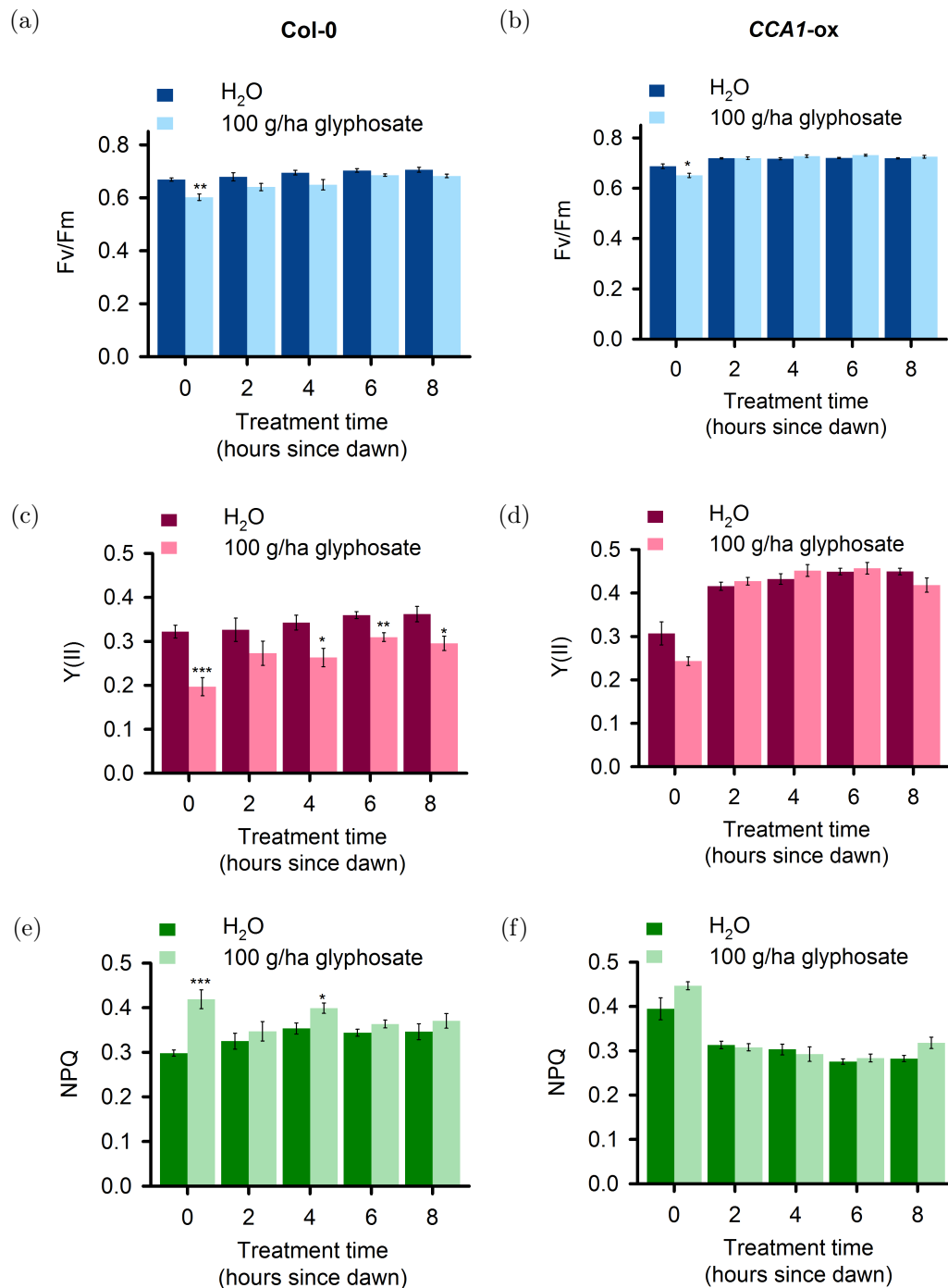


Figure 3.4.8: Applications of glyphosate at different times of day cause differing responses of chlorophyll fluorescence. 100 g/ha glyphosate was applied to 11 day old plants at five time points throughout the day and chlorophyll fluorescence was measured 24 hours later in both *Col-0* and *CCA1-ox*. 100 g/ha glyphosate reduced Fv/Fm the most when applied at dawn in both *Col-0* (a) and *CCA1-ox* (b). 100 g/ha glyphosate reduced Y(II) the most at dawn in *Col-0* (c), but had a reduced effect in *CCA1-ox* (d). NPQ was increased the most at dawn in *Col-0* treated with 100 g/ha glyphosate (e) but had little effect in *CCA1-ox* (f). Values shown are the mean of six rings of 12 plants ± SEM. Asterisks indicate statistically significant difference between control and treated plants determined by *t*-test at each time point where: * = $P \leq 0.05$, ** = $P \leq 0.01$, *** = $P \leq 0.001$. No asterisk indicates a non-significant difference.

Glyphosate treatment at dawn had the greatest effect on Y(II) in Col-0 where Y(II) was reduced by 0.12 (Fig. 3.4.8c). Treatments at other time points resulted in a smaller reduction in Y(II), with a mean of 0.07. In *CCA1-ox*, glyphosate had no significant effect on Y(II) (Fig. 3.4.8d). In Col-0, glyphosate application at dawn caused the greatest increase in NPQ (0.12) (Fig. 3.4.8e), whereas other time points glyphosate had minimal effect on NPQ (0.03). Glyphosate had no effect on NPQ in *CCA1-ox* at any time point (Fig. 3.4.8f). Overall, glyphosate applications at dawn had the greatest effect on chlorophyll fluorescence in Col-0, and a reduced effect in *CCA1-ox* plants.

Mesotrione

Mesotrione treatment at all times caused significant alterations in Fv/Fm in Col-0 (Fig. 3.4.9a). Treatments at 0 h - 6 h after dawn reduced Fv/Fm by a mean of 0.31, but the treatment at 8 h after dawn only reduced Fv/Fm by 0.17, suggesting this may be a less effective treatment time. A two-way ANOVA indicated that there was a significant interaction between treatment and time ($F(4, 50) = 5.53, P < 0.001$), suggesting that the time of treatment is important for the effectiveness. In *CCA1-ox*, the mesotrione treatment at dawn had the greatest effect on Fv/Fm (Fig. 3.4.9b) reducing it by 0.21. Treatments at other times of the day reduced Fv/Fm by approximately 0.1. The treatment with the smallest effect was 8 hours after dawn, similar to in Col-0 however a two-way ANOVA did not determine a significant interaction between treatment and time, suggesting that time does not affect the extent of the treatment.

Treatments at all times of day had a great impact on Y(II) in both Col-0 and *CCA1-ox* (Figures 3.4.9c to 3.4.9d). The only treatment time that did not completely inhibit Y(II) in Col-0 was dawn, therefore this was slightly less effective than the other treatment times, however there was no significant interaction between treatment and time (two-way ANOVA). In *CCA1-ox*, the opposite time of day response was observed. The greatest effect on Y(II) occurred in dawn treatments, with decreased efficacy of treatments later in the day, and the least effective treatment at dusk, but there was

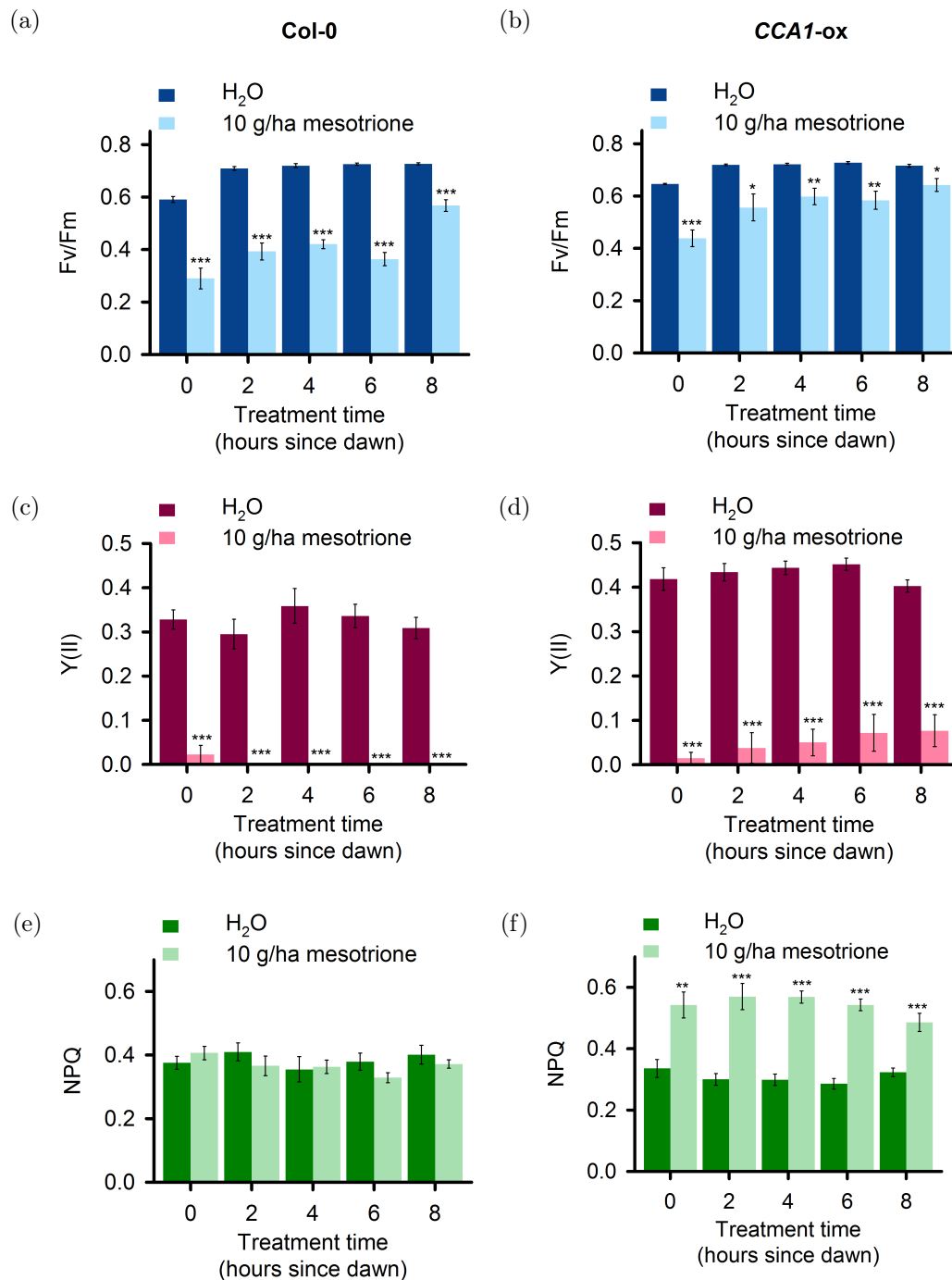


Figure 3.4.9: Applications of mesotrione at different times of day cause differing responses of chlorophyll fluorescence. 10 g/ha mesotrione was applied to 11 day old plants at five time points throughout the day and chlorophyll fluorescence was measured 2 hours later in both Col-0 and *CCA1-ox*. 10 g/ha mesotrione significantly reduced Fv/Fm at all time points for both Col-0 (a) and *CCA1-ox* (b). Y(II) was abolished by 10 g/ha mesotrione at time points except dawn in Col-0 (c), whereas dawn had the lowest Y(II) in *CCA1-ox* (d). NPQ was not affected by 10 g/ha mesotrione in Col-0 (e) but was significantly increased at all time points in *CCA1-ox* (f). Values shown are the mean of six rings of 12 plants \pm SEM. Asterisks indicate statistically significant difference between control and treated plants determined by *t*-test at each time point where: * = $P \leq 0.05$, ** = $P \leq 0.01$, *** = $P \leq 0.001$. No asterisk indicates a non-significant difference.

not a significant interaction between treatment and time (two-way ANOVA). In Col-0, mesotrione treatments at different times of day had no effect on NPQ (Fig. 3.4.9e). In *CCA1-ox*, mesotrione treatments increased NPQ (Fig. 3.4.9f). The responses were similar, irrespective of the treatment time, and there was no significant interaction between treatment and time (two-way ANOVA). There did not appear to be a distinct time of day response in Col-0 to mesotrione, and there were some inconsistencies between the parameters measured. For example, 8 h after dawn was the least effective treatment time when measuring Fv/Fm, whereas for Y(II), treatments 8 h after dawn was one of the more effective treatment times.

Terbutylazine

TBA treatments at all times of day significantly altered Fv/Fm in Col-0 (Fig. 3.4.10a). Treatments at all times of day except from 2 h after dawn gave a mean reduction of 0.16 in Fv/Fm, whereas treatment 2 h after dawn reduced Fv/Fm by 0.06, suggesting this treatment time was less effective. There was a significant interaction between treatment and time (two-way ANOVA, $F(4, 50) = 6.05$, $P < 0.001$), suggesting that the effect of the treatment is determined by the time of the application. In *CCA1-ox*, all treatment times had a significant effect on Fv/Fm with similar magnitudes of reduction and no significant interaction between treatment and time (two-way ANOVA; Fig. 3.4.10b).

TBA treatments in Col-0 at different times of day all reduced Y(II) (Fig. 3.4.10c). The treatment at 2 h after dawn was the least effective, and there was a significant interaction between treatment and time ($F(4, 50) = 4.06$, $P = 0.006$). In *CCA1-ox*, treatment time had little effect on TBA efficacy (Fig. 3.4.10d); treatment time caused a similar level of reduction in Y(II) regardless of treatment time (no significant interaction between treatment and time, two-way ANOVA). The treatment at dawn was perhaps less effective, but the control value was lower for this time point. TBA reduced NPQ in Col-0 at all time points (Fig. 3.4.10e). The control values varied somewhat between time points. However, the least effective time point was 4 h after

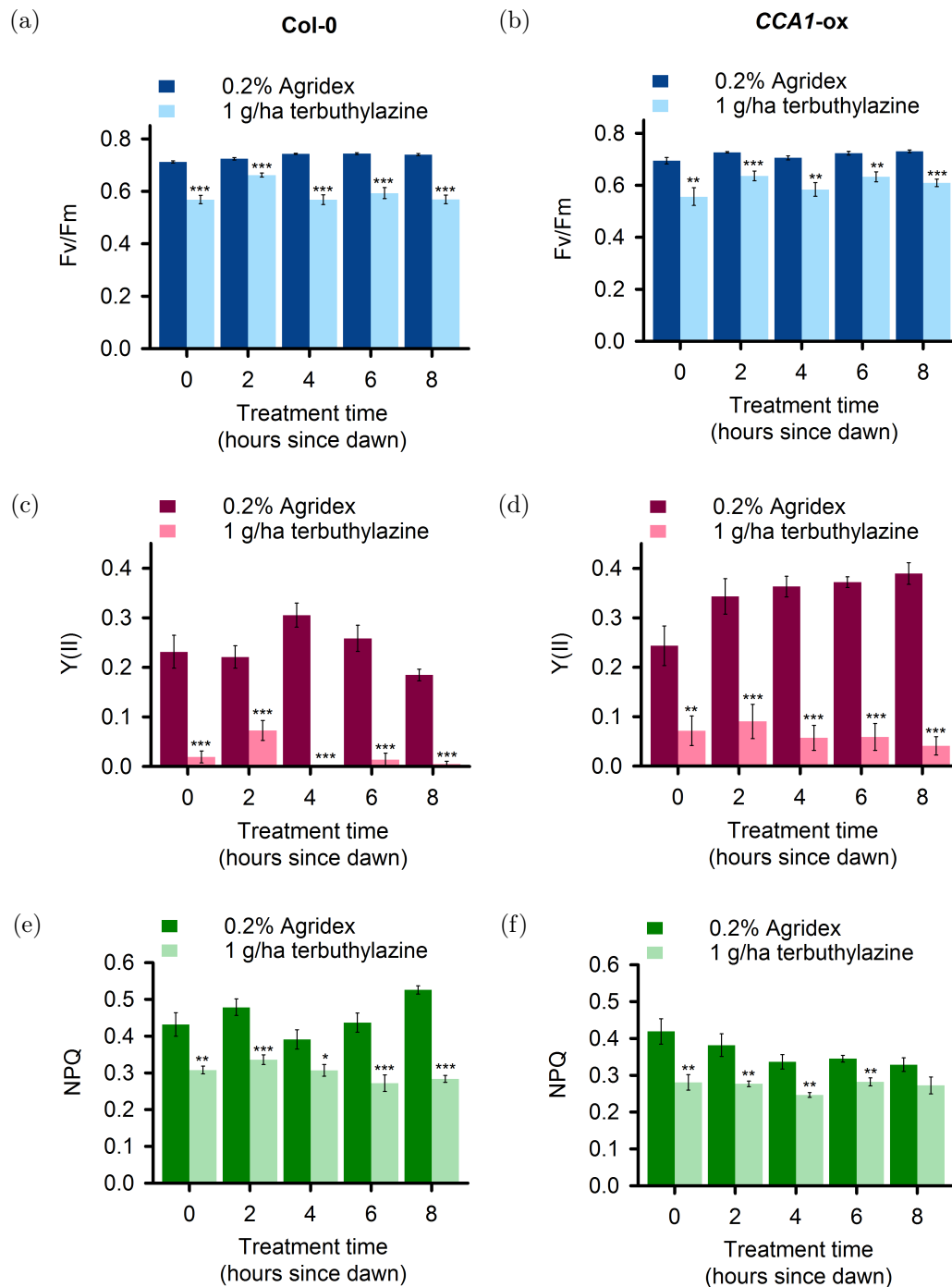


Figure 3.4.10: Applications of terbuthylazine at different times of day cause differing responses of chlorophyll fluorescence. 1 g/ha TBA or 0.2% Agridex control were applied to 11 day old plants at five time points throughout the day and chlorophyll fluorescence was measured immediately in both Col-0 and *CCA1-ox*. 1 g/ha TBA significantly reduced Fv/Fm at all time points in both Col-0 (a) and *CCA1-ox* (b). 1 g/ha TBA abolished Y(II) at some time points in Col-0 (c) but this did not occur in *CCA1-ox* (d). 1 g/ha TBA reduced NPQ the most at treatment times later in the day in Col-0 (e) but these times were least effective in *CCA1-ox* (f). Values shown are the mean of six rings of 12 plants \pm SEM. Asterisks indicate statistically significant difference between control and treated plants determined by *t*-test at each time point where: * = $P \leq 0.05$, ** = $P \leq 0.01$, *** = $P \leq 0.001$. No asterisk indicates a non-significant difference.

dawn (0.08), and the most effective was 8 h after dawn (0.24). A significant interaction between treatment and time was seen for Col-0 (two-way ANOVA $F(4, 50) = 3.47$, $P = 0.014$). TBA treatments to *CCA1-ox* reduced NPQ (Fig. 3.4.10f). The greatest reduction occurred in response to a dawn treatment (0.14), and the smallest reduction followed a dusk treatment (0.06); however, there was no statistically significant interaction between treatment and time (two-way ANOVA). In Col-0, similarities between the treatment being less effective 2 h after dawn for both Fv/Fm and Y(II) suggest there could be a time of day response to TBA and two-way ANOVAs determined there were significant interactions between treatment and time for all fluorescence parameters in Col-0. In contrast, in *CCA1-ox* there were reduced time of day differences in response to TBA treatment and no significant interactions between treatment and time were determined.

3.5 Identification of glyphosate marker genes

We reasoned that one method to measure the rapid effects that herbicides have on a plant is to quantify the changes in the transcript abundance of certain genes. Some transcripts, not necessarily in the pathway directly affected by the herbicide, are up- or down-regulated in response to herbicide treatment (Faus et al., 2015; Das et al., 2010). Measuring such alterations in the transcriptome could be a useful reporter to determine whether there is a certain time of day when a herbicide is more effective.

The Gene Expression Omnibus (<https://www.ncbi.nlm.nih.gov/geo/>) was searched to identify deposited microarray datasets for experiments where *Arabidopsis* was treated with the herbicides of interest: glyphosate, mesotrione and TBA. Two studies had data available for glyphosate (Faus et al., 2015; Das et al., 2010), but no datasets were available for the two other herbicides. The two glyphosate experiments differed slightly in the methods used to collect the data: Faus et al. (2015) exposed 16-day-old Landsberg *erecta* plants to 200 μM glyphosate (approximately 6 g/ha) for

1 min and analysed gene expression 6 h after treatment and Das et al. (2010) applied 10 g/ha glyphosate and sampled 14-day-old Columbia-0 plants 24 h after treatment for microarray analysis.

The two datasets containing genes with significant changes in expression after glyphosate treatment (Faus et al., 2015; Das et al., 2010) were compared using an online tool (nemates.org/MA/progs/Compare.html). 27 common genes were identified. Five genes were excluded due to a disagreement in whether the transcript level increased or decreased in each dataset. The remaining 22 genes were examined for the magnitude in change of gene expression and lack of circadian regulation. The \log_2 values from the two microarray datasets were compared for each transcript to assess the change in gene expression. To ensure that in the control plants transcripts would have the same level of expression at all time points, genes that did not have rhythmic expression were identified by searching DIURNAL (Mockler et al., 2007) and eFP browser (Winter et al., 2007). Five genes were chosen as potential glyphosate marker genes in Arabidopsis: *OUTER MITOCHONDRIAL MEMBRANE PROTEIN OF 66 KDA* (*OM66*; AT3G50930), *PECTIN METHYLESTERASE 5* (*PME5*; AT5G47500), *URIDINE DIPHOSPHATE GLYCOSYLTRANSFERASE 74E2* (*UGT74E2*; AT1G05680), *PLEIOTROPIC DRUG RESISTANCE 12* (*PDR12*; AT1G15520), and *DETOXIFICATION1* (*DTX1*; AT2G04040). The expression of *PME5* was repressed after glyphosate treatment, the other marker genes were induced following glyphosate treatment. *ACTIN2* (*ACT2*; AT3G18780) expression was stable in both the glyphosate microarray datasets with and without treatment, suggesting this is an acceptable reference gene for qPCR analysis.

3.5.1 Glyphosate takes 6 hours to alter transcript abundance

An initial experiment was conducted to determine how long glyphosate took to affect the marker gene transcripts, and to validate the results from published arrays under our experimental conditions. 11 day old seedlings (Col-0) were treated (100 μ L

100 g/ha glyphosate or water control) at dawn and sampled at set time points after treatment (0 h, 1 h, 2 h, 4 h, 6 h, 9 h, 12 h and 24 h).

All transcripts responded to glyphosate treatment, suggesting that they were suitable marker genes (Fig. 3.5.1). There were varying magnitudes of responses but generally a similar trend was observed for the marker genes. *OM66* transcripts had a very strong response to glyphosate treatment (Fig. 3.5.1a). There was a significant increase in *OM66* transcript abundance 2 h after application (Fig. 3.5.1a). There was no difference between control and glyphosate-treated samples 4 h after treatment, but at all time points sampled after this glyphosate treatment caused a significant increase in transcript abundance. The effect of glyphosate on *PME5* transcript abundance was significant after 24 h only (Fig. 3.5.1b). *PME5* transcripts were down-regulated in response to glyphosate treatment, and the magnitude of the response was quite small. *UGT74E2* transcripts responded strongly to glyphosate application (Fig. 3.5.1c). Glyphosate treatment caused a significant increase in *UGT74E2* transcript abundance 4 h, 6 h, 12 h and 24 h after application but not 9 h after application. Transcript abundance of *PDR12* (Fig. 3.5.1d) and *DTX1* (Fig. 3.5.1e) was significantly increased 6 h after glyphosate treatment and at each time point after.

The transcript abundance was significantly altered for most of these genes 6 h after glyphosate application suggesting that this represents suitable treatment length for subsequent experiments.

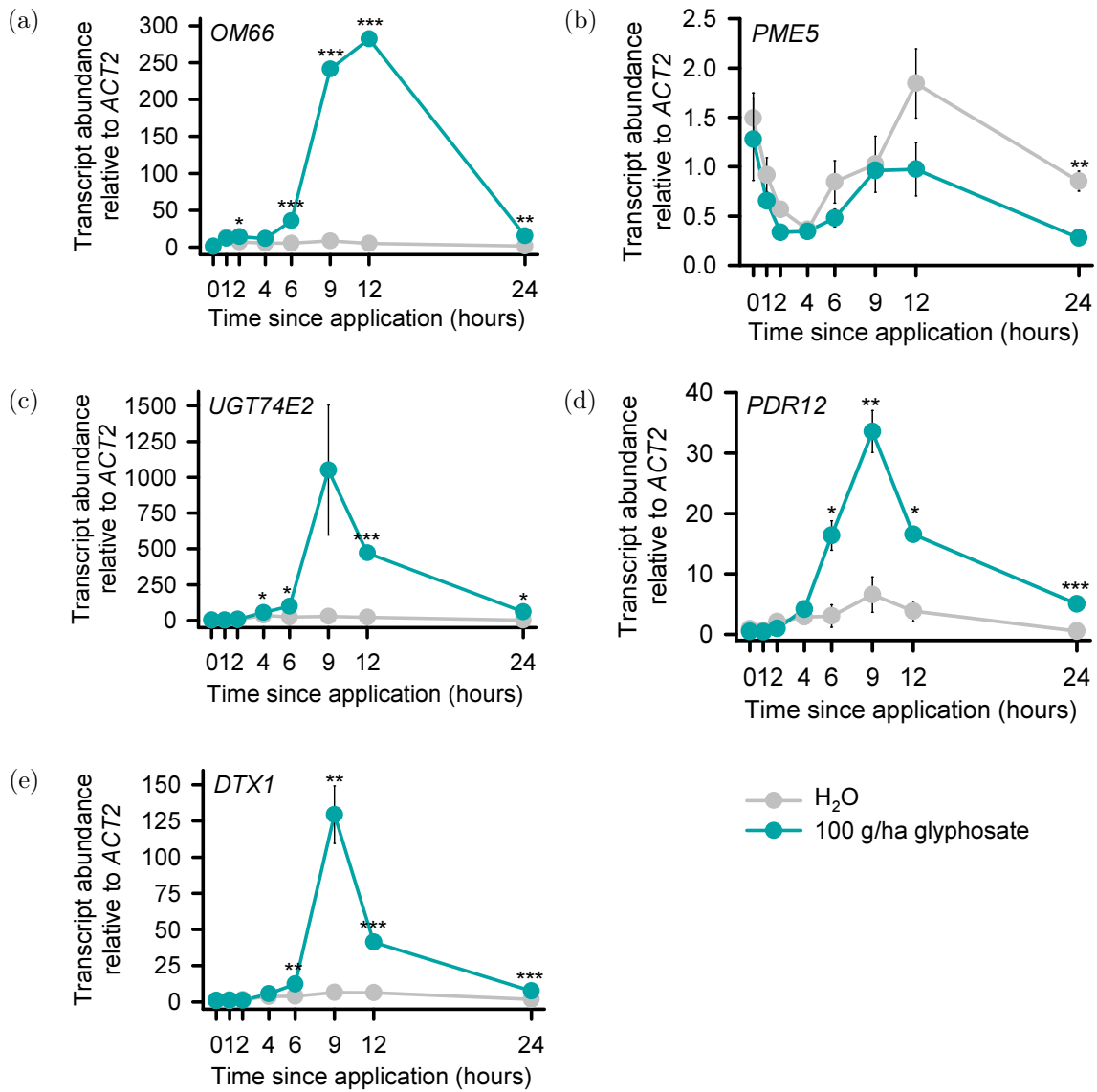


Figure 3.5.1: Glyphosate treatment significantly altered the abundance of selected marker genes within 24 hours. 100 g/ha glyphosate increased the expression of (a) *OM66* after 2 hours, (b) *PME5* after 24 hours, (c) *UGT74E2* after 4 hours, (d) *PDR12* after 6 hours and (e) *DTX1* after 6 hours. *ACT2* was used as a reference transcript. Data are the mean of 2-3 biological replicates per time point \pm SEM. Asterisks indicate statistically significant difference between control and treated samples determined by *t*-test at each time point where: * = $P \leq 0.05$, ** = $P \leq 0.01$, *** = $P \leq 0.001$. No asterisk indicates a non-significant difference.

3.5.2 Glyphosate alters marker gene transcript abundance in a time-of-day-dependent manner under light-dark cycles

To determine the effect of glyphosate treatment time on the transcript abundance of marker genes, 11 day old plants (Col-0 and *CCA1-ox*) were treated at one of five time points throughout the 8-hour light period and samples were obtained 6 h later.

The marker genes in Col-0 plants responded to glyphosate with time of day sensitivity (Fig. 3.5.2). There was no effect of glyphosate on *OM66* transcript abundance when treatment occurred at dawn, but glyphosate treatments at all other times of day caused a significant increase in transcript abundance (Fig. 3.5.2a). The increase in *OM66* transcript abundance was greater with treatments later in the day (Fig. 3.5.2a, bottom). There was a significant interaction between glyphosate treatment and treatment time (two-way ANOVA; $F(4, 17) = 37.61$, $P < 0.001$). This suggests that treatments later in the day were more effective at increasing *OM66* transcript abundance.

Glyphosate applied 6 h after dawn was the least effective time point in reducing *PME5* transcript abundance as there was no significant difference between control and treated samples (Fig. 3.5.2b). Treatments of glyphosate at all other time points caused a significant decrease of *PME5* transcript relative to the control (Fig. 3.5.2b). Glyphosate applied at dawn and 2 h after dawn had a small effect, whereas treatment at dusk was the most effective time point where *PME5* transcript abundance was reduced the most. There was a significant interaction between glyphosate treatment and the time of treatment ($F(4, 20) = 8.71$, $P < 0.001$), suggesting that the time of glyphosate treatment is important for its efficacy.

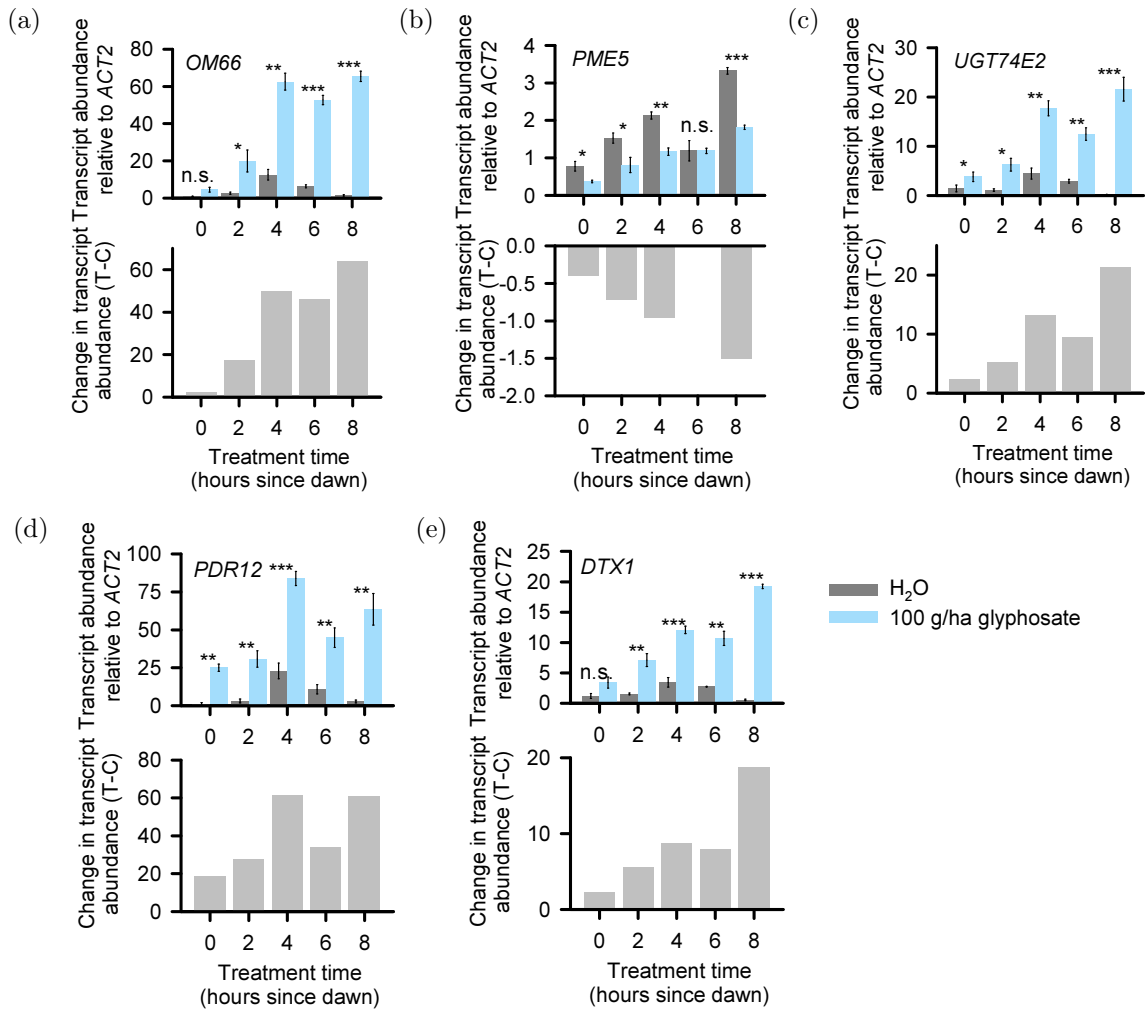


Figure 3.5.2: Glyphosate affects the abundance of marker gene transcripts in a time of day dependent manner under light-dark cycles for Col-0 plants. Graphs show mean relative transcript abundance (top) and change in mean transcript abundance between control and treated samples (bottom) for *OM66* (a), *PME5* (b), *UGT74E2* (c), *PDR12* (d) and *DTX1* (e). *ACT2* was used as a reference transcript. Data are the mean of 2-3 biological replicates per time point \pm SEM. Asterisks indicate statistically significant difference between control and treated samples determined by *t*-test at each time point where: * = $P \leq 0.05$, ** = $P \leq 0.01$, *** = $P \leq 0.001$. n.s. indicates a non-significant difference. C = water control, T = glyphosate treatment.

The effect of glyphosate on *UGT74E2* and *PDR12* transcripts had similar responses where application at all time points gave a significant increase in transcript abundance (Figs. 3.5.2c and 3.5.2d). The smallest increase in the transcript abundance was seen at dawn and generally increased throughout the day with the greatest change seen at the dusk application (Figs. 3.5.2c and 3.5.2d). The response of *DTX1* transcripts was similar to *UGT74E2* and *PDR12*, however there was no significant effect of glyphosate application at dawn (Fig. 3.5.2e). There was a significant interaction between glyphosate treatment and treatment time for *UGT74E2* ($F(4, 20) = 19.52$, $P < 0.001$), *PDR12* ($F(4, 19) = 5.99$, $P = 0.003$) and *DTX1* ($F(4, 20) = 41.38$, $P < 0.001$) measured by two-way ANOVA, suggesting that the timing of glyphosate application is important.

In *CCA1-ox* plants (Fig. 3.5.3) under light-dark cycles, the time of day sensitivity to glyphosate was similar to that of Col-0 (Fig. 3.5.2) whereby the sensitivity increased with treatment time points throughout the day. The response of *OM66* (Fig. 3.5.3a), *UGT74E2* (Fig. 3.5.3c), *PDR12* (Fig. 3.5.3d), and *DTX1* (Fig. 3.5.3e) were similar where the response of the marker gene transcript to glyphosate treatment at dawn was smallest and the greatest response was observed at dusk. Glyphosate had a significant effect on the transcript abundance of *PME5* only when applied at midday (Fig. 3.5.3b). This was a different response to that seen in the wild-type where the greatest effect was seen when glyphosate was applied at dusk.

There was a significant interaction between glyphosate treatment and treatment time for all marker genes: *OM66* ($F(4, 19) = 24.78$, $P < 0.001$), *PME5* ($F(4, 20) = 8.80$, $P < 0.001$), *UGT74E2* ($F(4, 20) = 11.65$, $P < 0.001$), *PDR12* ($F(4, 20) = 11.97$, $P < 0.001$) and *DTX1* ($F(4, 20) = 19.88$, $P < 0.001$), tested by two-way ANOVA. Therefore, the time of glyphosate application had an effect of the efficacy of the treatment.

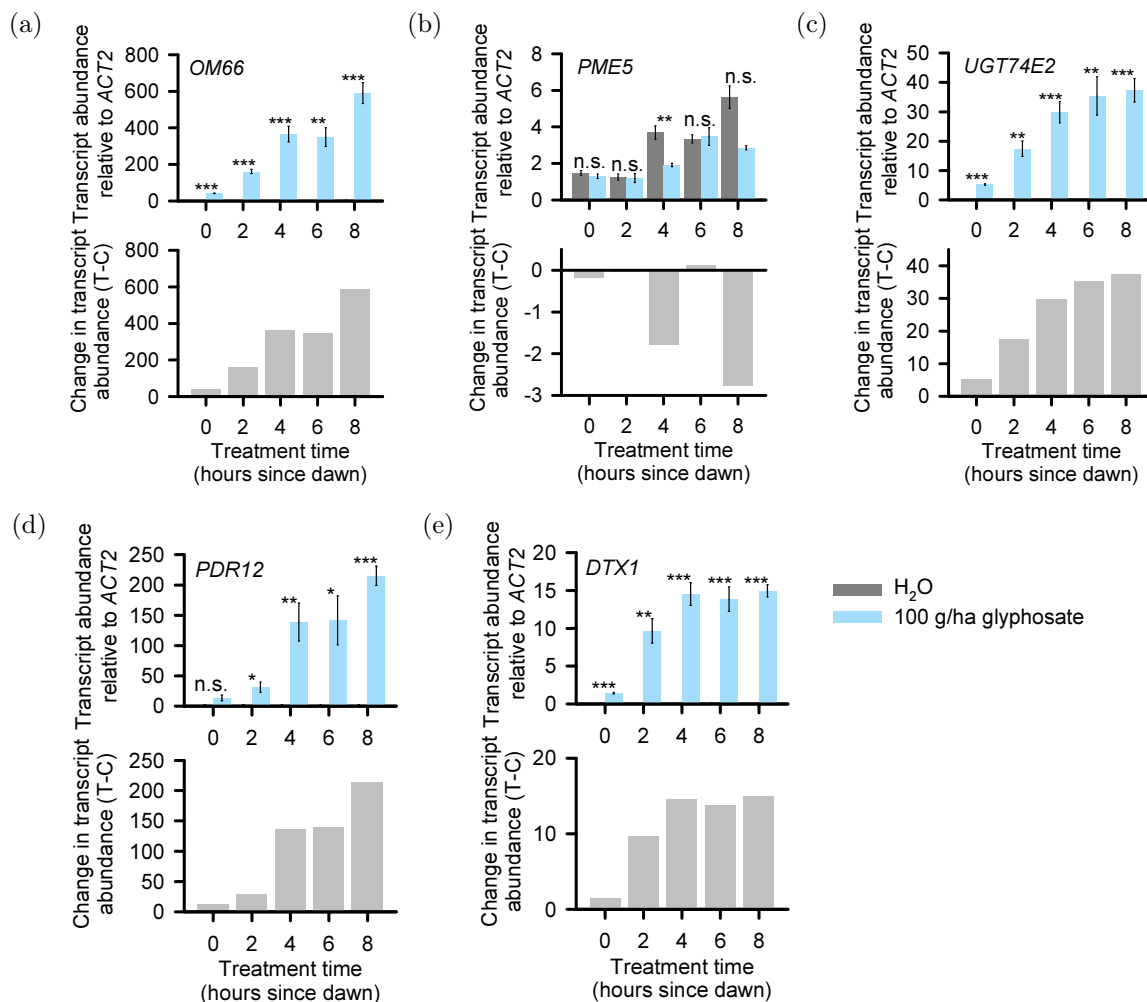


Figure 3.5.3: Glyphosate affects the abundance of marker gene transcripts in a time of day dependent manner under light-dark cycles for *CCA1*-ox plants. Graphs show mean relative transcript abundance (top) and change in mean transcript abundance between control and treated samples (bottom) for *OM66* (a), *PME5* (b), *UGT74E2* (c), *PDR12* (d) and *DTX1* (e). *ACT2* was used as a reference transcript. Data are the mean of 2-3 biological replicates per time point \pm SEM. Asterisks indicate statistically significant difference between control and treated samples determined by *t*-test at each time point where: * = $P \leq 0.05$, ** = $P \leq 0.01$, *** = $P \leq 0.001$. n.s. indicates a non-significant difference. C = water control, T = glyphosate treatment.

Under light-dark cycles the response of the marker gene transcripts to glyphosate was similar for both Col-0 and *CCA1-ox* plants where there was an increased sensitivity to glyphosate later in the day. A similar response in *CCA1-ox* to the wild type could suggest that the circadian oscillator is not involved in the time of day sensitivity of the marker gene transcripts to glyphosate, however, *CCA1-ox* plants can remain rhythmic under light-dark cycles (Green et al., 2002).

3.5.3 The circadian oscillator is involved in the time-of-day sensitivity of glyphosate marker genes

Under free-running conditions (constant light), the circadian oscillator causes rhythmic regulation of processes in the absence of external cues (Greenham and McClung, 2015). To determine the sensitivity of the marker genes to glyphosate under free-running conditions, 10 day old plants (Col-0 and *CCA1-ox*) were transferred from 8 h light /16 h dark cycles into constant light. After 24 h in constant light, plants were treated (100 g/ha glyphosate or water control) at nine time points throughout the subsequent 24 h period (ZT 24, 26, 28, 30, 32, 34, 38, 42 and 46). Tissue was sampled 6 h after each treatment.

In Col-0 wild type plants, the response of the glyphosate marker gene transcripts under constant light was different to the response under light-dark cycles (Fig. 3.5.4). Under light-dark cycles, the effect of glyphosate on the marker transcripts was greatest when applied at the end of the day, but this pattern did not repeat under constant light conditions. Under constant light, subjective dawn was one of the more sensitive time points but glyphosate treatments at subjective midday, and for some transcripts subjective night, also had a strong response (Fig. 3.5.4). Although the patterns of marker gene transcript abundance were different to that under light-dark cycles, some of the transcripts responded in the same way as each other.

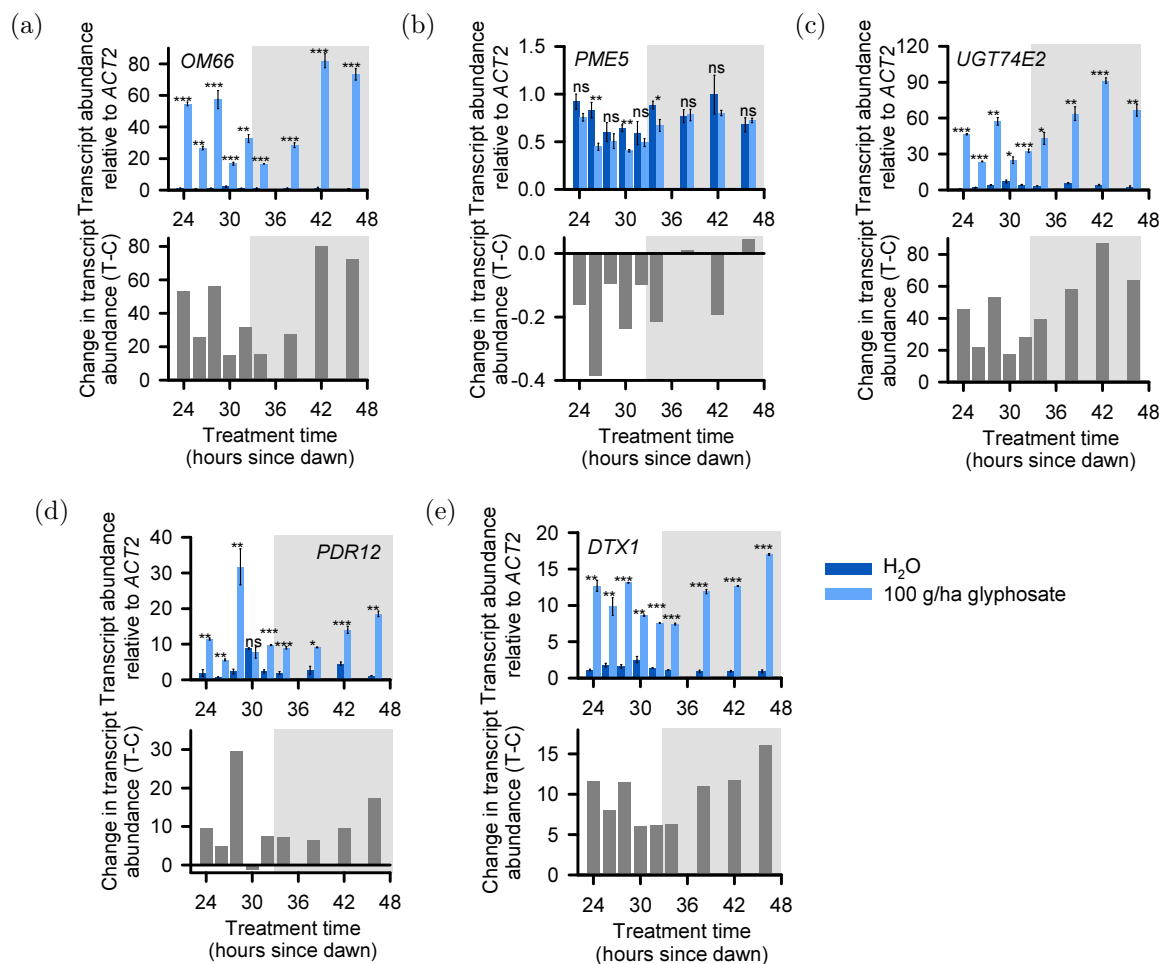


Figure 3.5.4: Glyphosate affects the abundance of marker gene transcripts in a time-of-day-dependent manner under constant light for Col-0 plants. Graphs show mean relative transcript abundance (top) and change in mean transcript abundance between control and treated samples (bottom) for *OM66* (a), *PME5* (b), *UGT74E2* (c), *PDR12* (d) and *DTX1* (e). *ACT2* was used as a reference transcript. Data are the mean of 2-3 biological replicates per time point \pm SEM. Asterisks indicate statistically significant difference between control and treated samples determined by *t*-test at each time point where: * = $P \leq 0.05$, ** = $P \leq 0.01$, *** = $P \leq 0.001$. n.s. indicates a non-significant difference. C = water control, T = glyphosate treatment.

The responses of *OM66*, *UGT74E2* and *DTX1* to glyphosate were most sensitive to applications in the subjective night and least sensitive at the end of the subjective day (Figs. 3.5.4a, 3.5.4c and 3.5.4e). *PDR12* transcript abundance was less sensitive to the time of glyphosate application because the response was similar after applications at most time points, aside from 4 h after subjective dawn (Fig. 3.5.4d). This was also the time of greatest sensitivity for *PDR12* under light dark cycles. The effect of glyphosate was dependent on the time of application for *OM66*, *UGT74E2*, *PDR12* and *DTX1* (determined by two-way ANOVA where $F(8, 26) = 70.2$, $P < 0.001$, $F(8, 20) = 49.81$, $P < 0.001$, $F(8, 25) = 28.48$, $P < 0.001$ and $F(8, 26) = 70.2$, $P < 0.001$, respectively).

Glyphosate treatment only had a significant effect on *PME5* transcripts when applied 2 h and 6 h after subjective dawn and 2 h after subjective dusk (Fig. 3.5.4b). Glyphosate treatment 2 h after subjective dawn caused the greatest reduction in *PME5* transcript abundance. Under light-dark cycles, the response of *PME5* to glyphosate was most sensitive at the end of the day, therefore there was a different response under constant light conditions. A two-way ANOVA did not determine there to be a significant interaction between treatment and time for *PME5* ($F(8, 32) = 1.18$, $P = 0.34$) therefore, under constant conditions there does not appear to be circadian regulation in the response of *PME5* to glyphosate treatment.

Under constant light, the response of the marker genes in *CCA1-ox* plants to glyphosate treatments at different times of day was different to the response in Col-0 plants, but it was similar to the response of *CCA1-ox* under light-dark cycles (Fig. 3.5.5).

Generally, the marker gene transcripts were least sensitive to glyphosate applied at subjective dawn, and increased in sensitivity throughout the day with the most sensitive time points in the subjective night (Figs. 3.5.5a, 3.5.5c, 3.5.5d, 3.5.5e). These responses were similar to the results under light-dark cycles where the marker transcripts were most sensitive to glyphosate treatment at dusk. A significant interaction

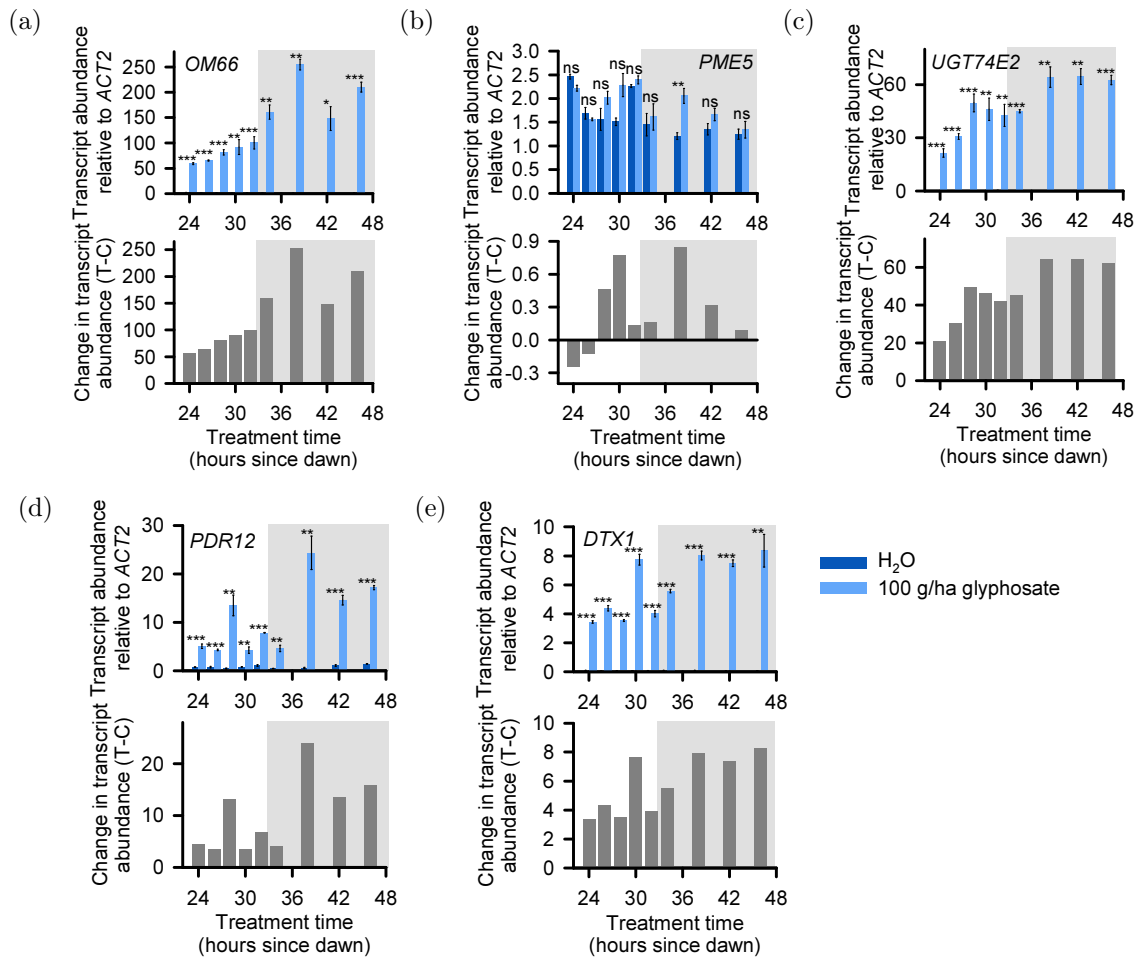


Figure 3.5.5: Glyphosate affects the abundance of marker gene transcripts in a time-of-day-dependent manner under constant light for *CCA1*-ox plants. Graphs show mean relative transcript abundance (top) and change in mean transcript abundance between control and treated samples (bottom) for *OM66* (a), *PME5* (b), *UGT74E2* (c), *PDR12* (d) and *DTX1* (e). *ACT2* was used as a reference transcript. Data are the mean of 2-3 biological replicates per time point \pm SEM. Asterisks indicate statistically significant difference between control and treated samples determined by *t*-test at each time point where: * = $P \leq 0.05$, ** = $P \leq 0.01$, *** = $P \leq 0.001$. n.s. indicates a non-significant difference. C = water control, T = glyphosate treatment.

between the application of glyphosate and the timing of the application was identified for these marker genes (two-way ANOVA; *OM66* $F(8, 25) = 23.24$, $P < 0.001$, *UGT74E2* $F(8, 27) = 8.83$, $P < 0.001$, *PDR12* $F(8, 29) = 41.85$, $P < 0.001$ and *DTX1* $F(8, 29) = 18.51$, $P < 0.001$).

Glyphosate application had little effect on *PME5* transcript abundance in *CCA1*-ox plants under constant light (Fig. 3.5.5b). *PME5* transcript abundance was only significantly altered when glyphosate was applied 6 h after subjective dusk. This caused an increase in *PME5* transcripts, where previously glyphosate reduced the expression of *PME5*. While there was only one time point where glyphosate significantly altered *PME5* transcript abundance, there was an interaction between glyphosate application and the timing of the treatment (two-way ANOVA; $F(8, 30) = 3.0$, $P = 0.014$).

The results from the constant light experiments suggest that there was circadian regulation of the marker genes in the Col-0 wild type in the response to glyphosate applied at different times of day for two reasons: (i) the response is not the same under light-dark cycles as under constant light conditions and (ii) there were differences in the response when glyphosate was applied at different times of day. There appeared to be some involvement of the circadian oscillator because the response of the *CCA1*-ox plants was different to that of the wild type plants under constant light conditions, suggesting that a correctly functioning circadian oscillator was required for the time of day responses in wild type.

3.6 Discussion

3.6.1 Herbicides appear to cause small time-of-day-dependent differences to Arabidopsis physiology

The visual injuries to the rosettes were as expected of the three herbicides: glyphosate caused chlorosis with necrosis in higher concentrations or after a longer period of time

(Lassiter et al., 2007), mesotrione caused bleaching of the meristematic tissue and later necrosis (McCurdy et al., 2009; Abendroth et al., 2006), TBA caused yellowing of lamina tissue followed by necrosis and disintegration (Blancard, 2017) (Fig. 3.2.1). There are few published studies that examine the physiology in response to herbicide treatment in detail, the majority of experiments state the percentage of weed control (e.g. Table 3.2.1) but no measurements aside from this. Therefore the method employed here is more objective, and could be used more widely.

Some small indications were obtained for time of day sensitivity to the herbicides used here. Several field studies have identified dawn and dusk as being the least effective times for glyphosate weed control, with the middle of the day being the most effective (Norsworthy et al., 1999; Martinson et al., 2002; Stopps et al., 2013; Waltz et al., 2004). In the literature, responses are variable with differences between species and concentrations. This follows a similar trend for the lower concentrations in this work, where the dawn and dusk treatments were less effective, but not for the highest concentration tested (Fig. 3.2.4d). However, these experiments in the literature were not conducted in a controlled environment but in the field, making it difficult to elucidate the underlying mechanisms. Many factors could be responsible for time of day responses in the field including temperature (Martinson et al., 2002), humidity, and leaf angle (Waltz et al., 2004). In the field Waltz et al. (2004) found that velvetleaf (*Abutilon theophrasti*) control by glyphosate was maximal around midday. However, in controlled environment conditions, the time of day sensitivity changed. Velvetleaf biomass and height were more susceptible to glyphosate after applications after dusk compared to applications pre-dawn. These experiments were conducted in constant temperature and humidity, and leaf angle was kept constant, also; therefore, the light cycle has a role in the effectiveness of glyphosate. It is suggested that because photosynthetic photon flux density (PPFD) increases throughout the day in the field, photosynthesis would increase, and this results in more translocation of glyphosate through the plant (Waltz et al., 2004). Again, this was not specifically measuring the same parameters as those measured in this work.

There is only one published study that has used *Arabidopsis* physiology to test the response to treatment time of day (Sharkhuu et al., 2014). The authors found that glyphosate applications earlier in the day were most effective, and later in the day were less effective. However this was measuring inflorescence extension, rather than damage to the rosette. No records could be found that compare mesotrione or terbuthylazine application times for physiological parameters, therefore the results here are novel and insightful.

The results presented here were at times inconsistent and variable. One reason for this variation was due to difficulty to quantify the rosette area in some images as it was the same colour as the background (seen in Fig. 3.2.1). This was particularly problematic for plants where the tissue had become necrotic and was disintegrating. One of the major issues with these experiments was the variation in the control plants within an experiment at different time points, and also across experiments. For example, the control plants in TBA and glyphosate experiments only reached around 450 mm² in area, whereas in the mesotrione experiment they reached around 700 mm². This could be due to growth conditions changing slightly, such as inconsistent watering. This variation is likely to also be due to low replicate number, particularly for the mesotrione and TBA experiments. Furthermore, a major consideration is that the treatment application was not an entirely consistent or appropriate mechanism for applying herbicides to mature plants. This spraying method could have led to some of the variation observed between replicates within one treatment group, particularly for the control plants that were saturated with water.

All herbicide concentrations applied had a clear visual effect on the *Arabidopsis* rosettes, and these effects could be quantified through image analysis. Some small differences were evident in the damage caused by treatments at different times of day. Therefore, this method and the use of *Arabidopsis* are suitable models for testing these time of day responses.

3.6.2 Herbicides affect photosynthetic measurements with time-of-day-dependent efficacy

The initial experiments using chlorophyll fluorescence determined effective concentrations of each herbicide, and the length of time the herbicides took to become effective. Preliminary experiments were conducted to determine any indications as to time of day effects of the herbicides on chlorophyll fluorescence. These experiments found that: glyphosate appeared to be most effective when applied at dawn, mesotrione did not have one distinct treatment time point that was most or least effective, and TBA appeared to be possibly most effective when applied later in the day and least effective 2 h after dawn.

The modes of action of mesotrione and TBA involve the inhibition of photosynthesis (Mitchell et al., 2001; LeBaron et al., 2008), so it is logical that effects on chlorophyll fluorescence would occur. Glyphosate does not have a direct effect on the photosynthetic apparatus in *Arabidopsis*, therefore it is interesting that alterations in photosynthesis occurred in these experiments (Figs. 3.4.2, 3.4.5, 3.4.8).

The effects of glyphosate on photosynthesis appear to be threefold: firstly, when glyphosate binds to EPSPS, erythrose-4-phosphate (E4P) is diverted into the shikimate pathway, inhibiting the reduction of ribulose 1,5-bisphosphate (RuBP). Carbon (in the form of E4P) is diverted away from the Calvin cycle lowering the level of RuBP thus leading to over-reduction of the photosynthetic electron chain and ultimately photoinhibition of PSII (Christensen et al., 2003). Secondly, the inhibition of EPSPS also leads to the inhibition of homogentisic acid production, a metabolite required for reduction of plastoquinone (PQ). PQ is required for both the electron transfer chain plus the activation of photo-protective carotenoids (Christensen et al., 2003; Olesen and Cedergreen, 2010). Therefore glyphosate causes over-reduction and photo-inhibition of PSII, while simultaneously inhibiting the photo-protection via carotenoids.

The response of chlorophyll fluorescence to glyphosate in *Arabidopsis* has been re-

ported previously (Barbagallo et al., 2003), however experimental differences, such as different concentrations of glyphosate, make the experiments difficult to compare. The majority of other research concerning glyphosate and chlorophyll fluorescence was conducted in species other than *Arabidopsis* e.g. soyabean (*Glycine max*) (Silva et al., 2015), wheat (*Triticum aestivum* L.) (Ireland et al., 1986), ryegrass (*Lolium perenne*) (Yannicari et al., 2012), and barley (*Hordeum vulgare* L.) (Olesen and Cedergreen, 2010).

At the highest concentration tested, glyphosate did not completely inhibit PSII (Fv/Fm and Y(II), Fig. 3.4.2), unlike mesotrione and TBA (Figures 3.4.3 to 3.4.4). Photosynthesis still occurred, and thermal dissipation increased, suggesting that glyphosate might have caused a stress response. This is in accordance with a study on white mustard and sugar beet, where glyphosate did not completely inhibit photosynthesis (Christensen et al., 2003). Although not entirely inhibitory, glyphosate did have a measurable effect on chlorophyll fluorescence and time-of-day effects were identified in this study. While the mechanism behind how glyphosate can have an effect on photosynthesis is understood, there have been no reports of how time of day applications of glyphosate could differ or be regulated.

At the highest two concentrations tested, mesotrione inhibited the ability of the plant to use any light energy to drive photosynthesis (Fig. 3.4.3). NPQ was also greatly reduced or inhibited, suggesting that the plant was unable to diffuse excess light energy and to prevent formation of ROS. Mesotrione inhibits carotenoid biosynthesis indirectly through the inhibition of the HPPD enzyme. HPPD converts hydroxyphenylpyruvate to homogentisate, which synthesize α -tocopherols and plastoquinone. Plastoquinone is required as a cofactor for phytoene desaturase, which is a component of the carotenoid biosynthesis pathway (Mitchell et al., 2001; Hall et al., 2001b; Abendroth et al., 2006). Carotenoids, in particular zeaxanthin, are involved in the quenching of excess light energy by inducing changes in PSII structure (Demmig-Adams et al., 1989; Murchie and Lawson, 2013). Therefore, a decrease in carotenoids resulting from mesotrione treatment may explain the reduction in NPQ

where F_v/F_m is also reduced. Where NPQ usually increases following a decrease in F_v/F_m , this may not be possible due to the inability to produce carotenoids needed to make conformational changes in PSII. Therefore, this may be the cause of reduced NPQ.

Effects of mesotrione upon photosynthesis have been reported in a variety of species including Palmer amaranth (*Amaranthus palmeri*) (Godar et al., 2015), ryegrass (*Lolium perenne*) (McCurdy et al., 2008) large crabgrass (*Digitaria sanguinalis*) (McCurdy et al., 2009) and sweet corn (*Zea mays* var. *rugosa*) (Kopsell et al., 2011). However there are no previous reports in Arabidopsis.

Temperature can affect the response of photosynthesis to certain concentrations of mesotrione such that at higher temperatures, mesotrione has less effect on F_v/F_m (Godar et al., 2015). However, other studies using different species found that temperature had no effect on mesotrione efficacy (McCurdy et al., 2008, 2009). Additionally, while mesotrione had a significant effect on F_v/F_m in some grass species, the plants were able to recover after a longer period of time, suggesting the possibility of transient effects of mesotrione on chlorophyll fluorescence (McCurdy et al., 2008, 2009). It is evident that multiple factors may affect the response of chlorophyll fluorescence to mesotrione including species, temperature and length of time between treatment and measurement. Therefore, these factors could affect the impact of mesotrione on photosynthesis.

Terbutylazine had the greatest effect of the three herbicides on $Y(II)$, meaning that it had the greatest inhibitory effect on the ability of the plant to use light energy for PSII photochemistry, and by proxy photosynthesis. TBA, as a triazine herbicide, inhibits plastoquinone binding in PSII, so electrons cannot be accepted or passed on to the reaction centre (Fuerst and Norman, 1991). This explains why TBA had such a significant, and fast, impact on chlorophyll fluorescence, particularly when used at high concentrations and for long periods of time. When excited chlorophyll molecules cannot lose their electrons, they form triplet chlorophylls, which consequently form

reactive oxygen species (ROS) (Fuerst and Norman, 1991). Increased ROS has been reported to decrease NPQ in other species (Hideg et al., 2008; del Hoyo et al., 2011), therefore this could be the explanation for reduced NPQ in TBA treated plants.

While TBA is a direct PSII inhibitor, there is little published research using chlorophyll fluorescence as a parameter to measure the effects of TBA, especially in *Arabidopsis* and in response to applications at different times of day. Existing evidence is somewhat conflicting. In young olive (*Olea europaea*) plants 3 kg/ha TBA significantly decreased photosynthetic parameters, but it took 60 days to see a quantifiable difference (Cañero et al., 2011). In contrast, Abbaspoor et al. (2006) found that in sugar beet (*Beta vulgaris*) there was an initial decrease for the first 7 days following 28 g/ha TBA treatment, subsequently Fv/Fm increased to the original value. It is likely these different results are in part due to different concentrations of TBA used, application methods, and ages of plants.

In the field, multiple factors affect the rate of photosynthesis throughout the day, such as light intensity, humidity, stress and temperature (Iio et al., 2004; Koyama and Takemoto, 2014). Therefore, changes in efficacy of herbicides that affect photosynthesis at different times of day may be unsurprising. However, under controlled environmental conditions such as those used here, there must be an underlying mechanism that accounts for the changes in time of day. Due to differences between the wild type and a line with an arrhythmic circadian oscillator (*CCA1-ox*), it is likely that there is at least some circadian regulation involved which could explain this.

Chlorophyll fluorescence is a suitable assay for measuring the effects of the three herbicides of interest. Optimal concentrations and treatment durations have been identified for each herbicide for experimental work, with potential treatment time of day effects. Therefore, further experiments could be conducted using chlorophyll fluorescence as a measure. Differences were also observed between wild-type and circadian arrhythmic plants. This indicates that there may be some involvement of the circadian oscillator in these time of day responses to the herbicides. Future experiments are required to un-

derstand the cellular mechanisms behind the time of day effects which were observed for the herbicides.

3.6.3 Circadian gating may lead to time-of-day sensitivity of glyphosate marker genes

The results from the glyphosate marker gene experiments found that when measured an appropriate time after application, the selected marker gene transcripts have different magnitudes of response depending on the time of the treatment. Generally, the marker gene transcripts increased in sensitivity to glyphosate throughout the day under light-dark cycles for both Col-0 and *CCA1-ox*. This was a different time of day response to that observed for the chlorophyll fluorescence data, where plants were most sensitive to glyphosate treatment at dawn (Fig. 3.4.8). Under constant light conditions, the sensitivity of the marker genes in the subjective day was different for Col-0 (Fig. 3.5.4) compared to that observed under light-dark cycles (Fig. 3.5.2), but it remained similar for *CCA1-ox* (Figs. 3.5.3 and 3.5.5). Furthermore, both genotypes had increased sensitivity in the subjective night.

These marker transcripts were shown previously to respond to glyphosate (Faus et al., 2015; Das et al., 2010), and were selected because they had the greatest response to glyphosate. Therefore, it was expected that there should be a significant increase or decrease in transcript abundance in response to glyphosate in these experiments. However, there were differences in the magnitudes of the responses. For example, two of the marker genes (*OM66* and *UGT74E2*) had a very strong response to the glyphosate treatment, whereas *PME5* had a weak response to glyphosate. There are various explanations for this; for example, the level of transcript abundance is relative to the control value and the expression of the transcript in the control could already be quite high, therefore it may not increase much more. Additionally, the magnitude of the increase in transcript abundance does not necessarily equate to the level of protein

translation and, as such, the variation in transcript abundance between the marker genes does not necessarily correlate to any differences at the protein level.

The marker genes were selected because they are not circadian regulated and there should not be any difference in the expression of the marker genes in the water-treated control samples at different times of day. However, this was not the case as there were small fluctuations in the control sample transcript levels under constant light conditions, particularly around mid-day. These differences were controlled for by accounting for the difference between the control and treated values for each time point.

The greater efficacy of glyphosate at the end of the day and during the subjective night has not been reported previously. Reports of time of day sensitivity to glyphosate generally found that applications in the middle of the day were more effective, however these experiments were conducted in the field in species other than *Arabidopsis* (Norsworthy et al., 1999; Martinson et al., 2002; Stopps et al., 2013; Waltz et al., 2004).

The marker genes that were selected participate in several processes within the plant such as cell death (*OM66*) (Zhang et al., 2014a), auxin homeostasis (*UGT74E2*) (Tognetti et al., 2010), ABA transport (*PDR12*) (Kang et al., 2010), detoxification (*DTX1*) (Li et al., 2002) and cell wall modification (*PME5*) (Bethke et al., 2014). It is interesting that all the marker genes responded with a similar temporal pattern of glyphosate sensitivity when they are involved in such diverse cellular processes. If glyphosate were to have downstream effects on each of these pathways individually, then it may be expected that they would not show the same trend in sensitivity, regardless of light conditions. Therefore, it seems likely that there is another upstream explanation for how glyphosate can cause these genes to alter in expression with the same temporal pattern. One potential explanation is the circadian gating of the marker gene response to glyphosate. Such gated stress responses have been reported previously, for example, a drought stress response was most effective at the end of

the day (Wilkins et al., 2010). This suggests that even though glyphosate did not alter the expression of circadian oscillator transcripts specifically, other transcripts can have a greater sensitivity at certain times of day due to circadian regulation of those transcripts (Hotta et al., 2007). This gives further evidence to suggest that the time of day efficacy of glyphosate is circadian regulated. The circadian experiment conducted here, a time of day response experiment under constant light, showed different responses of the marker genes to glyphosate when treated at different times of day. This suggests that there is circadian gating of the response of Arabidopsis to glyphosate. If there were no gating, the response of the marker genes would be the same regardless of the time of the treatment. Furthermore, the result seen in the *CCA1-ox* line is different to the response of wild-type plants. Therefore, when the plant does not have a properly functioning circadian oscillator, the response was altered.

Overall, these data suggest that there is time of day sensitivity to glyphosate, which is likely due to circadian gating of the response. These experiments confirmed that using marker genes was a useful method of detecting the time of day response to a herbicide. This method could be used for other herbicides and also in other species, depending on the genetic resources available. Finally, that it is important to investigate why and how this differential time of day sensitivity occurs in order to potentially exploit this and utilise it in the field.

3.7 Conclusions

In summary, preliminary experiments were conducted to test different methods of identifying and quantifying time of day variation in the effects of herbicides. The experiments identified suitable concentrations of herbicides to use and length of herbicide treatments, with some initial time of day effectiveness indicators. Furthermore, this work identified that Arabidopsis is a suitable experimental model for investigating these questions. A new piece of equipment was developed for future experiments in-

investigating the application of herbicides at different times of day to plants at a variety of developmental stages.

Chapter 4

Photoperiodic and circadian regulation of responses to glyphosate

4.1 Introduction

The plant circadian oscillator is responsible for coordinating the timing of many physiological processes in plants including stomatal opening (Kreps and Kay, 1997; Somers et al., 1998b), hypocotyl elongation (Dowson-Day and Millar, 1999), leaf movement (Kim et al., 1993), and photoperiodic flowering (Hamner and Takimoto, 1964; Somers et al., 1998b; Samach and Coupland, 2000). The circadian oscillator regulates these processes largely through transcriptional regulation. While the number of genes that comprise the circadian oscillator itself is quite small, the oscillator is responsible for causing a significant proportion of the transcriptome to have rhythmic regulation (Salomé et al., 2008). Studies have reported 6%-15% of the Arabidopsis transcriptome is regulated by the circadian oscillator (Harmer et al., 2000; Edwards et al., 2006). Another, much higher, estimate from 11 different experimental conditions (thermocycles, photocycles and circadian conditions) found that 89% of the Arabidopsis transcrip-

tome can have rhythmic expression under at least one of these conditions (Michael et al., 2008). These rhythmically expressed genes are involved in diverse plant processes including the response to light and photosynthesis, and numerous metabolic pathways in addition to physiological processes (Harmer et al., 2000; Edwards et al., 2006). By regulating plant processes to occur at particular times of day, the circadian oscillator is optimising plant fitness (Dodd et al., 2005; Michael et al., 2008).

Another aspect of circadian regulation is circadian gating. Circadian gating occurs when the same stimulus applied at different times of day results in responses of different magnitudes (Hotta et al., 2007). It is thought that plants evolved this mechanism in order to respond most appropriately to the changing environment to which they are constantly subjected (Hotta et al., 2007). Circadian gating of a pathway can function through regulating the levels of signalling intermediates, regulating the activity of signalling molecules, or regulating the availability of metabolites (Hotta et al., 2007). Outputs of the oscillator can be directly involved in the signalling pathway that is gated, or, the pathway regulated by the oscillator can be responsible for regulating other pathways resulting in gating of the response (Hotta et al., 2007). Since the oscillator is capable of regulating so many processes in *Arabidopsis*, and because gating of responses can occur, it is reasonable to hypothesise that the circadian oscillator might influence the ability of the plant to respond to a herbicide. Targets of the herbicide could themselves be regulated by the circadian oscillator, or alternatively other pathways that are involved in the response to the herbicide could be regulated by the oscillator. This could mean that the effect of the herbicide could be exacerbated at certain times of day, or alternatively there could be a reduced effect at other times of day.

The magnitude of the effect of glyphosate has previously been reported to vary dependent on the time of the application (Martinson et al., 2002; Miller et al., 2003; Mohr et al., 2007; Sharkhuu et al., 2014) and preliminary results in previous chapters support this (Chapter 3). As such, we hypothesised that the circadian oscillator is responsible for gating the response to glyphosate. To test this, the aim of the re-

search in this chapter was to determine the extent of underlying circadian regulation in the response to glyphosate and to determine whether glyphosate could be used more effectively at certain times of day.

4.2 Glyphosate-regulated transcripts are rhythmic

To identify why the efficacy of glyphosate might depend on the application time, publicly available datasets were analysed. 3243 glyphosate-regulated transcripts (Faus et al., 2015) were compared to circadian- and light-dark-regulated transcriptomes to identify any overlaps in rhythmically-regulated transcripts that could be responsible for time-of-day responses to glyphosate (Fig. 4.2.1).

The glyphosate-regulated transcript list was compared to two different light-dark regulated transcript sets (Bläsing et al., 2005; Smith et al., 2004) (Fig. 4.2.1a). The first light-dark-regulated dataset contained 4576 transcripts (Bläsing et al., 2005), 979 of which overlapped with the glyphosate-regulated transcripts, more than the 660 transcripts that would be expected to occur in a chance overlap ($P = 6.7 \times 10^{-48}$; Fig. 4.2.1a, left). The second light-dark-regulated dataset contained 5538 transcripts (Smith et al., 2004), of which 971 overlapped with the glyphosate-regulated dataset. This overlap contained more transcripts than would be expected by chance (798 transcripts, $P = 1.2 \times 10^{-14}$; Fig. 4.2.1a, right).

Next, the glyphosate-regulated dataset was compared to three circadian regulated datasets (Dodd et al., 2007; Edwards et al., 2006; Covington and Harmer, 2007) (Fig. 4.2.1b). The first dataset contained 2283 circadian-regulated transcripts of which 415 overlapped with the glyphosate-regulated dataset (Dodd et al., 2007). The next contained 3501 circadian-regulated transcripts (Edwards et al., 2006), of which 819 transcripts overlapped with the glyphosate-regulated list. The third transcript list contained 1706 circadian-regulated transcripts (Covington and Harmer, 2007), of which 451 overlapped with the glyphosate-regulated transcript list. These three overlaps were

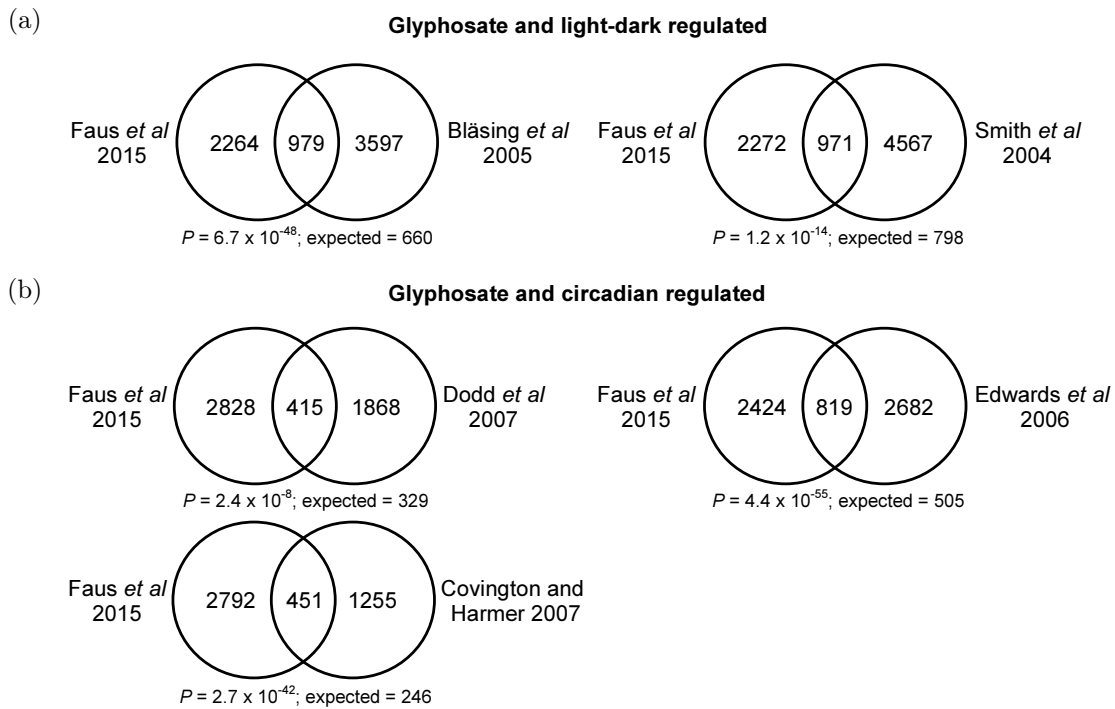


Figure 4.2.1: Identification of glyphosate-regulated rhythmic transcripts. (a) Glyphosate-regulated transcripts (Faus *et al.*, 2015) significantly overlap with transcripts from two light-dark regulated transcriptomes (Bläsing *et al.*, 2005; Smith *et al.*, 2004). (b) Glyphosate-regulated transcripts significantly overlap with those from three circadian-regulated transcriptomes (Dodd *et al.*, 2007; Edwards *et al.*, 2006; Covington and Harmer, 2007). Statistical analysis conducted using hypergeometric analysis, number of transcripts expected to overlap by chance provided below each Venn diagram.

considered statistically significant ($P = 2.4 \times 10^{-8}$, 4.4×10^{-55} , and 2.7×10^{-42} , respectively) and greater than the number of transcripts that would be expected to overlap by chance (329, 505 and 246, respectively), determined by hypergeometric analysis.

The transcripts that were consistently glyphosate- and light-dark-regulated were pooled to form a list of 538 transcripts. The transcripts that were consistently glyphosate- and circadian-regulated were pooled to form a list of 137 transcripts. The lists were sub-divided into whether the glyphosate-regulated transcripts were up- or down-regulated in response to glyphosate treatment and compared across the light conditions (Fig. 4.2.2a). The expression timing of these transcripts was examined because genes involved in common processes are usually expressed with the same phase (Mil-

lar, 2004), suggesting the phase may be important for the function of the process (Fig. 4.2.2b).

The transcripts that were light-dark-regulated and glyphosate-induced were compared to the circadian-regulated and glyphosate-induced transcripts resulting in 18 transcripts ($P = 1.4 \times 10^{-28}$). This number of transcripts was greater than the 0.3 transcripts expected by a chance overlap. These 18 glyphosate-induced, rhythmically-regulated genes are listed in Table 4.2.1, four of these genes have an unknown function. 72% of these genes clustered with peak abundance at dawn (Fig. 4.2.2b, top).

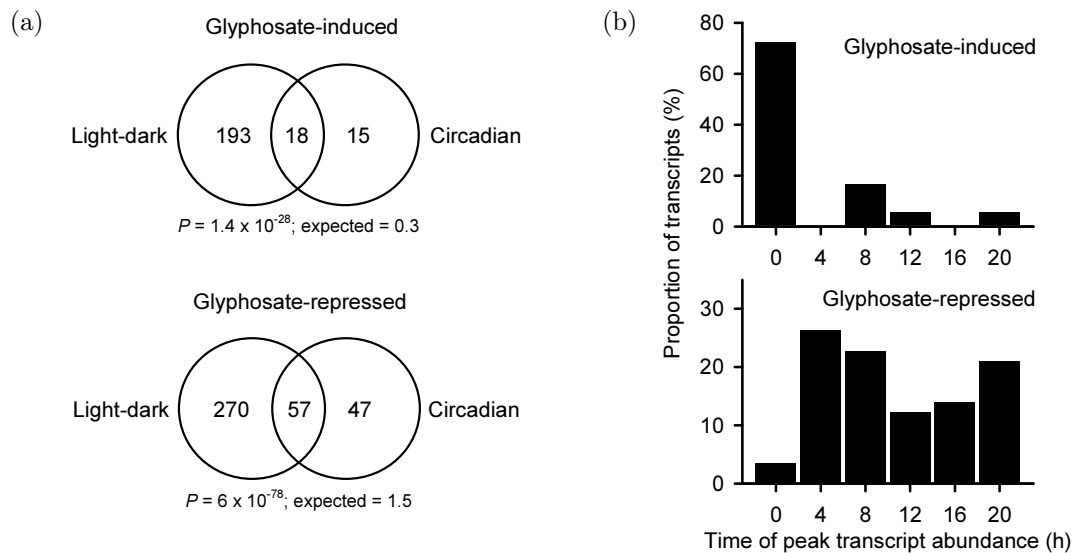


Figure 4.2.2: Regulation and phase analysis of the glyphosate-responsive and rhythmic transcripts. (a) A significant number of rhythmic transcripts are glyphosate-induced (18) and glyphosate-repressed (57). (b) Phase clustering of glyphosate-induced and glyphosate-repressed rhythmic transcripts. Statistical analysis of the overlap was conducted using hypergeometric analysis, number of transcripts expected to overlap by chance provided below each Venn diagram. Phase of transcripts derived from data of Smith et al. (2004).

Table 4.2.1: Summary of the light-dark- and circadian-regulated transcripts induced by glyphosate. Gene information from TAIR.

Locus	Name
AT4G11570	<i>ATPYRP2</i>
AT2G37970	<i>SOUL-1</i>
AT1G07180	<i>ALTERNATIVE NAD(P)H DEHYDROGENASE 1 (NDA1)</i>
AT5G49480	<i>CA2+-BINDING PROTEIN 1 (CP1)</i>
AT5G15850	<i>CONSTANS-LIKE 1 (COL1)</i>
AT1G79270	<i>EVOLUTIONARILY CONSERVED C-TERMINAL REGION 8 (ECT8)</i>
AT3G24170	<i>GLUTATHIONE-DISULFIDE REDUCTASE (GR1)</i>
AT1G78600	<i>LIGHT-REGULATED ZINC FINGER PROTEIN 1 (LZF1)</i>
AT5G11670	<i>NADP-MALIC ENZYME 2 (NADP-ME2)</i>
AT2G23420	<i>NICOTINATE PHOSPHORIBOSYLTRANSFERASE 2 (NAPRT2)</i>
AT1G06570	<i>PHYTOENE DESATURATION 1 (PDS1)</i>
AT1G55920	<i>SERINE ACETYLTRANSFERASE 2;1 (SERAT2;1)</i>
AT2G18700	<i>TREHALOSE PHOSPHATASE/SYNTHASE 11 (TPS11)</i>
AT3G22420	<i>WITH NO LYSINE (K) KINASE 2 (WNK2)</i>
AT5G50100	Unknown
AT4G17840	Unknown
AT5G43440	Unknown
AT2G28200	Unknown

The transcripts that were light-dark-regulated and glyphosate-repressed were compared to the circadian-regulated and glyphosate-repressed transcripts, resulting in 57 transcripts ($P = 6 \times 10^{-78}$). This number was greater than the 1.5 transcripts expected by a chance overlap. These 57 glyphosate-repressed, rhythmically-regulated transcripts are listed in Table 4.2.2, 17 of these genes have an unknown function. The glyphosate-repressed, rhythmic transcripts were phased to a variety of times with a cluster phased towards the middle of the day and another at the end of the night (Fig. 4.2.2b, bottom).

Table 4.2.2: Summary of the light-dark- and circadian-regulated transcripts repressed by glyphosate. Gene information from TAIR.

Locus	Name
AT5G23660	<i>(SWEET12)</i>
AT5G64940	<i>ABC2 HOMOLOG 13 (ATH13)</i>
AT1G16880	<i>ACT DOMAIN REPEATS 11 (ACR11)</i>
AT4G22570	<i>ADENINE PHOSPHORIBOSYL TRANSFERASE 3 (APT3)</i>
AT1G23740	<i>ALKENAL/ONE OXIDOREDUCTASE (AOR)</i>
AT3G29320	<i>ALPHA-GLUCAN PHOSPHORYLASE 1 (PHS1)</i>
AT3G46970	<i>ALPHA-GLUCAN PHOSPHORYLASE 2 (PHS2)</i>
AT2G32480	<i>ARABIDOPSIS SERIN PROTEASE (ARASP)</i>
AT1G26560	<i>BETA GLUCOSIDASE 40 (BGLU40)</i>
AT4G15560	<i>CLOROPLASTOS ALTERADOS 1 (CLA1)</i>
AT2G07050	<i>CYCLOARTENOL SYNTHASE 1 (CAS1)</i>
AT4G19120	<i>EARLY-RESPONSIVE TO DEHYDRATION 3 (ERD3)</i>
AT2G30390	<i>FERROCHELATASE 2 (FC2)</i>
AT2G21330	<i>FRUCTOSE-BISPHOSPHATE ALDOLASE 1 (FBA1)</i>
AT1G74670	<i>GA-STIMULATED ARABIDOPSIS 6 (GASA6)</i>
AT3G59400	<i>GENOMES UNCOUPLED 4 (GUN4)</i>
AT5G20630	<i>GERMIN 3 (GER3)</i>
AT2G18300	<i>HOMOLOG OF BEE2 INTERACTING WITH IBH 1 (HBI1)</i>
AT4G26670	<i>HYPOTHETICAL PROTEIN 20 (HP20)</i>
AT3G08940	<i>LIGHT HARVESTING COMPLEX PHOTOSYSTEM II (LHCB4.2)</i>
AT2G34430	<i>LIGHT-HARVESTING CHLOROPHYLL-PROTEIN COMPLEX II SUBUNIT B1 (LHB1B1)</i>
AT1G13270	<i>METHIONINE AMINOPEPTIDASE 1B (MAP1C)</i>
AT3G26570	<i>PHOSPHATE TRANSPORTER 2;1 (PHT2;1)</i>
AT3G01440	<i>PHOTOSYNTHETIC NDH SUBCOMPLEX L 3 (PnsL3)</i>
AT1G03130	<i>PHOTOSYSTEM I SUBUNIT D-2 (PSAD-2)</i>
AT1G52230	<i>PHOTOSYSTEM I SUBUNIT H2 (PSAH2)</i>
AT3G27690	<i>PHOTOSYSTEM II LIGHT HARVESTING COMPLEX GENE 2.3 (LHCB2.3)</i>
AT2G43010	<i>PHYTOCHROME INTERACTING FACTOR 4 (PIF4)</i>
AT1G70940	<i>PIN-FORMED 3 (PIN3)</i>

Continued on next page

Table 4.2.2 – continued

Locus	Name
AT5G06970	<i>PROTON ATPASE TRANSLOCATION CONTROL 1 (PATROL1)</i>
AT2G05620	<i>PROTON GRADIENT REGULATION 5 (PGR5)</i>
AT4G04340	<i>REDUCED HYPEROSMOLALITY, INDUCED CA²⁺ INCREASE 1 (OSCA1) (OSCA1)</i>
AT3G55800	<i>SEDOHEPTULOSE-BISPHOSPHATASE (SBPASE)</i>
AT5G18060	<i>SMALL AUXIN UP RNA 23 (SAUR23)</i>
AT1G29440	<i>SMALL AUXIN UP RNA 63 (SAUR63)</i>
AT1G29430	<i>SMALL AUXIN UPREGULATED RNA 62 (SAUR62)</i>
AT5G51970	<i>SORBITOL DEHYDROGENASE (ATSDH)</i>
AT2G29630	<i>THIAMINC (THIC)</i>
AT1G10200	<i>WLIM1 (WLIM1)</i>
AT3G02830	<i>ZINC FINGER PROTEIN 1 (ZFN1)</i>
AT4G26130	Unknown
AT5G16030	Unknown
AT1G22850	Unknown
AT3G01660	Unknown
AT1G07050	Unknown
AT5G02830	Unknown
AT2G35260	Unknown
AT1G13930	Unknown
AT1G73470	Unknown
AT4G14270	Unknown
AT5G56850	Unknown
AT4G12980	Unknown
AT1G70820	Unknown
AT4G16140	Unknown
AT4G30650	Unknown
AT3G46630	Unknown
AT4G26370	Unknown

These comparisons suggest that there could be circadian regulation in the response to glyphosate and that the response could be phased to pre-dawn, dawn, or around the middle of the day.

4.3 Glyphosate-responsive rhythmic transcripts are enriched for auxin signalling

A Gene Ontology (GO) term analysis of the 137 glyphosate- and circadian-regulated transcripts identified a significant overlap between these transcripts and an auxin GO term (GO:0060918; $P = 0.024$, Benjamini Hochberg correction). This is logical since glyphosate inhibits EPSPS (Herrmann, 1995). EPSPS is involved in the biosynthesis of the aromatic amino acids including tryptophan, the precursor for indole-3-acetic acid (IAA; auxin) biosynthesis (Jaworski, 1972; Tao et al., 2008), and glyphosate has previously been proposed to interact with auxin signalling (Baur, 1979).

To further understand the interaction between rhythmic glyphosate regulation and auxin, an auxin-related gene list was compiled. This was conducted by obtaining all of the gene names for each of the different auxin GO terms available using AmiGO (amigo.geneontology.org/amigo). The GO accessions and associated terms that were identified are listed in Table 4.3.1. Every gene that was identified for each of these GO terms was saved and a list of the unique genes (549 genes) was compiled to form the auxin-related gene list.

Table 4.3.1: Auxin Gene Ontology (GO) terms and the associated number of genes for each term that were used to create an auxin-regulated gene list. Individual genes occurred in multiple GO terms. A list of 549 genes was compiled where each gene only occurred once. GO terms obtained from AmiGO (amigo.geneontology.org/amigo).

GO Accession	GO Term	Number of genes identified for GO term
GO:0038198	Auxin receptor activity	1
GO:0010601	Positive regulation of auxin biosynthetic process	5
GO:0010600	Regulation of auxin biosynthetic process	6
GO:0010541	Acropetal auxin transport	3

Continued on next page

Table 4.3.1 – continued

GO Accession	GO Term	Number of genes identified for GO term
GO:0010540	Basipetal auxin transport	19
GO:1901703	Protein localization involved in auxin polar transport	7
GO:0080161	Auxin transmembrane transporter activity	1
GO:0080162	Intracellular auxin transport	1
GO:0071365	Cellular response to auxin stimulus	21
GO:0009851	Auxin biosynthetic process	33
GO:0009850	Auxin metabolic process	12
GO:0009852	Auxin catabolic process	2
GO:0010929	Positive regulation of auxin mediated signaling pathway	4
GO:0009734	Auxin-activated signaling pathway	186
GO:0009733	Response to auxin	297
GO:0009672	Auxin:proton symporter activity	14
GO:0009926	Auxin polar transport	56
GO:0060919	Auxin unflux	3
GO:0060918	Auxin transport	10
GO:0060774	Auxin mediated signaling pathway involved in phyllotactic patterning	3
GO:2000012	Regulation of auxin polar transport	23
GO:0090355	Positive regulation of auxin metabolic process	1
GO:0010011	Auxin binding	6
GO:0010249	Auxin conjugate metabolic process	1
GO:0010252	Auxin homeostasis	34
GO:0010315	Auxin efflux	13
GO:0010329	Auxin efflux transmembrane transporter activity	18
GO:0010328	Auxin influx transmembrane transporter activity	6
GO:0010928	Regulation of auxin mediated signaling pathway	10
GO:0010930	Negative regulation of auxin mediated signaling pathway	2
GO:0080024	Indolebutyric acid metabolic process	5
GO:0010013	N-1-naphthylphthalamic acid binding	2
GO:0010178	IAA-amino acid conjugate hydrolase activity	4

This auxin-related gene list was compared to the 75 transcripts that were consistently glyphosate regulated (both induced and repressed) and light-dark- and circadian-regulated (Fig. 4.2.2 and Tables 4.2.1 and 4.2.2). This analysis identified a significant overlap of five genes that were involved in the rhythmic response to glyphosate and auxin ($P = 0.03$, 1.8 transcripts would be expected to overlap by chance; Table 4.3.2).

Table 4.3.2: Genes that were common to the glyphosate-, rhythmic- and auxin-regulated lists.

Locus	Name
AT2G43010	<i>PHYTOCHROME INTERACTING FACTOR 4 (PIF4)</i>
AT1G70940	<i>PIN-FORMED 3 (PIN3)</i>
AT5G18060	<i>SMALL AUXIN UP RNA 23 (SAUR23)</i>
AT1G29440	<i>SMALL AUXIN UP RNA 63 (SAUR63)</i>
AT1G29430	<i>SMALL AUXIN UPREGULATED RNA 62 (SAUR62)</i>

Auxin signalling is circadian regulated (Covington and Harmer, 2007). Therefore, it is possible that the timing of auxin signalling coincides with the time of greatest glyphosate efficacy since there appears to be a link between auxin, glyphosate and circadian regulation.

4.4 Response to glyphosate has time of day sensitivity under light-dark cycles

Since there were significant overlaps between glyphosate-regulated transcripts, rhythmic transcripts and auxin-regulated transcripts, and all steps of auxin signalling are circadian regulated (Covington and Harmer, 2007), an auxin-dependent process was used as a model to test for a rhythmic response to glyphosate.

Hypocotyl elongation is the elongation of the cells in the hypocotyl that occurs largely between 2 and 5 days after germination (Gendreau et al., 1997). In the light, phytochrome perceive light and interact with PIFs, in particular PIF4 (Nomoto et al., 2012), which become phosphorylated and targeted for degradation. HY5 is stabilised, and promotes expression of photomorphogenesis genes, and hypocotyl elongation is suppressed (Mazzella et al., 2014). In the dark, photoreceptors are inactive and HY5 is targeted for degradation by COP1 and SPA1 (Mazzella et al., 2014). PIFs (PIF4 and PIF5 in particular) accumulate and promote expression of skotomorphogenesis genes including auxin biosynthesis, transport and response genes (such as *YUCCA8*, *PIN3* and *IAA29*, respectively), leading to hypocotyl elongation (Jensen et al., 1998; Reed et al., 2018).

The circadian oscillator is involved in hypocotyl elongation at multiple levels. Under continuous light, hypocotyl elongation is rhythmic where peak elongation occurs at subjective dusk (Dowson-Day and Millar, 1999). In *cca1* and *elf3*, there is no daily elongation arrest and seedlings have a long hypocotyl (Dowson-Day and Millar, 1999). Under short days, peak hypocotyl elongation occurs at dawn (Nozue et al., 2007). This is because the clock regulates levels of *PIF4* and *PIF5* transcript abundance, whereas in the day, light regulates these at the protein level (Nozue et al., 2007; Kunihiro et al., 2011). Furthermore, when there is no light repression of the PIFs early in the night, the evening complex (EC; ELF3, ELF4 and LUX) binds to the promoters of *PIF4* and *PIF5*, preventing their promotion of elongation. Therefore, the EC underlies the molecular basis for circadian gating of hypocotyl elongation at the onset of darkness (Nusinow et al., 2011).

Therefore, because of the identified over-representation of rhythmic and auxin-related transcripts, and since hypocotyl elongation is circadian regulated, it was hypothesised that glyphosate application could prevent the elongation of the hypocotyl and that the timing of hypocotyl elongation could determine timing of glyphosate sensitivity.

4.4.1 Hypocotyl length is most sensitive to glyphosate when applied at dawn in wild type *Arabidopsis*

To test whether the magnitude of inhibition of hypocotyl elongation by glyphosate might depend on the time of day, glyphosate treatments were applied at five time points throughout the light period of the day. Treatments were applied on day 3 as this is when elongation is greatest (Gendreau et al., 1997).

Glyphosate treatments applied at dawn had the greatest effect on hypocotyl length in wild type Col-0 plants (Fig. 4.4.1a), inhibiting hypocotyl length by about 26%. Effectiveness of glyphosate decreased throughout the day with treatments at dusk being ineffective. Two-way ANOVA identified a significant interaction between glyphosate treatment and the time of treatment ($F(4, 184) = 6, P < 0.001$).

Glyphosate treatment at all application times caused a significant reduction in hypocotyl length of *CCA1-ox* plants (Fig. 4.4.1b). The greatest reductions in hypocotyl length were when glyphosate was applied at midday and dusk (45% reduction). The least effective times of glyphosate application were 2 h after dawn and dawn (20% reduction). The interaction between glyphosate treatment and application time was significant (two-way ANOVA, $F(4, 240) = 18, P < 0.001$).

Dawn and 2 h after dawn were the only times where glyphosate treatment had a significant effect (12% and 15% reduction, respectively) on the length of the hypocotyl in *TOC1-ox* plants (Fig. 4.4.1c). Two-way ANOVA indicated a significant interaction between glyphosate treatment and time ($F(4, 188) = 3, P = 0.04$).

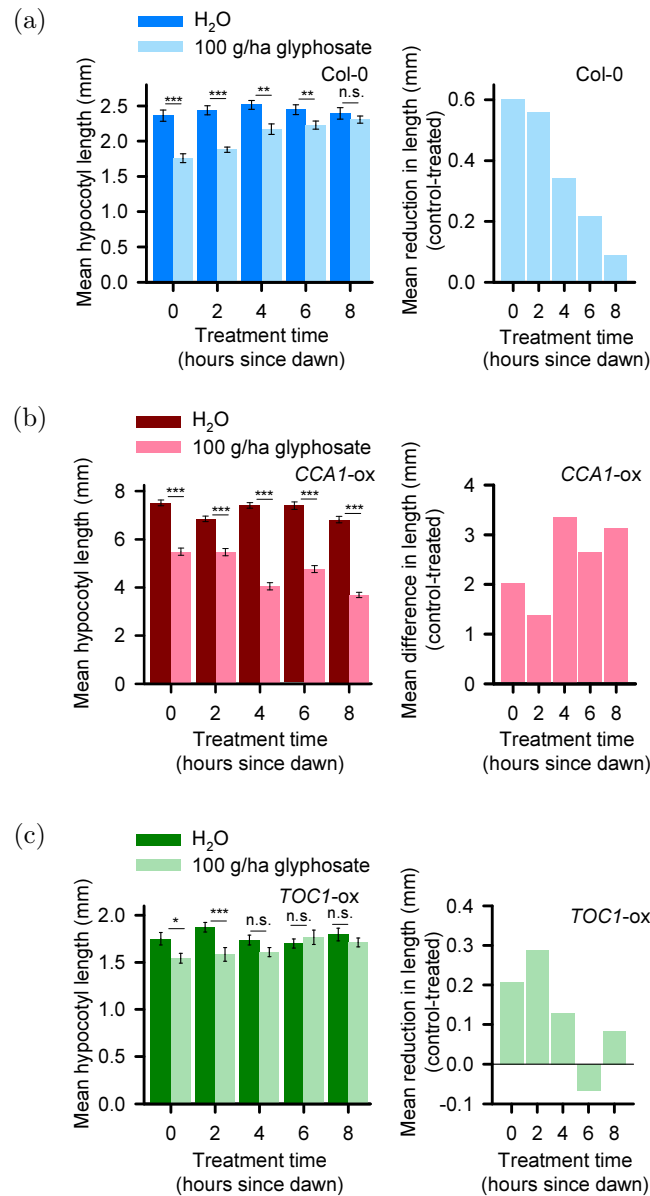


Figure 4.4.1: Response of hypocotyl length to glyphosate is rhythmic. Under light-dark cycles hypocotyls are shorter after 100 g/ha glyphosate treatment. Figures show mean hypocotyl length for control and glyphosate-treated plants at each treatment time point (left) and the change in mean length between the control and treated lengths (right). (a) Hypocotyl length was shortest after glyphosate application at dawn in Col-0, and reduced in sensitivity throughout the day. (b) *CCA1-ox* plants had altered sensitivity to glyphosate compared to wild-type plants. (c) Sensitivity to glyphosate was similar to wild type in *TOC1-ox* plants, with reduced sensitivity. Values are mean \pm SEM where $n = 18-25$. Asterisks indicate significant difference between control and treated value, calculated by t -test where $* = P \leq 0.05$, $** = P \leq 0.01$ and $*** = P \leq 0.001$. n.s. = no statistically significant difference.

Overall, the time of day responses in the length of the hypocotyl to glyphosate differed between the three genotypes, indicating potential involvement of the circadian oscillator. While the two-way ANOVAs for all three lines suggest that the effect of treatment was dependent on the application time, there were differences in which time points were more or less effective. To test the involvement of the circadian oscillator further, it would be necessary to conduct the experiment under constant light conditions.

4.4.2 Validation of experimental methods

Several control experiments were conducted to validate the experimental methods used for hypocotyl elongation assays. Firstly, while different concentrations of glyphosate had been tested previously (Chapter 3), it was necessary to determine the concentration of glyphosate that would have a detectable, but not lethal, effect on the hypocotyl (Fig. 4.4.2a). The response of hypocotyl length to increasing concentrations of glyphosate was not linear, suggesting that the effect of glyphosate upon hypocotyl elongation became saturated with higher concentrations. The 100 g/ha glyphosate concentration was suitable because this concentration was not too high that subtle time of day differences would be missed. A similar concentration has been reported to be the midpoint of a damage score dose-response curve for *Arabidopsis* (Yang et al., 2017).

The Touchdown Total formulation of glyphosate that was used in these experiments contains an adjuvant. A formulation that contained the adjuvant but no glyphosate active ingredient was produced by Syngenta. The adjuvant did not reduce hypocotyl elongation (Fig. 4.4.2b). Therefore, the inhibition of hypocotyl elongation was solely due to the glyphosate active ingredient in the formulation.

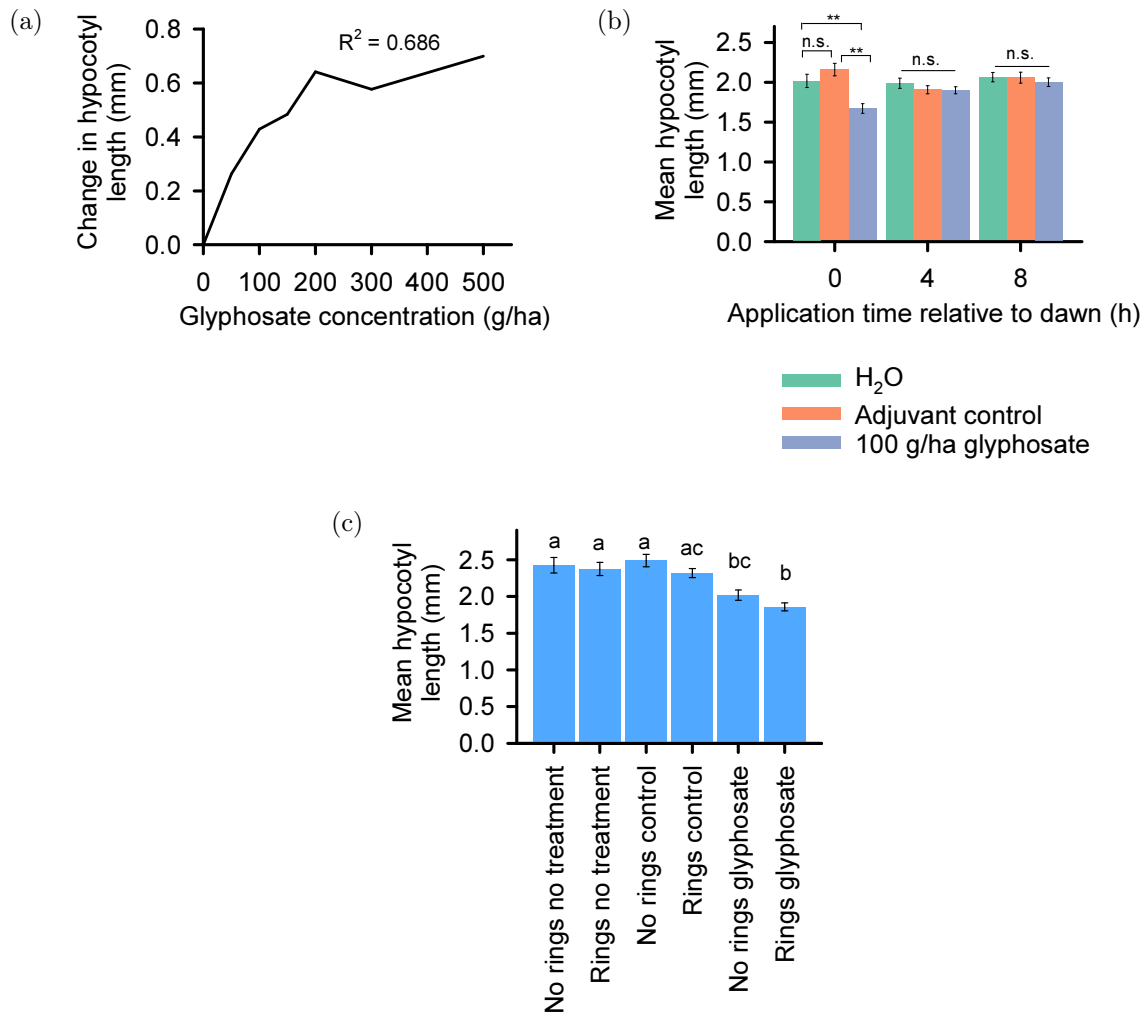


Figure 4.4.2: Validation of experimental methods. (a) Length of hypocotyl reduced with increasing glyphosate concentration. R^2 value from linear regression. (b) The adjuvant component of the glyphosate formulation did not cause the inhibition of hypocotyl elongation. (c) The plastic rings used for equal treatment application did not have a negative effect on the hypocotyl length. Statistical analysis conducted using one-way ANOVA per time point (a) or across all samples (c). Asterisks or letters indicate significant difference. Values are mean \pm SEM where $n = 19-20$.

The nature of the experimental set up (Chapter 2.1; Fig. 2.1.1) involved growing seedlings in plastic rings. It was determined that there was no difference in the length of hypocotyl when grown in the rings compared to growth without rings (Fig. 4.4.2c). Therefore, the method was acceptable, and the reported hypocotyl lengths in non-treated plants were a result of the general growth conditions (light intensity, photoperiod, temperature).

Measurements for all treatment times were usually taken around dawn on day 7. Consequently, there could have been differences in hypocotyl lengths depending on whether the hypocotyls were measured at dawn, or at a later time point. A test was conducted where all hypocotyls were measured at the same time (dawn) regardless of treatment time (Fig. 4.4.3a) or they were measured at the time at which they were treated, where all treatments regardless of treatment time were exactly the same length (Fig. 4.4.3b). There was a small difference in the effect of measurement time, where glyphosate treatment did not cause a significant difference in hypocotyl length at mid-day when measured at mid-day. The overall result was the same: that hypocotyls treated at dawn were most sensitive to glyphosate treatment and hypocotyls treated at dusk were least sensitive to glyphosate treatment. It was not possible in all experiments to always measure at exactly the same time because the number of hypocotyls to measure in some experiments was too large.

4.4.3 Plants have increased sensitivity to glyphosate pre-dawn and post-dusk

The daily fluctuation in sensitivity to glyphosate under 8 h photoperiods (Fig. 4.4.1a) was also apparent under 12 h photoperiods (Fig. 4.4.4a) and 16 h photoperiods (Fig. 4.4.4b). Under 12 h light/12 h dark cycles, glyphosate application at dawn was the most effective (20% shorter than controls; Fig. 4.4.4a). Glyphosate application 9 hours after dawn caused no significant difference in hypocotyl length between the treatment and control, and glyphosate treatment at dusk increased the length of the hypocotyl compared to the control (Fig. 4.4.4a). Two-way ANOVA determined a significant interaction between treatment and time ($F(4, 190) = 7.97, P < 0.001$).

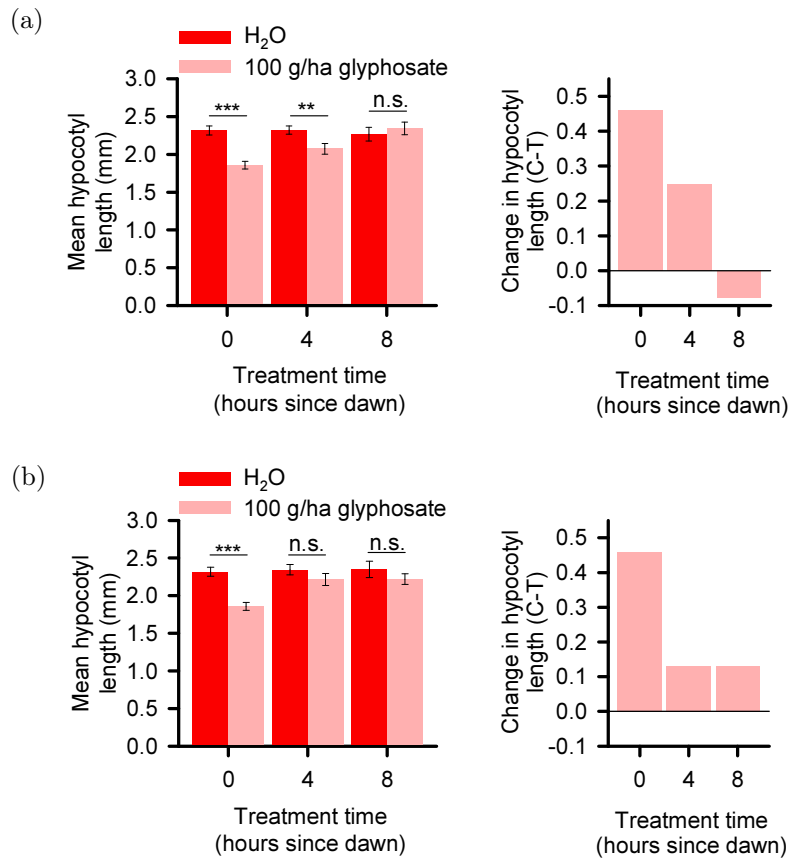


Figure 4.4.3: Measurement time did not affect the time of day sensitivity to glyphosate. Dawn was the most sensitive time of glyphosate application regardless of when the hypocotyls were measured where (a) hypocotyls were imaged at dawn on the final day of the experiment or (b) hypocotyls were imaged at the respective treatment time on the final day of the experiment. Figures show mean hypocotyl length for control and glyphosate-treated plants at each treatment time point (left) and the change in mean length between the control and treated lengths (right). Values are mean \pm SEM where $n = 18-20$. Significance determined by two-way ANOVA, (a) $F(2, 114) = 7.3$, $P = 0.001$, (b) $F(2, 112) = 3.1$, $P = 0.048$, and pairwise comparisons by t -test where $** = P \leq 0.01$, $*** = P \leq 0.001$ and n.s. = no statistically significant difference.

Under 16 h light/8 h dark cycles, the greatest inhibition of hypocotyl elongation occurred when glyphosate was applied at dawn (29% shorter than control; Fig. 4.4.4b). Glyphosate application was least effective under long days when applied at dusk (18% reduction). Two-way ANOVA determined a significant interaction between treatment and time ($F(4, 190) = 2.74$, $P = 0.03$).

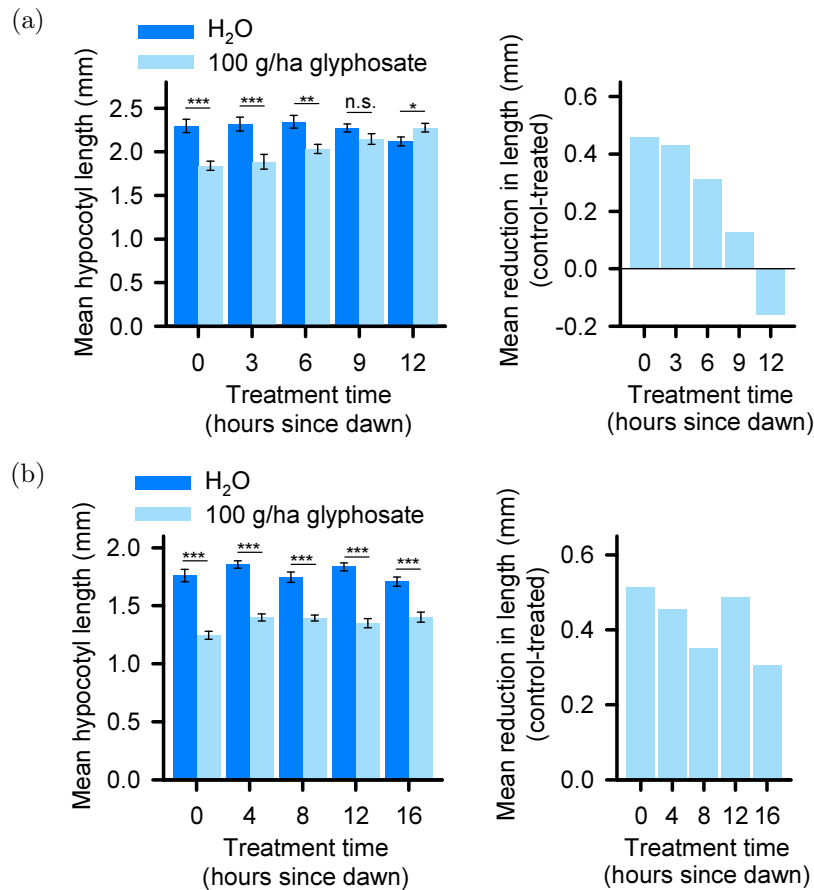


Figure 4.4.4: Sensitivity to glyphosate was greatest at dawn regardless of photoperiod. 100 g/ha glyphosate was applied at five time points throughout the light period of the day under (a) 12 h light /12 h dark cycles and (b) 16 h light /8 h dark cycles. Figures show mean hypocotyl length for control and glyphosate-treated plants at each treatment time point (left) and the change in mean length between the control and treated lengths (right). Values are mean \pm SEM where $n = 20$. Asterisks indicate significant difference between control and treated value, calculated by t -test where * = $P \leq 0.05$, ** = $P \leq 0.01$ and *** = $P \leq 0.001$. n.s. = no statistically significant difference.

Subsequent experiments were conducted under short photoperiods because the longer length of hypocotyls grown under short photoperiods was likely to emphasise any subtle differences between treatment time points and therefore, the subtle effects of glyphosate were more easily discernible.

Whilst it may not be relevant to field applications, we thought it would be informative to also determine the effect of glyphosate in the dark (Fig. 4.4.5). Although glyphosate

treatment at dusk was the least effective at inhibiting the length of the hypocotyl (Fig. 4.4.1a, 4.4.5), application of glyphosate just after dusk significantly inhibited elongation of the hypocotyl (12% shorter compared to the control (Fig. 4.4.5)). The two glyphosate application time points in the middle of the night had no effect on the hypocotyl length. Application of glyphosate at the end of the night (pre-dawn) also had a significant effect on length of the hypocotyl, reducing hypocotyl length by 13%. The post-dusk and pre-dawn time points did not inhibit the length of the hypocotyl to the same extent as the dawn application (20% reduction in length). Two-way ANOVA determined a significant interaction between treatment and time ($F(6, 266) = 5.39$, $P < 0.001$).

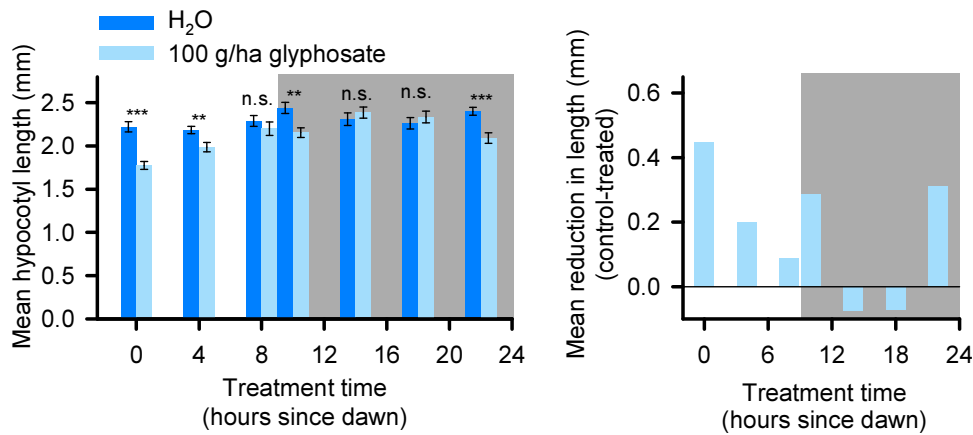


Figure 4.4.5: Hypocotyls were sensitive to glyphosate at the beginning and end of the night. Under light-dark cycles, 100 g/ha glyphosate applied to hypocotyls caused a reduction in hypocotyl length compared to the controls when applied just after the onset of darkness and just before dawn, but not at time points in between. Figures show mean hypocotyl length for control and glyphosate-treated plants at each treatment time point (left) and the change in mean length between the control and treated lengths (right). Values are mean \pm SEM where $n = 20$. Asterisks indicate significant difference between control and treated value, calculated by t -test where $* = P \leq 0.05$, $** = P \leq 0.01$ and $*** = P \leq 0.001$. n.s. = no statistically significant difference. Grey shading indicates dark period.

4.4.4 Glyphosate reduced hypocotyl elongation rate when applied at dawn but not at dusk

Experiments to this point measured end-point hypocotyl lengths. We thought it would be interesting to determine whether there were transient effects at a specific time point during the elongation of the hypocotyl that led to the different end-point lengths. Therefore, infra-red time-lapse imaging was used (Chapter 2.5.3) to measure the effect of glyphosate on hypocotyl elongation rate after glyphosate treatment at either dawn (Fig. 4.4.6a) or dusk (Fig. 4.4.6b).

To allow a detailed analysis of the elongation rate within each light or dark period, data were plotted as the mean rate of elongation for each light or dark period per cycle (Figs. 4.4.6c and 4.4.6d). This identified that the elongation rate was significantly lower in the first dark cycle after dawn glyphosate treatment compared to the control (Fig. 4.4.6c). This did not occur in the same cycle for the dusk glyphosate-treated seedlings (Fig. 4.4.6d). After glyphosate treatment at dusk, elongation rate was never lower for treated plants than the corresponding control. Therefore, the small effect in the dawn glyphosate-treated seedlings in the first dark period seems to be responsible for the final hypocotyl length being shorter in dawn-treated seedlings, compared to the dusk-treated seedlings.

The data from these experiments were noisy and there were differences in the control plants for the two treatment times. There were peaks where elongation was occurring, but subsequent experiments were conducted using hypocotyl length rather than elongation rate experiments for greater consistency, reliability and throughput.

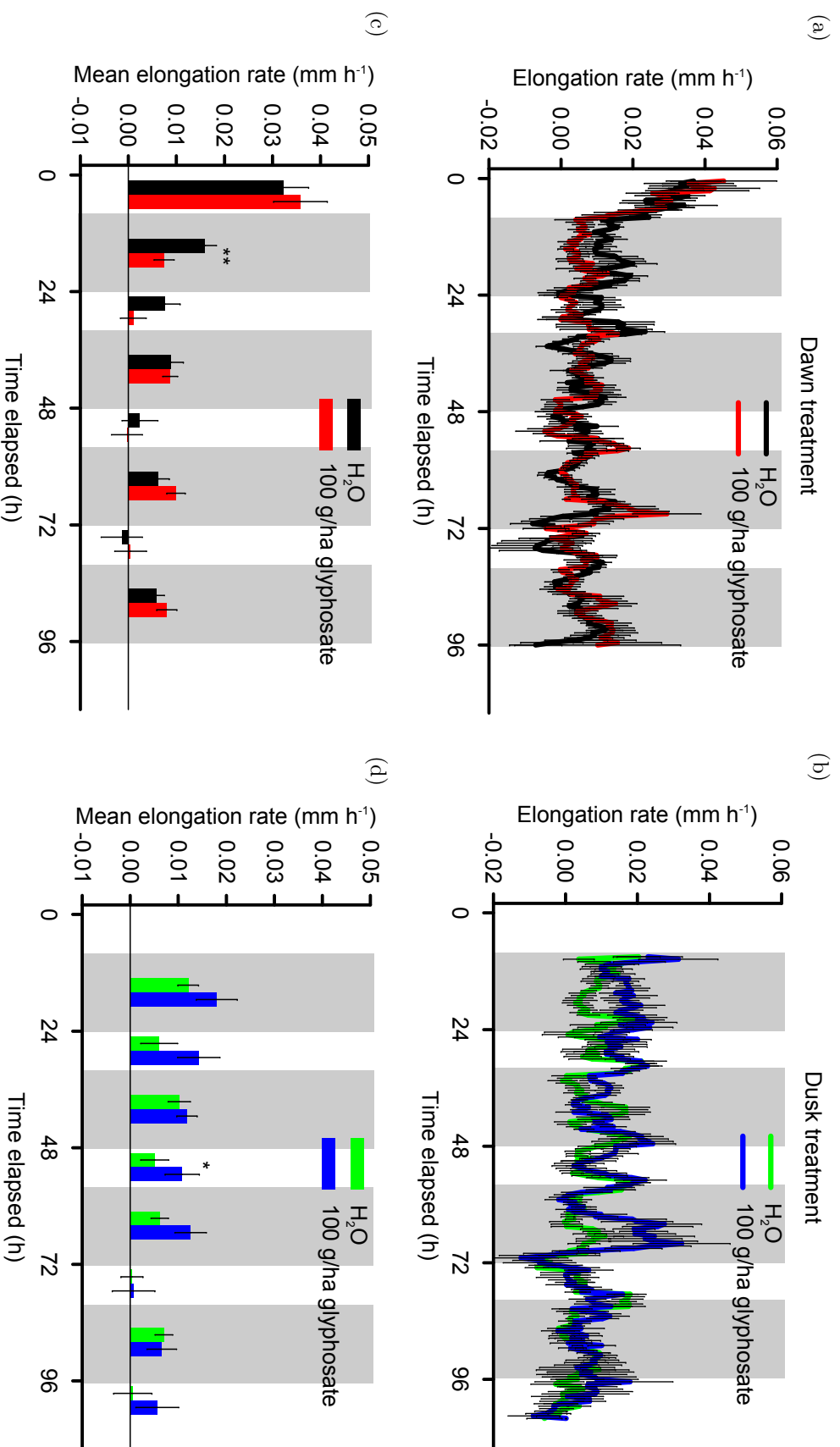


Figure 4.4.6: The effect of glyphosate applied at either dawn or dusk on hypocotyl elongation rate. Trace of hypocotyl elongation rate in Col-0 (a) and *CCA1-ox* (b) under light-dark cycles. The mean elongation rate in the light or dark period per cycle for Col-0 (c) and *CCA1-ox* (d). Glyphosate was applied at either dawn or dusk on day 3. Values are mean \pm SEM where $n = 10$. Significant differences in mean elongation rate per light or dark period in each cycle determined by *t*-test where * = $P \leq 0.05$ and ** = $P \leq 0.01$. Grey shading indicates dark period.

4.4.5 Higher glyphosate concentrations are required at dusk than dawn to cause the same inhibition of hypocotyl elongation

Glyphosate was consistently most effective when applied at dawn under light-dark cycles, therefore we wanted to know what concentration of glyphosate was required at dusk to result in an equivalent attenuation of the hypocotyl length. A titration experiment identified that at least 150 g/ha glyphosate was required at dusk to give the same inhibition in hypocotyl length as 100 g/ha applied at dawn (Fig. 4.4.7). At least 1.5 times more active ingredient was required at dusk, and as such, less chemical could be used at a more effective treatment time of day.

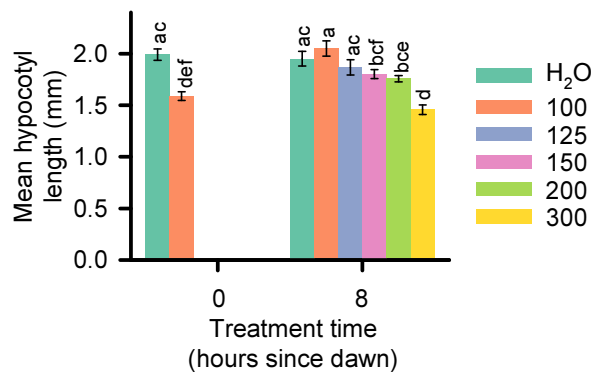


Figure 4.4.7: 1.5 times more glyphosate is required at dusk to give the same level of attenuation in hypocotyl length as 100 g/ha glyphosate at dawn. Different concentrations of glyphosate were applied to elongating hypocotyls at dusk to determine the concentration required to cause the same phenotype as 100 g/ha glyphosate at dawn. Significance determined using one-way ANOVA with Tukey post-hoc test. Different letters indicate a significant difference. Values are mean \pm SEM where $n = 18-20$.

4.4.6 Seedlings have decreased sensitivity to glyphosate applied at dusk

Previous experiments concluded when seedlings were 7 days old, which was 4 days after glyphosate treatment. We wondered what the long-term effects of glyphosate treatments at dawn or dusk would be on the seedlings. Seedlings that had been treated with glyphosate at either dawn or dusk on day 3 were left for a further six weeks (Fig. 4.4.8). Seedlings that were treated at dusk grew larger than the seedlings treated at dawn. All seedlings treated with glyphosate at dusk produced new leaves, whereas only 58% of dawn-treated seedlings produced new leaves (Fig. 4.4.8). This growth suggests that seedlings were less sensitive to glyphosate application at dusk. While the dusk treated seedlings continued to grow, they did not appear healthy. None of the seedlings appeared to be dead, but the concentration of glyphosate was intentionally not lethal.

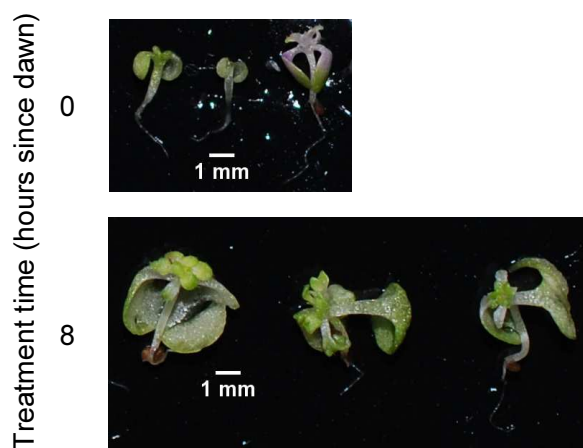


Figure 4.4.8: Representative images of the long term effects of glyphosate on the hypocotyl when applied at either dawn or dusk. Hypocotyls treated at dawn were smaller than those treated at dusk, and produced fewer new leaves. Images are representative of two independent experiments, $n= 21-22$.

4.5 Sensitivity to glyphosate at dawn is circadian-regulated

Experiments to this point were conducted under light-dark cycles. These results were informative because plants cultivated agriculturally would be exposed to light-dark cycles in the environment. However, it is not possible to ascertain the involvement of the circadian oscillator in such conditions. Therefore, similar experiments were conducted under constant light conditions.

4.5.1 Glyphosate sensitivity is rhythmic under constant light conditions in wild-type *Arabidopsis*

In order to conduct similar experiments under constant light conditions, it was necessary to verify the rhythmicity of seedlings after only one light-dark cycle, before plants were exposed to constant light in a hypocotyl length assay (Fig. 4.5.1). Measuring *CCA1::LUC* bioluminescence determined that one cycle of light-dark was sufficient to entrain the circadian oscillator (Fig. 4.5.1a). Immediately after seedlings emerged they were rhythmic with a period of approximately $24.2 \text{ h} \pm 0.1$ (Fig. 4.5.1b). Therefore, plants could be exposed to one cycle of light-dark before transfer to constant light for one cycle and treatments could be applied on day 3, as in the light-dark experiments (Fig. 4.4.1).

46 h after the onset of constant light, sets of plants were treated at specified time points over two cycles of subjective day and night (Fig. 4.5.2). Glyphosate treatment significantly reduced hypocotyl elongation at all treatment time points (Fig. 4.5.2), unlike under light-dark cycles (Fig. 4.4.1). Application of glyphosate at dawn caused the greatest inhibition in hypocotyl length in both cycles (Fig. 4.5.2a). Hypocotyls were least sensitive to glyphosate at dusk, as they were under light-dark cycles. A two-way ANOVA determined a significant interaction between glyphosate treatment and time of treatment ($F(17, 683) = 6, P < 0.001$).

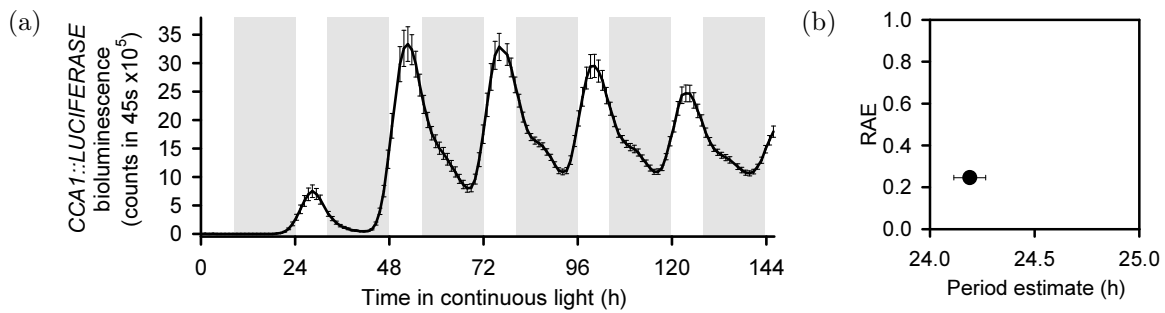


Figure 4.5.1: Seedlings were rhythmic after entrainment under one cycle of light-dark. Plates of vernalised *CCA1::LUC* seedlings were placed into a growth chamber for one cycle of light-dark before being placed into constant light for bioluminescence imaging. The bioluminescence of *CCA1::LUC* was rhythmic after the seedling emerged from the seed (a). The parameters of the *CCA1::LUC* bioluminescence determined that the seedlings were rhythmic with a period of 24.2 h (b). RAE is the relative amplitude error, parameters are derived from Fast Fourier Transform-nonlinear least-squares analysis. Values are mean \pm SEM where $n = 8$. Shaded panels indicate subjective night.

In *CCA1-ox* plants there was no time of day sensitivity to glyphosate (Fig. 4.5.2b). The length of the hypocotyls after glyphosate treatment were similar regardless of treatment time. However, a two-way ANOVA determined that there was a significant interaction between treatment and time ($F(17, 677) = 3, P < 0.001$). Together, these results suggest that circadian regulation underlies the response of the hypocotyl to glyphosate.

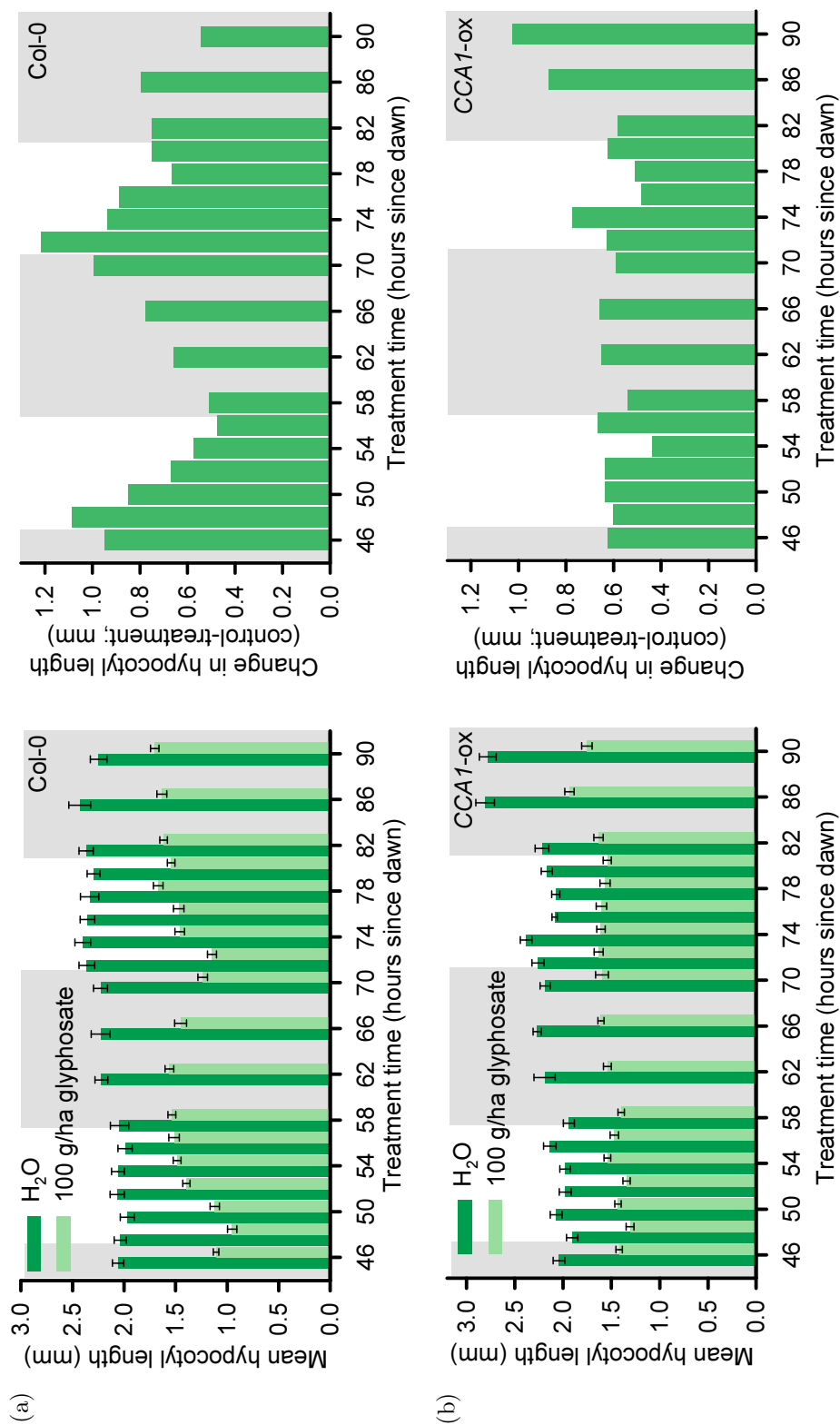


Figure 4.5.2: Sensitivity to glyphosate is rhythmic under constant light conditions. After one light-dark cycle, seedlings were placed into constant light; application of 100 g/ha glyphosate began after two days in constant light. Figures show the mean hypocotyl length for control and treated seedlings (left) and the mean change in hypocotyl length between control and treated plants per time point (right). (a) *Col-0* plants had a rhythmic sensitivity to glyphosate where hypocotyl length after glyphosate treatment was shortest at dawn across the two cycles. (b) *CCA1-ox* plants responded in a similar manner to glyphosate regardless of the treatment application time. Values are mean \pm SEM where $n = 18-20$. Shaded panels indicate subjective night.

4.5.2 Plants that have altered circadian oscillators are not sensitive to different concentrations of glyphosate

Because there were circadian rhythms in the sensitivity of hypocotyls to glyphosate, we wondered how this would affect the effective dose of glyphosate (Fig. 4.5.3). In the wild type, 125 g/ha glyphosate was required at subjective dusk to give the same change in hypocotyl length as 100 g/ha glyphosate at subjective dawn. This was lower than the 150 g/ha required at dusk under light-dark cycles (Fig. 4.4.7).

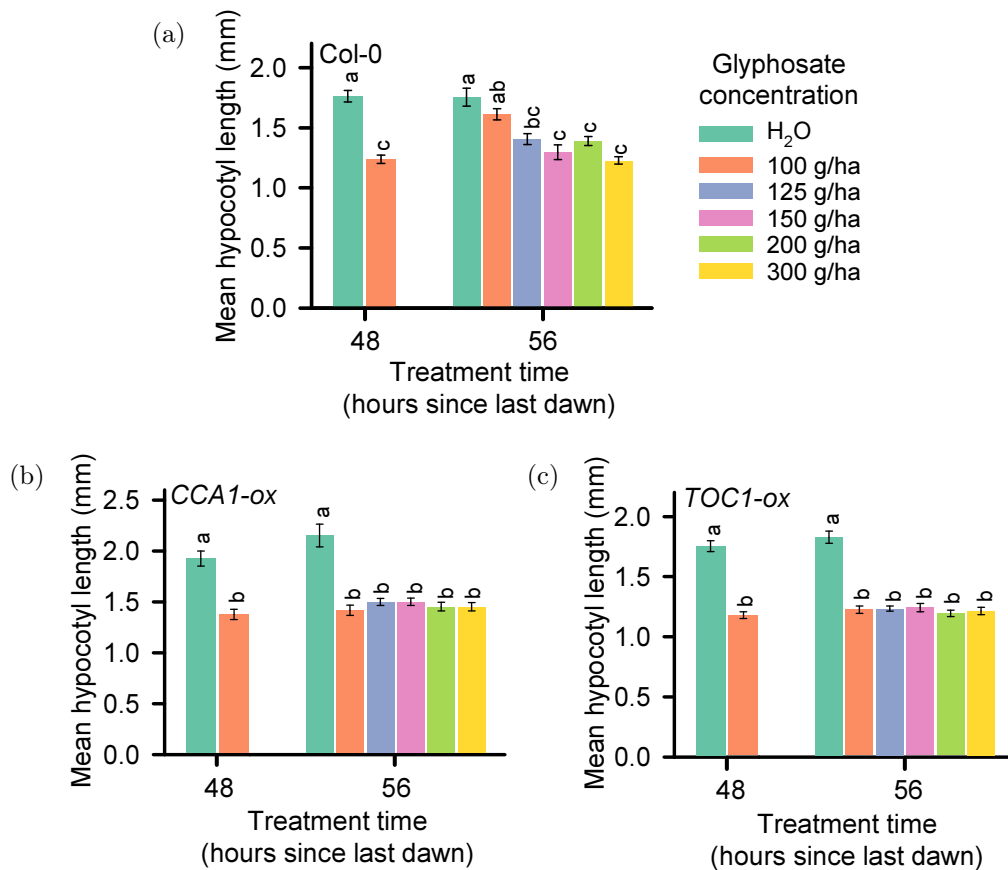


Figure 4.5.3: The effective concentration of glyphosate is regulated by the circadian oscillator. (a) In Col-0 plants, 125 g/ha glyphosate was required at subjective dusk to cause the same inhibition in hypocotyl elongation as 100 g/ha glyphosate applied at subjective dawn. In *CCA1-ox* (b) and *TOC1-ox* (c), there was no difference in the effect of glyphosate on hypocotyl length regardless of treatment time or concentration. Significance determined by one-way ANOVA and Tukey post-hoc analysis indicated by different letters. Values are mean \pm SEM where $n = 19-20$.

In contrast, in *CCA1-ox* and *TOC1-ox*, the response to glyphosate was the same regardless of the treatment time or concentration (Fig. 4.5.3b and 4.5.3c). This suggests that a correctly functioning circadian oscillator was required for the alteration in efficacy of glyphosate in Col-0 under constant light conditions, and under light-dark cycles. Furthermore, glyphosate can be used more effectively at a lower concentration when applied at an optimal time of day.

4.6 Cell death markers have circadian responses to glyphosate

Glyphosate applications were most effective at dawn and this could have been due to the interaction between auxin and circadian regulation. We wanted to know whether the same time of day sensitivity existed when measuring parameters that measure cell death, which is likely being caused by herbicide application.

4.6.1 Glyphosate appears to increase programmed cell death with circadian regulation

Programmed cell death (PCD) involves a sequence of events that leads to the controlled and organised destruction of the cell, crucial for defence responses (Reape and McCabe, 2008). It has been reported that herbicides can alter the expression of genes involved in PCD (Chen and Dickman, 2004; Graham, 2005; Zhu et al., 2009; Faus et al., 2015). It was reasoned that glyphosate application may cause changes in PCD-related genes, and that such responses may change dependent on the time of herbicide application.

Candidate PCD marker genes were identified by obtaining all the genes that were associated with GO terms related to programmed cell death (GO:0012502, GO:0043066, GO:0043068, GO:0042981 and GO:0043067; AmiGO). This identified 71 genes. The

glyphosate-regulated dataset (Faus et al., 2015) was compared to these PCD genes to determine whether any were regulated by glyphosate. This identified 12 genes up-regulated by glyphosate, and 5 genes down-regulated by glyphosate. One gene from each of these lists was selected as a glyphosate-regulated PCD marker gene: *METACASPASE1* (*MC1*) and *DEFENDER AGAINST APOPTOTIC DEATH1* (*DAD1*). These genes were chosen as they were known to have a primary role in PCD (Coll et al., 2010; Danon et al., 2004), while most other genes that had been identified had alternative primary functions.

MC1 is a positive regulator of cell death (Coll et al., 2010) whereby, if the gene is expressed, the cell is inducing PCD. *MC1* was up-regulated by glyphosate treatment (Faus et al., 2015), suggesting that glyphosate is initiating programmed cell death. Conversely, *DAD1* is a negative regulator of PCD (Danon et al., 2004), and an increase in expression is intended to suppress cell death. *DAD1* was suppressed by glyphosate treatment (Faus et al., 2015), suggesting that increased PCD could occur.

The effect of glyphosate on the abundance of the two PCD marker genes was tested at the most and least effective time points from the hypocotyl elongation experiments, dawn and dusk. Under light-dark cycles in the wild type, transcript abundance of *MC1* was significantly increased in response to glyphosate treatment at dawn, but not after glyphosate treatment at dusk (Fig. 4.6.1a, top). However there was no significant interaction between treatment and time. There was a significant decrease in transcript abundance of the negative regulator of cell death, *DAD1*, at dawn but not at dusk (Fig. 4.6.1a, bottom), and there was a significant interaction between treatment and time.

The response was the same as the wild type for *CCA1*-ox plants (Fig. 4.6.1b). There was a significant increase in *MC1* transcript abundance when glyphosate was applied at dawn but not at dusk. *DAD1* transcript abundance significantly decreased when glyphosate was applied at dawn but not at dusk (Fig. 4.6.1b, bottom). In *TOC1*-ox plants, glyphosate application did not significantly alter the transcript abundance

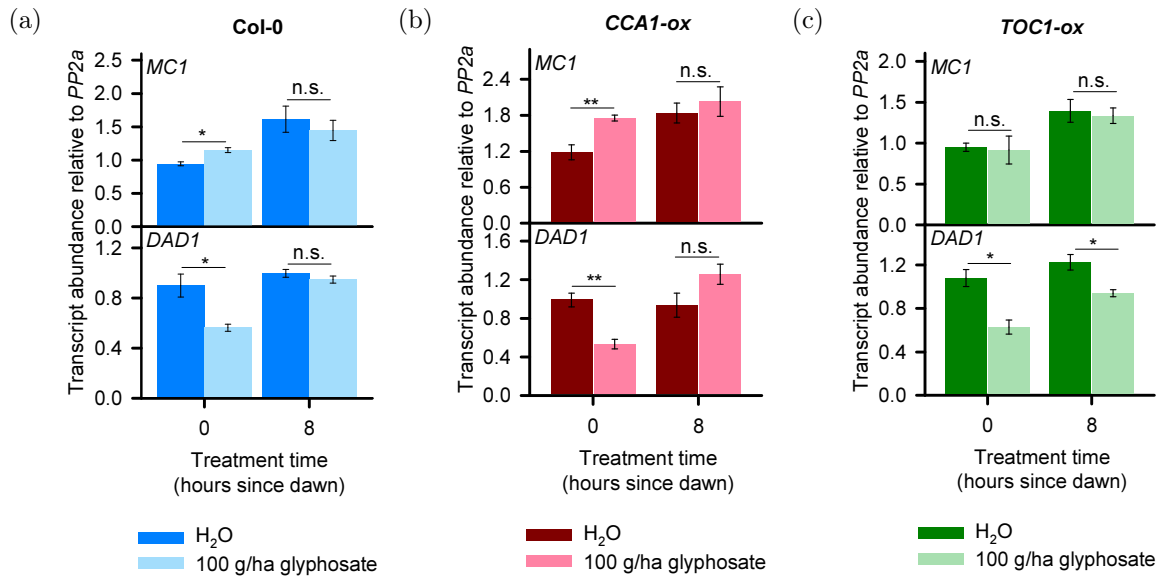


Figure 4.6.1: Glyphosate alters the abundance of transcripts involved in programmed cell death under light-dark cycles in a time-of-day-dependent manner. (a) In Col-0 plants, *MC1* (top) was up-regulated in response to glyphosate at dawn but not at dusk, however there was no significant interaction between treatment and time (two-way ANOVA). *DAD1* (bottom) was down-regulated in response to glyphosate at dawn but not at dusk, there was a significant interaction between treatment and time (two-way ANOVA, $F(1, 8) = 7.48$, $P = 0.03$). (b) In *CCA1-ox* plants, a similar response was seen as in Col-0. There was not a significant interaction between treatment and time for *MC1*, but there was for *DAD1* ($F(1, 8) = 18$, $P = 0.003$, two-way ANOVA). (c) In *TOC1-ox*, glyphosate had no effect on *MC1* transcript abundance at dawn or dusk (top), and glyphosate caused a significant decrease in *DAD1* transcript abundance (bottom) when applied at dawn and dusk (no significant interaction between treatment and time, two-way ANOVA). Tissue was sampled from 5 day old seedlings, 6 hours after glyphosate treatment at either dawn or dusk. Transcripts relative to *PP2a* reference gene. Values are mean \pm SEM where $n = 2-3$. Significant differences between treatment and control per time point determined by *t*-test where * = $P \leq 0.05$, ** = $P \leq 0.01$ and n.s. indicates no significant difference.

of *MC1* when applied at dawn or dusk (Fig. 4.6.1c). *DAD1* transcript abundance significantly decreased after glyphosate application at dawn and at dusk. Therefore, there are differences in the response of PCD marker genes after glyphosate application at different times of day. This suggests that there could be diel regulation of PCD in response to glyphosate.

To determine circadian oscillator involvement in the time-of-day-specific response of PCD marker genes (Fig. 4.6.1), the same experiment was conducted under constant light conditions (Fig. 4.6.2). Glyphosate significantly altered the abundance of both *MC1* and *DAD1* transcripts between control and treated samples at all time points tested (Fig. 4.6.2). However, there were differences in the magnitude of the responses.

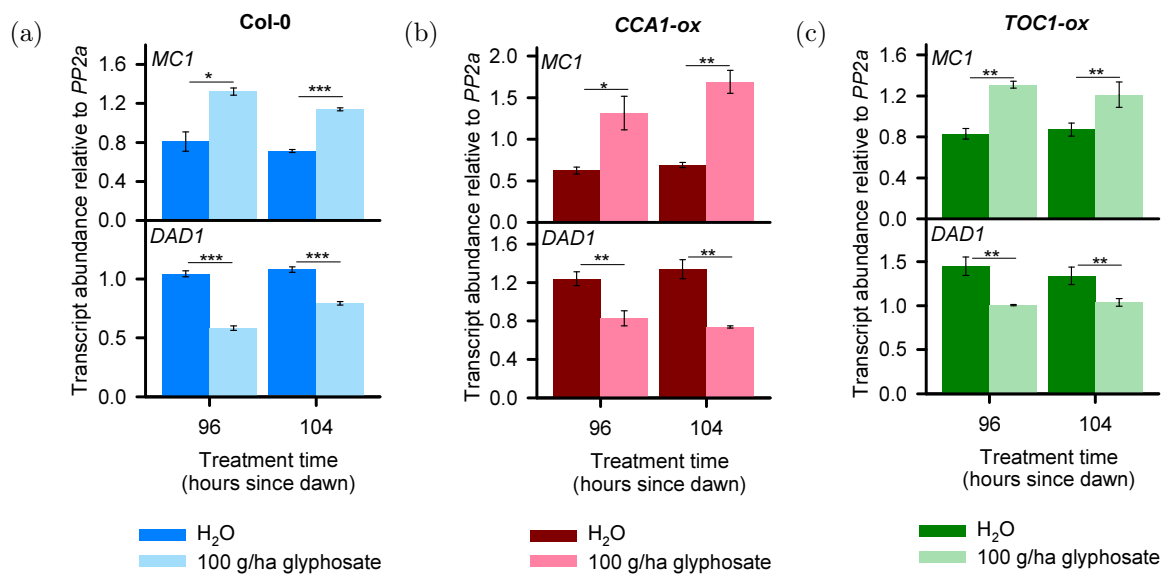


Figure 4.6.2: Glyphosate alters the abundance of transcripts involved in programmed cell death under constant light. 100 g/ha glyphosate applied at subjective dawn or dusk altered transcripts involved in programmed cell death in a time of day-dependent manner. In Col-0 (a), *CCA1-ox* (b) and *TOC1-ox* (c) plants *MC1* transcript abundance was up-regulated in response to glyphosate at subjective dawn and subjective dusk (top), and *DAD1* transcripts were significantly reduced at subjective dawn and at subjective dusk (bottom). There was a significant interaction between glyphosate treatment and the timing of glyphosate treatment in Col-0 for *DAD1* (two-way ANOVA, $F(1, 8) = 17$, $P = 0.003$), but not for any other treatments. Tissue was sampled from 5 day old seedlings, 6 hours after glyphosate treatment at either subjective dawn or subjective dusk. Transcripts relative to *PP2a* reference gene. Values are mean \pm SEM where $n = 2-3$. Significant differences between treatment and control per time point determined by *t*-test where * = $P \leq 0.05$, ** = $P \leq 0.01$ and *** = $P \leq 0.001$.

In Col-0, *MC1* transcript abundance significantly increased after glyphosate treatment at dawn and dusk (Fig. 4.6.2a), and there was not a significant interaction between treatment and time. Glyphosate significantly reduced *DAD1* transcript abundance

after applications at both dawn and dusk (Fig. 4.6.2a). The magnitude of the change was slightly greater at dawn, consistent with the result under light-dark cycles.

In both *CCA1*-ox (Fig. 4.6.2b) and *TOC1*-ox (Fig. 4.6.2c), *MC1* transcript abundance increased after glyphosate treatment at dawn and dusk, and *DAD1* transcript abundance decreased after glyphosate treatment at both dawn and dusk. There were no significant interactions between glyphosate treatment and treatment time. This suggests that a properly functioning circadian oscillator was required for the time-of-day-dependent effects on PCD marker transcripts that were observed in the wild type. Furthermore, studying PCD genes in response to herbicide treatment appeared to be a useful method for determining time of day sensitivity and circadian regulation.

4.6.2 Glyphosate does not affect electrolyte leakage under our experimental conditions

When plant cells die, membrane integrity is lost and electrolytes leak from the cell (Whitlow et al., 1992; Hatsugai and Katagiri, 2018). Electrolyte leakage is a common stress related phenotype, and can be used to quantify relative plant stress (Demidchik et al., 2014). Electrolyte leakage has previously been used as a method to detect the stress response to herbicides (Vanstone and Stobbe, 1977; Falk et al., 2006). Therefore, we hypothesised that this could be used to investigate whether these are time of day-dependent cell death responses to glyphosate.

An initial electrolyte leakage experiment was conducted to determine how long it took glyphosate to have a measurable effect on electrolyte leakage (Fig. 4.6.3). Electrolyte leakage increased after longer periods of glyphosate or control treatment. It appeared that glyphosate had a small change on the extent of electrolyte leakage after 16 hours (Fig. 4.6.3a). Glyphosate treatment appeared to cause a small, but not statistically significant, increase in electrolyte leakage when applied at dawn compared to the control treated plants (Fig. 4.6.3b). The level of electrolyte leakage for the dusk treated plants was more similar for glyphosate and control treated plants (Fig. 4.6.3b).

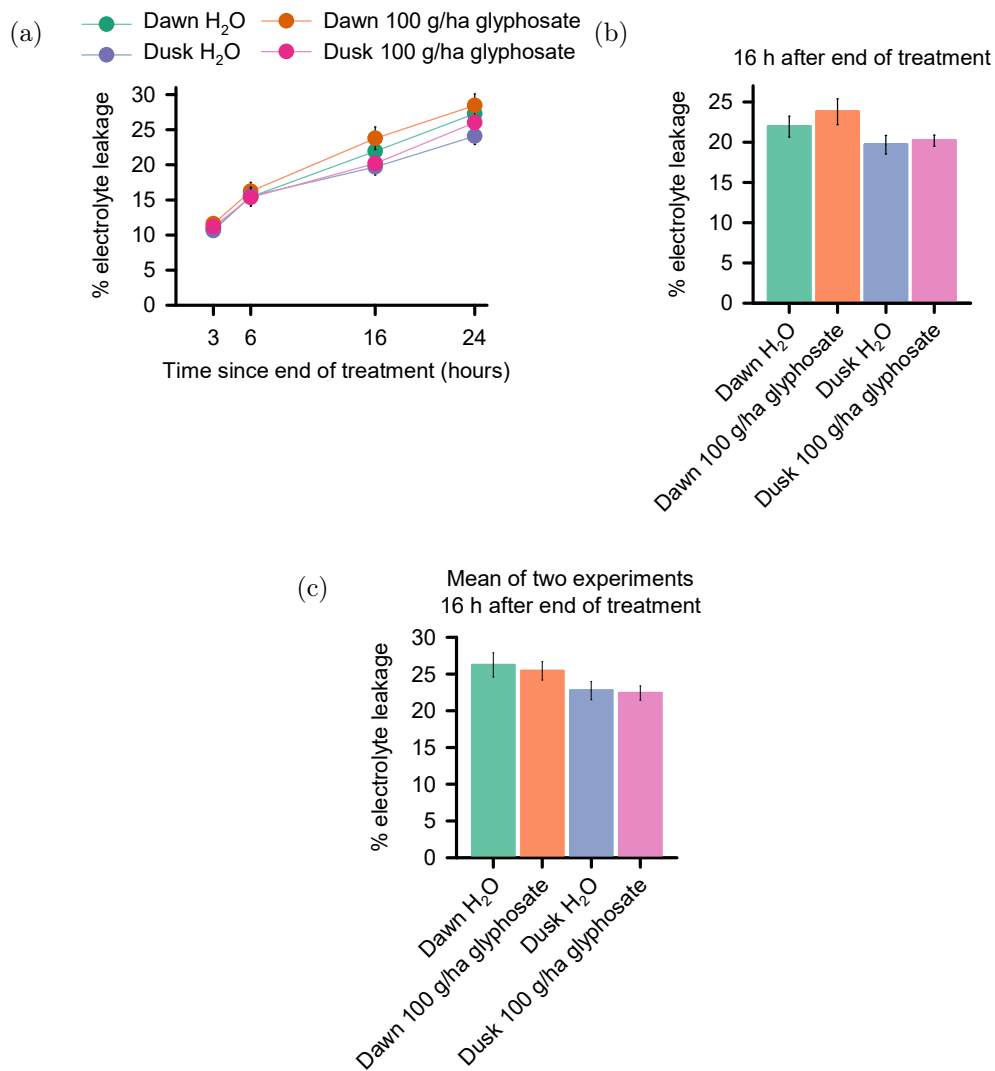


Figure 4.6.3: Glyphosate does not appear to significantly affect the extent of electrolyte leakage. (a) The percentage of electrolyte leakage was quantified in specified time points after a 6 hour 100 g/ha glyphosate application. (b) 16 h after the end of glyphosate treatment, glyphosate appeared to cause a small but not significant increase in electrolyte leakage when applied at dawn. (c) After replication, glyphosate did not significantly alter electrolyte leakage. Values are mean \pm SEM where $n = 6$ (a, b) and 12 (c). Significant differences between treatment and control per time point determined by t -test, but differences were not significant.

The initial experiment was repeated with an increased number of replicates (Fig. 4.6.3c). 16 h after the end of the glyphosate treatment at either dawn or dusk, there was no statistically significant difference in the extent of electrolyte leakage between control or glyphosate treated plants, regardless of treatment time (Fig. 4.6.3c). These data suggest that electrolyte leakage may not be an appropriate method for determining the effect of glyphosate, so was not pursued further.

4.6.3 Glyphosate alters pigment composition in a time-of-day-dependent manner

Pigment composition can change in response to stress (Lichtenthaler and Babani, 2004) and thus quantification of pigments can be used as a plant-health indicator (Lichtenthaler, 1996). Chlorosis is caused by a reduction in chlorophyll and occurs as part of cell death (Hörtensteiner and Kräutler, 2011). Glyphosate causes chlorosis, therefore, it is likely that there is an interaction between glyphosate and pigment content that could be quantified, and this has been previously identified in some plant species (Zobiolo et al., 2011; Ralph, 2000). To extend this further, it would be interesting to know whether glyphosate could affect pigment composition when applied at different times of day.

Glyphosate significantly reduced the amount of chlorophyll *a* in the seedlings (Fig. 4.6.4a). This reduction of chlorophyll *a* appeared to be greater when glyphosate was applied at dawn compared to at dusk. However, there was not a significant interaction between glyphosate treatment and treatment time (determined by two-way ANOVA). Glyphosate application had no effect on chlorophyll *b* content when applied at dawn or dusk (Fig. 4.6.4b). Glyphosate reduced the total chlorophyll content when applied at dawn, but had no effect on total chlorophyll content when applied at dusk (Fig. 4.6.4c). Glyphosate also significantly reduced the carotenoid content when applied at dawn but not at dusk (Fig. 4.6.4d). Finally, there was no effect of glyphosate application on the ratio of chlorophyll *a* to *b* at either time point (Fig. 4.6.4e). These data indicate that glyphosate has very specific effects on pigments, whereby some are reduced, and that some (e.g. chlorophyll *a* and carotenoids) could involve circadian regulation in response to glyphosate whereas the others may not.

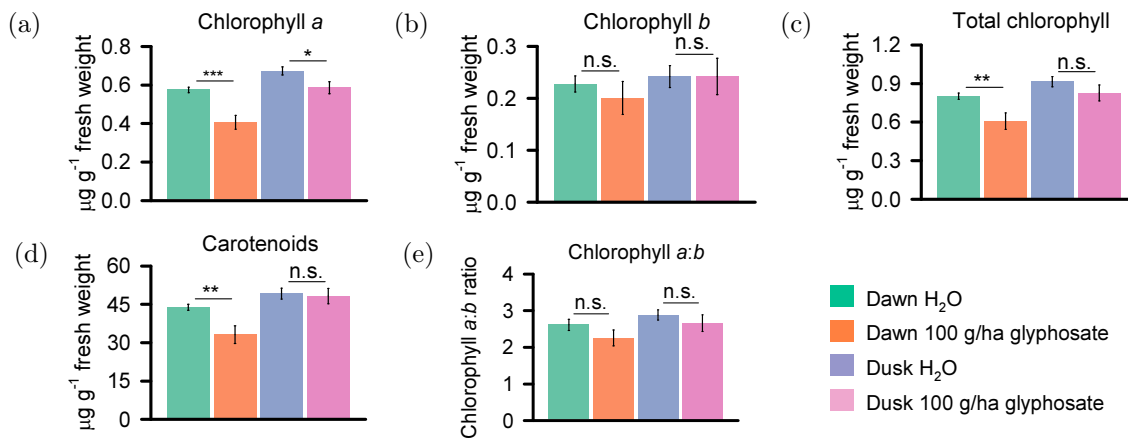


Figure 4.6.4: Glyphosate alters pigment content in a time-of-day-dependent manner. 100 g/ha glyphosate applied at dawn altered the chlorophyll *a* content to a greater extent than glyphosate applied at dusk (a). Chlorophyll *b* was not altered by glyphosate application at either application time (b). Total chlorophyll was significantly altered at dawn but not at dusk (c). Carotenoid content was significantly reduced when glyphosate was applied at dawn but not at dusk (d). Chlorophyll *a*:*b* was not affected by glyphosate application (e). Values are mean \pm SEM where $n = 6$. Significant differences between treatment and control per time point determined by *t*-test where $* = P \leq 0.05$, $** = P \leq 0.01$ and $*** = P \leq 0.001$. n.s. indicates non-significant difference.

4.7 Discussion

4.7.1 Circadian regulation in the response to glyphosate could lead to agricultural chronotherapy

Fluctuations in the effective dose of glyphosate were identified under both light-dark cycles and constant light, and this was controlled by the circadian oscillator (Figs. 4.4.7 and 4.5.3). 1.25-1.5 times more glyphosate was required at the least effective time of day to give the same response as the most effective time of day. This is an important finding since this could lead to lower concentrations of chemicals being used, but more effectively. This would mean there could be less resistance evolving, lower cost to farmers, less leaching into the environment, while having the required effect on weed species and allowing greater crop yields (Harding and Raizada, 2015; Otto et al., 2016).

In the field of chronotherapeutics, many of the highest-grossing and commonly-taken drugs have circadian-regulated targets (Zhang et al., 2014b). There are several studies from the 1960-70s that investigated circadian regulation of toxicity of pharmaceutical drugs (Ballesta et al., 2017). One of the earliest studies found that morphine has altered efficacy dependent on the time of application, where efficacy was 28% at the least effective time of day, compared to 67% at the most effective time of day (Morris and Lutsch, 1967). Therefore, the application timing is of great importance for drug efficacy, in addition to the half-life of the chemical (Zhang et al., 2014b). Identifying circadian regulation of drug efficacy or drug targets is not common practice in drug-testing (Zhang et al., 2014b). However, it is becoming more studied since inter-patient variability in response to treatment is becoming more apparent (Ballesta et al., 2017).

The same principle can be applied to plants for the application of herbicides, and also has the potential for fertiliser applications. The circadian regulation of herbicide and fertiliser targets has not been studied extensively, but the results produced here for glyphosate provide a basis for agricultural chronotherapy. It should be noted that other factors are likely to arise in the environment, such as temperature fluctuations and species specificity, that could affect this response and, as such, could be tested further.

4.7.2 Glyphosate treatment causes an increase in PCD-promoting transcripts

Glyphosate application at dawn appeared to induce PCD by up-regulating the positive regulator of PCD, *MC1* and down-regulating the negative regulator of PCD, *DAD1* (Figs. 4.6.1 and 4.6.2). The response, at least for *DAD1*, was dependent on a correctly functioning circadian oscillator. Herbicides can alter the expression of genes involved in PCD (Chen and Dickman, 2004; Graham, 2005; Zhu et al., 2009; Faus et al., 2015). *METACASPASE1* and another positive regulator of PCD, *ACCELERATED CELL*

DEATH, increased after atrazine treatment in soybean (Zhu et al., 2009). Also in soybean, a transient response of another positive cell death marker gene *HS203J* was observed in response to a different mode of action herbicide (lactofen, a protoporphyrinogen oxidase-targeting herbicide) (Graham, 2005). These previous studies, in addition to the data presented here, suggest that part of the general response to herbicides is to increase PCD through increasing the abundance of transcripts that are positive regulators of PCD. The repression of negative regulators of PCD in response to stress does not seem to be as well-studied. Further, the response of these genes to glyphosate, specifically, are not well-reported.

Both *MC1* and *DAD1* appear to have rhythmic transcript accumulation, with the phase dependant on entrainment conditions (Mockler et al., 2007). This suggests that the circadian oscillator could be responsible for gating the time of day promotion or inhibition of PCD. Pathogen resistance defence in Arabidopsis is reported to be regulated by CCA1, whereby plants have the ability to anticipate and respond best to a pathogen attacks at the time it is most likely to occur (Wang et al., 2011). However, the circadian regulation of PCD under other circumstances does not appear to be well-understood. Therefore, further work could be conducted to determine the mechanism through which glyphosate can specifically alter the expression of these genes, and more extensively the involvement of the circadian oscillator in PCD.

4.7.3 Glyphosate does not increase electrolyte leakage in these experimental conditions

Glyphosate did not affect electrolyte leakage when applied at either dawn or dusk (Fig. 4.6.3), suggesting that glyphosate does not affect membrane permeability (Cañal et al., 1990) under our experimental conditions and time scales. Electrolyte leakage occurs when plant cells die and electrolytes are able to leak out of the cell (Whitlow et al., 1992; Hatsugai and Katagiri, 2018). Previously this has been used as a method to detect the stress response to herbicides (Vanstone and Stobbe, 1977; Falk et al.,

2006). In particular, glyphosate has been shown to cause electrolyte leakage (Lee et al., 2008; Silva et al., 2014; Singh et al., 2017). However, published data are conflicting, because other studies have found that glyphosate did not cause electrolyte leakage (Wells, 1989; Cañal et al., 1990). It is likely that the concentration of glyphosate and treatment length needed to increase in order to detect a significant increase in electrolyte leakage, which could be tested in future.

4.7.4 Glyphosate increases chlorophyll degradation and causes an increase in ROS toxicity through reduced quenching by carotenoids

Glyphosate application significantly reduced chlorophyll *a*, total chlorophyll and carotenoids more when applied at dawn compared to at dusk (Fig. 4.6.4). Previous studies have found that total chlorophyll (Kitchen et al., 1981), and chlorophyll *a*, chlorophyll *b* and carotenoids were all reduced after treatment with glyphosate (Mateos-Naranjo et al., 2009; Huang et al., 2012a). It was interesting that there was no effect in this work on chlorophyll *b*, but also that the effect of glyphosate appeared to be dependent on the time of application.

Reduced levels of chlorophylls in response to herbicide treatment can either be due to increased chlorophyll degradation or decreased chlorophyll synthesis (Gomes et al., 2017). Pheophytin is a degradation product of chlorophyll (Matile et al., 1999) and can be measured to infer whether reduced levels of chlorophyll are due to degradation or reduced chlorophyll synthesis. Previously, glyphosate was shown to increase the level of pheophytin (Gomes et al., 2016), suggesting that glyphosate causes an increase in chlorophyll degradation. Therefore, this is likely to be occurring here, at least for chlorophyll *a* (Fig. 4.6.4). Chlorophyll *b* must first be converted back to chlorophyll *a* before degradation (Hörtensteiner et al., 1995; Sato et al., 2015). This requires two stages with different reductase enzymes (Sato et al., 2015). Therefore, this could account for the fact that there was no apparent degradation of chlorophyll *b*, but

there was degradation of chlorophyll *a*. Furthermore, since there is a higher level of chlorophyll *a* than chlorophyll *b* in plant tissues (Palta, 1990) this probably accounts for the significant reduction in total chlorophyll that was quantified (Fig. 4.6.4).

The abundance of chlorophylls may be under the regulation of the circadian oscillator since the concentrations have been shown to vary significantly throughout a 24 h light-dark cycle (Pan et al., 2015). Levels of chlorophyll *a* are lower at dawn compared to at dusk, whereas chlorophyll *b* content was similar at dawn and dusk (Pan et al., 2015). This rhythmicity also correlates to the regulation of genes associated with chlorophyll synthesis and the light-harvesting reactions of photosynthesis (Harmer et al., 2000). Some of these photosynthesis and chlorophyll biosynthesis genes have also been shown to be down-regulated in response to glyphosate (Faus et al., 2015). Glyphosate could potentially be able to down-regulate the synthesis of chlorophylls more at dawn compared to at dusk in addition to being able to degrade chlorophylls.

The effect of glyphosate on carotenoid content has previously been discussed in relation to the effect of glyphosate on chlorophyll fluorescence (Chapter 3.6.2). Briefly, inhibition of the shikimate pathway inhibits plastoquinone biosynthesis, which directly relates to reduced carotenoids (Gomes et al., 2017). Consequently, glyphosate causes, through a reduction in photoprotective carotenoids, photodestruction of plastid components (Kim et al., 1999; Frankart et al., 2003; Mateos-Naranjo et al., 2009). Since carotenoids are involved in quenching reactive oxygen species and triplet chlorophyll (Knox and Dodge, 1985), the results (Fig. 4.6.4) suggest that when glyphosate is applied at dawn, a reduction in carotenoids may mean that plants were less able to tolerate the ROS produced. The previous chlorophyll fluorescence data (Fig. 3.4.8) indicated that after glyphosate application at dawn, F_v/F_m and $Y(II)$ decreased, which could be consistent with decreased chlorophyll content. However, NPQ increased suggesting that in the chlorophyll fluorescence data, the reduced photosynthetic capacity could have been due to increased quenching of chlorophyll.

Chlorophylls are degraded faster than carotenoids (Lichtenthaler and Babani, 2004),

so it is interesting that carotenoid content was significantly decreased at dawn whereas chlorophyll *b* was not. However, this could further relate to the fact that chlorophyll *b* requires more steps in its degradation (Sato et al., 2015). It has also been reported that carotenoid content may be dependent on chlorophyll biosynthesis and that the two share a common precursor (Welsch et al., 2000; Bohne and Linden, 2002; Gomes et al., 2016). Therefore, if chlorophyll is reduced, carotenoids would subsequently be reduced, which could be the case in these results where chlorophyll *a* was reduced at dawn, as were carotenoids (Fig. 4.6.4).

The results from this pigment analysis appear to be logical given the mechanism through which glyphosate works. Further experimentation could be conducted to extend this work and understand it better. It is unclear how glyphosate has a time of day effect on carotenoids at dawn. As such, it would be interesting to determine whether there are specific carotenoids that are affected by glyphosate and whether there is circadian regulation of plastoquinone synthesis. Finally, it would be interesting to test the involvement of the circadian oscillator. Therefore, pigment analysis could also be conducted under constant light conditions, in addition to quantifying the effect of glyphosate on transcripts encoding pigment biosynthesis proteins. Photosynthetic pigments could also be quantified for the other herbicides of interest, since others also affect carotenoid biosynthesis.

4.7.5 The interaction between glyphosate, auxin and hypocotyl elongation is regulated by the circadian oscillator

Under both light-dark cycles of different photoperiods and under constant light, hypocotyls were most sensitive at dawn or subjective dawn and least sensitive at dusk or subjective dusk (Figs. 4.4.1, 4.4.4, 4.4.5, and 4.5.2). Hypocotyl length assays were chosen to measure the effectiveness of glyphosate applied at different times of day since this is an auxin-dependent process (Jensen et al., 1998). Furthermore, the initial ana-

lysis conducted here determined there to be a significant overlap between rhythmic, glyphosate-regulated transcripts and auxin-regulated transcripts (Section 4.3).

The fact that glyphosate efficacy appears to relate to auxin in some way is logical since glyphosate is likely to indirectly inhibit auxin biosynthesis. By inhibiting EPSPS, glyphosate prevents the formation of chorismate, from which the aromatic amino acids are produced (Steinrücken and Amrhein, 1980; Herrmann, 1995). Tryptophan, the main precursor for auxin biosynthesis requires chorismate (Jaworski, 1972). Therefore, glyphosate probably indirectly inhibits auxin biosynthesis. This has been suggested previously (Baur, 1979; Jiang et al., 2013), but the efficacy of glyphosate at different times of day has not been previously investigated in depth.

Auxin signalling and responses are circadian regulated (Covington and Harmer, 2007), as is hypocotyl elongation (Dowson-Day and Millar, 1999). Therefore, the circadian oscillator is functioning at multiple levels in this response (Dowson-Day and Millar, 1999). The light conditions determine the phase of hypocotyl elongation whereby under short days, the majority of elongation occurs at dawn (Nozue et al., 2007), and under constant (low) light, elongation occurs largely at subjective dusk with an arrest in elongation around subjective dawn (Dowson-Day and Millar, 1999). Many auxin-related transcripts are rhythmic, with a range of phases (Covington and Harmer, 2007), but it would also be useful to know whether there are rhythms of free IAA throughout a 24 h cycle.

While timing of both glyphosate sensitivity and hypocotyl elongation coincide under short day conditions, this may not be the case under the other photoperiods tested, or under constant light. It is plausible that glyphosate is inhibiting auxin biosynthesis and consequently signalling and hypocotyl elongation when applied at dawn under short day conditions. An alternative process must occur under the other light conditions if elongation is inhibited but glyphosate is still able to have the same effect on hypocotyl elongation. One suggestion is that auxin biosynthesis could always occur around dawn regardless of photoperiod, and glyphosate could still inhibit this process, but the

signalling of auxin required for hypocotyl elongation changes under different light conditions.

An interesting comparison here, is that in Chapter 3 *UGT74E2*, an auxin homeostasis gene, and *DTX1* a detoxification gene, were both up-regulated in response to glyphosate treatment to the greatest extent at the end of the day under light-dark cycles (Fig. 3.5.2). This relates to the response of hypocotyls to glyphosate because at the end of the day, hypothetically, the plant could be increasing auxin content through *UGT74E2* and causing the reduced effect on hypocotyl length. Furthermore, the plant may be able to increase detoxification of glyphosate through increasing *DTX1*, and causing a reduced effect of glyphosate at the end of the day. However, the opposite response was seen for these marker genes under constant light conditions (Fig. 3.5.4), further suggesting another mechanism is occurring under constant light to cause the same time of day response of the hypocotyls to glyphosate as under light-dark cycles.

There were differences in the magnitudes of the responses to glyphosate in the lines over-expressing components of the circadian oscillator (Fig. 4.4.1). *CCA1-ox* hypocotyls failed to elongate more than those of *TOC1-ox* and Col-0 after glyphosate treatment (Fig. 4.4.1). In general *CCA1-ox* plants are longer than Col-0 and *TOC1-ox* are shorter. Altering the circadian oscillator is known to cause severe morphological phenotypes since the oscillator has widespread regulation in physiology (Dowson-Day and Millar, 1999). *CCA1-ox* is known to cause a long hypocotyl phenotype and this is due to the lack of elongation arrest (Dowson-Day and Millar, 1999). Since long hypocotyl phenotypes have a greater ability to elongate, it is not surprising that a chemical causing elongation arrest causes a more drastic reduction in length, as seen in these data (Fig. 4.4.1). Aside from understanding the mechanism behind the link between glyphosate and auxin (tested and discussed in more depth in the following chapter), further experiments could be conducted under conditions where hypocotyl elongation is promoted further where a response to glyphosate may be more pronounced, for example under low light or a low R:FR.

4.8 Conclusions

The research in this chapter initially identified sets of transcripts that are glyphosate-regulated and overlap with rhythmic transcriptomes. The transcripts that were up-regulated in response to glyphosate were mainly phased to dawn. This coincided with the greatest sensitivity of the auxin-dependent hypocotyl elongation to glyphosate occurring at dawn, and this response was dependent on the circadian oscillator. One of the key findings was that the minimum effective dose of glyphosate depends on the application time of day, and this opens the possibility of the field of agricultural chronotherapy. Other markers of cell death also support the fact that glyphosate was most effective at dawn, therefore the response is not solely due to auxin involvement. Further work is required to elucidate the mechanism through which glyphosate interacts with auxin, which is reported in the following chapter.

Chapter 5

Circadian regulation of a glyphosate response is potentially due to rhythmic auxin signalling

5.1 Introduction

Glyphosate inhibits EPSPS in the shikimate pathway, preventing proper pathway function (Fig. 1.6.2) (Steinrücken and Amrhein, 1980). The final product of the shikimate pathway is chorismate, from which the aromatic amino acids are produced (Fig. 1.6.3) (Herrmann, 1995). Consequently, glyphosate indirectly inhibits aromatic amino acid biosynthesis (Fig. 1.6.3) (Jaworski, 1972). Furthermore, tryptophan is the precursor for indole-3-acetic acid (IAA; auxin) biosynthesis in *Arabidopsis* (Fig. 1.6.3), the primary plant auxin (Zhang et al., 2008; Tao et al., 2008; Mano and Nemoto, 2012). As such, it is likely that glyphosate down-regulates the production of auxins. This has been reported previously in corn and soybean, but not in *Arabidopsis* (Baur, 1979; Jiang et al., 2013).

The circadian oscillator is involved in many aspects of auxin signalling and response (Covington and Harmer, 2007). For example, auxin signal transduction, regu-

lation of auxin-induced genes and exogenous auxin-induced growth are all controlled, and gated, by the circadian oscillator (Covington and Harmer, 2007). An oscillator-regulated transcription factor, REVEILLE1, has been shown to be responsible for circadian regulation of free auxin levels (Rawat et al., 2009), associated with auxin biosynthesis, providing further association between auxin and circadian regulation. Additionally, hypocotyl elongation is circadian-regulated (Nozue et al., 2007). It was also determined that there was a significant overlap between transcripts that were rhythmic, auxin- and glyphosate-regulated, and that glyphosate had an effect on the auxin-dependent process of hypocotyl elongation (Chapter 4).

Overall, these concepts led to the formation of the hypothesis that circadian regulation of auxin biosynthesis and signalling underlies the gated response to glyphosate applied at different times of day. In order to test this hypothesis, the aims of the research in this chapter were to elucidate the mechanism behind the time of day sensitivity to glyphosate in Chapter 4, and to determine the extent of different aspects of auxin biosynthesis and signalling in these responses.

5.2 Glyphosate appears to alter hypocotyl elongation through inhibition of auxin signalling

Since there is an intersection between glyphosate, circadian, and auxin response genes (Chapter 4), it was hypothesised that glyphosate could have been affecting auxin biosynthesis because glyphosate indirectly inhibits tryptophan biosynthesis. Experiments utilising auxin biosynthesis and transport inhibitors, analogs and transport mutants were conducted to further elucidate the effect of glyphosate in a time-of-day-dependent manner.

5.2.1 Hypocotyls are most sensitive to the auxin biosynthesis inhibitor L-kynurenine at dawn

L-kynurenine (kyn) is a small molecule that decreases auxin biosynthesis (He et al., 2011). Kyn competitively inhibits the activity of the TRYPTOPHAN AMINOTRANSFERASE OF ARABIDOPSIS1 (TAA1), TRYPTOPHAN AMINOTRANSFERASE RELATED1 (TAR1) and TAR2 proteins in the indole-3-pyruvic acid (IPyA) pathway of auxin biosynthesis (He et al., 2011). Since glyphosate may reduce auxin biosynthesis through inhibition of tryptophan biosynthesis (Baur, 1979; Jiang et al., 2013), upstream of the IPyA pathway, we reasoned that the response of hypocotyls to kyn may respond in the same way as glyphosate.

The first experiment tested the concentration of kyn that is required to give the same attenuation in hypocotyl length as glyphosate. Treatment occurred at dawn to determine the concentration needed to give the same magnitude in reduction as glyphosate did at its most effective time point. 300 μM kyn caused a significant reduction (approximately 14% reduction) in hypocotyl length compared to the control (Fig. 5.2.1a). However, the change in length was not of the same magnitude as the change in length of the hypocotyl after glyphosate treatment at that time (26% reduction). Therefore, the highest concentration, 500 μM , of kyn was used for further experiments because this resulted in a shorter hypocotyl.

Next, kyn was applied at different times of day to determine the extent of similarity to glyphosate time-of-day sensitivity (Fig. 5.2.1b). Kyn caused a significant reduction in hypocotyl length when applied at dawn and 6 h after dawn, but not at any other time point (Fig. 5.2.1b). The treatment at dawn appeared the most effective as it caused a greater inhibitory effect on hypocotyl length than the treatment later in the day. A two-way ANOVA determined no significant interaction between kyn treatment and the time of treatment.

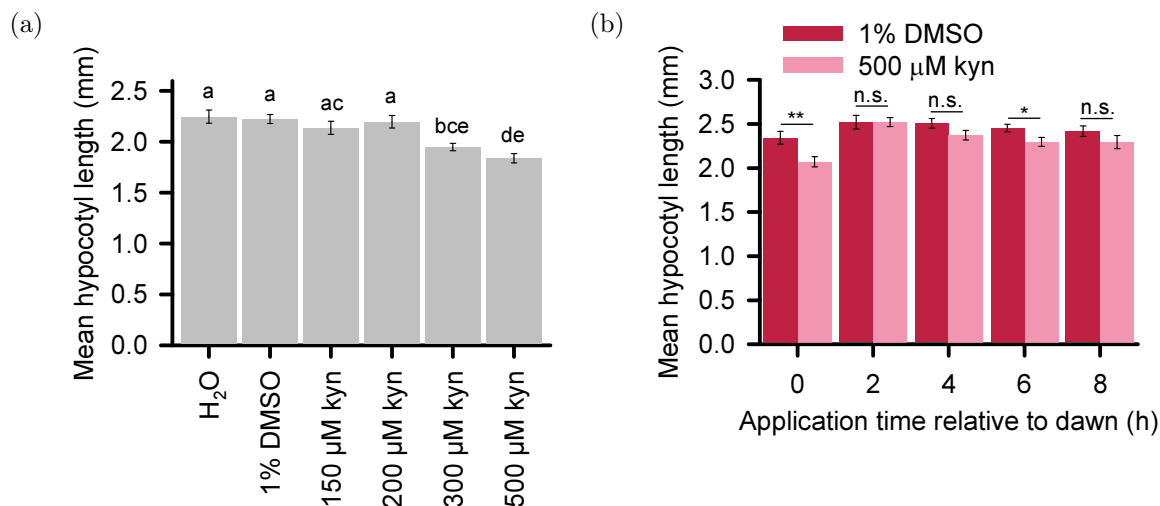


Figure 5.2.1: The IAA biosynthesis inhibitor L-kynurenine inhibits hypocotyl elongation. (a) 300 μM L-kyurenine (kyn) was required to significantly attenuate hypocotyl length. (b) 500 μM kyn applied at different times of the day caused the most inhibition of hypocotyl elongation when applied at dawn. Values are mean ± SEM where $n = 20$. (a) Lettering indicates significant difference between values determined by one-way ANOVA followed by tukey post-hoc test. (b) Asterisks indicate significant difference between control and treated value, calculated by t -test where $* = P \leq 0.05$, $** = P \leq 0.01$ and n.s. = no statistically significant difference.

Kyn had a similar effect on the hypocotyl as glyphosate, and while the time of day sensitivity was reduced, it seemed that dawn may have been the most sensitive to kyn application, as it was for glyphosate applications. This could mean that there are similarities in the way in which the two chemicals function.

5.2.2 Exogenous auxin overcomes the effect of glyphosate

Since the effect of kyn can be overcome with exogenous auxin (He et al., 2011) and we hypothesise that glyphosate may be acting in a similar way to kyn, we thought it would be interesting to test whether the effect of glyphosate could be overcome with the addition of an exogenous auxin. To do this, we used the synthetic auxin NAA, a more stable analog of IAA (Flasiński and Hąc-Wydro, 2014; Dunlap et al., 1986).

Firstly, a concentration of NAA that could rescue the effect of kyn upon hypocotyl length was determined (Fig. 5.2.2a). 1 μM -10 μM NAA caused significantly longer hypocotyls compared to the kyn-only treatment (Fig. 5.2.2a). Addition of 50 μM NAA caused the hypocotyl to be significantly longer than the kyn-only treatment, and the same length as the controls. 100 μM NAA increased the hypocotyl length to greater than that of the controls, therefore, this concentration was too high (Fig. 5.2.2a). Subsequent experiments were conducted with 50 μM NAA.

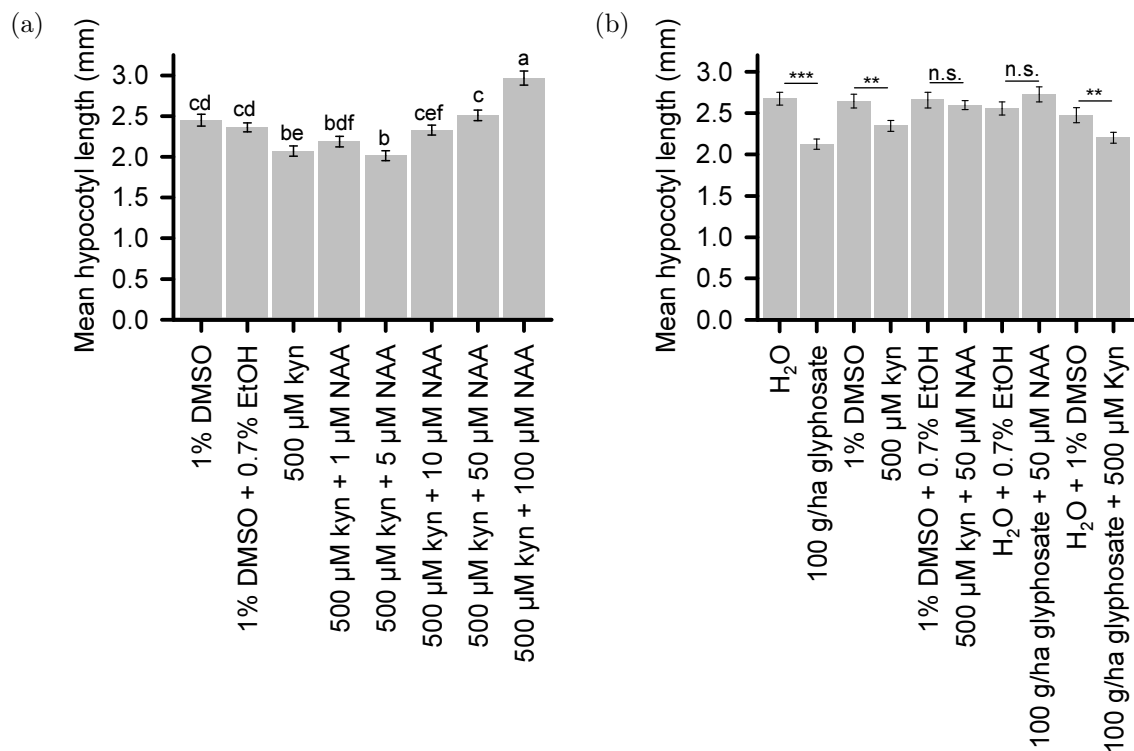


Figure 5.2.2: Exogenous auxin overcomes the effect of glyphosate. (a) 50 μM NAA prevented the inhibitory effect of 500 μM L-kynurenine (kyn) when applied simultaneously. (b) 50 μM NAA prevented the inhibitory effect of 100 g/ha glyphosate on hypocotyl length. Furthermore, glyphosate and kyn did not appear to have an additive effect. Treatments were applied at dawn on day 3 and hypocotyls were measured on day 7. Values are mean \pm SEM where $n = 19-20$. Significant differences between means were calculated using (a) one-way ANOVA followed by Tukey post-hoc test, and (b) t -test between treatment and control. Significant differences shown by different letters or asterisks were ** = $P \leq 0.01$, *** = $P \leq 0.001$ and n.s. = no statistically significant difference.

Next, the combined effect of NAA and glyphosate were examined (Fig. 5.2.2b). The addition of NAA overcame the inhibitory effect on hypocotyl length seen with glyphosate application alone (Fig. 5.2.2b). Therefore, an exogenous auxin was able to overcome the effect of glyphosate. The application of glyphosate in combination with kyn was also tested (Fig. 5.2.2b). There was no additive effect of the two chemicals, suggesting that they could be involved in the same pathway. If the chemicals operated on different pathways, an additive effect may be expected, and the length of the hypocotyl could have been reduced to a greater extent than the length observed for each chemical individually.

5.2.3 Auxin transport is required for the rhythmic response to glyphosate

To test the requirement of auxin transport in the response of the hypocotyl to glyphosate, the response to glyphosate was compared to that of the polar auxin transport inhibitor NPA (Ching et al., 1956; Hertel et al., 1983). 100 μ M NPA inhibited hypocotyl elongation only when applied at dawn (Fig. 5.2.3), and not after the dusk application. There was a significant interaction between the effect of NPA treatment and the time of treatment (two-way ANOVA, $F(1, 76) = 5.7$, $P = 0.02$). This response was the same as the effect of glyphosate application at the two treatment times, indicating a possible similar mechanism.

Since glyphosate applied at different times of day had the same effect on the hypocotyl as NPA, we wanted to compare the response in an auxin transport mutant. This was particularly interesting as one of the key proteins involved in polar auxin efflux in the hypocotyl, PIN-FORMED3 (PIN3) (Keuskamp et al., 2010; Rakusová et al., 2011; Ding et al., 2011), was also identified as one of the rhythmic and glyphosate regulated transcripts (Table 4.3.2). *pin3-3* hypocotyl elongation was inhibited significantly when glyphosate was applied 2 h after dawn, but not at any other time of application (Fig. 5.2.3b).

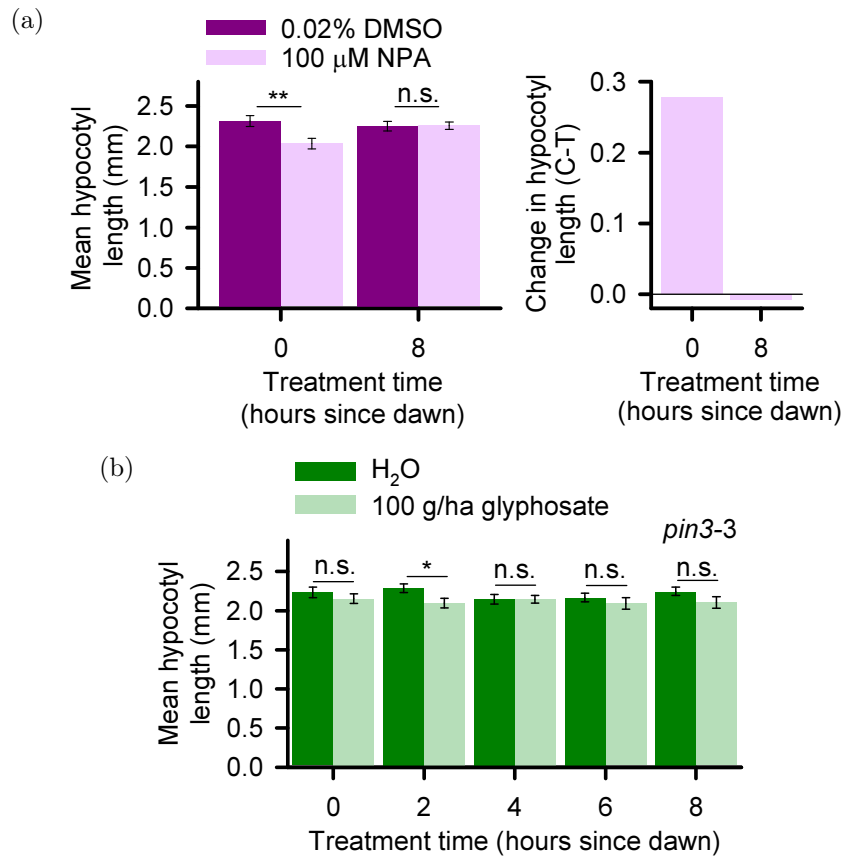


Figure 5.2.3: Glyphosate may have an indirect effect through auxin transport. (a) Application of the auxin transport inhibitor NPA was most effective at reducing hypocotyl length when applied at dawn. Figure shows mean hypocotyl length of control and treated plants per time point (left) and change in hypocotyl length caused by NPA (right). (b) Auxin transport mutant *pin3-3* had reduced sensitivity to glyphosate applications. Values are mean \pm SEM where $n = 20$. Asterisks indicate significant difference between control and treated value, calculated by *t*-test where $* = P \leq 0.05$, $** = P \leq 0.01$ and n.s. = no statistically significant difference.

A two-way ANOVA did not determine there to be an interaction between glyphosate application and the time of application. This result suggests that correct auxin efflux via PIN3 is required for the response of wild type *Arabidopsis* hypocotyls to glyphosate, with particular sensitivity when applied at dawn.

Another herbicide, diflufenzopyr (DFF), is reported to inhibit auxin transport (Wehtje, 2008). Therefore, we wanted to know whether the same time of day sensitivity existed for DFF as it did for NPA and also glyphosate (Fig. 5.2.4). DFF application to Col-0 at all three time points caused a significant reduction in the length of the

hypocotyl (Fig. 5.2.4a), but the greatest change in hypocotyl length was observed at dawn. The sensitivity decreased throughout the day. There was a significant interaction between DFF treatment and the time of treatment (two-way ANOVA, $F(2, 114) = 8.52$, $P < 0.001$). Therefore, plants had the same time of day sensitivity to DFF as to glyphosate.

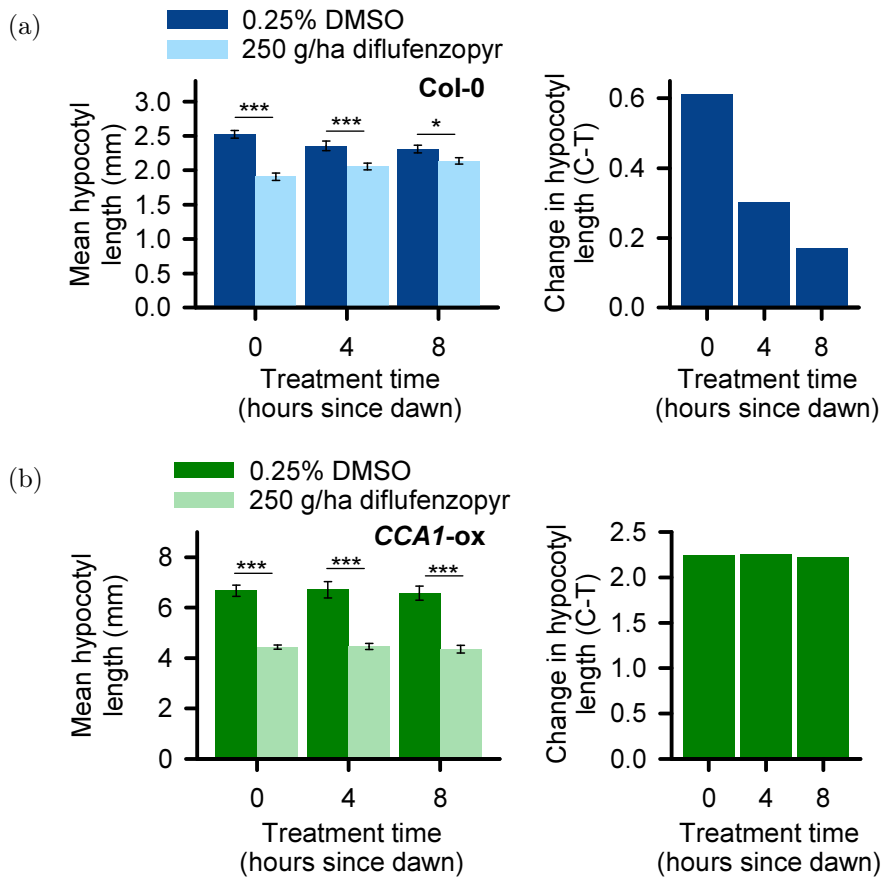


Figure 5.2.4: The response of Arabidopsis to the auxin transport-inhibiting herbicide diflufenzopyr is time of day-dependent. (a) Col-0 hypocotyls treated with 250 g/ha diflufenzopyr (DFF) were most sensitive at dawn, and least sensitive at dusk. (b) CCA1-ox hypocotyls had the same response to DFF regardless of treatment time. Figures show mean hypocotyl length of control and treated plants per time point (left) and change in hypocotyl length caused by DFF (right). 0.25% DMSO was used as a carrier control. Values are mean \pm SEM where $n = 20$. Asterisks indicate significant difference between control and treated value, calculated by t -test where $* = P \leq 0.05$ and $*** = P \leq 0.001$. Data collected through supervision of undergraduates A. Jackson and F. Schanschweif.

Conversely, DFF applied to *CCA1-ox* caused a significant attenuation of hypocotyl elongation at all treatment times (Fig. 5.2.4b), and there was not a significant interaction between treatment and time. This suggests that a properly functioning circadian oscillator was required for the response to DFF seen in the wild type plants. Furthermore, the response of glyphosate is similar to that of a known auxin-transport inhibiting herbicide.

5.2.4 PhyB mutation does not confer resistance to glyphosate

Previously published data concluded that a phytochromeB (phyB) mutation was responsible for glyphosate-resistance (Sharkhuu et al., 2014). We thought this was interesting since phyB is involved in light perception and subsequently inhibits the auxin biosynthesis pathway (Xu et al., 2018). Since a similar same time of day response was reported with *phyB* as that in our results, we wanted to test the response of *phyB* to glyphosate using our hypocotyl elongation method.

The wild type ecotype *L. er* had the same time of day sensitivity to glyphosate as Col-0 (Fig. 5.2.5a). Glyphosate treatments at dawn caused the greatest inhibition of hypocotyl elongation, and treatments later in the day were less effective. Mutation of phyB did not alter the time of day sensitivity to glyphosate, where glyphosate application at dawn remained the most sensitive (Fig. 5.2.5b). The effect of treatment was dependent on the time for both genotypes (two-way ANOVA, *L. er*: $F(2, 113) = 7, P = 0.001$, *phyB*: $F(2, 114) = 6, P = 0.004$). Therefore, phyB does not appear to be involved in the time of day sensitivity to glyphosate, and while hypocotyls were overall longer in *phyB*, the plants remained sensitive to glyphosate.

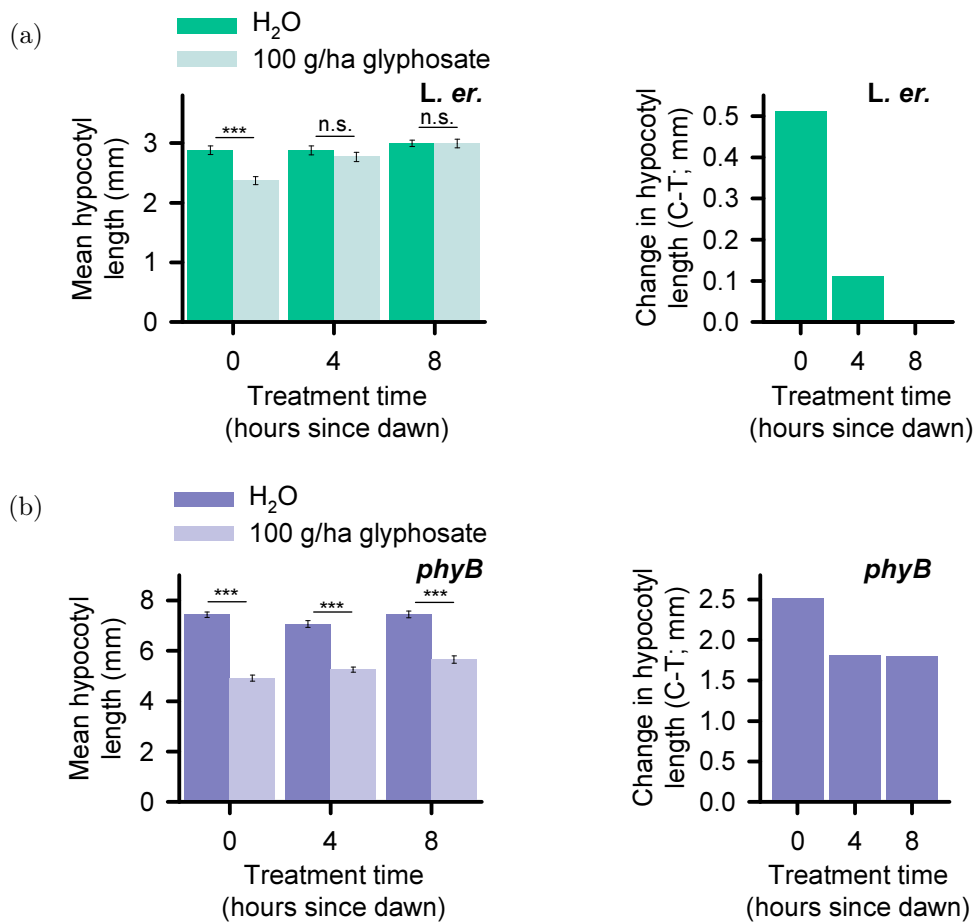


Figure 5.2.5: Mutation in *phyB* does not confer glyphosate resistance. (a) *L. er* ecotype was most sensitive to 100 g/ha glyphosate at dawn, and decreased in sensitivity throughout the day. (b) *phyB* plants were susceptible to 100 g/ha glyphosate and had the same time of day sensitivity as wild type plants. Values are mean \pm SEM where $n = 19-20$. Asterisks indicate significant difference between control and treated value, calculated by *t*-test where *** = $P \leq 0.001$ and n.s. indicates no significant difference.

5.3 Glyphosate has variable effects on DR5::GUS

DR5::GUS plants contain seven repeats of an auxin-responsive element, a 35S promoter and the β -glucuronidase (GUS) reporter gene (Ulmasov et al., 1997). The auxin-responsive element binds auxin responsive factors and responds only to active auxins (Ulmasov et al., 1997). Histochemical staining of the plant allows visualisation of this readout and it is possible to infer the quantity of free auxin (Tao et al., 2008). Since glyphosate may inhibit IAA biosynthesis, we hypothesised that glyphosate may decrease the amount of free auxin, and as such, this could be visualised in DR5::GUS plants.

Histochemical staining of DR5::GUS seedlings 5 days after glyphosate treatment determined that glyphosate can prevent GUS accumulation (Fig. 5.3.1a, right). In control plants (Fig. 5.3.1a, left), blue staining indicated the presence of free auxin in the apical meristem and hypocotyl of seedlings. The synthetic DR5 promoter is auxin-responsive, therefore this result suggests that in glyphosate-treated plants there was a lack of auxin. However, these results were variable and inconsistent between experimental repeats.

To further ascertain whether glyphosate had an effect on GUS and to eliminate the possibility that results from inconsistency derived from GUS staining, the abundance of *GUS* transcript was measured (Fig. 5.3.1b). Application of glyphosate at dawn had no effect on *GUS* transcript abundance (Fig. 5.3.1b), but the positive control (NAA application) increased markedly. Application of glyphosate at dusk appeared to have a small but not significant decrease on *GUS* transcript abundance (Fig. 5.3.1b), whereas NAA application at dusk significantly increased *GUS* transcript abundance. These results indicated that glyphosate did not have an effect on *GUS* transcript accumulation.

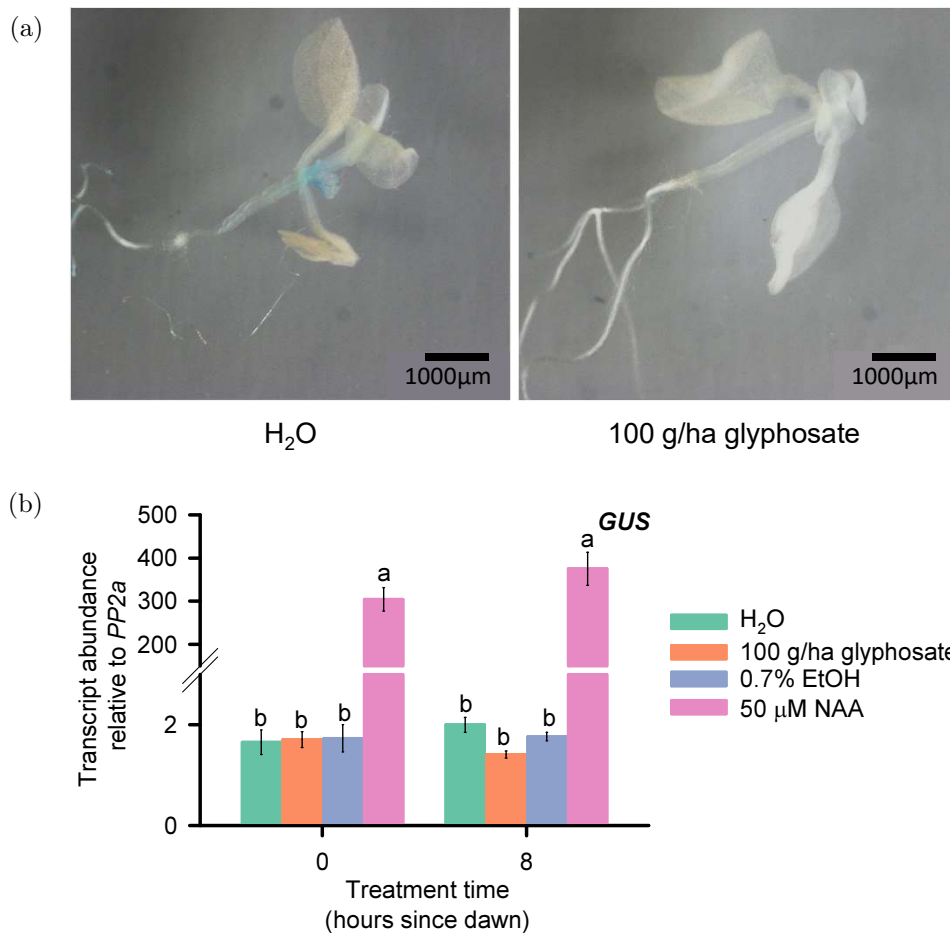


Figure 5.3.1: Glyphosate had an inconsistent effect on GUS. (a) Histochemical staining of *DR5::GUS* was reduced after glyphosate treatment. (b) *GUS* transcript abundance was not significantly reduced by glyphosate treatment regardless of treatment time. Values are mean \pm SEM where $n = 8$ (a) and 8-9 (b, average of three independent experiments). Significance determined by one-way ANOVA within each time point followed by Tukey post-hoc test.

5.4 Glyphosate does not alter *DR5::VENUS* fluorescence or transcript accumulation

VENUS is a type of fast maturing yellow fluorescent protein that can be used as a reporter (Brunoud et al., 2012). Two *VENUS* reporters are commonly used to study auxin abundance and activity: *DR5::VENUS* and *DII-VENUS*. The *DR5::VENUS* reporter contains the *DR5* synthetic promoter fused to three copies of *VENUS* (Heisler et al., 2005). Therefore, plants fluoresce when the auxin-responsive element is ex-

pressed. The DII-VENUS sensor contains the auxin interaction domain (domain II; DII) of Aux/IAA genes fused to VENUS (Brunoud et al., 2012). When auxin binds to the DII domain of Aux/IAs, they are targeted for degradation by ubiquitin (Brunoud et al., 2012). Hence, DII-VENUS is degraded in the presence of auxin (Brunoud et al., 2012). It was hypothesised that if glyphosate was interfering with auxin biosynthesis, the levels of auxin within the plants may change, and that this could be visualised through the use of the fluorescent reporters.

Preliminary tests with the fluorescent reporters were conducted in the leaf, where there was a greater surface area and more cells compared to the hypocotyl. In the control H₂O-treated leaves, green spots indicate DII-VENUS fluorescence in cells (Fig. 5.4.1, top left). After treatment with the synthetic auxin NAA, DII-VENUS fluorescence was depleted (Fig. 5.4.1, top right). After treatment with the auxin biosynthesis inhibitor kyn, visible DII-VENUS fluorescence increased relative to the control leaf (Fig. 5.4.1, bottom left). In response to glyphosate, there appeared to be slightly fewer areas of DII-VENUS fluorescence compared to the control (Fig. 5.4.1, bottom right). DII-VENUS responded as expected with NAA or kyn treatment, but suggested that there was no effect of glyphosate on auxin using this reporter.

The DR5::VENUS leaf treated with H₂O had areas of visible VENUS fluorescence, indicating areas where auxin was present (Fig. 5.4.2, top left). Addition of NAA markedly increased VENUS fluorescence compared to the control leaf, indicating an increase in auxin (Fig. 5.4.2, top right). Application of kyn to the leaf appeared to decrease fluorescence, indicating that kyn was inhibiting auxin (Fig. 5.4.2, bottom left). The leaf that was exposed to glyphosate appeared to fluoresce less than the leaf treated with NAA, but more than the leaf treated with kyn (Fig. 5.4.2, bottom right). The fluorescence in the glyphosate-treated leaf was comparable to the level of fluorescence in the H₂O-treated leaf, suggesting glyphosate did not have a significant effect on the auxin levels in the leaf under these experimental conditions.

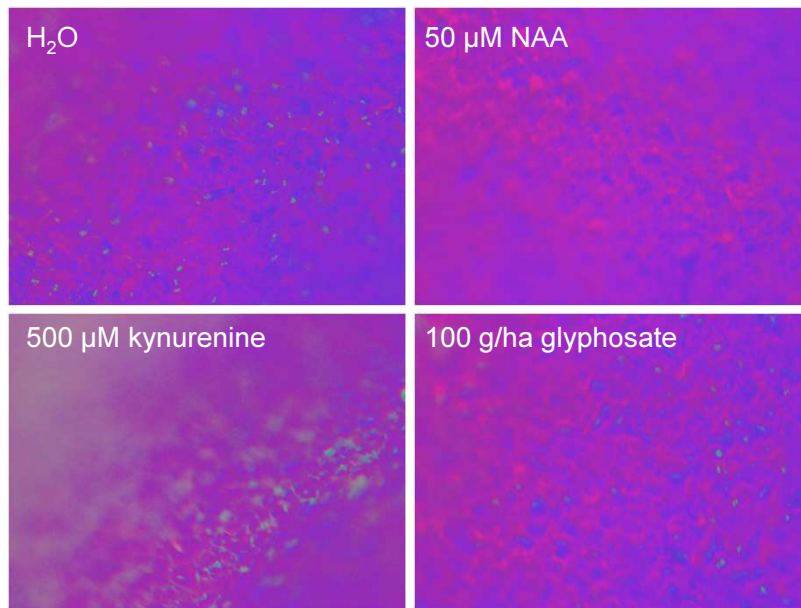


Figure 5.4.1: Glyphosate appeared to reduce DII-VENUS fluorescence in the leaf. 50 μM NAA decreased DII-VENUS fluorescence compared to the H_2O control and 500 μM kyn increased DII-VENUS fluorescence. However, 100 g/ha glyphosate may have also decreased DII-VENUS fluorescence compared to the H_2O control. Image brightness and contrast adjusted to show fluorescence; all images were adjusted in exactly the same way. Images are all to scale.

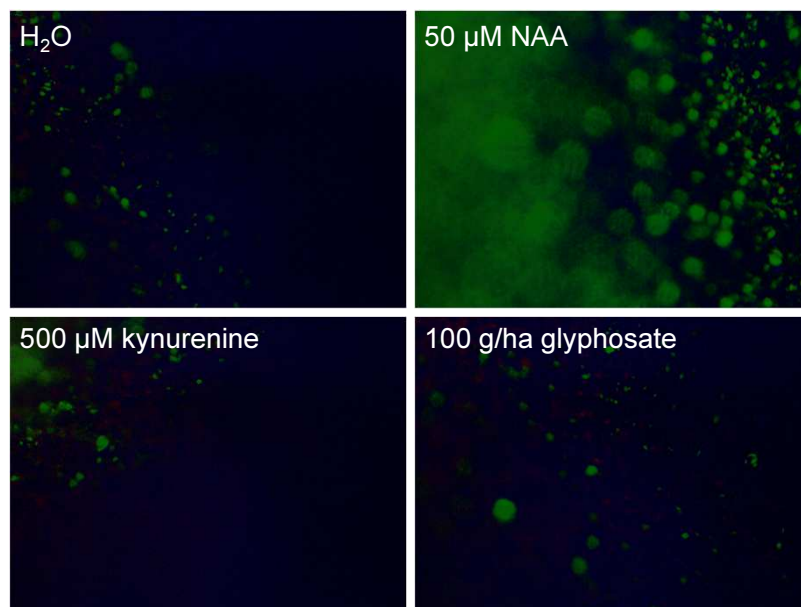


Figure 5.4.2: Glyphosate did not have a clear effect on DR5::VENUS in the leaf 50 μM NAA increased DR5::VENUS fluorescence compared to the H_2O control and 500 μM kyn appeared to decrease DR5::VENUS fluorescence. 100 g/ha glyphosate did not appear to have a clear visible effect on DR5::VENUS fluorescence compared to the H_2O control. Image brightness and contrast adjusted to show fluorescence. All images were adjusted in exactly the same way. Images are all to scale.

Since fluorescence of DR5::VENUS was much brighter than DII-VENUS, this was used to test the effect of glyphosate in the hypocotyl. The intensity of DR5::VENUS fluorescence in hypocotyls appeared similar after treatment with H₂O, EtOH, DMSO, kyn and glyphosate (Fig. 5.4.3a). Quantification of the fluorescence intensity from the images supported this (Fig. 5.4.3b). Application of NAA to the hypocotyl increased the intensity of DR5::VENUS fluorescence (Figs. 5.4.3a, 5.4.3b). The treatments had the same effect on DR5::VENUS regardless of treatment time. The results suggested that only application of NAA affects the level of auxin in the seedlings.

VENUS transcript abundance was also quantified (Brunoud et al., 2012). There was no difference between the abundance of *VENUS* transcripts after H₂O, glyphosate, EtOH, DMSO, or kyn treatments applied at dawn (Fig. 5.4.3c). Although kyn did appear to reduce *VENUS* abundance, this was not a statistically significant result (Fig. 5.4.3c). Application of the exogenous auxin, NAA, caused a significant increase in *VENUS* transcript abundance (Fig. 5.4.3c). Glyphosate application at dusk also had no effect on *VENUS* transcript abundance compared to the control (Fig. 5.4.3c).

These results suggest that glyphosate did not have a quantifiable effect on auxin reporters. However, kyn also had no significant effect on these reporters, which had been seen in other experimental methods. It was expected that glyphosate may have the same effect as kyn. As such, it may be that these reporters are not appropriate for detecting these changes in the predicted reduction in auxin, at least over these timescales.

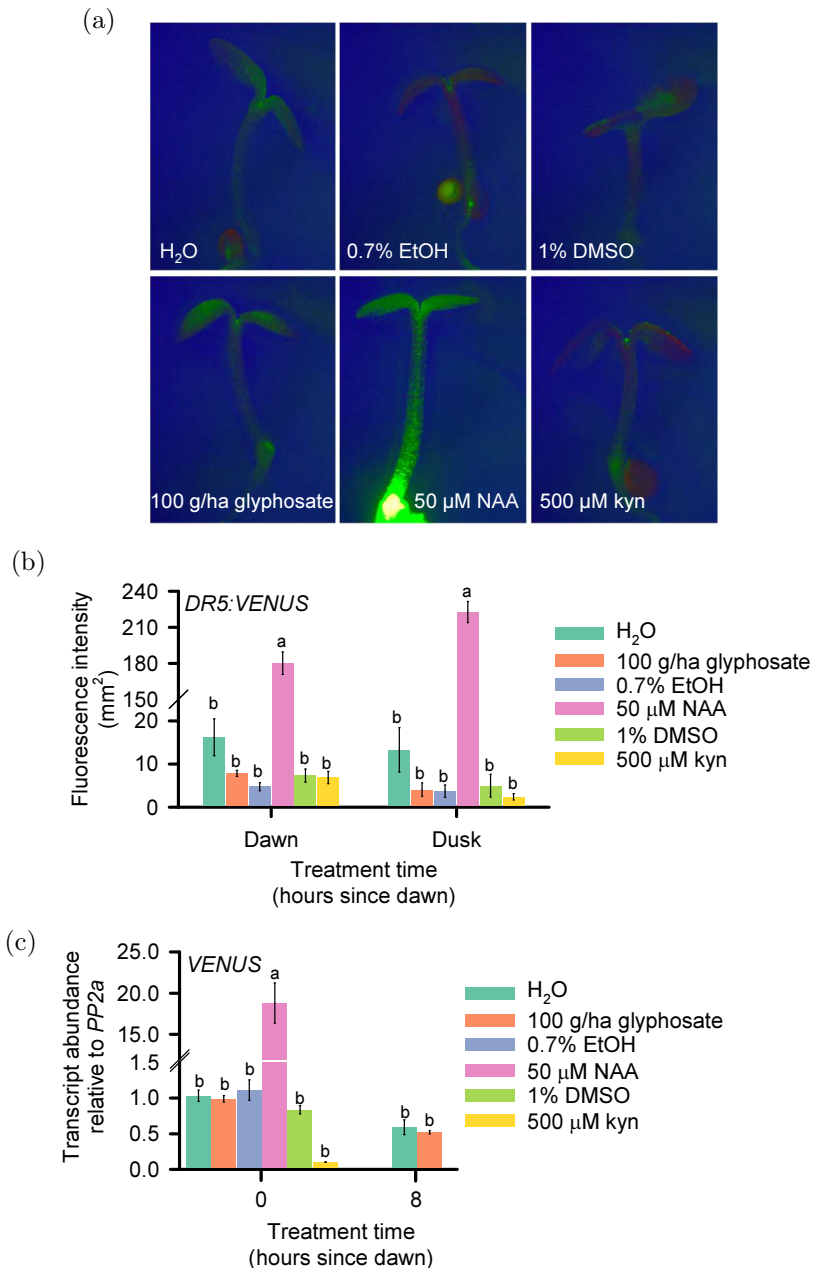


Figure 5.4.3: Glyphosate did not have a significant effect on DR5::VENUS in the hypocotyl when measured through fluorescence intensity or VENUS transcript abundance. (a) Example fluorescence images of DR5::VENUS hypocotyls that had been treated at dawn with either H₂O, 0.7% EtOH, 1% DMSO, 100 g/ha glyphosate, 50 μM NAA or 500 μM kyn. All images are to the same scale. Image brightness and contrast was adjusted to show fluorescence, all images were adjusted identically. (b) 100 g/ha glyphosate or 500 μM kyn did not cause a significant reduction in DR5::VENUS fluorescence intensity in the hypocotyl, whereas 50 μM NAA caused a significant increase in DR5::VENUS fluorescence intensity, regardless of treatment time. Image intensity derived from the images in (a). (c) 100 g/ha glyphosate or 500 μM kyn did not cause a significant reduction in VENUS transcript abundance, whereas 50 μM NAA caused a significant increase in VENUS transcript abundance. Tissue samples taken from DR5::VENUS seedlings. Values are mean ± SEM where $n = 5$ (a, b) and 3 (c). Significance determined by one-way ANOVA within each time point and Tukey post-hoc test. Lettering indicates significance.

5.5 Glyphosate has time-of-day-dependent effects on auxin-related transcripts

To further elucidate the interaction between glyphosate and auxin, I investigated the effect of glyphosate on auxin-related transcripts. Several genes were selected that are involved in different aspects of auxin biosynthesis, perception, transport and signalling. Several genes, such as *INDOLE-3-ACETIC ACID INDUCIBLEs* (*IAAs*) and *GRETCHEN HAGEN-3s* (*GH3s*), exhibit rapid responses to auxin and, as such, are well-known auxin-inducible genes (Quint and Gray, 2006; Gao et al., 2015). YUCCA (*YUC*) proteins are involved in the auxin biosynthesis pathway where they oxidise IPyA to IAA (Dai et al., 2013; Nishimura et al., 2014). Any decreases in these transcripts could indicate that glyphosate was reducing auxin biosynthesis, or vice versa. PHYTOCHROME-INTERACTING FACTOR4 (*PIF4*) binds to phyB (Huq and Quail, 2002), and is known to regulate auxin levels (Franklin et al., 2011). phyB has previously been reported to be involved in the resistance to glyphosate (Sharkhuu et al., 2014). EXPANSIN8 (*EXPA8*) is involved in cell elongation in the hypocotyl (Gangappa and Kumar, 2017) and PIN3 is one of the PIN proteins involved in auxin efflux within the hypocotyl (Friml et al., 2002). Therefore the altered abundance of these genes could be responsible for the morphological changes in the hypocotyl in response to glyphosate. The abundance of these transcripts was quantified after glyphosate treatment at either dawn or dusk (Fig. 5.5.1 and 5.5.2).

Glyphosate application had no effect on *YUC8* transcript abundance regardless of treatment time (Fig. 5.5.1a). *YUC9* transcript abundance was not altered by glyphosate treatment at dawn, but there was a significant increase in *YUC9* transcript abundance when glyphosate was applied at dusk (Fig. 5.5.1b). There was a significant interaction between glyphosate treatment and treatment time for *YUC9* transcript abundance (two-way ANOVA, $F(1, 5) = 33.8$, $P = 0.002$). There was a significant decrease in *IAA29* transcript abundance when glyphosate was applied at dawn, but a significant increase in *IAA29* transcript abundance after glyphosate was applied at

dusk (Fig. 5.5.1c). There was a significant interaction between glyphosate treatment and treatment time for *IAA29* transcript abundance (two-way ANOVA, $F(1, 6) = 49.2$, $P < 0.001$). There was no effect of glyphosate on *GH3.3* transcript abundance when applied at dawn, but a significant increase in *GH3.3* transcript abundance when glyphosate was applied at dusk (Fig. 5.5.1d). Therefore, the effect of the glyphosate treatment was dependent on the application time (two-way ANOVA, $F(1, 5) = 62.7$, $P < 0.001$). These genes involved in auxin biosynthesis and signalling generally had a similar response where there was no effect, or a decrease in transcript abundance when glyphosate was applied at dawn, but an increase in the transcript abundance of these genes when applied at dusk (aside from *YUC8*).

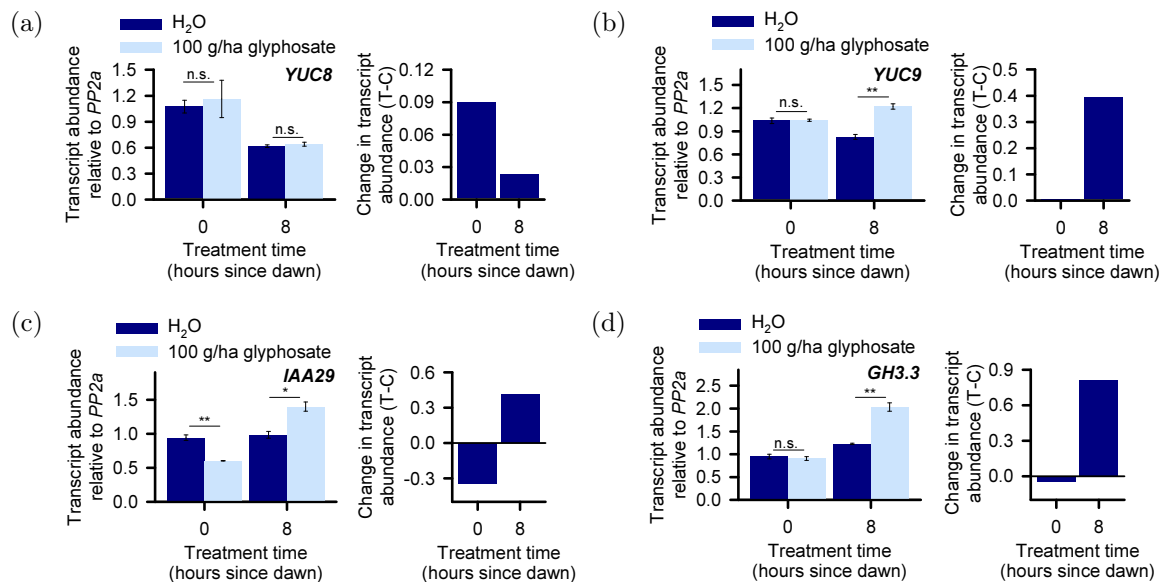


Figure 5.5.1: Glyphosate changes the transcript abundance of auxin signalling-related genes. 100 g/ha glyphosate had no significant effect on (a) *YUC8*. 100 g/ha glyphosate caused time of day-dependent changes in (b) *YUC9*, (c) *IAA29* and (d) *GH3.3*. Figures show mean transcript abundance for control and glyphosate treated samples relative to *PP2a* reference transcripts (left), and mean change in transcript abundance between control and treated samples (right). Values are mean \pm SEM where $n = 2-3$. Asterisks indicate significant difference between control and treated value, calculated by t -test where * = $P \leq 0.05$, ** = $P \leq 0.01$ and n.s. indicates no significant difference.

There was an increase in *PHYB* transcript abundance in response to glyphosate applied at either dawn or dusk (Fig. 5.5.2a). The response at both time points had a similar magnitude and, as such, there was no effect of treatment time in the response of *PHYB* to glyphosate treatment. *PIF4* transcript abundance decreased in response to glyphosate treatment at dawn, but there was no effect on *PIF4* transcript abundance to glyphosate applied at dusk (Fig. 5.5.2b). The time of day of the treatment was responsible for the difference in the magnitude of the response to glyphosate (two-way ANOVA, $F(1, 8) = 41.5$, $P < 0.001$). There was a small but significant decrease in *EXPA8* transcript abundance when glyphosate was applied at dawn, but no effect of glyphosate treatment on *EXPA8* transcripts after dusk treatment (Fig. 5.5.2c). Therefore, the time of the glyphosate treatment determined the response of *EXPA8* (two-way ANOVA, $F(1, 4) = 27.4$, $P = 0.006$).

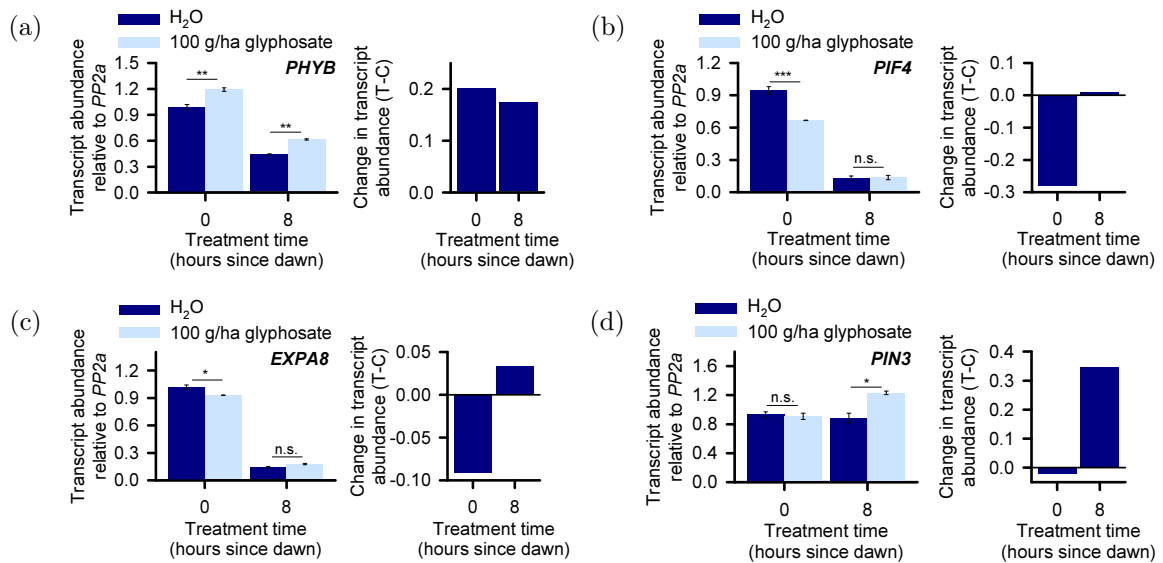


Figure 5.5.2: Glyphosate changes the transcript abundance of auxin-related genes. 100 g/ha glyphosate caused time of day-dependent changes in (a) *PHYB*, (b) *PIF4*, (c) *EXPA8* and (d) *PIN3*. Figures show mean relative transcript abundance for control and glyphosate treated samples relative to *PP2a* reference transcripts (left), and mean change in transcript abundance between control and treated samples (right). Values are mean \pm SEM where $n = 2-3$. Asterisks indicate significant difference between control and treated value, calculated by t -test where $* = P \leq 0.05$, $** = P \leq 0.01$, $*** = P \leq 0.001$, and n.s. indicates no significant difference.

There was no effect of glyphosate on *PIN3* transcript abundance when glyphosate was applied at dawn, but there was a significant increase in *PIN3* transcript abundance when glyphosate was applied at dusk (Fig. 5.5.2d). Therefore, there was a significant interaction between glyphosate treatment and the timing of the treatment (two-way ANOVA, $F(1, 6) = 16.5$, $P = 0.007$).

5.6 Discussion

5.6.1 Glyphosate is likely to inhibit all auxin biosynthesis pathways

Application of an exogenous auxin biosynthesis inhibitor, L-kynurenine, inhibited the elongation of the hypocotyl (Fig. 5.2.1a) and this had time of day sensitivity (Fig. 5.2.1b). Dawn was the most sensitive time point, as it was for glyphosate application (Fig. 4.4.1a). However, the pattern in the time of day sensitivity was slightly different to that of glyphosate, where kyn was only effective at reducing the length of the hypocotyl when applied at dawn and 6 hours after dawn. The reason behind this reduced sensitivity could relate to the pathway that kyn affects. Kyn competitively inhibits TAA1 activity in the tryptophan-dependent IPyA IAA biosynthesis pathway (He et al., 2011). However, there are other pathways of IAA biosynthesis that could still occur in the presence of kyn (Soeno et al., 2010; Mano and Nemoto, 2012). For example, there is the indole-3-acetaldoxime (IAOx) pathway, which is possibly brassicaceae-specific (Mano and Nemoto, 2012), the indole-3-acetamide (IAM) pathway (Suzuki et al., 2015), and the tryptamine (TAM) pathway (Suzuki et al., 2015). These pathways are all tryptophan-dependent, but there is also a tryptophan-independent IAA biosynthesis pathway that requires indole (Nonhebel, 2015). Indole is a product of chorismic acid, downstream of EPSPS (Soeno et al., 2010; Ljung, 2013). Therefore, in experiments that used kyn, there are several other possible routes of IAA biosynthesis. In contrast, after glyphosate treatment, all of these possible routes are likely to be

inhibited. Hence, glyphosate may have an overall greater effect on an auxin-dependent process compared to kyn.

The effect of glyphosate on *pin3-3* hypocotyl length was only significant when applied 2 h after dawn (Fig. 5.2.3b), suggesting that there was reduced sensitivity to glyphosate, and that PIN3 was required for the response to glyphosate in the wild type. This result was somewhat unexpected since there is functional redundancy between the PIN proteins (Vieten et al., 2005; Wang et al., 2015). *pin3* hypocotyls are defective in gravitropic and phototropic responses, and hypocotyls can be shorter than the wild type (Friml et al., 2002). PIN3 also localises to the hypocotyl, proving that PIN3 is involved of auxin efflux in the hypocotyl specifically (Friml et al., 2002). This, and the fact that *PIN3* was identified as one of the transcripts that was regulated by glyphosate, auxin, and was rhythmic (Table 4.3.2) further suggests that PIN3 is important in the time of day sensitivity to glyphosate, that is likely to involve auxin.

The use of other mutants for auxin biosynthesis and signalling was also considered for the work in this chapter. The auxin biosynthesis mutants *wei8 tar2* and *yuc1 yuc2 yuc4 yuc6* exist as segregating populations (Stepanova et al., 2011) making it very difficult to conduct the experiments according to the protocol used. However, these mutations are only involved in the IPyA pathway of auxin biosynthesis (Stepanova et al., 2011), therefore glyphosate could still have an effect on the alternative pathways of IAA biosynthesis. *superroot1* and *superroot2* cause auxin overproduction (Boerjan et al., 2007; Barlier et al., 2000) and have long hypocotyl phenotypes. The mutations prevent IAOx converting to indolic glucosinolates (Zhao, 2010) and consequently accumulate IAA (Ljung, 2013). Therefore, these mutations are not directly involved in auxin biosynthesis and would not mimic the response of glyphosate, but could provide an interesting result if tested in future.

5.6.2 *phyB* is more susceptible to glyphosate due to its longer hypocotyls

phyB seedlings were sensitive to glyphosate at all treatment times, with treatments applied at dawn causing a slightly greater effect on hypocotyl elongation (Fig. 5.2.5). This is not in accordance with a previous publication that concluded a mutation in phyB caused glyphosate resistance (Sharkhuu et al., 2014). It would appear that the results in the previous publication were not compared to the relative length of a glyphosate-free control for each time point. In doing this, *phyB* mutants treated with glyphosate would appear longer than the wild-type and, as such, it could be misinterpreted as indicating that this mutant is glyphosate resistant. This is not the case, and in contrast, the *phyB* mutation actually causes greater sensitivity to glyphosate since the magnitude of the response is much greater in *phyB*. The maximum change in hypocotyl length after glyphosate treatment in *phyB* was 34% (Fig. 5.2.5) whereas in the wild type it was 18% (Fig. 5.2.5a).

The response in the elongating *phyB* lines is reminiscent to that of *CCA1-ox* (Fig. 4.4.1b) where the magnitude of the response was also greater. *CCA1-ox* hypocotyls also elongate since the mis-regulation of the circadian oscillator prevents the arrest of elongation (Dowson-Day and Millar, 1999). Interestingly, *PHYB* gene expression is circadian regulated (Hall et al., 2002), and is responsible for preventing elongation of the hypocotyl through auxin biosynthesis (Reed et al., 1993; Nomoto et al., 2012). Light perception through phyB inhibits hypocotyl elongation (Franklin and Quail, 2010), therefore in the absence of phyB, this arrest on hypocotyl elongation does not exist, and the hypocotyl can continue to elongate. Glyphosate appears to have such a great effect on the hypocotyl, as it did for *CCA1-ox*, because more elongation is occurring in these genotypes.

While mutation in phyB does not cause glyphosate resistance, the same time of day sensitivity to glyphosate was detected here as reported by Sharkhuu et al. (2014), although a different measure was used. Therefore, the results in this work compare

well to previous studies that also extend the effect of glyphosate to the circadian oscillator and the red/far-red, phyB, and auxin signalling pathways.

5.6.3 Effect of glyphosate on reporters could have been masked by the inhibition of protein synthesis

Glyphosate application caused inconsistent histochemical staining of DR5::GUS seedlings (Fig. 5.3.1a). In some seedlings, accumulation of GUS was absent, indicating that glyphosate was inhibiting the expression of the auxin-induced promoter, *DR5*. However, the results were inconsistent and in some seedlings GUS was expressed.

The lack of GUS staining could be explained by reasons other than glyphosate reducing auxin content in the seedlings. For example, glyphosate inhibits protein synthesis (Cebeci and Budak, 2009), since aromatic amino acid biosynthesis is blocked after glyphosate application (Petersen et al., 2007; Zulet et al., 2013; Carbonari et al., 2014). Therefore, this could account for the inability of the plants to form GUS. However, the use of the GUS reporter has previously been used successfully in combination with glyphosate, at least in lettuce (Torres et al., 1999). To help elucidate the response of DR5::GUS to glyphosate, it would have been useful to compare the results with application of the positive control NAA and also the known auxin inhibitor, kyn. However this would not test for the proposed lack of protein synthesis. Quantification of the *GUS* gene also indicated that there was no difference in the free auxin level in response to glyphosate, regardless of treatment time (Fig. 5.3.1b). It may have been better to study the response of DR5::GUS to glyphosate under conditions where auxin was naturally increased, or to have have taken samples from only tissue that would have been enriched in auxin, e.g. the hypocotyl.

Glyphosate application was expected to increase VENUS fluorescence in DII-VENUS plants, since there may be lower free auxin. This was not the case for glyphosate treatments, whereas application of kyn did increase VENUS fluorescence (Fig. 5.4.1).

This response could have been due to the inability of the glyphosate-treated plants to synthesise new proteins, as it may have been in the DR5::GUS plants.

Since glyphosate is hypothesised to reduce auxin content, we thought that glyphosate treatment would reduce DR5::VENUS fluorescence and, as such, the response in DR5::VENUS depends on degradation of the fluorescent protein. Non-treated control plants were fluorescent (Figs. 5.4.2 and 5.4.3), indicating that there was auxin present. Therefore, enough time would have to have passed in order to detect a difference in lower fluorescence levels. However, fluorescence imaging occurred two days after treatment in the hypocotyl experiment. Therefore, this should have been sufficient time for normal protein degradation of VENUS, and no more VENUS to have been synthesised if there were no auxin driving the promotion of *DR5*. There was also no change in the abundance of *VENUS* transcripts, therefore, these results suggest that glyphosate did not affect DR5::VENUS. Interestingly, the response to kyn also did not show the expected reduction in VENUS fluorescence, and perhaps this is not a suitable method for measuring a reduction in auxin content. Again, these experiments may have yielded more promising results had they been conducted under different, auxin biosynthesis-promoting conditions.

5.6.4 The effect of glyphosate on auxin-related transcript abundance correlates with the function of the genes in auxin biosynthesis and hypocotyl elongation

The expression of auxin-related transcripts that could be reporters of the time of day response to glyphosate were examined. In general, where there was a change in transcript abundance of these reporters in response to glyphosate treatment, the response seemed logical. This is because there was generally an up-regulation of genes involved in auxin biosynthesis or signalling after treatment at the end of the day, or a decrease in transcript abundance following glyphosate treatment at dawn (Figs. 5.5.1

and 5.5.2). This correlated to the effect of glyphosate on hypocotyl length, which is regulated by auxin.

The YUCCA family of flavin monooxygenases participate in the conversion of IPyA to IAA (Tao et al., 2008; Stepanova et al., 2011), and elevated expression of *YUCCA* genes increases auxin production (Cheng et al., 2006). Here, *YUC9* transcript abundance increased in response to glyphosate at dusk, but not at dawn (Fig. 5.5.1). Therefore, the elevated *YUC9* at dusk indicates that the plant responded in a way that could promote elongation of the hypocotyl even though it usually would not be producing auxin at that time.

GH3.3 contains an auxin-responsive promoter (Ulmasov et al., 1997) and is involved in regulating the response of the hypocotyl through phyB mediated signals (Park et al., 2007). *GH3.3* is also involved in conjugating amino acids to IAA (Staswick et al., 2005; Mellor et al., 2016). *GH3.3* transcripts responded in the same way as *YUC9*. Since *GH3.3* contains an auxin-responsive element, the elevation in transcript abundance at dusk may indicate that there is more auxin after glyphosate treatment at that time, and perhaps the plant attempts to produce more auxin at this time but this was not possible after dawn glyphosate treatment.

IAA29 is also an auxin-inducible gene that is a positive regulator for the elongation of hypocotyls (Kunihiro et al., 2011). Under normal growth conditions, *IAA29* is reportedly increased at the end of the night, pre-dawn (Kunihiro et al., 2011). This would correlate to the increase in hypocotyl elongation at dawn (Nozue et al., 2007). However, after glyphosate treatment at dawn *IAA29* was down-regulated. After glyphosate treatment at dusk, there was an increase in *IAA29* transcript abundance, indicating that hypocotyl elongation was promoted at that time, also correlating to the longer hypocotyls after dusk glyphosate treatments.

Previously, *YUC9*, *GH3.3* and *IAA29* have been shown to respond in the same way to conditions that promote the expression of these transcripts (Hayes et al., 2014). This

was generally seen here, aside from *IAA29* transcript abundance, which decreased at dawn while the others were not affected by glyphosate.

PIF4 is regulated by the circadian oscillator (Kunihiro et al., 2011) and is reported to be involved in the circadian regulation of hypocotyl elongation, but possibly only under certain light conditions (Nozue et al., 2007; Choi and Oh, 2016). *PIF4* also promotes hypocotyl elongation (Choi and Oh, 2016). *PIF4* was down-regulated in response to glyphosate treatment at dawn (Fig. 5.5.2), which correlates to the shorter hypocotyls after glyphosate treatment at dawn. However, the mechanism through which this response occurs is unclear, since *PIF4* regulation of the hypocotyl occurs largely at the protein level (Section 4.3). Interestingly, the response of *IAA29* depends on *PIF4* (Kunihiro et al., 2011). Therefore, if *PIF4* is down-regulated in response to glyphosate, it is logical that *IAA29* transcript abundance was also reduced, but it may have been expected that there would be a delay in the response, rather than the same time of day effect seen for both transcripts.

EXPANSINs (EXPAs) are often involved in turgor-driven expansion and processes where the cell wall requires modification (Sasidharan et al., 2010). EXPAs are expressed in tomato hypocotyls and the transcripts are up-regulated in response to exogenous auxin (Caderas et al., 2000). Glyphosate application at dawn caused a reduction in *EXPA8* transcript abundance (Fig. 5.5.2). *EXPA8* transcript abundance was higher in the control at that time, suggesting more of the protein may have been required to modify the cell walls to allow hypocotyl elongation. Interestingly, *EXPA8* and other EXPAs were reported previously to be down regulated by glyphosate application (Das et al., 2010).

Overall, it seems that the transcripts involved in auxin biosynthesis are a good marker for the response of the elongating hypocotyls to glyphosate. It is logical that the plant would try to increase auxin biosynthesis if glyphosate were inhibiting it, and this may be the case in the results obtained for these transcripts. These results are somewhat difficult to interpret since the pathways work at different levels (protein

and transcript) and it is unexpected that the same timing response was seen for all aspects in a pathway. It is necessary to note that samples were taken several hours after the treatment at that time point, hence in the controls, the expression levels of transcripts may not be as expected in terms of the rhythmicity. For example, *IAA29* would be expected to be higher at the dawn time point compared to the dusk time point. This in general is one of the caveats of these experiments, because it would be useful to see what the genes were doing at the time that the treatments were applied. Further work could be conducted to elucidate further the mechanisms of glyphosate on these components. For example, determining how glyphosate could regulate these genes, whether glyphosate regulates them all individually, or whether there is a knock-on effect at the top of the pathway. Use of mutants of these transcripts would be beneficial for this. Furthermore, a greater understanding of the circadian regulation in the response of these transcripts would be beneficial, since many of these genes are circadian regulated.

5.7 Conclusion

This chapter aimed to elucidate the mechanism through which glyphosate and auxin interact to inhibit hypocotyl elongation in a time of day dependent manner. The use of an exogenous auxin biosynthesis inhibitor, exogenous auxin, an auxin transport inhibitor and an auxin efflux mutant suggest that glyphosate has the same effect on the elongation of the hypocotyl as a lack of auxin in the plant. The result with kyn suggested that glyphosate may have more of a complete inhibition of auxin biosynthesis, since the magnitude and time of day sensitivity was reduced with kyn compared to that of glyphosate. Use of the *pin3* mutant suggested that the response to glyphosate was dependent on PIN3, and auxin efflux in the hypocotyl.

Quantifying the abundance of auxin-related transcripts further strengthened the argument that glyphosate has an effect on the pathways that lie upstream of hypocotyl elongation. These transcripts were affected in a way that is consistent with de-

creased hypocotyl elongation at dawn, and increased hypocotyl elongation after dusk glyphosate applications, consistent with the glyphosate-treated hypocotyl elongation results.

Use of auxin reporters (DR5::GUS, DR5::VENUS, DII-VENUS) did not necessarily support the hypothesis that glyphosate was inhibiting auxin biosynthesis. However, further understanding of the mechanisms behind glyphosate and the reporters suggest that the results could have been due to how glyphosate works, and that it can inhibit protein synthesis. Additionally, the known inhibitor of auxin biosynthesis also did not show the expected result with these markers, suggesting that this was not necessarily a good choice of experimental methodology.

While the results do not unequivocally demonstrate that glyphosate inhibits auxin biosynthesis, there are multiple lines of evidence that suggest it does, both here and in previously-published work. Further experiments could extend this research, such as the quantification of IAA after glyphosate applications at different times of day. Furthermore, using these methods with more circadian oscillator over-expressors or mutants would be beneficial to elucidate the contribution of the oscillator in these responses, since the oscillator acts at multiple levels in the regulation of auxin and the response to glyphosate.

Chapter 6

Extending findings to older plants and agriculturally-relevant species

6.1 Introduction

As the world's most widely used herbicide, with over 125 million kilograms used per year in the USA alone (Benbrook, 2016), glyphosate could be used more effectively. In order for glyphosate use to be optimised in the field, the mechanisms through which it works could be better understood. Glyphosate is used on numerous plant species including grain crops, fruits and vegetables, plus the many weed species that grow alongside these, in addition to uses outside of agriculture (Benbrook, 2016). Therefore, it is informative to understand the mechanisms through which glyphosate affects species other than the model plant species *Arabidopsis*. Glyphosate is applied at different times of the year for various purposes (Kumar and Jha, 2015) and, as such, is applied to plants of different ages and growth stages.

The aim of this chapter was identify whether the findings from Chapters 4 and 5, where circadian regulation and auxin signalling were found to be involved in the time of day response to glyphosate, extrapolated to (i) older plants and (ii) species other than *Arabidopsis*, which may be more relevant to field conditions.

6.2 Glyphosate inhibits petiole elongation

Herbicides need to be effective on plants of all ages and growth stages. The hypocotyl elongation experiments conducted in seedlings (Chapter 4.3) tested the time of day response to glyphosate of an auxin-dependent process, since it appeared that glyphosate indirectly affects auxin biosynthesis and signalling (Chapter 5). Therefore, experiments were designed to determine whether the time of day responses found in *Arabidopsis* hypocotyls extended to older plants. To do this, another auxin-dependent process that occurs in older plants was identified: petiole elongation. The petiole joins the leaf blade to the stem and determines the leaf position that is optimal for light perception and photosynthesis (Kozuka et al., 2010). Petiole elongation is promoted by a low R:FR ratio such as that found in shade conditions (Vince-Prue et al., 1976) as part of the shade avoidance syndrome (SAS) and this response is auxin-dependent (Kozuka et al., 2010). It has also been reported that other factors responsible for leaf morphology in SAS, such as a suppression of leaf blade expansion, are auxin dependent (Kozuka et al., 2010). However, these processes also occur as part of normal growth. Petiole elongation, and leaf blade morphology were measured 7 days after 100 g/ha glyphosate treatment in both Col-0 and *CCA1*-ox plants.

Petiole length was significantly shorter than controls in response to 100 g/ha glyphosate treatment in both Col-0 (Fig. 6.2.1a) and *CCA1*-ox plants (Fig. 6.2.1b), however there were no differences in effect between the times of application (determined by two-way ANOVA). Overall, petioles were longer in control *CCA1*-ox plants compared to the control Col-0 plants, but glyphosate treatment caused petioles of both genotypes to be approximately the same length (2.5 mm).

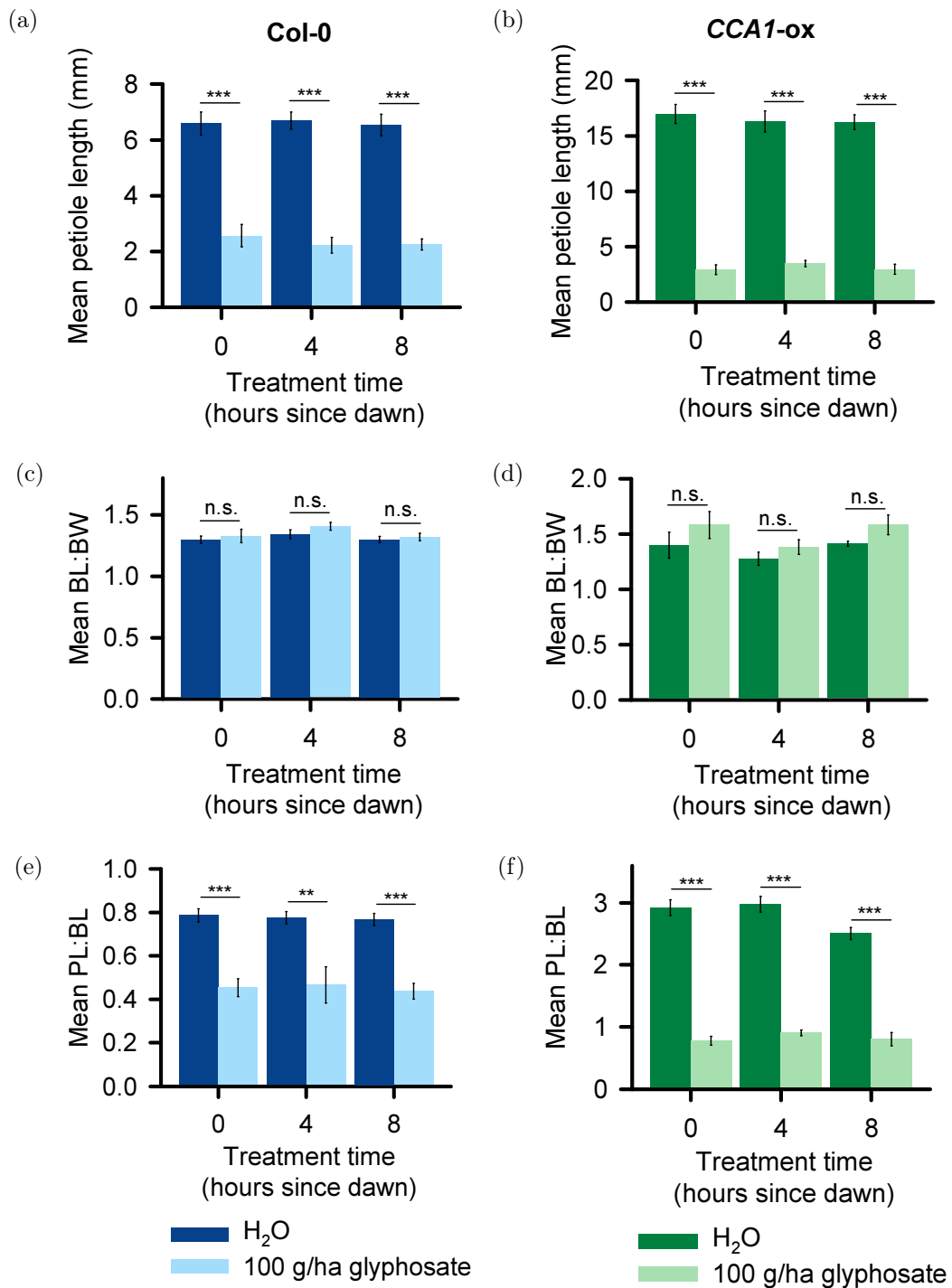


Figure 6.2.1: Glyphosate application inhibits elongation of the *Arabidopsis* petiole but is not time of day-dependent. The petioles of the fifth leaf of Col-0 (a) and *CCA1-ox* (b) did not elongate after application of 100 g/ha glyphosate, but there were no differences in the effect after different times of application. The blade length (BL): blade width (BW) ratio was not changed in response to glyphosate in Col-0 (c) and *CCA1-ox* plants (d). The petiole length (PL): blade length (BL) ratio was significantly reduced following glyphosate treatment at all treatment times in Col-0 (e) and *CCA1-ox* (f) plants. Measurements were taken 7 days after glyphosate application. Data shown are the mean of 13-15 plants per time point \pm SEM. Asterisks indicate statistically significant difference between control and treated plants determined by *t*-test at each time point where: ** = $P \leq 0.01$, *** = $P \leq 0.001$, n.s. indicates a non-significant difference.

Like petiole length, mean blade lengths and mean blade widths were reduced in glyphosate-treated plants compared to control plants (Table 6.2.1), but there was no difference between the effect of glyphosate treatments at different times of day (determined by two-way ANOVA). Blade lengths and widths were reduced in *CCA1-ox* control plants compared to Col-0 control plants, suggesting the leaves were in general smaller in *CCA1-ox* plants.

Table 6.2.1: Mean leaf blade length and mean leaf blade width after glyphosate treatments at different times of day in Col-0 and *CCA1-ox*. Treatment time in hours since dawn. Control (C) is water treatment, Treated (T) is 100 g/ha glyphosate treatment. n = 13-15 plants.

Genotype	Treatment time (h)	Control or Treated	Mean blade length \pmSEM	Mean blade width \pmSEM
Col-0	0	C	8.32 \pm 0.37	6.38 \pm 0.21
		T	5.29 \pm 0.39	4.00 \pm 0.28
	4	C	8.69 \pm 0.36	6.48 \pm 0.22
		T	4.94 \pm 0.33	3.51 \pm 0.22
	8	C	8.50 \pm 0.34	6.55 \pm 0.23
		T	5.15 \pm 0.24	3.94 \pm 0.21
<i>CCA1-ox</i>	0	C	5.95 \pm 0.36	4.40 \pm 0.21
		T	3.60 \pm 0.20	2.42 \pm 0.21
	4	C	5.67 \pm 0.45	4.37 \pm 0.22
		T	3.81 \pm 0.15	2.78 \pm 0.08
	8	C	6.52 \pm 0.22	4.61 \pm 0.12
		T	3.64 \pm 0.16	2.38 \pm 0.16

I also investigated whether there were differences in the leaf shape following glyphosate treatment. This was because a variety of factors regulate different aspects of the leaf morphology, and glyphosate could be responsible for altering some aspects but not others. The blade length (BL): blade width (BW) ratio did not have any differing responses to glyphosate depending on the time of day in Col-0 plants (Fig. 6.2.1c) or *CCA1-ox* plants (Fig. 6.2.1d). There were small but non-significant increases in BL:BW of glyphosate-treated *CCA1-ox* plants, suggesting slightly longer, less round leaves after glyphosate treatment.

The petiole length (PL): blade length (BL) ratio provides information regarding the morphology of the whole leaf, including the petiole. Glyphosate application significantly reduced PL:BL for both Col-0 plants (Fig. 6.2.1e) and *CCA1*-ox plants (Fig. 6.2.1f) at all time points. This suggests that there was a shorter petiole compared to the blade length after glyphosate treatment, and that the petiole was longer than the blade length in control plants. Furthermore, this suggests that the shorter petiole seen after glyphosate treatment (Figs. 6.2.1a and 6.2.1b) was not due to complete inhibition of growth of all leaf parameters. While these plants were not grown in shade-avoiding conditions, auxin would be required for the normal elongation and growth in the petiole and leaf blade, hence these results suggest that glyphosate could be inhibiting auxin in the petiole because petiole length was not able to elongate in the glyphosate-treated plants.

6.3 Glyphosate reduces hypocotyl and coleoptile elongation in species additional to *Arabidopsis*

In the field, herbicides must be effective on a variety of plant species, including both dicotyledons and monocotyledons. Therefore, it would be informative to know whether the time of day sensitivity to glyphosate identified in *Arabidopsis* (Chapter 4.3) extended to other species. To make comparisons between species, the same experimental method of hypocotyl length measurement was used to test the time of day sensitivity of other species to glyphosate. Hypocotyl elongation remains an auxin dependent process across species (Kelly and Bradford, 1986; Walker and Key, 1982). Monocotyledons do not have a hypocotyl, instead they possess a coleoptile. The elongation of the coleoptile in monocotyledonous species is also auxin-dependent (Ishizawa and Esashi, 1983).

Several species were selected (in conjunction with Syngenta) to investigate the effect of glyphosate on hypocotyl or coleoptile elongation. The criteria for selection were: small seeds, relationship to weed species in the field, relationship to *Arabidopsis*, and the physical availability of seeds. These species included: *Raphanus raphanistrum* (wild radish), *Sinapis arvensis* (wild mustard), *Brassica napus* (oilseed rape), *Amaranthus palmeri* (Palmer's amaranth), *Papaver rhoeas* (poppy), *Chenopodium album* (lamb's quarters), *Panicum miliaceum* (proso millet), *Alopecurus myosuroides* (blackgrass), and *Lolium perenne* (perennial rye-grass). There was very poor germination in many of these species or inconsistent rates of germination and growth. Hypocotyl elongation experiments require all seeds to germinate on exactly the same day in order for treatments to occur at exactly the same growth stage. Ultimately, three species were chosen to conduct time of day sensitivity experiments with glyphosate. These were: *Brassica napus*, *Sinapis arvensis*, and *Panicum miliaceum*.

Hypocotyls of *B. napus* were significantly reduced after glyphosate application at all application time points (Fig. 6.3.1a, left). The change in *B. napus* hypocotyl length (Fig. 6.3.1a, right) suggested that dawn was the most effective treatment time point, because the hypocotyl was shortest compared to the control at that time point (41%). The dusk glyphosate treatment caused the smallest difference in length between control and treated plants (30%), however, a two-way ANOVA did not indicate a significant interaction between treatment and time.

100 g/ha glyphosate prevented the elongation of the hypocotyl significantly in *S. arvensis* at all treatment time points (Fig. 6.3.1b, left). The mean change in length between control and treated hypocotyls (Fig. 6.3.1b, right) was greatest at dawn (17%), suggesting this was the time where glyphosate was more effective. Conversely, the smallest mean change in hypocotyl length between control and treated *S. arvensis* was after dusk glyphosate applications (14%). However, a two-way ANOVA did not identify a significant interaction between treatment and time.

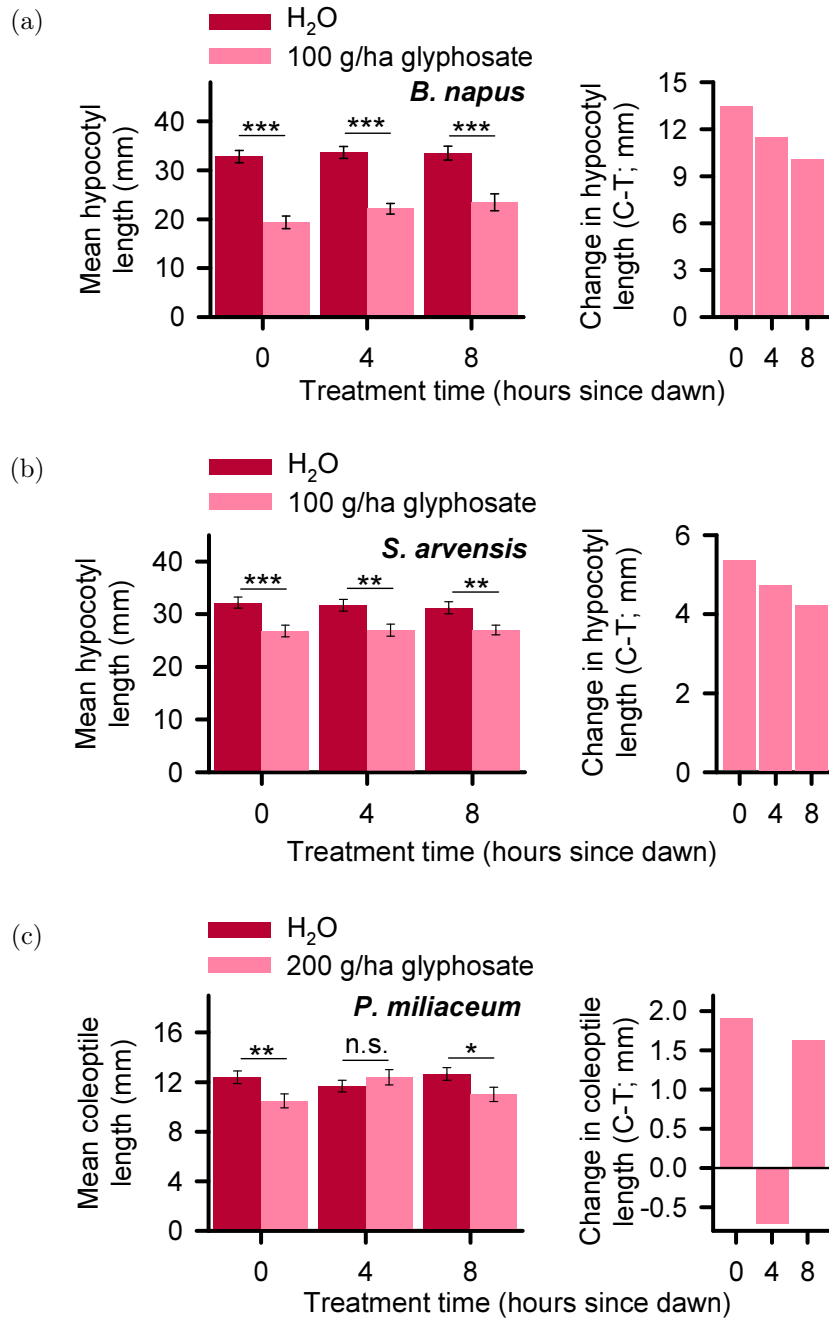


Figure 6.3.1: Glyphosate significantly reduced the hypocotyls and coleoptiles of agriculturally-relevant species. 100 g/ha glyphosate significantly reduced the hypocotyl at all application time points in *Brassica napus* (a) and *Sinapis arvensis* (b). 200 g/ha glyphosate significantly reduced the coleoptile of *Panicum miliaceum* (c) at dawn and dusk. Values are mean \pm SEM where $n = 20-45$. Two-way ANOVAs were conducted to determine significant interactions between treatment and time: (a) $F(2, 237) = 0.8$, $P = 0.45$, (b) $F(2, 252) = 0.14$, $P = 0.87$, and (c) $F(2, 387) = 3.08$, $P = 0.05$. Asterisks indicate significant difference between control and treated value, calculated by t -test where $* = P \leq 0.05$ and $** = P \leq 0.01$. n.s. = no statistically significant difference.

A higher concentration of glyphosate (200 g/ha) was required to prevent the coleoptile elongation in *P. miliaceum*, a monocotyledon. Glyphosate treatment at midday had no effect on the length of the coleoptile of *P. miliaceum*, but glyphosate treatments at dawn and dusk caused a significant reduction in coleoptile length (Fig. 6.3.1c, left). The mean change in coleoptile length between control and treated plants after glyphosate treatment appeared to be marginally greater at dawn (14%) compared to dusk (7%, Fig. 6.3.1c, right). A two-way ANOVA concluded that there was a significant interaction between glyphosate treatment and treatment time ($F(2, 387) = 3.08, P = 0.05$).

Overall, these data indicate that glyphosate does have an effect on hypocotyl and coleoptile length in other species. The mean change in length values supported the hypocotyl data in *Arabidopsis* where glyphosate treatments at dawn were slightly more effective than other time points. However, these small changes in length caused by different treatment times were not all statistically significant.

6.4 Discussion

6.4.1 Regulation of petiole elongation is determined by growth conditions

Petiole elongation was inhibited by the application of glyphosate, however there did not appear to be time of day sensitivity in the response. This might be due to different underlying regulatory mechanisms. While hypocotyl and petiole elongation are both auxin-regulated processes, different pathways of genes could be involved in regulating each individual process. As such, there could be different circadian regulation of such process-specific genes, or a lack of circadian regulation of the genes involved in petiole elongation.

CONSTITUTIVELY PHOTOMORPHOGENIC1 (*COP1*) and *SUPPRESSOR OF PHYA* (*SPA*) genes (particularly *SPA1* and *SPA4*) are essential for petiole elongation in response to simulated shade and also under white light (Rolauffs et al., 2012). It appears that the lack in time of day sensitivity of the petioles to glyphosate treatment cannot be due to a lack of circadian regulation of these genes as *COP1*, *SPA1* and *SPA4* are circadian regulated with peak expression around dawn, or 2 hours after dawn (Mockler et al., 2007). Furthermore, the peak expression of these genes coincides with the period of maximum petiole elongation (Dornbusch et al., 2014). Therefore, the circadian regulation of petiole elongation appears to be consistent with that in hypocotyl elongation (Nozue et al., 2007) where glyphosate application did have time of day sensitivity.

Rhythmic regulation of petiole elongation and the genes that drive such elongation indicate that this is not the reason for the absence of time of day sensitivity to glyphosate in the petiole. Therefore, perhaps other factors involved in petiole elongation were preventing time of day sensitivity. Auxin and brassinosteroids (BR) are reported to act together to promote petiole elongation in the shade (Kozuka et al., 2010) and an additive effect of mutations in each pathway was not observed, supporting the fact the two pathways could be working cooperatively (Kozuka et al., 2010). Perhaps if glyphosate inhibits auxin signalling in some way, and BR were still available, the BR would prevent the inhibition of petiole elongation to a certain extent and prevent the detection of time of day responses.

Much of the research surrounding petiole elongation has focussed on its involvement in shade avoidance. In shade conditions, auxin could be the major regulator of the response whereas under normal growth conditions, petiole elongation could be a combination of multiple growth regulators. This is supported by the fact that the auxin transport inhibitor NPA was only able to inhibit petiole elongation under low R:FR and had no effect under high R:FR (Kozuka et al., 2010). The data providing the elongation rate of the petiole (Dornbusch et al., 2014) prove that petiole elongation is rhythmic even in the absence of shade conditions and that petiole elongation occurs

in normal growth conditions. Although there is some involvement of auxin in petiole elongation, perhaps the auxin-dependence is only prevalent under shade conditions, and a rhythmic response to glyphosate would therefore be more evident under shade conditions. Therefore, it would be interesting to test whether there could be time of day sensitivity of petiole elongation to glyphosate under low R:FR where the petiole would usually be elongating more. It would also be of interest to determine the sensitivity of the petiole to glyphosate under circadian conditions. Furthermore, it is interesting that the same concentration of glyphosate that was used on the hypocotyls (100 g/ha glyphosate) had such a significant response on the petiole, perhaps a lower concentration would equate to more subtle time of day effects.

6.4.2 Multiple factors regulate coleoptile elongation

Hypocotyls of *B. napus* and *S. arvensis*, and the coleoptiles of *P. miliaceum* were sensitive to glyphosate treatments. This response was logical since the elongation of the hypocotyl and coleoptiles are auxin-dependent, glyphosate has previously been shown to inhibit auxin transport in corn coleoptiles (Baur, 1979), and glyphosate appears to indirectly inhibit the biosynthesis or transport of auxin (Chapter 5). Therefore there are similarities between these species and Arabidopsis. However, there was reduced time of day sensitivity in the response to glyphosate in these other species.

It is difficult to speculate on the rhythmic regulation of auxin in these other species because, as non-model organisms, the molecular mechanisms are poorly understood. However, there might be species-specific differences in the circadian regulation of auxin signalling, and this could influence the differences in the time of day sensitivity to glyphosate compared with Arabidopsis.

Signalling by other hormones might contribute to the differences in the time of day sensitivity between Arabidopsis and these other species. For example, in rice, exogenous and endogenous ethylene can promote elongation of the coleoptile (Ishizawa and Esashi, 1983). Therefore, ethylene could be responsible for elongating the hypocotyls

or coleoptiles in the absence of auxin, and reducing the time of day effects. However, ethylene is reported to be produced in response to IAA, and therefore IAA would need to be present in order for ethylene to be produced (Ishizawa and Esashi, 1983).

The experiments in *B. napus*, *S. arvensis*, and *P. miliaceum* were somewhat inconsistent and the data were noisy but glyphosate was capable of inhibiting an auxin-dependent process. It is possible that more subtle effects could be seen with different concentrations of glyphosate, however, the change in length was already quite small for *S. arvensis* and *P. miliaceum*. It would be interesting to understand the molecular mechanisms behind the interactions between auxin and the circadian oscillator in these species. Further optimisation could also be conducted for experiments with additional species.

6.5 Conclusion

Glyphosate affected processes that are known to be auxin-regulated in both older *Arabidopsis* plants and in seedlings of additional species, but with reduced time of day responses. These were exploratory experiments to investigate how the responses in *Arabidopsis* seedlings might extend to older plants and agriculturally-relevant species. Other methods of measuring time of day responses in older plants could be tested in more depth, including quantifying the effects of glyphosate on transcripts relating to the auxin-dependent petiole elongation at different times of day. Furthermore, experiments under constant conditions would be useful for a more thorough investigation of circadian regulation of glyphosate sensitivity in other species.

Chapter 7

RNA-sequencing of *Arabidopsis* treated with mesotrione and terbuthylazine

7.1 Introduction

Whilst transcriptome data can be used simply to determine differential expression between samples (Zhang et al., 2017), extensive manipulation of the data can provide much greater depth of information. For example, comparing transcriptomes of different samples can identify pathways common, or unique, to the samples (Khandelwal et al., 2008) and additionally, circadian regulation or rhythms in data (Michael et al., 2008). Furthermore, RNA-sequencing (RNA-seq) has been employed to investigate the effects of herbicides on the transcriptome, in particular how weed species can develop resistance to herbicides. For example, glyphosate-resistance in goosegrass (*Eleusine indica*) (Chen et al., 2017), nicosulfuron-susceptibility in maize (Liu et al., 2015), and diclofop-resistance in *Lolium rigidum* (Gaines et al., 2014). However, there has not been any published reports on the transcriptomic responses to mesotrione or TBA, specifically in *Arabidopsis*. Without these data, it can be difficult to identify genes

and pathways of interest in relation to underlying interactions between the herbicide treatment and circadian regulation.

RNA-seq allows an unbiased quantification of the transcriptome with the ability to quantify low-abundance transcripts and sequence variants, while simultaneously analysing multiple samples (Zhu et al., 2013; Weber, 2015). RNA-seq has a multitude of uses, for example: (i) *de novo* sequencing of non-model species such as *Eucalyptus* (Mizrachi et al., 2010), sweet potato (*Ipomoea batatas*) (Wang et al., 2010), and chickpea (*Cicer arietinum* L.) (Garg et al., 2011). (ii) RNA-seq can be used to improve the annotation of existing model organism species, including alternative splicing patterns, such as *Arabidopsis* (Filichkin et al., 2010) and rice (*Oryza sativa*) (Lu et al., 2010). (iii) RNA-seq can be employed to compare transcriptomes across growth stages to identify development-specific genes for example in radish (*Raphanus sativum*) (Wang et al., 2012), and grapevine (*Vitis vinifera*) (Zenoni et al., 2010) or across organ or tissue types (Begara-Morales et al., 2014; Loraine et al., 2013).

The aim of this Chapter was to identify transcriptomic changes in response to mesotrione, TBA, and the adjuvant required in combination with TBA, Agridex. Further analyses identified pathways that were affected by these herbicides, identified common promoter motifs, and finally the relationship between these genes and circadian regulation.

7.2 RNA-sequencing data collection

Treatments were applied at dawn and samples were taken 4 hours later. RNA was extracted from control or treated seedlings, checked for quality and purity, and RNA-seq was conducted (Chapter 2.16). The RNA-seq method chosen increased coverage of the transcriptome by increasing read length through paired-ends, and through detection of anti-sense transcription using stranded sequencing (Martin et al., 2013; Ozsolak

and Milos, 2011). Bioinformatics analysis was performed using Partek Flow, using the TopHat2 pipeline, followed by downstream analysis using online tools.

7.3 Principal component analysis separates samples into clusters by treatment

To obtain RNA-seq datasets, 12 cDNA libraries were prepared, three for each treatment: H₂O (CT), 10 g/ha mesotrione (TM), 0.2% Agridex (CT) and 1 g/ha TBA (TT). Samples were run on the Illumina NextSeq simultaneously to avoid between-run variation. Post-sequencing, bases were trimmed from each end of the reads to remove poor quality sequence, followed by removal of Illumina adapter sequences. 38 - 61 million reads were generated with a mean read length of 75 bases (Table 7.3.1). Sequences were aligned to the TAIR10-all chromosomes reference genome.

The use of paired-end sequencing generated 75 - 124 million alignments (Table 7.3.1). Each fragment is read in both directions, consequently the total alignments are approximately double the total reads. Reads can align more than once, hence the total alignments can be more than double the total reads. A high percentage of reads were aligned to the reference genome, with a minimum of 97.23% (Trapnell et al., 2012; Conesa et al., 2016) (Table 7.3.1). 90% of alignments had both ends of a read pair uniquely mapped to the reference genome. The average coverage depth ranged from 52 - 87 for all bases in the sample. Furthermore, an average of 65% of the bases across the samples are covered at least once and 34% of the bases in the reference are covered at least 20 times. The mean quality score for the samples was 34.55 (based on Phred-33 format), meaning that the chance of an incorrect base read was 1 in 1000. Finally, the TAIR10 reference genome coverage had a mean of 35% (Partek, 2019).

Table 7.3.1: Summary of RNA-seq reads and mapping results. Three samples were sequenced per treatment: CM (H₂O), TM (10 g/ha mesotrione), CT (0.2% Agridex) and TT (1 g/ha TBA).

Sample	Total reads	Total alignments	Aligned (%)	Unique paired (%)	Average coverage depth
CM1	41 169 411	82 605 120	97.23	90.20	57.55
CM2	51 598 302	104 042 685	97.82	90.52	73.49
CM3	38 463 591	75 958 276	97.35	87.98	52.91
TM1	44 854 454	90 778 776	97.41	89.54	87.24
TM2	42 872 606	86 411 152	97.59	89.97	84.07
TM3	45 924 140	92 982 482	97.91	90.58	64.40
CT1	61 480 116	124 231 949	98.02	90.84	62.37
CT2	58 925 816	119 300 989	97.93	90.73	59.52
CT3	45 487 720	91 846 570	98.17	91.14	64.72
TT1	52 769 337	106 750 902	97.98	90.78	75.55
TT2	49 317 746	99 275 023	97.84	90.23	70.10
TT3	48 919 709	98 342 290	97.56	90.24	69.55

To ensure samples were comparable, transcripts per million (TPM) normalisation (Wagner et al., 2012) was applied to mapped transcript counts. A principal component analysis was conducted on normalised counts in order to identify underlying structure in the data. Clustering by sample occurred (Fig. 7.3.1). Principal component 1 (PC1), the component with highest variance (30%), determined that H₂O-treated samples (CM) are further away from the other samples (Fig. 7.3.1). Adjuvant (CT)-, Mesotrione (TM)-, and TBA (TT)- treated samples had less variance explained by PC1. H₂O and adjuvant samples had the least variance in PC2, whereas TBA and mesotrione samples had more variance explained by PC2.

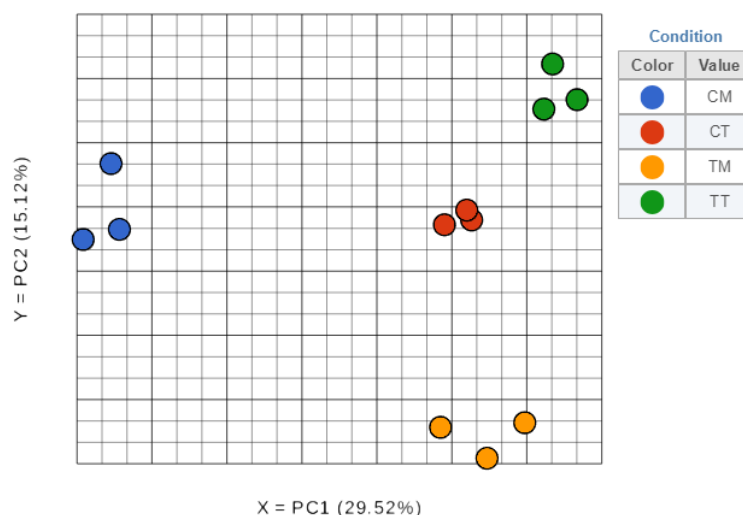


Figure 7.3.1: Principal component analysis of the 12 RNA-seq samples separates samples by treatment. x- and y-axis show principal component (PC) 1 and 2, respectively. PC1 explains variance in H₂O- treated samples (CM, blue dots) compared to other samples. PC2 explains variance between H₂O- and adjuvant- treated samples (CT, red dots) and TBA-treated samples (TT, green dots) and mesotrione-treated samples (TM, orange dots). The value in parentheses is the fraction of explained variance of that dimension.

7.4 Mesotrione, Agridex and TBA treatments cause differential gene expression

Prior to differential expression detection, statistics were applied to the normalised data. Gene specific analysis (GSA) was employed to test multiple fits for each gene to calculate *P*-value and fold-change, and feature lists were created. Due to the large number of statistical tests implemented, a correction for false-discovery rates (FDR) was applied (0.05). Furthermore, fold change was constrained to ≤ -2 - and ≥ 2 -fold for output feature lists.

Hierarchical clustering was used to cluster samples within treatments (Figures 7.4.1 to 7.4.2). The dendrogram on the left of each figure shows the hierarchy of the clusters. In order to give all features equal weight, expression data was standardised so that the mean expression for each gene is zero and the standard deviation is 1 (Partek, 2019). Standardised gene expression is shown for each sample in the heat maps (Figures 7.4.1

to 7.4.2) with genes along the x-axis in chromosomal sequential order. Each gene can be compared in standardised abundance across the treatments. Colours show difference in expression of genes across the samples and treatments, where green is a lower expression of a gene relative to the mean, and red is a higher expression relative to the mean. Overall, mesotrione-treated (TM) samples appeared to have higher expression of the majority of genes compared to H₂O- treated samples (CM; Fig. 7.4.1). Adjuvant-treated samples (CT) appeared to have the highest expression of genes, this was clustered most closely to TBA-treated samples (TT), and H₂O-treated samples (CM) had lower gene expression levels (Fig. 7.4.2). This hierarchical clustering appears to be in accordance with the principal components identified in Fig. 7.3.1.

Lists of differentially expressed features for each relevant treatment comparison were downloaded from PartekFlow for interpretation. Gene annotations were obtained using ThaleMine from ARAPORT (araport.org/search/thalemine; accessed 13/12/16), which produced lists of genes, some with unknown names or functions (Tables 7.4.1 to 7.4.3). Two levels of filtering were applied to the original lists of differentially expressed genes, to identify (i) those having a predicted function and (ii) those that were fully annotated. The latter lists were used for subsequent analyses.

Mesotrione-treated seedlings had the greatest number of differentially expressed genes compared to the control treatment with 1132 fully annotated genes being differentially expressed (Table 7.4.1). The majority of these differentially expressed genes (751) were up-regulated. Adjuvant-treated seedlings also had a greater number of up-regulated genes, 736 out of 1058 (Table 7.4.2). TBA-treated seedlings had the fewest differentially expressed genes (315 fully annotated; Table 7.4.3), however these TBA samples would also have included those that were differentially expressed in the adjuvant versus water comparison. Furthermore, 299 of the TBA-treated differentially expressed genes were down-regulated and only 16 were up-regulated.

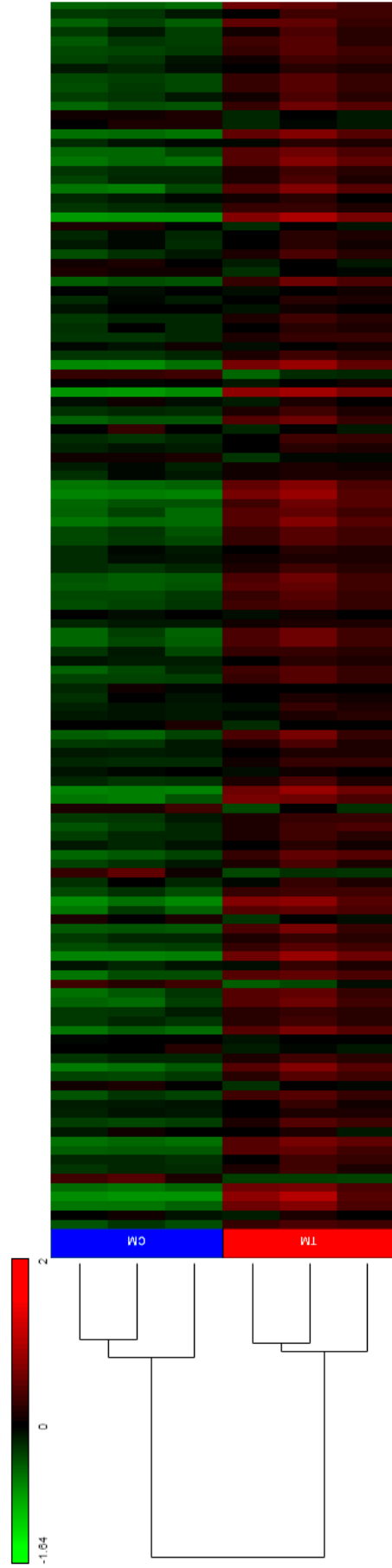


Figure 7.4.1: Hierarchical clustering and heat map comparison of H₂O- and mesotrione-treated RNA-seq samples. Standardisation of gene expression occurred for each gene across treatments, where the mean was set to 0, and the standard deviation was 1. Mesotrione-treated samples (TM) generally have higher normalised gene expression (shown by red colouring) compared to H₂O-treated samples (CM) having lower gene expression (green colouring). Genes are along the x-axis in chromosomal order.

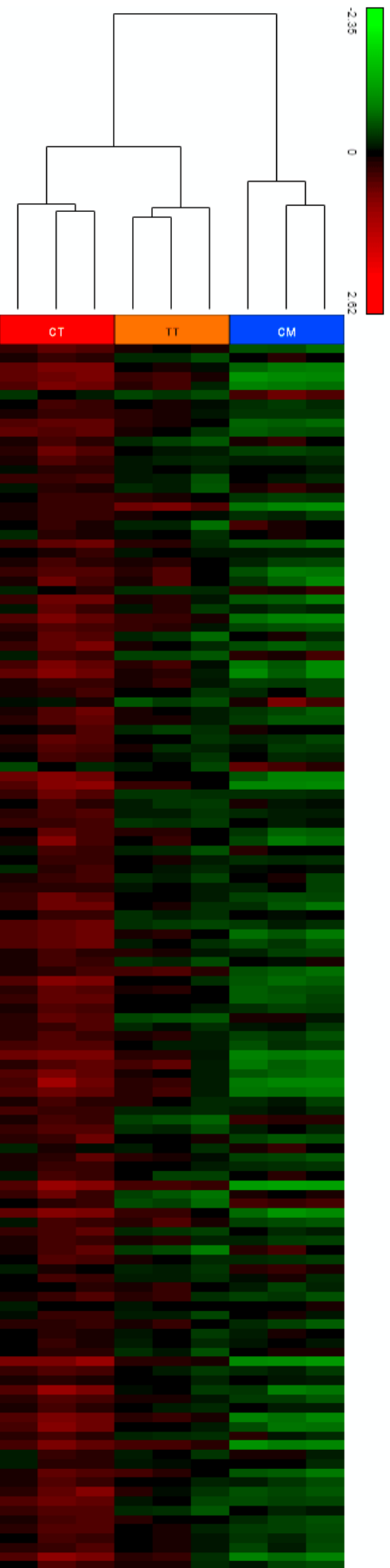


Figure 7.4.2: Hierarchical clustering and heat map comparison of H₂O-, adjuvant-, and TBA-treated RNA-seq samples. Standardisation of gene expression occurred for each gene across treatments, where the mean was set to 0, and the standard deviation was 1. The dendrogram clustered adjuvant- (CT) and TBA-treated (TT) samples more closely than H₂O-treated samples. Adjuvant-treated samples had higher levels of normalised gene expression (shown by red colouring) compared to H₂O-treated samples, which had the lowest overall gene expression (green colouring). Genes are along the x-axis in chromosomal order.

Table 7.4.1: Summary of the differential gene expression in response to mesotrione treatment. Two levels of filtering were applied to the feature lists: (i) to only include those with predicted gene functions, and (ii) to only include those that were fully annotated. A greater number of genes were up-regulated compared to those down-regulated.

	All	Up-regulated	Down-regulated
All differentially expressed genes	2128	1353	775
Genes with predicted function	1807	1166	641
Fully annotated genes	1132	751	381

Table 7.4.2: Summary of the differential gene expression in response to adjuvant treatment. Two levels of filtering were applied to the feature lists: (i) to only include those with predicted gene functions, and (ii) to only include those that were fully annotated. A greater number of genes were up-regulated compared to down-regulated.

	All	Up-regulated	Down-regulated
All differentially expressed genes	1905	1312	593
Genes with predicted function	1637	1132	505
Fully annotated genes	1058	736	322

Table 7.4.3: Summary of the differential gene expression in response to TBA treatment. Two levels of filtering were applied to the feature lists: (i) to only include those with predicted gene functions, and (ii) to only include those that were fully annotated. Many more genes were down-regulated in response to TBA compared to the number that were up-regulated.

	All	Up-regulated	Down-regulated
All differentially expressed genes	561	51	510
Genes with predicted function	481	36	445
Fully annotated genes	315	16	299

The genes with the 10 greatest fold changes, both up-regulated and down-regulated, for each treatment in comparison to the controls are listed in Tables 7.4.4 to 7.4.9. *PDR12* was the most highly differentially expressed gene relative to the control, with a fold change of >2400. The other nine most highly up-regulated genes increased by 88-770-fold (Table 7.4.4). The most down-regulated gene in response to mesotrione treatment compared to H₂O-treated seedlings was *PER69* which decreased 13-fold, the other most down-regulated genes decreased by 5-8-fold (Table 7.4.5).

Table 7.4.4: Summary of the 10 genes with greatest fold increase in response to meso-trione treatment relative to H₂O treatment.

Locus	Name	Function	Fold change
AT1G15520	<i>PDR12</i>	Pleiotropic drug resistance 12	2.43×10^3
AT4G34410	<i>RRTF1</i>	Redox responsive transcription factor 1	7.74×10^2
AT2G35980	<i>YLS9</i>	Late embryogenesis abundant (LEA) hydroxyproline-rich glycoprotein family	4.16×10^2
AT2G47520	<i>HRE2</i>	Integrase-type DNA-binding superfamily protein	3.58×10^2
AT1G05100	<i>MAPKKK18</i>	Mitogen-activated protein kinase kinase kinase 18	2.59×10^2
AT5G67080	<i>MAPKKK19</i>	Mitogen-activated protein kinase kinase kinase 19	1.56×10^2
AT1G71520	<i>ERF020</i>	Integrase-type DNA-binding superfamily protein	1.40×10^2
AT2G29470	<i>ATGSTU3</i>	Glutathione S-transferase tau 3	1.12×10^2
AT5G24110	<i>WRKY30</i>	WRKY DNA-binding protein 30	9.17×10^1
AT1G53540	<i>HSP17.6C</i>	HSP20-like chaperones superfamily protein	8.79×10^1

Table 7.4.5: Summary of the 10 genes with greatest fold decrease in response to mesotrione treatment relative to H₂O treatment.

Locus	Name	Function	Fold change
AT5G64100	<i>PER69</i>	Peroxidase superfamily protein	-13.3
AT5G43350	<i>ATPT1</i>	Phosphate transporter 1	-8.48
AT2G17230	<i>EXL5</i>	EXORDIUM like	-7.57
AT1G74670	<i>GASA6</i>	Gibberellin-regulated family protein	-7.27
AT3G13610	<i>F6'H1</i>	2-oxoglutarate (2OG) and Fe(II)-dependent oxygenase superfamily protein	-6.84
AT1G19510	<i>ATRL5</i>	RAD-like	-5.47
AT1G20190	<i>ATEXPA11</i>	Expansin 11	-5.38
AT2G23130	<i>AGP17</i>	Arabinogalactan protein 17	-5.34
AT5G14920	<i>GASA14</i>	Gibberellin-regulated family protein	-5.31
AT3G23810	<i>SAHH2</i>	S-adenosyl-l-homocysteine (SAH) hydrolase 2	-5.28

PDR12 was also the most highly up-regulated gene in response to adjuvant treatment increasing 1640-fold compared to H₂O treatment (Table 7.4.6). The other most up-regulated genes in response to mesotrione increased by 39-450-fold. Eight out of the 10 most up-regulated genes for adjuvant treatment were the same as those for mesotrione treatment. The gene most down-regulated in response to adjuvant treatment was *GASA6*, with an 18-fold decrease (Table 7.4.7). Other down-regulated genes decreased 7-13-fold. Two of the 10 most down-regulated were the same as those for mesotrione-treated.

Table 7.4.6: Summary of the 10 genes with greatest fold increase in response to adjuvant treatment relative to H₂O treatment.

Locus	Name	Function	Fold change
AT1G15520	<i>PDR12</i>	Pleiotropic drug resistance 12	1.64×10^3
AT2G35980	<i>YLS9</i>	Late embryogenesis abundant (LEA) hydroxyproline-rich glycoprotein family	4.50×10^2
AT2G47520	<i>HRE2</i>	Integrase-type DNA-binding superfamily protein	1.46×10^2
AT2G29470	<i>ATGSTU3</i>	Glutathione S-transferase tau 3	1.32×10^2
AT5G24110	<i>WRKY30</i>	WRKY DNA-binding protein 30	5.43×10^1
AT5G59570	<i>PCLL</i>	Homeodomain-like superfamily protein	5.16×10^1
AT1G05100	<i>MAPKKK18</i>	Mitogen-activated protein kinase kinase kinase 18	4.71×10^1
AT1G71520	<i>ERF020</i>	Integrase-type DNA-binding superfamily protein	4.42×10^1
AT4G34410	<i>RRTF1</i>	Redox responsive transcription factor 1	4.23×10^1
AT1G69930	<i>ATGSTU11</i>	Glutathione S-transferase tau 11	3.88×10^1

Table 7.4.7: Summary of the 10 genes with greatest fold decrease in response to adjuvant treatment relative to H₂O treatment.

Locus	Name	Function	Fold change
AT1G74670	<i>GASA6</i>	Gibberellin-regulated family protein	-18.5
AT3G03780	<i>ATMS2</i>	Methionine synthase 2	-13.2
AT3G23810	<i>SAHH2</i>	S-adenosyl-l-homocysteine (SAH) hydrolase 2	-10.6
AT3G04290	<i>ATLTL1</i>	Li-tolerant lipase 1	-9.19
AT1G51680	<i>4CL1</i>	4-coumarate:CoA ligase 1	-8.95
AT3G55120	<i>TT5</i>	Chalcone-flavanone isomerase family protein	-8.14
AT1G30530	<i>UGT78D1</i>	UDP-glucosyl transferase 78D1	-7.95
AT1G24020	<i>MLP423</i>	MLP-like protein 423	-7.79
AT1G73602	<i>CPuORF32</i>	Conserved peptide upstream open reading frame 32	-7.49
AT2G37040	<i>PAL1</i>	PHE ammonia lyase 1	-7.48

Only 16 genes were up-regulated in response to TBA treatment compared to adjuvant-treated (Table 7.4.8). The most up-regulated was *PDX1L4*, but only 2.8-fold (Table 7.4.8). All TBA up-regulated genes had a small fold increase. Many more genes were down-regulated in response to TBA. The most down-regulated gene was *HSP70-2* that decreased 9-fold (Table 7.4.9). The other nine most down-regulated ranged from 5-8 fold decreases.

Table 7.4.8: Summary of the 10 genes with greatest fold increase in response to TBA treatment relative to adjuvant treatment.

Locus	Name	Function	Fold change
AT2G38210	<i>PDX1L4</i>	Putative PDX1-like protein 4	2.81
AT3G61060	<i>AtPP2-A13</i>	Phloem protein 2-A13	2.64
AT2G42530	<i>COR15B</i>	Cold regulated 15b	2.58
AT3G07650	<i>COL9</i>	CONSTANS-like 9	2.56
AT2G28630	<i>KCS12</i>	3-ketoacyl-CoA synthase 12	2.43
AT5G66520	<i>PCMP-H61</i>	Tetratricopeptide repeat (TPR)-like superfamily protein	2.30
AT1G47655	<i>DOF1.6</i>	Dof-type zinc finger DNA-binding family protein	2.26
AT1G65870	<i>F12P19.3</i>	Disease resistance-responsive (dirigent-like protein) family protein	2.25
AT3G47430	<i>PEX11B</i>	Peroxin 11B	2.14
AT1G12240	<i>ATBETA-FRUCT4</i>	Glycosyl hydrolases family 32 protein	2.12

Table 7.4.9: Summary of the 10 genes with greatest fold decrease in response to TBA treatment relative to adjuvant treatment.

Locus	Name	Function	Fold change
AT5G02490	<i>HSP70-2</i>	Heat shock protein 70 (Hsp 70) family protein	-9.66
AT1G16410	<i>CYP79F1</i>	Cytochrome p450 79f1	-8.07
AT3G45140	<i>LOX2</i>	Lipoxygenase 2	-7.96
AT4G21680	<i>NRT1.8</i>	Nitrate transporter 1.8	-6.83
AT4G21850	<i>ATMSRB9</i>	Methionine sulfoxide reductase B9	-6.59
AT4G04610	<i>APR1</i>	APS reductase 1	-6.51
AT3G58990	<i>IPMI1</i>	Isopropylmalate isomerase 1	-6.32
AT3G44860	<i>FAMT</i>	Farnesoic acid carboxyl-O-methyltransferase	-6.27
AT1G53540	<i>HSP17.6C</i>	HSP20-like chaperones superfamily protein	-6.23
AT4G34588	<i>CPuORF2</i>	Conserved peptide upstream open reading frame 2	-5.42

7.5 Genes representing many metabolic pathways were enriched by herbicide treatment

Obtaining differentially expressed gene lists alone makes it difficult to assign biological relevance to the wider effect of the treatment (Martin et al., 2013). Assigning biological function to lists of genes through pathway enrichment aids this interpretation. Therefore, pathway enrichment was performed on differentially expressed gene lists using the Kyoto Encyclopedia of Genes and Genomes (KEGG) pathway database KEGG mapper tool (www.genome.jp/kegg/tool/map_pathway1.html). This identifies metabolic pathways that are represented by the input genes.

A large number of pathways were identified for each treatment: 90 up-regulated for mesotrione, 70 down-regulated for mesotrione, 74 up-regulated for adjuvant, 90 down-

regulated for adjuvant, 14 up-regulated for TBA and 74 down-regulated for TBA. However, many only identified one gene involved in a metabolic pathway therefore, a minimum overlap of five genes to each pathway was used as an inclusion cutoff. After this filtering, hypergeometric tests were conducted to compare the number of genes identified in the overlap to the RNA-seq dataset and the total number of genes listed in each pathway to establish whether the enrichment was greater than would be expected by chance. This identified the pathways listed in Tables 7.5.1 to 7.5.5. Pathways are listed in order of the overlap between the input gene list and the pathway identified.

Mesotrione treatment significantly up-regulated genes involved in 20 metabolic pathways (Table 7.5.1). Four of these pathways were unique to this treatment: endocytosis, glycerophospholipid metabolism, glycine, serine and threonine metabolism, and glycerolipid metabolism. Mesotrione significantly down-regulated genes involved in eight metabolic pathways (Table 7.5.2). Two of these pathways were unique to this treatment: phagosome, and amino sugar and nucleotide sugar metabolism.

Table 7.5.1: Mesotrione treatment significantly up-regulated genes involved in 20 metabolic pathways. Pathways were identified using the KEGG mapper tool restricted to a minimum of five overlapping genes. Significant overlaps were determined using hypergeometric analyses. Asterisks (*) indicate a pathway was unique to mesotrione treatment, compared with adjuvant or TBA treatment.

Pathway	Overlap	<i>P</i>
Plant hormone signal transduction	24	1.12×10^{-5}
Glutathione metabolism	23	7.72×10^{-14}
Biosynthesis of amino acids	21	6.30×10^{-5}
Carbon metabolism	20	3.51×10^{-4}
Protein processing in ER	19	6.17×10^{-5}
Plant pathogen interaction	19	3.24×10^{-6}
Alpha-linolenic acid metabolism	12	9.85×10^{-10}
Phenylpropanoid biosynthesis	10	2.84×10^{-2}
Endocytosis	9	2.97×10^{-2} *
Glycolysis/Gluconeogenesis	8	2.39×10^{-2}
Carbon fixation	7	6.00×10^{-2}
2-Oxocarboxylic acid metabolism	6	2.53×10^{-2}
Glycerophospholipid metabolism	6	4.79×10^{-2} *
Arginine and proline metabolism	6	6.94×10^{-2}
Sulfur metabolism	6	1.87×10^{-2}
Glycine, serine and threonine metabolism	6	2.05×10^{-2} *
Alanine, aspartate and glutamate metabolism	5	1.77×10^{-2}
Nitrogen metabolism	5	1.09×10^{-2}
Phenylalanine, tyrosine and tryptophan biosynthesis	5	2.79×10^{-2}
Glycerolipid metabolism	5	3.13×10^{-2} *

Table 7.5.2: Mesotrione treatment significantly down-regulated genes involved in eight metabolic pathways. Pathways were identified using the KEGG mapper tool restricted to a minimum of five overlapping genes. Significant overlaps were determined using hypergeometric analyses. Asterisks (*) indicate a pathway was unique to mesotrione treatment, compared with adjuvant or TBA treatment.

Pathway	Overlap	<i>P</i>
Phenylpropanoid biosynthesis	11	1.01×10^{-4}
Plant hormone signal transduction	9	2.53×10^{-2}
Carbon metabolism	8	4.40×10^{-2}
Phagosome	6	2.21×10^{-3} *
Amino sugar and nucleotide sugar metabolism	6	1.72×10^{-2} *
Fatty acid elongation	5	3.03×10^{-4}
Cysteine and methionine metabolism	5	3.25×10^{-2}
Glutathione metabolism	5	1.85×10^{-2}

Adjuvant treatment significantly up-regulated genes involved in 12 metabolic pathways (Table 7.5.3). Five of these pathways were unique to this treatment: ribosome, flavonoid biosynthesis, purine metabolism, phenylalanine metabolism, and ribosome biogenesis in eukaryotes. 17 pathways contained a significant number of genes that were down-regulated by adjuvant mesotrione treatment (Table 7.5.4). Three of these pathways were unique to this treatment: starch and sucrose metabolism, ascorbate and aldrate metabolism, and cyanoamino acid metabolism.

Table 7.5.3: Adjuvant treatment significantly up-regulated genes involved in 12 metabolic pathways. Pathways were identified using the KEGG mapper tool restricted to a minimum of five overlapping genes. Significant overlaps were determined using hypergeometric analyses. Asterisks (*) indicate a pathway was unique to adjuvant treatment, compared with mesotrione or TBA treatment.

Pathway	Overlap	<i>P</i>
Phenylpropanoid biosynthesis	15	1.55×10^{-8}
Biosynthesis of amino acids	13	4.94×10^{-5}
Ribosome	13	1.58×10^{-3} *
Fatty acid elongation	8	3.29×10^{-8}
Flavonoid biosynthesis	7	1.59×10^{-8} *
Carbon metabolism	7	4.86×10^{-2}
Purine metabolism	7	5.62×10^{-3} *
Phenylalanine, tyrosine and tryptophan biosynthesis	6	1.31×10^{-4}
Cysteine and methionine metabolism	6	4.92×10^{-3}
Phenylalanine metabolism	6	2.96×10^{-5} *
Glutathione metabolism	5	1.01×10^{-2}
Ribosome biogenesis in eukaryotes	5	1.18×10^{-2} *

Table 7.5.4: Adjuvant treatment significantly down-regulated genes involved in 17 metabolic pathways. Pathways were identified using the KEGG mapper tool restricted to a minimum of five overlapping genes. Significant overlaps were determined using hypergeometric analyses. Asterisks (*) indicate a pathway was unique to adjuvant treatment, compared with mesotrione or TBA treatment.

Pathway	Overlap	<i>P</i>
Glutathione metabolism	22	4.71×10^{-13}
Plant-pathogen interaction	20	6.11×10^{-7}
Carbon metabolism	17	3.46×10^{-3}
Plant hormone signal transduction	15	1.75×10^{-2}
Biosynthesis of amino acids	13	3.07×10^{-2}
Protein processing in ER	11	4.19×10^{-2}
Alpha-linolenic acid metabolism	10	1.43×10^{-7}
Starch and sucrose metabolism	9	2.98×10^{-2} *
Phenylpropanoid biosynthesis	9	4.88×10^{-2}
Ascorbate and aldrate metabolism	7	5.77×10^{-4} *
Glycolysis/gluconeogenesis	7	4.82×10^{-2}
2-Oxocarboxylic acid metabolism	6	2.35×10^{-2}
Alanine, aspartate and glutamate metabolism	6	4.06×10^{-3}
Arginine and proline metabolism	6	6.36×10^{-3}
Nitrogen metabolism	6	2.16×10^{-3}
Carbon fixation	6	1.80×10^{-2}
Cyanoamino acid metabolism	5	4.59×10^{-2} *

No more than 2 genes were found in any TBA treated up-regulated pathway, therefore there were no pathways that were deemed a significant overlap. Ten pathways were identified that had a significant overlap with the TBA-treated down-regulated genes (Table 7.5.5). One of these pathways was unique to this treatment: pyruvate metabolism.

Table 7.5.5: TBA treatment significantly down-regulated genes involved in 10 metabolic pathways. Pathways were identified using the KEGG mapper tool restricted to a minimum of five overlapping genes. Significant overlaps were determined using hypergeometric analyses. Asterisks (*) indicate a pathway was unique to TBA treatment, compared with mesotrione or adjuvant treatment.

Pathway	Overlap	<i>P</i>
Protein processing in ER	19	2.97×10^{-7}
Biosynthesis of amino acids	13	2.86×10^{-3}
2-Oxocarboxylic acid metabolism	11	7.41×10^{-7}
Alpha-linolenic acid metabolism	10	1.72×10^{-7}
Glutathione metabolism	8	1.07×10^{-2}
Cysteine and methionine metabolism	7	2.70×10^{-3}
Carbon metabolism	7	1.93×10^{-6}
Plant pathogen interaction	6	4.37×10^{-2}
Pyruvate metabolism	5	1.15×10^{-2} *
Sulfur metabolism	5	9.09×10^{-3}

7.6 Three core promoter motifs were enriched in herbicide-treated seedlings

Each cluster of genes either up- or down-regulated by a treatment contains genes that are co-expressed (Brown et al., 2013). It is likely that the gene clusters may contain some common regulatory features, such as transcription factor binding sites (TFBS) (Brown et al., 2013). TFBS are important components of gene promoter sequences that allow proteins (specifically, transcription factors) to bind to the sequence and regulate the expression of the gene, either by initiating or repressing the transcription (Cartharius et al., 2005).

The MEME-LaB (MEME Launcher and Browser) web tool (Brown et al., 2013) was

used to identify motifs that are over-represented in the promoter regions of the lists of herbicide-regulated genes. The lists of differentially-regulated genes either up- or down-regulated by the treatment were uploaded. Promoter sequences of the relevant genes were retrieved, and compared to known TFBS motifs. The input parameters were as follows: promoter maximum length = 500 nucleotides (nt), promoter minimum length = 100 nt, number of motifs per cluster = 10 nt, maximum motif width = 14 nt, minimum motif width = 6 nt. Furthermore, results were filtered to be in >5% of sites within the input cluster, and to have an E-value (number of motifs expected to be found by chance) of <0.05.

Four promoter motifs were identified that met these parameters. Two motifs were identified for mesotrione-treated plants that were in the cluster of up-regulated genes (Fig. 7.6.1). The MCACGTGKCA (where M is C or A, and K is T or G) motif (Fig. 7.6.1a) was found in 60 sites (14%) with an E-value of 2.9×10^{-28} . The motif is found 40 times on the positive stand and 20 times on the negative strand. The YYTCTTCTYY (where Y is C or T) motif (Fig. 7.6.1b) was identified in 103 sites (24%) with an E-value of 4.9×10^{-14} . The motif is found 68 times on the positive stand and 35 times on the negative strand.

Two motifs were identified that were in the adjuvant-treated down-regulated gene list (Fig. 7.6.2). The RRAGAAGAAR (where R is A or G) motif (Fig. 7.6.2a) was found in 92 sites (26%) with an E-value of 7×10^{-12} . This motif was found 30 times on the positive stand and 62 times on the negative strand. Finally, the ATGMCACGTGK motif (Fig. 7.6.2b) was found in 24 sites (7%) with an E-value of 2×10^{-2} . The motif was found 7 times on the positive stand and 17 times on the negative strand. The MCACGTGKCA motif found in the mesotrione treatment (Fig. 7.6.1a) and the ATGMCACGTGK motif found in the adjuvant treatment (Fig. 7.6.2b) contain the same core CACGTG hexamer, known as a G-box (Giuliano et al., 1988).

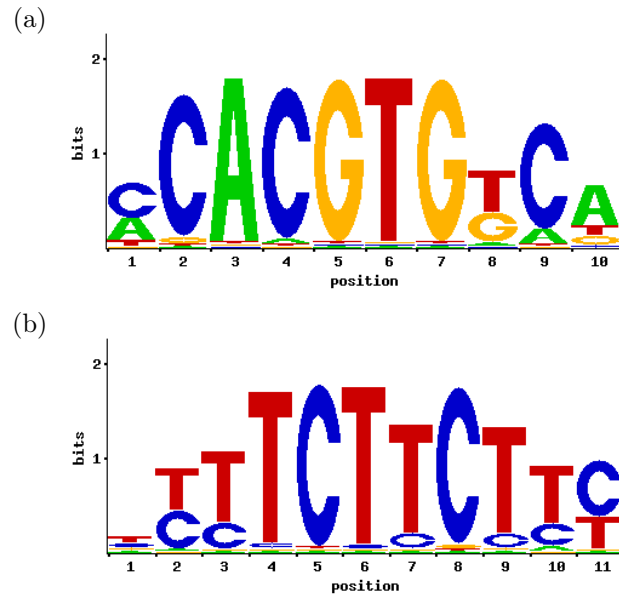


Figure 7.6.1: Two promoter motifs were over-represented in the mesotrione up-regulated gene list. (a) The MCACGTGKCA motif was found in 60 sites. (b) The YYTCTTCTYY motif was found in 103 sites. Motif sequence logos produced by MEME-LaB.

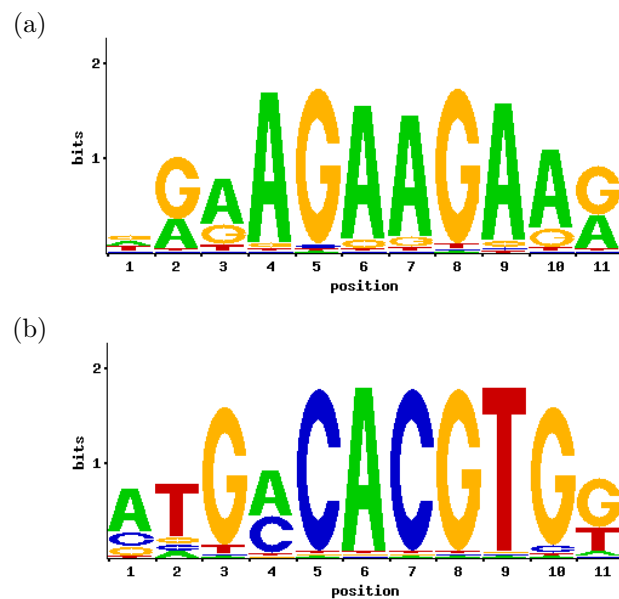


Figure 7.6.2: Two promoter motifs were over-represented in the adjuvant down-regulated gene lists. (a) The RRAGAAGAAR motif was found in 92 sites. (b) The ATGMCACGTGK motif was found in 24 sites. Motif sequence logos produced by MEME-LaB.

7.7 Significant overlaps of herbicide-response genes and nycthemeral and circadian regulated transcript sets

To identify potential interactions between the effect of these herbicides and treatment time of day effects, a meta-analysis was conducted. The mesotrione-, adjuvant-, and TBA-regulated gene lists were compared to published gene lists for nycthemeral-regulated genes (Smith et al., 2004; Bläsing et al., 2005), circadian-regulated genes (Edwards et al., 2006; Dodd et al., 2007; Covington and Harmer, 2007), or the genes that appear in both the nycthemeral and circadian lists.

227 mesotrione-regulated genes significantly overlapped with nycthemeral-regulated genes, which is more than the 121 expected by chance (Fig. 7.7.1). 62 mesotrione-regulated genes significantly overlapped with circadian-regulated genes, whereas 26 were expected by chance (Fig. 7.7.1). 35 mesotrione-regulated genes significantly overlapped with both circadian- and nycthemeral-regulated genes, whereas 15 were expected by chance (Fig. 7.7.1). Of these 35, 17 genes were up-regulated and 18 were down-regulated in response to mesotrione.

205 genes were identified that significantly overlap between adjuvant-treated and nycthemeral-regulated genes, more than the 113 expected by chance (Fig. 7.7.2). 52 genes significantly overlapped between the adjuvant-treated and circadian-regulated genes, whereas 25 were expected by chance (Fig. 7.7.2). 28 genes significantly overlapped between adjuvant-treated genes and both circadian- and nycthemeral-regulated genes, whereas 14 were expected by chance (Fig. 7.7.2). Of these 28 adjuvant-, circadian-, and nycthemeral-regulated genes, 13 were up-regulated and 15 were down-regulated.

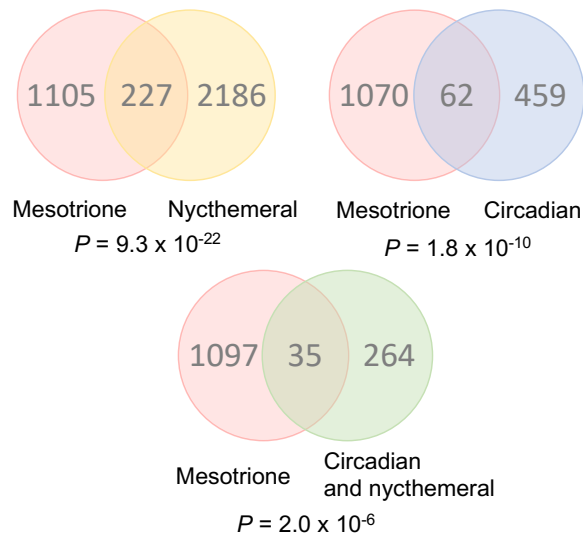


Figure 7.7.1: Mesotrione-regulated genes overlap significantly with nycthemeral, circadian, and circadian and nycthemeral genes. Nycthemeral dataset compiled from genes common to Smith et al. (2004) and Bläsing et al. (2005), circadian dataset compiled from genes common to Edwards et al. (2006), Dodd et al. (2007) and Covington and Harmer (2007). *P* values obtained by hypergeometric analyses.

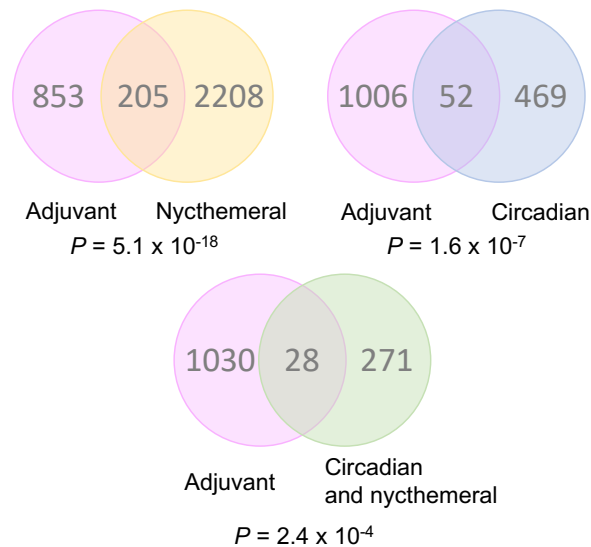


Figure 7.7.2: Adjuvant-regulated genes overlap significantly with nycthemeral, circadian, and circadian and nycthemeral genes. Nycthemeral dataset compiled from genes common to Smith et al. (2004) and Bläsing et al. (2005), circadian dataset compiled from genes common to Edwards et al. (2006), Dodd et al. (2007) and Covington and Harmer (2007). *P* values obtained by hypergeometric analyses.

105 genes significantly overlapped between the TBA-regulated gene list and the nycthemeral-regulated gene list, where 60 were expected by chance (Fig. 7.7.3). 26 genes overlapped significantly between the TBA-regulated list and the circadian-regulated gene list, with 13 genes expected by chance (Fig. 7.7.3). There were 13 genes that overlapped between the TBA-regulated gene list and both the circadian and nycthemeral gene lists, whereas 7 were expected by chance (Fig. 7.7.3). Of these 13, one was up-regulated by TBA, and 12 were down-regulated by TBA.

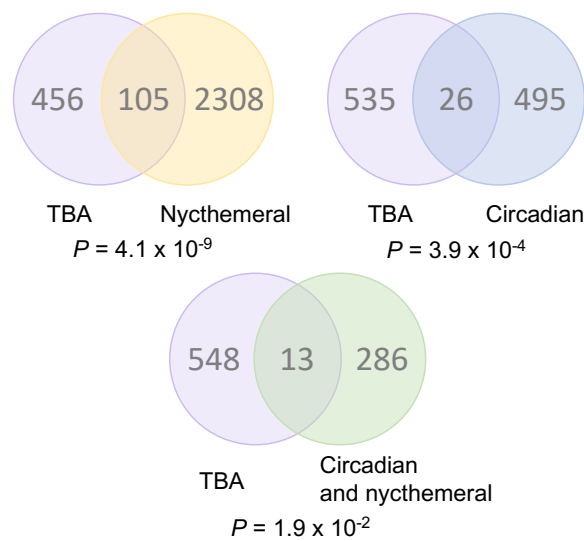


Figure 7.7.3: TBA-regulated genes overlap significantly with nycthemeral, circadian, and circadian and nycthemeral genes. Nycthemeral dataset compiled from genes common to Smith et al. (2004) and Bläsing et al. (2005), circadian dataset compiled from genes common to Edwards et al. (2006), Dodd et al. (2007) and Covington and Harmer (2007). P values obtained by hypergeometric analyses.

7.8 Discussion

RNA-sequencing was conducted to identify differential gene expression in response to mesotrione, Agridex, and TBA treatment in Arabidopsis. The sequencing produced good quality reads and alignment to the reference genome. There were small differences in the total reads and genome coverage between replicates of the same treatment. This could have been due to differential degradation of the RNA in samples pre-sequencing. The coverage of the reference genome had a mean of 35%. This appears low, however not all genes in the genome would be expressed at one time due to factors including: nycthemeral regulation of transcripts, growth stage-specific expression and tissue-specific expression.

Following sequencing, further analysis was conducted with the aim of understanding the biological importance of the results. Some genes with the highest fold change were unique to that treatment, for example: *ARTL5*, *PDX1L4*, and *ATPP2-A13*. These unique genes mostly occurred in the TBA treated samples. TBA treated samples would have also had the same genes changing in expression as the adjuvant-only treatment, as the adjuvant is a component of the TBA treatment. Most of these unique genes have little published about their function in the literature, therefore it is difficult to understand their wider context and importance. Conversely, some genes that were up- or down-regulated were common to more than one treatment suggesting they are involved in a common stress response. It is interesting to understand what role each gene family has, whether they map to any of the KEGG pathways identified and how they relate to circadian regulation. As such, this discussion focusses on the latter.

7.8.1 *PDR12* is a detoxifying gene highly up-regulated in response to mesotrione and adjuvant

The highest up-regulated gene in response to both mesotrione and adjuvant was

PLEIOTROPIC DRUG RESISTANCE 12 (PDR12) (Tables 7.4.4 and 7.4.6). PDR12 is a member of the ATP-binding cassette (ABC) proteins, a large superfamily of proteins involved in many types of substrate transport across membranes, including abscisic acid (Rea, 2007; Van Den Brûle and Smart, 2002). There are 129 ABC proteins in *Arabidopsis* organised into 13 subfamilies (Sánchez-Fernández et al., 2001). PDR homologs are one of these ABC subfamilies, with 15 genes encoding PDRs in *Arabidopsis* (Van Den Brûle and Smart, 2002). *Arabidopsis* PDR12 is closely related to *Spirodela polyrrhiza* TUR2 and *Nicotiana plumbaginifolia* ABC1 (Van Den Brûle and Smart, 2002). Early research found that *SpTUR2* expression accumulates in response to high salt and cold (Smart and Fleming, 1996). More recently, *Arabidopsis PDR12* was shown to be involved in the resistance to lead (Lee et al., 2005), and has since been referred to as a detoxifying gene. *PDR12* has also been shown to be induced by cold, drought and oxidative stress (Sham et al., 2014). Therefore, PDR12 is involved in transport of toxic metabolites across membranes in response to stress, and it is logical that it should be up-regulated in response to the herbicide or adjuvant treatments, and is non-specific in the response to these particular chemicals.

7.8.2 *WRKY30* and *MAPKKKs* could be components of the same stress-response signalling cascade

WRKY30 was up-regulated in response to both mesotrione and adjuvant treatment (Tables 7.4.4 and 7.4.6). WRKY proteins are TFs, named after the WRKY amino acid sequence of the DNA-binding domain (Rushton et al., 1996). *Arabidopsis* has 74 *WRKY* genes divided into 8 subfamilies (Ülker and Somssich, 2004). The majority of research involving WRKY TFs has examined their extensive involvement in biotic stress responses (Rushton et al., 2010). However, WRKYs are also involved in other plant processes including germination and senescence, and in response to abiotic stresses such as drought, heat, cold and salinity (Rushton et al., 2010; Chen et al., 2012). Induction of *WRKY* genes has been reported to be fast and transient and does not appear to require synthesis of regulatory factors (Hara et al., 2000; Eulgem

et al., 2000). Additionally, one WRKY TF can regulate the plant response to multiple factors and as such may be non-specific to types of abiotic stress (Chen et al., 2012).

Interestingly, several WRKYs are phosphorylated when co-expressed with mitogen-activated protein kinases (MAPK) and MAPK kinases (MAPKK) (Popescu et al., 2009). Here, *MITOGEN-ACTIVATED PROTEIN KINASE KINASE KINASE (MAPKKK) 18* and *MAPKKK19* were up-regulated in response to both mesotrione and adjuvant treatments (Tables 7.4.4 and 7.4.6). Therefore, hypothetically, the *MAPKKKs* induced by herbicide treatment could be responsible for signalling cascades that allow a downstream MAPK to phosphorylate WRKY30, subsequently causing transcriptomic changes in response to the mesotrione or adjuvant treatment.

MAPKKK18 and *WRKY30* have previously been collectively identified in a set of 12-oxo-phytodienoic acid (OPDA)-specific response genes (Taki et al., 2005). OPDA is a precursor in the jasmonate biosynthetic pathway that has its own signalling properties in biotic and abiotic stress responses (Taki et al., 2005; Dave et al., 2011, 2016). Therefore, because these two genes have been shown to be in the same response pathway previously, this further suggests that they could be components of the same signalling cascade, although there is no direct evidence to support this. *MAPKKK18* and *19* and *WRKY30* are poorly understood so it is interesting that they have consistently been highly up-regulated in response to the abiotic stresses caused by the application of mesotrione and adjuvant.

WRKY TFs are frequently up-regulated in response to pathogenic attack, hence these genes could be components of the plant pathogen interaction metabolic KEGG pathway that was found to be up-regulated in response to mesotrione (Table 7.5.1). MAPK and WRKY TFs have been found to show nycthemeral and circadian-regulated expression (Bhardwaj et al., 2011). For example, the *Neurospora* circadian oscillator component WCC binds directly to a *MAPKKK* promoter and regulates phosphorylation rhythms (Lamb et al., 2011) and is responsible for cellular growth (Bennett et al.,

2013). In plants, some protein kinases are regulated by the circadian oscillator (Nakamichi et al., 2002; Kumar et al., 2011), and consequently may restrict their ability to phosphorylate downstream targets. Therefore, WRKY30 or MAPKKK18 and 19 could be involved in some circadian regulation in the response to mesotrione or adjuvant, however, there is currently no evidence to support this but it would be interesting to investigate further.

7.8.3 Herbicide-induced oxidative stress is regulated through *ERFs* and *GSTs*

Ethylene is a plant hormone involved in biotic and abiotic plant stress signalling (Müller and Munné-Bosch, 2015). Plant hormones such as ethylene function as signals in the stress-response cascade to adapt the plant to stress environments (Müller and Munné-Bosch, 2015). The APETALA 2 (AP2)/ethylene-responsive element binding factor (ERF) superfamily of TFs have been shown to respond to pathogen attack, cold, heat, drought and salinity (Mizoi et al., 2012; Müller and Munné-Bosch, 2015). These TFs contain the AP2/ERF DNA-binding domain that is 60-70 amino acids in length (Nakano et al., 2006). There are four major families of AP2/ERFs based on their overall structure and binding domains: AP2, RAV, ERF, dehydration-responsive element-binding (DREB) protein (Sakuma et al., 2002; Mizoi et al., 2012). The DREB subfamily is more closely related to the ERF subfamily than the other subfamilies and has led to different family classifications (Nakano et al., 2006; Mizoi et al., 2012). In total there are 145 AP2/ERF genes and 122 in the ERF and DREB subfamilies in Arabidopsis (Sakuma et al., 2002; Nakano et al., 2006; Mizoi et al., 2012). Three *AP2/ERF* genes were up-regulated in response to both mesotrione and adjuvant treatment. Two of these genes are in the ERF subfamily: *HYPOXIA RESPONSIVE ERF GENE 2* (*HRE2*; also known as *ERF71*) and *REDOX-RESPONSIVE TF1* (*RRTF1*, also known as *ERF109*), and one is in the DREB subfamily: *ERF020* (Sakuma et al., 2002).

ERF020 is a member of the A-5 subgroup of DREBs (Sakuma et al., 2002). These proteins have a specific ERF-associated amphiphilic repression (EAR) motif that is potentially involved in negative feedback regulation of DREB1/CBF (A-1 subgroup) and DREB2 pathways (Tsutsui et al., 2009; Mizoi et al., 2012). Interestingly, *ERF8* (another member of the A-5 subgroup) is a target of TOC1, therefore is circadian regulated (Grundy et al., 2015). Furthermore, the DREB1 TFs, involved in cold responses, are circadian regulated (Fowler et al., 2005). It seems the main regulatory role of these A-5 group proteins is not in directly initiating a response pathway of their own, but binding to other ERFs.

HRE2 is in the B-2 subgroup of ERFs (Sakuma et al., 2002). Despite being an ERF, *HRE2* is not induced by ethylene. Instead, *HRE2* was one of two ERF genes identified that was up-regulated in response to low O₂, hence it was named hypoxia-responsive (Licausi et al., 2010). Hypoxia is caused by an oxygen shortage due to reduced intracellular oxygen transport that can occur due to external oxygen becoming unavailable if the plant is submerged in water (Licausi et al., 2010). *HRE2* is largely expressed in roots (Licausi et al., 2010; Eysholdt-Derzso and Sauter, 2019), however roots were not sampled in this work. It is interesting that an oxygen starvation response might have been perceived by the herbicide-treated plants. It is possible that the method of treatment application could have caused a hypoxic environment, but it would therefore also have occurred in the water-treated control. Alternatively, it could have been that the water treatment still contained sufficient oxygen whereas the other treatments did not.

RRTF1 is in the B-4 subgroup of ERFs (Sakuma et al., 2002). *RRTF1* is involved in regulating the response to redox stress (Khandelwal et al., 2008), and is induced by different abiotic stresses such as salt (Soliman and Meyer, 2019) and jasmonic acid (Cai et al., 2014). The up-regulation of *RRTF1* is logical since many stresses, particularly these herbicides, induce ROS accumulation. *RRTF1* becomes activated in response to ROS after photosynthetic perturbations to help achieve redox homeostasis (Matsuo et al., 2015; Soliman and Meyer, 2019). Under oxidative stress conditions, *RRTF1*

drives expression of *BAX INHIBITOR 1 (BI-1)*, a cell death suppressor (Bahieldin et al., 2018) to prevent programmed cell death. RRTF-regulated genes are reported to be involved in three pathways: phenylalanine, tyrosine and tryptophan biosynthesis, tryptophan metabolism, and plant hormone signal transduction. Two of these KEGG pathways were up-regulated in response to mesotrione and adjuvant (Tables 7.5.1 and 7.5.3). Interestingly, RRTF was also found to be involved in regulating families of ROS scavenging enzymes (Bahieldin et al., 2018). One of these enzymes is the glutathione S-transferases (GST). These GSTs further prevent the induction of PCD by inhibiting Bax protein, a PCD initiator (Baek et al., 2004).

Glutathione S-transferases (GSTs) catalyse the conjugation of glutathione to an electrophilic substance, either endogenous or exogenous (Wagner et al., 2002). GSTs can also act as glutathione peroxidases where they protect cells from oxygen toxicity (Edwards et al., 2000; Wagner et al., 2002). There are 55 genes in the GST superfamily, divided into seven classes including the plant-specific tau and phi classes (Wagner et al., 2002; Sappl et al., 2009; Gallé et al., 2019). 28 of the Arabidopsis GST genes are of the tau class, two of which were up-regulated in response to mesotrione and adjuvant, *ATGSTU3* and *ATGSTU11* (Tables 7.4.4 and 7.4.6). It has been shown that the GST phi class are involved in the protection against oxidative stress, but it is unclear whether this extends to the tau class (Sappl et al., 2009). However, a rice tau *GST* gene (*OsGSTU4*) expressed in Arabidopsis conferred an increased tolerance to oxidative stress, due to lower accumulation of ROS (Sharma et al., 2014). Therefore, there is potentially a relationship between the up-regulation of *RRTF1*, *ATGSTU3*, and *ATGSTU11* in the response to mesotrione and adjuvant to prevent oxidative damage.

In the presence of oxidants, biological membrane stability decreases and subsequent changes in the composition of the membrane, such as an increase in saturated fatty acids, act as protective mechanisms (Quinn and Williams, 1978). Antioxidant enzymes, such as GSTs, can decelerate the peroxidation of lipids, enhancing membrane stability. Malondialdehyde (MDA) is produced when ROS react with unsatur-

ated fatty acids in the membrane damaging the cell. Membrane fatty acid composition can prevent lipid peroxidation and MDA production (Prione et al., 2016). Mesotrione has been shown to increase saturated fatty acids and decrease membrane permeability while enhancing GST activity in the bacteria *Pantoea ananatis* and *Escherichia coli* (Prione et al., 2016; Olchanheski et al., 2014). Adjuvants in those experiments interfered with the structure of the lipid membrane, which is logical as they assist getting chemicals into the cell. It is suggested that GSTs are involved in the degradation of mesotrione in a bacteria where high activity of the GST corresponds with reduced mesotrione concentration (Prione et al., 2016). The KEGG pathways up-regulated in response to mesotrione include glycerophospholipid metabolism and glycerolipid metabolism, suggesting that the plant is increasing production of lipids for the membrane, in addition to the up-regulation of GSTs.

ROS-related pathways were also over-represented in response to herbicides. Glutathione metabolism is represented in mesotrione, adjuvant and TBA treated plants, both up and down regulated. Glutamate metabolism was down-regulated in response to adjuvant, and up-regulated in response to mesotrione, and ascorbate and aldrate metabolism was down-regulated in response to adjuvant. These pathways are all involved in plant responses to ROS (Noctor and Foyer, 1998). Dehydroascorbate reductase (DHAR) is involved in all three of these pathways and could potentially be the common enzyme limiting ROS detoxification (Hasanuzzaman et al., 2017).

There appears to be circadian regulation of ROS production and subsequently the ability of plants to cope with oxidative stress. ROS production peaks at ZT7 (noon), and the H₂O₂ scavenger, catalase, also peaks at ZT7 (Lai et al., 2012). This further coincides with when photosynthesis peaks. 140 ROS-responsive genes, with the majority peaking at noon, were also identified coinciding with when the gene regulators peaked (Lai et al., 2012). When plants had an improperly functioning circadian oscillator they are less able to tolerate oxidative stress (Lai et al., 2012). Therefore, the plant is more able to cope with ROS production at certain times of day, namely when it is expecting it, around noon. A herbicide that is increasing ROS production could

be more effective at a time when the plant is less able to respond and counteract the elevated levels of ROS.

Glutathione levels have also been shown to have nycthemeral regulation in Arabidopsis with glutathione increasing in the first 4 h of light, and decreasing in concentration in the night (Huseby et al., 2013). Therefore, this nycthemeral regulation can be responsible for redox control (Gallé et al., 2019). Studies have reported nycthemeral expression of GSTs (Sosa Alderete et al., 2018); one study in tobacco found the phi class of GSTs had nycthemeral expression patterns with peaks at the end of the light phase (Sosa Alderete et al., 2018). Little else is known about circadian regulation of GSTs (Gallé et al., 2019), but cycling of detoxification enzymes suggests that the plant is more susceptible to ROS toxicity when GSTs are low. Mutants with higher GST activity were found to have higher ability to detoxify and have enhanced tolerance to fluorodifen, a herbicide (Dixon et al., 2003). Further, herbicide safeners have been shown to up-regulate tau and phi GSTs (Skipsey et al., 2011). Therefore, this could be a useful factor to consider when engineering crops to have herbicide resistance.

7.8.4 CPuORFs regulate translation of downstream genes in response to herbicide treatments

Two conserved peptide upstream open reading frames (CPuORFs) were identified in the most highly down-regulated genes in response to adjuvant and TBA (Tables 7.4.7 and 7.4.9), *CPuORF32* and *CPuORF2*, respectively. The 5' untranslated region (UTR) of transcripts can contain a uORF (Ito and Chiba, 2013). This uORF contains a specific amino acid sequence that interacts in the nascent state with the ribosome during translation causing translation arrest (Ito and Chiba, 2013). These uORFs function to regulate gene expression of the downstream transcript through translation regulation (Jorgensen and Dorantes-Acosta, 2012; Ito and Chiba, 2013). If the initiation codon in the uORF is weak, the translation of the uORF may be skipped due to leaky scanning of the transcript by the ribosome, and translation will occur

from the main ORF (Rahmani et al., 2009; Yamashita et al., 2017). Often an effector, such as a signalling molecule, is required for the ribosome to start, and subsequently stop, translation at the uORF preventing translation of the main ORF, consequently regulating gene expression (Yamashita et al., 2017). Currently there are 58 genes in Arabidopsis known to contain CPuORFs, these genes are divided into at least 27 families of CPuORF homology groups (Jorgensen and Dorantes-Acosta, 2012). The majority of these families (33%) are involved in signalling processes such as protein kinases and biosynthesis or catabolism of small molecule signals. The next largest family (26%) encode TFs (Jorgensen and Dorantes-Acosta, 2012). These TFs encode important regulatory proteins that respond to the environment and are involved in growth and development (Jorgensen and Dorantes-Acosta, 2012).

CPuORF2 (Table 7.4.9) is a uORF in the *bZIP11* transcript, and is assigned to the HG1 family of CPuORFs (Jorgensen and Dorantes-Acosta, 2012). The bZIP11 TF is involved in reprogramming amino acid metabolism in response to sucrose and light, and regulates sugar-related genes (Hanson et al., 2008; Rahmani et al., 2009). bZIP11 is a component of the stress-dependent SnRK1 protein kinase adaption pathway (Rahmani et al., 2009). Sucrose acts as a signalling molecule that modulates the translation of bZIP11 in response to altered sucrose concentrations. Under high sucrose concentrations translation of CPuORF is enhanced and the nascent peptide causes ribosome arrest, consequently repressing bZIP11 at the level of translation (Rook et al., 1998; Wiese et al., 2004; Rahmani et al., 2009; Yamashita et al., 2017).

CPuORF2 was down-regulated in TBA-treated plants compared to control plants. This could mean that the control plants were photosynthesising as normal, and had a high level of sucrose that was then able to signal to initiate translation at the uORF. As TBA inhibits photosynthesis, it is logical that there would be less sucrose signalling, subsequently the bZIP11 uORF was not receiving sucrose signals, and translation initiated at the main ORF. This suggests there were lower levels of the CPuORF2. The biosynthesis of amino acids KEGG pathway was reduced in TBA-treated plants

(Table 7.5.5). There was potentially more bZIP11 protein being translated from the main ORF, as bZIP11 is known to be involved in amino acid metabolism.

CPuORF32 is a uORF in the *PHOSPHOETHANOLAMINE METHYLTRANSFERASE 3 (NMT3)* transcript. The main ORF encodes a phosphoethanolamine N-methyltransferase which is involved in the methylation of phosphoethanolamine to phosphocholine which is an intermediate to phosphatidylcholine, an abundant phospholipid in plasma membranes (Alatorre-Cobos et al., 2012). Little is understood about the translational regulation of NMT3 by *CPuORF32*. A closely related gene, *XIPOTL1*, begins translation at *uORF30* in the presence of phosphocholine, and subsequently represses translation of the main ORF (Alatorre-Cobos et al., 2012). Many reports state that the three NMTs in Arabidopsis are essential for phosphatidylcholine biosynthesis and growth (Liu et al., 2019; Chen et al., 2018; Liu et al., 2018; Chen et al., 2019). However, if the translation of one is inhibited by the translation at the uORF, it does not mean all three are simultaneously being translated at the uORF and inhibiting phosphatidylcholine. Furthermore, there is tissue-specificity of NMT expression (Alatorre-Cobos et al., 2012). The uORF which arrests production of the methyltransferase, was down-regulated after adjuvant treatment. Potentially the plant is compensating for a negative effect the adjuvant is having on the phospholipid membrane, ensuring there is higher methyltransferase production from the main ORF to increase phosphatidylcholine production.

While no evidence is currently apparent of circadian interactions with CPuORFs in Arabidopsis, the *Neurospora* circadian oscillator protein FREQUENCY (FRQ) has two isoforms regulated by translation of a uORF (Diernfellner et al., 2005). Both FRQ isoforms are crucial for rhythmicity and temperature compensation. Thermosensitive trapping of ribosomes leads to translation at the uORF, and reduced accumulation of the main ORF. This regulates FRQ levels in response to temperature where higher temperatures lead to higher levels of the long protein, and the uORF is more efficiently translated in lower temperatures. This is an example of direct involvement of differential translation and circadian rhythmicity. This could mean there is similar

regulation of CPuORFs in Arabidopsis that could be affected by herbicide-induced signalling components.

While these hypotheses are interesting, uORFs are involved in translational regulation rather than at the mRNA level, therefore it is unclear why there is a down-regulation in the mRNAs if the effects would not be seen at this level. There are other examples where herbicide treatments have had a significant effect on the differential gene expression of CPuORFs. For example, *OsCPuORF25* and *OsCPuORF26* transcripts were down-regulated in response to atrazine in rice (Zhang et al., 2012).

Further on the topic of translation, KEGG pathways ribosome and ribosome biogenesis in eukaryotes were up-regulated in response to adjuvant treatment, and not other treatments. The ribosome pathway includes the genes that comprise the large and small units of the ribosome, whereas the ribosome biogenesis pathway is the production of the components required for synthesising the mature ribosome (Kanehisa and Goto, 2000). The ribosome is the site for protein synthesis, therefore under stress, the plants could be increasing protein translation to synthesise stress response proteins discussed above (Weis et al., 2015). Furthermore, in order for the plants to continue growing newly synthesised proteins are required, consequently more ribosomes would need to be produced (Lastdrager et al., 2014).

7.8.5 G-box motifs could determine circadian regulation of differentially expressed genes

Two over-represented promoter motifs were identified for both the mesotrione up-regulated and adjuvant down-regulated differentially expressed gene lists. One of these core motifs was common to both treatments (Figs. 7.6.1a and 7.6.2b), CACGTG, a highly conserved G-box DNA-binding site (Giuliano et al., 1988). Over 2000 genes in Arabidopsis are reported to contain pure G-box sequences within 500 bp upstream of the transcription start site (Ezer et al., 2017).

Basic helix-loop-helix (bHLH) and basic leucine zipper (bZIP) families of transcription factor (TF) bind to G-boxes in many organisms, including plants (Meier and Grissem, 1994; Ezer et al., 2017). These TFs are responsible for initiating gene expression changes in response to light, temperature, drought, during growth, and other factors (Choi and Oh, 2016; Gangappa et al., 2013; Jung et al., 2016; Ezer et al., 2017). At least 78 G-box binding bHLH have been identified in *Arabidopsis* (Carretero-Paulet et al., 2010), and at least 8 of the 75 known bZIPs contain definite G-box binding sites (Jakoby et al., 2002). Therefore, there are a high number of potential TF-G-box binding combinations and relatively little is known about the specificity of TF-binding to G-boxes.

bZIP TFs are able to differentiate perfect G-boxes between genes (Ezer et al., 2017). The G-box flanking sequences could be responsible for determining such TF specificity. One study identified that a G two bases upstream, or a C two bases downstream of the G-box were important genomic features for determining bZIP homodimer binding (Ezer et al., 2017). This downstream C was found in the motif in response to mesotrione treatment (Fig. 7.6.1a) and the upstream G was found in the motif in response to adjuvant (Fig. 7.6.2b). However, the specific TFs or responses to the binding to this G-box and the flanking sequence is not known. Another study found that PhyA specifically bound to one flanking sequence of a G-box where the following gene was up-regulated, and a different G-box flanking sequence for those genes that PhyA down-regulated (Hudson and Quail, 2003).

A multitude of factors can affect TF binding, including flanking sequences and DNA shape (Ezer et al., 2017). Binding of a TF does not necessarily mean that the TF is affecting transcription. As G-boxes are present in genes that are involved in pathways of co-expressed genes, and the specific binding TFs are unknown, it is unclear how the presence of a G-box is biologically important in the responses to mesotrione and adjuvant.

A particularly interesting aspect is that the presence of G-box motifs are over-represented in circadian-regulated genes (Michael and McClung, 2003; Hudson and Quail, 2003; Ezer et al., 2017). The interaction of G-boxes and circadian regulation was initially identified by light-induced expression of the circadian genes *CCA1* and *LHY*. The bHLH PHYTOCHROME INTERACTING FACTOR 3 (PIF3) binds to a G-box in the circadian gene, that can then be bound by the phytochrome (Martínez-García et al., 2000). The G-box was the second most-represented promoter motif in circadian-regulated genes, after the evening element (AAAATATCT) (Hudson and Quail, 2003). In particular, circadian genes phased to the morning have been shown to be over-represented with G-box motifs (Michael and McClung, 2003). The G-box was also over-represented in nycthemeral- and light-regulated genes, and under-represented in dark-induced genes (Michael and McClung, 2003). It is also common for the G-box to be present alongside other circadian-related promoters in circadian controlled genes, such as the CCA1-binding site (AAAAATCT), or the evening element (Michael and McClung, 2003).

Compiling over 200 RNA-seq samples from different conditions, nearly all of the genes downstream of a G-box were expressed with a nycthemeral pattern (Ezer et al., 2017). These genes were clustered into two main groups of expression time: one clustered with gene expression late at night or dawn and one cluster was expressed 1 h after dawn (Ezer et al., 2017). Furthermore, there were corresponding peaks of TF expression. PIFs in particular were found to be key TFs linking the expression of the gene clusters by binding the the promoter G-boxes in these circadian-regulated genes (Ezer et al., 2017). It was also found that the G-box was over-represented in the rapidly induced PhyA-response genes, compared to being under-represented in the PhyA slow-response genes (Hudson and Quail, 2003). This suggests that the response genes are one of the primary components of the response pathways instead of genes further down the cascade.

Together, this suggests that while possession of a G-box in the mesotrione- or adjuvant-treated genes does not elucidate the related response pathway, the sets of

co-expressed genes could be circadian regulated. Furthermore, this regulation of expression could be restricted to the morning phase. Other circadian-related promoters were not enriched within these gene groups, which could have enhanced the effect of the G-box motif, but are not necessary in the response.

7.8.6 Core promoter hexamers could be causing a pathogen-like response after both mesotrione and adjuvant treatment

The other two enriched motifs identified for both mesotrione up-regulated, with a TCTTCT core motif (Fig. 7.6.1b), and adjuvant down-regulated, with an AGAAGA core motif (Fig. 7.6.2a), are not as well reported as the G-box promoter motif.

One study investigating TATA-box variants identified the TCTTCT motif in 418 Arabidopsis promoters (Bernard et al., 2010). The genes containing these motifs were involved in protein metabolism more than in any other gene class, based on Gene Ontology analysis. This is quite a basic biological process compared to the specific roles of TATA-containing genes. However, this study was only identifying hexamers near the TATA-box region -39 to -26 upstream of the transcription start site. The wider context and interpretation of this result is consequently quite limited, however it can be noted that protein metabolism as a metabolic pathway was not identified as over-represented alongside the presence of the TCTTCT motif in this work.

The TCTTCT motif is conserved across species being reported in rice and soybean in addition to Arabidopsis (Maruyama et al., 2012). This motif was one of the most over-represented hexamers in cold- and dehydration-inducible promoters in these species and caused both up- and down-regulation of the genes within which it occurs (Maruyama et al., 2012). It is unclear whether there were co-expressed genes involved in specific pathways that contained this motif, but the genes or pathways may be

similar to the ones identified in this study. Alternatively the motif could be present in genes that are involved in a more general stress response.

A protein-binding promoter element, termed *TL1* (CTGAAGAAGAA), was identified in the salicylic acid induction of pathogenesis-related and secretion-related genes, via the NPR1 (Nonexpressor of pathogenesis-related genes 1) protein (Wang et al., 2005). This *TL1* motif is thought to be related to the LURP^A motif, involved in the induction of genes in response to pathogenic oomycetes (Knoth et al., 2009). The LURP^A motif was identified in clusters of genes enriched with an inversely repeated sequence (5'-ATTGTTTTCTTCTGTAGAAGACCAT-3'). Knoth et al. (2009) found that DNA-binding factors interacted mainly with the second inverted repeat, AGAAGA. They found that one copy of the motif is sufficient for inducing the expression of the gene, but two copies of the motif enhance the defence response. The *TL1* motif contains different flanking nucleotides, which could be responsible for determining specificity of the TF, although both motifs are reported to be involved in a pathogenic response. Perhaps it is the core AGAAGA hexamer that is the key component of this promoter motif. Interestingly, these two hexamer sequences were two of the motifs that were enriched in the present work (Figures 7.6.1b to 7.6.2a; underlined), but it is unclear why a pathogen-induced response would be similar to a herbicide-induced response.

Up-regulation of the pathogenesis genes by *TL1* included those involved in the secretory pathway and ER-localised proteins. One of the mesotrione up-regulated KEGG pathways identified was protein processing in ER (Table 7.5.1), potentially there is a link between the TCTTCT motif found in the mesotrione up-regulated genes and the ER. The same KEGG pathway was identified in the adjuvant down-regulated pathway where the AGAAGA motif was enriched (Table 7.5.4). Furthermore, plant-pathogen interaction was also enriched in the KEGG pathways for these treatments. This suggests that the herbicide response within the plant is similar to that of a pathogen infection. A point of note is that the motifs identified by herbicide or adjuvant treatment do not have the same flanking sequences as *TL1* or LURP^A. Therefore, it

could only be the core hexamers that would be responsible for the pathogen-related responses.

The AGAAGA motif has been also been reported as a binding site for serine/arginine-rich proteins that are important splicing factors. Two proteins in Arabidopsis, SC35 and SC35-like (SCL), preferentially bind to this motif and enhance pre-mRNA splicing in the target mRNA (Yan et al., 2017). Therefore, it could be that down-regulation by adjuvant of the genes identified in the current work, is preventing the genes from being spliced, although it is unknown why this could be.

Overall, it seems that the TCTTCT and AGAAGA motifs are present in the promoters of co-expressed genes that are involved in a stress response similar to that caused by a pathogen infection. It could be that the flanking sequences specify the TF that would bind to the motif that separates the mesotrione and adjuvant response from actual pathogen responses.

7.9 Conclusion

RNA-seq was conducted in Arabidopsis to determine the effect of mesotrione, Agri-dex and TBA on the transcriptome. This has not previously been conducted. Various changes in gene expression occurred that link to stress response pathways and promoter elements. The pathways identified can largely be interpreted as consistent with the stress response expected when herbicide mode of action is considered, for example oxidative stress.

What was particularly interesting was that the adjuvant alone caused a strong stress response. This is important because the adjuvant could be applied to genetically modified, herbicide-resistant crops and could still have a significant impact on the health and, importantly, yield of those plants.

The greater fold-increase in certain genes does not necessarily equate to a high level of protein abundance. Therefore it would be more robust to complement the RNA-seq

data with proteomics and /or metabolomics. It was however good for an initial approximation of protein abundance as high mRNA levels have been shown to correlate to high protein levels (Ponnala et al., 2014).

Further validation of these results could be conducted through qPCR. Treatments of varying lengths could be tested to determine the effect on the gene expression. It would also be particularly interesting to investigate the effect of different times of treatments to determine whether or not there is circadian gating of the responses. It is also possible, due to the sequencing method employed, to examine the alternative splicing events caused by the treatments.

Chapter 8

Herbicides alter circadian period and phase

8.1 Introduction

Plants, as sessile organisms, are required to adapt to their changing growth environments and in doing so evolved circadian oscillators (Millar, 2004). When the plant circadian oscillator is correctly synchronised to its environment, fitness is enhanced (Dodd et al., 2005). In order to time biological processes to the phase that is most beneficial, plants perceive environmental signals, such as light and temperature, to set the circadian phase to the correct time of day and the period to 24 hours through a process known as entrainment (Harmer et al., 2001; Eriksson and Millar, 2003). Such environmental entrainment signals are also known as inputs to the oscillator; consequential actions of the oscillator, such as changes in gene expression, are termed outputs (Hsu and Harmer, 2014).

Under constant conditions the period can change due to the absence of phase setting by such entrainment signals (Eriksson and Millar, 2003). Factors such as metabolites and ions also have the ability to alter the circadian period. For example, nicotinamide, Ca^{2+} and 3'-phosphoadenosine 5'-phosphate can lengthen the period (Dodd et al.,

2007; Martí Ruiz et al., 2018; Litthauer et al., 2018), whereas ethylene, sucrose and Fe^{3+} are able to shorten the circadian period (Haydon et al., 2017, 2013; Salomé et al., 2013; Webb et al., 2019). In a natural environment a plant would not be exposed to constant environmental conditions but a change in period can consequently affect entrainment under light-dark cycles (Webb et al., 2019).

A notable example of the relationship between circadian period and phase was identified by Hearn et al. (2018). A forward genetic screen identified a *BIG* mutant as circadian period-hypersensitive to exogenous nicotinamide. The mutation also caused a significantly shorter period under constant low light and, importantly, an early entrained phase (Hearn et al., 2018). Therefore, the altered phase under light/dark cycles, caused by the change in period, suggests that *BIG* is fundamental for correct circadian entrainment. Two principles have been proposed as to how period affects entrainment: (i) a stimulus could alter the activity of components in the pathway of the oscillator, changing the speed at which the circadian oscillator is running and changing the ability of the plant to respond to the entrainment signal (Aschoff, 1960). Or, (ii) the change in period could be because of a large change in an oscillator component altering the phase directly without affecting the speed at which the oscillator is running (Pittendrigh and Daan, 1976). These theories are known as parametric- and non-parametric entrainment, respectively (Johnson et al., 2003; Webb et al., 2019). The example of *BIG* emphasises the importance of reporting the activity of the plant circadian oscillator under both constant conditions and light-dark cycles in response to stimuli, to determine whether such a stimuli affects the ability of the plant to have a correct phase relationship with the environment.

A commonly used method for detecting oscillations of circadian genes is the luciferase reporter system. The luciferase assay system provides a non-invasive, real-time report of promoter activity (Millar et al., 1992). The system originally exploited the naturally occurring *LUCIFERASE* (*LUC*) gene from the North American firefly *Photinus pyralis* (Leeuwen et al., 2000), however more recently a modified brighter *LUC*, *LUC+*, is used (Welsh et al., 2005). Transgenic plants are produced with the promoter from

the gene of interest (here, a circadian oscillator gene) fused to the *LUC* gene (Millar et al., 1992). Exogenous luciferin is applied to the plant and, when the *LUC* gene is expressed via the promoter of interest, LUC catalyses the oxidative decarboxylation of the luciferin (Millar et al., 1992). This reaction releases a photon which can be imaged with a highly sensitive camera (Leeuwen et al., 2000). This method has multiple benefits: unlike other biological reporters, external illumination is unnecessary making it useful in circadian assays in the absence of light. The lack of light required also prevents the exposure to toxic high energy photons, necessary for other reporters. The light emitted from the reaction is very low intensity, and is in the green portion of the visible light spectrum (560 nm). Therefore, the light produced from the reaction will not affect the experimental light conditions, which is essential for circadian experiments, and also will not be able to entrain the circadian oscillator or drive photosynthesis (Welsh et al., 2005).

Time course experiments are usually conducted after a period of entrainment followed by at least four cycles of constant conditions (Welsh et al., 2005). Bioluminescence data are obtained and manipulated to determine the emergent properties of the circadian oscillator (Dodd et al., 2014). Such properties include the circadian period, phase and amplitude. To obtain period estimations, one method of analysis is the fast Fourier transform-nonlinear least-squares (FFT-NLLS) algorithm. The central concept of this method is that data are fitted to a series of linearly damped cosine curves (Straume et al., 2002; Welsh et al., 2005). The algorithm gives confidence levels for period and amplitude, and can determine data as arrhythmic if no period is detected (Zielinski et al., 2014). Furthermore, phase can be calculated under entrainment conditions by measuring the time of the peak in each cycle.

The aim of this chapter was to examine the effects of the herbicides and their adjuvants on the promoters of core circadian oscillator components, and to measure the resulting emergent properties of the circadian rhythm. The importance of this is twofold: herbicides could alter the metabolites within a weed species that could alter the circadian oscillator of the weed and prevent it from being matched to the environment

and, therefore, having a lower fitness. Alternatively, if a herbicide did have negative effects on the phase-relationship of the circadian oscillator to the environment, and the herbicide is sprayed onto herbicide-resistant plants, this could negatively impact the non-target crop species. Furthermore, the adjuvants in the herbicide formulations could also have off-target effects on the circadian oscillator. This has not been investigated previously in plants for the chemicals of interest.

8.2 Bioluminescence data collection and analysis

Data were collected as described in Chapter 2.11. After collection, data were normalised within the first 24 h for each individual treatment where the peak value was set to 1 and the trough to 0. Unless stated otherwise, the mean of 12-18 rings of seedlings from across two or three separate experiments was calculated and plotted. For experiments under constant light, emergent properties were calculated from 48 h after the onset of constant conditions, 24 h after the application of treatment. Data are also presented in the form of a heat map from one representative experiment to visualise the peaks, troughs and effect on bioluminescence caused by treatments, where white indicates highest bioluminescence and red indicates lowest bioluminescence. Each square within a heat map represents one time point; data were transformed using amplitude and baseline detrending using BioDare2 (Zielinski et al., 2014).

8.3 Some herbicides alter circadian period, depending on the reporter

To investigate the effect of herbicides on the promoters of the circadian oscillator, experiments were conducted under free-running conditions. First, the effects of 100 g/ha glyphosate on *CCA1::LUC* were examined (Fig. 8.3.1). Glyphosate had visible effects on *CCA1::LUC* bioluminescence after the second cycle after treatment (approximately

56 h after exposure to continuous light) where the bioluminescence signal appeared weaker (Fig. 8.3.1a). This damping in bioluminescence became more pronounced with time, where the greatest difference between control and treated signal was 106 h after measurement commenced. Glyphosate-treated plants appeared to remain rhythmic (Fig. 8.3.1a). This was supported by the mean RAE value of approximately 0.12 for both glyphosate-treated plants and control plants (Fig. 8.3.1b). RAE values below 0.5 are considered rhythmic (Welsh et al., 2005). The period of *CCA1::LUC* appeared to become shorter with glyphosate treatment; control plants had a mean period of 25.8 h \pm 0.1 and glyphosate-treated plants had a mean period of 25.5 h \pm 0.16, however this was not a significant shortening. Glyphosate significantly reduced the amplitude of *CCA1::LUC* bioluminescence to almost half the value of the control plants (Fig. 8.3.1c), consistent with the damping of signal observed in the bioluminescence trace (Fig. 8.3.1a) suggesting that glyphosate reduced *CCA1* promoter activity. Alternatively, the reduced signal could be due to lower luciferase enzyme translation or lower ATP availability for luciferase activity. The time of peak *CCA1::LUC* bioluminescence signal was later with each cycle for both control and treated plants (Fig. 8.3.1d). However, the dynamics of this were slightly different between the control and glyphosate-treated plants where glyphosate-treated peaked slightly later in cycle 3, control and glyphosate-treated peak time was similar in cycle 4 and glyphosate-treated peaked earlier in cycle 5 (Fig. 8.3.1d). *CCA1::LUC* bioluminescence peaked approximately 1.5 h later in each cycle for control plants. This was consistent with the shorter period seen for glyphosate-treated plants. The difference in peak bioluminescence per cycle for the two different treatments can also be visualised in the heat map (Fig. 8.3.1e), where the period appears to be shorter in glyphosate-treated plants.

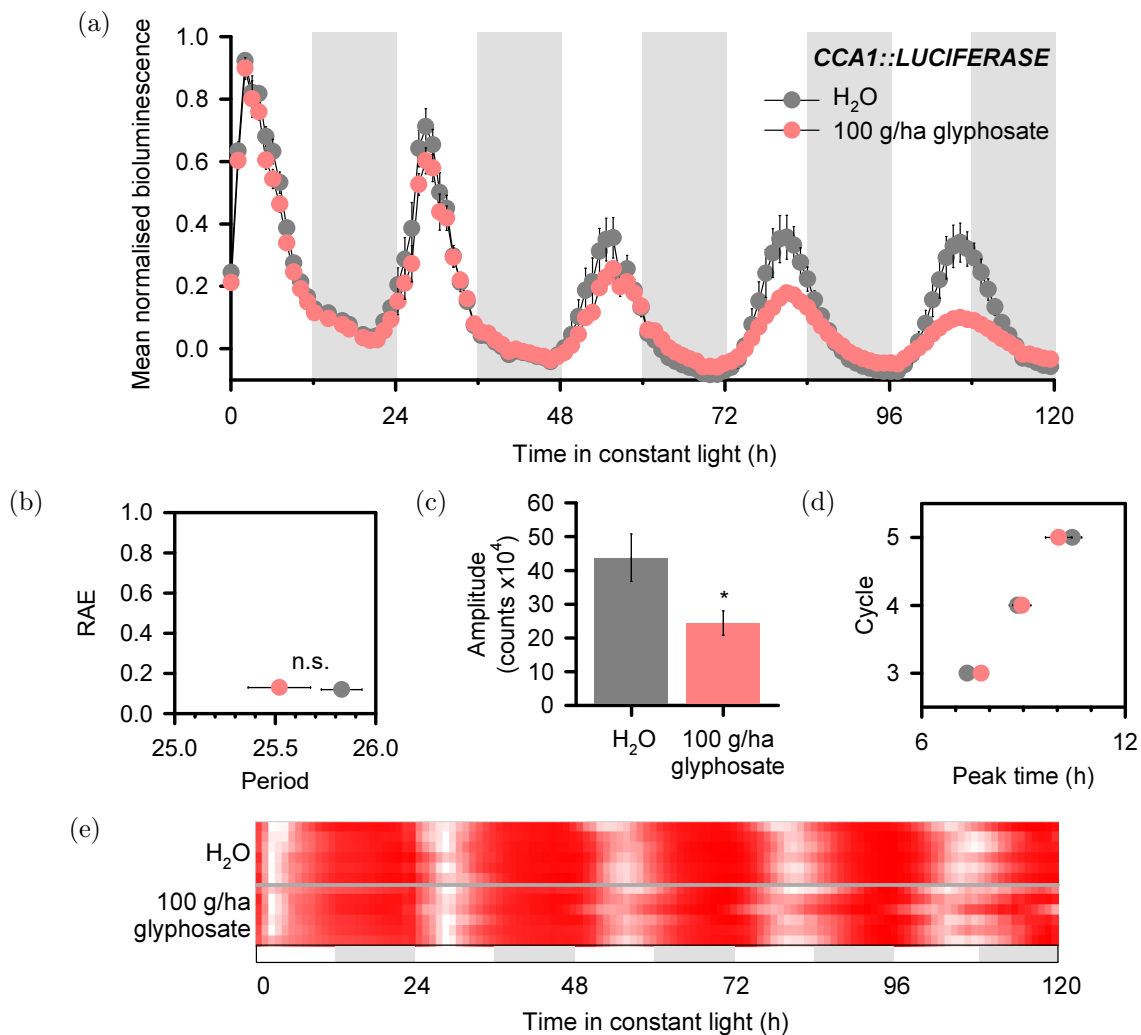


Figure 8.3.1: Glyphosate affects *CCA1::LUCIFERASE* activity under constant light conditions. Plants were dosed with luciferin on day 10. On day 11, imaging began under constant light conditions for 24 h. At dawn on day 12 plants were treated with either 100 g/ha glyphosate (pink) or a water control (grey) followed by a further 96 hours imaging under constant light. (a) Glyphosate application affected *CCA1::LUC* bioluminescence 48 h after application. (b) Glyphosate caused an earlier period phenotype, with no effect on RAE. (c) Glyphosate reduced *CCA1::LUC* amplitude. (d) Glyphosate did not significantly affect time of peak *CCA1::LUC* bioluminescence. (e) The effect of glyphosate on *CCA1::LUC* bioluminescence can be seen in the final two cycles of the heat map. Period, RAE and amplitude were derived from FFT-NLLS analysis conducted using BioDare2 after baseline and amplitude detrending. Shaded areas indicate subjective night. Data are the mean of 18 replicates from three independent experiments \pm SEM. Heat map data is from one representative experiment. Asterisks indicate significant difference between control and treated value, calculated by *t*-test where $* = P \leq 0.05$.

The effect of 100 g/ha glyphosate on *TOC1::LUC* was also examined (Fig. 8.3.2). Glyphosate appeared to have little effect on rhythms of *TOC1::LUC* bioluminescence (Fig. 8.3.2a). The bioluminescence signals were similar for both glyphosate-treated and control plants over the four cycles post-treatment and appeared to remain rhythmic. The mean RAE values were the same for both control and treated, at 0.2 (Fig. 8.3.2b). There was also no significant difference in the period between control and glyphosate-treated plants, possibly due to a large SEM for control plants (0.77). A small, but not significant decrease in amplitude occurred after glyphosate treatment (Fig. 8.3.2c). The mean peak time for each cycle was similar in glyphosate-treated plants between 19-20 h, whereas the peak time for control plants was approximately 1.5 h later in each cycle for control plants (Fig. 8.3.2d). However these differences were not significant. The bioluminescence signal appeared later with time in the control plants compared to the glyphosate-treated plants (Fig. 8.3.2e). This was consistent with the peak time and the potential shorter period in glyphosate-treated plants. The variability and inconsistent peak time between replicates that can be seen for control plants was likely to be causing the large period SEM.

While there appeared to be small changes to period, and peak time after glyphosate treatment for both *CCA1::LUC* and *TOC1::LUC*, only *CCA1::LUC* amplitude was significantly reduced (Fig. 8.3.2c). Therefore it appears that glyphosate does not have a particularly significant impact on the circadian oscillator under these experimental conditions. Results also summarised in Table 8.3.1.

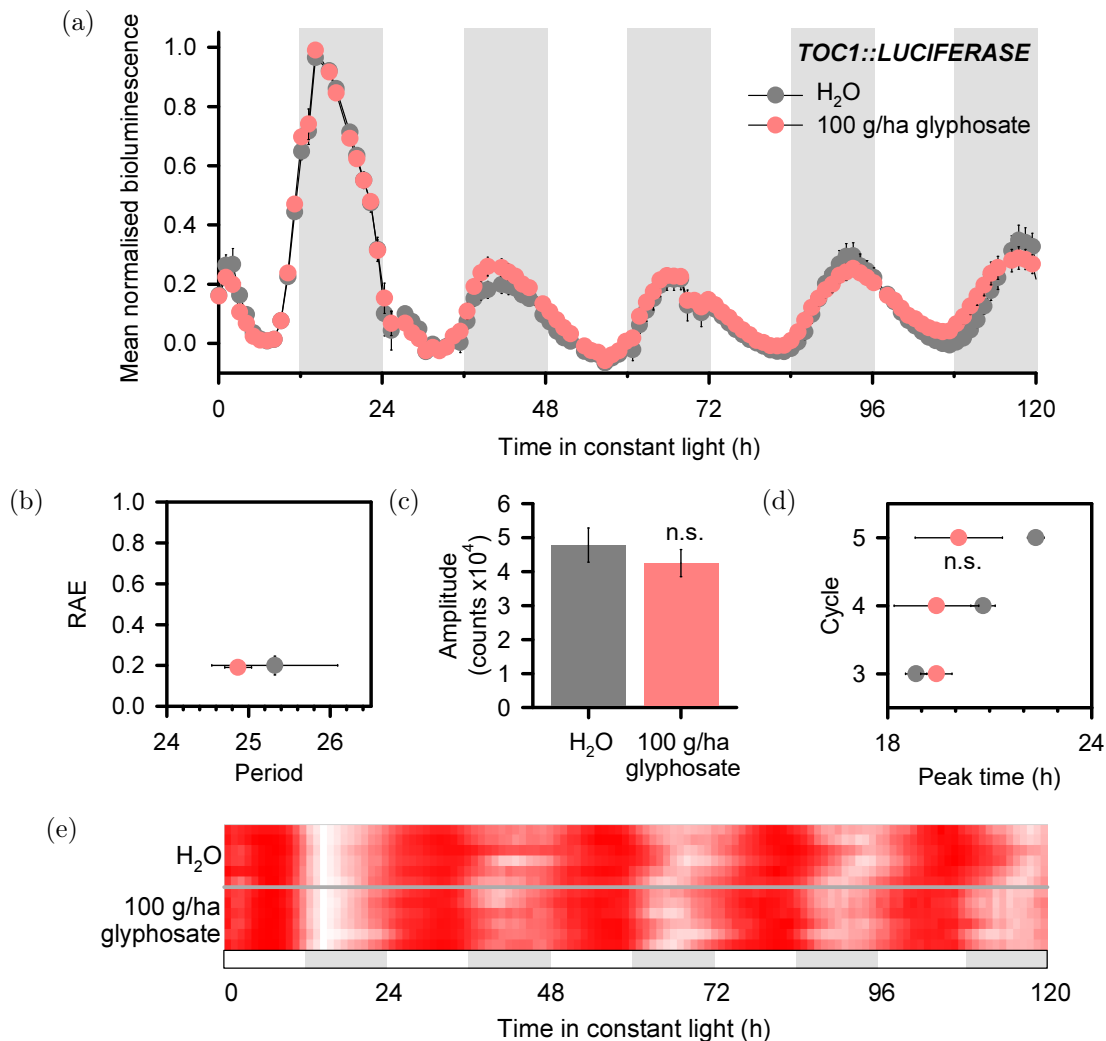


Figure 8.3.2: Glyphosate has little effect on *TOC1::LUCIFERASE* activity under constant light conditions. Plants were dosed with luciferin on day 10. On day 11, imaging began under constant light conditions for 24 h. At dawn on day 12 plants were treated with either 100 g/ha glyphosate (pink) or a water control (grey) followed by a further 96 hours imaging under constant light. (a) Glyphosate application had no clear visible effect on *TOC1::LUC* bioluminescence. (b) Glyphosate did not affect period length or RAE. (c) Glyphosate caused a small reduction in *TOC1::LUC* amplitude. (d) *TOC1::LUC* peak bioluminescence appeared to be slightly earlier with glyphosate application in cycle 5. (e) The effect of glyphosate on *TOC1::LUC* bioluminescence can be seen in the final two cycles of the heat map. Period, RAE and amplitude were derived from FFT-NLLS analysis conducted using BioDare2 after baseline and amplitude detrending. Shaded areas indicate subjective night. Data are the mean of 17 replicates from three independent experiments \pm SEM. Heat map data is from one representative experiment.

Next, the effects of 10 g/ha mesotrione on *CCA1::LUC* and *TOC1::LUC* were examined (Figs. 8.3.3 and 8.3.4). Mesotrione had an immediate effect on *CCA1::LUC*, such that the bioluminescence was damped compared to that of the control (Fig. 8.3.3a). Mesotrione had a greater effect on the promoter of *CCA1::LUC* over time, where the peaks of control plants remained constant over cycles 3, 4 and 5, the signal from the mesotrione-treated plants damped with each cycle. Mesotrione did not significantly affect the rhythmicity of the plants, where the mean RAE in mesotrione-treated plants was 0.15 ± 0.01 , compared to 0.12 ± 0.004 in control plants (Fig. 8.3.3b). Mesotrione treatment significantly increased the period of *CCA1::LUC* by half an hour from $25.8 \text{ h} \pm 0.1$ in control plants to $26.3 \text{ h} \pm 0.18$ (Fig. 8.3.3b). Mesotrione treatment reduced amplitude significantly, by a mean of 45% across the cycles 24 h after treatment (Fig. 8.3.3c). The peak of *CCA1::LUC* bioluminescence was later over the cycles in control and mesotrione-treated plants, however this was more pronounced in the mesotrione-treated plants (Fig. 8.3.3d). The peak of *CCA1::LUC* bioluminescence was significantly later than that of the control plants for each cycle, corresponding to the longer period observed. These later peaks were also seen in the heat map, particularly at 84 h and 108 h (Fig. 8.3.3e).

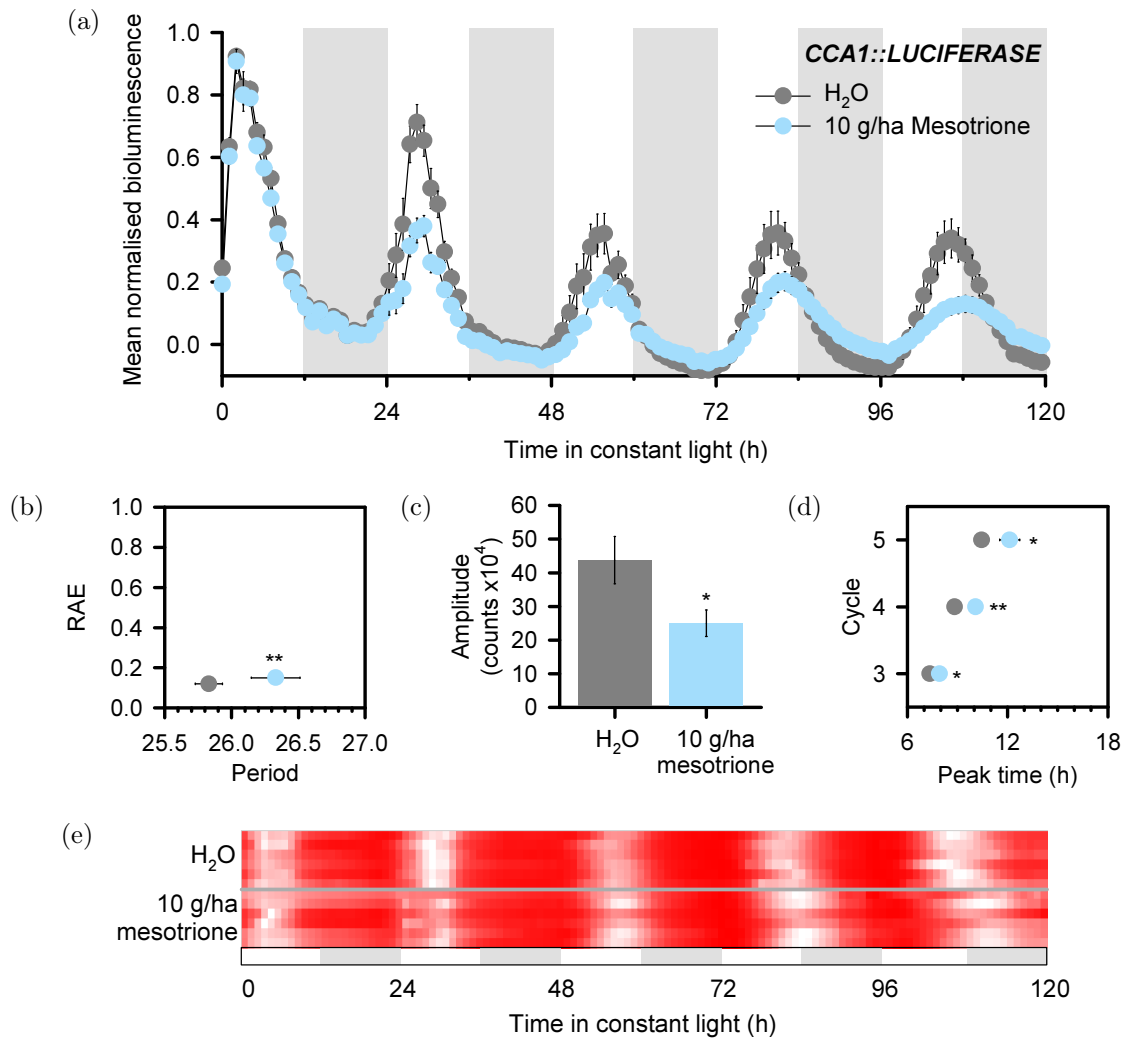


Figure 8.3.3: Mesotrione affects *CCA1::LUCIFERASE* activity under constant light conditions. Plants were dosed with luciferin on day 10. On day 11, imaging began under constant light conditions for 24 h. At dawn on day 12 plants were treated with either 10 g/ha mesotrione (blue) or a water control (grey) followed by a further 96 hours imaging under constant light. (a) Mesotrione application affected *CCA1::LUC* bioluminescence immediately after application. (b) Mesotrione caused a later period phenotype, with no effect on RAE. (c) Mesotrione reduced *CCA1::LUC* amplitude. (d) Mesotrione delayed the time of peak *CCA1::LUC* bioluminescence in all three cycles measured. (e) The effect of mesotrione on *CCA1::LUC* bioluminescence can be seen in the final two cycles of the heat map. Period, RAE and amplitude were derived from FFT-NLLS analysis conducted using BioDare2 after baseline and amplitude detrending. Shaded areas indicate subjective night. Data are the mean of 18 replicates from three independent experiments \pm SEM. Heat map data is from one representative experiment. Asterisks indicate significant difference between control and treated value, calculated by *t*-test where * = $P \leq 0.05$ and ** = $P \leq 0.01$.

Mesotrione treatment did not appear to have an inhibitory effect on *TOC1::LUC* bioluminescence, in comparison to *CCA1::LUC* (Fig. 8.3.4). Interestingly, mesotrione appeared to increase *TOC1* bioluminescence, particularly in the fifth cycle under constant light (Fig. 8.3.4a). No differences were observed between mesotrione-treated and control plants for RAE, period or amplitude (Figs. 8.3.4b and 8.3.4c). While the peak of *TOC1::LUC* bioluminescence for control plants was later over time, the peak for the last cycle of mesotrione-treated plants was significantly earlier than the control and also earlier than the other time points (Fig. 8.3.4d). *TOC1::LUC* bioluminescence appeared to peak slightly earlier than the control in the fourth and fifth subjective nights (Fig. 8.3.4e). It appeared that mesotrione had somewhat opposite effects on *CCA1* and *TOC1*, in particular for the effect on bioluminescence peak time where it was delayed for *CCA1::LUC* and advanced for *TOC1::LUC*. Results also summarised in Table 8.3.1.

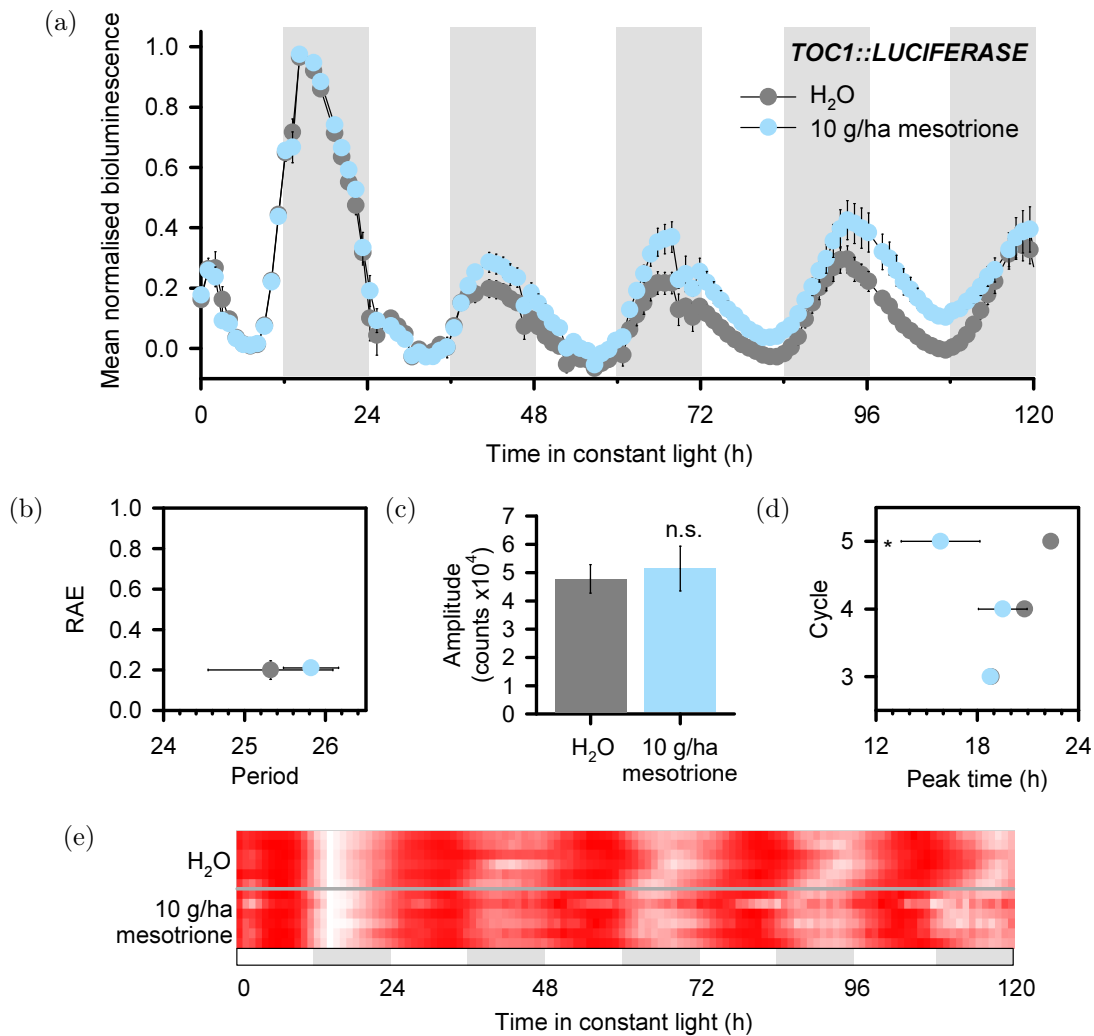


Figure 8.3.4: Mesotrione affects *TOC1::LUCIFERASE* activity under constant light conditions. Plants were dosed with luciferin on day 10. On day 11, imaging began under constant light conditions for 24 h. At dawn on day 12 plants were treated with either 10 g/ha mesotrione (blue) or a water control (grey) followed by a further 96 hours imaging under constant light. (a) Mesotrione application affected *TOC1::LUC* bioluminescence 14 h after application. (b, c) Mesotrione had no effect on *TOC1::LUC* period, RAE or amplitude. (d) Mesotrione advanced the time of peak *TOC1::LUC* bioluminescence in the final cycle measured. (e) The effect of mesotrione on *TOC1::LUC* bioluminescence can be seen in the final three cycles of the heat map. Period, RAE and amplitude were derived from FFT-NLLS analysis conducted using BioDare2 after baseline and amplitude detrending. Shaded areas indicate subjective night. Data are the mean of 16-17 replicates from three independent experiments \pm SEM. Heat map data is from one representative experiment. Asterisks indicate significant difference between control and treated value, calculated by *t*-test where * = $P \leq 0.05$.

Next, the effect of 1 g/ha TBA and its corresponding adjuvant control, 0.2% Agridex, were investigated for their effects on rhythms of *CCA1::LUC* (Fig. 8.3.5) and *TOC1::LUC* (Fig. 8.3.6). Effects of both TBA and Agridex were particularly obvious after 48 h in constant light (24 h after treatment) where the *CCA1::LUC* signal was damped (Fig. 8.3.5a). The mean RAE was 0.3 ± 0.02 for TBA-treated plants and 0.35 ± 0.004 for Agridex-treated plants (Fig. 8.3.5b), suggesting that the plants were less rhythmic than water-treated control plants (RAE = 0.15; Figs. 8.3.1b and 8.3.3b). TBA and Agridex treatments caused a long period phenotype, but TBA did not significantly lengthen the period relative to the Agridex control (Fig. 8.3.5b). No difference was seen between the effect of Agridex and TBA on *CCA1::LUC* amplitude (Fig. 8.3.5c) however, the mean amplitude was lower for both treatments compared to that of a water-treated control (Figs. 8.3.1c and 8.3.3c). While comparisons have been drawn between TBA and Agridex treatment, and a water control, these experiments were conducted on separate occasions. The peak time of *CCA1::LUC* bioluminescence after Agridex and TBA treatment was later with each cycle (Fig. 8.3.5d). After Agridex treatment, *CCA1::LUC* peaked approximately 2.5 h later with each cycle, which was lengthened by approximately 1 h more per cycle than in water-treated controls. TBA caused the peak to be even later, particularly in cycle 4, where it was 2 h later than the Agridex control, and 3 h later than in water-treated control plants. The differences between TBA and Agridex appeared to be reduced in cycle 5, suggesting either transient effects of the TBA in cycle 3 and 4, or perhaps the treatment effect was saturated at that point. *CCA1::LUC* bioluminescence maintains clear oscillations for at least three cycles following Agridex and TBA treatment (Fig. 8.3.5e). In the fourth cycle for Agridex treated plants, the level of bioluminescence was higher for a longer period of time than in previous cycles, represented by the white in the heat map. The Agridex peak was wider, or the signal was constant at a higher level, suggesting changes in the dynamics of the circadian rhythm in these plants. The higher levels of *CCA1::LUC* bioluminescence after TBA treatment appeared later than for Agridex treatment, corresponding to the peak time result (Fig. 8.3.5d).

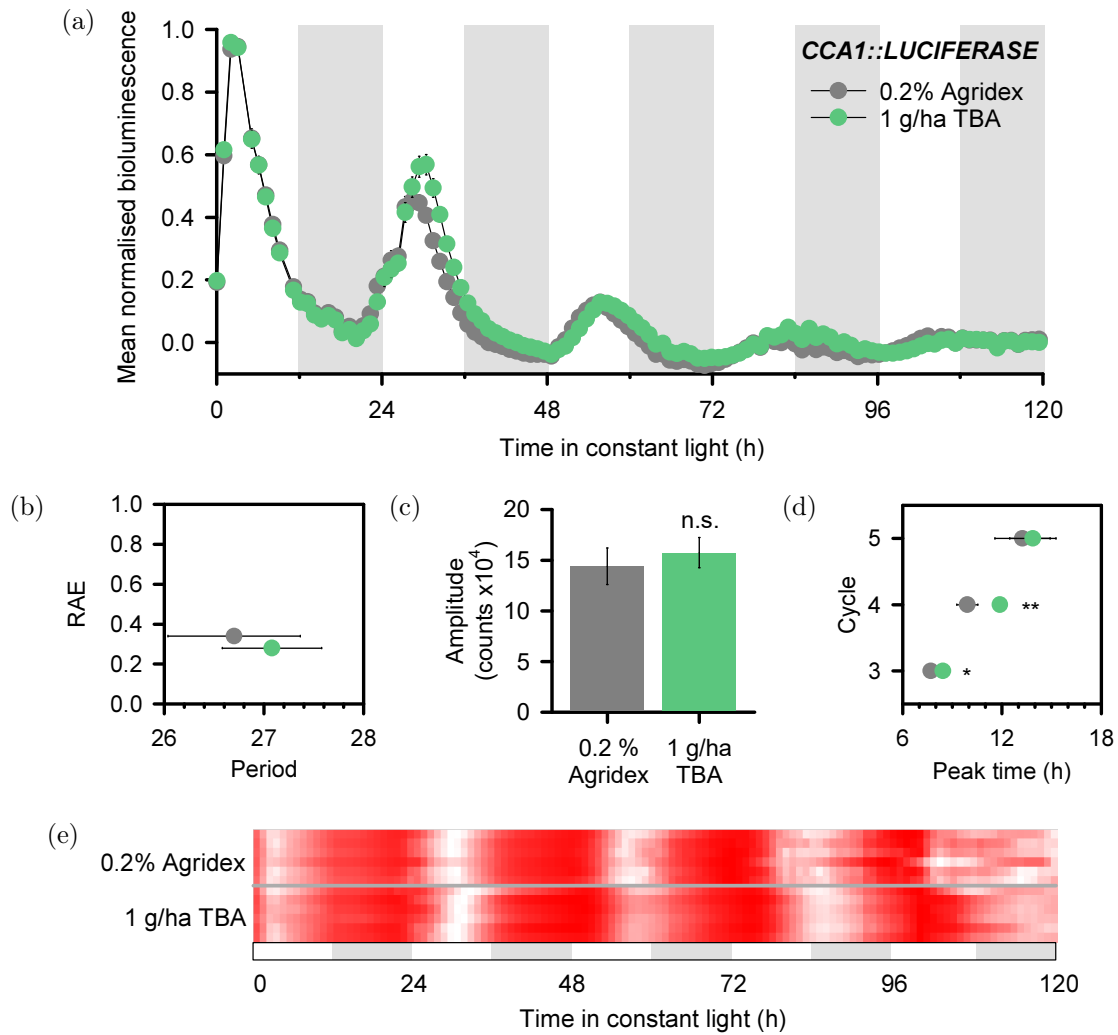


Figure 8.3.5: Terbutylazine affects *CCA1::LUCIFERASE* activity under constant light conditions. Plants were dosed with luciferin on day 10. On day 11, imaging began under constant light conditions for 24 h. At dawn on day 12 plants were treated with either 1 g/ha terbutylazine (green) or a 0.2% Agridex control (grey) followed by a further 96 hours imaging under constant light. (a) TBA application affected *CCA1::LUC* bioluminescence 6 h after application. (b, c) TBA had no significant effect on *CCA1::LUC* period, RAE or amplitude relative to Agridex. (d) TBA delayed the time of peak *CCA1::LUC* bioluminescence in the third and fourth cycles of constant light. (e) The effect of TBA on *CCA1::LUC* bioluminescence can be seen in all cycles of the heat map. Period, RAE and amplitude were derived from FFT-NLLS analysis conducted using BioDare2 after baseline and amplitude detrending. Shaded areas indicate subjective night. Data are the mean of 17-18 replicates from three independent experiments \pm SEM. Heat map data is from one representative experiment. Asterisks indicate significant difference between control and treated value, calculated by *t*-test where * = $P \leq 0.05$ and ** = $P \leq 0.01$.

TBA and Agridex had a similar effect on *TOC1::LUC* bioluminescence (Fig. 8.3.6). The rhythmicity of *TOC1* was affected by Agridex and TBA where the mean RAE values were 0.45 ± 0.04 and 0.3 ± 0.03 , respectively (Fig. 8.3.6b). Agridex had a greater effect on the rhythmicity than TBA, where the change in RAE of 0.15 was significant. Neither treatment appeared to alter the period of *TOC1::LUC* ($25.1 \text{ h} \pm 0.38$ for Agridex and $25.4 \text{ h} \pm 0.2$ for TBA; Fig. 8.3.6b) and there was no significant change between the treatments. The period was similar to that of water-treated control plants seen previously (25.3 h ; Fig. 8.3.4b). *TOC1::LUC* amplitude was higher in TBA-treated plants compared to Agridex-treated plants (Fig. 8.3.6c). The amplitudes appeared to be lower for both TBA and Agridex treatments compared to water-treated controls, that were previously approximately 4.8×10^4 counts. The timing of mean peak *TOC1::LUC* bioluminescence after Agridex treatment was approximately 4 h later from cycle 3 to 4, and then remained at approximately 23 h in cycle 5 (Fig. 8.3.6d). After TBA treatment, mean peak *TOC1::LUC* bioluminescence was slightly earlier in cycle 4 (19 h) than in cycle 3 (20 h), but in cycle 5 was later (23 h) than it was in cycle 3. The length of time where *TOC1::LUC* bioluminescence was a higher level was greater in later cycles, shown by wider areas of white colouring (Fig. 8.3.6d). This suggests changes in the shape of the oscillation, where the promoter activity was at trough levels for a shorter period of time. Overall, the results for TBA and Agridex treatment show that the adjuvant alone had an effect on the circadian oscillator, and that the differences between the herbicide and its adjuvant were small. Results are also summarised in Table 8.3.1.

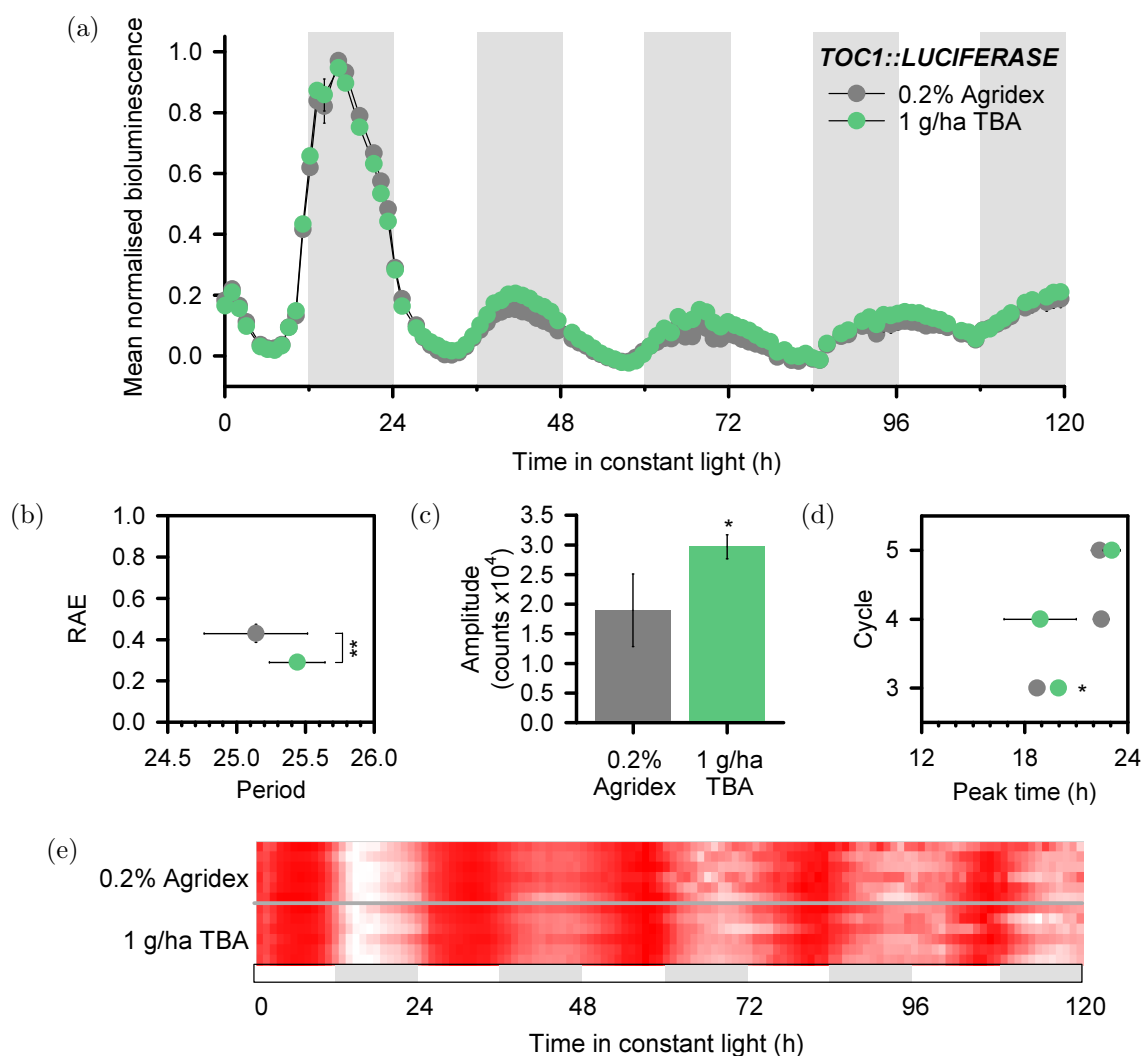


Figure 8.3.6: Terbutylazine affects *TOC1::LUCIFERASE* activity under constant light conditions. Plants were dosed with luciferin on day 10. On day 11, imaging began under constant light conditions for 24 h. At dawn on day 12 plants were treated with either 1 g/ha terbutylazine (green) or a 0.2% Agridex control (grey) followed by a further 96 hours imaging under constant light. (a) TBA application had small effects on *TOC1::LUC* bioluminescence. (b) TBA caused *TOC1::LUC* to be more rhythmic than Agridex treated plants. (c) TBA increased *TOC1::LUC* amplitude relative to Agridex. (d) TBA delayed the time of peak *TOC1::LUC* bioluminescence in the third cycle of constant light. (e) The effect of TBA on *CCA1::LUC* bioluminescence can be seen in the fourth cycle of the heat map. Period, RAE and amplitude were derived from FFT-NLLS analysis conducted using BioDare2 after baseline and amplitude detrending. Shaded areas indicate subjective night. Data are the mean of 17-18 replicates from three independent experiments \pm SEM. Heat map data is from one representative experiment. Asterisks indicate significant difference between control and treated value, calculated by *t*-test where * = $P \leq 0.05$ and ** = $P \leq 0.01$.

Table 8.3.1: Summary of the effects of herbicides under constant light conditions. Effect of herbicide is compared to the relevant control: water for glyphosate and mesotrione, and Agridex for TBA. Only statistically significant results are included. Phase result was not always consistent across multiple cycles.

Treatment	Reporter	Period	RAE	Amplitude	Phase
Glyphosate	<i>CCA1::LUC</i>	-	-	Reduced	-
	<i>TOC1::LUC</i>	-	-	-	-
Mesotrione	<i>CCA1::LUC</i>	Long	-	Reduced	Late
	<i>TOC1::LUC</i>	-	-	-	Early
TBA	<i>CCA1::LUC</i>	-	-	-	Late
	<i>TOC1::LUC</i>	-	Increased	Increased	Late

8.4 The adjuvant components of herbicide formulations alter the properties of the circadian oscillator under free-running conditions

Components of the herbicide formulations other than the active ingredient could also affect the circadian oscillator, therefore these were also investigated. Three concentrations of the glyphosate adjuvant were tested and compared to the water-treated control for the effects on *CCA1::LUC* and *TOC1::LUC* (Figs. 8.4.1 and 8.4.2). The three concentrations were: 840 g/ha glyphosate equivalent (field rate), 100 g/ha glyphosate equivalent (concentration of glyphosate used for the majority of this work), and a lower concentration of 25 g/ha glyphosate equivalent.

The effect of 840 g/ha equivalent adjuvant was apparent immediately after application (Fig. 8.4.1a), where *CCA1::LUC* bioluminescence damped. The effects of 840 g/ha equivalent adjuvant were apparent throughout the subsequent cycles where the bioluminescence signal was low, and did not have clear oscillations. The effects of the

other concentrations of glyphosate adjuvant were not apparent until the cycle after treatment. 100 g/ha equivalent adjuvant appeared to reduce the *CCA1::LUC* bioluminescence in cycle 3 and 4, however this was not apparent in cycle 5, therefore this could have been a transient effect. 25 g/ha equivalent adjuvant appeared to increase *CCA1::LUC* bioluminescence in cycle 5. Rhythmicity of *CCA1::LUC* was significantly affected by the 840 g/ha adjuvant treatment, where mean RAE increased from 0.17 ± 0.01 in control-treated plants to 0.3 ± 0.04 (Fig. 8.4.1b). The other two concentrations of adjuvant had no effect on rhythmicity, but the 25 g/ha equivalent adjuvant caused the period to be half an hour shorter. 840 g/ha equivalent adjuvant was the only concentration to have a significant effect on *CCA1::LUC* amplitude, decreasing it from a mean of $35 \times 10^4 \pm 5.46 \times 10^4$ to $5 \times 10^4 \pm 8.6 \times 10^3$ (Fig. 8.4.1c). *CCA1::LUC* peak bioluminescence was later in each cycle for each treatment (Fig. 8.4.1d). However 840 g/ha equivalent adjuvant treatment peaked significantly earlier than the control in cycle 3, but not in later cycles. In cycle 5, the 25 g/ha equivalent adjuvant treatment peaked earlier than the control, corresponding to the earlier period (Fig. 8.4.1b). The 840 g/ha equivalent adjuvant treatment had the greatest effect on *CCA1::LUC* bioluminescence (Fig. 8.4.1e). This was clear at 24 h when the treatment was applied (Fig. 8.4.1e). The peak for this treatment was earlier than the control, and immediately after this point, the signal decreased and was very inconsistent between replicates. There were also not clear oscillations in signal intensity, which related to the increased RAE (Fig. 8.4.1b). The earlier peak time in cycle 5 for the 25 g/ha adjuvant treatment was also observed (Fig. 8.4.1e).

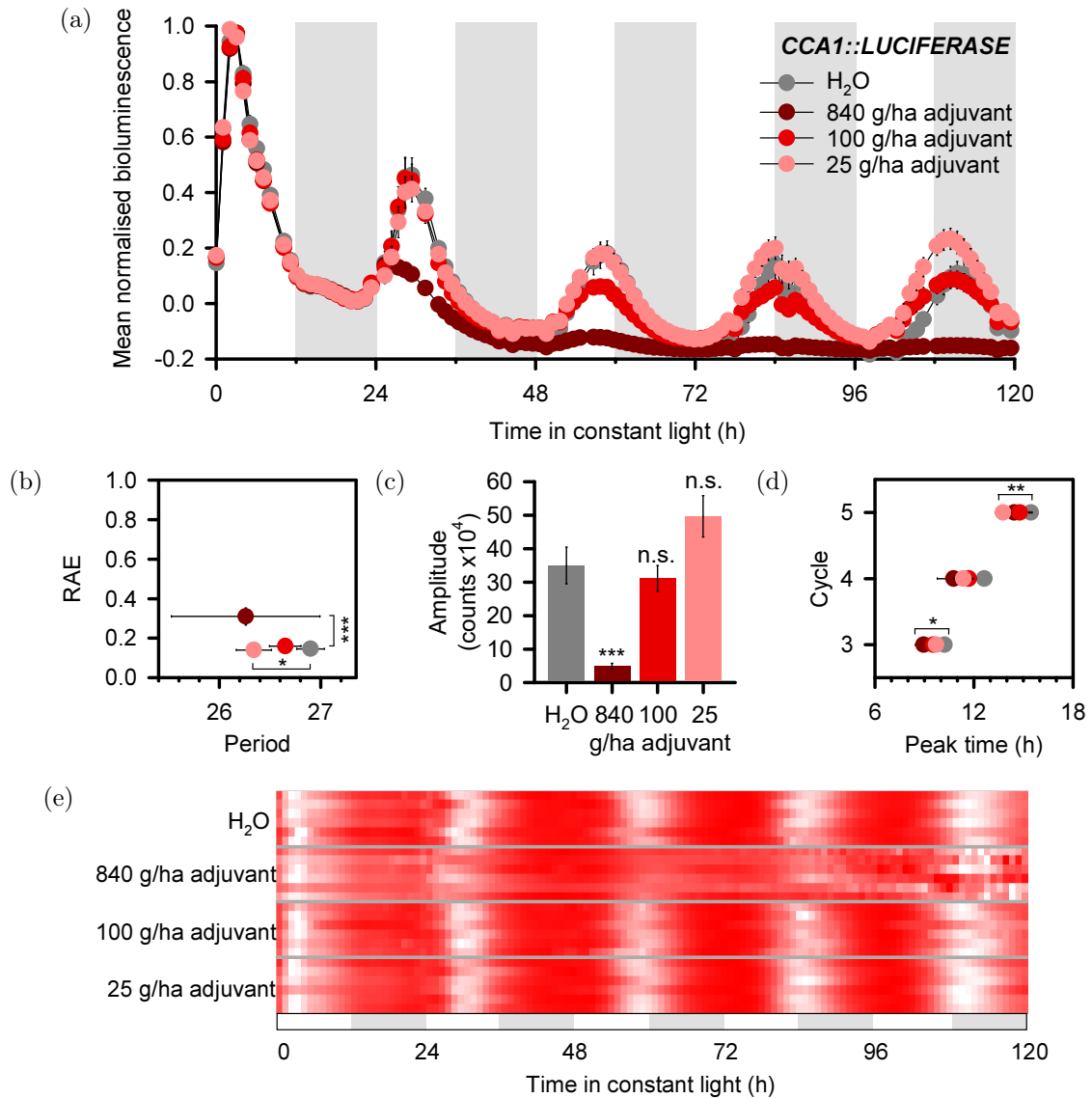


Figure 8.4.1: Glyphosate adjuvant alone affects *CCA1::LUCIFERASE* activity under constant light conditions. Plants were dosed with luciferin on day 10. On day 11, imaging began under constant light conditions for 24 h. At dawn on day 12 plants were treated with the equivalent of 840 g/ha glyphosate adjuvant (maroon), 100 g/ha glyphosate adjuvant (red), 25 g/ha glyphosate adjuvant (pink) or a water control (grey) followed by a further 96 hours imaging under constant light. (a) 840 g/ha adjuvant application affected *CCA1::LUC* bioluminescence immediately after application. (b) 840 g/ha adjuvant increased *CCA1::LUC* RAE and 25 g/ha adjuvant advanced the period of *CCA1::LUC* relative to the control. (c) 840 g/ha adjuvant reduced *CCA1::LUC* amplitude. (d) 840 g/ha adjuvant advanced *CCA1::LUC* peak time in the cycle after application, 25 g/ha adjuvant caused *CCA1::LUC* peak time to be earlier in the final cycle. (e) The effect of 840 g/ha adjuvant on *CCA1::LUC* bioluminescence can be seen immediately after application. Period, RAE and amplitude were derived from FFT-NLLS analysis conducted using BioDare2 after baseline and amplitude detrending. Shaded areas indicate subjective night. Data are the mean of 12 replicates from two independent experiments \pm SEM. Heat map data is from one representative experiment. Asterisks indicate significant difference between control and treated value, calculated by *t*-test where * = $P \leq 0.05$, ** = $P \leq 0.01$, and *** = $P \leq 0.001$.

The effect of the glyphosate adjuvants on *TOC1::LUC* bioluminescence were not apparent until approximately 10 h after application where the control-, 100 g/ha adjuvant-, and 25 g/ha adjuvant-treated plants began to increase in bioluminescence and the 840 g/ha adjuvant-treated did not (Fig. 8.4.2a). Instead, the signal from the 840 g/ha adjuvant-treated plants decreased over the next 24 h, and remained around the same level (Fig. 8.4.2a). There did not appear to be any effect of the lower two concentrations of the adjuvant on *TOC1::LUC* bioluminescence. The mean RAE for 840 g/ha was 0.6 ± 0.08 , higher than the 0.5 threshold for rhythmicity (Fig. 8.4.2b). 100 g/ha and 25 g/ha adjuvant had no effect on RAE or period, suggesting no effect on *TOC1::LUC* rhythms compared to the control. Only the 840 g/ha treatment had a significant effect on *TOC1::LUC* amplitude, reducing the mean value from $4.5 \times 10^4 \pm 1.2 \times 10^4$ to almost 0 (Fig. 8.4.2c). Mean peak *TOC1::LUC* bioluminescence was later for each cycle for all treatments, with 25 g/ha and 100 g/ha adjuvant treatments peaking slightly later than the control in each cycle (Fig. 8.4.2d). Conversely, the 840 g/ha adjuvant treatment caused *TOC1::LUC* to peak earlier than the control in each cycle. This difference between peak time for control and 840 g/ha was 5 h to 9 h earlier depending on the cycle. The oscillations in *TOC1::LUC* bioluminescence after 840 g/ha adjuvant treatment were less apparent than for *CCA1::LUC* (Figs. 8.4.2e and 8.4.1e); no clear consistent areas of high bioluminescence could be seen after 840 g/ha adjuvant treatment. 100 g/ha and 25 g/ha adjuvant did not appear much different from the control-treated *TOC1::LUC* bioluminescence, with defined waves of high and low bioluminescence at approximately the same times as control bioluminescence. These results are also summarised in Table 8.4.1.

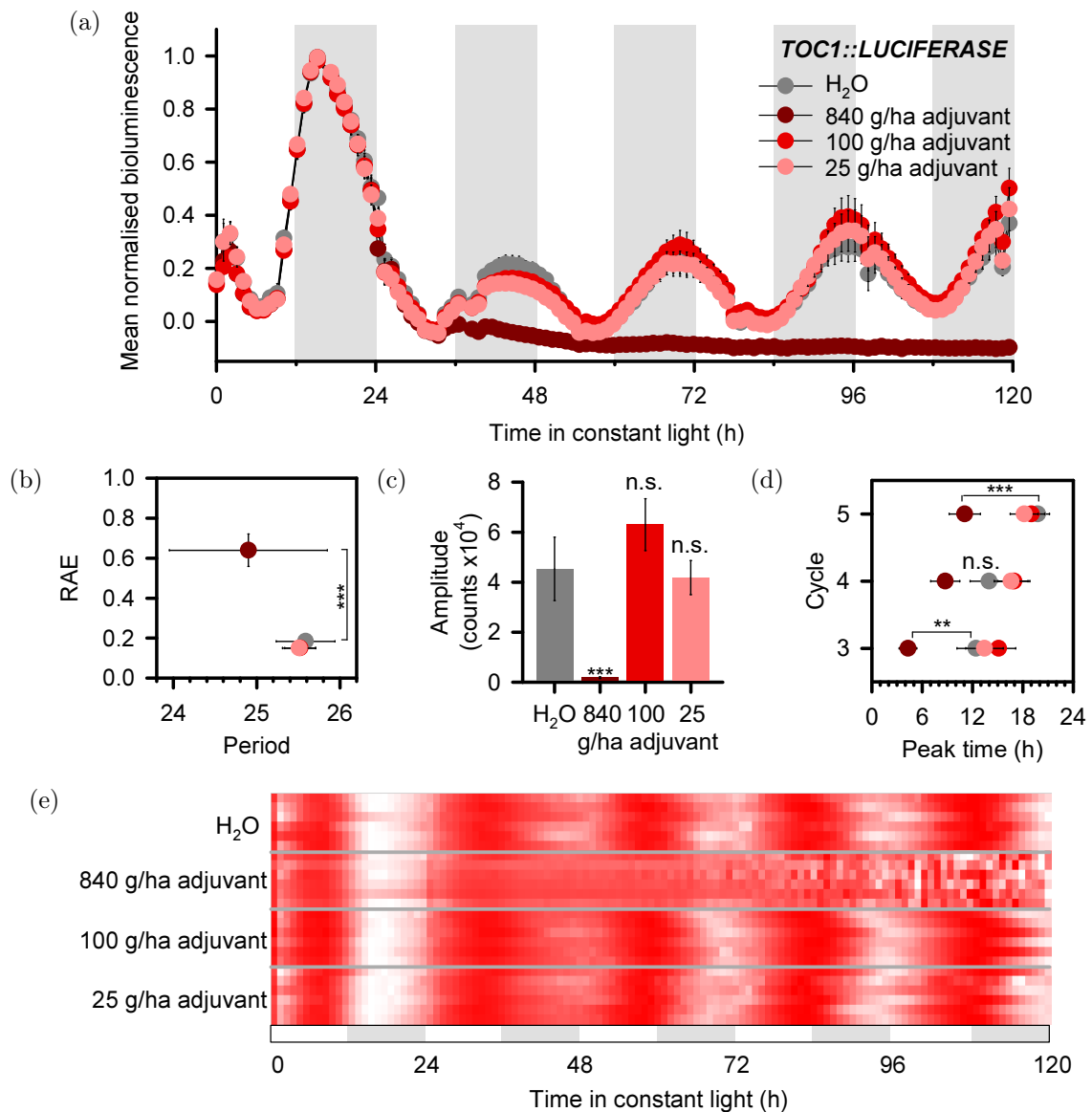


Figure 8.4.2: Glyphosate adjuvant alone affects *TOC1::LUCIFERASE* activity under constant light conditions. Plants were dosed with luciferin on day 10. On day 11, imaging began under constant light conditions for 24 h. At dawn on day 12 plants were treated with the equivalent of 840 g/ha glyphosate adjuvant (maroon), 100 g/ha glyphosate adjuvant (red), 25 g/ha glyphosate adjuvant (pink) or a water control (grey) followed by a further 96 hours imaging under constant light. (a) 840 g/ha adjuvant application affected *TOC1::LUC* bioluminescence 8 h after application. (b) 840 g/ha adjuvant increased *TOC1::LUC* RAE, but the adjuvants had no effect on *TOC1::LUC* period. (c) 840 g/ha adjuvant reduced *TOC1::LUC* amplitude. (d) 840 g/ha adjuvant advanced *TOC1::LUC* peak time in all cycles after application. (e) The effect of 840 g/ha adjuvant on *TOC1::LUC* bioluminescence can be seen immediately after application. Period, RAE and amplitude were derived from FFT-NLLS analysis conducted using BioDare2 after baseline and amplitude detrending. Shaded areas indicate subjective night. Data are the mean of 12 replicates from two independent experiments \pm SEM. Heat map data is from one representative experiment. Asterisks indicate significant difference between control and treated value, calculated by *t*-test where * = $P \leq 0.05$, ** = $P \leq 0.01$, and *** = $P \leq 0.001$.

The visual effect of the glyphosate adjuvant on Arabidopsis was also observed (Fig. 8.4.3). 840 g/ha glyphosate adjuvant caused severe bleaching of the seedlings, 100 g/ha glyphosate adjuvant caused plants to be paler than control plants and 25 g/ha glyphosate adjuvant had little effect on plants. Therefore, the adjuvant affects plant health in addition to the circadian oscillator. Bioluminescence rhythms were detected in *CCA1::LUC* plants treated with 840 g/ha glyphosate adjuvant, therefore they were not dead. These results suggest that the high concentration of adjuvant was detrimental to the plant, but comparing the adjuvant and the herbicide at 100 g/ha, it was only the glyphosate active ingredient affecting the circadian oscillator.

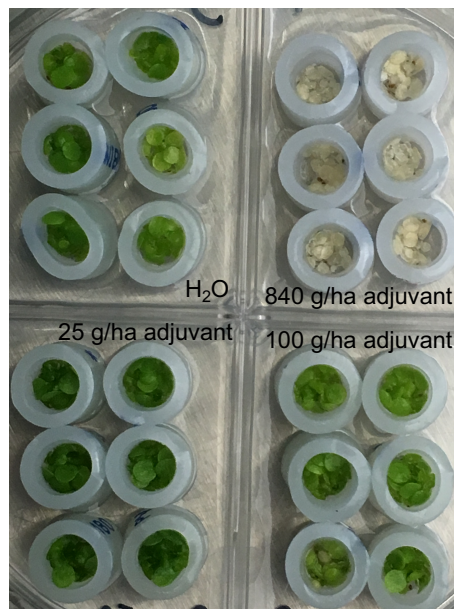


Figure 8.4.3: Glyphosate adjuvant alone causes damage to Arabidopsis. Four days after application, the recommended field rate of 840 g/ha adjuvant causes complete bleaching of Arabidopsis tissue. Lower concentrations of the adjuvant do not have the same effect. Image taken at the end of 5 days luciferase imaging under constant light conditions.

The effect of Agridex, the adjuvant for TBA, was investigated for the effect upon the circadian oscillator. Previously, Agridex was compared to TBA but not to a water control. Agridex appeared to have an effect on the oscillator alone, therefore these effects were investigated at different concentrations (Figs. 8.4.4 and 8.4.5). The three concentrations of Agridex caused immediate damping of *CCA1::LUC* bioluminescence

(Fig. 8.4.4a). This was more pronounced with increasing Agridex concentrations. *CCA1::LUC* bioluminescence continued to peak in the second cycle after Agridex treatment to approximately the same level as water-treated plants, but this diminished in the following two cycles. Agridex delayed the period of *CCA1::LUC* (Fig. 8.4.4b). The mean period increased from approximately $26.9 \text{ h} \pm 0.14$ in water-treated control plants to approximately 30.5 h for all concentrations of Agridex. Agridex did not have an effect on the rhythmicity of *CCA1* (Fig. 8.4.4b). The three concentrations of Agridex decreased *CCA1::LUC* amplitude by a mean of 45%, with little difference between concentrations (Fig. 8.4.4c). *CCA1::LUC* bioluminescence peaked at later time points with each cycle (Fig. 8.4.4d). The three concentrations of Agridex caused *CCA1::LUC* bioluminescence to peak at the same time as the water-treated control plants in cycle 3, but in later cycles, *CCA1::LUC* bioluminescence peaked later, correlating to concentration where the highest concentration peaked latest. *CCA1::LUC* bioluminescence appeared to increase at the same time as control plants around 54 h and 84 h (Fig. 8.4.4e). The bioluminescence remained at a higher level for longer than control plants, this becomes most evident around 108 h where the control plants begin to increase in bioluminescence again, but treated plants are only just reducing *CCA1::LUC* activity. This correlates to the longer period phenotype and later peak times calculated.

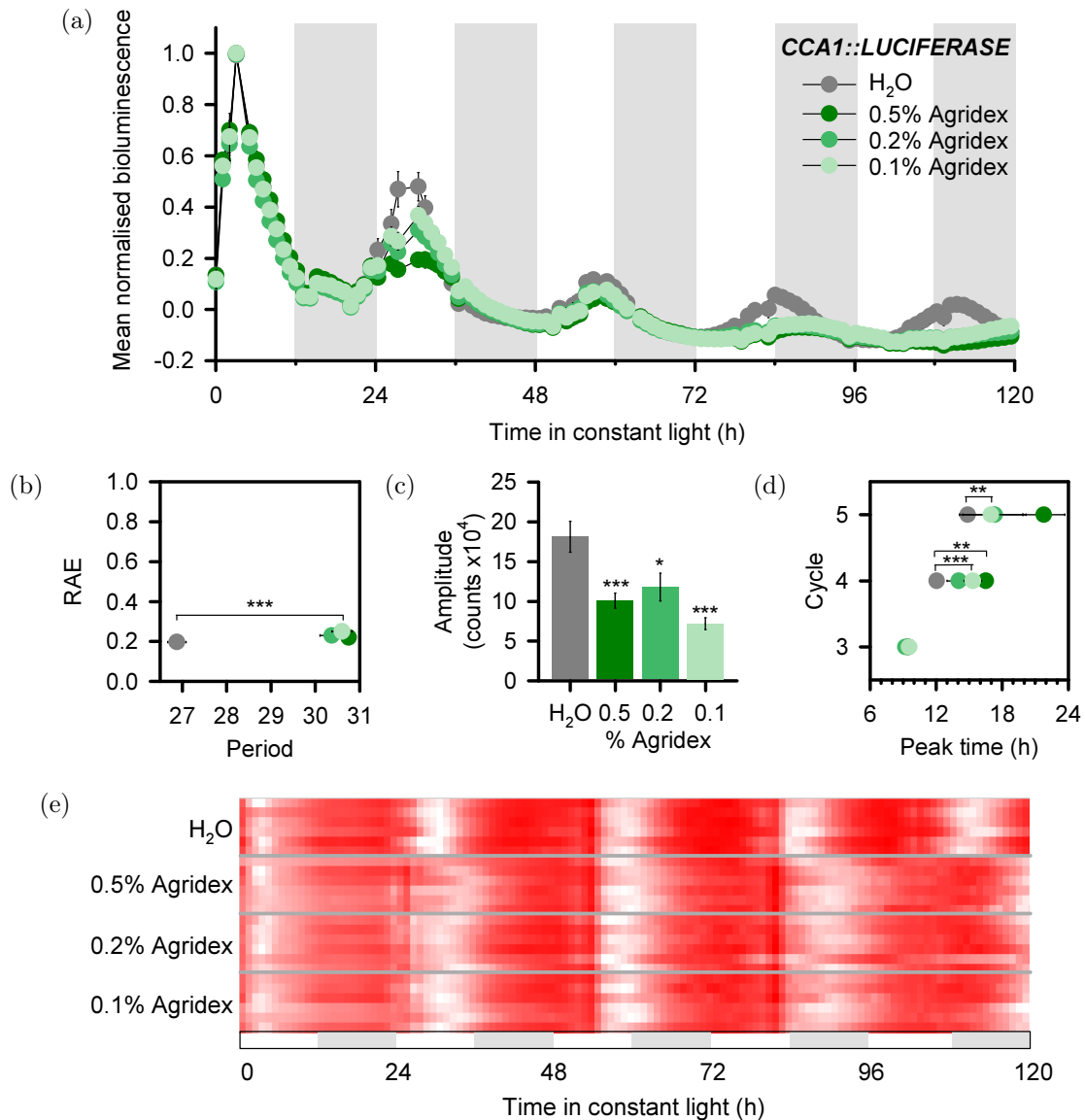


Figure 8.4.4: Agridex alone affects *CCA1::LUCIFERASE* activity under constant light conditions. Plants were dosed with luciferin on day 10. On day 11, imaging began under constant light conditions for 24 h. At dawn on day 12 plants were treated with one of three concentrations of Agridex: 0.5% (dark green), 0.2% (green), 0.1% (pale green), or a water control (grey) followed by a further 96 hours imaging under constant light. (a) Agridex application affected *CCA1::LUC* bioluminescence immediately after application. (b) Agridex application increased the period of *CCA1::LUC*, but did not affect rhythmicity. (c) Agridex reduced *CCA1::LUC* amplitude. (d) Agridex delayed *CCA1::LUC* peak time to various extents in cycles 4 and 5 under constant light. (e) The effect of Agridex on *CCA1::LUC* bioluminescence can be seen immediately after application. Period, RAE and amplitude were derived from FFT-NLLS analysis conducted using BioDare2 after baseline and amplitude detrending. Shaded areas indicate subjective night. Data are the mean of 12 replicates from two independent experiments \pm SEM. Heat map data is from one representative experiment. Asterisks indicate significant difference between control and treated value, calculated by *t*-test where * = $P \leq 0.05$, ** = $P \leq 0.01$, and *** = $P \leq 0.001$.

Increasing concentrations of Agridex had a greater effect on *TOC1::LUC* bioluminescence (Fig. 8.4.5a). The effect of Agridex was most evident from 62 h in constant light onwards, when *TOC1::LUC* bioluminescence in the control-treated plants peaked, and the bioluminescence signal in Agridex-treated plants was damped. Agridex caused a significant reduction in the rhythmicity of plants, where mean RAE increased from around 0.17 ± 0.01 in control plants to 0.4-0.55 in Agridex-treated plants (Fig. 8.4.5b). The mean period was shorter in Agridex-treated plants, with a significantly shorter period in the 0.5% Agridex-treated plants (Fig. 8.4.5b). Agridex decreased *TOC1::LUC* amplitude in a concentration-dependent manner (Fig. 8.4.5c). *TOC1::LUC* bioluminescence activity in water-treated control plants peaked at similar times across the three cycles measured (Fig. 8.4.5d). In cycles 3 and 4, Agridex treatment caused *TOC1::LUC* to peak earlier. In cycle 5, peak bioluminescence occurred at the same time for all treatments. This correlated with the final time point, therefore if the signal continued to increase after this time point it would not be measured, so no differences may be visible. 0.1% Agridex had a similar pattern of *TOC1::LUC* bioluminescence as the water-treated control (Fig. 8.4.5e). The effects of the higher concentrations of Agridex on *TOC1::LUC* activity were particularly distinct after approximately 90 h in constant light (Fig. 8.4.5e). After this point, the oscillations of high and low *TOC1::LUC* activity were less visible. These results are also summarised in Table 8.4.1.

Overall, Agridex had a clear detrimental effect on promoter activity of *CCA1* and *TOC1*. For some measures, such as rhythmicity, the effects were more profound in *TOC1::LUC*. The change in period of *CCA1::LUC* of around 4 hours would have a significant impact on the performance of the plant. This was the case for the lowest concentration of adjuvant tested, which was lower than the recommended field rate.

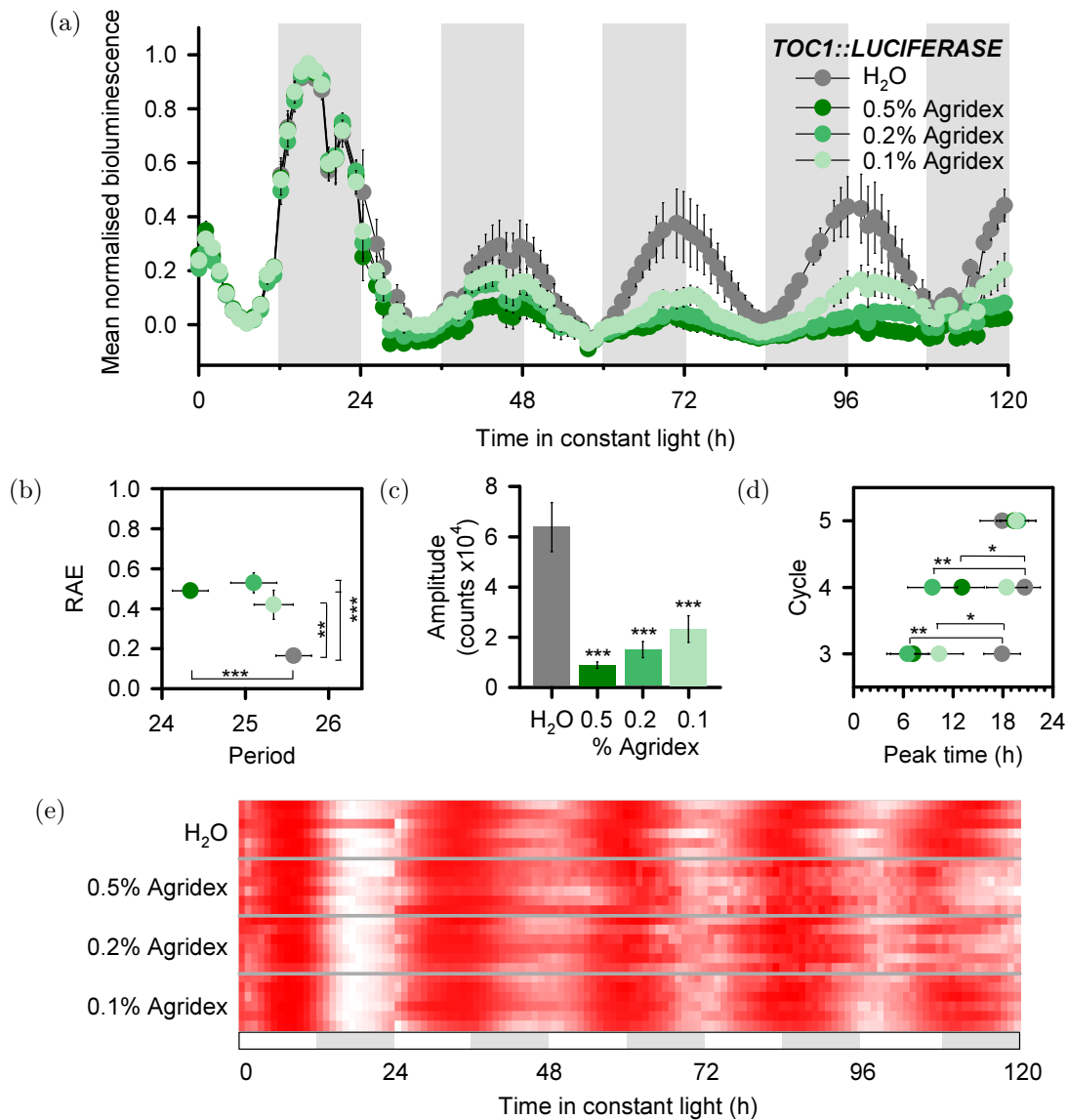


Figure 8.4.5: Agridex alone affects *TOC1::LUCIFERASE* activity under constant light conditions. Plants were dosed with luciferin on day 10. On day 11, imaging began under constant light conditions for 24 h. At dawn on day 12 plants were treated with one of three concentrations of Agridex: 0.5% (dark green), 0.2% (green), 0.1% (pale green), or a water control (grey) followed by a further 96 hours imaging under constant light. (a) Agridex application affected *TOC1::LUC* bioluminescence in the first peak post-application. (b) Agridex application increased *TOC1::LUC* RAE at all concentrations, and shortened the period with 0.5% Agridex. (c) Agridex reduced *TOC1::LUC* amplitude. (d) Agridex advanced *TOC1::LUC* peak time to various extents in cycles 3 and 4 under constant light. (e) The effect of Agridex on *TOC1::LUC* bioluminescence can be seen around 96 h after application for 0.5% and 0.2% Agridex. Period, RAE and amplitude were derived from FFT-NLLS analysis conducted using BioDare2 after baseline and amplitude detrending. Shaded areas indicate subjective night. Data are the mean of 12 replicates from two independent experiments \pm SEM. Heat map data is from one representative experiment. Asterisks indicate significant difference between control and treated value, calculated by *t*-test where * = $P \leq 0.05$, ** = $P \leq 0.01$, and *** = $P \leq 0.001$.

Table 8.4.1: Summary of the effects of adjuvants under constant light conditions. Effect of adjuvant is compared to water control. Only statistically significant results are included. Phase result was not always consistent across multiple cycles.

Treatment	Reporter	Period	RAE	Amplitude	Phase
840 g/ha glyphosate adjuvant	<i>CCA1::LUC</i>	-	Increased	Reduced	Early
	<i>TOC1::LUC</i>	-	Increased	Reduced	Early
100 g/ha glyphosate adjuvant	<i>CCA1::LUC</i>	-	-	-	-
	<i>TOC1::LUC</i>	-	-	-	-
25 g/ha glyphosate adjuvant	<i>CCA1::LUC</i>	Short	-	-	Early
	<i>TOC1::LUC</i>	-	-	-	-
0.5% Agridex	<i>CCA1::LUC</i>	Long	-	Reduced	Late
	<i>TOC1::LUC</i>	Short	Increased	Reduced	Early
0.2% Agridex	<i>CCA1::LUC</i>	Long	-	Reduced	-
	<i>TOC1::LUC</i>	-	-	Reduced	Early
0.1% Agridex	<i>CCA1::LUC</i>	Long	-	Reduced	Late
	<i>TOC1::LUC</i>	-	Increased	Reduced	Early

8.5 Phase can be altered by herbicides under entrained conditions

In a natural environment, plants are exposed to light-dark cycles with a period of about 24 h, with strong entrainment signals at dawn (McClung, 2006). The period has the ability to determine the phase and it can be detrimental to the plant if the phase is not properly synchronised to that of the environment (Dodd et al., 2005). In the following experiments, the objective was to study the rhythmic behaviour of oscillator components under driven cycles, in the presence of herbicides.

There did not appear to be any immediate or transient effects of glyphosate or its adjuvant on *CCA1::LUC* under light dark cycles (Fig. 8.5.1). Longer-term alterations were observed two cycles after treatment (around 72 h) where *CCA1::LUC* bioluminescence was damped when treated with glyphosate, but not adjuvant (Fig. 8.5.1a). These effects were visible over the remainder of the cycles measured. In all cycles, there was a difference in bioluminescence signal between glyphosate-treated plants and adjuvant-treated plants in the pre-dawn period where bioluminescence was lower in the glyphosate-treated plants, and *CCA1::LUC* bioluminescence started to peak later. This was seen most clearly in cycle 6 (Fig. 8.5.1b), but no difference was observed between control and adjuvant-treated plants. Peak *CCA1::LUC* bioluminescence occurred around 2.5-3 h after dawn in control plants (Fig. 8.5.1c). In cycle 3 and 6 there was no difference in *CCA1::LUC* bioluminescence observed between the control and treated plants. In cycles 4 and 5, *CCA1::LUC* bioluminescence peaked significantly later (0.5 h) for adjuvant compared to the control, but there was no difference between the adjuvant and glyphosate treatments. It is interesting that the peak time was the same for glyphosate- and adjuvant-treated plants even though the bioluminescence of glyphosate-treated plants was much lower intensity. Clear cycles of high and low *CCA1::LUC* bioluminescence were observed for all treatments (Fig. 8.5.1d). The areas of high bioluminescence were narrow, indicating the peak was for a short amount of time. Slightly wider peaks can be seen around 72 h and 96 h for the glyphosate- and adjuvant-treated plants, correlating with the later peak times (Fig. 8.5.1d).

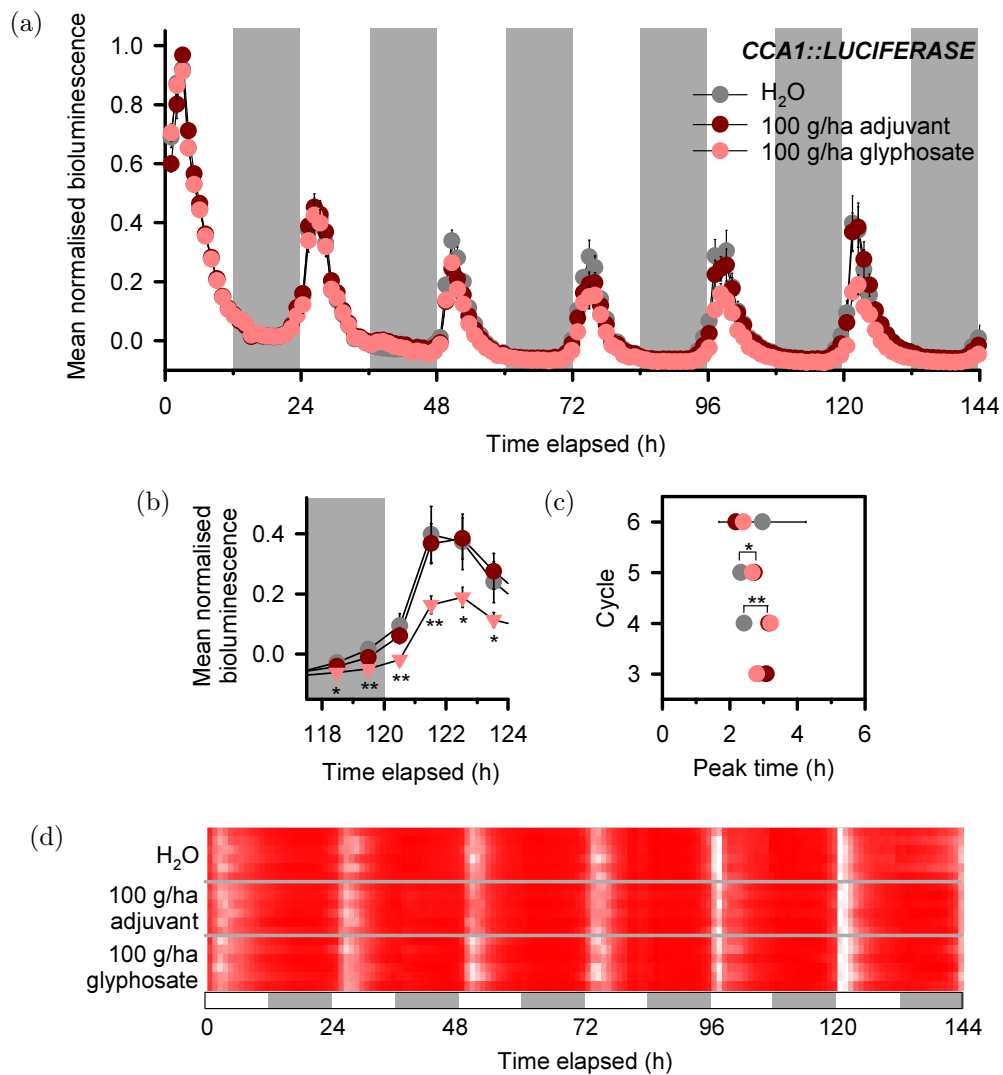


Figure 8.5.1: Glyphosate affects *CCA1::LUCIFERASE* activity under light-dark cycles. Plants were dosed with luciferin on day 10. On day 11, imaging began under a 12 h light/ 12 h dark cycle. At dawn on day 12 plants were treated with either 100 g/ha glyphosate (pink), 100 g/ha equivalent adjuvant (maroon) or a water control (grey) followed by a further 5 days imaging under 12 h light/ 12 h dark cycles. (a) Glyphosate application affected *CCA1::LUC* bioluminescence 24 h after application. (b) Glyphosate reduced *CCA1::LUC* bioluminescence relative to the adjuvant. (c) Glyphosate adjuvant delayed the time of peak *CCA1::LUC* bioluminescence in cycles 3 and 4. (d) The effect of glyphosate on *CCA1::LUC* bioluminescence can be seen in the final two cycles of the heat map. Grey areas indicate night. Data are the mean of 18 replicates from three independent experiments \pm SEM. Heat map data is from one representative experiment. Asterisks indicate significant difference between control and adjuvant or adjuvant and glyphosate, calculated by *t*-test where * = $P \leq 0.05$ and ** = $P \leq 0.01$.

Glyphosate and its adjuvant did not appear to have much impact on *TOC1::LUC* oscillations under light-dark cycles (Fig. 8.5.2). There were no transient effects after application, or during the first peak after application at around 34 h (Fig. 8.5.2a). The greatest effect was in the peak in the final cycle measured, around 132 h (Fig. 8.5.2b). However, even where the treatment had the greatest effect, the changes were small. There was little effect of glyphosate on *TOC1::LUC* peak time (Fig. 8.5.2c). In cycle 5, the bioluminescence in the adjuvant-treated plants peaked significantly earlier than the control, and there was no difference between adjuvant and glyphosate treatment. Bioluminescence of adjuvant-treated plants appeared to begin to peak earlier than the water-treated control in cycles 4, 5 and 6. This suggests that the shape of the peak changed, but it only affected actual peak time in cycle 5 (Fig. 8.5.2d).

Overall, glyphosate did not appear to have a significant impact on *CCA1::LUC* and *TOC1::LUC* oscillations under light dark cycles. These results are summarised in Table 8.5.1. This was consistent with the results from the constant light experiments (Figs. 8.3.1 and 8.3.2). Therefore it seems that glyphosate did not have any significant effect on altering the circadian oscillator in Arabidopsis, at least under these experimental conditions.

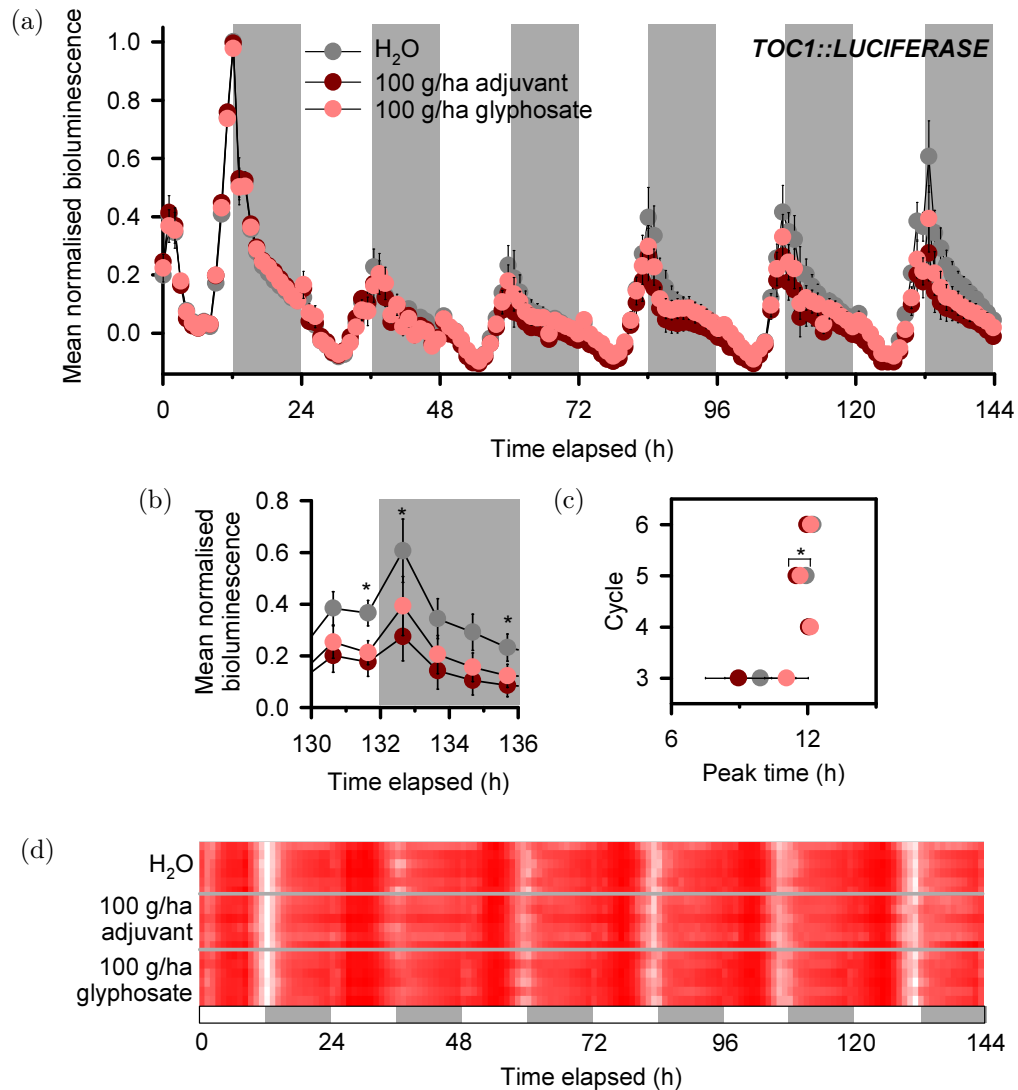


Figure 8.5.2: Glyphosate affects *TOC1::LUCIFERASE* activity under light-dark cycles. Plants were dosed with luciferin on day 10. On day 11, imaging began under a 12 h light/ 12 h dark cycle. At dawn on day 12 plants were treated with either 100 g/ha glyphosate (pink), 100 g/ha equivalent adjuvant (maroon) or a water control (grey) followed by a further 5 days imaging under 12 h light/ 12 h dark cycles. (a) Glyphosate application affected *TOC1::LUC* bioluminescence 84 h after application. (b) Glyphosate and adjuvant slightly reduced *TOC1::LUC* bioluminescence relative to the control. (c) Glyphosate adjuvant advanced the time of peak *TOC1::LUC* bioluminescence in cycle 5. (d) The effect of glyphosate on *TOC1::LUC* bioluminescence is difficult to determine in the heat map. Grey areas indicate night. Data are the mean of 12 replicates from two independent experiments \pm SEM. Heat map data is from one representative experiment. Asterisks indicate significant difference between control and adjuvant or adjuvant and glyphosate, calculated by *t*-test where $* = P \leq 0.05$.

Mesotrione treatment appeared to have a transient effect on *CCA1::LUC* under light-dark cycles (Fig. 8.5.3). There was no apparent effect of mesotrione during the first 24 h after treatment (Fig. 8.5.3a). The most obvious effect of mesotrione appeared in the cycle after treatment (48 h) where *CCA1::LUC* bioluminescence was lower than the control plants. The bioluminescence traces for the two treatments in the following two cycles appeared quite similar, but signal intensity was slightly lower in the final cycle. The greatest change was seen in cycle 3 where the response of *CCA1::LUC* to mesotrione was clearly different than the water-treated control plants (Fig. 8.5.3b). The mesotrione-treated plants had a lower bioluminescence signal at dawn, and peaked much earlier than control plants. This difference in peak time was also evident in the following two cycles. While mesotrione treatment caused a significantly earlier *CCA1::LUC* peak time in cycles 3, 4 and 5, this difference was greatest in cycle 3 (1.5 h; Fig. 8.5.3c). This phase advance reduced by approximately 30 minutes with each following cycle, where in cycle 6 there was no difference. This phase difference was also seen when represented as a heat map of the bioluminescence signal (Fig. 8.5.3d). At 48 h, the mesotrione-treated *CCA1::LUC* bioluminescence signal increased before the water-treated control, whereas at 120 h, both treatments increased in signal at the same time.

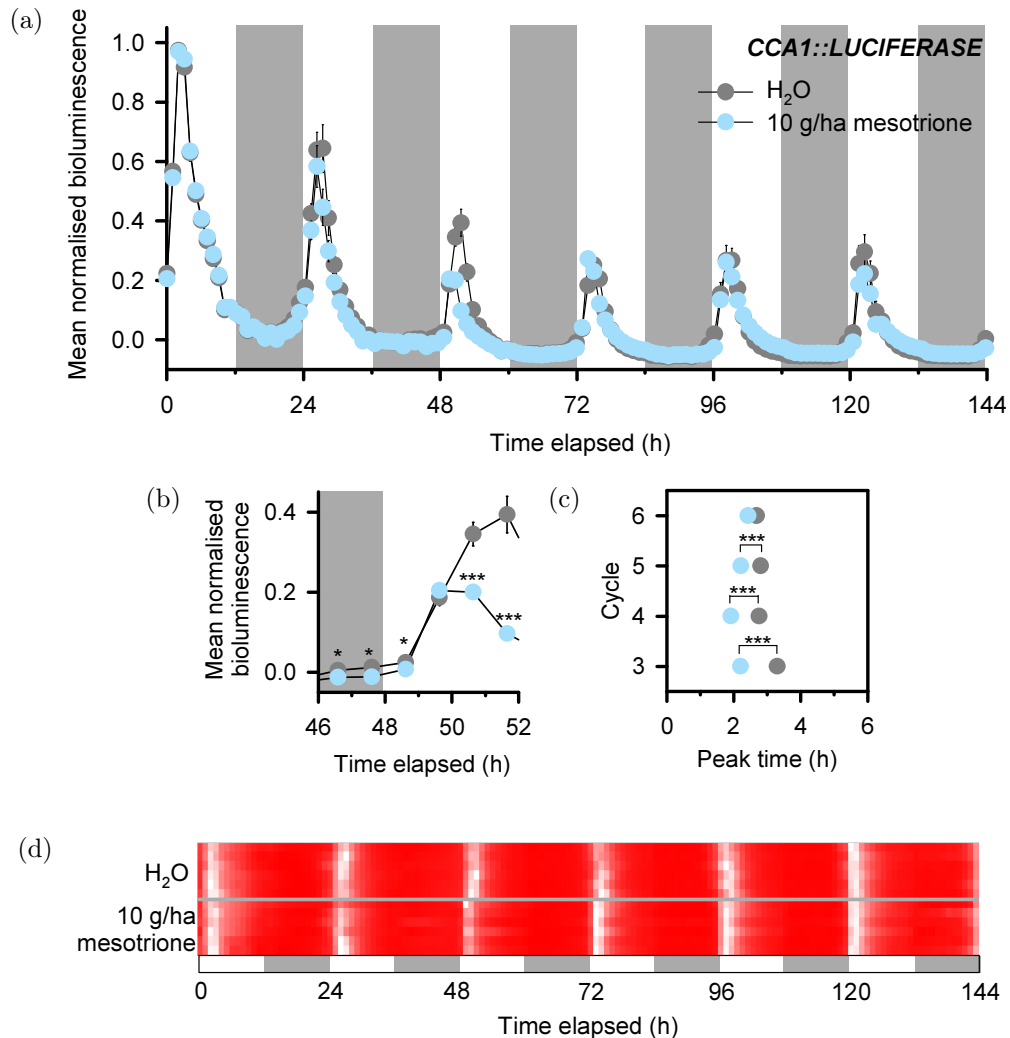


Figure 8.5.3: Mesotrione affects *CCA1::LUCIFERASE* activity under light-dark cycles. Plants were dosed with luciferin on day 10. On day 11, imaging began under a 12 h light/ 12 h dark cycle. At dawn on day 12 plants were treated with either 10 g/ha mesotrione (blue) or a water control (grey) followed by a further 5 days imaging under 12 h light/ 12 h dark cycles. (a) Mesotrione application affected *CCA1::LUC* bioluminescence 24 h after application. (b) Mesotrione altered the response of *CCA1::LUC* bioluminescence. (c) Mesotrione advanced the time of peak *CCA1::LUC* bioluminescence in cycles 3, 4 and 5. (d) The earlier peak of *CCA1::LUC* bioluminescence can be seen around 48 h and 72 h in the heat map. Grey areas indicate night. Data are the mean of 12 replicates from two independent experiments \pm SEM. Heat map data is from one representative experiment. Asterisks indicate significant difference between control and mesotrione calculated by *t*-test where * = $P \leq 0.05$, ** = $P \leq 0.01$ and *** = $P \leq 0.001$.

The effects of mesotrione on *TOC1::LUC* bioluminescence were different compared to *CCA1::LUC* under light-dark cycles (Fig. 8.5.4). Mesotrione appeared to have an effect on *TOC1::LUC* bioluminescence after 3 days, where the signal was damped compared to the control (Fig. 8.5.4a). This was also observed during the following cycle, where mesotrione-treated plants had significantly lower *TOC1::LUC* bioluminescence (Fig. 8.5.4b). There was no difference between mesotrione-treated and water-treated peak *TOC1::LUC* bioluminescence times for any of the cycles (Fig. 8.5.4c), unlike the response seen in *CCA1::LUC*. Mesotrione appeared to change the dynamic of the *TOC1::LUC* bioluminescence peaks, such that the level of bioluminescence was higher for longer, suggesting the peaks were wider and less distinct (Fig. 8.5.4d).

Overall, mesotrione had interesting effects on the circadian oscillator under light-dark cycles. These results are summarised in Table 8.5.1. Mesotrione appeared to have a transient effect on *CCA1::LUC* such that peak time was affected, but a longer term effect on *TOC1::LUC* whereby the characteristics of the oscillations were altered.

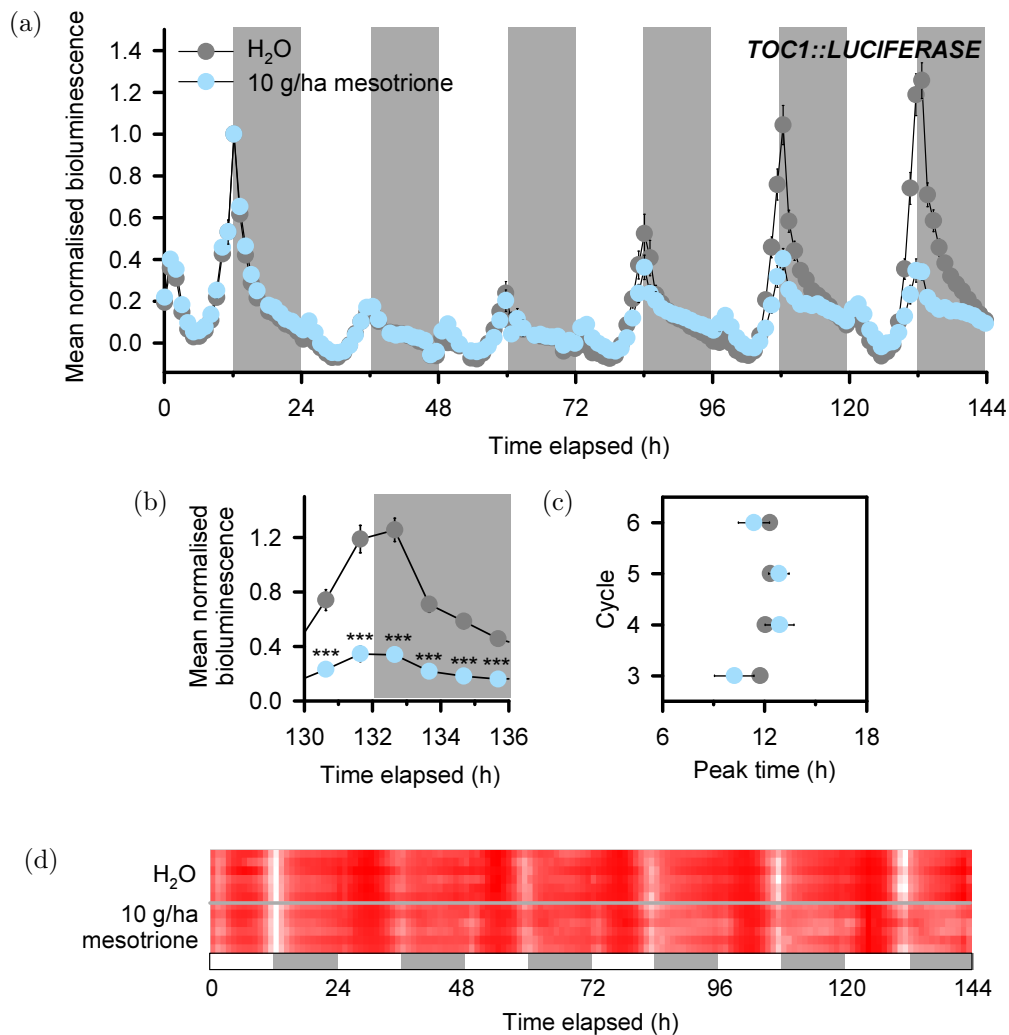


Figure 8.5.4: Mesotrione affects *TOC1::LUCIFERASE* activity under light-dark cycles. Plants were dosed with luciferin on day 10. On day 11, imaging began under a 12 h light/ 12 h dark cycle. At dawn on day 12 plants were treated with either 10 g/ha mesotrione (blue) or a water control (grey) followed by a further 5 days imaging under 12 h light/ 12 h dark cycles. (a) Mesotrione application affected *TOC1::LUC* bioluminescence 84 h after application. (b) Mesotrione decreased *TOC1::LUC* bioluminescence. (c) Mesotrione was without effect on the time of peak *TOC1::LUC* bioluminescence. (d) Mesotrione treatment effected the characteristics of *TOC1::LUC* bioluminescence, particularly from 84 h onwards. Grey areas indicate night. Data are the mean of 12 replicates from two independent experiments \pm SEM. Heat map data is from one representative experiment. Asterisks indicate significant difference between control and mesotrione calculated by *t*-test where *** = $P \leq 0.001$.

Next the effects of TBA and its adjuvant Agridex upon *CCA1::LUC* and *TOC1::LUC* were examined under light-dark cycles (Figs. 8.5.5 and 8.5.6). The effects of TBA and its adjuvant on *CCA1::LUC* bioluminescence were observed in the cycle after the application of the treatment (Fig. 8.5.5a). Although the signal did peak in the Agridex and TBA treated plants, the increase in signal was much smaller compared to that of the control. A very similar response occurred across all subsequent cycles. This response is illustrated in detail in Fig. 8.5.5b for cycle 6. The treated plants appeared to anticipate dawn less accurately because the bioluminescence did not start to increase until the light period. The adjuvant treatment had a significant effect on *CCA1::LUC*, where the signal was much lower than the control plants. The effect of TBA treatment was only different from the effect of adjuvant treatment at the time of peak *CCA1::LUC* bioluminescence. TBA and Agridex treatments caused *CCA1::LUC* activity to peak earlier in cycles 5 (1 h) and 6 (1.5 h), however there was no difference between the TBA and Agridex treatments (Fig. 8.5.5c). The characteristics of the *CCA1::LUC* oscillations appeared to be altered by Agridex and TBA treatments (Fig. 8.5.5d). Around 48 h the bioluminescence was not very clear for the Agridex-treated, suggesting that the peak was not very strong at this point. At 96 h, the earlier peak in *CCA1::LUC* for Agridex- and TBA-treated plants was seen; TBA also had an effect on the shape of the peak where it seemed wider than the water-treated control plants. Around 144 h, *CCA1::LUC* bioluminescence in TBA-treated plants appeared to have an early increase in signal from the previous cycle, which was not seen for the control nor Agridex treatments.

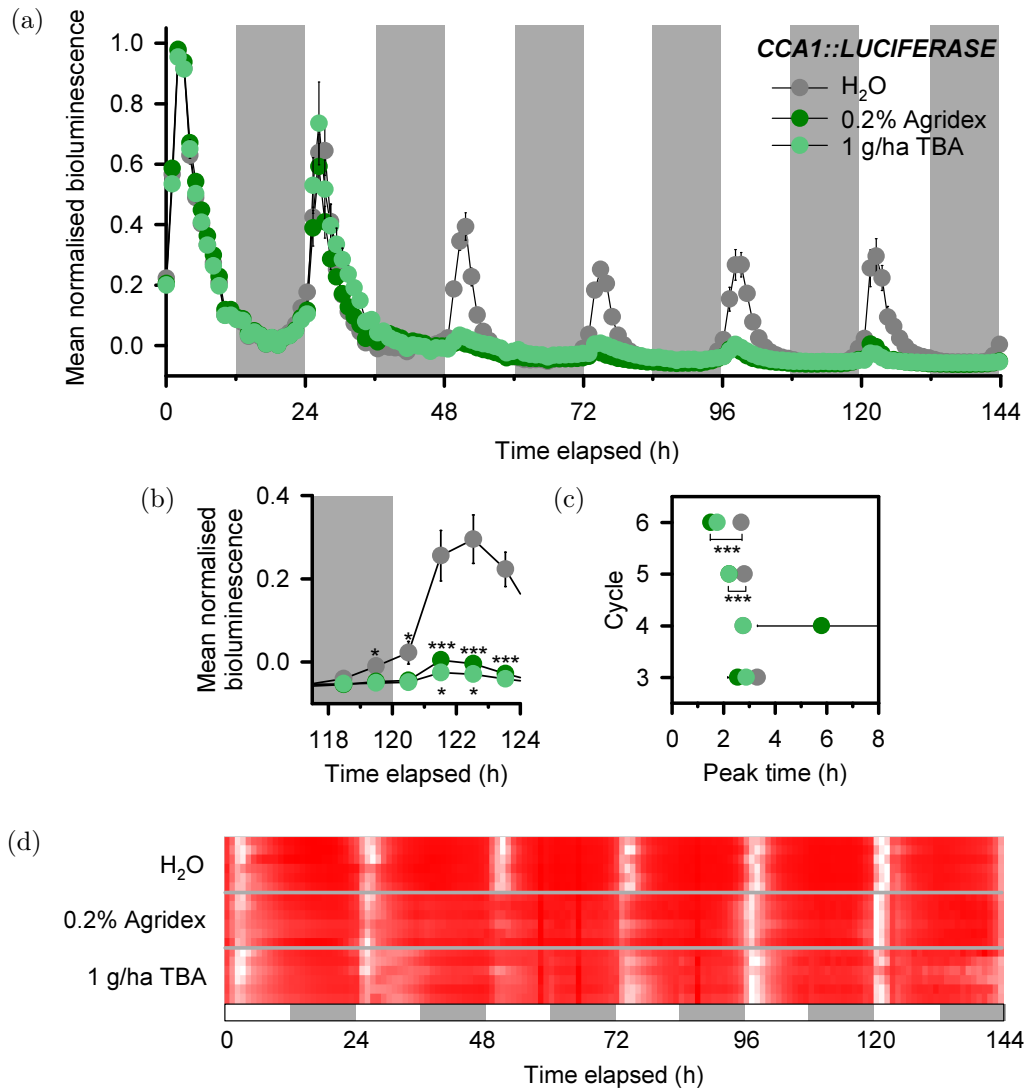


Figure 8.5.5: TBA and Agridex affect *CCA1::LUCIFERASE* activity under light-dark cycles. Plants were dosed with luciferin on day 10. On day 11, imaging began under a 12 h light/ 12 h dark cycle. At dawn on day 12 plants were treated with either 1 g/ha TBA (light green), 0.2% Agridex (dark green) or a water control (grey) followed by a further 5 days imaging under 12 h light/ 12 h dark cycles. (a) TBA and Agridex applications affected *CCA1::LUC* bioluminescence 24 h after application. (b) TBA and Agridex reduced *CCA1::LUC* bioluminescence relative to the water control. (c) Agridex advanced the time of peak *CCA1::LUC* bioluminescence in cycles 5 and 6, but there was no difference between Agridex and TBA peak times. (d) The effect of TBA on *CCA1::LUC* bioluminescence can be seen from 24 h in the heat map. Grey areas indicate night. Data are the mean of 12 replicates from two independent experiments \pm SEM. Heat map data is from one representative experiment. Asterisks indicate significant difference between control and adjuvant or adjuvant and glyphosate, calculated by *t*-test where * = $P \leq 0.05$, ** = $P \leq 0.01$, and *** = $P \leq 0.001$.

The effect of TBA treatment on *TOC1::LUC* bioluminescence was observed in the first 12 h after treatment where TBA-treated plants did not have a significant bioluminescence peak at the end of the day as would be typical for *TOC1::LUC* (Fig. 8.5.6a). The effect of Agridex treatment was not seen until the next cycle, but at this time point, the *TOC1::LUC* signals for both Agridex- and TBA-treated plants were similar. The effects of these treatments were more obvious over time, where the difference between water control plants and both Agridex- and TBA-treated plants was greater. The greatest change was in cycle 6 where the bioluminescence signal from Agridex-treated plants was much lower than that of water-treated plants, and the response of *TOC1::LUC* with TBA treatment was significantly lower than that of Agridex-treated plants (Fig. 8.5.6b). The peak for TBA-treated plants was almost indiscernible. In cycle 3, Agridex treatment caused a significantly earlier peak, of 6 h, in *TOC1::LUC* bioluminescence compared to the control plants, however TBA treatment did not have the same effect (Fig. 8.5.6c). In cycle 4, Agridex caused the *TOC1::LUC* peak to be slightly later, but there was no difference in the effect between Agridex and TBA treatments. In cycles 5 and 6, *TOC1::LUC* peaked at the same time for all treatments, therefore it is possible that the effect of treatments on the peak time was transient. At approximately 36 h, the *TOC1::LUC* peak for TBA-treated plants was not apparent (Fig. 8.5.6d). After 108 h, the shape of the *TOC1::LUC* bioluminescence peaks was different after both Agridex and TBA treatments when compared to the water-treated control plants. While all three treatments caused *TOC1::LUC* to peak around the same time, TBA and Agridex treatments did not have the same distinct on/off in signal that occurred in the control plants. However, this response could be due to the change in signal not being substantial, therefore the relative change in signal was not as obvious.

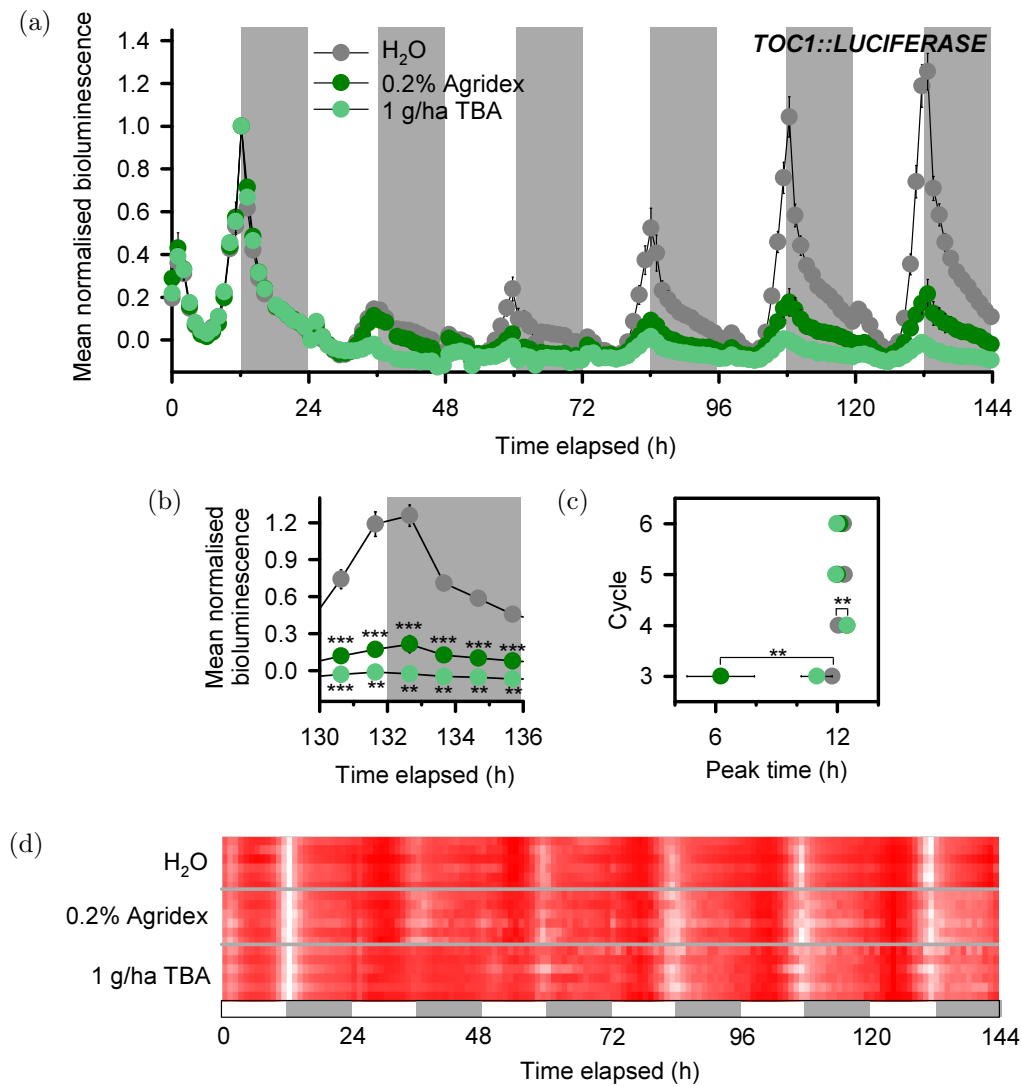


Figure 8.5.6: TBA and Agridex affect *TOC1::LUCIFERASE* activity under light-dark cycles. Plants were dosed with luciferin on day 10. On day 11, imaging began under a 12 h light/ 12 h dark cycle. At dawn on day 12 plants were treated with either 1 g/ha TBA (light green), 0.2% Agridex (dark green) or a water control (grey) followed by a further 5 days imaging under 12 h light/ 12 h dark cycles. (a) TBA affected *TOC1::LUC* bioluminescence 12 h after application. (b) Agridex reduced *TOC1::LUC* bioluminescence relative to the water control, and TBA reduced *TOC1::LUC* to a greater extent than Agridex. (c) Agridex advanced the time of peak *TOC1::LUC* bioluminescence in cycles 3, but delayed the peak in cycle 4. TBA had no effect relative to Agridex. (d) The effects of Agridex and TBA on *TOC1::LUC* bioluminescence can be seen from 24 h in the heat map. Grey areas indicate night. Data are the mean of 12 replicates from two independent experiments \pm SEM. Heat map data is from one representative experiment. Asterisks indicate significant difference between control and adjuvant or adjuvant and glyphosate, calculated by *t*-test where * = $P \leq 0.05$, ** = $P \leq 0.01$, and *** = $P \leq 0.001$.

Overall, the effect of TBA and Agridex under light-dark cycles appears different between *CCA1::LUC* and *TOC1::LUC*. These results are summarised in Table 8.5.1. The effects were more apparent later in the time course for *CCA1::LUC*, whereas they were earlier in *TOC1::LUC*. However, different parameters were affected for the two reporters. The peaks were still clearly defined in *CCA1::LUC*, but the effect of peak time was more apparent. For *TOC1::LUC*, there were transient effects on peak time, but the characteristics of the peaks were altered later in the time course.

Table 8.5.1: Summary of the effects of herbicides and adjuvants under light-dark cycles. Effect of glyphosate is compared to its adjuvant and effect of glyphosate adjuvant is compared to water control. Effect of mesotrione is compared to water control. Effect of TBA is compared to Agridex and effect of Agridex is compared to water control. Only statistically significant results are included. Phase result was not always consistent across multiple cycles.

Treatment	Reporter	Phase
Glyphosate	<i>CCA1::LUC</i>	Late
	<i>TOC1::LUC</i>	-
Glyphosate adjuvant	<i>CCA1::LUC</i>	Late
	<i>TOC1::LUC</i>	Late
Mesotrione	<i>CCA1::LUC</i>	Early
	<i>TOC1::LUC</i>	-
TBA	<i>CCA1::LUC</i>	Early
	<i>TOC1::LUC</i>	-
Agridex	<i>CCA1::LUC</i>	Early
	<i>TOC1::LUC</i>	Early

8.6 Exogenous sucrose rescues the effect of mesotrione on entrained phase and circadian period

Previous work identified, through the use of the photosynthesis inhibitor DCMU, a range of circadian mutants and supplemental sucrose applications, that sugars from photosynthesis provide metabolic entrainment to the oscillator (Haydon et al., 2013). Therefore, I hypothesised that certain herbicides could be preventing the correct entrainment of the oscillator by interfering with the normal accumulation of photosynthetic sugars. Experiments were conducted with exogenous sucrose supplementation to determine whether the effect of herbicides on the circadian oscillator could be overcome. The effect of mesotrione and TBA on *CCA1::LUC* under light dark cycles was initially examined to determine the effect under entrainment conditions (Figs. 8.6.1 and 8.6.3).

Mesotrione treatment of *CCA1::LUC* plants on media supplemented with either sorbitol or sucrose had no immediate effect on bioluminescence (Fig. 8.6.1a). There were few differences in the peak height for mesotrione treatment on either media, however both water and mesotrione treatments in the presence of sucrose had a higher *CCA1::LUC* bioluminescence peak than the responses on sorbitol. In cycles 4, 5 and 6, for the sucrose plus mesotrione treatment, the bioluminescence peaks were higher than the sucrose without mesotrione. As on MS, the mesotrione treatment caused little effect on peak height. Importantly, the *CCA1::LUC* bioluminescence of mesotrione-treated plants on sorbitol peaked earlier than the water control (Fig. 8.6.1b), but with sucrose supplementation, there was no difference in the response of plants to mesotrione (Fig. 8.6.1c). This difference in peak time was only present in the two cycles after mesotrione treatment (Fig. 8.6.1d), being greater in cycle 3 (1.5 h) compared to cycle 4 (1 h).

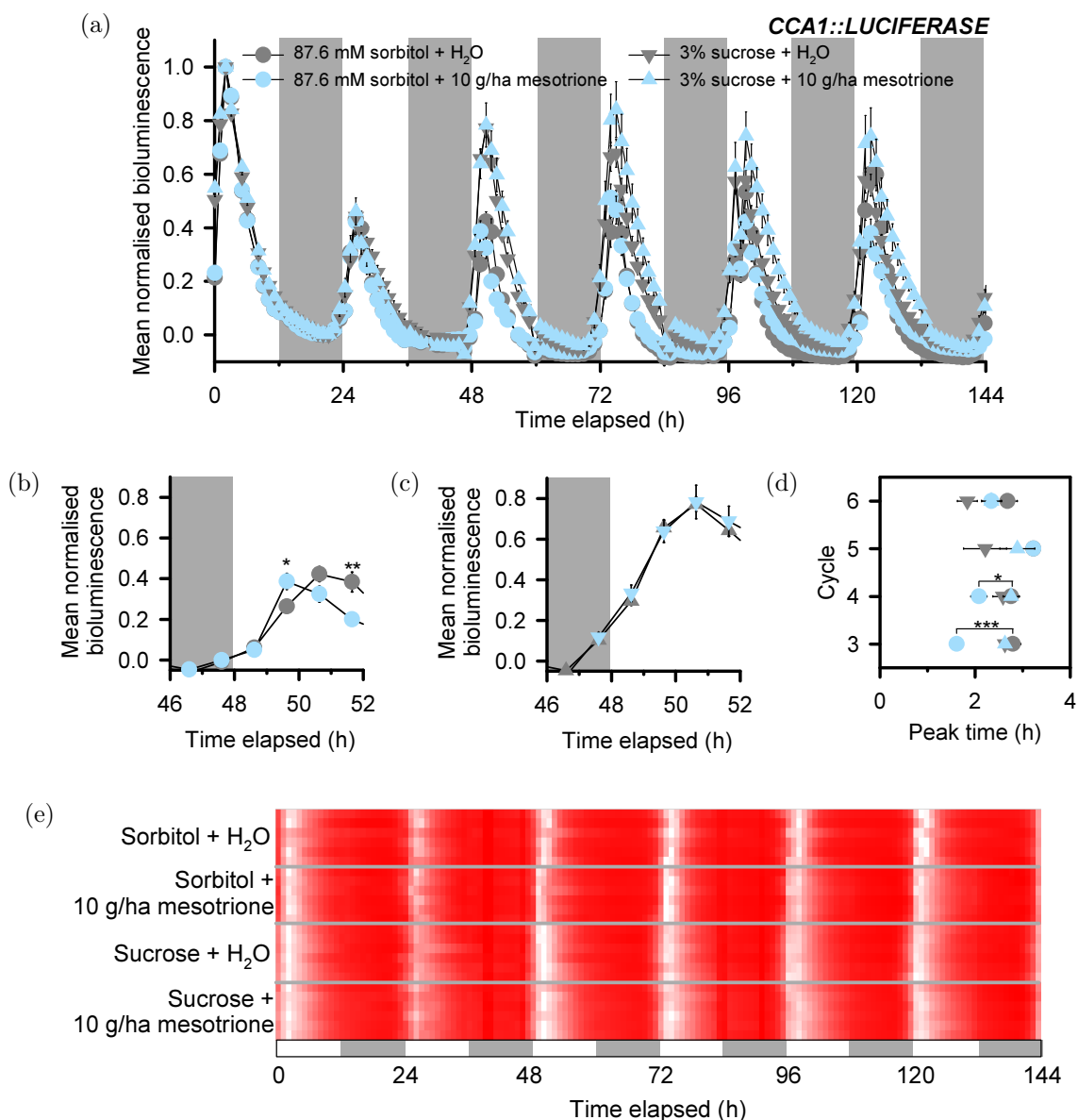


Figure 8.6.1: Exogenous sucrose inhibits the effects of mesotrione on *CCA1::LUC* under light-dark cycles. Plants were grown on media supplemented with either 87.6 mM sorbitol (circles) or 3% sucrose (triangles). Plants were dosed with luciferin on day 10. On day 11, imaging began under a 12 h light/ 12 h dark cycle. At dawn on day 12 plants were treated with either 10 g/ha mesotrione (blue) or a water control (grey) followed by a further 5 days imaging under 12 h light/ 12 h dark cycles. (a) Mesotrione application without sucrose affected *CCA1::LUC* bioluminescence 24 h after application. (b) Mesotrione altered the response of *CCA1::LUC* bioluminescence in the absence of sucrose, but not in the presence of sucrose (c). (d) Mesotrione advanced the time of peak *CCA1::LUC* bioluminescence in cycles 3 and 4, but this was absent in the presence of sucrose. (e) The earlier peak of *CCA1::LUC* bioluminescence can be seen around 48 h in the heat map. The addition of sucrose alters *CCA1::LUC* response to mesotrione. Grey areas indicate night. Data are the mean of 6 replicates from one representative experiment \pm SEM. Asterisks indicate significant difference between control and mesotrione calculated by *t*-test where * = $P \leq 0.05$, ** = $P \leq 0.01$ and *** = $P \leq 0.001$.

There were no differences in peak time for the control and mesotrione treatments on sucrose-supplemented media. Supplemental sucrose caused changes in the characteristics of the peaks, where they appeared wider compared to sorbitol (Fig. 8.6.1e). However, there were no obvious differences between the control and mesotrione treatments on sucrose. Conversely, in cycle 3 for the response on sorbitol, the earlier peak caused by mesotrione treatment could be seen (Fig. 8.6.1e). This was an interesting response because it suggests that a lack of photosynthetic sugar could be causing the effect on the oscillator in mesotrione treated plants. These results are summarised in Table 8.6.1.

Sucrose appeared to rescue the effect of mesotrione on the phase, however the effect of mesotrione did not appear to be completely rescued based on visual inspection of the plants (Fig. 8.6.2). Plants grown on sucrose-supplemented media were larger than those grown on MS. On MS, mesotrione caused bleaching of the plants, as expected. Sucrose supplementation prevented bleaching to a certain extent but mesotrione still caused bleaching of the plants.

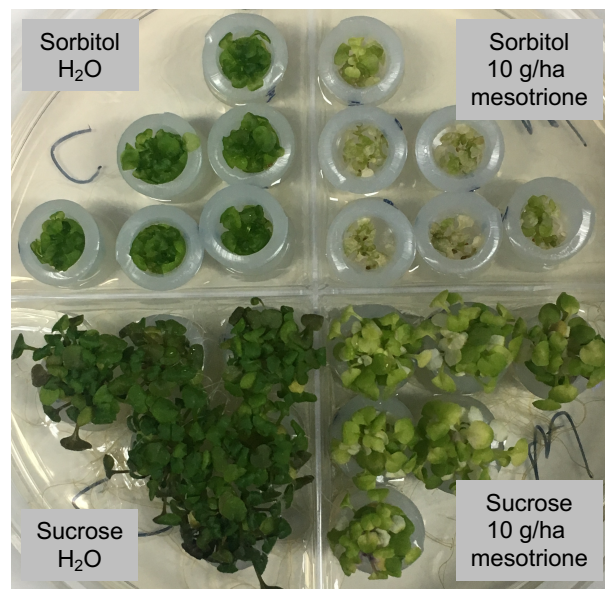


Figure 8.6.2: Mesotrione-induced bleaching of Arabidopsis tissue was reduced in the presence of sucrose. Five days after treatment, 10 g/ha mesotrione caused typical bleaching on media supplemented with 87.6 mM sorbitol, but this was reduced with 3% sucrose supplementation. 3% sucrose increased growth of Arabidopsis overall, but this caused the effect of mesotrione to be reduced. Image taken at the end of 6 days luciferase imaging under 12 h light/ 12 h dark cycles.

The greatest effects of TBA and Agridex were observed from 24 h after treatment onwards (Fig. 8.6.3a), consistent with previous experiments (Figs. 8.5.5 and 8.5.6). TBA and Agridex on sorbitol caused significant damping of *CCA1::LUC* bioluminescence for the remainder of the time course. The response was transient in the presence of sucrose, because after three cycles of treatment, the bioluminescence signal for all three treatments had similar peak height, unlike the response on sorbitol. In cycle 3, there was a significant reduction in the bioluminescence between control and Agridex, but no difference between Agridex and TBA (Fig. 8.6.3b). There was also a difference in the anticipation of dawn by treated plants such that the treated plants appeared less able to predict the changes in light conditions (Fig. 8.6.3b). However, in the presence of supplemental sucrose, the plants retained the ability to anticipate dawn (Fig. 8.6.3c). There were some inconsistencies between the timing of peak *CCA1::LUC* bioluminescence results here (Fig. 8.6.3d) and those reported earlier (Fig. 8.5.5c). In this experiment, the adjuvant caused *CCA1::LUC* bioluminescence to peak significantly earlier than the control in cycle 3, which did not occur previously. Furthermore, in the previous experiment Agridex caused a significantly earlier peak in cycles 5 and 6 which did not occur here. However, there were no overall effects of Agridex or TBA on *CCA1::LUC* peak times in the presence of sucrose. There was an absence of a clear peak in this experiment (Fig. 8.6.3e) unlike in the previous TBA LD experiment at 48 h. There was an unexpected peak around 108 h in Agridex and TBA treatments on sorbitol, which was not seen previously. There were some inconsistencies between replicates for Agridex and TBA effects on *CCA1::LUC* on sorbitol, but these occurred from before the application of treatments. The treatments in the presence of sucrose did not appear any different to the control, consistent with the peak time data. These results are summarised in Table 8.6.1.

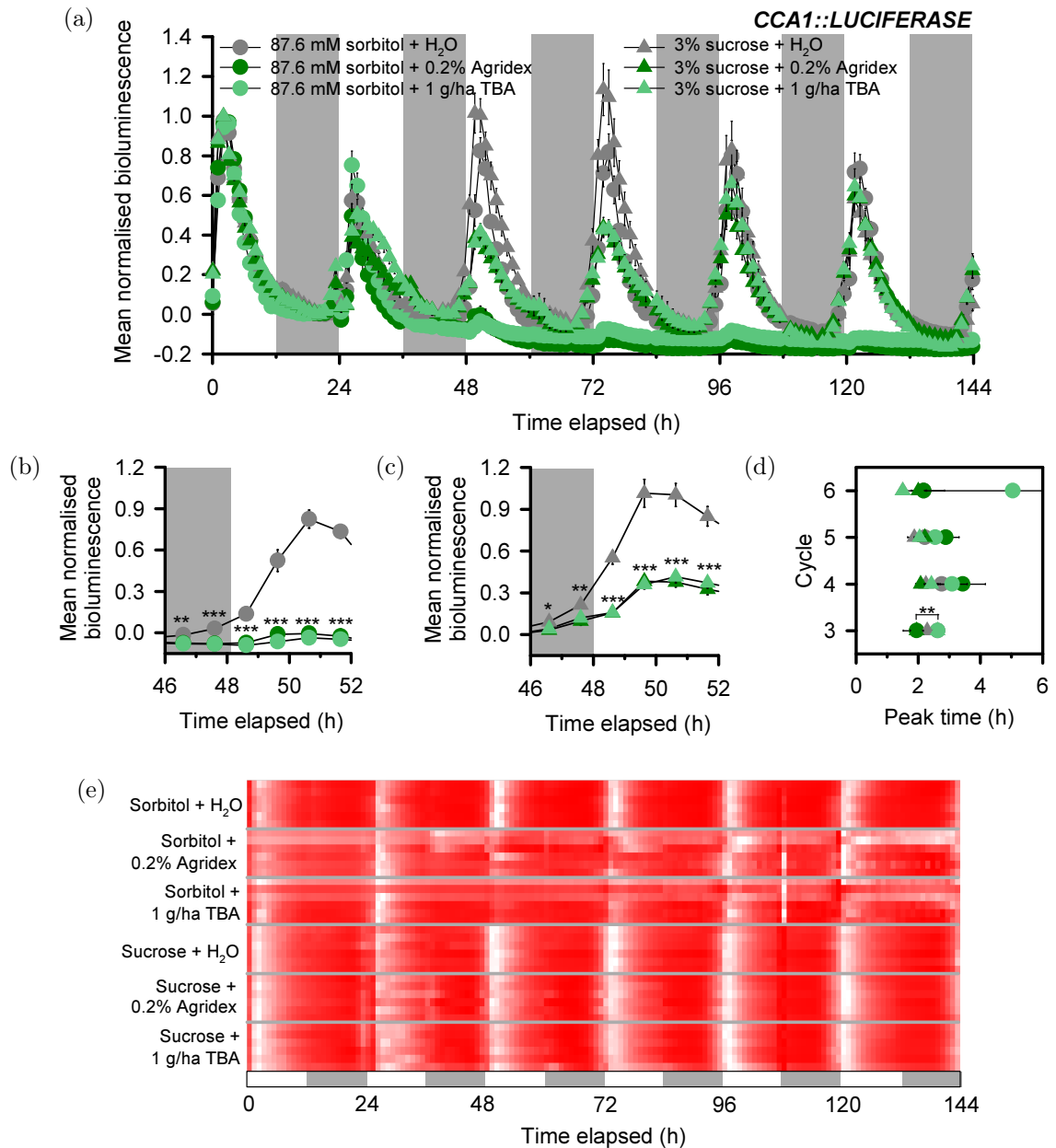


Figure 8.6.3: Exogenous sucrose inhibits the effect of Agridex and TBA on *CCA1::LUC* after a transient period. Plants were grown on media supplemented with either 87.6 mM sorbitol (circles) or 3% sucrose (triangles). Plants were dosed with luciferin on day 10. On day 11, imaging began under a 12 h light/ 12 h dark cycle. At dawn on day 12 plants were treated with either 1 g/ha TBA (light green), 0.2% Agridex (dark green) or a water control (grey) followed by a further 5 days imaging under 12 h light/ 12 h dark cycles. (a) TBA and Agridex applications affected *CCA1::LUC* bioluminescence after 24 h. After 96 h, there was no difference between the treatments and control in the presence of sucrose. (b) TBA and Agridex reduced *CCA1::LUC* bioluminescence relative to the water control, but to a lesser extent in the presence of sucrose (c). (d) Agridex advanced the peak time of *CCA1::LUC* in cycle 3 only in the absence of sucrose. (e) The effect of Agridex and TBA on *CCA1::LUC* bioluminescence can be seen from 24 h in the heat map, the addition of sucrose inhibited these effects. Grey areas indicate night. Data are the mean of 6 replicates from one representative experiment \pm SEM. Asterisks indicate significant difference between control and Agridex or Agridex and TBA, calculated by *t*-test where * = $P \leq 0.05$, ** = $P \leq 0.01$, and *** = $P \leq 0.001$.

Table 8.6.1: Summary of the effects of herbicides with sucrose supplementation on *CCA1::LUC* under light-dark cycles. Effect of mesotrione is compared to water control. Effect of TBA is compared to Agridex and effect of Agridex is compared to water control. Only statistically significant results are included. Phase result was not always consistent across multiple cycles.

Treatment	Phase
Sorbitol mesotrione	Early
Sucrose mesotrione	-
Sorbitol TBA	-
Sucrose TBA	-
Sorbitol Agridex	-
Sucrose Agridex	-

TBA and its adjuvant, Agridex, caused bleaching to the plant, but in the presence of exogenous sucrose this bleaching was reduced (Fig. 8.6.4). This was interesting because after several days in the presence of sucrose, the effect of TBA and Agridex were similar to that of the sorbitol controls. After transient effects of TBA and Agridex, the addition of exogenous sucrose did appear to overcome the effect of the treatments. However, due to inconsistencies across experiments, it is difficult to interpret the results and make conclusions.

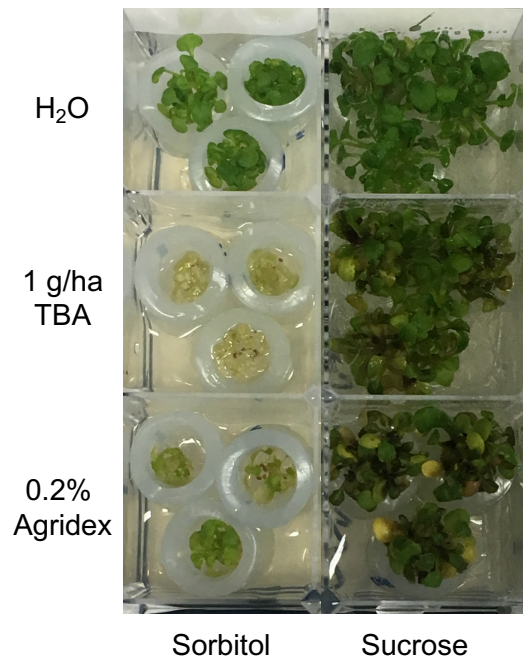


Figure 8.6.4: TBA-induced bleaching of tissue and growth inhibition of *Arabidopsis* was reduced in the presence of sucrose. Five days after treatment, 1 g/ha TBA caused typical bleaching and inhibition of growth on media supplemented with 87.6 mM sorbitol, but this was almost completely overcome with 3% sucrose supplementation. 0.2% Agridex also caused some bleaching and growth inhibition on sorbitol. This was largely overcome by 3% sucrose supplementation however some bleaching still occurred. Image taken at the end of 6 days luciferase imaging under 12 h light/ 12 h dark cycles.

The results from the interaction of mesotrione and sucrose supplementation were interesting and consistent, therefore the effect of mesotrione in the presence of sucrose was examined under constant light. The effect of mesotrione treatment on *CCA1::LUC* in the presence of sucrose was detected easily from around 96 h onwards, where the peaks of bioluminescence appeared to be enhanced by mesotrione treatment (Fig. 8.6.5a). The peaks of *CCA1::LUC* bioluminescence in the absence of sucrose did not seem to be affected by mesotrione as much as it had been previously (Fig. 8.3.3a), as there was little damping over time. There was no difference between the rhythmicity of plants for any of the treatments, they all had a mean RAE value of approximately 0.1-0.15 (Fig. 8.6.5b). Sucrose shortened the period of *CCA1::LUC* (Fig. 8.6.5b). There was no significant difference between period for control and mesotrione-treated plants in the presence of sucrose, whereas mesotrione caused a lengthening of the period in

the absence of sucrose (Fig. 8.6.5b). On sorbitol, mesotrione did not have a significant effect on the amplitude of *CCA1::LUC* although it appeared to reduce it (Fig. 8.6.5c), whereas previously on MS it reduced the amplitude (Fig. 8.3.3c). In the presence of sucrose, mesotrione appeared to increase the amplitude, but again this was not a significant increase. The later peak time across the cycles observed previously (Fig. 8.3.3d) was not evident in this experiment (Fig. 8.6.5d). However, differences were observed in the presence of sucrose, where the peak time was significantly later in the presence of mesotrione and sucrose (Fig. 8.6.5d). Interestingly, the peak time in the absence of sucrose was later with each cycle, however this did not occur in the presence of sucrose. The difference in peak time between mesotrione and control in the presence of sucrose was evident in the bioluminescence (Fig. 8.6.5e), where the mesotrione caused *CCA1::LUC* to peak later. The difference between the period in the presence or absence of sucrose could also be seen where the peaks for sucrose were closer together than they were in the absence of sucrose. These results are summarised in Table 8.6.2.

Table 8.6.2: Summary of the effect of mesotrione with sucrose supplementation on *CCA1::LUC* under constant light. Effect of mesotrione is compared to water control. Only statistically significant results are included. Phase result was not always consistent across multiple cycles.

Treatment	Period	RAE	Amplitude	Phase
Sorbitol mesotrione	Long	-	-	-
Sucrose mesotrione	-	-	-	Late

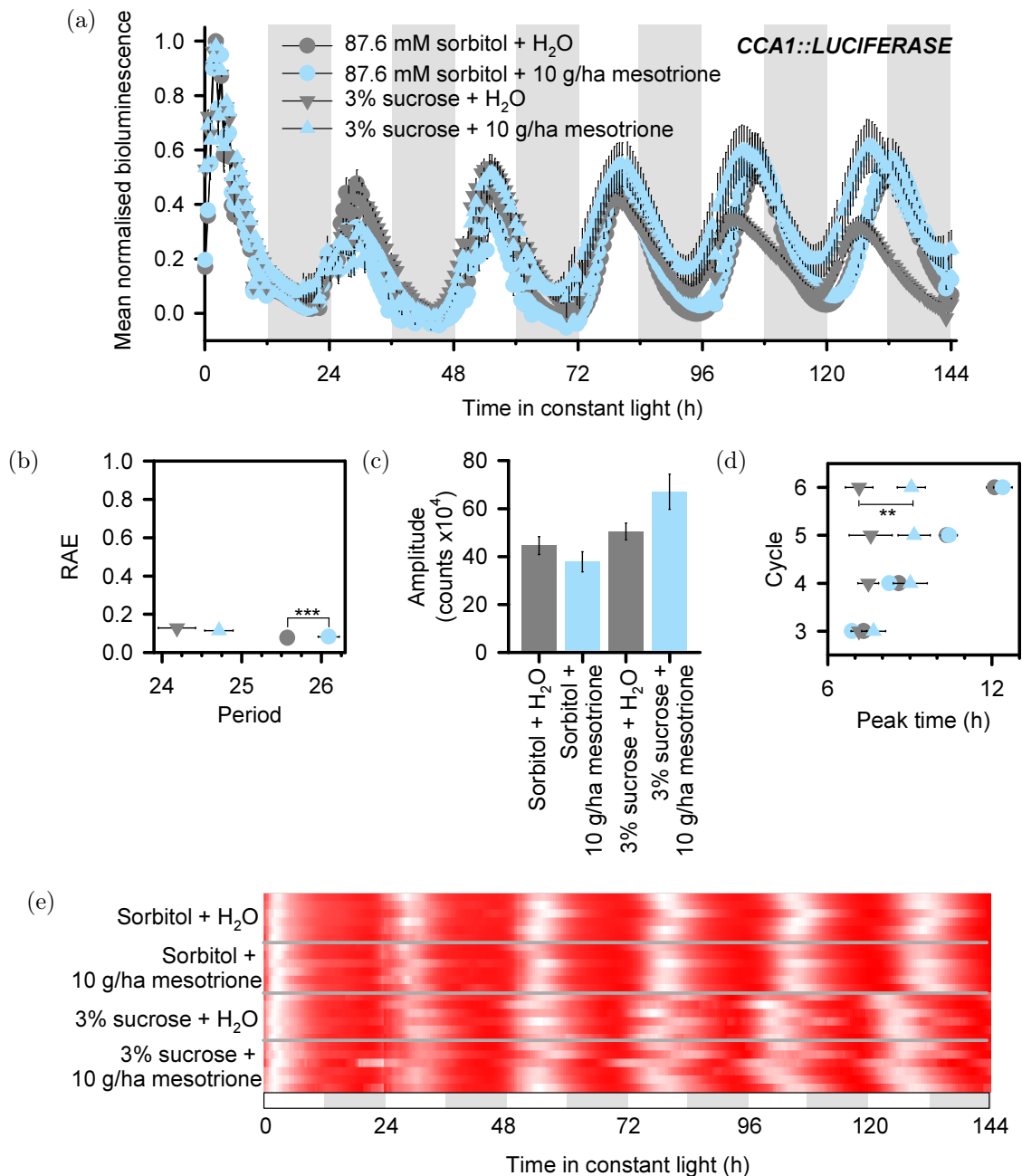


Figure 8.6.5: Exogenous sucrose inhibits the effects of mesotrione on *CCA1::LUC* under constant light. Plants were grown on media supplemented with either 87.6 mM sorbitol (circles) or 3% sucrose (triangles). Plants were dosed with luciferin on day 10. On day 11, imaging began under constant light conditions for 24 h. At dawn on day 12 plants were treated with either 10 g/ha mesotrione (blue) or a water control (grey) followed by a further 5 days imaging under constant light. (a) Effects of mesotrione on *CCA1::LUC* bioluminescence became apparent 96 h after application. (b) Mesotrione increased *CCA1::LUC* period only in the absence of sucrose. (c) Mesotrione had no effect on *CCA1::LUC* amplitude. (d) Mesotrione was without effect on *CCA1::LUC* bioluminescence in the absence of sucrose, but delayed the peak time in cycle 6 in the presence of sucrose. (e) The effect of sucrose on *CCA1::LUC* bioluminescence can be seen in the heat map. Grey areas indicate subjective night. Data are the mean of 12 replicates from two independent experiments \pm SEM. Asterisks indicate significant difference between control and mesotrione calculated by *t*-test where * = $P \leq 0.05$, ** = $P \leq 0.01$ and *** = $P \leq 0.001$.

The effect of sucrose on the circadian oscillator is more pronounced under low light conditions (Haydon et al., 2013). Therefore, the response to mesotrione could be more obvious under low light conditions. Under constant low light, the effect of mesotrione was apparent immediately after application (Fig. 8.6.6a). Mesotrione caused damping of *CCA1::LUC* bioluminescence in the presence of MS, sorbitol and sucrose, although these effects were small and transient. In the presence of sorbitol, *CCA1::LUC* RAE was significantly higher after mesotrione treatment (Fig. 8.6.6b), but was still considered rhythmic. Mesotrione treatment had no effect on *CCA1::LUC* RAE on MS and sucrose (Fig. 8.6.6b). Under low LL, mesotrione treatment had no significant effect on *CCA1::LUC* period, whereas previously period was increased with mesotrione treatment in the absence of sucrose (Fig. 8.6.6b), but not in the presence of sucrose. There were no differences between the control and mesotrione-treated *CCA1::LUC* amplitudes for any of the growth media under low LL (Fig. 8.6.6c). Under low LL, the *CCA1::LUC* peak bioluminescence per cycle was later in each cycle for all controls (Fig. 8.6.6d). In cycle 5 on MS, mesotrione treatment caused the peak time to be significantly earlier. This was the opposite to the effect observed under higher light conditions (Fig. 8.3.3d). In the presence of sucrose under low light, there was no difference between the peak times, whereas under high light, mesotrione caused the peak to occur later in the presence of sucrose (Fig. 8.6.5d). Under low LL, peak time per cycle increased more compared to under higher light conditions. For example, under high light the control peak time per cycle in the absence of sucrose shifted about 2 h per cycle, whereas under low light in the absence of sucrose, peak time shifted approximately 3 h later with each cycle. The *CCA1::LUC* peak on MS was almost absent when mesotrione was applied, but there were strong oscillations in later cycles (Fig. 8.6.6e). In the presence of sucrose, there appeared to be inconsistencies between replicates, but the addition of sucrose and the earlier peak time was seen around 96 h and 120 h, corresponding to the earlier period with the addition of sucrose (Fig. 8.6.6e). These results are summarised in Table 8.6.3.

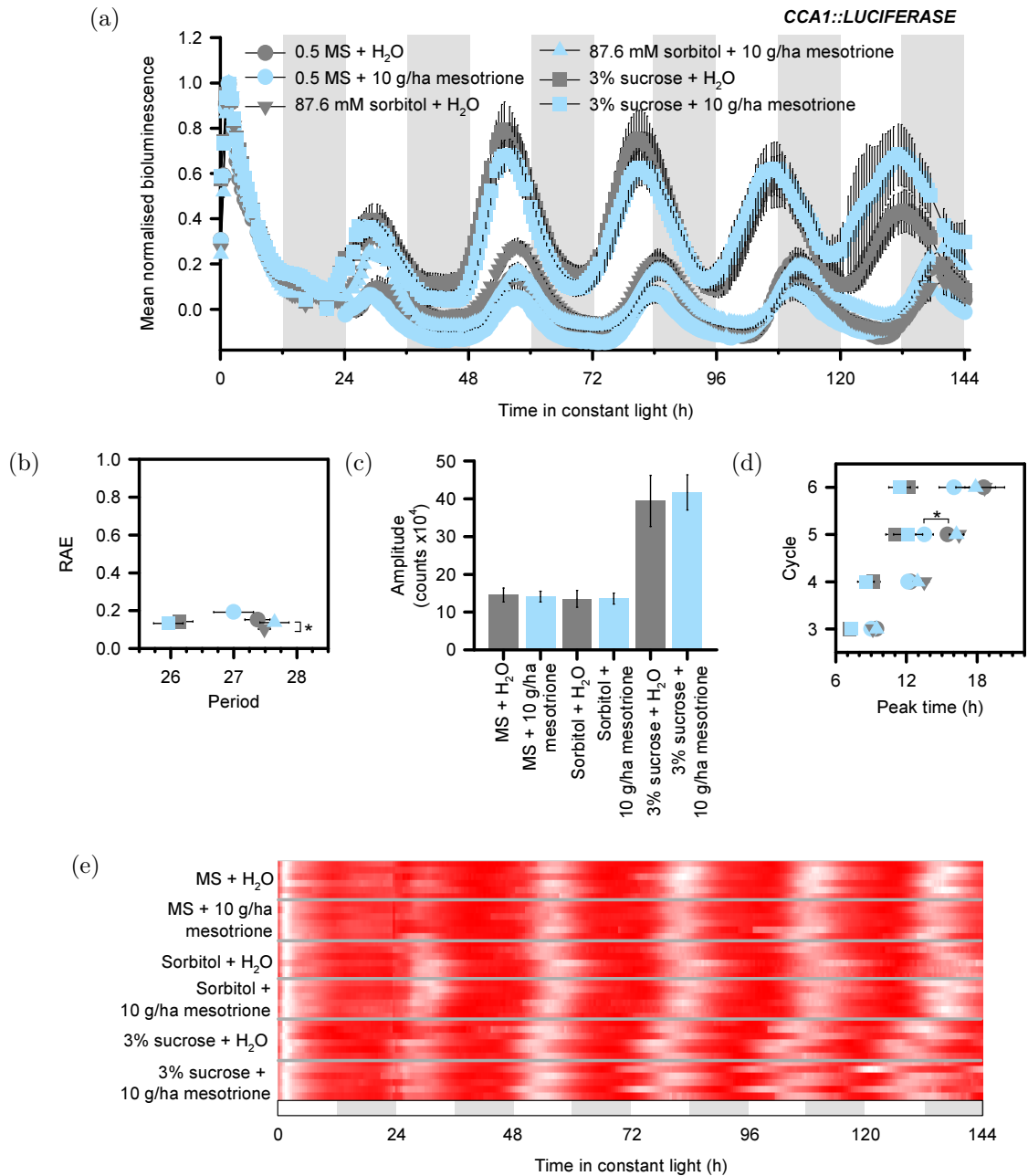


Figure 8.6.6: Exogenous sucrose inhibits the effects of mesotrione on *CCA1::LUC* under constant low light. Plants were grown on media supplemented with either 87.6 mM sorbitol (triangles), 3% sucrose (squares), or no supplementation (circles). Plants were dosed with luciferin on day 10. On day 11, imaging began under constant low light conditions ($10 \mu\text{mol m}^{-2} \text{s}^{-1}$) for 24 h. At dawn on day 12 plants were treated with either 10 g/ha mesotrione (blue) or a water control (grey) followed by a further 5 days imaging under constant light. (a) Effects of mesotrione on *CCA1::LUC* bioluminescence became apparent immediately after application. (b) Mesotrione decreased *CCA1::LUC* rhythmicity only in the presence of sorbitol and had no effect on period, or amplitude (c). (d) Mesotrione advanced *CCA1::LUC* bioluminescence peak time on MS in cycle 5, but otherwise was without effect. (e) The effect of sucrose on *CCA1::LUC* bioluminescence can be seen in the heat map. Grey areas indicate subjective night. Data are the mean of 12 replicates from two independent experiments \pm SEM. Asterisks indicate significant difference between control and mesotrione calculated by *t*-test where $* = P \leq 0.05$.

Table 8.6.3: Summary of the effect of mesotrione with sucrose supplementation on *CCA1::LUC* under constant low light. Effect of mesotrione is compared to water control. Only statistically significant results are included. Phase result was not always consistent across multiple cycles.

Treatment	Period	RAE	Amplitude	Phase
MS mesotrione	-	-	-	Early
Sorbitol mesotrione	-	Increased	-	-
Sucrose mesotrione	-	-	-	-

Overall, these results indicated that under constant low light, *CCA1::LUC* period was longer in the absence of sucrose. Mesotrione had a reduced effect at low light because there was no effect on amplitude or period. However, mesotrione did cause an earlier *CCA1::LUC* bioluminescence peak in one cycle on MS, but this was not present with exogenous sucrose, nor sorbitol.

8.7 Discussion

Measuring the activity of the circadian oscillator through bioluminescence reporters after herbicide application found that herbicides can alter the circadian period and the phase under entrained conditions. The mechanism through which the herbicides have such an effect on the oscillator is currently unknown, but it is likely that it is dependent on the herbicide active ingredient. Glyphosate application caused a slightly shorter circadian period, and a late entrained phase under light-dark, whereas mesotrione and TBA caused a long circadian period phenotype, but an earlier entrained phase under light-dark. The adjuvants for glyphosate and TBA also had considerable effect on the circadian oscillator promoter activity when applied alone. To our knowledge, this is the first investigation of effects of herbicides and adjuvants on the plant circadian oscillator. In the absence of biochemical detail of the interactions between

these chemicals and the circadian oscillator, we interpret the findings in the context of other factors known to regulate the circadian oscillator.

8.7.1 Herbicides cause different effects on the circadian oscillator under constant conditions compared to entrainment conditions

Under constant conditions, TBA and mesotrione caused a long circadian period compared to water controls, which led to an early phase under entrained conditions. It is logical that the long period under constant conditions would cause a later phase under entrained conditions because if a factor is causing period to increase, the phase would also get later. This is known as dynamic plasticity of the oscillator, and confers an advantage to the plant (Webb et al., 2019). It would be expected that under entrainment conditions, if a factor were able to affect the period, and also the system is not correctly entrained each dawn by the zeitgeber, that the period change would cause the phase to move in the same direction as the change in period under constant conditions (Salomé et al., 2013; Hearn et al., 2018). This was not the result observed here. Instead, the phase was altered in the opposite direction to that expected based on the period under constant conditions. For example, mesotrione caused a long period and late phase under constant light for *CCA1::LUC*, but under entrainment conditions an early phase was observed. Currently, this effect does not appear to have been reported in the literature. This could be because many studies only conduct circadian experiments under constant conditions, and do not report the effects under entrainment conditions and would therefore not know whether the circadian response has any effect under entrainment. It is important to extrapolate the findings under constant conditions to those under entrainment conditions, as this is what the plant experiences in the natural environment.

8.7.2 Photosynthesis-inhibiting herbicides may affect metabolic entrainment of the circadian oscillator

Sugar from photosynthesis is a rhythmic output of the circadian oscillator that, in turn, is able to provide entrainment signals to the oscillator, entraining the oscillator to a “metabolic dawn” (Haydon et al., 2013). Exogenous sucrose can shorten the period of the oscillator under constant light (Knight et al., 2008) and sustain rhythms in constant darkness (Dalchau et al., 2011), where most oscillator reporters without sucrose supplementation would become arrhythmic. Because exogenous sugar is known to affect the oscillator, the reliance of the oscillator on endogenous sugar from photosynthesis was identified using 3-(3,4-dichlorophenyl)-1, 1-dimethylurea (DCMU) (Haydon et al., 2013). DCMU is a urea-derived herbicide that inhibits plastoquinone binding in PSII (Oettmeier and Soll, 1983), therefore leading to inhibition of metabolic signalling by endogenous sugar, and changes the entrainment of the oscillator (Haydon et al., 2013). The effect of DCMU on circadian period was dependent on the reporter, such that DCMU caused reduced rhythmicity and a shorter period in *CCA1::LUC*, a lengthening in period for *PRR7::LUC* and *PRR9::LUC*, but had no effect on *TOC1::LUC*. Furthermore, the effects were emphasised by lower light levels (Haydon et al., 2013).

DCMU and TBA work through a similar mechanism, where TBA displaces plastoquinone from the binding site on the D1 protein of PSII (LeBaron et al., 2008). Therefore, it was hypothesised that if TBA had the same effect as DCMU, TBA might alter the metabolic entrainment of the circadian oscillator. Mesotrione also has an indirect effect on photosynthesis because it prevents the production of plastoquinone that is required for photosynthesis, therefore it could be affecting the circadian oscillator in a similar way. In this work, TBA and mesotrione caused a long period in *CCA1::LUC* under constant light. Therefore, this was the opposite effect to DCMU for *CCA1::LUC*, but the same as *PRR7::LUC* and *PRR9::LUC*, however treatments

were applied differently across the experiments, making direct comparisons difficult (Haydon et al., 2013).

The effect of DCMU upon the circadian oscillator was rescued with the application of exogenous sucrose, and the plants could be entrained by the exogenous sugar (Haydon et al., 2013). Therefore, I reasoned that the application of exogenous sucrose could also rescue the effect of TBA and mesotrione on metabolic entrainment through photosynthetic sugars, and this could explain the effect TBA and mesotrione had upon the oscillator. While exogenous sucrose is reported to shorten the period of the oscillator, the response appears to depend on experimental conditions. The period of Col-0 leaf movement was 0.7 h shorter in the presence of sucrose compared to no sucrose under $50 \mu\text{mol m}^{-2} \text{s}^{-1}$ light (Knight et al., 2008); conversely, it was also reported that sucrose only had an effect on *CCA1::LUC* circadian period under $10 \mu\text{mol m}^{-2} \text{s}^{-1}$ light, but no effect at $50 \mu\text{mol m}^{-2} \text{s}^{-1}$ (Haydon et al., 2013). Furthermore, the effect of sucrose on the oscillator appears to depend on the reporter, for example 90 mM sucrose increased the period of *TOC1::LUC* under constant light but decreased the period of *GI::LUC* (Dalchau et al., 2011). In summary, there are inconsistencies in the literature. In this work, sucrose reduced *CCA1::LUC* period by 1.3 h under $50 \mu\text{mol m}^{-2} \text{s}^{-1}$ light (Fig. 8.6.5).

The response to sucrose was first tested under light-dark cycles (Figs. 8.6.1, 8.6.3), to determine whether the response was altered in entraining conditions. Sucrose rescued the effect of mesotrione and TBA on the early phase phenotype (Figs. 8.6.1, 8.6.3). The control was inconsistent for TBA and was not investigated further. When experiments with exogenous sucrose were conducted under constant light with the application of mesotrione, the long period and late phase phenotype were rescued by the addition of exogenous sucrose (Fig. 8.6.5). This suggests that the exogenous sucrose could have been providing the sugars that may be inhibited by the herbicide affecting photosynthesis, and that the inhibition of sugars was affecting photosynthetic entrainment of the oscillator. Therefore, the addition of exogenous sucrose can rescue both

the long period and late phase under constant light conditions, and also the sucrose can rescue the early phase phenotype evident under light-dark cycles.

It is not known whether the effect of the herbicides is solely through the inhibition of synthesis or signalling by photosynthetic sugars, so further experiments should test this. For example, the endogenous sugars could be measured to determine if they are affected by mesotrione and TBA, although it is very likely they are depleted in TBA treatments. Furthermore, mutants of known components of the photosynthetic entrainment pathway such as *bzip63*, *tps1* and *prr7*, could be investigated to test whether they are insensitive to the effect of the herbicides on the oscillator (Frank et al., 2018; Haydon et al., 2013).

8.7.3 Mesotrione has no effect upon circadian period under constant low light

It appeared that inhibition of metabolic sugar entrainment could be causing the effect of mesotrione on the circadian oscillator because the long period and early phase was rescued with sucrose supplementation. It has been reported that the shortening of period by exogenous sugar is exaggerated under constant low light ($10 \mu\text{mol m}^{-2} \text{s}^{-1}$) (Haydon et al., 2013). Sucrose may be altering the oscillator period at lower light intensities because with less sugar production from photosynthesis, sugar signalling is not saturated and so sucrose addition can affect the oscillator (Haydon et al., 2013). Therefore the effects of constant low light and mesotrione with and without exogenous sucrose were tested.

Period was longer in control plants in the absence of sucrose under the low light intensity. This is consistent with Aschoffs Rule, which predicts that a decrease in light intensity lengthens the period (Aschoff, 1979; Devlin and Kay, 2000). Addition of sucrose to control plants shortened the period by approximately 1.4 hours. The shortening of period by sucrose was only slightly more pronounced in these experiments compared to at the higher light intensity tested, in contrast to previous reports

(Haydon et al., 2013). Haydon et al. (2013) reported that the effect of DCMU upon period did not change much under different light intensities. However it appeared that DCMU caused approximately a 1 h shortening of *CCA1::LUC* period under low light, but this was dependent on the reporter. While mesotrione caused a 0.5 h lengthening of period under higher light conditions, intriguingly mesotrione was without effect on period at the low light intensity (Fig. 8.6.6). This was surprising because if a treatment were affecting photosynthesis, it may be expected that inhibition and consequent effect on circadian period would occur no matter what the light intensity (Haydon et al., 2013). However, this is similar to previous results measuring a different reporter line. *GI::LUC* period was lengthened by DCMU treatment at $50 \mu\text{mol m}^{-2} \text{s}^{-1}$ but was not affected under $10 \mu\text{mol m}^{-2} \text{s}^{-1}$ light (Haydon et al., 2013), similar to the response of *CCA1::LUC* to mesotrione. It is unclear why there are differences in the effect of DCMU on circadian period depending on the reporter.

Because the magnitude of the response was not the same for *CCA1::LUC* with mesotrione treatment as the response of the oscillator to DCMU treatment, perhaps the effects observed were not solely due to the effect of mesotrione on metabolic entrainment. While it has been suggested that a photosynthesis inhibitor would have the same effect regardless of light intensity (Haydon et al., 2013), it would be interesting to determine how mesotrione would affect the oscillator under higher light intensities. Perhaps because mesotrione is indirectly involved in photosynthesis, under conditions such as higher light where a higher rate of photosynthesis would be occurring, the effect of mesotrione would be greater and thus have a greater effect on the circadian oscillator. The response to sucrose and low light suggests that there is another mechanism through which mesotrione is having an effect on the circadian oscillator that requires further investigation.

8.7.4 Herbicides could be affecting the circadian oscillator through oxidative stress

While mesotrione and TBA could be affecting the entrainment of the oscillator through inhibition of signalling by photosynthetic sugars, there were differences between the results obtained in the current work and the literature, that could suggest otherwise. For example, the difference in the effect on whether the period was shortened or lengthened in response to treatment. Furthermore, the differences in the effect of the herbicides under constant conditions and those seen under entrainment conditions suggest that the herbicides could be having multiple effects on the oscillator. Therefore, it is possible that there are other mechanisms through which the herbicides can affect the oscillator.

Metabolic stress in the chloroplast is known to affect nuclear circadian rhythms (Litthauer et al., 2018), and it is plausible that mesotrione and TBA are causing metabolic stress in the chloroplast since they are likely to increase ROS production when inhibiting photosynthesis. Oxidative damage induced by perturbations in metabolism caused by abiotic factors is usually first perceived in the chloroplast (Mittler et al., 2011; Litthauer et al., 2018). Therefore the herbicides could cause oxidative stress that is signalled to the nucleus and affects circadian rhythms. A signalling component that could be involved in the integration of chloroplast stress status to the nuclear circadian oscillator is SAL1 phosphatase (Litthauer et al., 2018). When the chloroplast is experiencing oxidative stress, redox-induced impairment of SAL1 leads to accumulation of 3'-phosphoadenosine 5'-phosphate (PAP), inhibiting exoribonuclease activity (Litthauer et al., 2018). Such oxidative stress causes PAP to increase and is accompanied by a 1 hour increase in circadian period (Litthauer et al., 2018). Through mutating *SAL1*, circadian period is increased further and there is a greater level of PAP. Induced oxidative stress, through application of methyl viologen was also found to lengthen the circadian period (Litthauer et al., 2018), supporting this

theory. Therefore, probable oxidative stress in the chloroplast caused by mesotrione and TBA could be affecting the circadian period through an increase of PAP.

Under dim blue light, there was no difference in the circadian period of wild type and *sal1* mutant allele plants that have increased levels of PAP; however, increasing the fluence rate caused a longer period in *sal1* alleles compared to WT (Litthauer et al., 2018). Increased fluence rates are thought to increase PAP accumulation. This is reminiscent of mesotrione treatment under the two light intensities, where there was no effect of the treatment under low light (Fig. 8.6.5), but at higher light intensity mesotrione caused a longer period (Fig. 8.6.5). Interestingly, the response of *sal1* period was blue-light dependent, suggesting that there could be involvement of the CRYPTOCHROME1 (CRY1), CRY2 or ZEITLUPE (ZTL) photoreceptors (Litthauer et al., 2018). Therefore it is hypothesised that the application of mesotrione, and potentially TBA, are causing oxidative stress in the chloroplast that is initiating a signalling pathway to the nucleus through the accumulation of PAP, and consequently affecting circadian period. This could explain the response of the circadian period, and the abolished effect of mesotrione under low light. Furthermore this could potentially be blue light-dependent. This mechanism could be responsible for the altered effect under entrainment conditions, if the photoreceptors are affected by herbicide treatment. It remains unclear how this mechanism could advance the phase under entrainment conditions, as opposed to delaying it, as Litthauer et al. (2018) do not report the effect of PAP accumulation under light-dark cycles. Therefore it is not possible to compare the different responses seen under constant light and light-dark cycles.

In the experiments by Litthauer et al. (2018) referred to above, mannitol was used as an osmoticum to cause oxidative stress. An osmotic control for sucrose application was used in this work, and with this osmoticum (sorbitol) the circadian period was not altered. This could be due to differences in the osmotic potential and application methods across the studies.

Interestingly, *GIGANTEA* (*GI*) mutants have been shown to have resistance to

butafenacil, which is a herbicide that inhibits protoporphyrinogen IX oxidase, within the chlorophyll/heme biosynthetic pathway (Cha et al., 2019). Butafenacil application causes ROS accumulation, but this was absent in *gi-1* and *gi-2* (Cha et al., 2019). This suggests a role for GI in chloroplast biogenesis, and perhaps there is a link between GI, oxidative stress and the effect of oxidative stress on the circadian oscillator. This is further made interesting because of the effect of DCMU on *GI::LUC* found by Haydon et al. (2013) indicating an interaction between *GI* as a component of the circadian oscillator, photosynthesis and ROS that could link to the effect of mesotrione and TBA.

This hypothesis suggests further experiments that could be used to determine the effect of oxidative stress-induced PAP accumulation by the herbicides. For example, it would be interesting to measure: the levels of PAP after herbicide treatment, the effect of herbicides under high light, the effects of herbicides under different wavelengths of light, and the effect of the herbicides on the blue-light photoreceptors, including the use of photoreceptor mutants. If the herbicides affect photoreceptors this could explain the effect on entrainment in the dark to light transition under light-dark cycles, where phase was advanced. Because this mechanism of PAP accumulation requires retrograde signalling from the chloroplast to the nucleus, further work could investigate the effect of the herbicides on those signals and the involvement of *GI*. Alternatively, this phenomenon could still relate to the involvement of metabolic sugars, and there may be a recovery time during the dark period, when photosynthesis is not occurring, when the herbicides have a reduced effect.

8.7.5 Herbicides may influence de-synchronisation of oscillator components

There were differences in the effect of herbicide treatments upon the promoters of different oscillator components. Treatment with glyphosate under constant light conditions and light-dark cycles had no obvious effect on *TOC1::LUC*, whereas the effect was more visible on *CCA1::LUC*. Furthermore, the adjuvant for glyphosate also

had a greater effect on the *CCA1::LUC* reporter compared to the *TOC1::LUC* reporter. Under constant light, mesotrione had a greater effect on *CCA1::LUC* where there was a significant effect on all measured parameters. For *TOC1::LUC*, mesotrione caused a significantly earlier peak time in the fifth cycle, the opposite to that observed for *CCA1::LUC*. Under light-dark cycles, mesotrione had no effect on the phase of *TOC1::LUC*, but had a significant effect on *CCA1::LUC*. Finally, there were few differences between the effect of TBA compared to its adjuvant on *CCA1::LUC* and *TOC1::LUC* under constant light conditions. The effect of the TBA adjuvant under constant light conditions was the opposite for the two reporters, where Agridex caused a significantly longer period and later phase for *CCA1::LUC* (Fig. 8.4.4) but an earlier period and phase for *TOC1::LUC* (Fig. 8.4.5). Under light-dark cycles, TBA had a greater effect on *CCA1::LUC* in the later cycles, whereas TBA had the greatest effect on peak time in the first two cycles for *TOC1::LUC*. These results suggest that there could be some asynchrony between different components of the oscillator.

Due to the tightly interlinked mechanism of the circadian oscillator, it would be expected that an effect on one oscillator component would lead to alterations in the rhythms of downstream components. For example, if a stressor affected CCA1, it may be expected that the effect on CCA1 would cause an effect on TOC1, as CCA1 negatively regulates TOC1 (Alabadí et al., 2001). The subsequent effect might be seen for all elements of the oscillator, given its cyclical nature. This has been reported previously where iron deficiency caused a long period phenotype under constant conditions in *CCA1::LUC*, *PRR7::LUC*, *TOC1::LUC* and *CAB2::LUC* reporters. The period delay caused a phase delay under entrained conditions, and this was to the same extent for each reporter (Salomé et al., 2013). Such iron deficiency caused an equal phase delay to all components of the oscillator that were measured. Conversely, reports have shown that some treatments can have different effects on different oscillator components. For example, an early period was observed after DCMU treatment on *CCA1::LUC*, but a later period for *PRR7::LUC*, *PRR9::LUC*, and *GI::LUC*, whereas there was little effect on *TOC1::LUC* (Haydon et al., 2013). Therefore, evidence also exists of one

treatment having differing effects on the oscillator components, comparable to the results found in the present work.

It is assumed that all cells contain an individual circadian oscillator (Takahashi et al., 2015), however the extent of coupling between the oscillators of different cells is unknown. If there is uncoupling of the oscillators between cells, this could suggest why there are differences between the responses of different reporters to the same stimuli. Endo et al. (2014) proposed that there are tissue-specific oscillators that asymmetrically regulate each other in *Arabidopsis*. The morning loop consists of mesophyll-rich genes whereas the evening loop consists of vasculature rich genes. The vasculature oscillator is distinct and robust, and can control the mesophyll cells that are next to the vasculature (Endo et al., 2014). This suggests that the plant circadian oscillator can vary across tissue types and that the rhythm present in one tissue type could be regulating the rhythm in another tissue type. Moreover, Takahashi et al. (2015) found that the shoot apex may act as a master oscillator that influences rhythms in roots. Excised organs showed different rhythms and emergent properties of bioluminescence, in particular the shoot and the root had very different rhythms, where roots were less rhythmic than shoots (Takahashi et al., 2015). Therefore, the shoot is required for the rhythm in the root. Different periods have also been estimated from the leaf from distinct physiological parameters (Dodd et al., 2004). The circadian control of stomatal conductance and CO₂ assimilation can be uncoupled in certain mutants, further suggesting that individual cells contain their own oscillator that runs autonomously (Dodd et al., 2004). Together, these data indicate that the components of the oscillator could reside in different parts of the plant and respond differently to a stimuli, and consequently produce a different response when measured through bioluminescence. The different responses in the promoter activity could be due to differences in the cell types where each reporter is predominantly active.

It has been suggested that a period change under constant conditions will affect the phase of evening genes more than morning genes due to the strong resetting signal of dawn, where a shorter period equates to the earlier expression of evening

genes (Salomé and McClung, 2005a). This did not appear to be the case here where *CCA1* was affected more than *TOC1*. However, it could be that the responses would be seen to a greater extent in output genes rather than the promoters of oscillator components themselves. It could be that plasticity within the oscillator buffers the effect of the morning component upon the evening component, if the change in the morning component is relatively small (Webb et al., 2019).

An alternative explanation for the differences in effect of treatments across reporters is that the timing of the treatments cause a greater effect on a certain component of the oscillator. The treatments were applied at dawn, and as such are closest to the time of the morning phase of the oscillator, and this could be why there were greater effects observed on *CCA1*. Treatments later in the day may have a greater effect on *TOC1* and a lesser effect on *CCA1*, therefore this could be tested in further work. This was apparent in the experiments by Qian et al. (2014), where atrazine had the greatest effect on the oscillator of *Microcystis aeruginosa* when applied at the onset of the light phase (measured by the impact on cell growth). The key components of the *M. aeruginosa* oscillator are morning phased, hence this could also be why the effects were greatest at this time. The reasoning behind the effect at one time is likely related to the mechanism of the herbicide or adjuvant component and how it is interacting within the cell to affect the circadian oscillator component at that time. However, this may not explain de-synchronisation of the oscillator and why there are opposite effects observed for the circadian period or entrained phase on the different oscillator elements.

8.7.6 Further observations

Interestingly, the adjuvants for both glyphosate and TBA had profound effects on the bioluminescence of the circadian reporters when applied alone. The highest concentrations significantly reduced rhythmicity in the plants, but this could have been due to plant death, based on visual inspection of the plants (Figs. 8.4.3 and 8.6.4). It

is unknown why or how the adjuvants cause such a response on the circadian oscillator, but it might be related to stress responses. Furthermore, the adjuvants affected some emergent properties of the circadian system but not others. For example, the glyphosate adjuvant did not cause a reduction in the peaks of the signal but it did cause a later phase of *CCA1::LUC* under light-dark cycles (Fig. 8.5.1). There also appeared to be asynchrony between the components of the oscillator in response to the adjuvant treatments, whereby *TOC1::LUC* was affected more than *CCA1::LUC* for both glyphosate and TBA adjuvants. Further experimentation is required to better understand what processes are causing this, but the fact that the adjuvants can cause such an effect is fundamental for field applications where the adjuvant could be applied to herbicide-resistant crops.

Some of the responses of the reporters to herbicides appear to be transient changes or long term responses. For example, TBA affects the phase of *CCA1::LUC* in cycles 5 and 6 under light-dark cycles (Fig. 8.5.5), whereas it affects *TOC1::LUC* phase on cycles 3 and 4 (Fig. 8.5.6). This response could be related to the mechanism through which the chemicals are affecting the oscillator and entrainment, but without further experimentation this is speculative.

8.8 Conclusions

It has been suggested that a long period and late phase in the circadian system reduces metabolism in the plant, enhancing survival under suboptimal conditions (Syed et al., 2015; Litthauer et al., 2018). This is in accordance with the effect of mesotrione and TBA in this work under constant light conditions. This suggests that stress signals are perceived by the plant, and the plant responds by adjusting the circadian rhythm to cope with the unfavourable environment. However, this does not appear to be the case under light-dark cycles. Mechanisms for these responses have been proposed that include the herbicides inhibiting metabolic entrainment through photosynthetic sugars or the accumulation of PAP through oxidative stress signalling from the chloroplast to

the nucleus altering the circadian oscillator. The intriguing effect of these herbicides on phase under light-dark cycles remains unclear.

Overall, these herbicides and their adjuvants have an impact on the circadian oscillator in *Arabidopsis*. This is important because: (i) when the oscillator is not correctly synchronised to the environment, plant fitness is reduced. This is beneficial if the herbicide were to only affect weed species, however non-target crops could also be affected in the field. (ii) In herbicide-resistant crops, the crop is resistant to the mode of action of the active ingredient of the herbicide, but not to the subsequent effects on the circadian oscillator. (iii) The adjuvant components of the formulations also have a distinct affect on plant circadian rhythms, therefore herbicide-resistant crops would be receiving the effects of the adjuvant, reducing the fitness of the crop through altering the circadian rhythm, and preventing the plant from being synchronised to the environment.

In addition to the aforementioned experiments that could be conducted to understand the mechanisms in greater detail, further experiments could extend this work. Different entrainment photoperiods could exaggerate, or reduce, the effect of herbicides on both circadian period and entrainment (Hearn et al., 2018). Additional reporters of the circadian oscillator could be measured to determine the effect of herbicides on more components of the oscillator. Transcripts of the oscillator components could be quantified as the effect on the promoter measured by the luciferase reporter does not necessarily equate to transcript or protein levels. Finally, the effects of the herbicides and adjuvants could be examined in other species, and also in herbicide-resistant plants to examine the extent of phase asynchrony between the treated plants and the environment to determine the cost in fitness.

Chapter 9

General discussion

9.1 Summary of novel findings

Overall, this research identified two key novel findings surrounding the interaction between circadian regulation and herbicides: (i) circadian regulation of signalling or metabolism might cause daily fluctuations in the effectiveness of herbicides applied at different times of day and (ii) herbicides have an effect on the emergent properties of the plant circadian oscillator. These findings are summarised in Figure 9.1.1.

This research was focussed on testing three different mode of action herbicides that were of interest to Syngenta, the collaborators of this work: glyphosate, mesotrione and terbuthylazine. Since these herbicides function differently within the plant, various experimental approaches were used to test for time of day sensitivity to the herbicides (Chapter 3). Preliminary data provided evidence to suggest there was regulation of the response, dependent on a properly functioning circadian oscillator, and that *Arabidopsis* was a suitable species in which to conduct this work.

The existence of time of day variation in the responses to herbicides is not a new concept (Martinson et al., 2002; Miller et al., 2003; Waltz et al., 2004; Mohr et al., 2007; Stewart et al., 2009; Stopps et al., 2013; Sharkhuu et al., 2014). However, until now, there has not been a clear, definite connection between the plant circadian oscillator

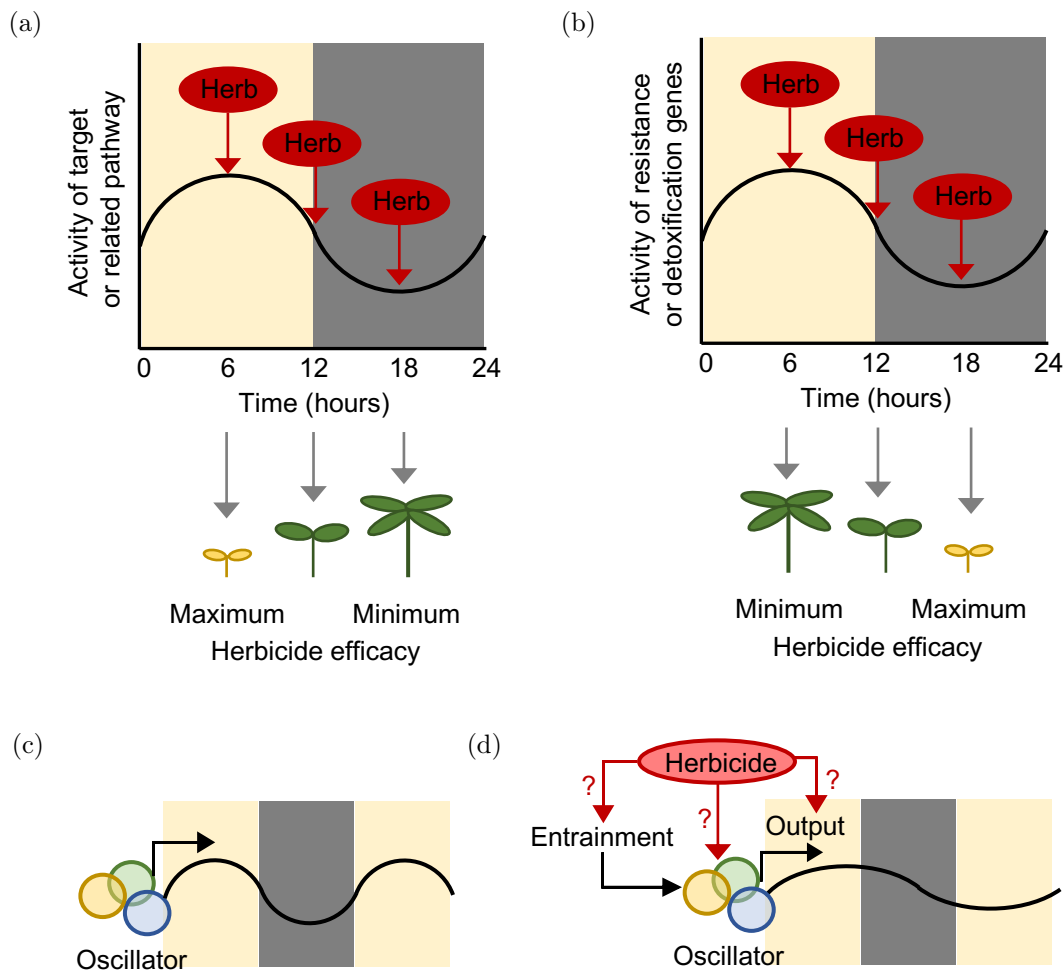


Figure 9.1.1: Overview of the interactions between the circadian oscillator and herbicides. Circadian rhythms and herbicides have been shown to interact in two ways: (i) the response to a herbicide could be gated by the circadian oscillator (a, b). This could be due to cyclic activity of either the herbicide target (a) or resistance or detoxification genes (b) whereby the application of a herbicide at different times of day can result in different magnitudes of herbicide efficacy and consequently, different effects on the survival of the plant. (ii) Rhythmic properties of the circadian oscillator (c) might be altered by the herbicide (d) in one of three ways (indicated by “?”), the herbicide could: affect the input pathway to the oscillator, affect the oscillator components directly, or affect the oscillator outputs. As such, the herbicide can cause changes in entrainment phase, period, and, consequently, physiology. Yellow, green and blue circles represent the circadian oscillator. Shaded areas indicate day (yellow) and night (grey). Red circles and Herb indicate application of a herbicide. (a, b) Figure concept adapted from Hotta et al. (2007).

and herbicide efficacy. Furthermore, the majority of research has been conducted with glyphosate in the field. The research presented here provides the first evidence that the circadian oscillator is responsible for variation in the efficacy of herbicides at different times of day (Figs. 9.1.1a and 9.1.1b). This circadian regulation might occur through: (i) rhythmic activity of the herbicide target, where maximum herbicide efficacy occurs when application coincides with when the herbicide target is at a peak (Fig. 9.1.1a) or (ii) rhythmic activity of resistance or detoxification genes, with maximum herbicide efficacy occurring when such activity is at low levels (Fig. 9.1.1b). Equally, rhythmic efficacy of the herbicide could be due to a combination of both factors.

The mechanism behind the circadian regulation of the response to glyphosate was investigated in depth (Chapters 4, 5 and 6). Experiments identified a link between the inhibitory effect of glyphosate on tryptophan biosynthesis (Baur, 1979) and consequently auxin biosynthesis and signalling, and circadian regulation. While a link between glyphosate and inhibition of auxin biosynthesis has been previously described (Baur, 1979; Jiang et al., 2013), the relationship between this and time of day sensitivity is novel. Importantly, we determined that such circadian regulation determines that the concentration of glyphosate required to give a certain level of control alters with application timing. Consequently, a reduced concentration of herbicide can be applied at a certain time of day that is more effective (Figs. 4.4.7 and 4.5.3). This circadian regulation of the response to agrochemicals has not been reported previously.

Preliminary experiments were conducted with mesotrione and TBA to attempt to identify time of day variation in the response to the herbicides, and circadian regulation was apparent (Chapter 3). Elucidation of further mechanisms behind such circadian regulation for these two chemicals was difficult since very little existing data were available to analyse as an initial starting point. By obtaining mesotrione- and TBA-regulated transcriptomes (Chapter 7) and performing extensive analysis of these data, we have a better understanding of the effects of these chemicals and how an interaction between the herbicide and circadian regulation may occur. These new

transcriptomes and the findings from the analyses will be useful for further research into understanding the circadian regulation of these herbicides.

Finally, until this point there was, to our knowledge, no evidence for the effects of herbicides on plant circadian rhythms. Some research exists on the effect of atrazine on a cyanobacterial circadian oscillator (Qian et al., 2014), but nothing similar had been conducted in plants. We identified that mesotrione, TBA, and the adjuvant Agridex had significant effects on the emergent properties of the *Arabidopsis* circadian oscillator (Chapter 8, Figs. 9.1.1c and 9.1.1d). Such alterations in the properties of the circadian oscillator suggest that the plant will be unable to correctly temporally synchronise to its surrounding environment, and fitness may be reduced. While this may be a positive aspect of herbicide application to weeds, this may not be beneficial to herbicide-resistant crops. In particular, the significant effect of the adjuvant applied alone has not been reported previously, and could be detrimental to crops in the field.

9.2 Broad implications of these findings for agriculture

Since this research has a basis in agriculture, it is important to extrapolate these findings to consider their meaning in such a context. Questions to address this are discussed below, outlining potential areas for future work.

9.2.1 How do these findings extend to field conditions?

In a field environment there are numerous factors that fluctuate throughout each 24 h cycle. One major fluctuation is the transition between light and dark. The effect of this on herbicide efficacy was tested in this work (Fig. 4.4.1). The response to herbicide treatments at different times of day under different photoperiods was also tested (Fig. 4.4.4). This is relevant to the altered photoperiods in different growing seasons, or

at different latitudes for farming in different parts of the world. We found that the time of day that glyphosate was most effective in our assay was the same regardless of photoperiod, suggesting that this could be relevant to multiple types of field conditions where light conditions fluctuate. The time of day when plants were most sensitive to glyphosate was dawn. If the time that was most sensitive to glyphosate had been during the dark period, this may have been less relevant to the field since farmers are less likely to spray fields at night.

Temperature fluctuates by different extents dependent on location and season. Temperature can also entrain the circadian oscillator (Heintzen et al., 1994). Therefore, changes in temperature may alter the daily timing in sensitivity to herbicides, since many processes within the plant are controlled by the oscillator. However, temperature compensation by the circadian oscillator (Harmer et al., 2001) means that fluctuations in temperature do not usually alter the circadian period, and therefore the outputs of the oscillator may not change with fluctuating temperature. Furthermore, light is the predominant daily timing cue over temperature and, as such, in the field temperature may have little effect on herbicide sensitivity. Nevertheless, it would be interesting to determine the effect of fluctuating temperature on the responses to herbicides alone, and in combination with fluctuating light conditions. Within the plant, temperature would not affect the circadian oscillator alone, it would also affect other processes, such as changing the expression of genes. Therefore, there could be changes to the transcriptome, including the targets of the herbicide, or resistance and detoxification genes, which would alter the time of day sensitivity to herbicides.

In the field, weather conditions such as wind, dew and rain contribute to herbicide efficacy. These factors can all vary throughout the day. As such, the timing of these factors could conflict with the time that herbicides are most effective in controlled environments. Wind is usually lower around dawn and dusk (Mohr et al., 2007), and this is when herbicides are usually sprayed in order to avoid drift to non-target species. Wind is reported to also help dry, and concentrate, the herbicide on the leaf, increasing uptake. Dew can be present early in the morning and late at night (Mohr et al., 2007).

Dew can re-wet the surface of the leaf, increasing uptake (Thompson and Slife, 1969), alternatively, dew can dilute the herbicide and make it less effective or make it run off the leaf (Stopps et al., 2013). Therefore, these factors could increase the time of day effectiveness of herbicides, if the timing coincided with environmental factors that also aid the uptake of the herbicide. Rain can occur at any time of day and a farmer would not apply herbicides during rain. If it was raining during the most effective herbicide time point on one particular day, the findings from this work would not necessarily be useful. However, herbicide formulations contain surfactants that increase rainfastness (Field and Bishop, 1988; Roggenbuck et al., 1990), and such formulations are usually taken into the plant within 2 h. The most effective time of herbicide application could still be relevant when rain needs to be taken into consideration if such effective time point still allows 2 h before predicted rainfall.

These weather conditions may be responsible for altering herbicide efficacy overall, but they are not likely to affect the circadian regulation of responses to herbicides. As such, the time of day effectiveness of herbicides reported in this work remain relevant to the field.

9.2.2 What species are these results important for?

In the field, herbicides have many targets including: numerous species of weeds growing in competition with crops, crops themselves for desiccation and harvest management (Orson and Davies, 2007), and cover crops (Reddy et al., 2003). The majority of this research was conducted using *Arabidopsis*. *Arabidopsis* itself is not commonly a target of herbicides in the field. While *Arabidopsis* as a Brassicaceae is related to some crop and weed species, and similarities are likely to exist in the relevant biochemical and molecular pathways, there are many other plant families that could have species-specific effects. This is a limitation of this work, and as such, more work should be conducted to test the time of day sensitivity to herbicides in other species in order to use herbicides as efficiently as possible.

Herbicides are also sprayed on herbicide-resistant crops. This is a major consideration since herbicides and their adjuvants can have a detrimental effect on the plant via the effects on the circadian oscillator (Chapter 8, Figs. 9.1.1c and 9.1.1d). While the herbicide-resistant crop may be resistant to the main herbicide target, damage could still be caused by the adjuvant component of the formulation due to the indirect effect on the oscillator. Such effects are unlikely to have been considered previously. Misregulation of the circadian oscillator can cause changes in the plant fitness and yield (Dodd et al., 2005). Therefore, if the herbicide were to affect the circadian oscillator indirectly in a herbicide-resistant crop, the yield or other traits such as flowering time, could still be negatively impacted.

9.2.3 Can we use these results to reduce agrochemical use?

The quantities of herbicides used creates problems for the environment by leaching into waterways, and creating selection pressure on weeds, leading to resistance. Thus, it would be beneficial to reduce the amount of agrochemicals used (Otto et al., 2016). One of the key outcomes of this research is that the time of day of herbicide application can determine the effective amount of herbicide that is required (Figs. 4.4.7 and 4.5.3). For example, 1.5 times more glyphosate was required at the least effective time of application to give the same effect on a seedling at the most effective application time (Fig. 4.4.7). In principle, if herbicides are applied at the most appropriate time of day, this could lead to reduced levels of chemicals being used overall. We have proposed the term agricultural chronotherapy to explain this concept. While this requires further testing before application to the field (Section 9.2.1), and a better understanding for more mode of action herbicides, we think that this concept could also be extended further to other agrochemicals such as fertilisers and safeners, and can reduce overall agrochemical use.

9.3 Application of these findings to new products

This research was not intended to provide evidence to inform the design of new products. However, several outcomes of this research have resulted in new ideas that could hypothetically be used in new agrochemical products or to provide guidance on certain aspects of agrochemical testing.

9.3.1 Have these results provided recommendations for testing new agrochemicals?

Since we found that the time of day that a herbicide is applied to a plant alters the efficacy of the herbicide (Figs. 4.4.1 and 4.5.2), we would recommend that this could be considered as an element of testing new formulations. Further, we found that the concentration of herbicide required to give a certain degree of effect can change at different times of day (Figs. 4.4.7 and 4.5.3). Therefore, the required or recommended amount of new herbicide could vary depending on the time of day that tests were conducted. The same concept has been recommended in medical chronotherapeutics (Zhang et al., 2014b) since many drug targets are circadian regulated, and also have short half lives.

There are many ways in which time of day testing could be conducted as a component of herbicide trials. For example, the simplest test could be applying herbicides at different times of day, and physiological parameters of the plant could be measured a specified time after application. Measuring chlorophyll fluorescence is another method that could be used. This method is beneficial since it is a non-invasive method, and is not overly time-consuming. While primarily used to measure the effects of factors on photosynthesis, the herbicide of interest does not have to directly affect photosynthesis since chlorophyll fluorescence can simply measure stress, as reported in response to glyphosate (Chapter 3). Finally, quantifying the abundance of programmed cell death-related transcripts would be a useful measure of time of day efficacy. This relies on

some knowledge of the transcriptome of the species of interest, whereas other suggested methods do not.

These tests could be conducted under a variety of environmental conditions that would be relevant to the field, and not solely whether the response is due to light-dark or circadian regulation. Some optimisation tests would be necessary to ensure the concentration of herbicide is not too high that it would mask such time of day differences. Overall, we feel that including such testing would benefit the producers of agrochemicals in that the quantity of chemical could be optimised to potentially minimise unintentional environmental exposure.

9.3.2 Could the circadian oscillator be a target for agrochemicals?

The circadian oscillator could potentially be a useful tool for other agrochemicals. Firstly, the oscillator could be used as a target for new mode of action herbicides. Since dissonance between the circadian oscillator and the environment is known to be detrimental for plant fitness (Dodd et al., 2005), exploiting this could make a good herbicidal chemical. As the circadian oscillator is a complex mechanism, it could be difficult to identify what specifically could be targeted effectively. Recently, a chemical biology screen using a library of 90 small synthetic molecules was used to determine the effects on circadian period in *Arabidopsis* (Uehara et al., 2019). One such compound was found to lengthen the period of both *CCA1::LUC* and *TOC1::LUC*, and furthermore, caused growth retardation (Uehara et al., 2019). Therefore, such an approach could be used to identify an oscillator-targeting herbicide. While attempting to create a novel herbicide targeting the circadian oscillator would be a complex task, it has the potential to be a powerful agrochemical.

Secondly, the circadian oscillator could be the target of agrochemicals intended to alter the properties of the plant, without having herbicidal activity. The circadian oscillator responds to changing photoperiods and regulates plant development in re-

sponse (Seaton et al., 2015). One such example is the regulation of flowering time (Hicks et al., 1996). Flowering time could potentially be manipulated by agrochemical application in crops to enhance yields, or alter traits. For example, delaying flowering time could allow for increased vegetative growth, and consequently an increased yield of vegetative crops. Conversely, initiating flowering could speed up production of seed and potentially allow for more harvests per year. Traits such as this are usually altered through breeding, but there is potential that an agrochemical could be applied to chemically alter the oscillator function and initiate, or delay, flowering. Such research could also be conducted through the use of chemical biology screens (Uehara et al., 2019). This could provide a further mechanism through which the circadian oscillator could be manipulated to benefit the agrochemical industry.

9.4 Overall conclusions

This has been an insightful and useful topic to research with clear agricultural applications, tackling an overarching aim of aiding the global issue of food security. This research has been somewhat preliminary in places, and was restricted to three mode of action herbicides and largely one plant species. However, it has opened a new field of research, which we have termed agricultural chronotherapy. We do recognise that there are limitations to this work, primarily the effect of environmental factors and species-specific effects. Therefore, further work is required before the concept of agricultural chronotherapy can be applied fully to the field. We hope that the results obtained from this work will lead to further research surrounding this new field, since it has applications that reach further than we initially anticipated. For example, these principles could be useful for testing the efficacy of new chemicals and further, to aid the use of chemicals more effectively and safely in the field.

Chapter 10

Appendix

Select papers I have had published throughout the duration of this PhD.


1. Belbin et al (2019).
2. Belbin and Dodd (2018).
3. Belbin et al (2017).

ARTICLE

<https://doi.org/10.1038/s41467-019-11709-5>

OPEN

Plant circadian rhythms regulate the effectiveness of a glyphosate-based herbicide

Fiona E. Belbin¹, Gavin J. Hall², Amelia B. Jackson¹, Florence E. Schanschieff¹, George Archibald², Carl Formstone² & Antony N. Dodd¹ 

Herbicides increase crop yields by allowing weed control and harvest management. Glyphosate is the most widely-used herbicide active ingredient, with \$11 billion spent annually on glyphosate-containing products applied to >350 million hectares worldwide, using about 8.6 billion kg of glyphosate. The herbicidal effectiveness of glyphosate can depend upon the time of day of spraying. Here, we show that the plant circadian clock regulates the effectiveness of glyphosate. We identify a daily and circadian rhythm in the inhibition of plant development by glyphosate, due to interaction between glyphosate activity, the circadian oscillator and potentially auxin signalling. We identify that the circadian clock controls the timing and extent of glyphosate-induced plant cell death. Furthermore, the clock controls a rhythm in the minimum effective dose of glyphosate. We propose the concept of agricultural chronotherapy, similar in principle to chronotherapy in medical practice. Our findings provide a platform to refine agrochemical use and development, conferring future economic and environmental benefits.

¹School of Biological Sciences, University of Bristol, Bristol BS8 1TQ, UK. ²Syngenta, Jealott's Hill International Research Centre, Warfield, Bracknell RG42 6EY, UK. Correspondence and requests for materials should be addressed to A.N.D. (email: antony.dodd@bristol.ac.uk)

Global food requirements demand crop production increases of 100–110% by 2050¹. Weeds cause estimated yield losses of 34%², with herbicides being a tool to tackle these losses and also enhance harvest management³. Glyphosate (*N*-(phosphonomethyl) glycine) is the most widely used herbicide active ingredient, with \$5 billion and \$11 billion spent annually on glyphosate-containing products in the USA and worldwide, respectively⁴. Glyphosate-based formulations are used on >350 million hectares worldwide, involving about 8.6 billion kg of glyphosate annually⁴. This scale of glyphosate use makes strategies to enhance its utility commercially and environmentally attractive.

Intriguingly, the herbicidal effectiveness of glyphosate can depend upon the time of day of application^{5–8}. One mechanism that influences the timing of responses of plants to their environment is the circadian clock. Circadian rhythms are biological cycles with a period of about 24 h that persist in the absence of external cues. In plants, circadian rhythms are generated by a series of interlocked transcription-translation loops and post-translational mechanisms that are known collectively as the circadian oscillator. The phase of the circadian oscillator is adjusted to match the phase of the environment through the process of entrainment in response to light, temperature and metabolic cues, and the circadian oscillator regulates metabolism, development and physiology primarily through regulation of gene expression. The circadian oscillator also modulates the responses of plants to a variety of environmental cues so that the response depends on the time of day, through a process known as circadian gating.

We hypothesised that circadian regulation might underlie certain rhythmic responses of plants to glyphosate because the circadian clock co-ordinates the timing of many physiological and developmental processes in plants^{9,10}. In *Arabidopsis*, 6–15%^{9,11} of the transcriptome is circadian-regulated with up to 89%¹² having the potential for rhythmic behaviour under a range of environments. The resulting rhythms of metabolism and development present a variety of potential rhythmic targets for agrochemicals. This is reminiscent of over half of the 100 highest grossing prescribed drugs in the USA having circadian-regulated targets in the mouse¹³, providing a basis for temporal variation in drug sensitivity that underpins chronotherapy. We reasoned that pervasive circadian regulation in plants might underlie rhythmic responses to certain chemical applications, and tested this notion for glyphosate-based herbicides due to their widespread use. This is an important question, because rhythmic responses of plants to agrochemicals introduce novel opportunities to refine or reduce agrochemical use.

Results

A subset of glyphosate-responsive transcripts are rhythmic. We wished to establish why the effectiveness of glyphosate (*N*-(phosphonomethyl)glycine) can depend on the time of day of application^{5–8}. Glyphosate inhibits 5-enolpyruvyl-shikimate-3-phosphate synthase (EPSPS) within the shikimate pathway¹⁴, eventually killing the plant (Supplementary Fig. 1). We identified cellular processes influenced by both circadian rhythms and glyphosate, by interrogating transcriptome data from the experimental model *Arabidopsis thaliana*. A subset of glyphosate-responsive transcripts¹⁵ oscillate under light-dark cycles (Supplementary Fig. 2A)^{16,17} or are circadian-regulated (Supplementary Fig. 2B)^{11,18,19}. From these, we identified glyphosate-responsive transcripts that are consistently diel- and circadian-regulated (Supplementary Fig. 2C). This identified 18 and 57 rhythmic transcripts that are glyphosate-induced and repressed, respectively (Supplementary Fig. 2C; Supplementary Data 1). Seventy two percent of glyphosate-induced rhythmic

transcripts reach peak abundance at dawn (Supplementary Fig. 2D), whereas rhythmic glyphosate-repressed transcripts oscillate with a range of phases (Supplementary Fig. 2D).

A gene ontology (GO)-term analysis of the 137 transcripts that are glyphosate- and circadian-regulated identified a significant enrichment of this transcript set with an auxin transport GO term (GO:0060918; $P=0.024$; Benjamini Hochberg correction), whereas the 538 transcripts that are glyphosate- and light/dark regulated is not enriched significantly for auxin-related GO terms. Examining this further, we identified a statistically significant overlap between the set of 75 transcripts that are consistently glyphosate-responsive and both circadian- or light/dark regulated (Supplementary Fig. 2C) and the 549 unique transcripts present within all of the auxin-related GO terms in the *Arabidopsis* genome (Supplementary Data 1; $P=0.03$). These overlaps between glyphosate-responsive and auxin-related transcripts might occur because glyphosate inhibits EPSPS, preventing synthesis of the auxin precursor tryptophan²⁰, or because glyphosate can inhibit auxin transport²¹. Auxin signalling is circadian-regulated¹⁹, so we reasoned that interaction between auxin signalling, glyphosate and circadian rhythms might underlie certain nycthemeral or circadian responses to glyphosate. An informative proxy to study this is seedling hypocotyl elongation, which is regulated by the circadian oscillator and phytohormones including auxin²². Therefore, we hypothesised that such rhythms might underlie a rhythmic sensitivity of hypocotyl length to glyphosate.

Rhythms in the sensitivity of hypocotyl length to glyphosate.

Glyphosate applied at dawn caused the greatest reduction in hypocotyl length compared with control treatments, whereas hypocotyl length was unaffected by glyphosate applied at dusk (Fig. 1a). This greater sensitivity of hypocotyl length to glyphosate applied at dawn corresponds to a time of elevated auxin signalling¹⁹. The daily fluctuation in glyphosate sensitivity occurred under 8, 12 and 16 h photoperiods (Fig. 1a, Supplementary Fig. 3 A, B; two-way ANOVA identified a significant interaction between glyphosate treatment and time upon hypocotyl length under 8 h ($P<0.001$), 12 h ($P<0.001$) and 16 h ($P=0.03$) photoperiods, respectively). We performed subsequent experiments under 8 h photoperiods, because the hypocotyls were longer under this photoperiod. During the dark period, hypocotyl length was reduced most by glyphosate applied immediately after dusk and in the pre-dawn period (Supplementary Fig. 3C). The measurements described involved glyphosate application on day 3 after germination. This daily pattern of increased glyphosate sensitivity at dawn occurred also when glyphosate was applied at dawn or dusk on day 5 after germination (Supplementary Fig. 3D). Combined with the predawn increase in glyphosate sensitivity during the dark period (Supplementary Fig. 3C), these data suggest that there are daily cycles of glyphosate sensitivity of hypocotyl length during this period of development, irrespective of any decrease in hypocotyl elongation rate during this period of time.

Circadian arrhythmic *CCA1-ox*²³ changed the timing of this response, causing a greater reduction of hypocotyl length when glyphosate was applied around dusk (Fig. 1b; significant interaction between treatment and time; $P<0.001$). Overexpressing the oscillator component *TOC1-ox*²⁴ did not appear to cause a substantial change in time of greatest glyphosate sensitivity compared with the wild type (Fig. 1c; significant interaction between treatment and time; $P=0.04$). The greatest decrease in hypocotyl length caused by glyphosate in the Col-0 wild type (26%) was smaller than the greatest decrease in *CCA1-ox* (46%) and more than the greatest decrease in *TOC1-ox* (15%)

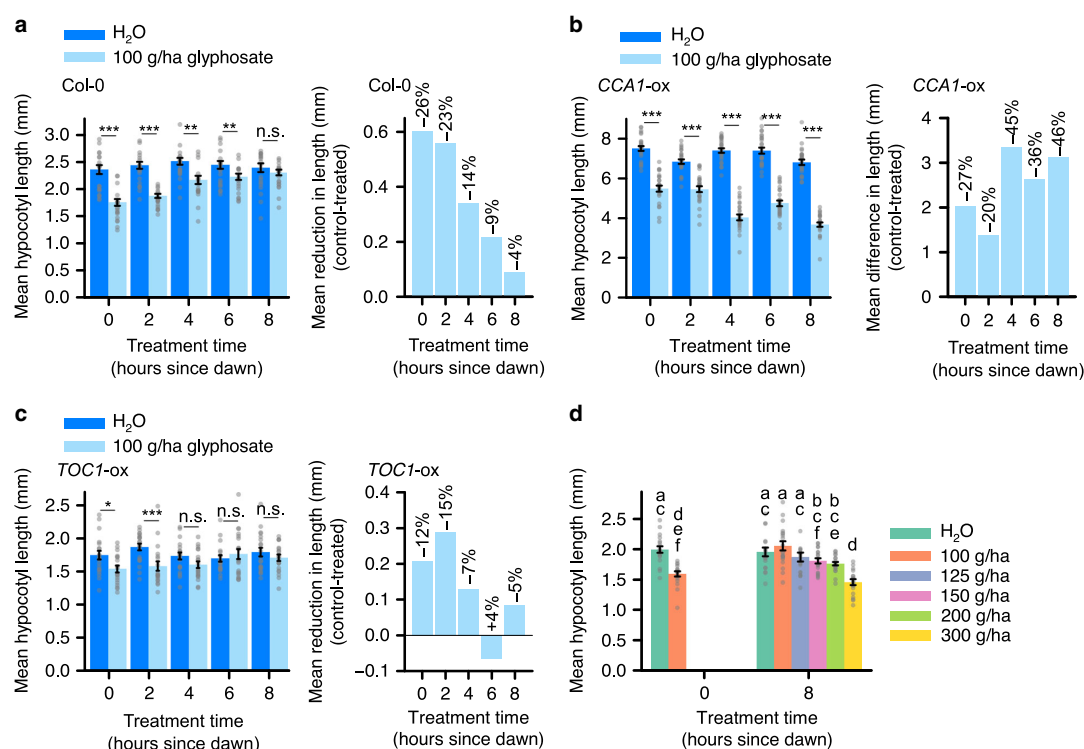


Fig. 1 Daily rhythms in glyphosate effectiveness. **a–c** Under light/dark cycles, hypocotyls are shorter in seedlings treated with 100 g/ha glyphosate compared with controls at times specified, in **a** Col-0, **b** CCA1-ox and **c** TOC1-ox seedlings. Graphs show (left) hypocotyl length and (right) change in hypocotyl length caused by glyphosate. **d** Titration of glyphosate concentration required to cause equivalent decrease in hypocotyl length at dawn and dusk in the Col-0 background. **a–d** Significance determined by **a–c** two-way ANOVA and *t*-tests between control and treatment at each timepoint; **d** one-way ANOVA and Tukey post-hoc analysis. n.s. = not statistically significant, * $P \leq 0.05$, ** $P \leq 0.01$, *** $P \leq 0.001$. Data are mean \pm s.e.m; $n = 18–25$. Source data are provided in the Source Data file

(Fig. 1a–c). These differing responses of CCA1-ox and TOC1-ox to glyphosate might reflect differences in their elongation response to light compared with the wild type²⁵. Reduction of hypocotyl length was caused by glyphosate, not the herbicide adjuvants (Supplementary Fig. 3E). Together, this indicates that the circadian oscillator underlies a daily rhythm in glyphosate efficacy under light/dark cycles.

We reasoned that this daily cycle in the effectiveness of glyphosate might be due to a transient effect of glyphosate upon hypocotyl elongation. To test this, we used time-lapse imaging to monitor the rate of hypocotyl elongation following glyphosate treatment under light/dark cycles. After glyphosate treatment at dawn, the mean hypocotyl elongation rate was reduced significantly compared with the control during the first dark period after glyphosate treatment (Supplementary Fig. 4A, B). In contrast, the mean hypocotyl elongation rate was not decreased during this period when seedlings were treated with glyphosate at dusk (Supplementary Fig. 4C, D). Although the data are noisy, this suggests that glyphosate causes a transient reduction in hypocotyl elongation and the occurrence of this transient reduction depends upon the time of glyphosate treatment.

We identified daily fluctuations in the effective dose of glyphosate. Increasing the dusk glyphosate concentration to 150 g/ha caused an equivalent reduction in hypocotyl length as 100 g/ha at dawn (Fig. 1d). Therefore, using the decrease in hypocotyl length as a measure of glyphosate effectiveness, 1.5

times more glyphosate was required at dusk to have the same effectiveness as at dawn. This suggests that plant growth is less sensitive to a dusk glyphosate application.

Circadian regulation of a response to glyphosate. Next, we identified a circadian rhythm in the response of hypocotyl length to glyphosate. First, we verified that germinating seedlings receiving one 8 h light/16 h dark cycle had a free-running circadian rhythm, by measuring rhythms of CCA1::LUCIFERASE bioluminescence in seedlings receiving this treatment (Supplementary Fig. 5A, B; period 24.2 ± 0.1 h). The phase of CCA1::LUCIFERASE was consistent with previous reports under free running conditions^{26–28}, with promoter activity increasing before subjective dawn and peaking around the middle of the subjective day (Supplementary Fig. 5A, B). Sets of seedlings were treated with 100 g/ha glyphosate at intervals across two 24 h cycles, beginning 46 h after the onset of constant conditions. The wild type had a circadian rhythm in the decrease in hypocotyl length caused by glyphosate (Fig. 2a, Supplementary Fig. 5C). Greatest glyphosate sensitivity occurred at subjective dawn, similar to the phase of maximum glyphosate sensitivity of hypocotyl length under light/dark cycles (Fig. 1a). In CCA1-ox, there was no rhythm in the decrease in hypocotyl length caused by glyphosate (Fig. 2b, Supplementary Fig. 5D). This identifies that the circadian oscillator underlies a circadian rhythm in the response of hypocotyl length to glyphosate.

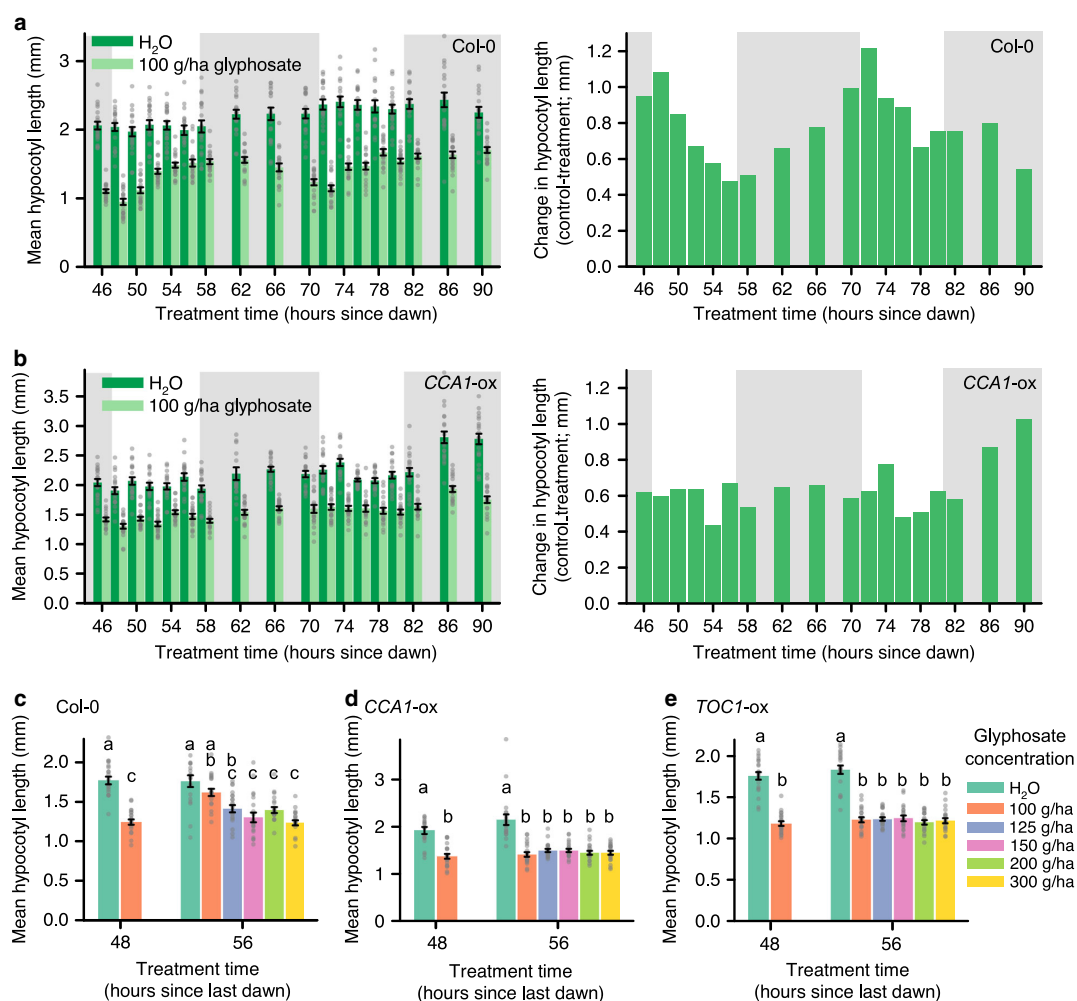


Fig. 2 Circadian regulation of the sensitivity of plants to glyphosate. **a, b** Under constant light conditions, hypocotyl length of seedlings treated with 100 g/ha glyphosate at times specified, in **a** Col-0 and **b** CCA1-ox seedlings. Graphs show (left) hypocotyl length and (right) change in hypocotyl length caused by glyphosate. Grey shading indicates subjective night. **c-e** Glyphosate concentration required to produce equivalent attenuation of hypocotyl length at subjective dawn (48 h) and subjective dusk (56 h) in **c** Col-0, **d** CCA1-ox and **e** TOC1-ox. Significance determined by **a, b** two-way ANOVA **c-e** one-way ANOVA and post-hoc Tukey analysis. Different letters indicate significant differences between means. Data are mean \pm s.e.m; $n = 18-20$. Source data are provided in the Source Data file

Under constant light conditions, in the wild type 125 g/ha glyphosate was required at subjective dusk to attenuate hypocotyl length by the same magnitude as 100 g/ha glyphosate applied at subjective dawn (Fig. 2c). In contrast, in both CCA1-ox and TOC1-ox, glyphosate caused equivalent attenuation of hypocotyl elongation regardless of the glyphosate concentration or application time (Fig. 2d, e). Therefore, there is a circadian rhythm in the minimum effective dose of glyphosate that is controlled by the circadian oscillator.

Rhythmic glyphosate sensitivity and auxin signalling. We identified that auxin signalling-related transcripts have a rhythmic response to glyphosate. We examined the transcript abundance of *YUCCA9* (*YUC9*), which encodes a protein involved in an auxin biosynthesis pathway^{29,30}, *INDOLE-3-ACETIC ACID INDUCIBLE29* (*IAA29*)³¹, which is induced rapidly by auxin, and

EXPANSIN A8 (*EXPA8*), which encodes an auxin-induced cell wall-modifying enzyme involved in turgor-driven cell expansion^{32,33}. Glyphosate applied at dawn significantly decreased the transcript abundance of *YUC9* and *EXPA8*, but not *IAA29* (Fig. 3a-c). Furthermore, glyphosate applied at dusk significantly increased the abundance of *YUC9*, *IAA29* and *EXPA8* transcripts (Fig. 3a-c). The decrease in *YUC9* and *EXPA8* transcript abundance in response to glyphosate applied at dawn might suggest that auxin signalling becomes downregulated in response to glyphosate applied at this time, potentially explaining the greater sensitivity of hypocotyl elongation to glyphosate applied at dawn.

We found that the daily rhythm in the sensitivity of hypocotyl length to glyphosate might derive from inhibition of processes upstream of auxin signalling. Under light/dark cycles, the auxin biosynthesis inhibitor L-kynurenine³⁴ caused the greatest

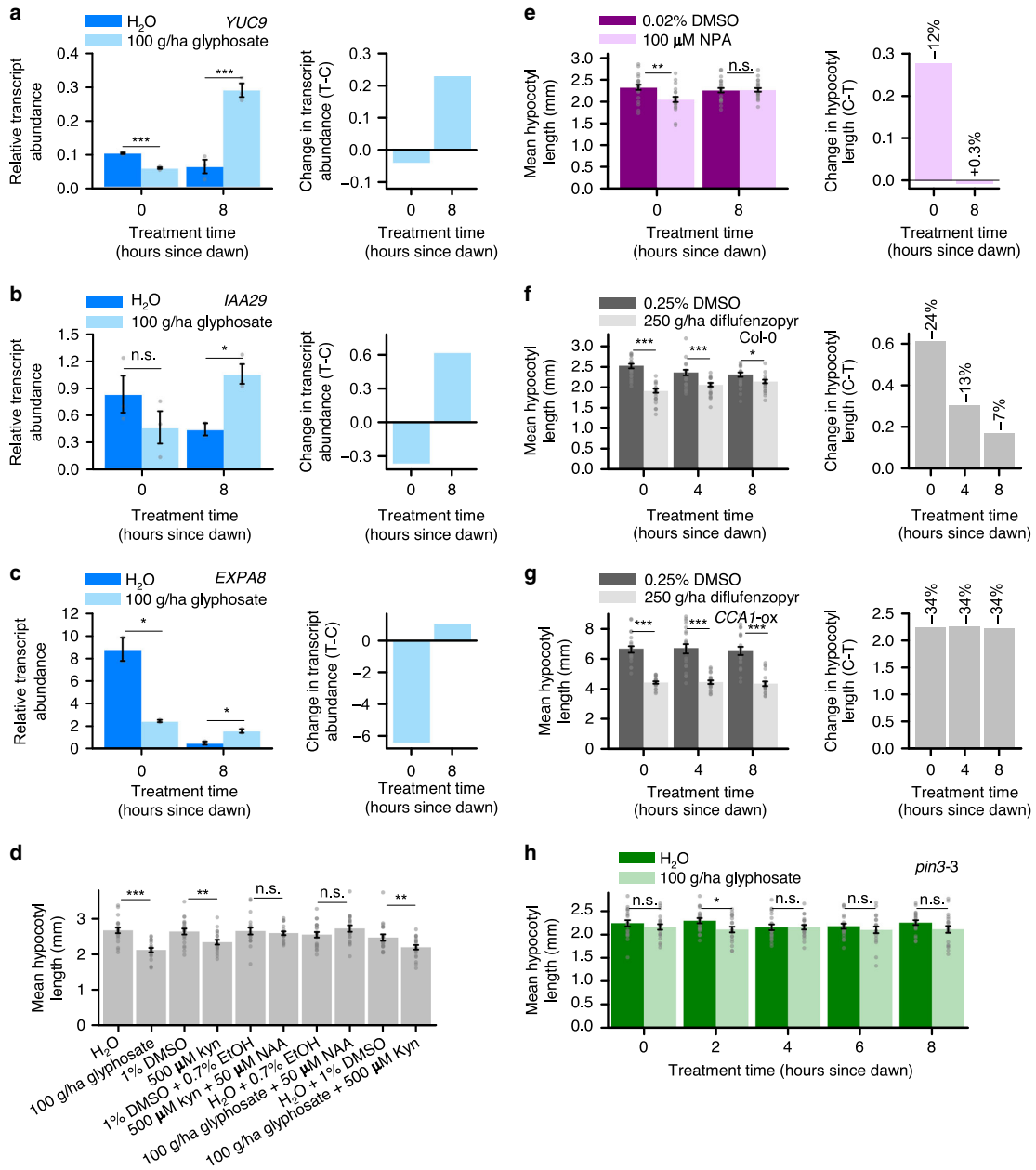


Fig. 3 Processes associated with auxin signalling might underlie rhythmic sensitivity of hypocotyl length to glyphosate. **a–c** 100 g/ha glyphosate-induced alterations in auxin signalling transcript abundance depends on treatment time. Graphs show (left) relative transcript abundance and (right) change in transcript abundance caused by glyphosate. Reference transcript was *PP2AA3*. **d** Mean hypocotyl length of seedlings treated with either glyphosate, kynurenine (kyn), kyn + NAA, glyphosate + NAA, or glyphosate + kyn at dawn. **e** Mean hypocotyl lengths of seedlings treated with NPA or DMSO vehicle control at dawn or dusk. **f, g** Attenuation of hypocotyl length by 250 g/ha diflufenzopyr or DMSO vehicle control applied at 4 h intervals, in **f** *Col-0* and **g** *CCA1-ox* seedlings under 8 h photoperiods. Chemical treatments were on day 3 and measurements on day 7. **g** Mean hypocotyl length of *pin3-3* seedlings treated with 100 g/ha glyphosate at 2 h intervals throughout the photoperiod. Significance determined by **a–c**; **e–h** two-way ANOVA and *t*-test comparisons and **d** *t*-tests. n.s. = not statistically significant, **P* ≤ 0.05, ***P* ≤ 0.01, ****P* ≤ 0.001. Data are mean ± s.e.m.: *n* = 2–3 (transcript analysis); *n* = 20 (hypocotyl measurements). Transcript abundance change expressed as treated (T) – control (**c**). Source data are provided in the Source Data file

attenuation of hypocotyl elongation when applied at dawn (Supplementary Fig. 6A, B), mimicking the timing of maximum sensitivity of elongation to glyphosate (Fig. 1a). Exogenous auxin (1-naphthaleneacetic acid; NAA) rescued the decrease in hypocotyl length caused by both kynurenine and glyphosate (Fig. 3d, Supplementary Fig. 6C), and glyphosate and kynurenine in combination did not cause additive reductions in hypocotyl length (Fig. 3d). One explanation for this result is that glyphosate and kynurenine might be acting upon the same pathway to alter hypocotyl length. As with glyphosate, the commonly used inhibitor of polar auxin transport 1-N-naphthylphthalamic acid (NPA)³⁵ decreased hypocotyl length when applied at dawn but not when applied at dusk (Fig. 3e; two-way ANOVA identified statistically significant interaction of treatment with time; $P = 0.02$).

Because we identified differences between the length of hypocotyls following topical NPA application at dawn and dusk, we investigated the temporal response of hypocotyl length to diflufenzopyr. This herbicide active ingredient is thought to inhibit auxin transport³⁶. We performed this experiment because we were interested to know whether there might be daily rhythms of sensitivity to herbicide active ingredients that inhibit aspects of auxin signalling. As with glyphosate, at the end of the experiment hypocotyls were shorter following 250 g/ha diflufenzopyr applied at dawn compared to the hypocotyl length following diflufenzopyr applied at dusk (Fig. 3f; two-way ANOVA identifies a significant interaction between the treatment and time; $P \leq 0.001$). Therefore, the magnitude of the change in hypocotyl length in response to diflufenzopyr depends on treatment time even though diflufenzopyr causes a significant reduction in hypocotyl length at all times. In comparison, in *CCA1-ox* diflufenzopyr application reduced the hypocotyl length at all times tested, but the magnitude of decrease in hypocotyl length did not depend on the time of diflufenzopyr application (Fig. 3g; $P = 0.99$, two-way ANOVA). Taken together, these data suggest that inhibition by glyphosate of processes related to auxin signalling might underlie the rhythmic sensitivity of hypocotyl length to glyphosate. This inhibition of auxin signalling by glyphosate might be indirect because auxin biosynthesis shares initial steps with the biosynthesis of aromatic amino acids, which is suppressed by glyphosate.

We identified that auxin transport has potential involvement in the rhythmic sensitivity of elongating hypocotyls to glyphosate. PIN-FORMED3 (PIN3) participates in polar auxin transport within hypocotyls^{37–39}, and PIN3 transcripts are rhythmic and glyphosate-responsive (Supplementary Data 1). In *pin3-3*, the hypocotyl length at the end of the experiment was not altered significantly in response to glyphosate applied at most times tested during the light period of light/dark cycles. Furthermore, the daily rhythms of glyphosate sensitivity of hypocotyl length that occur in the wild type were absent from *pin3-3* (Fig. 3h; $P = 0.69$, two-way ANOVA). Therefore, PIN3-mediated auxin transport might be required for rhythmic sensitivity of elongating hypocotyls to glyphosate under light-dark cycles. This was surprising, because PIN3 is reported to have functional redundancy with PIN1 and PIN7 in elongating hypocotyls^{40,41}. Other auxin biosynthesis mutants, such as *yuc1 yuc2 yuc4 yuc6*, *wei8 tar2* and *rooty* are impractical for this type of experiment because it is problematic to work with segregating populations in this type of assay. We also found that long hypocotyls of glyphosate-treated *phyB* arise from the long hypocotyl phenotype of *phyB*⁴² rather than proposed glyphosate resistance⁸ (Supplementary Fig. 7A–D).

Circadian and diel responses of cell death to glyphosate. We found that markers of cell death have rhythmic responses to

glyphosate. Under light/dark cycles, glyphosate applied to the wild type at dawn but not dusk significantly increased the abundance of transcripts encoding the positive regulator of cell death *METACASPASE1* (*MCI*)⁴³ (Fig. 4a; significant interaction between glyphosate treatment and application time, $P < 0.001$). In contrast, *MCI* transcripts were increased by glyphosate at both dawn and dusk in *CCA1-ox* (Fig. 4b; significant interaction between glyphosate treatment and application time, $P < 0.001$), and glyphosate did not increase *MCI* transcripts in *TOC1-ox* when applied at either dawn or dusk (Fig. 4c; $P = 0.3$).

Under constant light conditions, glyphosate significantly increased the abundance of *MCI* transcripts when applied at subjective dawn, whereas *MCI* transcript abundance was reduced by glyphosate application at subjective dusk (Fig. 4d; significant interaction between glyphosate treatment and application time $P < 0.001$). In contrast, *MCI* transcripts did not increase in *CCA1-ox* or *TOC1-ox* when glyphosate was applied at either subjective dawn or subjective dusk (Fig. 4e, f). We also investigated the response to glyphosate of the negative regulator of cell death (*DEFENDER AGAINST APOPTOTIC DEATH1* (*DADI*)⁴⁴), but found that *DADI* did not respond to glyphosate under our experimental conditions in the genotypes that we tested (Supplementary Fig. 7E–J). Overall, the response of *MCI* transcripts to glyphosate is consistent with the notion that glyphosate applied to wild type plants at dawn or subjective dawn might cause greater cell death than when applied at dusk or subjective dusk (Fig. 4a–f).

Another marker for cell death is a reduction in the concentration of chlorophyll⁴⁵, with chlorophyll degradation also being induced by glyphosate^{8,46,47}. Under light-dark cycles, glyphosate application to wild type plants at dawn but not dusk significantly decreased the chlorophyll concentration (Fig. 4g). In addition to ROS and lipid peroxidation⁴⁷, decreased abundance of transcripts encoding *GENOMES UNCOUPLED4* (*GUN4*) (Supplementary Data 1)¹⁵ might represent a mechanism by which glyphosate reduces chlorophyll concentration, because *gun4* mutants have reduced chlorophyll accumulation⁴⁸. Taken together, two indicators of cell death (*MCI* transcripts and chlorophyll concentration) report that glyphosate application at dawn causes cell death more rapidly than when applied at dusk, with circadian regulation potentially underlying this response.

Species-specificity of rhythmic responses to glyphosate.

Rhythmic developmental responses to glyphosate also occur in certain agriculturally relevant species. In dicotyledonous *Brassica napus* and *Sinapis arvensis*, glyphosate caused a significant decrease in hypocotyl length. Although a dawn glyphosate application caused a greater reduction in hypocotyl length compared to a dusk glyphosate application, the interaction between glyphosate and treatment time was not statistically significant (Fig. 4h, i; $P = 0.45$ and $P = 0.87$ from two-way ANOVA for *B. napus* and *S. arvensis*, respectively). In contrast, in monocotyledonous *Panicum miliaceum*, glyphosate applied at dawn and dusk caused a significant decrease in coleoptile length, but not when applied in the middle of the photoperiod (Fig. 4j; $P = 0.05$ from two-way ANOVA) (monocot coleoptile elongation is also auxin-regulated⁴⁹). This identifies that under laboratory conditions, there are species-dependent differences in the time of day variation in the response of seedling growth to glyphosate.

Discussion

We identified that the circadian clock controls the sensitivity of plant development and cell death to glyphosate. With the exception of varieties that have evolved glyphosate tolerance, glyphosate is generally not degraded by plants^{50,51} but appears to

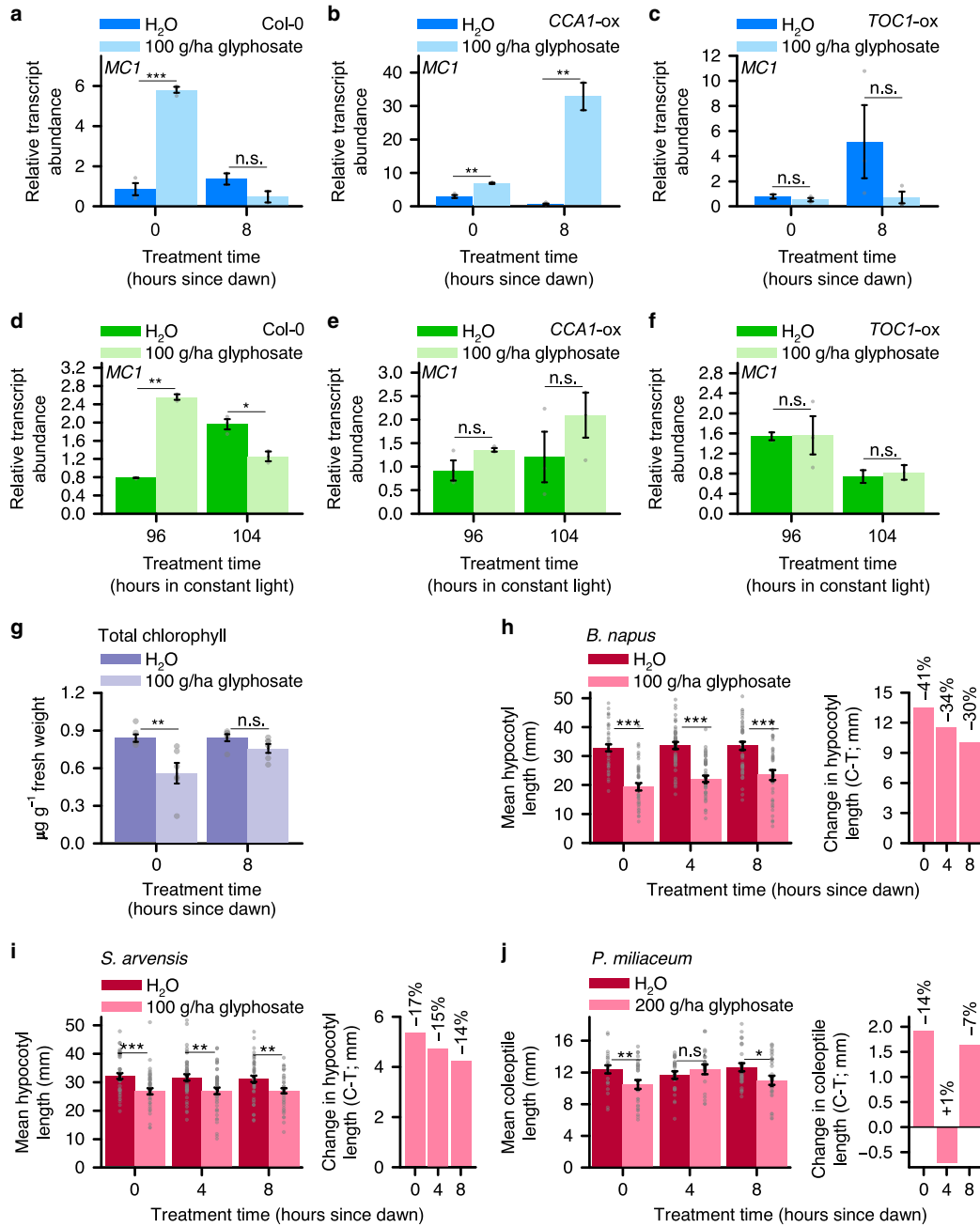


Fig. 4 Impact upon plants of daily and circadian rhythms of glyphosate efficacy. **a–f** 100 g/ha glyphosate alters programmed cell death transcript *MC1* in a time of day-dependent manner under both light-dark cycles (**a–c**) and constant light (**d–f**). Reference transcript was *PP2AA3*. **g** 100 g/ha glyphosate alters total chlorophyll content depending on the time of day of application. **h–j** Diel changes in sensitivity of hypocotyl or coleoptile length to glyphosate in agriculturally relevant species. **h, i** Mean hypocotyl length of *B. napus* and *S. arvensis* and treated with 100 g/ha glyphosate and **j** mean coleoptile length of *P. miliaceum* treated with 200 g/ha glyphosate. Graphs show (left) hypocotyl/coleoptile length and (right) hypocotyl/coleoptile length change caused by glyphosate. A greater glyphosate concentration was required to alter coleoptile length in *P. miliaceum* (200 g/ha) compared with hypocotyl length in the dicots (100 g/ha), possibly because monocots and dicots have differing auxin responses⁸⁰. Significance determined by two-way ANOVA and *t*-test comparisons between control and treatment at each timepoint. n.s. = not statistically significant, **P* ≤ 0.05, ***P* ≤ 0.01, ****P* ≤ 0.001. Data are mean ± s.e.m.; *n* = 2–3 (transcript analysis), *n* = 20–45 (data from multiple experiments, hypocotyl measurements). Source data are provided in the Source Data file

have transient effects that underlie its rhythmic efficacy (e.g. Supplementary Fig. 4). In nature, microbial metabolism of glyphosate^{52,53} might alter or enhance these transient effects compared with the data that we obtained under sterile laboratory conditions. In the field, fluctuations in glyphosate translocation, leaf angle and environmental conditions might contribute to daily rhythms of glyphosate effectiveness^{5–7}. Furthermore, environmental conditions can also determine the time when growers decide to spray. Transport processes and leaf position can be circadian-regulated in plants^{54,55}, so it is possible that circadian regulation contributes to plant glyphosate responses through multiple mechanisms. In future, it will be informative to identify the exact mechanism by which glyphosate might attenuate hypocotyl elongation and/or auxin signalling, and the extent to which this could scale to an agricultural context.

There are circadian rhythms of stomatal opening that are regulated by the circadian oscillator^{10,56}, but we think it unlikely that such rhythms of stomatal opening contribute to daily cycles of glyphosate sensitivity in our experiments. Firstly, in *Arabidopsis* under laboratory conditions of light/dark cycles and constant light the stomata reach peak conductance around the middle of the day^{10,57}, whereas peak glyphosate sensitivity occurred around dawn (Fig. 1a; Fig. 2a). Therefore, the phase of maximum stomatal conductance and maximum glyphosate sensitivity appear to be different. Second, because our experiments used agar-grown seedlings enclosed within petri dishes in growth chambers to provide a consistent and reproducible experimental environment, the daily fluctuations in humidity, growth medium moisture and temperature that cause midday stomatal closure were absent. Finally, herbicide formulations tend to enter leaves through the stomatal flooding only when combined with an organosilicone superwetter such as Silwet L77^{58,59}, which is commercially uncommon due to cost. The adjuvant within the formulation that we used was a standard mix of alkylamine ethoxylate and a co-surfactant, which will cause cuticular rather than stomatal uptake. The very narrow capillary formed by the stomatal pore combined with surface tension generally prevents stomatal entry of water, otherwise leaves would flood when it rains.

Overall, our data indicate that there is circadian regulation of the sensitivity of plants to chemicals that affect biological processes, in a manner comparable to rhythmic responses to drugs in mammals¹³. This could extend the concept of chronotherapy to agriculture. The pervasive influence of circadian regulation upon plant metabolism suggests that the principle we identify might scale to other agrochemicals. The circadian regulation of plant responses to agrochemicals provides a basis to refine agrochemical development and use, through this novel concept of agricultural chronotherapy, to optimise crop protection for food security.

Methods

Identification of rhythmic glyphosate-responsive transcripts. Lists of transcripts that are either glyphosate-induced or repressed¹⁵ were compared with those that oscillate with a circadian or diel rhythm^{11,16–19} to identify transcripts that are both glyphosate- and circadian/diel-regulated. Statistical significance was determined using hypergeometric tests. Each of these transcripts was also assigned to bins of 4 h according to its circadian phase, using phase data from a previous report¹⁸. Gene descriptions were extracted using The *Arabidopsis* Information Resource (TAIR) (accessed 11/05/18). GO-term analysis of the set of glyphosate-responsive and rhythmic transcripts was performed using ThaleMine on the *Araport* platform using version 11 of the *Arabidopsis* genome (Araport11). The subset of overlapping glyphosate and circadian/diel regulated transcripts was compared with an auxin-related GO term list. For this comparison, 549 unique transcripts were identified from 33 different auxin-related GO terms in the *Arabidopsis* genome (Supplementary Data 1), using AmiGO2 (accessed 11/05/18).

Glyphosate formulation. A glyphosate formulation (Touchdown Total, Syngenta) containing glyphosate and a proprietary adjuvant was used for this work. In

agriculture, herbicide concentration is expressed as the mass of active ingredient per hectare (g/ha) based on a typical spray volume application rate of 200 l/ha, so we used this convention here. Glyphosate formulations that are used at the typical field rate of 840 g/ha contain 24.8 mM of glyphosate. Since our experiments involved the topical application of glyphosate to agar-cultivated seedlings several days after germination, we measured the dose response of hypocotyl length to glyphosate to select a suitable experimental concentration. We selected a concentration of glyphosate for the majority of our experiments (100 g/ha, equivalent to 2.95 mM; Supplementary Fig. 8A) that caused partial attenuation of hypocotyl elongation, because we reasoned that this would allow us to detect potential daily variations in the response of hypocotyl length to glyphosate (Supplementary Fig. 8A). The glyphosate concentration that we used (100 g/ha) is lower than a reported ED50 for glyphosate in *Arabidopsis* of 350 g/ha⁶⁰.

Plant material and growth conditions. Unless stated otherwise, seeds were surface sterilised with 70% (v/v) ethanol for 1 min, 20% (v/v) domestic bleach for 12 min, followed by two washes with sterile distilled H₂O. Seeds were subsequently re-suspended in 0.1% (w/v) agar for pipetting. Growth media comprised half-strength (2.15 g l⁻¹) Murashige and Skoog nutrient mix (basal salts without vitamins, Duchefa Biochimie, Haarlem, Netherlands; pH 6.8) and 0.8% (w/v) agar, using sterile plastic rings embedded in media to allow equal dosing of seedlings with chemicals. Approximately 12 seeds were sown per ring. Seeds were stratified in darkness for 3 days at 4 °C before transfer to growth chambers (8 h light/16 h dark, 12 h light/12 h dark, or 16 h light/8 h dark; 19 °C, ~100 μmol m⁻² s⁻¹ photon flux density; MLR-352 chambers, Panasonic, Osaka, Japan). Genotypes used were Col-0, *L. er*, *CCA1-ox*²³, *TOC1-ox*²⁴, *pin3-361*, *phyB*^{62,63} and *CCA1::LUCIFERASE*⁶⁴.

To examine the effect of glyphosate on mature *Arabidopsis* plants (Supplementary Fig. 1), seedlings grown as above were transplanted after 7 days onto compost (Levington Advance F2 Seed & Modular, ICL) and transferred into a different growth chamber (12 h light/12 h dark, 19 °C, ~100 μmol m⁻² s⁻¹ photon flux density; 70% relative humidity; Snijders Labs Micro Climate-Series). Plants were treated with the recommended field rate of glyphosate (840 g/ha) at the six true leaf stage and photographed 14 days later (Nikon D80 DSLR).

Hypocotyl length measurement. Seeds were prepared as above, with two plastic rings on each petri dish and two petri dishes per chemical treatment per time point. Plants were treated on day 3 or day 5 after germination (for each plastic ring of 12 seedlings, this comprised 20 μl 100 g/ha glyphosate, water control, or other treatment) at specified time points, and returned to the growth cabinet. 4 days after treatment, 18–25 plants were measured per treatment, per time point by positioning plants on 1% (w/v) agar and taking photographs, followed by manual analysis of hypocotyl length using the image analysis programme ImageJ⁶⁵. Hypocotyls were measured from the shoot apical meristem to the shoot–root junction. We treated seedlings with glyphosate on day 3 and measured hypocotyl length on day 7 after germination because the intervening period is one of rapid hypocotyl elongation²², therefore providing the opportunity to detect variation in the impact of glyphosate upon hypocotyl elongation. Hypocotyls ranged 2–4 mm under our short day conditions (8 h photoperiod, 100 μmol m⁻² s⁻¹ photon flux density; 19 °C), which is positioned within the range of hypocotyl lengths (2–7 mm) reported for *Arabidopsis* seedlings under short day conditions^{66–69}. Hypocotyl length was not altered by either topical addition of liquid to the seedlings, nor the presence of plastic rings embedded within the media that were used to direct the chemical application (Supplementary Fig. 8B). Hypocotyls were measured as one batch, rather than staggered according to the time that they were treated with glyphosate. Hypocotyl length was measured at approximately dawn on day 7 after germination. We verified that irrespective of whether the hypocotyl length was measured in one batch or staggered according to time of treatment, hypocotyl elongation was attenuated more in response to glyphosate treatment at dawn than at dusk (Supplementary Fig. 8C, D). Exact numbers of replicate plants for each treatment and experiment are provided in Supplementary Data 2. For clarity, many figures show actual hypocotyl length, the change in hypocotyl length resulting from glyphosate treatment (calculated as the difference between the mean control hypocotyl length and mean treated hypocotyl length), and the proportional change in hypocotyl length.

For experiments with *l*-kynurenine (kyn; Sigma-Aldrich), kyn was applied using 1% (v/v) dimethyl sulfoxide (DMSO) as a vehicle control (for the highest volume DMSO). For experiments with 1-naphthaleneacetic acid (NAA; Sigma-Aldrich), seedlings were treated with 500 μM kyn supplemented with NAA. This concentration was consistent with the range of concentrations used by previous studies involving hypocotyl length measurements^{70,71}. The vehicle control was 0.7% (v/v) EtOH + 1% (v/v) DMSO. For experiments with diflufenzopyr (Syngenta), 250 g/ha was chosen because it caused similar attenuation in hypocotyl length as 100 g/ha glyphosate, using 0.25% (v/v) DMSO as a vehicle control (Supplementary Fig. 8E). The concentration range of NAA used (1–100 μM) was consistent with other studies^{72–74}. For experiments with 1-*N*-naphthylphthalamic acid (NPA; Sigma), 100 μM NPA was chosen because this concentration gave a similar level of attenuation in hypocotyl length as glyphosate and this concentration has been used reliably by other studies^{35,75,76}. 0.02% (v/v) DMSO was used as a vehicle control for NPA. To investigate whether the adjuvant within the glyphosate formulation affected hypocotyl elongation (Supplementary Fig. 3B),

a glyphosate adjuvant control formulation was produced (Syngenta). This control formulation was used at the equivalent mass of adjuvant present within the 100 g/ha glyphosate treatment.

Hypocotyl elongation rate measurement. To measure the rate of hypocotyl elongation, seeds were sown individually onto petri dishes which, after stratification, were positioned vertically within the growth chamber. Chemical treatments occurred at either dawn or dusk on day 3 after germination, and imaging commenced after the chemical treatment. 1.6 μL of either water or 100 g/ha glyphosate was applied to each seedling, which was an equivalent volume to other treatments. Time lapse images were captured with a Nikon D80 DSLR with its infra-red (IR) blocking filter removed, and replaced with an IR pass filter (>850 nm) (Zomei, Jiangsu, China). Plates were backlit with a custom-built IR LED array (880 nm) to allow images to be captured in darkness. Images were captured every 30 min following chemical treatment, for 96 h. Ten seedlings were measured per treatment. Hypocotyl lengths were measured manually from the time-series using ImageJ. The physical differences between the apparatus used to measure elongation rates and perform endpoint hypocotyl length measurements means that data such as the magnitude of changes in hypocotyl length over time is not identically comparable between the two assay types.

Investigation of circadian rhythms in emerging seedlings. Stratified Col-0 *CCA1::LUCIFERASE* seeds were placed into 8 h light/16 h dark conditions for 1 day, and then transferred to continuous light. 24 h before imaging, seeds were dosed with 100 μL 5 mM luciferin (potassium salt of D-luciferin; Melford Laboratories Ltd). Luciferase bioluminescence was imaged for 6 days using a Lumintek EM-CCD imaging system (Photek) controlled by Image32 software (Photek). This involved 45-s integrations of the bioluminescence signal at hourly intervals, with the EM gain on the camera set to 2700. This was followed by analysis of rhythmic features within the data using the fast Fourier transform-nonlinear least-squares (FFT-NLLS) algorithm within BRASS software (millar.bio.ed.ac.uk; University of Edinburgh).

Effect of glyphosate on transcript abundance. To measure transcript abundance, seedlings were cultivated as above. Aerial tissue was sampled 3 h (*YUC9*, *IAA29*, *EXPA8*) or 6 h (*MCI*, *DAD1*) after chemical treatment. For each RNA sample, the aerial tissue of ~20 seedlings was harvested from across two petri dishes of seedlings (i.e. about ten seedlings from each petri dish). RNA was isolated using the Nucleospin II RNA extraction kit (Machery-Nagel), with subsequent cDNA synthesis conducted with the High-Capacity cDNA Synthesis kit (Thermo-Fisher), both according to manufacturer's instructions. qRT-PCR analysis was performed using HOT FIREPol EvaGreen qPCR reagents (Solis BioDyne) and Agilent Mx3005P qPCR instrument. Amplification efficiency was determined from individual PCR reactions using a linear regression on the straight-line portion of log (fluorescence) during the PCR amplification, using LinRegPCR (version 2018.0)⁷⁷. Ct was determined using a threshold Rn of 0.2. Transcript abundance was determined relative to *PP2AA3* as a reference transcript⁶⁶ using a calculation (Equation 1) that incorporates the efficiency of each amplification^{28,78}. We verified that *PP2AA3* reference transcript amplification was unaltered by glyphosate treatment (control Ct = 27.17 \pm 0.10; glyphosate Ct = 27.05 \pm 0.09; $n = 6$; $P = 0.37$ from two-sample t test). Primer sequences are provided in Supplementary Table 1.

$$\text{RTA}(\text{GOI}) = (\text{RE}_{\text{RG}})^{C_{\text{RG}}} \times (\text{RE}_{\text{GOI}})^{-C_{\text{GOI}}} \quad (1)$$

Determination of relative transcript abundance. Calculation determines relative transcript abundance of gene of interest (GOI), where RE_{RG} and RE_{GOI} are the mean amplification efficiencies of the reference gene and gene of interest for each sample, and C_{RG} and C_{GOI} are the mean C_{t} values for the reference gene and gene of interest for each sample, respectively.

Chlorophyll content analysis. Total chlorophyll was extracted from elongating hypocotyls four days after glyphosate treatment, at either dawn or dusk, with 80% (v/v) buffered aqueous acetone⁷⁹. Total chlorophyll (chlorophyll *a* and *b*) was calculated as by Porra et al. (Eq. 2)⁷⁹.

$$\text{Chl}_{\text{total}} (\text{mg g}^{-1}) = \frac{V(17.76A^{646} + 7.34A^{663})}{1000W} \quad (2)$$

Determination of total chlorophyll content. V is the volume of 80% (v/v) acetone, A is the absorbency at 646 nm and 663 nm, and W is the tissue weight in grams.

Hypocotyl and coleoptile elongation in non-model species. Non-sterile seeds of rapeseed (*Brassica napus*), wild mustard (*Sinapis arvensis*) and proso millet (*Panicum miliaceum*) were placed onto water-saturated filter paper in petri dishes for 3 days (*S. arvensis*, *P. miliaceum*) or 5 days (*B. napus*) at room temperature under constant light. Seeds were then transplanted onto 3:1 compost and sand mixture and placed into growth chambers with conditions of 8 h light/16 h dark, 19 °C, ~100 $\mu\text{mol m}^{-2} \text{s}^{-1}$ photon flux density; 70% relative humidity (Snijders Labs Micro Climate-Series chamber). After 3 days plants were sprayed with glyphosate (100 g/ha, or 200 g/ha for *P. miliaceum*) using a custom-built laboratory-

sized track sprayer, at dawn, midday, or dusk. 4 days after treatments, plants were imaged and hypocotyls or coleoptiles were measured as in previous hypocotyl assays. Data shown are the mean of multiple experimental repeats.

Data analysis. Statistical analysis was performed with Sigmaplot 13.0, except hypergeometric tests were performed in Excel to investigate the intersection of transcriptomes. Fast Fourier transform (non-linear least squares method) (FFT-NLLS) analysis of bioluminescence imaging data was performed using BRASS (millar.bio.ed.ac.uk; University of Edinburgh). Output from all statistical analyses, including sample sizes and P values, are provided in Supplementary Data 2.

Reporting summary. Further information on research design is available in the Nature Research Reporting Summary linked to this article.

Data availability

All relevant data are included in the figures, supplementary information files, and Source Data file. The source data underlying Figs. 1–4 and Supplementary Figs. 3–8 are provided as a Source Data file. Bioinformatics and statistical analyses are in Supplementary Data 1 and Supplementary Data 2, respectively.

Received: 5 December 2018 Accepted: 31 July 2019

Published online: 16 August 2019

References

- Tilman, D., Balzer, C., Hill, J. & Befort, B. L. Global food demand and the sustainable intensification of agriculture. *Proc. Natl Acad. Sci.* **108**, 20260 (2011).
- Oerke, E. C. Crop losses to pests. *J. Agric. Sci.* **144**, 31–43 (2005).
- Orson, J., Davies, D. K. H. & Norfolk, N. R. Pre-harvest glyphosate for weed control and as a harvest aid in cereals. (Home-Grown Cereals Authority, 2007).
- Benbrook, C. M. Trends in glyphosate herbicide use in the United States and globally. *Environ. Sci. Eur.* **28**, 3 (2016).
- Martinson, K. B., Sothorn, R. B., Koukari, W. L., Durgan, B. R. & Gunsolus, J. L. Circadian response of annual weeds to glyphosate and glufosinate. *Chronobiol. Int.* **19**, 405–422 (2002).
- Miller, R. P., Martinson, K. B., Sothorn, R. B., Durgan, B. R. & Gunsolus, J. L. Circadian response of annual weeds in a natural setting to high and low application rates of four herbicides with different modes of action. *Chronobiol. Int.* **20**, 299–324 (2003).
- Mohr, K., Sellers, B. A. & Smeda, R. J. Application time of day influences glyphosate efficacy. *Weed Technol.* **21**, 7–13 (2007).
- Sharkhuu, A. et al. A red and far-red light receptor mutation confers resistance to the herbicide glyphosate. *Plant J.* **78**, 916–926 (2014).
- Harmer, S. L. et al. Orchestrated transcription of key pathways in *Arabidopsis* by the circadian clock. *Science* **290**, 2110–2113 (2000).
- Dodd, A. N. et al. Plant circadian clocks increase photosynthesis, growth, survival, and competitive advantage. *Science* **309**, 630–633 (2005).
- Edwards, K. D. et al. *FLOWERING LOCUS C* mediates natural variation in the high-temperature response of the *Arabidopsis* circadian clock. *Plant Cell* **18**, 639–650 (2006).
- Michael, T. P. et al. Network discovery pipeline elucidates conserved time-of-day-specific *cis*-regulatory modules. *PLoS Genet.* **4**, e14 (2008).
- Zhang, R., Lahens, N. F., Ballance, H. I., Hughes, M. E. & Hogenesch, J. B. A circadian gene expression atlas in mammals: Implications for biology and medicine. *Proc. Natl Acad. Sci. USA* **111**, 16219–16224 (2014).
- Steinrücken, H. C. & Amrhein, N. The herbicide glyphosate is a potent inhibitor of 5-enolpyruvylshikimic acid-3-phosphate synthase. *Biochem. Biophys. Res. Commun.* **94**, 1207–1212 (1980).
- Faus, I. et al. Protein kinase GCN2 mediates responses to glyphosate in *Arabidopsis*. *BMC Plant Biol.* **15**, 14 (2015).
- Bläsing, O. E. et al. Sugars and circadian regulation make major contributions to the global regulation of diurnal gene expression in *Arabidopsis*. *Plant Cell* **17**, 3257–3281 (2005).
- Smith, S. M. et al. Diurnal changes in the transcriptome encoding enzymes of starch metabolism provide evidence for both transcriptional and posttranscriptional regulation of starch metabolism in *Arabidopsis* leaves. *Plant Physiol.* **136**, 2687–2699 (2004).
- Dodd, A. N. et al. The *Arabidopsis* circadian clock incorporates a cADPR-based feedback loop. *Science* **318**, 1789–1792 (2007).
- Covington, M. F. & Harmer, S. L. The circadian clock regulates auxin signaling and responses in *Arabidopsis*. *PLoS Biol.* **5**, e222 (2007).
- Tao, Y. et al. Rapid synthesis of auxin via a new tryptophan-dependent pathway is required for shade avoidance in plants. *Cell* **133**, 164–176 (2008).

21. Baur, J. R. Effect of glyphosate on auxin transport in corn and cotton tissues. *Plant Physiol.* **63**, 882–886 (1979).
22. Nozue, K. et al. Rhythmic growth explained by coincidence between internal and external cues. *Nature* **448**, 358–361 (2007).
23. Wang, Z.-Y. & Tobin, E. M. Constitutive expression of the *CIRCADIAN CLOCK ASSOCIATED 1* (*CCA1*) gene disrupts circadian rhythms and suppresses its own expression. *Cell* **93**, 1207–1217 (1998).
24. Más, P., Alabadi, D., Yanovsky, M. J., Oyama, T. & Kay, S. A. Dual role of *TOC1* in the control of circadian and photomorphogenic responses in *Arabidopsis*. *Plant Cell* **15**, 223–236 (2003).
25. Niwa, Y., Yamashino, T. & Mizuno, T. The circadian clock regulates the photoperiodic response of hypocotyl elongation through a coincidence mechanism in *Arabidopsis thaliana*. *Plant Cell Physiol.* **50**, 838–854 (2009).
26. Ding, Z., Doyle, M. R., Amasino, R. M. & Davis, S. J. A complex genetic interaction between *Arabidopsis thaliana* *TOC1* and *CCA1/LHY* in driving the circadian clock and in output regulation. *Genetics* **176**, 1501–1510 (2007).
27. Doyle, M. R. et al. The *ELF4* gene controls circadian rhythms and flowering time in *Arabidopsis thaliana*. *Nature* **419**, 74–77 (2002).
28. Haydon, M. J., Mielczarek, O., Robertson, F. C., Hubbard, K. E. & Webb, A. A. R. Photosynthetic entrainment of the *Arabidopsis thaliana* circadian clock. *Nature* **502**, 689–692 (2013).
29. Hentrich, M. et al. The jasmonic acid signaling pathway is linked to auxin homeostasis through the modulation of *YUCCA8* and *YUCCA9* gene expression. *Plant J.* **74**, 626–637 (2013).
30. Dai, X. et al. The biochemical mechanism of auxin biosynthesis by an *Arabidopsis* *YUCCA* flavin-containing monooxygenase. *J. Biol. Chem.* **288**, 1448–1457 (2013).
31. Kunihiro, A. et al. PHYTOCHROME-INTERACTING FACTOR 4 and 5 (*PIF4* and *PIF5*) activate the homeobox *ATHB2* and auxin-inducible *IAA29* genes in the coincidence mechanism underlying photoperiodic control of plant growth of *Arabidopsis thaliana*. *Plant Cell Physiol.* **52**, 1315–1329 (2011).
32. Li, Y., Jones, L. & McQueen-Mason, S. Expansins and cell growth. *Curr. Opin. Plant Biol.* **6**, 603–610 (2003).
33. Gangappa, S. N. & Kumar, S. V. *DET1* and *COP1* modulate the coordination of growth and immunity in response to key seasonal signals in *Arabidopsis*. *Cell Rep.* **25**, 29–37.e23 (2018).
34. He, W. et al. A small-molecule screen identifies L-kynurenine as a competitive inhibitor of *TAA1/TAR* activity in ethylene-directed auxin biosynthesis and root growth in *Arabidopsis*. *Plant Cell* **23**, 3944–3960 (2011).
35. Nemhauser, J. L., Feldman, L. J. & Zambryski, P. C. Auxin and *ETTIN* in *Arabidopsis* gynoecium morphogenesis. *Development* **127**, 3877–3888 (2000).
36. Wehtje, G. Synergism of dicamba with diflufenzopyr with respect to turfgrass weed control. *Weed Technol.* **22**, 679–684 (2008).
37. Ding, Z. et al. Light-mediated polarization of the *PIN3* auxin transporter for the phototropic response in *Arabidopsis*. *Nat. Cell Biol.* **13**, 447–452 (2011).
38. Rakusová, H. et al. Polarization of *PIN3*-dependent auxin transport for hypocotyl gravitropic response in *Arabidopsis thaliana*. *Plant J.* **67**, 817–826 (2011).
39. Keuskamp, D. H., Pollmann, S., Voesenek, L. A. C. J., Peeters, A. J. M. & Pierik, R. Auxin transport through *PIN-FORMED 3* (*PIN3*) controls shade avoidance and fitness during competition. *Proc. Natl Acad. Sci. USA* **107**, 22740–22744 (2010).
40. Vieten, A. et al. Functional redundancy of *PIN* proteins is accompanied by auxin-dependent cross-regulation of *PIN* expression. *Development* **132**, 4521–4531 (2005).
41. Haga, K. & Sakai, T. *PIN* auxin efflux carriers are necessary for pulse-induced but not continuous light-induced phototropism in *Arabidopsis*. *Plant Physiol.* **160**, 763–776 (2012).
42. Somers, D. E., Sharrock, R. A., Tepperman, J. M. & Quail, P. H. The *hy3* long hypocotyl mutant of *Arabidopsis* is deficient in Phytochrome B. *Plant Cell* **3**, 1263–1274 (1991).
43. Coll, N. S. et al. *Arabidopsis* Type I metacaspases control cell death. *Science* **330**, 1393–1397 (2010).
44. Danon, A., Rotari, V. I., Gordon, A., Mailhac, N. & Gallois, P. Ultraviolet-C overexposure induces programmed cell death in *Arabidopsis*, which is mediated by caspase-like activities and which can be suppressed by caspase inhibitors, p35 and defender against apoptotic death. *J. Biol. Chem.* **279**, 779–787 (2004).
45. Hörtensteiner, S. & Kräutler, B. Chlorophyll breakdown in higher plants. *Biochim. Biophys. Acta* **1807**, 977–988 (2011).
46. Mateos-Naranjo, E., Redondo-Gómez, S., Cox, L., Cornejo, J. & Figueroa, M. E. Effectiveness of glyphosate and imazamox on the control of the invasive cordgrass *Spartina densiflora*. *Ecotoxicol. Environ. Saf.* **72**, 1694–1700 (2009).
47. Gomes, M. P. et al. Differential effects of glyphosate and aminomethylphosphonic acid (AMPA) on photosynthesis and chlorophyll metabolism in willow plants. *Pestic. Biochem. Physiol.* **130**, 65–70 (2016).
48. Larkin, R. M., Alonso, J. M., Ecker, J. R. & Chory, J. *GUN4*, a regulator of chlorophyll synthesis and intracellular signaling. *Science* **299**, 902–906 (2003).
49. Ishizawa, K. & Esashi, Y. Cooperation of ethylene and auxin in the growth regulation of rice coleoptile segments. *J. Exp. Bot.* **34**, 74–82 (1983).
50. Shaner, D. L. Role of translocation as a mechanism of resistance to glyphosate. *Weed Sci.* **57**, 118–123 (2009).
51. Duke, S. O. Glyphosate degradation in glyphosate-resistant and -susceptible crops and weeds. *J. Agric. Food Chem.* **59**, 5835–5841 (2011).
52. Torstensson, N. T. L. & Aamissepp, A. Detoxification of glyphosate in soil. *Weed Res.* **17**, 209–212 (1977).
53. Liu, C. M., McLean, P. A., Sookdeo, C. C. & Cannon, F. C. Degradation of the herbicide glyphosate by members of the family Rhizobiaceae. *Appl. Environ. Microbiol.* **57**, 1799–1804 (1991).
54. Dowson-Day, M. J. & Millar, A. J. Circadian dysfunction causes aberrant hypocotyl elongation patterns in *Arabidopsis*. *Plant J.* **17**, 63–71 (1999).
55. Haydon, M. J., Bell, L. J. & Webb, A. A. R. Interactions between plant circadian clocks and solute transport. *J. Exp. Bot.* **62**, 2333–2348 (2011).
56. Hennessey, T. L. & Field, C. B. Circadian rhythms in photosynthesis-oscillations in carbon assimilation and stomatal conductance under constant conditions. *Plant Physiol.* **96**, 831–836 (1991).
57. Dodd, A. N., Parkinson, K. & Webb, A. A. R. Independent circadian regulation of assimilation and stomatal conductance in the *ztl-1* mutant of *Arabidopsis*. *New Phytol.* **162**, 63–70 (2004).
58. Field, R. J. & Bishop, N. G. Promotion of stomatal infiltration of glyphosate by an organosilicone surfactant reduces the critical rainfall period. *Pestic. Sci.* **24**, 55–62 (1988).
59. Roggenbuck, F. C., Lowe, L., Penner, D., Petroff, L. & Burow, R. Increasing postemergence herbicide efficacy and rainfastness with silicone adjuvants. *Weed Technol.* **4**, 576–580 (1990).
60. Yang, X. et al. Effects of over-expressing a native gene encoding 5-enolpyruvylshikimate-3-phosphate synthase (EPSPS) on glyphosate resistance in *Arabidopsis thaliana*. *PLoS One* **12**, e0175820 (2017).
61. Friml, J., Wiśniewska, J., Benková, E., Mendgen, K. & Palme, K. Lateral relocation of auxin efflux regulator *PIN3* mediates tropism in *Arabidopsis*. *Nature* **415**, 806–809 (2002).
62. Koornneef, M., Rolff, E. & Spruit, C. J. P. Genetic control of light-inhibited hypocotyl elongation in *Arabidopsis thaliana* (L.) Heynh. *Z. Pflanzenphysiol.* **100**, 147–160 (1980).
63. Reed, J. W., Nagpal, P., Poole, D. S., Furuya, M. & Chory, J. Mutations in the gene for the red/far-red light receptor phytochrome B alter cell elongation and physiological responses throughout *Arabidopsis* development. *Plant Cell* **5**, 147–157 (1993).
64. Frank, A. et al. Circadian entrainment in *Arabidopsis* by the sugar-responsive transcription factor *bZIP63*. *Curr. Biol.* **28**, 2597–2606 (2018).
65. Hayes, S., Velanis, C. N., Jenkins, G. I. & Franklin, K. A. UV-B detected by the *UVR8* photoreceptor antagonizes auxin signaling and plant shade avoidance. *Proc. Natl Acad. Sci. USA* **111**, 11894–11899 (2014).
66. Simon, N. M. L. et al. The energy-signaling hub *SnRK1* is important for sucrose-induced hypocotyl elongation. *Plant Physiol.* **176**, 1299–1310 (2018).
67. Stewart, J. L., Maloof, J. N. & Nemhauser, J. L. *PIF* genes mediate the effect of sucrose on seedling growth dynamics. *PLoS One* **6**, e19894 (2011).
68. Boylan, M. T. & Quail, P. H. Phytochrome A overexpression inhibits hypocotyl elongation in transgenic *Arabidopsis*. *Proc. Natl Acad. Sci. USA* **88**, 10806–10810 (1991).
69. Wagner, D., Tepperman, J. M. & Quail, P. H. Overexpression of Phytochrome B induces a short hypocotyl phenotype in transgenic *Arabidopsis*. *Plant Cell* **3**, 1275–1288 (1991).
70. Stepanova, A. N. et al. The *Arabidopsis* *YUCCA1* flavin monooxygenase functions in the indole-3-pyruvic acid branch of auxin biosynthesis. *Plant Cell* **23**, 3961–3973 (2011).
71. Hersch, M. et al. Light intensity modulates the regulatory network of the shade avoidance response in *Arabidopsis*. *Proc. Natl Acad. Sci. USA* **111**, 6515–6520 (2014).
72. Wang, D., Pajeroska-Mukhtar, K., Culler, A. H. & Dong, X. Salicylic acid inhibits pathogen growth in plants through repression of the auxin signaling pathway. *Curr. Biol.* **17**, 1784–1790 (2007).
73. Bours, R., Kohlen, W., Bouwmeester, H. J. & van der Krol, A. Thermoperiodic control of hypocotyl elongation depends on auxin-induced ethylene signaling that controls downstream *PHYTOCHROME INTERACTING FACTOR3* activity. *Plant Physiol.* **167**, 517–530 (2015).
74. Park, J.-E., Kim, Y.-S., Yoon, H.-K. & Park, C.-M. Functional characterization of a small auxin-up RNA gene in apical hook development in *Arabidopsis*. *Plant Sci.* **172**, 150–157 (2007).
75. Heisler, M. G. et al. Patterns of auxin transport and gene expression during primordium development revealed by live imaging of the *Arabidopsis* inflorescence meristem. *Curr. Biol.* **15**, 1899–1911 (2005).

76. Ding, Z. et al. ER-localized auxin transporter PIN8 regulates auxin homeostasis and male gametophyte development in *Arabidopsis*. *Nat. Commun.* **3**, 941 (2012).
77. Ramakers, C., Ruijter, J. M., Deprez, R. H. L. & Moorman, A. F. M. Assumption-free analysis of quantitative real-time polymerase chain reaction (PCR) data. *Neurosci. Lett.* **339**, 62–66 (2003).
78. Talke, I. N., Hanikenne, M. & Krämer, U. Zinc-dependent global transcriptional control, transcriptional deregulation, and higher gene copy number for genes in metal homeostasis of the hyperaccumulator *Arabidopsis halleri*. *Plant Physiol.* **142**, 148–167 (2006).
79. Porra, R. J., Thompson, W. A. & Kriedemann, P. E. Determination of accurate extinction coefficients and simultaneous equations for assaying chlorophylls *a* and *b* extracted with four different solvents: verification of the concentration of chlorophyll standards by atomic absorption spectroscopy. *Biochim. Biophys. Acta.* **975**, 384–394 (1989).
80. McSteen, P. Auxin and monocot development. *Cold Spring Harb. Perspect. Biol.* **2**, a001479 (2010).

Acknowledgements

We thank Alan Cochran (Syngenta) for agrochemical spraying equipment advice and Kerry Franklin and Innes Cuthill (Bristol) for advice concerning data analysis and interpretation. This research was funded by the UK Biotechnology and Biological Sciences Research Council (BB/1005811/2; BB/M016900/1) and Syngenta.

Author contributions

F.E.B., A.B.J. and F.E.S. conducted experiments; G.A. provided technical support; F.E.B., G.J.H., C.F. and A.N.D. designed experiments, interpreted data and wrote the paper.

Additional information

Supplementary Information accompanies this paper at <https://doi.org/10.1038/s41467-019-11709-5>.

Competing interests: The authors declare the following competing interests: G.J.H., G.A. and C.F. are employed by Syngenta. The other authors declare no competing interests.

Reprints and permission information is available online at <http://npg.nature.com/reprintsandpermissions/>

Peer review information: *Nature Communications* thanks Philippe Juneau and other anonymous reviewers for their contribution to the peer review of this work.

Publisher's note: Springer Nature remains neutral with regard to jurisdictional claims in published maps and institutional affiliations.



Open Access This article is licensed under a Creative Commons Attribution 4.0 International License, which permits use, sharing, adaptation, distribution and reproduction in any medium or format, as long as you give appropriate credit to the original author(s) and the source, provide a link to the Creative Commons license, and indicate if changes were made. The images or other third party material in this article are included in the article's Creative Commons license, unless indicated otherwise in a credit line to the material. If material is not included in the article's Creative Commons license and your intended use is not permitted by statutory regulation or exceeds the permitted use, you will need to obtain permission directly from the copyright holder. To view a copy of this license, visit <http://creativecommons.org/licenses/by/4.0/>.

© The Author(s) 2019

Commentary

ABA signalling is regulated by the circadian clock component LHY

Circadian rhythms have widespread effects upon cellular and whole-plant physiology, from regulating a substantial proportion of the genome to controlling metabolism and enhancing fitness (Hsu & Harmer, 2014). Circadian regulation also increases the tolerance of plants to some environmental stresses and the nature and magnitude of stress responses (Grundy *et al.*, 2015). This circadian regulation of the magnitude of responses to environmental stimuli is termed circadian gating (Hotta *et al.*, 2007). The phytohormone abscisic acid (ABA) provides a core environmental stress signalling mechanism and regulator of plant development. In this issue of *New Phytologist*, Adams *et al.* (pp. 893–907) identified a new mechanism that couples the circadian oscillator with ABA signalling in *Arabidopsis*. The authors found that a component of the circadian oscillator called LATE ELONGATED HYPOCOTYL (LHY) binds directly to the promoters of a significant proportion of genes involved in ABA biosynthesis and responses. Furthermore, they identified a role for LHY in regulating the accumulation of ABA. This suggests a new mechanism connecting circadian regulation with drought and osmotic stress tolerance through ABA signalling.

Importantly, the expression of ABA stress-responsive genes is altered when LHY function is lost or LHY is overexpressed.

Circadian rhythms are self-sustaining biological cycles with a period of *c.* 24 h. A highly interconnected gene network, known as the circadian oscillator, generates plant circadian rhythms. This involves transcription–translation feedback loops and post-translational regulation. The phase of the circadian oscillator becomes synchronized with the environmental day: night cycle through the process of entrainment, whereby signalling pathways communicate environmental information to the circadian oscillator (Hsu & Harmer, 2014). Furthermore, the circadian oscillator communicates a measure of the time of day to circadian-regulated components of the cell, primarily through transcriptional regulation (Harmer *et al.*, 2000). The circadian oscillator is proposed to incorporate several loops of gene expression, characterized by the time of transcript accumulation or protein activity. LHY, identified

by Adams *et al.* as a regulator of ABA signalling, is thought to be positioned within the ‘morning’ loop of the circadian oscillator (Hsu & Harmer, 2014), reaching peak transcript abundance around dawn.

One way that circadian rhythms adapt plants to the fluctuating environment is to regulate environmental signalling pathways. There are many interactions between circadian rhythms and cell signalling pathways. In addition to circadian gating, there are interactions between the circadian oscillator and Ca²⁺ signalling (Martí Ruiz *et al.*, 2018), sugar signalling (Haydon *et al.*, 2013; Frank *et al.*, 2018), protein phosphorylation (Choudhary *et al.*, 2015), phytohormone signalling (Hanano *et al.*, 2006), and signalling between organelles (Noordally *et al.*, 2013). The circadian oscillator regulates auxin signals that control development (Covington & Harmer, 2007; Voß *et al.*, 2015), and there are bidirectional interactions between the circadian oscillator component TIMING OF CAB2 EXPRESSION1 (TOC1) and ABA signalling (Legnaioli *et al.*, 2009). There is also evidence that cytokinin, auxin and brassinosteroids cause small alterations in circadian oscillator function (Hanano *et al.*, 2006).

Adams *et al.* sought to understand the roles for LHY in gene regulation, and found that LHY binds to the promoter region of 519 genes in the genome of *Arabidopsis thaliana*. These promoters were enriched with the circadian-regulated ‘evening element’ (Harmer *et al.*, 2000), and cycling DOF factor and TCP transcription factor binding sites. Interestingly, the promoters are also enriched with the abscisic acid responsive-like element (ABRE), with similar and related elements also identified as circadian-regulated (Covington *et al.*, 2008). The set of LHY-binding genes is enriched with a variety of stress response genes, such as those involved in low temperature and drought/osmotic stress (Fig. 1). This includes several ABA receptor subunits, signal transduction proteins downstream of ABA, ABA-responsive transcription factors, and a 9-*cis*-epoxycarotenoid dioxygenase (NCED) enzyme that forms a rate limiting step in ABA biosynthesis (Fig. 1). This led Adams *et al.* to hypothesize that gene regulation by LHY might be integrated with ABA signalling. Testing this, they identified that ABA levels have daily rhythms under light: dark cycles combined with drought conditions, and that LHY inhibits ABA synthesis (Fig. 1). Importantly, the expression of ABA stress-responsive genes is altered when LHY function is lost or LHY is overexpressed.

The circadian oscillator component CIRCADIAN CLOCK ASSOCIATED1 (CCA1) has high sequence homology with LHY. Although this gene duplication event is thought to have occurred during the evolution of the Brassicaceae, a single CCA1/LHY-like gene is present in some land plants clades with similar duplications occurring in others (Linde *et al.*, 2017). In addition, CCA1/LHY form part of a larger REVEILLE-like transcription factor family (Farinas & Mas, 2011; Rawat *et al.*, 2011). Nagel *et al.* (2015) and

This article is a Commentary on Adams *et al.*, 220: 893–907.

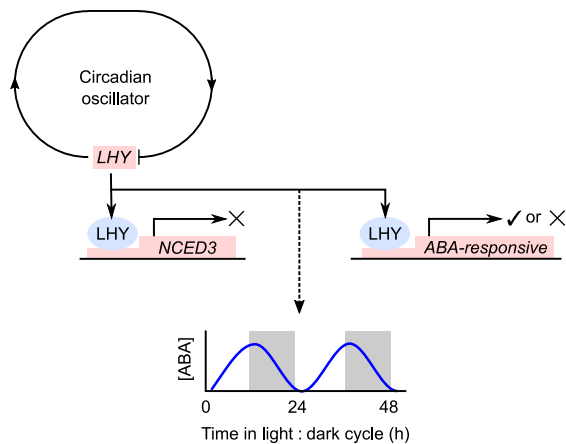


Fig. 1 Relationship between circadian oscillator component LATE ELONGATED HYPOCOTYL (LHY) and abscisic acid (ABA) signalling identified by Adams *et al.* (pp. 893–907) in this issue of *New Phytologist*. LHY binds to and suppresses transcription of *NCED3*, which encodes a 9-*cis*-epoxycarotenoid dioxygenase that participates in stress-induced ABA signalling. LHY also binds upstream of, and both induces and suppresses transcription of, ABA signalling-related genes. This may cause rhythms of ABA accumulation under light:dark cycles. Genes, pink boxes; proteins, blue circles. Broken line indicates indirect connection or emergent property. [ABA] indicates the relative concentration of ABA and shaded boxes on the timecourse of [ABA] indicate the dark period within the day:night cycle. The circadian oscillator is conceptualized as a simple cycle of gene expression.

Kamioka *et al.* (2016) previously investigated the binding targets of CCA1 and found that as with LHY, the majority of CCA1 target genes contained the evening element motif. The protein box element (PBE) and a G-box motif were also over-represented (Nagel *et al.*, 2015), but not the ABRE present within LHY targets (Adams *et al.*). Initially, this suggests specificity for LHY towards ABA-related target genes. Further examination of the CCA1 binding targets using gene ontology (GO) term analysis found that responses to internal and external stimuli and photosynthesis, response to biotic and abiotic stresses including low temperature and light, and response to cold, and cold acclimation were over-represented terms, further suggesting CCA1 targets are differentiated from those of LHY. However, enrichment of CCA1 target genes involved in the GO terms hormone responses, including ABA and response to salt stress (Nagel *et al.*, 2015; Kamioka *et al.*, 2016), might suggest some overlap for the roles of LHY and CCA1 in the regulation of ABA signalling-related genes.

LHY has been generally thought to be redundant with CCA1 within the functioning of the Arabidopsis circadian oscillator. However, by using transcriptome meta-analysis Adams *et al.* concluded that only 150 genes are common targets of both transcription factors. Therefore, although GO term analysis identified the enrichment of ABA-related terms in targets of both CCA1 and LHY, perhaps the sets of such target genes are different. For example, it is possible that genes within these same functional categories are targeted uniquely by either CCA1 or LHY, providing some specificity to each of these two transcription factors. Over-representation of the ABRE within only LHY targets provides an

example of such specificity (Adams *et al.*). A fascinating functional implication is that whilst CCA1/LHY might appear redundant within core oscillator function, it seems they have evolved to regulate different sets of circadian clock outputs. It would be interesting in future to examine whether, for example, a greater proportion of CCA1 targets participate in cold temperature and light signalling, whereas a greater proportion of LHY targets participate in ABA-related responses. Whilst this provides a basis for investigation of the control of specificity within circadian output pathways, it also provides insights into roles for gene duplication during the evolution of circadian clock transcription factors.

ORCID

Antony N. Dodd  <http://orcid.org/0000-0001-6859-0105>

Fiona E. Belbin and Antony N. Dodd* 

School of Biological Sciences, University of Bristol, Life Sciences Building, Bristol, BS8 1TQ, UK
(*Author for correspondence: tel +44 0117 394 1176; email antony.dodd@bristol.ac.uk)

References

- Adams S, Grundy J, Veflingstad SR, Dyer NP, Hannah MA, Ott S, Carré IA. 2018. Circadian control of ABA biosynthesis and signalling pathways revealed by genome-wide analysis of LHY binding targets. *New Phytologist* 220: 893–907.
- Choudhary MK, Nomura Y, Wang L, Nakagami H, Somers DE. 2015. Quantitative circadian phosphoproteomic analysis of Arabidopsis reveals extensive clock control of key components in physiological, metabolic, and signaling pathways. *Molecular & Cellular Proteomics* 14: 2243–2260.
- Covington MF, Harmer SL. 2007. The circadian clock regulates auxin signaling and responses in *Arabidopsis*. *PLoS Biology* 5: e222.
- Covington MF, Maloof JN, Straume M, Kay SA, Harmer SL. 2008. Global transcriptome analysis reveals circadian regulation of key pathways in plant growth and development. *Genome Biology* 9: R130.
- Farinas B, Mas P. 2011. Functional implication of the MYB transcription factor RVE8/LCL5 in the circadian control of histone acetylation. *The Plant Journal* 66: 318–329.
- Frank A, Matioli CC, Viana AJC, Hearn TJ, Kusakina J, Belbin FE, Newman DW, Yochikawa A, Cano-Ramirez DL, Chembath A *et al.* 2018. Circadian entrainment in *Arabidopsis* by the sugar-responsive transcription factor bZIP63. *Current Biology* 28: 2597–2606.
- Grundy J, Stoker C, Carré IA. 2015. Circadian regulation of abiotic stress tolerance in plants. *Frontiers in Plant Science* 6: 648.
- Hanano S, Domagalska MA, Nagy F, Davis SJ. 2006. Multiple phytohormones influence distinct parameters of the plant circadian clock. *Genes to Cells* 11: 1381–1392.
- Harmer SL, Hogenesch JB, Straume M, Chang H-S, Han B, Zhu T, Wang X, Kreps JA, Kay SA. 2000. Orchestrated transcription of key pathways in *Arabidopsis* by the circadian clock. *Science* 290: 2110.
- Haydon MJ, Mielczarek O, Robertson FC, Hubbard KE, Webb AAR. 2013. Photosynthetic entrainment of the *Arabidopsis thaliana* circadian clock. *Nature* 502: 689–692.
- Hotta CT, Gardner MJ, Hubbard KE, Baek SJ, Dalchau N, Suhita D, Dodd AN, Webb AAR. 2007. Modulation of environmental responses of plants by circadian clocks. *Plant, Cell & Environment* 30: 333–349.

- Hsu PY, Harmer SL. 2014. Wheels within wheels: the plant circadian system. *Trends in Plant Science* 19: 240–249.
- Kamioka M, Takao S, Suzuki T, Taki K, Higashiyama T, Kinoshita T, Nakamichi N. 2016. Direct repression of evening genes by CIRCADIAN CLOCK-ASSOCIATED1 in the Arabidopsis circadian clock. *The Plant Cell* 28: 696–711.
- Legnaioli T, Cuevas J, Mas P. 2009. TOC1 functions as a molecular switch connecting the circadian clock with plant responses to drought. *EMBO Journal* 28: 3745–3757.
- Linde AM, Eklund DM, Kubota A, Pederson ERA, Holm K, Gyllenstrand N, Nishihama R, Cronberg N, Muranaka T, Oyama T *et al.* 2017. Early evolution of the land plant circadian clock. *New Phytologist* 216: 576–590.
- Marti Ruiz MC, Hubbard KE, Gardner MJ, Jung HJ, Aubry S, Hotta CT, Mohd-Noh NI, Robertson FC, Hearn TJ, Tsai Y-C *et al.* 2018. Circadian oscillations of cytosolic free calcium regulate the Arabidopsis circadian clock. *Nature Plants* 4: 690–698.
- Nagel DH, Doherty CJ, Pruneda-Paz JL, Schmitz RJ, Ecker JR, Kay SA. 2015. Genome-wide identification of CCA1 targets uncovers an expanded clock network in Arabidopsis. *Proceedings of the National Academy of Sciences* 112: E4802–E4810.
- Noordally ZB, Ishii K, Atkins KA, Wetherill SJ, Kusakina J, Walton EJ, Kato M, Azuma M, Tanaka K, Hanaoka M *et al.* 2013. Circadian control of chloroplast transcription by a nuclear-encoded timing signal. *Science* 339: 1316.
- Rawat R, Takahashi N, Hsu PY, Jones MA, Schwartz J, Salemi MR, Phinney BS, Harmer SL. 2011. REVEILLE8 and PSEUDO-REPONSE REGULATORS5 form a negative feedback loop within the Arabidopsis circadian clock. *PLoS Genetics* 7: e1001350.
- Voß U, Wilson MH, Kenobi K, Gould PD, Robertson FC, Peer WA, Lucas M, Swarup K, Casimiro I, Holman TJ *et al.* 2015. The circadian clock rephases during lateral root organ initiation in Arabidopsis thaliana. *Nature Communications* 6: 7641.

Key words: abiotic stress, abscisic acid (ABA), circadian rhythms, gene regulation, signal transduction.



About New Phytologist

- *New Phytologist* is an electronic (online-only) journal owned by the New Phytologist Trust, a **not-for-profit organization** dedicated to the promotion of plant science, facilitating projects from symposia to free access for our Tansley reviews and Tansley insights.
- Regular papers, Letters, Research reviews, Rapid reports and both Modelling/Theory and Methods papers are encouraged. We are committed to rapid processing, from online submission through to publication 'as ready' via *Early View* – our average time to decision is <26 days. There are **no page or colour charges** and a PDF version will be provided for each article.
- The journal is available online at Wiley Online Library. Visit www.newphytologist.com to search the articles and register for table of contents email alerts.
- If you have any questions, do get in touch with Central Office (np-centraloffice@lancaster.ac.uk) or, if it is more convenient, our USA Office (np-usaoffice@lancaster.ac.uk)
- For submission instructions, subscription and all the latest information visit www.newphytologist.com

Integration of light and circadian signals that regulate chloroplast transcription by a nuclear-encoded sigma factor

Fiona E. Belbin¹, Zeenat B. Noordally², Sarah J. Wetherill³, Kelly A. Atkins¹, Keara A. Franklin¹ and Antony N. Dodd¹

¹School of Biological Sciences, University of Bristol, Bristol Life Sciences Building, 24 Tyndall Avenue, Bristol, BS8 1TQ, UK; ²Department of Botany and Plant Biology, University of Geneva, Geneva CH-1211, Switzerland; ³Department of Biology, University of York, York, YO10 5DD, UK

Author for correspondence:

Antony N. Dodd
Tel: +44 0117 394 1176
Email: antony.dodd@bristol.ac.uk

Received: 24 March 2016
Accepted: 28 July 2016

New Phytologist (2017) **213**: 727–738
doi: 10.1111/nph.14176

Key words: *Arabidopsis thaliana*, chloroplasts, circadian rhythms, photobiology, signal transduction.

Summary

- We investigated the signalling pathways that regulate chloroplast transcription in response to environmental signals. One mechanism controlling plastid transcription involves nuclear-encoded sigma subunits of plastid-encoded plastid RNA polymerase. Transcripts encoding the sigma factor SIG5 are regulated by light and the circadian clock. However, the extent to which a chloroplast target of SIG5 is regulated by light-induced changes in SIG5 expression is unknown. Moreover, the photoreceptor signalling pathways underlying the circadian regulation of chloroplast transcription by SIG5 are unidentified.
- We monitored the regulation of chloroplast transcription in photoreceptor and sigma factor mutants under controlled light regimes in *Arabidopsis thaliana*.
- We established that a chloroplast transcriptional response to light intensity was mediated by SIG5; a chloroplast transcriptional response to the relative proportions of red and far red light was regulated by SIG5 through phytochrome and photosynthetic signals; and the circadian regulation of chloroplast transcription by SIG5 was predominantly dependent on blue light and cryptochrome.
- Our experiments reveal the extensive integration of signals concerning the light environment by a single sigma factor to regulate chloroplast transcription. This may originate from an evolutionarily ancient mechanism that protects photosynthetic bacteria from high light stress, which subsequently became integrated with higher plant phototransduction networks.

Introduction

Plants are sessile autotrophs that require light for photosynthesis within chloroplasts, but experience continuous changes in their light environment. Predictable changes in light conditions arise from day–night cycles, and unpredictable changes include the effects of weather and shading by competitors. Phototransduction pathways and circadian clocks allow plants to anticipate, sense and respond to these environmental changes.

Both predictable and unpredictable changes in light conditions are perceived by photoreceptors, including phytochromes, cryptochromes, phototropins, other blue light-sensing light-oxygen-voltage (LOV)-domain photoreceptors and the UV-B photoreceptor UV RESISTANCE LOCUS8 (UVR8) (Casal, 2013). These elicit changes in gene expression that underlie global alterations in development and physiology (Casal, 2013). The action spectra of photoreceptors are allied closely with the wavelengths of light that are available for photosynthesis (Rockwell *et al.*, 2014), because photoreceptors regulate physiology and development to optimize photosynthetic light harvesting. Phototransduction pathways also synchronize the plant circadian oscillator with the day–night cycles of the environment (Somers *et al.*,

1998). The plant circadian oscillator comprises a network of interlocked transcription/translation feedback loops that produce a cellular estimate of the time of day (Nagel & Kay, 2012), which increases growth and fitness (Harmer *et al.*, 2000; Dodd *et al.*, 2005; Michael *et al.*, 2008).

Chloroplast transcription is regulated by light and the circadian clock (Gamble & Mullet, 1989; Klein & Mullet, 1990; Tsinoremas *et al.*, 1996; Noordally *et al.*, 2013), but knowledge of the mechanisms that integrate these signals is incomplete. Chloroplast genes are transcribed by two types of RNA polymerase: plastid-encoded plastid RNA polymerase (PEP) and nuclear-encoded plastid RNA polymerase (NEP) (Kanamaru *et al.*, 1999). PEP requires a bacterial-type σ^{70} subunit (sigma factor) to confer promoter specificity and initiate transcription. In higher plants, six sigma factors are encoded by the nuclear genome. It is thought that, during higher plant evolution, sigma factors transferred from the genomes of ancestral chloroplasts to the nuclear genome, and provide a mechanism for nuclear control of the specificity of chloroplast transcription (Kanamaru *et al.*, 1999; Ueda *et al.*, 2013).

Transcripts encoding *SIGMA FACTOR5* (*SIG5*) are regulated by several light signals in mature leaves (Ichikawa *et al.*, 2008;

Onda *et al.*, 2008; Mellenthin *et al.*, 2014) and during de-etiolation (Monte *et al.*, 2004; Tepperman *et al.*, 2006). This involves the cryptochrome, phytochrome and UVR8 photoreceptors (Monte *et al.*, 2004; Brown & Jenkins, 2008; Onda *et al.*, 2008; Mellenthin *et al.*, 2014). *SIG5* transcript abundance is also regulated by photosynthesis (Mellenthin *et al.*, 2014), abiotic stress (Nagashima *et al.*, 2004), retrograde signalling (Ankele *et al.*, 2007) and the circadian clock (Noordally *et al.*, 2013). Within chloroplasts, *SIG5* regulates transcription of the blue light-responsive promoter (BLRP) of *psbD* (*psbD* BLRP), which encodes the light-labile D2 protein of photosystem II (PSII) (Nagashima *et al.*, 2004), and transcripts with less well-characterized promoters (Noordally *et al.*, 2013). *psbD* BLRP is one of at least four differently sized transcripts that originate from the chloroplast *psbDC* operon in Arabidopsis (Hoffer & Christopher, 1997; Hanaoka *et al.*, 2003; Nagashima *et al.*, 2004). Here, we focused on *psbD* BLRP because it provides an experimentally tractable readout of chloroplast transcriptional regulation by *SIG5*.

Although sigma factors are known to be regulated by a variety of light signals, the extent to which this alters the transcription of sigma factor-regulated genes within chloroplasts is not known. We investigated this using nuclear-encoded *SIG5* and chloroplast-encoded *psbD* BLRP as a model. First, we report a series of new findings concerning the regulation of chloroplast transcription and the sigma factor *SIG5* by light. Second, we demonstrate that specific light signalling pathways are required for *SIG5* to maintain circadian rhythms of transcription of chloroplast *psbD* BLRP. We conclude that sigma factors integrate and communicate several types of information concerning the light environment to the chloroplast genome.

Materials and Methods

Plant materials and growth conditions

Seeds of *Arabidopsis thaliana* (L.) Heynh. were surface sterilized by exposure to 70% (v/v) ethanol for 1 min, 20% (v/v) domestic bleach for 12 min and then washed twice with sterile distilled H₂O. Seeds were resuspended in 0.1% (w/v) agar and sown individually onto half-strength (2.15 g l⁻¹) Murashige and Skoog nutrient mix (basal salts without vitamins, pH 6.8; Duchefa Biochimie, Haarlem, the Netherlands) in 0.8% (w/v) agar, without sucrose supplementation. For luciferase imaging, seeds were sown into sterile plastic rings embedded within growth medium (15 seeds per ring) to produce circular regions of luciferase bioluminescence (Love *et al.*, 2004; Noordally *et al.*, 2013; Dodd *et al.*, 2014). Seeds were stratified in the dark for 3 d at 4°C and then cultivated under 12 h : 12 h, light : dark cycles at 19°C and 90 μmol m⁻² s⁻¹ white light (MLR-352; Panasonic, Osaka, Japan). Modified conditions were required for comparable germination and growth of *phyABCDE* mutants, involving germination in 120 μmol m⁻² s⁻¹ white light (Microclima 1600E; Snijder Scientific, Tillburg, the Netherlands) at 20°C with 16 h : 8 h, light : dark cycles for 5 d, before transfer to standard growth conditions (as earlier). All photoreceptor mutants

described, except *phyABCDE*, were transformed with *SIG5::LUCIFERASE+* (Noordally *et al.*, 2013). T₃ generation *SIG5::LUCIFERASE+*-expressing homozygous seedlings were used for all experimentation. Multiple transgenic lines were screened to identify those having comparable luciferase bioluminescence, and then characterized using bioluminescence time course imaging to select lines for experimentation with representative circadian periods (Supporting Information Fig. S1). Eleven-day-old seedlings were used for all experiments.

Genotypes were Col-0, Landsberg *erecta* (L. *er.*), *sig5-3* (Noordally *et al.*, 2013), *phyA-201* (Nagatani *et al.*, 1993), *phyB-5* (Nagatani *et al.*, 1993), *phyA-201 phyB-5* (Reed *et al.*, 1994), *phyABCDE* (Hu *et al.*, 2013), *cry1-B104* (Bruggemann *et al.*, 1998), *cry2-1* (Guo *et al.*, 1998), *cry1 cry2 (hy4-1 fha-1)*, El-Assal *et al.*, 2003).

Transcript abundance

Aerial tissue was harvested 11 d after germination, as described previously (Noordally *et al.*, 2013). Total RNA was extracted using a NucleoSpin RNA extraction kit (Macherey-Nagel, Duren, Germany), from which cDNA was synthesized (High Capacity cDNA Reverse Transcription Kit, ThermoFisher, Waltham, MA, USA). Quantitative reverse transcription-polymerase chain reaction (qRT-PCR) analysis was performed using Brilliant III Ultra-Fast SYBR Green qRT-PCR Master Mix (Agilent Technologies, Santa Clara, CA, USA, using Agilent Mx3005P qRT-PCR instruments) and the primers described later. Transcript abundance was relative to *ACTIN2* (*ACT2*), an established reference for the study of this pathway (Noordally *et al.*, 2013), and calculated using the $\Delta\Delta C_t$ method. For light induction experiments, transcript abundance was measured 1 h (*SIG5*) and 4 h (*psbD* BLRP) after the start of light treatments, as a time delay exists between the upregulation of *SIG5* and *psbD* BLRP transcripts (Noordally *et al.*, 2013), and these times correspond with maximum *SIG5* and *psbD* BLRP transcript abundance attained after exposure to light of dark-adapted seedlings (Mochizuki *et al.*, 2004; Onda *et al.*, 2008; Noordally *et al.*, 2013). qRT-PCR primers were *SIG5* (GTGTTGGAGCTAATAACAGCAGACA (FP), TGTCGAA TAACCAGACTCTCTTTTCG (RP)); *psbD* BLRP (GGAAATC CGTCGATATCTCT (FP), CTCTCTTTCTCTAGGCAGGA AC (RP)) (Mochizuki *et al.*, 2004); *LHY* (*LATE ELONGATED HYPOCOTYL*) (ACGAAACAGGTAAGTGGCGACA (FP), TGGGAACATCTTGAACCGCGTT (RP)) (Noordally *et al.*, 2013); *ACT2* (TCAGATGCCAGAAAGTGTGTTCC (FP), CCGTACAGATCCCTTCCTGATATCC (RP), or TGAGAG ATTACAGATGCCAGAA (FP), TGGATTCCAGCAGCTT CCAT (RP) in Fig. 4(c) only (see later)).

Light conditions

Blue (B), red (R) and far red (FR) light manipulations used custom LED panels installed within temperature-controlled growth chambers, and custom Photek LB-1 R/FR/B LED panels controlled by the bioluminescence imaging system. Photosynthetically active radiation (PAR) and light spectra were quantified

with a spectroradiometer (Ocean Optics, Dunedin, FL, USA). Peak output wavelengths of R, B and FR LEDs were 660, 470 and 740 nm, respectively (Fig. S2). The R:FR ratio was calculated using PAR integrated from 660 to 670 nm divided by 725–735 nm (Franklin, 2008). Light induction experiments used $25 \mu\text{mol m}^{-2} \text{s}^{-1}$ total photon flux density (PFD) for each light colour treatment, except Fig. 4(c) only (see later), which used $10 \mu\text{mol m}^{-2} \text{s}^{-1}$ per treatment. In all figures, ***, $P < 0.001$; **, $P < 0.01$; *, $P < 0.05$; ns, not statistically significant. All light treatments commenced at zeitgeber time (ZT) 4, using dark-adapted seedlings, because *SIG5* has greatest sensitivity to B light pulses at ZT4 (Noordally *et al.*, 2013).

Bioluminescence imaging

Clusters of 10-d-old seedlings surrounded by sterile rings (e.g. Fig. S3) were dosed with $100 \mu\text{l}$ of 5 mM luciferin (potassium salt of D-luciferin; Melford Laboratories Ltd, Ipswich, UK) 24 h before imaging. Bioluminescence was measured using a Lumintek EM-CCD imaging system (Photek Ltd, St Leonards on Sea, UK) controlled by IMAGE32 software (Photek) and custom control scripts (45-s integrations, EM gain setting 2700). For experiments investigating *SIG5::LUCIFERASE* induction by light, 11-d-old seedlings were exposed to the light regime specified after dark adaptation for 24 h. Images were captured at 13-min intervals, preceded by a dark delay of 2 min to eliminate chlorophyll autofluorescence from the bioluminescence signal. Sequences of images lasted between 4 and 8 h, depending on the experiment; data on the figures represent peak *SIG5::LUCIFERASE* activity. Circadian time course imaging of *SIG5::LUCIFERASE* bioluminescence commenced at ZT0, using 11-d-old seedlings entrained previously to 12 h:12 h, light:dark cycles. Seedlings were exposed to two 12 h:12 h, light:dark cycles of the wavelength(s) under investigation before transfer to constant light, to reduce transitory effects. Bioluminescence images were captured approximately every hour. Imaging data were analysed using IMAGE32 software (Photek), with circadian time courses analysed further using the fast Fourier transform-nonlinear least-squares (FFT-NLLS) algorithm within BRASS software (Southern & Millar, 2005), downloaded in 2015 from <http://millar.bio.ed.ac.uk>. The first 24 h of data in constant light were discarded before FFT-NLLS analysis to remove transient responses to the final dark period.

Inhibitor experiments

For experiments with norflurazon (Sigma-Aldrich), growth medium was supplemented with $5 \mu\text{M}$ norflurazon and 1% (w/v) sucrose to allow growth in the absence of photosynthesis (e.g. Fig. S3a). For bioluminescence imaging experiments with 3-(3,4-dichlorophenyl)-1,1-dimethylurea (DCMU, Sigma-Aldrich), $20 \mu\text{M}$ DCMU was added to the $100 \mu\text{l}$ of 5 mM luciferin that was dosed onto seedlings. For RNA sampling, $100 \mu\text{l}$ of $20 \mu\text{M}$ DCMU was dosed onto seedlings. In both cases, DCMU was dosed onto seedlings 24 h before the start of light treatment. Inhibitors were dissolved in dimethylsulfoxide

(DMSO) (working concentrations of DMSO were 0.0025% (v/v) and 0.01% (v/v) with norflurazon and DCMU, respectively), and inhibitor controls contained an equal volume of DMSO without the inhibitor.

Results

We used the regulation of chloroplast *psbD* BLRP by nuclear-encoded *SIG5* as an experimental model. To provide a basis for subsequent experiments, we investigated the accumulation of chloroplast *psbD* BLRP transcripts in wild-type and *sig5-3* loss-of-function plants, under various light conditions, to determine the role of nuclear-encoded *SIG5* in the regulation of chloroplast *psbD* BLRP by light. Like *SIG5* transcripts, *SIG5* promoter activity and chloroplast-encoded *psbD* BLRP transcripts were induced most strongly by B light, other treatments including R light, and a combination of R and FR light with R:FR = 0.7 (Fig. 1a,b). *SIG5* transcripts and *SIG5* promoter activity were not induced by either R or FR light alone (Fig. 1a,b). The transcriptional responses of *psbD* BLRP were *SIG5* dependent because light treatments did not induce *psbD* BLRP in the *sig5-3* loss-of-function mutant (Fig. 1b). The behaviour of *SIG5* transcripts (Fig. 1b) was consistent with studies conducted under similar conditions (Mochizuki *et al.*, 2004; Nagashima *et al.*, 2004; Onda *et al.*, 2008; Noordally *et al.*, 2013). The regulation of *SIG5* promoter activity by light, measured with *SIG5::LUCIFERASE*, appeared to account largely for the regulation of *SIG5* transcript accumulation (Fig. 1a,b).

SIG5 communicates information concerning light intensity and quality to chloroplasts

We hypothesized that chloroplast transcription is regulated by *SIG5* in response to light intensity, as: (1) *SIG5* transcript abundance depends on B light intensity (Onda *et al.*, 2008); (2) *psbD* BLRP is regulated by *SIG5* in a dose-dependent manner (Onda *et al.*, 2008); and (3) we found that both B and R + FR light upregulation of *psbD* BLRP was dependent on *SIG5* (Fig. 1b). It is not known whether *SIG5* transcription is dependent on the intensity of R light, nor how these fluence responses of *SIG5* affect chloroplast transcription. To test this, we applied a range of intensities of either B or R + FR light to seedlings. Treatment with each light intensity commenced at ZT4, using separate batches of seedlings (we did not progressively increase light intensity over time, because that approach would be confounded by circadian gating). In both B and R + FR light, the magnitude of induction of chloroplast *psbD* BLRP transcripts was determined by PFD, and also required *SIG5* (Fig. 1c,d). The magnitude of induction of the *SIG5* promoter and *SIG5* transcript abundance were also determined by PFD (Fig. 1c,d). This suggests that, across the PFD range investigated, regulation of the *SIG5* promoter by PFD of both B and R + FR light controlled the accumulation of *SIG5* transcripts, causing the magnitude of chloroplast *psbD* BLRP transcript accumulation to be PFD dependent.

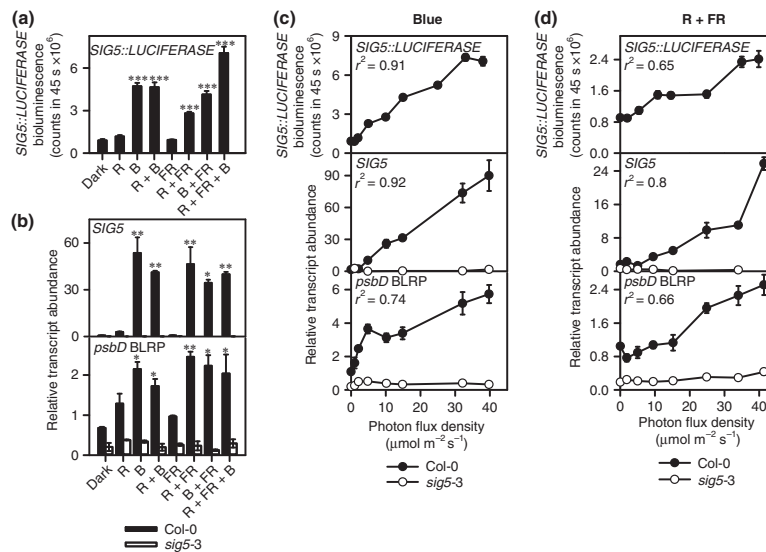


Fig. 1 Signalling of information concerning light intensity to the chloroplast genome by nuclear-encoded SIGMA FACTOR5 (SIG5) in *Arabidopsis thaliana*. (a, b) Relative induction of (a) *SIG5::LUCIFERASE* and (b) *SIG5* and *psbD* blue light-responsive promoter (BLRP) transcripts under several light conditions in dark-adapted wild-type and *sig5-3* seedlings (light conditions: R, red light; B, blue light; FR, far red light; and combinations of these with $25 \mu\text{mol m}^{-2} \text{s}^{-1}$ of each wavelength). (c, d) The magnitude of induction of *SIG5::LUCIFERASE* and the abundance of *SIG5* and *psbD* BLRP transcripts were dependent on light intensity under (c) blue light and (d) red and far red light (R : FR = 0.7). All light treatments commenced at zeitgeber time 4. (a, b) ANOVA and *post-hoc* Tukey analysis compared each light condition with dark control. ***, $P < 0.001$; **, $P < 0.01$; *, $P < 0.05$. (c, d) r^2 from linear regression. y axes in (c, d) are not comparable because experiments were analysed separately. Data are mean \pm SE: $n = 2-6$ (transcript abundance); $n = 5-12$ (*SIG5::LUCIFERASE*).

Photoreceptors and retrograde signals underlie the regulation of chloroplast transcription in response to light intensity by SIG5

Plant responses to light, including the transcription of *SIG5*, are mediated by photoreceptors and photosynthesis (Onda *et al.*, 2008; Mellenthin *et al.*, 2014). It is not known which of these light response pathways underlies the light intensity-dependent transcriptional response that we identified for *SIG5* and chloroplast *psbD* BLRP (Fig. 1c,d). Therefore, we investigated this question with a combination of photoreceptor mutants and photosynthetic inhibitors. Regulation of *SIG5* and *psbD* BLRP has been reported to involve the photoreceptors phytochromeA (*phyA*), cryptochrome1 (*cry1*) and *cry2* (Thum *et al.*, 2001; Ichikawa *et al.*, 2004; Onda *et al.*, 2008; Mellenthin *et al.*, 2014). Although *phyA* was required for *SIG5* induction by R + FR light and *phyB* may suppress *SIG5* transcript accumulation (Fig. S4b), *SIG5* was not regulated by R or FR light when applied alone (Fig. 1a,b; Mochizuki *et al.*, 2004; Onda *et al.*, 2008; Noordally *et al.*, 2013). A single report demonstrating *SIG5* induction in de-etiolated seedlings by R or FR light alone used sucrose-supplemented growth media (Mellenthin *et al.*, 2014). *SIG5* transcripts were induced by B light in the *phyA* mutant, presumably as a result of cryptochrome-mediated regulation of *SIG5* (Fig. S4d). However, as the regulation of *SIG5* by R and FR light is atypical for phytochrome signalling, we reasoned that additional mechanisms act alongside phytochromes to regulate chloroplast transcription by *SIG5* in response to the intensity of R + FR light.

We investigated the involvement of retrograde signalling in the control of chloroplast transcription by *SIG5* in response to PFD. B light activation of *SIG5::LUCIFERASE* was unaltered by norflurazon, which inhibits carotenoid biosynthesis, leading to photobleaching (e.g. Fig. S3a). By contrast, norflurazon inhibited the upregulation of *SIG5::LUCIFERASE* by R + FR light (Figs 2a, S3a). We also investigated the effect of DCMU, an inhibitor of photosynthetic electron transport between PSII and plastoquinone (PQ), on light activation of *SIG5*-mediated signals to chloroplasts. First, we determined the minimum effective dose for the inhibition of photosynthesis by DCMU under our experimental conditions using modulated PSII chlorophyll fluorescence (Imaging-PAM M, Walz, Germany). Seedlings grown exactly as for bioluminescence imaging and RNA sampling were dosed with 0, 5, 10, 15, 20, 35 or 50 μM DCMU (mixed with and without luciferin for Col-0 *SIG5::LUCIFERASE* and *L. er.*, respectively) and dark adapted for 24 h before determination of F_0 and F_m (intensity setting 1, frequency 4). Actinic light ($107 \mu\text{mol m}^{-2} \text{s}^{-1}$) was switched on for 10 min, after which the effective quantum yield of PSII ($Y(II)$) was calculated as $(F_m' - F')/F_m'$, where F_m' is the maximum fluorescence emission from the light-adapted seedling after a saturating pulse, and F' is the chlorophyll fluorescence emission from light-adapted seedlings. Based on these data, we used DCMU at a concentration of 20 μM , and luciferin did not alter the efficacy of DCMU.

DCMU treatment reduced R + FR light induction of *SIG5::LUCIFERASE* by 42%, whereas induction of *SIG5::*

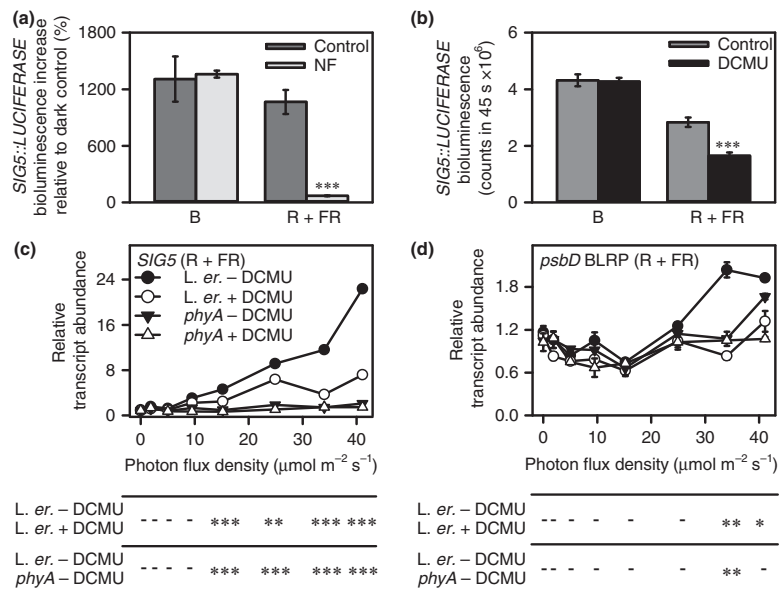


Fig. 2 Photosynthetic and phytochrome signals in *Arabidopsis thaliana* underlie SIGMA FACTOR5 (SIG5)-mediated signals to chloroplasts concerning red (R)/far red (FR) light intensity. (a, b) *SIG5::LUCIFERASE* induction by blue (B) and R + FR light in the presence of norflurazon (NF) or 3-(3,4-dichlorophenyl)-1,1-dimethylurea (DCMU), using $25 \mu\text{mol m}^{-2} \text{s}^{-1}$ of each wavelength. (a) Represented as proportional increase in bioluminescence relative to dark control (because inclusion of sucrose within growth media to allow growth in the presence of norflurazon, and cultivation on norflurazon, changed baseline bioluminescence). (c, d) Light intensity response of *SIG5* and *psbD* blue light-responsive promoter (BLRP) transcripts in R + FR light in wild-type (WT) and *phyA*-201 with DCMU supplementation. All light treatments commenced at zeitgeber time 4 (ZT4). Significance determined by (a, b) *t*-tests and (c, d) ANOVA and Tukey *post-hoc* analysis, comparing WT with and without DCMU and WT with DCMU and *phyA*-201 without DCMU. (a–d) ***, $P < 0.001$; **, $P < 0.01$; *, $P < 0.05$. (c, d) Hyphen indicates not statistically significant. Data are mean \pm SE; $n = 2–6$ (quantitative reverse transcription-polymerase chain reaction, qRT-PCR); $n = 5–12$ (*SIG5::LUCIFERASE*). R + FR, combination of red and far red light (R : FR = 0.7).

LUCIFERASE by B light was insensitive to DCMU (Fig. 2b). Together, these results indicated that a retrograde signal arising from photosynthetic electron transport was required for the regulation of the *SIG5* promoter by R + FR but not B light.

We used this information to investigate the contribution of phytochrome and photosynthetic signals to the regulation of chloroplast transcription in response to the intensity of R + FR light. There was some variation in the sensitivity of *psbD* BLRP transcripts to R + FR light; the PFD threshold for significant *psbD* BLRP upregulation by R + FR light was $25 \mu\text{mol m}^{-2} \text{s}^{-1}$ in Fig. 1(d) ($P = 0.001$) and $35 \mu\text{mol m}^{-2} \text{s}^{-1}$ in Fig. 2(d) ($P = 0.008$; two-sample *t*-tests relative to dark controls). *SIG5* and *psbD* BLRP were generally not induced significantly in *phyA* mutants at any PFD relative to dark controls (Fig. 2c,d), demonstrating that this response of *SIG5* to light intensity was dependent on *phyA*. A single exception was that, in *phyA*, *psbD* BLRP was induced by R + FR light at $40 \mu\text{mol m}^{-2} \text{s}^{-1}$ in the absence of DCMU, and this response was abolished when DCMU was added (Fig. 2d). Across the PFD range tested, DCMU reduced the slope estimate (r^2) of the R + FR PFD response of *SIG5* from 0.46 to 0.14, and of *psbD* BLRP from 0.03 to 0.01 (Fig. 2c,d). The absence of an effect of DCMU on B light activation of *SIG5::LUCIFERASE* (Fig. 2b) suggests that the DCMU sensitivity of R + FR light induction of *SIG5::LUCIFERASE* is a specific signalling response rather than a nonspecific consequence of

DCMU-induced oxidative damage. Overall, these data indicate that, although R + FR light activation of *psbD* BLRP by *SIG5* is dependent on *phyA*, a photosynthetic signal underlies the quantitative response of the pathway to R + FR light intensity.

Regulation of SIG5-mediated signalling to chloroplasts by the proportions of red and far red light

As R or FR light alone had little effect on chloroplast *psbD* BLRP transcription by *SIG5*, but R and FR light in combination induced this pathway (Fig. 1a,b), we reasoned that chloroplast *psbD* BLRP might be regulated by the relative proportions of R and FR light in a *SIG5*-dependent manner. In nature, R : FR light conditions provide plants with information concerning vegetational shade or the threat of vegetational shade, because vegetation absorbs R light and transmits and reflects FR light. The balance of R and FR light also affects plants because R and FR light preferentially excite PSII and PSI, respectively, altering the energy balance across the photosynthetic electron transport system and the redox state of the PQ pool (Pfannschmidt *et al.*, 1999; Bonardi *et al.*, 2005).

It is not known whether sigma factor-mediated signals to chloroplasts are regulated by the relative proportions of R and FR light. To test this, we exposed dark-adapted seedlings to R : FR light conditions in the range 0.02–1.4,

and monitored both *SIG5* promoter activity and *SIG5* and *psbD* BLRP transcript abundance (Fig. 3a). The magnitude of activation of *SIG5*, its promoter and chloroplast-encoded *psbD* BLRP was dependent on the relative proportions of R and FR light (Fig. 3a). *SIG5::LUCIFERASE* was induced strongly by R:FR in the range 0.46–0.96, and *SIG5* transcripts were induced most strongly by R:FR in the range 0.66–1.24 (Fig. 3a). *psbD* BLRP induction was reduced at very low R:FR and R:FR exceeding 1.2 (Fig. 3a). The *psbD* BLRP response to R:FR conditions was dependent on *SIG5*, as *psbD* BLRP was not induced in *sig5-3* (Fig. 3a). This was consistent with Fig. 1(a,b), where *SIG5* and *psbD* BLRP transcript accumulation was low under R or FR light alone, but high under R+FR light (R+FR=R:FR conditions of 0.7).

phyA promoted *SIG5* transcription under R+FR light (Fig. S4c), but the smallest induction of *SIG5::LUCIFERASE* and *SIG5* transcript abundance occurred under conditions of very low R:FR (Fig. 3a), when phyA signalling would be expected to be greatest (Martínez-García *et al.*, 2014). We explored this difference by testing the contribution of photosynthesis to R:FR responses of *SIG5*. DCMU had no effect on the small increase in *SIG5::LUCIFERASE* at low R:FR, yet inhibited *SIG5::LUCIFERASE* upregulation at

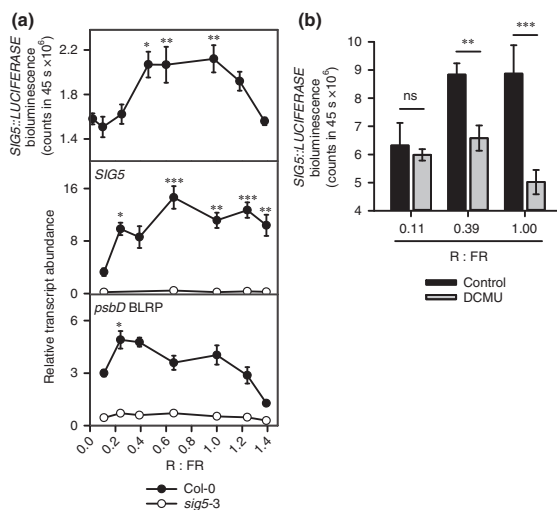


Fig. 3 Relative proportions of red (R) and far red (FR) light regulate SIGMA FACTOR5 (*SIG5*)-mediated signalling to chloroplasts in *Arabidopsis thaliana*. (a) *SIG5::LUCIFERASE* bioluminescence and abundance of transcripts encoding *SIG5* and *psbD* blue light-responsive promoter (BLRP) in dark-adapted seedlings exposed to a range of R:FR ratios (totalling 25 $\mu\text{mol m}^{-2} \text{s}^{-1}$). (b) Role of photosynthesis in R:FR response of *SIG5::LUCIFERASE* in seedlings treated with 3-(3,4-dichlorophenyl)-1,1-dimethylurea (DCMU). Analysis by (a) ANOVA and *post-hoc* Tukey test comparing lowest R:FR with all other R:FR; (b) two-sample *t*-tests within each R:FR, where: ***, $P < 0.001$; **, $P < 0.01$; *, $P < 0.05$; ns, not significant. Data are mean \pm SE; $n = 5$ –12 (*SIG5::LUCIFERASE*); $n = 2$ –6 (quantitative reverse transcription-polymerase chain reaction, qRT-PCR). Light treatments commenced at zeitgeber time 4.

higher R:FR conditions (Fig. 3b). The magnitude of *SIG5::LUCIFERASE* induction was dependent on the proportions of R and FR light, rather than simply R light intensity, because *SIG5* was not induced by R light alone (Fig. 1a,b).

Circadian signalling to chloroplasts by *SIG5* is primarily dependent on blue light and cryptochrome

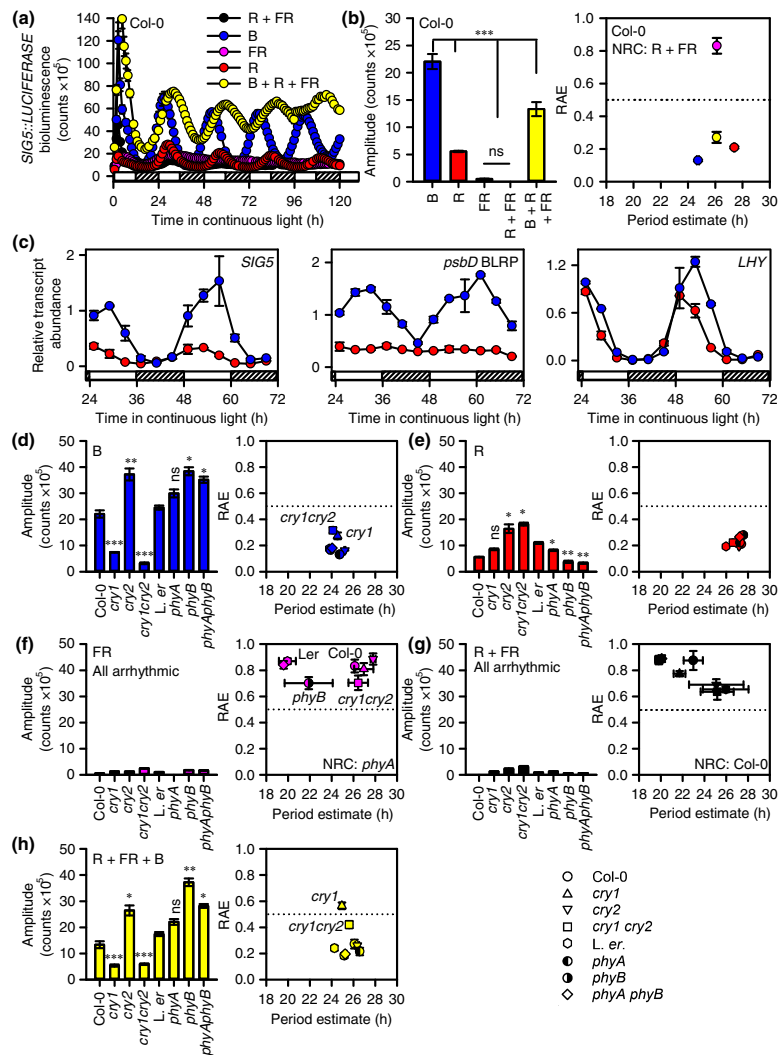
SIG5 communicates circadian timing information from the nuclear-encoded circadian oscillator to circadian-regulated chloroplast transcripts, including *psbD* BLRP (Nakahira *et al.*, 1998; Ichikawa *et al.*, 2008; Noordally *et al.*, 2013). Specific light conditions and photoreceptors regulate *SIG5* induction of *psbD* BLRP in dark-adapted seedlings (Figs 1, S4), the circadian clock gates transient B light induction of *SIG5* and *psbD* BLRP (Noordally *et al.*, 2013) and, in cycles of B light and darkness, cryptochromes contribute to the transcriptional patterns of a *SIG5* orthologue in *Physcomitrella* (Ichikawa *et al.*, 2004). It is not known which photoreceptor systems or light conditions underlie *SIG5*-mediated circadian signalling to chloroplasts, and so we investigated this with a combination of photoreceptor mutants and manipulations to the light conditions.

Circadian oscillations of *SIG5::LUCIFERASE* showed greatest amplitude under continuous B light, lower amplitude under a combination of B, R and FR light, and very low amplitude under continuous R light (Figs 4a,b, S5; see also Fig. S6 for these light conditions plotted separately for Col-0). The relative amplitude error (RAE) from analysis by FFT-NLLS indicates the quality of fit of a sine wave to the experimental data, from 0 (perfect fit) to 1 (no fit), where > 0.5 typically reflects arrhythmicity (Xu *et al.*, 2007) (Fig. 4b). Using this measure, *SIG5::LUCIFERASE* was arrhythmic under both R+FR and FR light alone (Figs 4a,b, S6), but was rhythmic when B light was added to R+FR (Fig. 4a). *SIG5::LUCIFERASE* has been shown elsewhere to be rhythmic under R+B light (Noordally *et al.*, 2013). Together, these data indicate that robust circadian oscillations of the *SIG5* promoter require B light.

To determine the relationship between the arrhythmicity of *SIG5::LUCIFERASE* under R and FR light and circadian oscillator function, we monitored circadian oscillations of *CCA1::LUCIFERASE* under combinations of R and FR light (Fig. S5b). *CCA1::LUCIFERASE* was rhythmic under R and R+FR light, but arrhythmic under FR light alone (Fig. S5b). The amplitude of oscillations of *CCA1::LUCIFERASE* was approximately six-fold greater under R than R+FR light (Fig. S5b).

Next, we investigated the role of selected wavelengths in the circadian regulation of *SIG5* and *psbD* BLRP transcripts (Fig. 4c). *SIG5* and *psbD* BLRP were rhythmic under B light and, under R light, there were low-amplitude oscillations of *SIG5* but *psbD* BLRP was arrhythmic (Fig. 4c). Circadian oscillations of *LHY* indicated that the circadian oscillator remained rhythmic under R light (Fig. 4c). It has been proposed that there is a minimum abundance of *SIG5* transcripts that is required for circadian oscillations of *psbD* BLRP (Noordally *et al.*, 2013), and so the low-amplitude oscillations of *SIG5* transcript abundance under R

Fig. 4 Blue (B) light and cryptochrome photoreceptors play major roles in SIGMA FACTOR5 (SIG5)-mediated circadian signalling to chloroplasts in *Arabidopsis thaliana*. Circadian oscillations of (a, b) *SIG5::LUCIFERASE* under five light regimes and (c) *SIG5*, *psbD* blue light-responsive promoter (BLRP) and *LHY* transcripts in continuous B and red (R) light. (d–h) Properties of circadian oscillations of *SIG5::LUCIFERASE* in photoreceptor mutants under five light regimes (Col-0 and *L. er.* backgrounds for *cry* and *phy*, respectively). Hatched bars in (a, c) indicate subjective darkness. Data are mean \pm SE; $n = 4$ circular clusters of seedlings; significance determined by ANOVA and Tukey *post-hoc* analysis. Statistical significance is indicated for comparisons of (b) all treatments and (d–h) each mutant against its background, except (f) and (h) where all genotypes had low rhythmic robustness, making amplitude comparisons uninformative. ***, $P < 0.001$; **, $P < 0.01$; *, $P < 0.05$; ns, not statistically significant. Light conditions: R, red light; B, blue light; FR, far red light (and combinations of these with $25 \mu\text{mol m}^{-2} \text{s}^{-1}$ of each wavelength). NRC, no rhythmic components detected; RAE, relative amplitude error derived from analysis by fast Fourier transform-nonlinear least-squares method.



light may have been below this threshold for *psbD* BLRP transactivation (Fig. 4c).

We investigated the photoreceptors that underlie circadian oscillations of *SIG5::LUCIFERASE*. Under continuous B light, the amplitude of circadian oscillations of *SIG5::LUCIFERASE* was reduced substantially in *cry1* and *cry1 cry2* relative to the wild-type (Figs 4d, S5), indicating that circadian oscillations of *SIG5* in B light were predominantly dependent on *cry1*. Under R light, the circadian amplitude of *SIG5::LUCIFERASE* was reduced slightly, but significantly, relative to the wild-type in *phyA*, *phyB* and *phyA phyB* (Fig. 4e). This suggests that *phyA* and *phyB* made small contributions to the amplitude of circadian oscillations of *SIG5* promoter activity, but were not essential for its rhythmicity. *SIG5::LUCIFERASE* was arrhythmic in all genotypes in FR and R + FR light (Fig. 4f,g). Under R + FR + B light, circadian oscillations of *SIG5::LUCIFERASE* required *cry1*,

because *SIG5::LUCIFERASE* was arrhythmic in *cry1* and had reduced rhythmic robustness in *cry1 cry2* (RAE = 0.42 ± 0.3 ; Fig. 4h) relative to other treatments. The greater amplitude of *SIG5::LUCIFERASE* oscillations in *cry2* relative to the wild-type in B and R + FR + B light suggests that there was antagonism between *cry1* and *cry2* in the circadian regulation of *SIG5* (Fig. 4d,h). In the presence of B light, *phyA* and *phyB* appeared to antagonize the circadian amplitude of *SIG5::LUCIFERASE* oscillations (Fig. 4d,h), possibly explaining why *SIG5::LUCIFERASE* had lower circadian amplitude in R + FR + B than B light alone (Fig. 4d,h).

The dynamics of *SIG5::LUCIFERASE* under light–dark cycles of five light conditions revealed two features within the daily regulation of the *SIG5* promoter under B light (Fig. 5). Under light–dark cycles of B light, *SIG5* promoter activity was induced rapidly following dawn (Fig. 5a, feature marked ‘A’), with a

second more slowly acting feature present during the middle of the photoperiod (Fig. 5a, feature marked 'B'). The 'spike-shoulder' dynamics were absent from the daily regulation of *SIG5* transcription under other light conditions tested (Fig. 5a). Under B light–dark cycles, the more slowly acting feature was absent in the *cry1* and *cry1 cry2* mutants, but present in *cry2* (Fig. 5b), suggesting that the feature arose from *cry1* activity. In addition, under light–dark cycles, there was clear anticipation of dawn by *SIG5::LUCIFERASE* under B + R + FR light conditions, but this was absent under B light alone (Fig. 5).

Discussion

We present new information concerning a mechanism that integrates light and circadian cues to regulate chloroplast transcription. We first examined the dynamics of this pathway during transition from dark to light, and subsequently investigated the involvement of light conditions in circadian regulation of the pathway. Previous studies have demonstrated that nuclear-encoded transcripts of the chloroplast RNA polymerase subunit *SIG5* are induced in *Arabidopsis* by B light, R light and UV-B (Monte *et al.*, 2004; Brown & Jenkins, 2008; Onda *et al.*, 2008; Mellenthin *et al.*, 2014). Likewise, orthologues of *Arabidopsis SIG5* in rice, *Physcomitrella* and *Marchantia* are light induced (Ichikawa *et al.*, 2004; Kubota *et al.*, 2007; Kanazawa *et al.*, 2013). Although the sigma factor *SIG5* appears to be conserved amongst land plants (Kanazawa *et al.*, 2013), in cyanobacteria and a species of red alga other sigma factors are light induced (Imamura *et al.*, 2003; Fujii *et al.*, 2015). Here, we demonstrated in *Arabidopsis* that light-induced changes in sigma factor transcript abundance lead to transcriptional changes in chloroplasts in response to various light signals. We also identified specific light signalling pathways underlying the circadian regulation of chloroplast transcription by *SIG5*. A general interpretation is that information concerning the light environment is integrated by, and communicated to, chloroplasts by nuclear-encoded sigma factors. *SIG5* appears to communicate information to the chloroplast genome concerning light intensity and light quality (Figs 1, 3), and this information is combined with B light and cryptochrome-dependent circadian timing cues (Fig. 4). An area for future investigation is to determine the role of the multiple transcription start sites (TSSs) within the *psbDC* operon in signal

integration, as the transcription or activity of other sigma factors is regulated by light conditions and the circadian oscillator (Onda *et al.*, 2008; Puthiyaveetil *et al.*, 2008, 2011; Shimizu *et al.*, 2010; Noordally *et al.*, 2013), and other *psbDC*TSSs are light regulated depending on the developmental stage (Hoffer & Christopher, 1997).

Circadian signalling to chloroplasts by *SIG5* requires specific light signalling pathways

The circadian oscillator is rhythmic under conditions of B and R light (Somers *et al.*, 1998) (see Fig. 4c for *LHY*), and so the B light dependence of circadian oscillations of *SIG5::LUCIFERASE* (Fig. 4a,c) is a specific feature of *SIG5*-mediated circadian signalling to chloroplasts, rather than a dependence of the circadian oscillator on B light. By contrast, arrhythmia of *SIG5::LUCIFERASE* under continuous FR light appears to arise from arrhythmia of the circadian oscillator, as *CCA1::LUCIFERASE* was arrhythmic under these conditions (Fig. S5b), rather than representing a specific feature of the circadian regulation of *SIG5*. A previous report has indicated that, under continuous FR light, the circadian oscillator is rhythmic with low amplitude and altered phase (Wenden *et al.*, 2011), whereas, under our experimental conditions, *CCA1::LUCIFERASE* was arrhythmic under continuous FR light (Fig. 5b). This difference could be because our experiments were conducted using sucrose-free growth medium, whereas Wenden *et al.* (2011) included 3% sucrose in the growth medium. As FR light has been proposed to act on the circadian oscillator through the evening loop component *ELF4* (Wenden *et al.*, 2011) and a long-term effect of sucrose on the circadian oscillator is mediated by the evening loop component *GIGANTEA* (Dalchau *et al.*, 2011), phytochrome and metabolite signals may interact to provide an input to the circadian oscillator via the evening loop. Circadian oscillations of *SIG5* transcript abundance were approximately coincident with the phasing to subjective day of circadian oscillations of the promoters and transcripts of *cry1*, *cry2* and *phyA-E* (Bognár *et al.*, 1999; Tóth *et al.*, 2001). However, as photoreceptor protein abundance may not cycle under constant light (Bognár *et al.*, 1999; Sharrock & Clack, 2002; Mockler *et al.*, 2003), rhythms of *SIG5* transcript abundance seem unlikely to be a direct consequence of oscillations of photoreceptor transcript abundance.

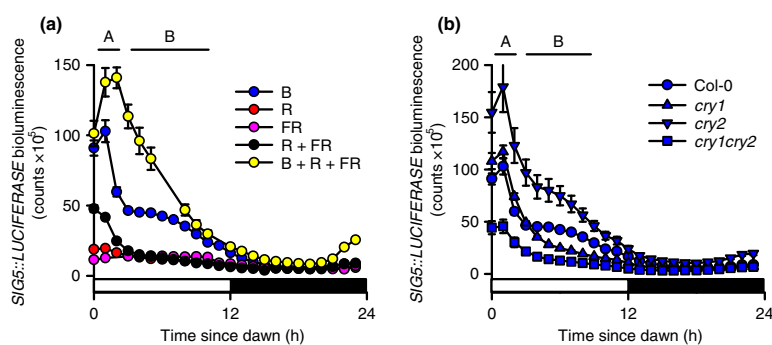


Fig. 5 Comparison of *SIG5::LUCIFERASE* dynamics under light–dark cycles of five light conditions in (a) the Col-0 background and (b) cryptochrome mutants of *Arabidopsis thaliana*. White and black bars on abscissa indicate light and dark periods, respectively. 'A' and 'B' above the graphs indicate two components within the *SIG5::LUCIFERASE* dynamics under monochromatic blue light. Data are mean \pm SE; $n = 4$. Light conditions: R, red light; B, blue light; FR, far red light (and combinations of these with $25 \mu\text{mol m}^{-2} \text{s}^{-1}$ of each wavelength).

cry1 cry2 SIG5::LUCIFERASE lacked the longer circadian period identified previously for the *CHLOROPHYLL A/B-BINDING PROTEIN2* promoter in *cry1 cry2* (Devlin & Kay, 2000). This might be explained by the temperature dependence of the period of *cry1 cry2* under conditions that include B light (Gould *et al.*, 2003). Gould *et al.* (2003) indicated that the experimental temperature of Devlin & Kay (2000) (22°C) would lengthen the period of *cry1 cry2* when B and R light are present, whereas the period may be indistinguishable from the wild-type at the lower temperature (19°C) used here (Fig. 4).

Under light–dark cycles, *SIG5* integrates several light signals that regulate chloroplast transcription

The presence of two features within the dynamics of *SIG5::LUCIFERASE* under light–dark cycles (Fig. 5a) suggests that the reduced experimental complexity provided by monochromatic B light alone (as opposed to a more complex spectrum) allowed the separation of light- and circadian-regulated components of *SIG5* promoter activity. The more slowly acting feature of *SIG5::LUCIFERASE* under these conditions (marked 'B' on Fig. 5a, b) may be caused by circadian regulation, because this feature requires *cry1* (Fig. 5b) and, under continuous B light, *cry1* contributes substantially to the amplitude of circadian *SIG5::LUCIFERASE* oscillations (Fig. 4d,h).

There are several possible explanations for the lack of dawn anticipation by *SIG5::LUCIFERASE* under B light–dark cycles, compared with clear anticipation of dawn under R + FR + B light (Fig. 5). The degree of dawn anticipation by circadian reporters under light–dark cycles can reflect differences in circadian period, whereby a longer period reduces the extent of dawn anticipation by morning-phased reporters, and a shorter period leads to more obvious anticipation of dawn (Dodd *et al.*, 2014). However, the circadian period of *SIG5::LUCIFERASE* was not longer under B light than under R + FR + B conditions (Fig. 4d,h), suggesting that period differences might not explain this variation in dawn anticipation. Another possibility is that increased photosynthetic energy availability in R + FR + B light relative to other treatments caused the *SIG5* promoter to assume an earlier phase, because increased energy availability can shorten the circadian period (Haydon *et al.*, 2013). We speculate that the anticipation of dawn by *SIG5* might be important to ensure appropriate rates of PSII D2 protein accumulation before the onset of photosynthesis. However, to better understand the adaptive significance of these results, it will be important to determine the contribution of the circadian oscillator to the dynamics of this pathway under lighting conditions more representative of natural environments.

Differences between the transcriptional response of *SIG5* to specific light conditions during acute induction and circadian free-run provide information about the contribution of circadian regulation to the functioning of this pathway under light–dark cycles, and about the role of specific light conditions around dawn. *SIG5* responded strongly to R + FR light in dark-adapted plants (Fig. 1a,b) and under light–dark cycles

(Fig. 5a), suggesting that, in nature, R + FR light might be an important regulator of *SIG5* around dawn. In comparison, B light and *cry1* help to maintain *SIG5* transcript accumulation longer term, such as during the circadian free-run (Fig. 4c,d, h) and the second half of the photoperiod (Fig. 5). Therefore, circadian regulation contributes to *SIG5* promoter activity during light–dark cycles. Under light–dark cycles, circadian regulation might be particularly important for gating the responses of *SIG5* to transient changes in light conditions in order to maintain optimum synthesis of PSII D2 (Noordally *et al.*, 2013).

Regulators of *SIG5* transcription in response to light include ELONGATED HYPOCOTYL5 (HY5) and HY5 HOMOLOG (HYH), which act redundantly to regulate *SIG5* transcript accumulation (Nagashima *et al.*, 2004; Brown & Jenkins, 2008; Melenthin *et al.*, 2014). Abscisic acid also upregulates *SIG5* transcripts, but may be without effect on chloroplast *psbD* under the same conditions (Yamburenko *et al.*, 2015). Although there are a variety of other light- and circadian-regulated *cis* elements within the *SIG5* promoter (Noordally *et al.*, 2013; Melenthin *et al.*, 2014), it is less clear which pathways underlie the circadian regulation of *SIG5*. For example, the high mean level of *SIG5* promoter activity in B + R + FR compared with B light (Fig. 4a) might reflect convergence on the *SIG5* promoter of distinct signals that regulate its activity. This could mean that, under certain lighting conditions, basal *SIG5* promoter activity might be increased to a point at which its circadian amplitude becomes reduced or masked. Although circadian oscillations of the *SIG5* promoter and *SIG5* transcript abundance are morning phased, the dawn-phased oscillator component CIRCADIAN CLOCK ASSOCIATED1 (CCA1) does not appear to bind the *SIG5* promoter (Nagel *et al.*, 2015).

The response of *SIG5* to the proportions of red and far red light may involve photosynthetic retrograde signals

The transcriptional response of *SIG5* and *psbD* BLRP to the relative proportions of R and FR light was atypical of regulation by phytochrome alone (Fig. 3). As $FR > c. 700 \text{ nm}$ has insufficient quantum energy to drive oxygenic photosynthesis (Chen & Blankenship, 2011), we reasoned that photosynthetic signals might contribute to this R:FR response because *SIG5* transcription can be regulated by photosynthesis (Melenthin *et al.*, 2014). Moreover, there was little alteration in *SIG5* promoter activity or transcript abundance across much of the R:FR range that induces shade avoidance responses, except for R:FR conditions typical of deeper shade (R:FR below *c.* 0.2) (Smith, 1982). *sig5-3* has been reported to have shorter hypocotyls and smaller cotyledons than the wild-type in either constant R or FR light, 4 d after germination (Khanna *et al.*, 2006). This was interpreted as a cell expansion defect rather than a photomorphogenic phenotype, potentially caused by increased sensitivity of *sig5-3* to light-induced damage (Khanna *et al.*, 2006), which is consistent with the slow recovery of PSII photochemistry after exposure of *sig5* mutants to high light (Nagashima *et al.*, 2004).

One interpretation of the response of *SIG5* to R and FR light is that, when a large proportion of light is FR, little energy is available to drive oxygenic photosynthesis. Under these conditions, the photosynthetic signal that regulates *SIG5* transcription is weak, inhibiting the *phyA* signal and suppressing *SIG5* transcription (Figs 2c, 4b). This would also explain the insensitivity of *SIG5* to DCMU under conditions of predominantly FR light (Fig. 3b), because DCMU inhibits photosynthetic electron transport from PSII to PQ, which decreases substantially under predominantly FR light in which PSII is less activated than PSI.

Interestingly, the differing R:FR response profiles of *SIG5* and *psbD* BLRP suggest that there is post-translational regulation of *SIG5* activity (Fig. 3). This is also supported by our findings that *SIG5* transcripts were not induced by R+FR light in the *phyA* mutant, whereas *psbD* BLRP was induced by higher intensity R+FR light in *phyA* (Fig. 2d); *phyA*-mediated activation of *psbD* BLRP by R+FR light required *phyB*, whereas *phyA*-mediated activation of *SIG5* did not require *phyB* (Fig. S4b); and B light induced *SIG5* through either *cry1* or *cry2*, whereas B light induction of *psbD* BLRP required both *cry1* and *cry2* (Fig. S4c). Post-translational regulation might involve phosphorylation of *SIG5* protein on one or more of its predicted serine/threonine phosphorylation sites, similar to redox-dependent regulation of *SIG1* and chloroplast transcription by PLASTID TRANSCRIPTION KINASE (PTK) and CHLOROPLAST SENSOR KINASE (CSK) (Baena-González *et al.*, 2001; Shimizu *et al.*, 2010). Another possibility is that there is light and/or redox regulation of *SIG5* chloroplast protein import (Küchler *et al.*, 2002; Hörmann *et al.*, 2004). In this context, future analysis of *SIG5* protein biology may be informative. Although there could also be *SIG5*-independent regulation of *psbD* BLRP, this is not supported by an analysis of *psbD* transcripts accumulating from all TSSs of the chloroplast *psbDC* operon (Nagashima *et al.*, 2004). In future, it will be informative to determine whether the regulation of chloroplast transcription by sigma factors contributes to photosynthetic adaptation to shade under light conditions more representative of natural environments, and to investigate the nature of the photosynthetic retrograde signal that regulates *SIG5* in response to changing light conditions.

Conclusions

The regulation of photosynthesis gene expression by sigma factors in response to light appears to be conserved throughout photosynthetic life. It is possible that this signalling pathway evolved as an adaptation to light stress. In cyanobacteria, sigma factors have an important role in maintaining optimum growth under high light conditions by regulating the expression of photosystem components (Hanaoka & Tanaka, 2008; Pollari *et al.*, 2009). This function appears to have been conserved following the endosymbiosis that led to the evolution of chloroplasts, because the regulation of chloroplast genes by sigma factors is important to maintain photosynthetic efficiency under very high light in *Arabidopsis* (Nagashima *et al.*, 2004). Our data suggest that, during evolution, this light stress response pathway has become rewired to also underpin subtle and sophisticated responses to the

light environment by the integration of a conserved signalling pathway with higher plant photoreceptor systems, retrograde signalling and the circadian clock.

Acknowledgements

Funding was from UK BBSRC (BB/I005811/2, BB/J014400/1), the Lady Emily Smyth Agricultural Research Station (Bristol) and the Wolfson Foundation. We thank Paul Devlin (Royal Holloway), Karen Halliday (Edinburgh), Akira Nagatani (Kyoto University) and Mitsumasa Hanaoka (Chiba University) for advice, Anthony Hall (Liverpool), Steven Penfield (John Innes Centre) and Alex Webb (Cambridge) for donating seeds, Dora Cano-Ramirez for assistance with spectrum measurements, and Kan Tanaka (Tokyo Institute of Technology), Alistair Hetherington (Bristol) and Jill Harrison (Bristol) for critical manuscript review. Thanks are also due to Kyoto University for a Guest Professorship (Joint Usage/Research Program of the Center for Ecological Research) and The Royal Society for awarding a University Research Fellowship.

Author contributions

F.E.B., Z.B.N., K.A.F. and A.N.D. conceived and designed the experiments. F.E.B. and Z.B.N. performed the experiments. S.J.W. prepared some transgenics. K.A.A. provided essential technical assistance (Fig. S3). F.E.B., Z.B.N., K.A.F. and A.N.D. interpreted the data and wrote the paper.

References

- Ankele E, Kindgren P, Pesquet E, Strand Å. 2007. *In vivo* visualization of Mg-protoporphyrinIX, a coordinator of photosynthetic gene expression in the nucleus and the chloroplast. *Plant Cell* 19: 1964–1979.
- Baena-González E, Baginsky S, Mulo P, Summer H, Aro E-M, Link G. 2001. Chloroplast transcription at different light intensities. Glutathione-mediated phosphorylation of the major RNA polymerase involved in redox-regulated organellar gene expression. *Plant Physiology* 127: 1044–1052.
- Bognár LK, Hall A, Adam É, Thain SC, Nagy F, Millar AJ. 1999. The circadian clock controls the expression pattern of the circadian input photoreceptor, phytochrome B. *Proceedings of the National Academy of Sciences, USA* 96: 14652–14657.
- Bonardi V, Pesaresi P, Becker T, Schleiff E, Wagner R, Pfannschmidt T, Jahns P, Leister D. 2005. Photosystem II core phosphorylation and photosynthetic acclimation require two different protein kinases. *Nature* 437: 1179–1182.
- Brown BA, Jenkins GI. 2008. UV-B signaling pathways with different fluence-rate response profiles are distinguished in mature *Arabidopsis* leaf tissue by requirement for UVR8, HY5, and HYH. *Plant Physiology* 146: 576–588.
- Bruggemann EP, Doan B, Handwerker K, Storz G. 1998. Characterization of an unstable allele of the *Arabidopsis* *HY4* locus. *Genetics* 149: 1575–1585.
- Casal JJ. 2013. Photoreceptor signaling networks in plant responses to shade. *Annual Review of Plant Biology* 64: 403–427.
- Chen M, Blankenship RE. 2011. Expanding the solar spectrum used by photosynthesis. *Trends in Plant Science* 16: 427–431.
- Dalchau N, Baek SJ, Briggs HM, Robertson FC, Dodd AN, Gardner MJ, Stancombe MA, Haydon MJ, Stan G-B, Gonçalves JM *et al.* 2011. The circadian oscillator gene *GIGANTEA* mediates a long-term response of the *Arabidopsis thaliana* circadian clock to sucrose. *Proceedings of the National Academy of Sciences, USA* 108: 5104–5109.

- Devlin PF, Kay SA. 2000. Cryptochromes are required for phytochrome signaling to the circadian clock but not for rhythmicity. *Plant Cell* 12: 2499–2509.
- Dodd AN, Dalchau N, Gardner MJ, Baek SJ, Webb AAR. 2014. The circadian clock has transient plasticity of period and is required for timing of nocturnal processes in Arabidopsis. *New Phytologist* 201: 168–179.
- Dodd AN, Salathia N, Hall A, Kévei E, Tóth R, Nagy F, Hibberd JM, Millar AJ, Webb AAR. 2005. Plant circadian clocks increase photosynthesis, growth, survival, and competitive advantage. *Science* 309: 630–633.
- El-Assal S, Alonso-Blanco C, Peeters AJM, Wagemaker C, Weller JL, Koornneef M. 2003. The role of cryptochrome 2 in flowering in Arabidopsis. *Plant Physiology* 133: 1504–1516.
- Franklin KA. 2008. Shade avoidance. *New Phytologist* 179: 930–944.
- Fujii G, Imamura S, Era A, Miyagishima S, Hanaoka M, Tanaka K. 2015. The nuclear-encoded sigma factor SIG4 directly activates transcription of chloroplast *psbA* and *ycf17* genes in the unicellular red alga *Cyanidioschyzon merolae*. *FEMS Microbiology Letters* 362: fnv063.
- Gamble PE, Mullet JE. 1989. Blue light regulates the accumulation of two *psbD-psbC* transcripts in barley chloroplasts. *EMBO Journal* 8: 2785–2794.
- Gould PD, Ugarte N, Domijan M, Costa M, Foreman J, MacGregor D, Rose K, Griffiths J, Millar AJ, Finkenzel B *et al.* 2003. Network balance via CR1 signalling controls the Arabidopsis circadian clock over ambient temperatures. *Molecular Systems Biology* 9: 650.
- Guo H, Yang H, Mockler TC, Lin C. 1998. Regulation of flowering time by Arabidopsis photoreceptors. *Science* 279: 1360–1363.
- Hanaoka M, Kanamaru K, Takahashi H, Tanaka K. 2003. Molecular genetic analysis of chloroplast gene promoters dependent on SIG2, a nucleus-encoded sigma factor for the plastid-encoded RNA polymerase, in Arabidopsis thaliana. *Nucleic Acids Research* 31: 7090–7098.
- Hanaoka M, Tanaka K. 2008. Dynamics of RpaB-promoter interaction during high light stress, revealed by chromatin immunoprecipitation (ChIP) analysis in *Synechococcus elongatus* PCC 7942. *Plant Journal* 56: 327–335.
- Harmer SL, Hogenesch JB, Straume M, Chang H-S, Han B, Zhu T, Wang X, Kreps JA, Kay SA. 2000. Orchestrated transcription of key pathways in Arabidopsis by the circadian clock. *Science* 290: 2110–2113.
- Haydon MJ, Mielczarek O, Robertson FC, Hubbard KE, Webb AAR. 2013. Photosynthetic entrainment of the Arabidopsis thaliana circadian clock. *Nature* 502: 689–692.
- Hoffer PH, Christopher DA. 1997. Structure and blue-light-responsive transcription of a chloroplast *psbD* promoter from Arabidopsis thaliana. *Plant Physiology* 115: 213–222.
- Hörmann F, Küchler M, Sveshnikov D, Oppermann U, Li Y, Soll J. 2004. Tic32, an essential component in chloroplast biogenesis. *Journal of Biological Chemistry* 279: 34756–34762.
- Hu W, Franklin KA, Sharrack RA, Jones MA, Harmer SL, Lagarias JC. 2013. Unanticipated regulatory roles for Arabidopsis phytochromes revealed by null mutant analysis. *Proceedings of the National Academy of Sciences, USA* 110: 1542–1547.
- Ichikawa K, Shimizu A, Okada R, Satbhai SB, Aoki S. 2008. The plastid sigma factor SIG5 is involved in the diurnal regulation of the chloroplast gene *psbD* in the moss *Physcomitrella patens*. *FEBS Letters* 582: 405–409.
- Ichikawa K, Sugita M, Imaizumi T, Wada M, Aoki S. 2004. Differential expression on a daily basis of plastid sigma factor genes from the moss *Physcomitrella patens*. Regulatory interactions among *PpSig5*, the circadian clock, and blue light signaling mediated by cryptochromes. *Plant Physiology* 136: 4285–4298.
- Imamura S, Yoshihara S, Nakano S, Shiozaki N, Yamada A, Tanaka K, Takahashi H, Asayama M, Shirai M. 2003. Purification, characterization, and gene expression of all sigma factors of RNA polymerase in a cyanobacterium. *Journal of Molecular Biology* 325: 857–872.
- Kanamaru K, Fujiwara M, Seki M, Katagiri T, Nakamura M, Mochizuki N, Nagatani A, Shinozaki K, Tanaka K, Takahashi H. 1999. Plastidic RNA polymerase σ factors in Arabidopsis. *Plant and Cell Physiology* 40: 832–842.
- Kanazawa T, Ishizaki K, Kohchi T, Hanaoka M, Tanaka K. 2013. Characterization of four nuclear-encoded plastid RNA polymerase sigma factor genes in the liverwort *Marchantia polymorpha*: blue-light- and multiple stress-responsive SIG5 was acquired early in the emergence of terrestrial plants. *Plant and Cell Physiology* 54: 1736–1748.
- Khanna R, Shen Y, Toledo-Ortiz G, Kikis EA, Johannesson H, Hwang Y-S, Quail PH. 2006. Functional profiling reveals that only a small number of phytochrome-regulated early-response genes in Arabidopsis are necessary for optimal deetiolation. *Plant Cell* 18: 2157–2171.
- Klein RR, Mullet JE. 1990. Light-induced transcription of chloroplast genes. *psbA* transcription is differentially enhanced in illuminated barley. *Journal of Biological Chemistry* 265: 1895–1902.
- Kubota Y, Miyao A, Hirochika H, Tozawa Y, Yasuda H, Tsunoyama Y, Niwa Y, Imamura S, Shirai M, Asayama M. 2007. Two novel nuclear genes, *OsSIG5* and *OsSIG6*, encoding potential plastid sigma factors of RNA polymerase in rice: tissue-specific and light-responsive gene expression. *Plant and Cell Physiology* 48: 186–192.
- Küchler M, Decker S, Hörmann F, Soll J, Heins L. 2002. Protein import into chloroplasts involves redox-regulated proteins. *EMBO Journal* 21: 6136–6145.
- Love J, Dodd AN, Webb AAR. 2004. Circadian and diurnal calcium oscillations encode photoperiodic information in Arabidopsis. *Plant Cell* 16: 956–966.
- Martínez-García JF, Gallemler M, Molina-Contreras MJ, Llorente B, Bevilacqua MRR, Quail PH. 2014. The shade avoidance syndrome in Arabidopsis: the antagonistic role of Phytochrome A and B differentiates vegetation proximity and canopy shade. *PLoS ONE* 9: e109275.
- Mellenthin M, Ellersiek U, Börger A, Baier M. 2014. Expression of the Arabidopsis sigma factor SIG5 is photoreceptor and photosynthesis controlled. *Plants* 3: 359–391.
- Michael TP, Mockler TC, Breton G, McEntee C, Byer A, Trout JD, Hazen SP, Shen R, Priest HD, Sullivan CM *et al.* 2008. Network discovery pipeline elucidates conserved time-of-day-specific cis-regulatory modules. *PLoS Genetics* 4: e14.
- Mochizuki T, Onda Y, Fujiwara E, Wada M, Toyoshima Y. 2004. Two independent light signals cooperate in the activation of the plastid *psbD* blue light-responsive promoter in Arabidopsis. *FEBS Letters* 571: 26–30.
- Mockler T, Yang H, Yu X, Parikh D, Cheng Y-C, Dolan S, Lin C. 2003. Regulation of photoperiodic flowering by Arabidopsis photoreceptors. *Proceedings of the National Academy of Sciences, USA* 100: 2140–2145.
- Monte E, Tepperman JM, Al-Sady B, Kaczorowski KA, Alonso JM, Ecker JR, Li X, Zhang Y, Quail PH. 2004. The phytochrome-interacting transcription factor, PIF3, acts early, selectively, and positively in light-induced chloroplast development. *Proceedings of the National Academy of Sciences, USA* 101: 16091–16098.
- Nagashima A, Hanaoka M, Shikanai T, Fujiwara M, Kanamaru K, Takahashi H, Tanaka K. 2004. The multiple-stress responsive plastid sigma factor, SIG5, directs activation of the *psbD* blue light responsive promoter (BLRP) in Arabidopsis thaliana. *Plant and Cell Physiology* 45: 357–368.
- Nagatani A, Reed JW, Chory J. 1993. Isolation and initial characterization of Arabidopsis mutants that are deficient in Phytochrome A. *Plant Physiology* 102: 269–277.
- Nagel DH, Doherty CJ, Prunedo-Paz JL, Schmitz RJ, Ecker JR, Kay SA. 2015. Genome-wide identification of CCA1 targets uncovers an expanded clock network in Arabidopsis. *Proceedings of the National Academy of Sciences, USA* 112: E4802–E4810.
- Nagel DH, Kay SA. 2012. Complexity in the wiring and regulation of plant circadian networks. *Current Biology* 22: R648–R657.
- Nakahira Y, Baba K, Yoneda A, Shiina T, Toyoshima Y. 1998. Circadian-regulated transcription of the *psbD* light-responsive promoter in wheat chloroplasts. *Plant Physiology* 118: 1079–1088.
- Noordally ZB, Ishii K, Atkins KA, Wetherill SJ, Kusakina J, Walton EJ, Kato M, Azuma M, Tanaka K, Hanaoka M *et al.* 2013. Circadian control of chloroplast transcription by a nuclear-encoded timing signal. *Science* 339: 1316–1319.
- Onda Y, Yagi Y, Saito Y, Takenaka N, Toyoshima Y. 2008. Light induction of Arabidopsis SIG1 and SIG5 transcripts in mature leaves: differential roles of cryptochrome 1 and cryptochrome 2 and dual function of SIG5 in the recognition of plastid promoters. *Plant Journal* 55: 968–978.
- Pannschmidt T, Nilsson A, Allen JF. 1999. Photosynthetic control of chloroplast gene expression. *Nature* 397: 625–628.

- Pollari M, Ruotsalainen V, Rantamäki S, Tyystjärvi E, Tyystjärvi T. 2009. Simultaneous inactivation of sigma factors B and D interferes with light acclimation of the cyanobacterium *Synechocystis* sp. strain PCC 6803. *Journal of Bacteriology* 191: 3992–4001.
- Puthiyaveetil S, Ibrahim IM, Allen JF. 2011. Oxidation–reduction signalling components in regulatory pathways of state transitions and photosystem stoichiometry adjustments in chloroplasts. *Plant, Cell & Environment* 35: 347–359.
- Puthiyaveetil S, Kavanagh TA, Cain P, Sullivan JA, Newell CA, Gray JC, Robinson C, van der Giezen M, Rogers MB, Allen JF. 2008. The ancestral symbiont sensor kinase CSK links photosynthesis with gene expression in chloroplasts. *Proceedings of the National Academy of Sciences, USA* 105: 10061–10066.
- Reed JW, Nagatani A, Elich TD, Fagan M, Chory J. 1994. Phytochrome A and Phytochrome B have overlapping but distinct functions in Arabidopsis development. *Plant Physiology* 104: 1139–1149.
- Rockwell NC, Duanmu D, Martin SS, Bachy C, Price DC, Bhattacharya D, Worden AZ, Lagarias JC. 2014. Eukaryotic algal phytochromes span the visible spectrum. *Proceedings of the National Academy of Sciences, USA* 111: 3871–3876.
- Sharrock RA, Clack T. 2002. Patterns of expression and normalized levels of the five Arabidopsis phytochromes. *Plant Physiology* 130: 442–456.
- Shimizu M, Kato H, Ogawa T, Kurachi A, Nakagawa Y, Kobayashi H. 2010. Sigma factor phosphorylation in the photosynthetic control of photosystem stoichiometry. *Proceedings of the National Academy of Sciences, USA* 107: 10760–10764.
- Smith H. 1982. Light quality, photoperception, and plant strategy. *Annual Review of Plant Physiology* 33: 481–518.
- Somers DE, Devlin PF, Kay SA. 1998. Phytochromes and cryptochromes in the entrainment of the Arabidopsis circadian clock. *Science* 282: 1488–1490.
- Southern MM, Millar AJ. 2005. Circadian genetics in the model higher plant *Arabidopsis thaliana*. *Methods in Enzymology* 393: 23–35.
- Tepperman JM, Hwang Y-S, Quail PH. 2006. phyA dominates in transduction of red-light signals to rapidly responding genes at the initiation of Arabidopsis seedling de-etiolation. *Plant Journal* 48: 728–742.
- Thum KE, Kim M, Christopher DA, Mullet JE. 2001. Cryptochrome 1, Cryptochrome 2, and Phytochrome A co-activate the chloroplast *psbD* blue light-responsive promoter. *Plant Cell* 13: 2747–2760.
- Tóth R, Kevei É, Hall A, Millar AJ, Nagy F, Kozma-Bognár L. 2001. Circadian clock-regulated expression of phytochrome and cryptochrome genes in Arabidopsis. *Plant Physiology* 127: 1607–1616.
- Tsinoremas NF, Ishiura M, Kondo T, Anderson CR, Tanaka K, Takahashi H, Johnson CH, Golden SS. 1996. A sigma factor that modifies the circadian expression of a subset of genes in cyanobacteria. *EMBO Journal* 15: 2488–2495.
- Ueda M, Takami T, Peng L, Ishizaki K, Kohchi T, Shikanai T, Nishimura Y. 2013. Subfunctionalization of sigma factors during the evolution of land plants based on mutant analysis of liverwort (*Marchantia polymorpha* L.). *MpSIG1. Genome Biology and Evolution* 5: 1836–1848.
- Wenden B, Kozma-Bognár L, Edwards KD, Hall AJW, Locke JCW, Millar AJ. 2011. Light inputs shape the Arabidopsis circadian system. *Plant Journal* 66: 480–491.
- Xu X, Hotta CT, Dodd AN, Love J, Sharrock R, Lee YW, Xie Q, Johnson CH, Webb AAR. 2007. Distinct light and clock modulation of cytosolic free Ca^{2+} oscillations and rhythmic *CHLOROPHYLL A/B BINDING PROTEIN2* promoter activity in Arabidopsis. *Plant Cell* 19: 3474–3490.
- Yamburenko MV, Zubo YO, Börner T. 2015. Abscisic acid affects transcription of chloroplast genes via protein phosphatase 2C-dependent activation of nuclear genes: repression by guanosine-3'-5'-bisdiphosphate and activation by sigma factor 5. *Plant Journal* 82: 1030–1041.

Supporting Information

Additional Supporting Information may be found online in the Supporting Information tab for this article:

Fig. S1 Initial circadian period characterization of multiple luciferase lines.

Fig. S2 Spectra of light treatments used in this study.

Fig. S3 Efficacy of 3-(3,4-dichlorophenyl)-1,1-dimethylurea (DCMU) and norflurazon under our experimental conditions.

Fig. S4 Analysis of photoreceptors involved in SIGMA FACTOR5 (SIG5)-mediated regulation of chloroplast *psbD* blue light-responsive promoter (BLRP).

Fig. S5 Circadian regulation of *SIG5::LUCIFERASE* by light quality and photoreceptors.

Fig. S6 Circadian regulation of *SIG5::LUCIFERASE* in the Col-0 background by light quality.

Please note: Wiley Blackwell are not responsible for the content or functionality of any Supporting Information supplied by the authors. Any queries (other than missing material) should be directed to the *New Phytologist* Central Office.

Bibliography

- Abbaspoor, M., Teicher, H. B., and Streibig, J. C. 2006. The effect of root-absorbed PSII inhibitors on Kautsky curve parameters in sugar beet. *Weed Research*, 46: 226–235.
- Abendroth, J. A., Martin, A. R., and Roeth, F. W. 2006. Plant Response to Combinations of Mesotrione and Photosystem II Inhibitors. *Weed Technology*, 20(1): 267–274.
- Adams, S., Manfield, I., Stockley, P., and Carré, I. A. 2015. Revised Morning Loops of the Arabidopsis Circadian Clock Based on Analyses of Direct Regulatory Interactions. *PLoS ONE*, 10(12).
- Alabadí, D., Oyama, T., Yanovsky, M. J., Harmon, F. G., Más, P., and Kay, S. A. 2001. Reciprocal regulation between TOC1 and LHY/CCA1 within the Arabidopsis circadian clock. *Science*, 293(5531):880–883.
- Alatorre-Cobos, F., Cruz-Ramírez, A., Hayden, C. A., Pérez-Torres, C.-A., Chauvin, A.-L., Ibarra-Laclette, E., Alva-Cortés, E., Jorgensen, R. A., and Herrera-Estrella, L. 2012. Translational regulation of Arabidopsis *XIPOTL1* is modulated by phosphocholine levels via the phylogenetically conserved upstream open reading frame 30. *Journal of Experimental Botany*, 63(13):5203–5221.
- Alibhai, M. F. and Stallings, W. C. 2001. Closing down on glyphosate inhibition - with a new structure for drug discovery. *Proceedings of the National Academy of Sciences*, 98(6):2944–2946.
- Amrhein, N., Deus, B., Gehrke, P., and Steinrücken, H. 1980. The site of the inhibition of the shikimate pathway by glyphosate. *Plant Physiology*, 66:830–834.
- Aper, J., Mechant, E., Rubin, B., Heyerick, A., Callebaut, G., Mangelinckx, S., Deforce, D., De Kimpe, N., Bulcke, R., and Reheul, D. 2012. Absorption, translocation and metabolism of metamitron in *Chenopodium album*. *Pest Management Science*, 68:209–216.
- Arregui, M. C., Lenardón, A., Sanchez, D., Maitre, M. I., Scotta, R., and Enrique, S. 2003. Monitoring glyphosate residues in transgenic glyphosate-resistant soybean. *Pest Management Science*, 60:163–166.
- Aschoff, J. 1960. Exogenous and Endogenous Components in Circadian Rhythms. *Cold Spring Harbor Symposia on Quantitative Biology*, 25:11–28.
- Aschoff, J. 1979. Circadian Rhythms: Influences of Internal and External Factors on

- the Period Measured in Constant Conditions. *Zeitschrift für Tierpsychologie*, 49: 225–249.
- Assalin, M. R., De Moraes, S. G., Queiroz, S. C. N., Ferracini, V. L., and Duran, N. 2010. Studies on degradation of glyphosate by several oxidative chemical processes: Ozonation, photolysis and heterogeneous photocatalysis. *Journal of Environmental Science and Health, Part B*, 45:89–94.
- Baek, D., Nam, J., Koo, Y. D., Kim, D. H., Lee, J., Jeong, J. C., Kwak, S. S., Chung, W. S., Lim, C. O., Bahk, J. D., Hong, J. C., Lee, S. Y., Kawai-Yamada, M., Uchimiyama, H., and Yun, D.-J. 2004. Bax-induced cell death of *Arabidopsis* is mediated through reactive oxygen-dependent and -independent processes. *Plant Molecular Biology*, 56:15–27.
- Bahieldin, A., Atef, A., Edris, S., Gadalla, N. O., Ramadan, A. M., Hassan, S. M., Al Attas, S. G., Al-Kordy, M. A., Al-Hajar, A. S. M., Sabir, J. S. M., Nasr, M. E., Osman, G. H., and El-Domyati, F. M. 2018. Multifunctional activities of ERF109 as affected by salt stress in *Arabidopsis*. *Scientific Reports*, 8(6403).
- Ballesta, A., Innominato, P. F., Dallmann, R., Rand, D. A., and Lévi, F. A. 2017. Systems Chronotherapeutics. *Pharmacological Reviews*, 69:161–199.
- Barbagallo, R. P., Oxborough, K., Pallett, K. E., and Baker, N. R. 2003. Rapid, Noninvasive Screening for Perturbations of Metabolism and Plant Growth Using Chlorophyll Fluorescence Imaging. *Plant Physiology*, 132:485–493.
- Barchanska, H., Kluza, A., Krajczewska, K., and Maj, J. 2016. Degradation study of mesotrione and other triketone herbicides on soils and sediments. *Journal of Soils and Sediments*, 16:125–133.
- Barlier, I., Kowalczyk, M., Marchant, A., Ljung, K., Bhalerao, R., Bennett, M., Sandberg, G., and Bellini, C. 2000. The *SUR2* gene of *Arabidopsis thaliana* encodes the cytochrome P450 CYP83B1, a modulator of auxin homeostasis. *Proceedings of the National Academy of Sciences*, 97(26):14819–14824.
- Baudry, A., Ito, S., Song, Y. H., Strait, A. A., Kiba, T., Lu, S., Henriques, R., Prunedapaz, J. L., Chua, N.-H., Tobin, E. M., Kay, S. A., and Imaizumi, T. 2010. F-Box proteins FKF1 and LKP2 act in concert with ZEITLUPE to control *Arabidopsis* clock progression. *The Plant Cell*, 22:606–622.
- Baur, J. R. 1979. Effect of Glyphosate on Auxin Transport in Corn and Cotton Tissues. *Plant Physiology*, 63:882–886.
- Beaudegnies, R., Edmunds, A. J. F., Fraser, T. E. M., Hall, R. G., Hawkes, T. R., Mitchell, G., Schaetzer, J., Wendeborn, S., and Wibley, J. 2009. Herbicidal 4-hydroxyphenylpyruvate dioxygenase inhibitors-A review of the triketone chemistry story from a Syngenta perspective. *Bioorganic & Medicinal Chemistry*, 17:4134–4152.
- Beckie, H. J. and Tardif, F. J. 2012. Herbicide cross resistance in weeds. *Crop Protection*, 35:15–28.
- Begara-Morales, J. C., Sánchez-Calvo, B., Luque, F., Leyva-Pérez, M. O., Leterrier, M., Corpas, F. J., and Barroso, J. B. 2014. Differential transcriptomic analysis by

- RNA-Seq of GSNO-responsive genes between *Arabidopsis* roots and leaves. *Plant and Cell Physiology*, 55(6):1080–1095.
- Beltran, J. C., Pannell, D. J., and Doole, G. J. 2012. Economic implications of herbicide resistance and high labour costs for management of annual barnyardgrass (*Echinochloa crus-galli*) in Philippine rice farming systems. *Crop Protection*, 31: 31–39.
- Benbrook, C. M. 2016. Trends in glyphosate herbicide use in the United States and globally. *Environmental Sciences Europe*, 28(3).
- Bennett, L. D., Beremand, P., Thomas, T. L., and Bell-Pedersen, D. 2013. Circadian activation of the mitogen-activated protein kinase MAK-1 facilitates rhythms in clock-controlled genes in *Neurospora crassa*. *Eukaryotic Cell*, 12(1):59–69.
- Bernal, J., Martin, M. T., Soto, M. E., Nozal, M. J., Marotti, I., Dinelli, G., and Bernal, J. L. 2012. Development and application of a liquid chromatography-mass spectrometry method to evaluate the glyphosate and aminomethylphosphonic acid dissipation in maize plants after foliar treatment. *Journal of Agricultural and Food Chemistry*, 60:4017–4025.
- Bernard, V., Brunaud, V., and Lecharny, A. 2010. TC-motifs at the TATA-box expected position in plant genes: a novel class of motifs involved in the transcription regulation. *BMC Genomics*, 11(116).
- Bethke, G., Grundman, R. E., Sreekanta, S., Truman, W., Katagiri, F., and Glazebrook, J. 2014. *Arabidopsis* PECTIN METHYLESTERASEs contribute to immunity against *Pseudomonas syringae*. *Plant Physiology*, 164:1093–107.
- Bhardwaj, V., Meier, S., Petersen, L. N., Ingle, R. A., and Roden, L. C. 2011. Defence responses of *Arabidopsis thaliana* to infection by *Pseudomonas syringae* are regulated by the circadian clock. *PLoS ONE*, 6(10).
- Blancard, D. Tobacco - Various chemical injuries, 2017.
- Bläsing, O. E., Gibon, Y., Günther, M., Höhne, M., Morcuende, R., Osuna, D., Thimm, O., Usadel, B., Scheible, W., and Stitt, M. 2005. Sugars and Circadian Regulation Make Major Contributions to the Global Regulation of Diurnal Gene Expression in *Arabidopsis*. *The Plant Cell*, 17:3257–3281.
- Boerjan, W., Cervera, M.-T., Delarue, M., Beeckman, T., Dewitte, W., Bellini, C., Caboche, M., van Onckelen, H., van Montagu, M., and Inze, D. 2007. *Superroot*, a recessive mutation in *Arabidopsis*, confers auxin overproduction. *The Plant Cell*, 7:1405–1419.
- Bohne, F. and Linden, H. 2002. Regulation of carotenoid biosynthesis genes in response to light in *Chlamydomonas reinhardtii*. *Biochimica et Biophysica Acta*, 1579:26–34.
- Bonnet, J. L., Bonnemoy, F., Dusser, M., and Bohatier, J. 2008. Toxicity assessment of the herbicides sulcotrione and mesotrione toward two reference environmental microorganisms: *Tetrahymena pyriformis* and *Vibrio fischeri*. *Archives of Environmental Contamination and Toxicology*, 55:576–583.

- Borggaard, O. K. and Gimsing, A. L. 2008. Fate of glyphosate in soil and the possibility of leaching to ground and surface waters: a review. *Pest Management Science*, 64:441–456.
- Boyes, D. C., Zayed, A. M., Ascenzi, R., McCaskill, A. J., Hoffman, N. E., Davis, K. R., and Görlach, J. 2001. Growth stage-based phenotypic analysis of Arabidopsis: a model for high throughput functional genomics in plants. *The Plant Cell*, 13:1499–510.
- Brotherton, J. E., Jeschke, M. R., Tranel, P. J., and Widholm, J. M. 2007. Identification of *Arabidopsis thaliana* variants with differential glyphosate responses. *Journal of Plant Physiology*, 164:1337–1345.
- Brown, P., Baxter, L., Hickman, R., Beynon, J., Moore, J. D., and Ott, S. 2013. MEME-LaB: Motif analysis in clusters. *Bioinformatics*, 29(13):1696–1697.
- Brunoud, G., Wells, D. M., Oliva, M., Larrieu, A., Mirabet, V., Burrow, A. H., Beckman, T., Kepinski, S., Traas, J., Bennett, M. J., and Vernoux, T. 2012. A novel sensor to map auxin response and distribution at high spatio-temporal resolution. *Nature*, 482:103–106.
- Caderas, D., Muster, M., Vogler, H., Mandel, T., Rose, J. K., McQueen-Mason, S., and Kuhlemeier, C. 2000. Limited correlation between Expansin gene expression and elongation growth rate. *Plant Physiology*, 123:1399–1414.
- Cai, X.-T., Xu, P., Zhao, P.-X., Liu, R., Yu, L.-H., and Xiang, C.-B. 2014. Arabidopsis ERF109 mediates cross-talk between jasmonic acid and auxin biosynthesis during lateral root formation. *Nature Communications*, 5(5833).
- Cañal, M. J., Sánchez Tamés, R., and Fernández, B. 1990. Glyphosate action on abscisic acid levels, stomatal response and electrolyte leakage in yellow nutsedge leaves. *Plant Physiology and Biochemistry*, 28(2):215–220.
- Cañero, A. I., Cox, L., Redondo-Gómez, S., Mateos-Naranjo, E., Hermosín, M. C., and Cornejo, J. 2011. Effect of the herbicides terbuthylazine and glyphosate on photosystem II photochemistry of young olive (*Olea europaea*) plants. *Journal of Agricultural and Food Chemistry*, 59:5528–5534.
- Carbonari, C. A., Gomes, G. L. G. C., Velini, E. D., Machado, R. F., Simões, P. S., and Macedo, G. 2014. Glyphosate Effects on Sugarcane Metabolism and Growth. *American Journal of Plant Sciences*, 5:3585–3593.
- Carles, L., Joly, M., and Joly, P. 2017. Mesotrione herbicide: Efficiency, effects, and fate in the environment after 15 years of agricultural use. *Clean - Soil, Air, Water*, 45(9).
- Carretero-Paulet, L., Galstyan, A., Roig-Villanova, I., Martinez-Garcia, J. F., Bilbao-Castro, J. R., and Robertson, D. L. 2010. Genome-wide classification and evolutionary analysis of the bHLH family of transcription factors in Arabidopsis, poplar, rice, moss, and algae. *Plant Physiology*, 153:1398–1412.
- Cartharius, K., Frech, K., Grote, K., Klocke, B., Haltmeier, M., Klingenhoff, A., Frisch, M., Bayerlein, M., and Werner, T. 2005. MatInspector and beyond: pro-

- moter analysis based on transcription factor binding sites. *Bioinformatics*, 21(13): 2933–2942.
- Casson, S. A. and Hetherington, A. M. 2014. Phytochrome B is required for light-mediated systemic control of stomatal development. *Current Biology*, 24(11):1216–1221.
- Cebeci, O. and Budak, H. 2009. Global expression patterns of three *Festuca* species exposed to different doses of glyphosate using the Affymetrix GeneChip Wheat Genome Array. *Comparative and Functional Genomics*.
- Cha, J.-Y., Lee, D.-Y., Ali, I., Jeong, S. Y., Shin, B., Ji, H., Kim, J. S., Kim, M.-G., and Kim, W.-Y. 2019. Arabidopsis *GIGANTEA* negatively regulates chloroplast biogenesis and resistance to herbicide butafenacil. *Plant Cell Reports*.
- Chen, J., Huang, H., Wei, S., Huang, Z., Wang, X., and Zhang, C. 2017. Investigating the mechanisms of glyphosate resistance in goosegrass (*Eleusine indica* (L.) Gaertn.) by RNA sequencing technology. *The Plant Journal*, 89:407–415.
- Chen, L., Song, Y., Li, S., Zhang, L., Zou, C., and Yu, D. 2012. The role of WRKY transcription factors in plant abiotic stresses. *Biochimica et Biophysica Acta*, 1819: 120–128.
- Chen, S. and Dickman, M. B. 2004. Bcl-2 family members localize to tobacco chloroplasts and inhibit programmed cell death induced by chloroplast-targeted herbicides. *Journal of Experimental Botany*, 55(408):2617–2623.
- Chen, W., Salari, H., Taylor, M. C., Jost, R., Berkowitz, O., Barrow, R., Masle, J., Qiu, D., Branco, R., and Masle, J. 2018. NMT1 and NMT3 *N*-Methyltransferase activity is critical to lipid homeostasis, morphogenesis and reproduction. *Plant Physiology*, 177:1605–1628.
- Chen, W., Taylor, M. C., Barrow, R. A., Croyal, M., and Masle, J. 2019. Loss of Phosphoethanolamine *N*-Methyltransferases Abolishes Phosphatidylcholine Synthesis and Is Lethal. *Plant Physiology*, 179:124–142.
- Chen, Y.-Y., Wang, Y., Shin, L.-J., Wu, J.-F., Shanmugam, V., Tsednee, M., Lo, J.-C., Chen, C.-C., Wu, S.-H., and Yeh, K.-C. 2013. Iron is involved in the maintenance of circadian period length in Arabidopsis. *Plant Physiology*, 161:1409–1420.
- Chen, Z. J. and Mas, P. 2019. Interactive roles of chromatin regulation and circadian clock function in plants. *Genome Biology*, 20(62).
- Cheng, Y., Dai, X., and Zhao, Y. 2006. Auxin biosynthesis by the YUCCA flavin monooxygenases controls the formation of floral organs and vascular tissues in Arabidopsis. *Genes & Development*, 20:1790–1799.
- Ching, T. T., Hamilton, R. H., and Bandurski, R. S. 1956. Selective inhibition of the geotropic response by *n*-1-Naphthylphthalamic acid. *Physiologia Plantarum*, 9: 546–558.
- Choi, H. and Oh, E. 2016. PIF4 integrates multiple environmental and hormonal signals for plant growth regulation in Arabidopsis. *Molecules and Cells*, 39(8): 587–593.

- Christensen, A. M. and Schaefer, J. 1993. Solid-state NMR determination of intra- and intermolecular ^{31}P - ^{13}C distances for shikimate 3-phosphate and $[1\text{-}^{13}\text{C}]$ glyphosate bound to enolpyruvylshikimate-3-phosphate synthase. *Biochemistry*, 32:2868–2873.
- Christensen, M. G., Teicher, H. B., and Streibig, J. C. 2003. Linking fluorescence induction curve and biomass in herbicide screening. *Pest Management Science*, 59: 1303–1310.
- Clor, M. A., Crafts, A. S., and Yamaguchi, S. 1963. Effects of high humidity on translocation of foliar-applied labeled compounds in plants. II. Translocation from starved leaves. *Plant Physiology*, pages 501–507.
- Cobb, A. H. and Reade, J. P. 2010. *Auxin-Type Herbicides, in Herbicides and Plant Physiology*.
- Coll, N. S., Vercammen, D., Smidler, A., Clover, C., Van Breusegem, F., Dangl, J. L., and Epple, P. 2010. Arabidopsis type I metacaspases control cell death. *Science*, 330(6009):1393–1397.
- Conesa, A., Madrigal, P., Tarazona, S., Gomez-Cabrero, D., Cervera, A., McPherson, A., Szczeniński, M. W., Gaffney, D. J., Elo, L. L., Zhang, X., and Mortazavi, A. 2016. A survey of best practices for RNA-seq data analysis. *Genome Biology*, 17 (13).
- Covington, M. F. and Harmer, S. L. 2007. The circadian clock regulates auxin signaling and responses in Arabidopsis. *PLoS Biology*, 5(8):1773–1784.
- Crouzet, O., Wiszniewski, J., Donnadieu, F., Bonnemoy, F., Bohatier, J., and Mallet, C. 2013. Dose-dependent effects of the herbicide mesotrione on soil cyanobacterial communities. *Archives of Environmental Contamination and Toxicology*, 64:23–31.
- Czechowski, T., Stitt, M., Altmann, T., Udvardi, M. K., and Scheible, W.-R. 2005. Genome-wide identification and testing of superior reference genes for transcript normalization in Arabidopsis. *Plant Physiology*, 139:5–17.
- Dai, X., Mashiguchi, K., Chen, Q., Kasahara, H., Kamiya, Y., Ojha, S., DuBois, J., Ballou, D., and Zhao, Y. 2013. The biochemical mechanism of auxin biosynthesis by an Arabidopsis YUCCA flavin-containing monooxygenase. *Journal of Biological Chemistry*, 288(3):1448–1457.
- Dalchau, N., Baek, S. J., Briggs, H. M., Robertson, F. C., Dodd, A. N., Gardner, M. J., Stancombe, M. A., Haydon, M. J., Stan, G.-B., Gonçalves, J. M., and Webb, A. A. R. 2011. The circadian oscillator gene *GIGANTEA* mediates a long-term response of the *Arabidopsis thaliana* circadian clock to sucrose. *Proceedings of the National Academy of Sciences*, 108(12):5104–5109.
- Daniel, X., Sugano, S., and Tobin, E. M. 2004. CK2 phosphorylation of CCA1 is necessary for its circadian oscillator function in Arabidopsis. *Proceedings of the National Academy of Sciences*, 101(9):3292–3297.
- Danon, A., Rotari, V. I., Gordon, A., Mailhac, N., and Gallois, P. 2004. Ultraviolet-C overexposure induces Programmed Cell Death in Arabidopsis, which is mediated by caspase-like activities and which can be suppressed by caspase inhibitors, p35

- and *Defender against Apoptotic Death*. *The Journal of Biological Chemistry*, 279 (1):779–787.
- Das, M., Reichman, J. R., Haberer, G., Welzl, G., Aceituno, F. F., Mader, M. T., Watrud, L. S., Pflieger, T. G., Gutiérrez, R. A., Schöffner, A. R., and Olszyk, D. M. 2010. A composite transcriptional signature differentiates responses towards closely related herbicides in *Arabidopsis thaliana* and *Brassica napus*. *Plant Molecular Biology*, 72:545–556.
- Dave, A., Hernández, M. L., He, Z., Andriotis, V. M., Vaistij, F. E., Larson, T. R., and Graham, I. A. 2011. 12-oxo-phytodienoic acid accumulation during seed development represses seed germination in *Arabidopsis*. *The Plant Cell*, 23:583–599.
- Dave, A., Vaistij, F. E., Gilday, A. D., Penfield, S. D., and Graham, I. A. 2016. Regulation of *Arabidopsis thaliana* seed dormancy and germination by 12-oxo-phytodienoic acid. *Journal of Experimental Botany*, 67(8):2277–2284.
- Dayan, F. E., Duke, S. O., Sauldubois, A., Singh, N., McCurdy, C., and Cantrell, C. 2007. *p*-Hydroxyphenylpyruvate dioxygenase is a herbicidal target site for β -triketones from *Leptospermum scoparium*. *Phytochemistry*, 68:2004–2014.
- de Carvalho, L. B., Alves, P. L. C. A., and Duke, S. O. 2013. Hormesis with glyphosate depends on coffee growth stage. *Anais da Academia Brasileira de Ciências*, 85(2): 813–821.
- de Mairan, J.-J. 1729. Observation botanique. *History of the Royal Academy of Sciences*.
- Dear, B. S., Sandral, G. A., Spencer, D., Khan, M. R., and Higgins, T. J. 2003. The tolerance of three transgenic subterranean clover (*Trifolium subterraneum* L.) lines with the *brn* gene to herbicides containing bromoxynil. *Australian Journal of Agricultural Research*, 54:203–210.
- del Hoyo, A., Álvarez, R., del Campo, E. M., Gasulla, F., Barreno, E., and Casano, L. M. 2011. Oxidative stress induces distinct physiological responses in the two *Trebouxia* phycobionts of the lichen *Ramalina farinacea*. *Annals of Botany*, 107: 109–118.
- Délye, C., Matějček, A., and Michel, S. 2008. Cross-resistance patterns to ACCase-inhibiting herbicides conferred by mutant ACCase isoforms in *Alopecurus myosuroides* Huds. (black-grass), re-examined at the recommended herbicide field rate. *Pest Management Science*, 63:1179–1186.
- Délye, C., Jasieniuk, M., and Le Corre, V. 2013. Deciphering the evolution of herbicide resistance in weeds. *Trends in Genetics*, 29(11):649–658.
- Demidchik, V., Straltsova, D., Medvedev, S. S., Pozhvanov, G. A., Sokolik, A., and Yurin, V. 2014. Stress-induced electrolyte leakage: the role of K⁺-permeable channels and involvement in programmed cell death and metabolic adjustment. *Journal of Experimental Botany*, 65(5):1259–1270.
- Demmig-Adams, B., Adams III, W. W., Winter, K., Meyer, A., Schreiber, U., Pereira, J. S., Krüger, A., Czygan, F.-C., and Lange, O. L. 1989. Photochemical efficiency of

- photosystem II, photon yield of O₂ evolution, photosynthetic capacity, and carotenoid composition during the midday depression of net CO₂ uptake in *Arbutus unedo* growing in Portugal. *Planta*, 177:377–387.
- Devlin, P. F. and Kay, S. A. 2000. Cryptochromes are required for phytochrome signaling to the circadian clock but not for rhythmicity. *The Plant Cell*, 12:2499–2509.
- Diernfellner, A. C. R., Schafmeier, T., Merrow, M. W., and Brunner, M. 2005. Molecular mechanism of temperature sensing by the circadian clock of *Neurospora crassa*. *Genes and Development*, 19:1968–1973.
- Dill, G. M., Sammons, R. D., Feng, P. C. C., Kohn, F., Kretzmer, K., Mehrsheikh, A., Bleeke, M., Honegger, J. L., Farmer, D., Wright, D., and Haupfear, E. A. Glyphosate: discovery, development, applications, and properties. In Nandula, V. K., editor, *Glyphosate Resistance in Crops and Weeds: History, Development, and Management*. John Wiley & Sons, Inc, Hoboken, NJ, USA, 2010.
- Ding, Z., Doyle, M. R., Amasino, R. M., and Davis, S. J. 2007. A complex genetic interaction between *Arabidopsis thaliana* TOC1 and CCA1/LHY in driving the circadian clock and in output regulation. *Genetics*, 176:1501–1510.
- Ding, Z., Galván-Ampudia, C. S., Demarsy, E., Łangowski, Ł., Kleine-Vehn, J., Fan, Y., Morita, M. T., Tasaka, M., Fankhauser, C., Offringa, R., and Friml, J. 2011. Light-mediated polarization of the PIN3 auxin transporter for the phototropic response in *Arabidopsis*. *Nature Cell Biology*, 13(4):447–452.
- Dixon, D. P., McEwen, A. G., Laphorn, A. J., and Edwards, R. 2003. Forced evolution of a herbicide detoxifying glutathione transferase. *The Journal of Biological Chemistry*, 278(26):23930–23935.
- Dodd, A. N., Parkinson, K., and Webb, A. A. R. 2004. Independent circadian regulation of assimilation and stomatal conductance in the *ztl-1* mutant of *Arabidopsis*. *New Phytologist*, 162:63–70.
- Dodd, A. N., Salathia, N., Hall, A., Kevei, E., Toth, R., Nagy, F., Hibberd, J. M., Millar, A. J., and Webb, A. A. R. 2005. Plant circadian clocks increase photosynthesis, growth, survival, and competitive advantage. *Science*, 309:630–633.
- Dodd, A. N., Gardner, M. J., Hotta, C. T., Hubbard, K. E., Dalchau, N., Love, J., Assie, J.-M., Robertson, F. C., Jakobsen, M. K., Gonçalves, J., Sanders, D., and Webb, A. A. R. 2007. The *Arabidopsis* circadian clock incorporates a cADPR-based feedback loop. *Science*, 318(5857):1789–1792.
- Dodd, A. N., Dalchau, N., Gardner, M. J., Baek, S.-J., and Webb, A. A. R. 2014. The circadian clock has transient plasticity of period and is required for timing of nocturnal processes in *Arabidopsis*. *New Phytologist*, 201:168–179.
- Dornbusch, T., Michaud, O., Xenarios, I., and Fankhauser, C. 2014. Differentially phased leaf growth and movements in *Arabidopsis* depend on coordinated circadian and light regulation. *The Plant Cell*, 26:3911–3921.
- Dowson-Day, M. J. and Millar, A. J. 1999. Circadian dysfunction causes aberrant hypocotyl elongation patterns in *Arabidopsis*. *Plant Journal*, 17(1):63–71.

- Du, S., Chen, L., Ge, L., and Huang, W. 2019. A novel loop: Mutual regulation between epigenetic modification and the circadian clock. *Frontiers in Plant Science*, 10(22).
- Dudek, C., Basler, E., and Santelmann, P. W. 1973. Absorption and translocation of terbutryn and propazine. *Weed Science*, 21(5):440–443.
- Duke, S. O. 2011. Glyphosate degradation in glyphosate-resistant and -susceptible crops and weeds. *Journal of Agricultural and Food Chemistry*, 59:5835–5841.
- Duke, S. O. 2012. Why have no new herbicide modes of action appeared in recent years? *Pest Management Science*, 68:505–512.
- Duke, S. O. and Powles, S. B. 2008. Glyphosate: a once-in-a-century herbicide. *Pest Management Science*, 64:319–325.
- Dunlap, J. R., Kresovich, S., and McGee, R. E. 1986. The effect of salt concentration on auxin stability in culture media. *Plant Physiology*, 81:934–936.
- Durand, S., Sancelme, M., Besse-Hoggan, P., and Combourieu, B. 2010. Biodegradation pathway of mesotrione: Complementarities of NMR, LC-NMR and LC-MS for qualitative and quantitative metabolic profiling. *Chemosphere*, 81:372–380.
- Edwards, K., Anderson, P., Hall, A., Salathia, N., Locke, J., Lynn, J., Straume, M., Smith, J., and Millar, A. J. 2006. *FLOWERING LOCUS C* mediates natural variation in the high-temperature response of the Arabidopsis circadian clock. *The Plant Cell*, 18:639–650.
- Edwards, R., Dixon, D. P., and Walbot, V. 2000. Plant glutathione S-transferases: enzymes with multiple functions in sickness and in health. *Trends in Plant Science*, 5(5):193–198.
- Endo, M., Shimizu, H., Nohales, M. A., Araki, T., and Kay, S. A. 2014. Tissue-specific clocks in Arabidopsis show asymmetric coupling. *Nature*, 515(7527):419–422.
- Eriksson, M. E. and Millar, A. J. 2003. The circadian clock. A plant's best friend in a spinning world. *Plant Physiology*, 132:732–738.
- Eulgem, T., Rushton, P. J., Robatzek, S., and Somssich, I. E. 2000. The WRKY superfamily of plant transcription factors. *Trends in Plant Science*, 5(5):199–206.
- European Food Safety Authority. 2011. Conclusion on pesticide peer review. *EFSA Journal*, 9(1).
- European Union. 2004. Commission Decision. *Official Journal of the European Union*, pages 53–55.
- Eysholdt-Derzsó, E. and Sauter, M. 2019. Hypoxia and the group VII ethylene response transcription factor HRE2 promote adventitious root elongation in Arabidopsis. *Plant Biology*, 21:103–108.
- Ezer, D., Shepherd, S. J., Brestovitsky, A., Dickinson, P., Cortijo, S., Charoensawan, V., Box, M. S., Biswas, S., Jaeger, K., and Wigge, P. A. 2017. The G-box transcriptional regulatory code in Arabidopsis. *Plant Physiology*, 175:628–640.

- Falk, J. S., Al-Khatib, K., and Peterson, D. E. 2006. Rapid assay evaluation of plant response to protoporphyrinogen oxidase (Protox)-inhibiting herbicides. *Weed Technology*, 20:104–112.
- FAO. 2009. How to Feed the World in 2050. *Insights from an expert meeting at FAO*.
- Farinas, B. and Más, P. 2011. Functional implication of the MYB transcription factor RVE8/LCL5 in the circadian control of histone acetylation. *Plant Journal*, 66(2): 318–329.
- Farré, E. M., Harmer, S. L., Harmon, F. G., Yanovsky, M. J., and Kay, S. A. 2005. Overlapping and distinct roles of PRR7 and PRR9 in the Arabidopsis circadian clock. *Current Biology*, 15:47–54.
- Faus, I., Zabalza, A., Santiago, J., Nebauer, S. G., Royuela, M., Serrano, R., and Gadea, J. 2015. Protein kinase GCN2 mediates responses to glyphosate in Arabidopsis. *BMC plant biology*, 15(14).
- Favory, J. J., Stec, A., Gruber, H., Rizzini, L., Oravec, A., Funk, M., Albert, A., Cloix, C., Jenkins, G. I., Oakeley, E. J., Seidlitz, H. K., Nagy, F., and Ulm, R. 2009. Interaction of COP1 and UVR8 regulates UV-B-induced photomorphogenesis and stress acclimation in Arabidopsis. *EMBO Journal*, 28:591–601.
- Feeney, K. A., Hansen, L. L., Putker, M., Olivares-Yañez, C., Day, J., Eades, L. J., Larrondo, L. F., Hoyle, N. P., O'Neill, J. S., and van Ooijen, G. 2016. Daily magnesium fluxes regulate cellular timekeeping and energy balance. *Nature*, 532(7599):375–379.
- Fehér, B., Kozma-Bognár, L., Kevei, É., Hajdu, A., Binkert, M., Davis, S. J., Schäfer, E., Ulm, R., and Nagy, F. 2011. Functional interaction of the circadian clock and UV RESISTANCE LOCUS 8-controlled UV-B signaling pathways in *Arabidopsis thaliana*. *Plant Journal*, 67(1):37–48.
- Field, R. J. and Bishop, N. G. 1988. Promotion of stomatal infiltration of glyphosate by an organosilicone surfactant reduces the critical rainfall period. *Pesticide Science*, 24:55–62.
- Filichkin, S. A., Priest, H. D., Givan, S. A., Shen, R., Bryant, D. W., Fox, S. E., Wong, W.-K., and Mockler, T. C. 2010. Genome-wide mapping of alternative splicing in *Arabidopsis thaliana*. *Genome Research*, 20:45–58.
- Flasiński, M. and Hąc-Wydro, K. 2014. Natural vs synthetic auxin: Studies on the interactions between plant hormones and biological membrane lipids. *Environmental Research*, 133:123–134.
- Fowler, S. G., Cook, D., and Thomashow, M. F. 2005. Low temperature induction of Arabidopsis *CBF1*, *2*, and *3* is gated by the circadian clock. *Plant Physiology*, 137: 961–8.
- Frank, A., Matioli, C. C., Viana, A. J., Hearn, T. J., Kusakina, J., Belbin, F. E., Wells Newman, D., Yochikawa, A., Cano-Ramirez, D. L., Chembath, A., Cragg-Barber, K., Haydon, M. J., Hotta, C. T., Vincentz, M., Webb, A. A., and Dodd, A. N. 2018. Circadian entrainment in Arabidopsis by the sugar-responsive transcription factor bZIP63. *Current Biology*, 28:2597–2606.

- Frankart, C., Eullaffroy, P., and Vernet, G. 2003. Comparative effects of four herbicides on non-photochemical fluorescence quenching in *Lemna minor*. *Environmental and Experimental Botany*, 49:159–168.
- Franklin, K., Lee, S. H., Patel, D., Kumar, S. V., Spartz, A. K., Gu, C., Ye, S., Yu, P., Breen, G., Cohen, J. D., Wigge, P. A., and Gray, W. M. 2011. PHYTOCHROME-INTERACTING FACTOR 4 (PIF4) regulates auxin biosynthesis at high temperature. *Proceedings of the National Academy of Sciences*, 108(50):20231–20235.
- Franklin, K. A. and Quail, P. H. 2010. Phytochrome functions in Arabidopsis development. *Journal of Experimental Botany*, 61(1):11–24.
- Friml, J., Wiśniewska, J., Benková, E., Mendgen, K., and Palme, K. 2002. Lateral relocation of auxin efflux regulator PIN3 mediates tropism in Arabidopsis. *Nature*, 415(6873):806–809.
- Fuerst, P. and Norman, M. A. 1991. Interactions of herbicides with photosynthetic electron transport. *Weed Science*, 39(3):458–464.
- Fujiwara, S., Wang, L., Han, L., Suh, S. S., Salomé, P. A., McClung, C. R., and Somers, D. E. 2008. Post-translational regulation of the Arabidopsis circadian clock through selective proteolysis and phosphorylation of pseudo-response regulator proteins. *Journal of Biological Chemistry*, 283(34):23073–23083.
- Gaines, T. A., Lorentz, L., Figge, A., Herrmann, J., Maiwald, F., Ott, M. C., Han, H., Busi, R., Yu, Q., Powles, S. B., and Beffa, R. 2014. RNA-Seq transcriptome analysis to identify genes involved in metabolism-based diclofop resistance in *Lolium rigidum*. *The Plant Journal*, 78:865–876.
- Gallé, Á., Czékus, Z., Bela, K., Horváth, E., Ördög, A., Csiszár, J., and Poór, P. 2019. Plant glutathione transferases and light. *Frontiers in Plant Science*, 9.
- Gangappa, S. N. and Kumar, S. V. 2017. DET1 and HY5 control PIF4-mediated thermosensory elongation growth through distinct mechanisms. *Cell Reports*, 18: 344–351.
- Gangappa, S. N., Maurya, J. P., Yadav, V., and Chattopadhyay, S. 2013. The regulation of the Z- and G-box containing promoters by light signaling components, SPA1 and MYC2, in Arabidopsis. *PLoS ONE*, 8(4).
- Gao, Y., Zhang, Y., Zhang, D., Dai, X., Estelle, M., and Zhao, Y. 2015. Auxin binding protein 1 (ABP1) is not required for either auxin signaling or Arabidopsis development. *Proceedings of the National Academy of Sciences*, 112(7):2275–2280.
- Garcia, I., Rodgers, M., Pepin, R., Hsieh, T.-F., and Matringe, M. 1999. Characterization and subcellular compartmentation of recombinant 4-hydroxyphenylpyruvate dioxygenase from Arabidopsis in transgenic tobacco. *Plant Physiology*, 119:1507–1516.
- Gardner, G. 1981. Azidoatrazine: Photoaffinity label for the site of triazine herbicide action in chloroplasts. *Science*, 211:937–940.
- Garg, R., Patel, R., Tyagi, A., and Jain, M. 2011. De novo assembly of chickpea transcriptome using short reads for gene discovery and marker identification. *DNA Research*, 18:53–63.

- Ge, X., D'Avignon, D., Ackerman, J. J. H., and Douglas Sammons, R. 2010. Rapid vacuolar sequestration: the horseweed glyphosate resistance mechanism. *Pest Management Science*, 66:345–348.
- Gendreau, E., Traas, J., Desnos, T., Grandjean, O., Caboche, M., and Höfte, H. 1997. Cellular basis of hypocotyl growth in *Arabidopsis thaliana*. *Plant Physiology*, 114: 295–305.
- Gendron, J. M., Pruneda-Paz, J. L., Doherty, C. J., Gross, A. M., Kang, S. E., and Kay, S. A. 2012. Arabidopsis circadian clock protein, TOC1, is a DNA-binding transcription factor. *Proceedings of the National Academy of Sciences*, 109(8):3167–3172.
- Giardi, M. T. and Pace, E. 2005. Photosynthetic proteins for technological applications. *Trends in Biotechnology*, 23(5):257–263.
- Gikas, E., Papadopoulos, N. G., Bazoti, F. N., Zalidis, G., and Tsarbopoulos, A. 2012. Use of liquid chromatography/electrospray ionization tandem mass spectrometry to study the degradation pathways of terbuthylazine (TER) by *Typha latifolia* in constructed wetlands: Identification of a new TER metabolite. *Rapid Communications in Mass Spectrometry*, 26:181–188.
- Gil, K. E. and Park, C. M. 2019. Thermal adaptation and plasticity of the plant circadian clock. *New Phytologist*, 221:1215–1229.
- Giuliano, G., Pichersky, E., Malik, V. S., Timko, M. P., Scolnik, P. A., and Cashmore, A. R. 1988. An evolutionarily conserved protein binding sequence upstream of a plant light-regulated gene. *Proceedings of the National Academy of Sciences of the United States of America*, 85:7089–93.
- Godar, A. S., Varanasi, V. K., Nakka, S., Prasad, P. V. V., Thompson, C. R., and Mithila, J. 2015. Physiological and molecular mechanisms of differential sensitivity of Palmer Amaranth (*Amaranthus palmeri*) to mesotrione at varying growth temperatures. *Plos One*, 10(5).
- Golden, S. S. and Haselkorn, R. 1985. Mutation to herbicide resistance maps within the *psbA* gene of *Anacystis nidulans* R2. *Science*, 229(4718):1104–1107.
- Gomes, M. P., Smedbol, E., Chalifour, A., Henault-Ethier, L., Labrecque, M., Lepage, L., Lucotte, M., and Juneau, P. 2014. Alteration of plant physiology by glyphosate and its by-product aminomethylphosphonic acid: an overview. *Journal of Experimental Botany*, 65(17):4691–4703.
- Gomes, M. P., Le Manac'h, S. G., Hénault-Ethier, L., Labrecque, M., Lucotte, M., and Juneau, P. 2017. Glyphosate-dependent inhibition of photosynthesis in Willow. *Frontiers in Plant Science*, 8(207).
- Gomes, M. P., Le Manac'h, S. G., Maccario, S., Labrecque, M., Lucotte, M., and Juneau, P. 2016. Differential effects of glyphosate and aminomethylphosphonic acid (AMPA) on photosynthesis and chlorophyll metabolism in willow plants. *Pesticide Biochemistry and Physiology*, 130:65–70.
- Gougler, J. A. and Geiger, D. R. 1981. Uptake and distribution of N-phosphonomethylglycine in sugar beet plants. *Plant physiology*, 68:668–672.

- Graham, M. Y. 2005. The diphenylether herbicide lactofen induces cell death and expression of defense-related genes in soybean. *Plant Physiology*, 139:1784–1794.
- Green, R. M., Tingay, S., Wang, Z.-Y., and Tobin, E. M. 2002. Circadian rhythms confer a higher level of fitness to Arabidopsis plants. *Plant Physiology*, 129:576–584.
- Greenberg, B. M., Gaba, V., Mattoo, A. K., and Edelman, M. 1987. Identification of a primary in vivo degradation product of the rapidly-turning-over 32 kd protein of photosystem II. *The EMBO journal*, 6(10):2865–2869.
- Greenham, K. and McClung, C. R. 2015. Integrating circadian dynamics with physiological processes in plants. *Nature Reviews Genetics*, 16:598–610.
- Grundy, J., Stoker, C., and Carré, I. A. 2015. Circadian regulation of abiotic stress tolerance in plants. *Frontiers in Plant Science*, 6(648).
- Grunstein, M. 1997. Histone acetylation in chromatin structure and transcription. *Nature*, 389(6649):349–352.
- Gutiérrez, R. A., Stokes, T. L., Thum, K., Xu, X., Obertello, M., Katari, M. S., Tanurdzic, M., Dean, A., Nero, D. C., McClung, C. R., and Coruzzi, G. M. 2008. Systems approach identifies an organic nitrogen-responsive gene network that is regulated by the master clock control gene *CCA1*. *Proceedings of the National Academy of Sciences*, 105(12):4939–4944.
- Hall, A., Kozma-Bognár, L., Tóth, R., Nagy, F., and Millar, A. J. 2001a. Conditional circadian regulation of *PHYTOCHROME A* gene expression. *Plant Physiology*, 127:1808–1818.
- Hall, A., Kozma-Bognár, L., Bastow, R. M., Nagy, F., and Millar, A. J. 2002. Distinct regulation of *CAB* and *PHYB* gene expression by similar circadian clocks. *Plant Journal*, 32:529–537.
- Hall, M. G., Wilks, M. F., McLean Provan, W., Eksborg, S., and Lumholtz, B. 2001b. Pharmacokinetics and pharmacodynamics of NTBC (2-(2-nitro-4-fluoromethylbenzoyl)-1,3-cyclohexanedione) and mesotrione, inhibitors of 4-hydroxyphenyl pyruvate dioxygenase (HPPD) following a single dose to healthy male volunteers. *British Journal of Clinical Pharmacology*, 52:169–177.
- Hamner, K. C. and Takimoto, A. 1964. Circadian rhythms and plant photoperiodism. *The American Naturalist*, 98(902):295–322.
- Hanson, J., Hanssen, M., Wiese, A., Hendriks, M. M. W. B., and Smeekens, S. 2008. The sucrose regulated transcription factor bZIP11 affects amino acid metabolism by regulating the expression of *ASPARAGINE SYNTHETASE1* and *PROLINE DEHYDROGENASE2*. *The Plant Journal*, 53:935–949.
- Hara, K., Yagi, M., Kusano, T., and Sano, H. 2000. Rapid systemic accumulation of transcripts encoding a tobacco WRKY transcription factor upon wounding. *Molecular and General Genetics*, 263:30–37.
- Harding, D. P. and Raizada, M. N. 2015. Controlling weeds with fungi, bacteria and viruses: a review. *Frontiers in Plant Science*, 6.

- Harmer, S. L. 2009. The circadian system in higher plants. *Annual Review of Plant Biology*, 60:357–377.
- Harmer, S. L., Hogenesch, J. B., Straume, M., Chang, H.-S., Han, B., Zhu, T., Wang, X., Kreps, J. A., and Kay, S. A. 2000. Orchestrated transcription of key pathways in *Arabidopsis* by the circadian clock. *Science*, 290:2110–2113.
- Harmer, S. L., Panda, S., and Kay, S. A. 2001. Molecular bases of circadian rhythms. *Annual Review of Cell and Developmental Biology*, 17:215–253.
- Hasanuzzaman, M., Nahar, K., Anee, T. I., and Fujita, M. 2017. Glutathione in plants: biosynthesis and physiological role in environmental stress tolerance. *Physiology and Molecular Biology of Plants*, 23(2):249–268.
- Hatfield, J., Takle, G., Grotjahn, R., Holden, P., Cesar Izaurralde, R., Mader, T., E. Marshall, and Liverman, D. Ch 6: Agriculture. In Melillo, J. M., Richmond, T., and Yohe, G. W., editors, *Climate Change Impacts in the United States: The Third National Climate Assessment*, pages 150–174. 2014.
- Hatsugai, N. and Katagiri, F. 2018. Quantification of plant cell death by electrolyte leakage assay. *Bio-Protocol*, 8(5).
- Haydon, M. J., Mielczarek, O., Robertson, F. C., Hubbard, K. E., and Webb, A. A. R. 2013. Photosynthetic entrainment of the *Arabidopsis thaliana* circadian clock. *Nature*, 502(7473):689–692.
- Haydon, M. J., Román, Á., and Arshad, W. 2015. Nutrient homeostasis within the plant circadian network. *Frontiers in Plant Science*, 6:1–6.
- Haydon, M. J., Mielczarek, O., Frank, A., Román, Á., and Webb, A. A. 2017. Sucrose and ethylene signaling interact to modulate the circadian clock. *Plant Physiology*, 175:947–958.
- Hayes, S., Velanis, C. N., Jenkins, G. I., and Franklin, K. A. 2014. UV-B detected by the UVR8 photoreceptor antagonizes auxin signaling and plant shade avoidance. *Proceedings of the National Academy of Sciences*, 111(32):11894–11899.
- He, W., Brumos, J., Li, H., Ji, Y., Ke, M., Gong, X., Zeng, Q., Li, W., Zhang, X., An, F., Wen, X., Li, P., Chu, J., Sun, X., Yan, C., Yan, N., Xie, D.-Y., Raikhel, N., Yang, Z., Stepanova, A. N., Alonso, J. M., and Guo, H. 2011. A small-molecule screen identifies L-Kynurenine as a competitive inhibitor of TAA1/TAR activity in ethylene-directed auxin biosynthesis and root growth in *Arabidopsis*. *The Plant Cell*, 23:3944–3960.
- Heap, I. International Survey of Herbicide Resistant Weeds, 2019.
- Hearn, T. J., Marti Ruiz, M. C., Abdul-Awal, S., Wimalasekera, R., Stanton, C. R., Haydon, M. J., Theodoulou, F. L., Hannah, M. A., and Webb, A. A. 2018. BIG regulates dynamic adjustment of circadian period in *Arabidopsis thaliana*. *Plant Physiology*, 178:358–371.
- Heintzen, C., Melzer, S., Fischer, R., Kappeler, S., Apel, K., and Staiger, D. 1994. A light- and temperature-entrained circadian clock controls expression of transcripts encoding nuclear proteins with homology to RNA-binding proteins in meristematic tissue. *The Plant Journal*, 5(6):799–813.

- Heisler, M. G., Ohno, C., Das, P., Sieber, P., Reddy, G. V., Long, J. A., and Meyerowitz, E. M. 2005. Patterns of auxin transport and gene expression during primordium development revealed by live imaging of the Arabidopsis inflorescence meristem. *Current Biology*, 15:1899–1911.
- Hemsley, P. A., Hurst, C. H., Kaliyadasa, E., Lamb, R., Knight, M. R., De Cothi, E. A., Steele, J. F., and Knight, H. 2014. The Arabidopsis mediator complex subunits MED16, MED14, and MED2 regulate mediator and RNA Polymerase II recruitment to CBF-responsive cold-regulated genes. *The Plant Cell*, 26:465–484.
- Herrmann, K. M. 1995. The shikimate pathway: early steps in the biosynthesis of aromatic compounds. *The Plant Cell*, 7:907–919.
- Herrmann, K. M. and Weaver, L. M. 1999. The shikimate pathway. *Annual Review of Plant Physiology and Plant Molecular Biology*, 50:473–503.
- Hertel, R., Lomax, T. L., and Briggs, W. R. 1983. Auxin transport in membrane vesicles from *Cucurbita pepo* L. *Planta*, 157:193–201.
- Hetherington, P. R., Reynolds, T. L., Marshall, G., and Kirkwood, R. C. 1999. The absorption, translocation and distribution of the herbicide glyphosate in maize expressing the CP-4 transgene. *Journal of Experimental Botany*, 50(339):1567–1576.
- Hicks, K. A., Millar, A. J., Carré, I. A., Somers, D. E., Straume, M., Meeks-Wagner, D. R., and Kay, S. A. 1996. Conditional circadian of the Arabidopsis *early-flowering 3* mutant. *Science*, 274:790–792.
- Hideg, É., Kós, P. B., and Schreiber, U. 2008. Imaging of NPQ and ROS formation in tobacco leaves: Heat inactivation of the water-water cycle prevents down-regulation of PSII. *Plant and Cell Physiology*, 49(12):1879–1886.
- Hilgenfeld, K. L., Martin, A. R., Mortensen, D. A., and Mason, S. C. 2004. Weed management in glyphosate resistant soybean: Weed emergence patterns in relation to glyphosate treatment timing. *Weed Technology*, 18(2):277–283.
- Hörtensteiner, S., Vicentini, F., and Matile, P. 1995. Chlorophyll breakdown in senescent cotyledons of rape, *Brassica napus* L.: Enzymatic cleavage of phaeophorbide *a* in vitro. *New Phytologist*, 129:237–246.
- Hörtensteiner, S. and Kräutler, B. 2011. Chlorophyll breakdown in higher plants. *Biochimica et Biophysica Acta 1807*, pages 977–988.
- Hotta, C. T., Gardner, M. J., Hubbard, K. E., Baek, S. J., Dalchau, N., Suhita, D., Dodd, A. N., and Webb, A. A. R. 2007. Modulation of environmental responses of plants by circadian clocks. *Plant, Cell and Environment*, 30:333–349.
- Hsu, P. Y. and Harmer, S. L. 2014. Wheels within wheels: The plant circadian system. *Trends in Plant Science*, 19(4):240–249.
- Hsu, P. Y., Devisetty, U. K., and Harmer, S. L. 2013. Accurate timekeeping is controlled by a cycling activator in Arabidopsis. *eLife*, 2(e00473).
- Huang, J., Silva, E. N., Shen, Z., Jiang, B., and Lu, H. 2012a. Effects of glyphosate on photosynthesis, chlorophyll fluorescence and physicochemical properties of cogon-grass (*Imperata cylindrical* L.). *Plant Omics Journal*, 5(2):177–183.

- Huang, W., Pérez-García, P., Pokhilko, A., Millar, A. J., Antoshechkin, I., Riechmann, J. L., and Mas, P. 2012b. Mapping the core of the Arabidopsis circadian clock defines the network structure of the oscillator. *Science*, 336(6077):75–79.
- Hudson, M. E. and Quail, P. H. 2003. Identification of promoter motifs involved in the network of phytochrome A-regulated gene expression by combined analysis of genomic sequence and microarray data. *Plant Physiology*, 133:1605–1616.
- Huq, E. and Quail, P. H. 2002. PIF4, a phytochrome-interacting bHLH factor, functions as a negative regulator of phytochrome B signaling in Arabidopsis. *The EMBO Journal*, 21(10):2441–2450.
- Huseby, S., Koprivova, A., Lee, B. R., Saha, S., Mithen, R., Wold, A. B., Bengtsson, G. B., and Kopriva, S. 2013. Diurnal and light regulation of sulphur assimilation and glucosinolate biosynthesis in Arabidopsis. *Journal of Experimental Botany*, 64(4):1039–1048.
- Iio, A., Fukasawa, H., Nose, Y., and Kakubari, Y. 2004. Stomatal closure induced by high vapor pressure deficit limited midday photosynthesis at the canopy top of *Fagus crenata* Blume on Naeba mountain in Japan. *Trees*, 18:510–517.
- Ireland, C. R., Percival, M. P., and Baker, N. R. 1986. Modification of the induction of photosynthesis in wheat by glyphosate, an inhibitor of amino acid metabolism. *Journal of Experimental Botany*, 37(176):299–308.
- Ishizawa, K. and Esashi, Y. 1983. Cooperation of ethylene and auxin in the growth regulation of rice coleoptile segments. *Journal of Experimental Botany*, 34(138):74–82.
- Ito, K. and Chiba, S. 2013. Arrest peptides: Cis-acting modulators of translation. *Annual Review of Biochemistry*, 82:171–202.
- Jakoby, M., Dröge-Laser, W., Vicente-Carbajosa, J., Tiedemann, J., Kroj, T., and Parcy, F. 2002. bZIP transcription factors in Arabidopsis. *TRENDS in Plant Science*, 7(3):106–111.
- James, A. B., Syed, N. H., Bordage, S., Marshall, J., Nimmo, G. A., Jenkins, G. I., Herzyk, P., Brown, J. W., and Nimmo, H. G. 2012. Alternative splicing mediates responses of the Arabidopsis circadian clock to temperature changes. *The Plant Cell*, 24(3):961–981.
- James, T. K., Rahman, A., and Hicking, J. 2006. Mesotrione – a new herbicide for weed control in maize. *New Zealand Plant Protection*, 59:242–249.
- Jaworski, E. G. 1972. Mode of action of N-phosphonomethylglycine. Inhibition of aromatic amino acid biosynthesis. *Journal of Agricultural and Food Chemistry*, 20(6):1195–1198.
- Jensen, P. J., Hangarter, R. P., and Estelle, M. 1998. Auxin transport is required for hypocotyl elongation in light-grown but not dark-grown Arabidopsis. *Plant physiology*, 116:455–462.
- Jiang, L. X., Jin, L. G., Guo, Y., Tao, B., and Qiu, L. J. 2013. Glyphosate effects on the gene expression of the apical bud in soybean (*Glycine max*). *Biochemical and Biophysical Research Communications*, 437:544–549.

- Johnson, B. C. and Young, B. G. 2002. Influence of Temperature and Relative Humidity on the Foliar Activity of Mesotrione. *Weed Science*, 50(2):157–161.
- Johnson, C. H., Elliott, J. A., and Foster, R. 2003. Entrainment of circadian programs. *Chronobiology International*, 20(5):741–774.
- Jordan, D., York, A., Griffin, J., Clay, P., Vidrine, P., and Reynolds, D. 1997. Influence of application variables on efficacy of glyphosate. *Weed Technology*, 11(2):354–362.
- Jorgensen, R. A. and Dorantes-Acosta, A. E. 2012. Conserved peptide upstream open reading frames are associated with regulatory genes in angiosperms. *Frontiers in Plant Science*, 3(191).
- Jung, J.-H., Domijan, M., Klose, C., Biswas, S., Ezer, D., Gao, M., Khattak, A. K., Box, M. S., Charoensawan, V., Cortijo, S., Kumar, M., Grant, A., Locke, J. C. W., Schäfer, E., Jaeger, K. E., and Wigge, P. A. 2016. Phytochromes function as thermosensors in Arabidopsis. *Science*, 354(6314):886–889.
- Kanehisa, M. and Goto, S. 2000. KEGG: Kyoto Encyclopedia of Genes and Genomes. *Nucleic Acids Research*, 28(1):27–30.
- Kang, J., Hwang, J.-U., Lee, M., Kim, Y.-Y., Assmann, S. M., Martinoia, E., and Lee, Y. 2010. PDR-type ABC transporter mediates cellular uptake of the phytohormone abscisic acid. *Proceedings of the National Academy of Sciences*, 107(5):2355–2360.
- Kelly, M. O. and Bradford, K. J. 1986. Insensitivity of the *Diageotropica* tomato mutant to auxin. *Plant Physiology*, 82:713–717.
- Keuskamp, D. H., Pollmann, S., Voeselek, L. A. C. J., Peeters, A. J. M., and Pierik, R. 2010. Auxin transport through PIN-FORMED 3 (PIN3) controls shade avoidance and fitness during competition. *Proceedings of the National Academy of Sciences*, 107(52):22740–22744.
- Khan, S., Rowe, S. C., and Harmon, F. G. 2010. Coordination of the maize transcriptome by a conserved circadian clock. *BMC Plant Biology*, 10(126).
- Khandelwal, A., Elvitigala, T., Ghosh, B., and Quatrano, R. S. 2008. Arabidopsis transcriptome reveals control circuits regulating redox homeostasis and the role of an AP2 transcription factor. *Plant Physiology*, 148:2050–2058.
- Kim, H. Y., Coté, G. G., and Crain, R. C. 1993. Potassium channels in *Samanea saman* protoplasts controlled by phytochrome and the biological clock. *Science*, 260(5110):960–962.
- Kim, J. S., Jung, S., Hwang, I. T., and Cho, K. Y. 1999. Characteristics of chlorophyll *a* fluorescence induction in cucumber cotyledons treated with diuron, norflurazon, and sulcotrione. *Pesticide Biochemistry and Physiology*, 65:73–81.
- Kim, W. Y., Fujiwara, S., Suh, S. S., Kim, J., Kim, Y., Han, L., David, K., Putterill, J., Nam, H. G., and Somers, D. E. 2007. ZEITLUPE is a circadian photoreceptor stabilized by GIGANTEA in blue light. *Nature*, 449(7160):356–360.
- Kitchen, L. M., Witt, W. W., and Rieck, C. E. 1981. Inhibition of chlorophyll accumulation by glyphosate. *Weed Science*, 29(4):513–516.

- Knight, H., Thomson, A. J., and McWatters, H. G. 2008. SENSITIVE TO FREEZING6 integrates cellular and environmental inputs to the plant circadian clock. *Plant Physiology*, 148:293–303.
- Knoth, C., Salus, M. S., Girke, T., and Eulgem, T. 2009. The synthetic elicitor 3,5-dichloroanthranilic acid induces *NPR1*-dependent and *NPR1*-independent mechanisms of disease resistance in *Arabidopsis*. *Plant Physiology*, 150:333–347.
- Knox, J. P. and Dodge, A. D. 1985. Singlet oxygen and plants. *Phytochemistry*, 24(5):889–896.
- Koornneef, M., Rolff, E., and Spruit, C. nov 1980. Genetic control of light-inhibited hypocotyl elongation in *Arabidopsis thaliana* (L.) Heynh. *Zeitschrift für Pflanzenphysiologie*, 100(2):147–160.
- Koornneef, M. and Meinke, D. 2010. The development of *Arabidopsis* as a model plant. *The Plant Journal*, 61:909–921.
- Kopsell, D. A., Armel, G. R., Abney, K. R., Vargas, J. J., Brosnan, J. T., and Kopsell, D. E. 2011. Leaf tissue pigments and chlorophyll fluorescence parameters vary among sweet corn genotypes of differential herbicide sensitivity. *Pesticide Biochemistry and Physiology*, 99:194–199.
- Koyama, K. and Takemoto, S. 2014. Morning reduction of photosynthetic capacity before midday depression. *Scientific Reports*, 4(4389).
- Kozuka, T., Kobayashi, J., Horiguchi, G., Demura, T., Sakakibara, H., Tsukaya, H., and Nagatani, A. 2010. Involvement of auxin and brassinosteroid in the regulation of petiole elongation under the shade. *Plant Physiology*, 153:1608–1618.
- Kreps, J. A. and Kay, S. A. 1997. Coordination of plant metabolism and development by the circadian clock. *The Plant Cell*, 9:1235–1244.
- Kristoffersen, P., Rask, A. M., Grundy, A. C., Franzen, I., Kempenaar, C., Raisio, J., Schroeder, H., Spijker, J., Verschwele, A., and Zarina, L. 2008. A review of pesticide policies and regulations for urban amenity areas in seven European countries. *Weed Research*, 48:201–214.
- Kumar, K., Rao, K. P., Biswas, D. K., and Sinha, A. K. 2011. Rice WNK1 is regulated by abiotic stress and involved in internal circadian rhythm. *Plant Signaling and Behavior*, 6(3):316–320.
- Kumar, V. and Jha, P. 2015. Influence of glyphosate timing on *Kochia scoparia* demographics in glyphosate-resistant sugar beet. *Crop Protection*, 76:39–45.
- Kunihiro, A., Yamashino, T., Nakamichi, N., Niwa, Y., Nakanishi, H., and Mizuno, T. 2011. PHYTOCHROME-INTERACTING FACTOR 4 and 5 (PIF4 and PIF5) activate the homeobox *ATHB2* and auxin-inducible *IAA29* genes in the coincidence mechanism underlying photoperiodic control of plant growth of *Arabidopsis thaliana*. *Plant and Cell Physiology*, 52(8):1315–1329.
- Kusakina, J. and Dodd, A. N. 2012. Phosphorylation in the plant circadian system. *Trends in Plant Science*, 17(10):575–583.

- Kusakina, J., Gould, P. D., and Hall, A. 2014. A fast circadian clock at high temperatures is a conserved feature across *Arabidopsis* accessions and likely to be important for vegetative yield. *Plant, Cell and Environment*, 37:327–340.
- Lai, A. G., Doherty, C. J., Mueller-Roeber, B., Kay, S. A., Schippers, J. H. M., and Dijkwel, P. P. oct 2012. *CIRCADIAN CLOCK-ASSOCIATED 1* regulates ROS homeostasis and oxidative stress responses. *Proceedings of the National Academy of Sciences*, 109(42):17129–17134.
- Lamb, T. M., Goldsmith, C. S., Bennett, L., Finch, K. E., and Bell-Pedersen, D. 2011. Direct transcriptional control of a p38 mapk pathway by the circadian clock in *Neurospora crassa*. *PLoS ONE*, 6(11).
- Lambrevia, M. D., Russo, D., Polticelli, F., Scognamiglio, V., Antonacci, A., Zobnina, V., Campi, G., and Rea, G. 2014. Structure/function/dynamics of photosystem II plastoquinone binding sites. *Current Protein & Peptide Science*, 15:285–295.
- Lassiter, B. R., Burke, I. C., Thomas, W. E., Pline-Srnić, W. a., Jordan, D. L., Wilcut, J. W., and Wilkerson, G. G. 2007. Yield and physiological response of peanut to glyphosate drift. *Weed Technology*, 21(4):954–960.
- Lastdrager, J., Hanson, J., and Smeekens, S. 2014. Sugar signals and the control of plant growth and development. *Journal of Experimental Botany*, 65(3):799–807.
- Lavieille, D., Ter Halle, A., Bussiere, P.-O., and Richard, C. 2009. Effect of a Spreading Adjuvant on Mesotrione Photolysis on Wax Films. *Journal of Agricultural and Food Chemistry*, 57:9624–9628.
- LeBaron, H. M., McFarland, J. E., and Burnside, O. C. 2008. *The Triazine Herbicides*. Elsevier, first edition.
- Lee, H. J., Lee, G. J., Kim, D. S., Kim, J.-B., Ku, J. H., and Kang, S.-Y. 2008. Selection and physiological characterization of glyphosate-tolerant Zoysiagrass mutants derived from a gamma ray irradiation. *Horticulture Science and Technology Journal*, 26(4):454–463.
- Lee, M., Lee, K., Lee, J., Noh, E. W., and Lee, Y. 2005. AtPDR12 contributes to lead resistance in *Arabidopsis*. *Plant Physiology*, 138:827–836.
- Leeuwen, W. V., Hagendoorn, M. J. M., Ruttink, T., Poecke, R. V., Plas, L. H. W. V. D., and Krol, A. R. V. D. 2000. The use of the luciferase reporter system for in planta gene expression studies. *Plant Molecular Biology Reporter*, 18:143a–144t.
- Legris, M., Klose, C., Burgie, E. S., Rojas, C. C. R., Neme, M., Hiltbrunner, A., Wigge, P. A., Schäfer, E., Vierstra, R. D., and Casal, J. J. 2016. Phytochrome B integrates light and temperature signals in *Arabidopsis*. *Science*, 354(6314):897–900.
- Li, G., Siddiqui, H., Teng, Y., Lin, R., Wan, X.-y., Li, J., Lau, O.-S., Ouyang, X., Dai, M., Wan, J., Devlin, P. F., Deng, X. W., and Wang, H. 2011. Coordinated transcriptional regulation underlying the circadian clock in *Arabidopsis*. *Nature Cell Biology*, 13(5):616–622.
- Li, L., He, Z., Pandey, G. K., Tsuchiya, T., and Luan, S. 2002. Functional cloning and characterization of a plant efflux carrier for multidrug and heavy metal detoxification. *Journal of Biological Chemistry*, 277(7):5360–5368.

- Licausi, F., Van Dongen, J. T., Giuntoli, B., Novi, G., Santaniello, A., Geigenberger, P., and Perata, P. 2010. *HRE1* and *HRE2*, two hypoxia-inducible ethylene response factors, affect anaerobic responses in *Arabidopsis thaliana*. *The Plant Journal*, 62: 302–315.
- Lichtenthaler, H. K. and Wellburn, A. R. 1983. Determinations of total carotenoids and chlorophylls *a* and *b* of leaf extracts in different solvents. *Biochemical Society Transactions*, 11:591–592.
- Lichtenthaler, H. K. 1996. Vegetation stress: an introduction to the stress concept in plants. *Journal of Plant Physiology*, 148:4–14.
- Lichtenthaler, H. K. and Babani, F. Light adaptation and senescence of the photosynthetic apparatus. Changes in pigment composition, chlorophyll fluorescence parameters and photosynthetic activity. In Papageorgiou, G. C. and Govindjee, editors, *Chlorophyll *a* Fluorescence: A signature of photosynthesis*, chapter 28, pages 713–736. 2004.
- Linde, A. M., Eklund, D. M., Kubota, A., Pederson, E. R., Holm, K., Gyllenstrand, N., Nishihama, R., Cronberg, N., Muranaka, T., Oyama, T., Kohchi, T., and Lagercrantz, U. 2017. Early evolution of the land plant circadian clock. *New Phytologist*, 216:576–590.
- Litthauer, S., Chan, K. X., and Jones, M. A. 2018. 3'-Phosphoadenosine 5'-phosphate accumulation delays the circadian system. *Plant Physiology*, 176:3120–3135.
- Liu, C.-M., McLean, P. A., Sookdeo, C. C., and Cannon, F. C. 1991. Degradation of the herbicide glyphosate by members of the family *Rhizobiaceae*. *Applied and environmental microbiology*, 57(6):1799–1804.
- Liu, X., Xu, X., Li, B., Wang, X., Wang, G., and Li, M. 2015. RNA-seq transcriptome analysis of maize inbred carrying nicosulfuron-tolerant and nicosulfuron-susceptible alleles. *International Journal of Molecular Sciences*, 16(3):5975–5989.
- Liu, Y.-c., Lin, Y. C., Kanehara, K., and Nakamura, Y. 2018. A pair of phospho-base methyltransferases important for phosphatidylcholine biosynthesis in *Arabidopsis*. *The Plant Journal*, 96:1064–1075.
- Liu, Y.-c., Lin, Y.-C., Kanehara, K., and Nakamura, Y. 2019. A methyltransferase trio essential for phosphatidylcholine biosynthesis and growth. *Plant Physiology*, 179:433–445.
- Livak, K. J. and Schmittgen, T. D. 2001. Analysis of relative gene expression data using real-time quantitative PCR and the $2^{-\Delta\Delta Ct}$ Method. *Methods*, 25:402–408.
- Ljung, K. 2013. Auxin metabolism and homeostasis during plant development. *Development*, 140:943–950.
- Lorraine, A. E., McCormick, S., Estrada, A., Patel, K., and Qin, P. 2013. RNA-Seq of *Arabidopsis* pollen uncovers novel transcription and alternative splicing. *Plant Physiology*, 162:1092–1109.
- Love, J., Dodd, A. N., and Webb, A. A. 2004. Circadian and diurnal calcium oscillations encode photoperiodic information in *Arabidopsis*. *The Plant Cell*, 16: 956–966.

- Lu, T., Lu, G., Fan, D., Zhu, C., Li, W., Zhao, Q., Feng, Q., Zhao, Y., Guo, Y., Li, W., Huang, X., and Han, B. 2010. Function annotation of the rice transcriptome at single-nucleotide resolution by RNA-seq. *Genome Research*, 20:1238–1249.
- Lupi, L., Miglioranza, K. S. B., Aparicio, V. C., Marino, D., Bedmar, F., and Wunderlin, D. A. 2015. Occurrence of glyphosate and AMPA in an agricultural watershed from the southeastern region of Argentina. *Science of the Total Environment*, 536: 687–694.
- Majumder, K., Selvapandiyan, A., Fattah, F. A., Arora, N., Ahmad, S., and Bhatnagar, R. K. 1995. 5-Enolpyruvylshikimate-3-phosphate synthase of *Bacillus subtilis* is an allosteric enzyme. *European Journal of Biochemistry*, 229:99–106.
- Malapeira, J., Khaitova, L. C., and Mas, P. 2012. Ordered changes in histone modifications at the core of the Arabidopsis circadian clock. *Proceedings of the National Academy of Sciences*, 109(52):21540–21545.
- Mano, Y. and Nemoto, K. 2012. The pathway of auxin biosynthesis in plants. *Journal of Experimental Botany*, 63(8):2853–2872.
- Martí Ruiz, M. C., Hubbard, K. E., Gardner, M. J., Jung, H. J., Aubry, S., Hotta, C. T., Mohd-Noh, N. I., Robertson, F. C., Hearn, T. J., Tsai, Y. C., Dodd, A. N., Hannah, M., Carré, I. A., Davies, J. M., Braam, J., and Webb, A. A. 2018. Circadian oscillations of cytosolic free calcium regulate the Arabidopsis circadian clock. *Nature Plants*, 4:690–698.
- Martin, L. B. B., Fei, Z., Giovannoni, J. J., and Rose, J. K. C. 2013. Catalyzing plant science research with RNA-seq. *Frontiers in Plant Science*, 4.
- Martínez-García, J. F., Huq, E., and Quail, P. H. 2000. Direct targeting of light signals to a promoter element-bound transcription factor. *Science*, 288(5467):859–863.
- Martinson, K. B., Sothorn, R. B., Koukkari, W. L., Durgan, B. R., and Gunsolus, J. L. 2002. Circadian response of annual weeds to glyphosate and glufosinate. *Chronobiology International*, 19(2):405–422.
- Maruyama, K., Todaka, D., Mizoi, J., Yoshida, T., Kidokoro, S., Matsukura, S., Takasaki, H., Sakurai, T., Yamamoto, Y. Y., Yoshiwara, K., Kojima, M., Sakakibara, H., Shinozaki, K., and Yamaguchi-Shinozaki, K. 2012. Identification of cis-acting promoter elements in cold- and dehydration- induced transcriptional pathways in Arabidopsis, rice, and soybean. *DNA Research*, 19:37–49.
- Más, P., Alabadí, D., Yanovsky, M. J., Oyama, T., and Kay, S. A. 2003. Dual role of TOC1 in the control of circadian and photomorphogenic responses in Arabidopsis. *The Plant Cell*, 15:223–236.
- Mateos-Naranjo, E., Redondo-Gómez, S., Cox, L., Cornejo, J., and Figueroa, M. E. 2009. Effectiveness of glyphosate and imazamox on the control of the invasive cordgrass *Spartina densiflora*. *Ecotoxicology and Environmental Safety*, 72:1694–1700.
- Matile, P., Hörtensteiner, S., and Thomas, H. 1999. Chlorophyll degradation. *Annual Review of Plant Physiology and Plant Molecular Biology*, 50:67–95.

- Matsuo, M., Johnson, J. M., Hieno, A., Tokizawa, M., Nomoto, M., Tada, Y., Godfrey, R., Obokata, J., Sherameti, I., Yamamoto, Y. Y., Böhmer, F.-D., and Oelmüller, R. 2015. High REDOX RESPONSIVE TRANSCRIPTION FACTOR1 levels result in accumulation of reactive oxygen species in *Arabidopsis thaliana* shoots and roots. *Molecular Plant*, 8:1253–1273.
- Maxwell, K. and Johnson, G. N. 2000. Chlorophyll fluorescence - a practical guide. *Journal of Experimental Botany*, 51(345):659–668.
- Mazur, B. J. and Falco, S. C. 1989. The development of herbicide resistant crops. *Annual Review of Plant Physiology and Plant Molecular Biology*, 40:441–470.
- Mazzella, M. a., Casal, J. J., Muschietti, J. P., and Fox, A. R. 2014. Hormonal networks involved in apical hook development in darkness and their response to light. *Frontiers in Plant Science*, 5:52.
- McClung, R. C. 2006. Plant circadian rhythms. *The Plant Cell*, 18:792–803.
- McCurdy, J. D., McElroy, J. S., Kopsell, D. A., Sams, C. E., and Sorochan, J. C. 2008. Effects of mesotrione on Perennial Ryegrass (*Lolium perenne* L.) carotenoid concentrations under varying environmental conditions. *Journal of Agricultural and Food Chemistry*, 56:9133–9139.
- McCurdy, J. D., McElroy, J. S., Kopsell, D. A., and Sams, C. E. 2009. Mesotrione control and pigment concentration of large crabgrass (*Digitaria sanguinalis*) under varying environmental conditions. *Pest Management Science*, 65:640–644.
- McWhorter, C. and Jordan, T. N. 1976. Effects of adjuvants and environment on the toxicity of dalapon to johnsongrass. *Weed Science*, 24(3):257–260.
- Meier, I. and Grussem, W. 1994. Novel conserved sequence motifs in plant G-box binding proteins and implications for interactive domains. *Nucleic Acids Research*, 22(3):470–478.
- Meinke, D. W., Cherry, J. M., Dean, C., Rounsley, S. D., and Koornneef, M. 1998. *Arabidopsis thaliana*: a model plant for genome analysis. *Science*, 282(5389):662–682.
- Mellor, N., Band, L. R., Pěňčík, A., Novák, O., Rashed, A., Holman, T., Wilson, M. H., Voß, U., Bishopp, A., King, J. R., Ljung, K., Bennett, M. J., and Owen, M. R. 2016. Dynamic regulation of auxin oxidase and conjugating enzymes AtDAO1 and GH3 modulates auxin homeostasis. *Proceedings of the National Academy of Sciences*, 113(39):11022–11027.
- Meyer, M. D., Pataky, J. K., and Williams II, M. M. 2010. Genetic factors influencing adverse effects of mesotrione and nicosulfuron on sweet corn yield. *Agronomy Journal*, 102(4):1138–1144.
- Meyerowitz, E. M. 1989. *Arabidopsis*, a useful weed. *Cell*, 56:263–269.
- Michael, T. P. and McClung, C. R. 2003. Enhancer trapping reveals widespread circadian clock transcriptional control in *Arabidopsis*. *Plant Physiology*, 132:629–639.

- Michael, T. P., Mockler, T. C., Breton, G., McEntee, C., Byer, A., Trout, J. D., Hazen, S. P., Shen, R., Priest, H. D., Sullivan, C. M., Givan, S. A., Yanovsky, M., Hong, F., Kay, S. A., and Chory, J. 2008. Network discovery pipeline elucidates conserved time-of-day-specific cis-regulatory modules. *PLoS Genetics*, 4(2).
- Millar, A. J. 2004. Input signals to the plant circadian clock. *Journal of Experimental Botany*, 55(395):277–283.
- Millar, A. J., Short, S. R., Chua, N.-H., and Kay, S. A. 1992. A novel circadian phenotype based on firefly luciferase expression in transgenic plants. *The Plant Cell*, 4:1075–1087.
- Miller, R. P., Martinson, K. B., Sothorn, R. B., Durgan, B. R., and Gunsolus, J. L. 2003. Circadian response of annual weeds in a natural setting to high and low application rates of four herbicides with different modes of action. *Chronobiology International*, 20(2):299–324.
- Mitchell, G., Bartlett, D. W., Fraser, T. E., Hawkes, T. R., Holt, D. C., Townson, J. K., and Wichert, R. A. 2001. Mesotrione: a new selective herbicide for use in maize. *Pest Management Science*, 57:120–128.
- Mittler, R., Vanderauwera, S., Suzuki, N., Miller, G., Tognetti, V. B., Vandepoele, K., Gollery, M., Shulaev, V., and Van Breusegem, F. 2011. ROS signaling: the new wave? *Trends in Plant Science*, 16(6):300–309.
- Mizoi, J., Shinozaki, K., and Yamaguchi-Shinozaki, K. 2012. AP2/ERF family transcription factors in plant abiotic stress responses. *Biochimica et Biophysica Acta 1819*, pages 86–96.
- Mizrachi, E., Hefer, C. A., Ranik, M., Joubert, F., and Myburg, A. A. 2010. De novo assembled expressed gene catalog of a fast-growing *Eucalyptus* tree produced by Illumina mRNA-Seq. *BMC Genomics*, 11(681).
- Mockler, T. C., Michael, T. P., Priest, H. D., Shein, R., Sullivan, C. M., Givan, S. A., McEntee, C., Kay, S. A., and Chory, J. 2007. The Diurnal project: diurnal and circadian expression profiling, model-based pattern matching, and promoter analysis. *Cold Spring Harbor Symposia on Quantitative Biology*, LXXII:353–363.
- Mohr, K., Sellers, B. A., and Smeda, R. J. 2007. Application time of day influences glyphosate efficacy. *Weed Technology*, 21(1):7–13.
- Monaco, T. J., Weller, S. C., and Ashton, F. M. 2002. *Weed Science: Principles and Practices*. Fourth edition.
- Morris, R. W. and Lutsch, E. F. 1967. Susceptibility to morphine-induced analgesia in mice. *Nature*, 216(5114):494–495.
- Müller, M. and Munné-Bosch, S. 2015. Ethylene Response Factors: a key regulatory hub in hormone and stress signaling. *Plant Physiology*, 169:32–41.
- Murchie, E. H. and Lawson, T. 2013. Chlorophyll fluorescence analysis: a guide to good practice and understanding some new applications. *Journal of Experimental Botany*, 64(13):3983–3998.

- Nakamichi, N., Murakami-Kojima, M., Sato, E., Kishi, Y., Yamashino, T., and Mizuno, T. 2002. Compilation and characterization of a novel WNK family of protein kinases in *Arabidopsis thaliana* with reference to circadian rhythms. *Bioscience, Biotechnology, and Biochemistry*, 66(11):2429–2436.
- Nakamichi, N., Kiba, T., Henriques, R., Mizuno, T., Chua, N.-H., and Sakakibara, H. 2010. PSEUDO-RESPONSE REGULATORS 9, 7, and 5 are transcriptional repressors in the Arabidopsis circadian clock. *The Plant Cell*, 22:594–605.
- Nakano, T., Suzuki, K., Fujimura, T., and Shinshi, H. 2006. Genome-wide analysis of the ERF gene family. *Plant Physiology*, 140:411–432.
- Ni, Y., Lai, J., Wan, J., and Chen, L. 2014. Photosynthetic responses and accumulation of mesotrione in two freshwater algae. *Environmental Science: Processes & Impacts*, 16:2288–2294.
- Nishimura, T., Hayashi, K. I., Suzuki, H., Gyohda, A., Takaoka, C., Sakaguchi, Y., Matsumoto, S., Kasahara, H., Sakai, T., Kato, J. I., Kamiya, Y., and Koshiba, T. 2014. Yucasin is a potent inhibitor of YUCCA, a key enzyme in auxin biosynthesis. *The Plant Journal*, 77:352–366.
- Noctor, G. and Foyer, C. H. 1998. Ascorbate and glutathione: Keeping active oxygen under control. *Annual Review of Plant Physiology and Plant Molecular Biology*, 49: 249–279.
- Nohales, M. A. and Kay, S. A. 2016. Molecular mechanisms at the core of the plant circadian oscillator. *Nature Structural and Molecular Biology*, 23(12):1061–1069.
- Nomoto, Y., Kubozono, S., Yamashino, T., Nakamichi, N., and Mizuno, T. 2012. Circadian clock-and PIF4-controlled plant growth: A coincidence mechanism directly integrates a hormone signaling network into the photoperiodic control of plant architectures in *Arabidopsis thaliana*. *Plant and Cell Physiology*, 53(11):1950–1964.
- Nonhebel, H. M. 2015. Tryptophan-independent indole-3-acetic acid synthesis: Critical evaluation of the evidence. *Plant Physiology*, 169:1001–1005.
- Noordally, Z. B., Ishii, K., Atkins, K. A., Wetherill, S. J., Kusakina, J., Walton, E. J., Kato, M., Azuma, M., Tanaka, K., Hanaoka, M., and Dodd, A. N. 2013. Circadian control of chloroplast transcription by a nuclear-encoded timing signal. *Science*, 339(6125):1316–1319.
- Norris, S. R., Barrette, T. R., and DellaPenna, D. 1995. Genetic dissection of carotenoid synthesis in *Arabidopsis* defines plastoquinone as an essential component of phytoene desaturation. *The Plant Cell*, 7:2139–2149.
- Norsworthy, J. K., Oliver, L. R., and Purcell, L. C. 1999. Diurnal leaf movement effects on spray interception and glyphosate efficacy. *Weed Technology*, 13(3):466–470.
- Nozue, K., Covington, M. F., Duek, P. D., Lorrain, S., Fankhauser, C., Harmer, S. L., and Maloof, J. N. 2007. Rhythmic growth explained by coincidence between internal and external cues. *Nature*, 448(7151):358–361.
- Nusinow, D. A., Helfer, A., Hamilton, E. E., King, J. J., Imaizumi, T., Schultz, T. F., Farré, E. M., and Kay, S. A. 2011. The ELF4-ELF3-LUX complex links the circadian clock to diurnal control of hypocotyl growth. *Nature*, 475(7356):398–402.

- Oerke, E.-C. 2006. Crop losses to pests. *The Journal of Agricultural Science*, 144: 31–43.
- Oettmeier, W. and Soll, H. J. 1983. Competition between plastoquinone and 3-(3,4-dichlorophenyl)-1,1-dimethylurea at the acceptor side of Photosystem II. *Biochimica et Biophysica Acta*, 724:287–290.
- Olchanheski, L. R., Dourado, M. N., Beltrame, F. L., Zielinski, A. A., Demiate, I. M., Pileggi, S. A., Azevedo, R. A., Sadowsky, M. J., and Pileggi, M. 2014. Mechanisms of tolerance and high degradation capacity of the herbicide mesotrione by *Escherichia coli* strain DH5- α . *PLoS ONE*, 9(6).
- Olesen, C. F. and Cedergreen, N. 2010. Glyphosate uncouples gas exchange and chlorophyll fluorescence. *Pest Management Science*, 66:536–542.
- Orellana-García, F., Álvarez, M. A., López-Ramón, V., Rivera-Utrilla, J., Sánchez-Polo, M., and Mota, A. J. 2014. Photodegradation of herbicides with different chemical natures in aqueous solution by ultraviolet radiation. Effects of operational variables and solution chemistry. *Chemical Engineering Journal*, 255:307–315.
- Orson, J. H. and Davies, D. H. K. 2007. Pre-harvest glyphosate for weed control and as a harvest aid in cereals. *Home Grown Cereals Authority*, 65.
- Otto, S., Pappalardo, S. E., Cardinali, A., Masin, R., Zanin, G., and Borin, M. 2016. Vegetated ditches for the mitigation of pesticides runoff in the Po Valley. *PLoS ONE*, 11(4).
- Ozsolak, F. and Milos, P. M. 2011. RNA sequencing: advances, challenges and opportunities. *Nature Reviews Genetics*, 12:87–98.
- Palta, J. P. 1990. Leaf chlorophyll content. *Remote Sensing Reviews*, 5(1):207–213.
- Pan, W. J., Wang, X., Deng, Y. R., Li, J. H., Chen, W., Chiang, J. Y., Yang, J. B., and Zheng, L. 2015. Nondestructive and intuitive determination of circadian chlorophyll rhythms in soybean leaves using multispectral imaging. *Scientific Reports*, 5(11108).
- Park, J. E., Seo, P. J., Lee, A. K., Jung, J. H., Kim, Y. S., and Park, C. M. 2007. An Arabidopsis *GH3* gene, encoding an auxin-conjugating enzyme, mediates Phytochrome B-regulated light signals in hypocotyl growth. *Plant and Cell Physiology*, 48(8):1236–1241.
- Partek. Post-alignment QA/QC - Flow Documentation - Partek® Documentation, 2019.
- Perales, M. and Más, P. 2007. A functional link between rhythmic changes in chromatin structure and the Arabidopsis biological clock. *The Plant Cell*, 19:2111–2123.
- Petersen, I. L., Hansen, H. C. B., Ravn, H. W., Sørensen, J. C., and Sørensen, H. 2007. Metabolic effects in rapeseed (*Brassica napus* L.) seedlings after root exposure to glyphosate. *Pesticide Biochemistry and Physiology*, 89:220–229.
- Pfister, K., Steinback, K., Gardner, G., and Arntzen, C. 1981. Photoaffinity labeling of an herbicide receptor protein in chloroplast membranes. *Proceedings of the National Academy of Sciences of the United States of America*, 78(2):981–985.

- Pittendrigh, C. S. and Daan, S. 1976. A functional analysis of circadian pacemakers in nocturnal rodents. *Journal of Comparative Physiology*, 106:333–355.
- Plank, L., Zak, D., Getzner, M., Follak, S., Essl, F., Dullinger, S., Kleinbauer, I., Moser, D., and Gattringer, A. 2016. Benefits and costs of controlling three allergenic alien species under climate change and dispersal scenarios in Central Europe. *Environmental Science & Policy*, 56:9–21.
- Ponnala, L., Wang, Y., Sun, Q., and van Wijk, K. J. 2014. Correlation of mRNA and protein abundance in the developing maize leaf. *The Plant Journal*, 78:424–440.
- Popescu, S. C., Popescu, G. V., Bachan, S., Zhang, Z., Gerstein, M., Snyder, M., and Dinesh-Kumar, S. P. 2009. MAPK target networks in *Arabidopsis thaliana* revealed using functional protein microarrays. *Genes & Development*, 23:80–92.
- Porra, R., Thompson, W., and Kriedemann, P. 1989. Determination of accurate extinction coefficients and simultaneous equations for assaying chlorophylls *a* and *b* extracted with four different solvents: verification of the concentration of chlorophyll standards by atomic absorption spectroscopy. *Biochimica et Biophysica Acta*, 975:384–394.
- Portolés, S. and Más, P. 2010. The functional interplay between protein kinase CK2 and CCA1 transcriptional activity is essential for clock temperature compensation in *Arabidopsis*. *PLoS Genetics*, 6(11).
- Preston, C. and Wakelin, A. M. 2008. Resistance to glyphosate from altered herbicide translocation patterns. *Pest Management Science*, 64:372–376.
- Prione, L. P., Olchanheski, L. R., Tullio, L. D., Santo, B. C. E., Reche, P. M., Martins, P. F., Carvalho, G., Demiate, I. M., Pileggi, S. A. V., Dourado, M. N., Prestes, R. A., Sadowsky, M. J., Azevedo, R. A., and Pileggi, M. 2016. GST activity and membrane lipid saturation prevents mesotrione-induced cellular damage in *Pantoea ananatis*. *AMB Express*, 6(70).
- Qian, H., Wei, Y., Bao, G., Huang, B., and Fu, Z. 2014. Atrazine affects the circadian rhythm of *Microcystis aeruginosa*. *Chronobiology International*, 31(1):17–26.
- Quinn, P. and Williams, W. 1978. Plant lipids and their role in membrane function. *Progress in Biophysics and Molecular Biology*, 34:109–173.
- Quint, M. and Gray, W. M. 2006. Auxin signaling. *Current Opinion in Plant Biology*, 9:448–453.
- Rahmani, F., Hummel, M., Schuurmans, J., Wiese-Klinkenberg, A., Smeekens, S., and Hanson, J. 2009. Sucrose control of translation mediated by an upstream open reading frame-encoded peptide. *Plant Physiology*, 150:1356–1367.
- Rakusová, H., Gallego-Bartolomé, J., Vanstraelen, M., Robert, H. S., Alabadí, D., Blázquez, M. A., Benková, E., and Friml, J. 2011. Polarization of PIN3-dependent auxin transport for hypocotyl gravitropic response in *Arabidopsis thaliana*. *The Plant Journal*, 67:817–826.
- Ralph, P. J. 2000. Herbicide toxicity of *Halophila ovalis* assessed by chlorophyll *a* fluorescence. *Aquatic Botany*, 66:141–152.

- Rawat, R., Schwartz, J., Jones, M. A., Sairanen, I., Cheng, Y., Andersson, C. R., Zhao, Y., Ljung, K., and Harmer, S. L. 2009. REVEILLE1, a Myb-like transcription factor, integrates the circadian clock and auxin pathways. *Proceedings of the National Academy of Sciences of the United States of America*, 106(39):16883–16888.
- Rawat, R., Takahashi, N., Hsu, P. Y., Jones, M. A., Schwartz, J., Salemi, M. R., Phinney, B. S., and Harmer, S. L. 2011. REVEILLE8 and PSEUDO-REPONSE REGULATOR5 form a negative feedback loop within the Arabidopsis circadian clock. *PLoS Genetics*, 7(3).
- Rea, P. A. 2007. Plant ATP-binding cassette transporters. *Annual Review of Plant Biology*, 58:347–375.
- Reape, T. J. and McCabe, P. F. 2008. Apoptotic-like programmed cell death in plants. *New Phytologist*, 180:13–26.
- Reddy, K. N., Zablotowicz, R. M., Locke, M. A., and Koger, C. H. 2003. Cover crop, tillage, and herbicide effects on weeds, soil properties, microbial populations, and soybean yield. *Weed Science*, 51(6):987–994.
- Reed, J. W., Nagpal, P., Poole, D. S., Furuya, M., and Chory, J. 1993. Mutations in the gene for the red/far-red light receptor phytochrome B alter cell elongation and physiological responses throughout Arabidopsis development. *The Plant Cell*, 5:147–157.
- Reed, J. W., Wu, M. F., Reeves, P. H., Hodgens, C., Yadav, V., Hayes, S., and Pierik, R. 2018. Three Auxin Response Factors Promote Hypocotyl Elongation. *Plant Physiology*, 178(2):864–875.
- Rizzini, L., Favory, J.-J., Cloix, C., Faggionato, D., O’Hara, A., Kaiserli, E., Baumeister, R., Schafer, E., Nagy, F., Jenkins, G. I., and Ulm, R. apr 2011. Perception of UV-B by the Arabidopsis UVR8 protein. *Science*, 332(6025):103–106.
- Rochaix, J. D. 2011. Regulation of photosynthetic electron transport. *Biochimica et Biophysica Acta 1807*, pages 375–383.
- Roggenbuck, F. C., Rowe, L., Penner, D., Petroff, L., and Burow, R. 1990. Increasing postemergence herbicide efficacy and rainfastness with silicone adjuvants. *Weed Technology*, 4(3):576–580.
- Rolauffs, S., Fackendahl, P., Sahm, J., Fiene, G., and Hoecker, U. 2012. Arabidopsis *COP1* and *SPA* genes are essential for plant elongation but not for acceleration of flowering time in response to a low red light to far-red light ratio. *Plant Physiology*, 160:2015–2027.
- Rook, F., Gerrits, N., Kortstee, A., van Kampen, M., Borrias, M., Weisbeek, P., and Smeekens, S. 1998. Sucrose-specific signalling represses translation of the Arabidopsis *ATB2* bZIP transcription factor gene. *The Plant Journal*, 15:253–263.
- Rueppel, M. L., Brightwell, B. B., Schaefer, J., and Marvel, J. T. 1977. Metabolism and degradation of glyphosate in soil and water. *Journal of Agricultural and Food Chemistry*, 25(3):517–528.

- Rushton, P. J., Tovar Torres, J., Parniske, M., Wernert, P., Hahlbrock, K., and Somssich, I. E. 1996. Interaction of elicitor-induced DNA-binding proteins with elicitor response elements in the promoters of parsley PR1 genes. *The EMBO Journal*, 15(20):5690–5700.
- Rushton, P. J., Somssich, I. E., Ringler, P., and Shen, Q. J. 2010. WRKY transcription factors. *Trends in Plant Science*, 15(5):247–258.
- Rutherford, A. W. and Krieger-Liszkay, A. 2001. Herbicide-induced oxidative stress in photosystem II. *Trends in Biochemical Sciences*, 26(11):648–653.
- Sahid, I. B. and Teoh, S. S. 1994. Persistence of terbuthylazine in soils. *Bulletin of Environmental Contamination and Toxicology*, 52:226–230.
- Sakuma, Y., Liu, Q., Dubouzet, J. G., Abe, H., Shinozaki, K., and Yamaguchi-Shinozaki, K. 2002. DNA-binding specificity of the ERF/AP2 domain of Arabidopsis DREBs, transcription factors involved in dehydration- and cold-inducible gene expression. *Biochemical and Biophysical Research Communications*, 290:998–1009.
- Salomé, P. A. and McClung, C. R. 2005a. What makes the Arabidopsis clock tick on time? A review on entrainment. *Plant, Cell and Environment*, 28:21–38.
- Salomé, P. A. and McClung, C. R. 2005b. PSEUDO-RESPONSE REGULATOR 7 and 9 are partially redundant genes essential for the temperature responsiveness of the Arabidopsis circadian clock. *The Plant Cell*, 17:791–803.
- Salomé, P. A., Xie, Q., and McClung, C. R. 2008. Circadian timekeeping during early Arabidopsis development. *Plant Physiology*, 147:1110–1125.
- Salomé, P. A., Oliva, M., Weigel, D., and Krämer, U. 2013. Circadian clock adjustment to plant iron status depends on chloroplast and phytochrome function. *The EMBO Journal*, 32:511–523.
- Salter, M. G., Franklin, K. A., and Whitelam, G. C. 2003. Gating of the rapid shade-avoidance response by the circadian clock in plants. *Nature*, 426:680–683.
- Samach, A. and Coupland, G. 2000. Time measurement and the control of flowering in plants. *BioEssays*, 22:38–47.
- Sanchez, S. E. and Kay, S. A. 2016. The plant circadian clock: From a simple timekeeper to a complex developmental manager. *Cold Spring Harbor Perspectives in Biology*, 8(12).
- Sánchez-Fernández, R., Davies, T. G., Coleman, J. O., and Rea, P. A. 2001. The *Arabidopsis thaliana* ABC protein superfamily, a complete inventory. *Journal of Biological Chemistry*, 276(32):30231–30244.
- Sappl, P. G., Carroll, A. J., Clifton, R., Lister, R., Whelan, J., Millar, A. H., and Singh, K. B. 2009. The Arabidopsis glutathione transferase gene family displays complex stress regulation and co-silencing multiple genes results in altered metabolic sensitivity to oxidative stress. *The Plant Journal*, 58:53–68.
- Sasidharan, R., Chinnappa, C. C., Staal, M., Elzenga, J. T. M., Yokoyama, R., Nishitani, K., Voesenek, L. a. C. J., and Pierik, R. 2010. Light quality-mediated

- petiole elongation in *Arabidopsis* during shade avoidance involves cell wall modification by xyloglucan endotransglucosylase/hydrolases. *Plant Physiology*, 154:978–990.
- Sato, R., Ito, H., and Tanaka, A. 2015. Chlorophyll *b* degradation by chlorophyll *b* reductase under high-light conditions. *Photosynthesis Research*, 126:249–259.
- Schönbrunn, E., Eschenburg, S., Shuttleworth, W. A., Schloss, J. V., Amrhein, N., Evans, J. N., and Kabsch, W. 2001. Interaction of the herbicide glyphosate with its target enzyme 5-enolpyruvylshikimate 3-phosphate synthase in atomic detail. *Proceedings of the National Academy of Sciences of the United States of America*, 98(4):1376–1380.
- Schrübbers, L. C., Valverde, B. E., Strobel, B. W., and Cedergreen, N. 2016. Glyphosate accumulation, translocation, and biological effects in *Coffea arabica* after single and multiple exposures. *European Journal of Agronomy*, 74:133–143.
- Seaton, D. D., Smith, R. W., Song, Y. H., MacGregor, D. R., Stewart, K., Steel, G., Foreman, J., Penfield, S., Imaizumi, T., Millar, A. J., and Halliday, K. J. 2015. Linked circadian outputs control elongation growth and development in response to photoperiod and temperature. *Molecular Systems Biology*, 11(776).
- Sellers, B. A., Smeda, R. J., and Johnson, W. 2003. Diurnal fluctuations and leaf angle reduce glufosinate efficacy. *Weed Technology*, 17(2):302–306.
- Sham, A., Al-Azzawi, A., Al-Ameri, S., Al-Mahmoud, B., Awwad, F., Al-Rawashdeh, A., Iratni, R., and AbuQamar, S. 2014. Transcriptome analysis reveals genes commonly induced by *Botrytis cinerea* infection, cold, drought and oxidative stresses in *Arabidopsis*. *PLoS ONE*, 9(11).
- Shaner, D. L. 2009. Role of translocation as a mechanism of resistance to glyphosate. *Weed Science*, 57:118–123.
- Sharkhuu, A., Narasimhan, M. L., Merzaban, J. S., Bressan, R. A., Weller, S., and Gehring, C. 2014. A red and far-red light receptor mutation confers resistance to the herbicide glyphosate. *The Plant Journal*, 78:916–926.
- Sharma, R., Sahoo, A., Devendran, R., and Jain, M. 2014. Over-expression of a rice tau class glutathione S-transferase gene improves tolerance to salinity and oxidative stresses in *Arabidopsis*. *PLoS ONE*, 9(3).
- Shifu, C. and Yunzhang, L. 2007. Study on the photocatalytic degradation of glyphosate by TiO₂ photocatalyst. *Chemosphere*, 67:1010–1017.
- Silva, F. M. L., Duke, S. O., Dayan, F. E., and Velini, E. D. 2015. Low doses of glyphosate change the responses of soyabean to subsequent glyphosate treatments. *Weed Research*.
- Silva, F. B., Costa, A. C., Pereira Alves, R. R., and Megguer, C. A. 2014. Chlorophyll fluorescence as an indicator of cellular damage by glyphosate herbicide in *Raphanus sativus* L. plants. *American Journal of Plant Sciences*, 5:2509–2519.
- Siminszky, B. 2006. Plant cytochrome P450-mediated herbicide metabolism. *Phytochemistry Reviews*, 5:445–458.

- Simon, N. M. L., Kusakina, J., Fernández-López, Á., Chembath, A., Belbin, F. E., and Dodd, A. N. 2018. The energy-signaling hub SnRK1 is important for sucrose-induced hypocotyl elongation. *Plant Physiology*, 176(2):1299–1310.
- Singh, H., Singh, N. B., Singh, A., Hussain, I., and Yadav, V. 2017. Physiological and biochemical roles of nitric oxide against toxicity produced by glyphosate herbicide in *Pisum sativum*. *Russian Journal of Plant Physiology*, 64(4):518–524.
- Singh, R., Sidhu, S. S., and McCullough, P. E. 2015. Physiological basis for triazine herbicide tolerance in bermudagrass, seashore paspalum, and zoysiagrass. *Crop Science*, 55:2334–2341.
- Skipsey, M., Knight, K. M., Brazier-Hicks, M., Dixon, D. P., Steel, P. G., and Edwards, R. 2011. Xenobiotic responsiveness of *Arabidopsis thaliana* to a chemical series derived from a herbicide safener. *Journal of Biological Chemistry*, 286(37):32268–32276.
- Skuterud, R., Bjugstad, N., Tyldum, A., and Semb Tørresen, K. 1998. Effect of herbicides applied at different times of the day. *Crop Protection*, 17(1):41–46.
- Smart, C. C. and Fleming, A. J. 1996. Hormonal and environmental regulation of a plant PDR5-like ABC transporter. *Journal of Biological Chemistry*, 271(32):19351–19357.
- Smith, S. M., Fulton, D. C., Chia, D., Thorneycroft, D., Chapple, A., Dunstan, H., Hylton, C., Zeeman, S. C., and Smith, A. M. 2004. Diurnal changes in the transcriptome encoding enzymes of starch metabolism provide evidence for both transcriptional and posttranscriptional regulation of starch metabolism in *Arabidopsis* leaves. *Plant Physiology*, 136:2687–2699.
- Soeno, K., Goda, H., Ishii, T., Ogura, T., Tachikawa, T., Sasaki, E., Yoshida, S., Fujioka, S., Asami, T., and Shimada, Y. 2010. Auxin biosynthesis inhibitors, identified by a genomics-based approach, provide insights into auxin biosynthesis. *Plant and Cell Physiology*, 51(4):524–536.
- Soliman, E. R. S. and Meyer, P. 2019. Responsiveness and adaptation to salt stress of the *REDOX-RESPONSIVE TRANSCRIPTION FACTOR 1 (RRTF1)* gene are controlled by its promoter. *Molecular Biotechnology*, 61:254–260.
- Somers, D. E., Devlin, P. F., and Kay, S. A. 1998a. Phytochromes and cryptochromes in the entrainment of the *Arabidopsis* circadian clock. *Science*, 282(5393):1488–1490.
- Somers, D. E., Webb, A. A., Pearson, M., and Kay, S. A. 1998b. The short-period mutant, *toc1-1*, alters circadian clock regulation of multiple outputs throughout development in *Arabidopsis thaliana*. *Development*, 125:485–494.
- Song, Y. H., Smith, R. W., To, B. J., Millar, A. J., and Imaizumi, T. 2012. FKF1 conveys timing information for CONSTANS stabilization in photoperiodic flowering. *Science*, 336:1045–1050.
- Sosa Alderete, L. G., Guido, M. E., Agostini, E., and Mas, P. 2018. Identification and characterization of key circadian clock genes of tobacco hairy roots: putative

- regulatory role in xenobiotic metabolism. *Environmental Science and Pollution Research*, 25:1597–1608.
- Southern, M. M. and Millar, A. J. 2005. Circadian genetics in the model higher plant, *Arabidopsis thaliana*. *Methods in Enzymology*, 393:23–35.
- Sprankle, P., Meggitt, W. F., and Penner, D. 1975a. Rapid inactivation of glyphosate in the soil. *Weed Science Society of America*, 23(3):224–228.
- Sprankle, P., Meggitt, W. F., and Penner, D. 1975b. Adsorption, mobility and microbial degradation of glyphosate in the soil. *Weed Science*, 23(3):229–234.
- Staswick, P. E., Serban, B., Rowe, M., Tiryaki, I., Maldonado, M. T., Maldonado, M. C., and Suza, W. 2005. Characterization of an Arabidopsis enzyme family that conjugates amino acids to indole-3-acetic acid. *The Plant Cell*, 17:616–627.
- Steinback, K. E., McIntosh, L., Bogoradt, L., and Arntzen, C. J. 1981. Identification of the triazine receptor protein as a chloroplast gene product. *Proceedings of the National Academy of Sciences of the United States of America*, 78(12):7463–7467.
- Steinrücken, H. and Amrhein, N. 1980. The herbicide glyphosate is a potent inhibitor of 5-enolpyruvylshikimic acid-3-phosphate synthase. *Biochemical and Biophysical Research Communications*, 94(4):1207–1212.
- Stepanova, A. N., Yun, J., Robles, L. M., Novak, O., He, W., Guo, H., Ljung, K., and Alonso, J. M. 2011. The Arabidopsis YUCCA1 flavin monooxygenase functions in the indole-3-pyruvic acid branch of auxin biosynthesis. *The Plant Cell*, 23:3961–3973.
- Sterling, T. M. 1994. Mechanisms of herbicide absorption across plant membranes and accumulation in plant cells. *Weed Science*, 42(2):263–276.
- Stewart, C. L., Nurse, R. E., and Sikkema, P. H. 2009. Time of day impacts postemergence weed control in corn. *Weed Technology*, 23(3):346–355.
- Stopps, G. J., Nurse, R. E., and Sikkema, P. H. 2013. The effect of time of day on the activity of postemergence soybean herbicides. *Weed Technology*, 27(4):690–695.
- Stratmann, T. and Más, P. 2008. Chromatin, photoperiod and the Arabidopsis circadian clock: A question of time. *Seminars in Cell and Developmental Biology*, 19:554–559.
- Straume, M., Frasier-Cadoret, S. G., and Johnson, M. L. 2002. *Topics in Fluorescence Spectroscopy*.
- Sugano, S., Andronis, C., Green, R. M., Wang, Z.-Y., and Tobin, E. M. 1998. Protein kinase CK2 interacts with and phosphorylates the Arabidopsis circadian clock-associated 1 protein. *Proceedings of the National Academy of Sciences*, 95:11020–11025.
- Sugano, S., Andronis, C., Ong, M. S., Green, R. M., and Tobin, E. M. 1999. The protein kinase CK2 is involved in regulation of circadian rhythms in Arabidopsis. *Proceedings of the National Academy of Sciences*, 96(22):12362–12366.
- Sugiyama, N., Izawa, T., Oikawa, T., and Shimamoto, K. 2001. Light regulation of circadian clock-controlled gene expression in rice. *The Plant Journal*, 26(6):607–615.

- Suzuki, M., Yamazaki, C., Mitsui, M., Kakei, Y., Mitani, Y., Nakamura, A., Ishii, T., Soeno, K., and Shimada, Y. 2015. Transcriptional feedback regulation of *YUCCA* genes in response to auxin levels in Arabidopsis. *Plant Cell Reports*, 34:1343–1352.
- Swanton, C. J., Nkoa, R., and Blackshaw, R. E. 2015. Experimental methods for crop–weed competition studies. *Weed Science*, 63(1):2–11.
- Syed, N. H., Prince, S. J., Mutava, R. N., Patil, G., Li, S., Chen, W., Babu, V., Joshi, T., Khan, S., and Nguyen, H. T. 2015. Core clock, *SUB1*, and *ABAR* genes mediate flooding and drought responses via alternative splicing in soybean. *Journal of Experimental Botany*, 66(22):7129–7149.
- Takahashi, N., Hirata, Y., Aihara, K., and Mas, P. 2015. A hierarchical multi-oscillator network orchestrates the Arabidopsis circadian system. *Cell*, 163:148–159.
- Taki, N., Sasaki-sekimoto, Y., Obayashi, T., Kikuta, A., Kobayashi, K., Ainai, T., Yagi, K., Sakurai, N., Suzuki, H., Masuda, T., Takamiya, K.-i., Shibata, D., Kobayashi, Y., and Ohta, H. 2005. 12-oxo-phytodienoic acid triggers expression of a distinct set of genes and plays a role in wound-induced gene expression in Arabidopsis. *Plant Physiology*, 139:1268–1283.
- Tao, Y., Ferrer, J. L., Ljung, K., Pojer, F., Hong, F., Long, J. A., Li, L., Moreno, J. E., Bowman, M. E., Ivans, L. J., Cheng, Y., Lim, J., Zhao, Y., Ballaré, C. L., Sandberg, G., Noel, J. P., and Chory, J. 2008. Rapid synthesis of auxin via a new tryptophan-dependent pathway is required for shade avoidance in plants. *Cell*, 133:164–176.
- Thompson, L. and Slife, F. W. 1969. Foliar and root absorption of atrazine applied postemergence to giant foxtail. *Weed Science*, 17(2):251–256.
- Tognetti, V. B., Van Aken, O., Morreel, K., Vandenbroucke, K., van de Cotte, B., De Clercq, I., Chiwocha, S., Fenske, R., Prinsen, E., Boerjan, W., Genty, B., Stubbs, K. a., Inzé, D., and Van Breusegem, F. 2010. Perturbation of indole-3-butyric acid homeostasis by the UDP-glucosyltransferase *UGT74E2* modulates Arabidopsis architecture and water stress tolerance. *The Plant Cell*, 22:2660–79.
- Torres, A. C., Nagata, R. T., Ferl, R. J., Bewick, T. A., and Cantliffe, D. J. 1999. In vitro assay selection of glyphosate resistance in lettuce. *Journal of the American Society for Horticultural Science*, 124(1):86–89.
- Trapnell, C., Roberts, A., Goff, L., Pertea, G., Kim, D., Kelley, D. R., Pimentel, H., Salzberg, S. L., Rinn, J. L., and Pachter, L. 2012. Differential gene and transcript expression analysis of RNA-seq experiments with TopHat and Cufflinks. *Nature Protocols*, 7(3):562–578.
- Tsutsui, T., Kato, W., Asada, Y., Sako, K., Sato, T., Sonoda, Y., Kidokoro, S., Yamaguchi-Shinozaki, K., Tamaoki, M., Arakawa, K., Ichikawa, T., Nakazawa, M., Seki, M., Shinozaki, K., Matsui, M., Ikeda, A., and Yamaguchi, J. 2009. DEAR1, a transcriptional repressor of DREB protein that mediates plant defense and freezing stress responses in Arabidopsis. *Journal of Plant Research*, 122:633–643.
- Tzin, V. and Galili, G. 2010. The biosynthetic pathways for shikimate and aromatic amino acids in *Arabidopsis thaliana*. *The Arabidopsis Book*.

- Uehara, T. N., Mizutani, Y., Kuwata, K., Hirota, T., Sato, A., Mizoi, J., Takao, S., Matsuo, H., Suzuki, T., Ito, S., Saito, A. N., Nishiwaki-Ohkawa, T., Yamaguchi-Shinozaki, K., Yoshimura, T., Kay, S. A., Itami, K., Kinoshita, T., Yamaguchi, J., and Nakamichi, N. 2019. Casein kinase 1 family regulates PRR5 and TOC1 in the Arabidopsis circadian clock. *Proceedings of the National Academy of Sciences*, 116 (23):11528–11536.
- Ülker, B. and Somssich, I. E. 2004. WRKY transcription factors: from DNA binding towards biological function. *Current Opinion in Plant Biology*, 7:491–498.
- Ulmasov, T., Murfett, J., Hagen, G., and Guilfoyle, T. J. 1997. Aux/IAA proteins repress expression of reporter genes containing natural and highly active synthetic auxin response elements. *The Plant Cell*, 9:1963–1971.
- Van Den Brûle, S. and Smart, C. C. 2002. The plant PDR family of ABC transporters. *Planta*, 216:95–106.
- Vanstone, D. E. and Stobbe, E. H. 1977. Electrolytic conductivity: a rapid measure of herbicide injury. *Weed Science*, 25(4):352–354.
- Vieten, A., Vanneste, S., Wiśniewska, J., Benková, E., Benjamins, R., Beeckman, T., Luschnig, C., and Friml, J. 2005. Functional redundancy of PIN proteins is accompanied by auxin-dependent cross-regulation of PIN expression. *Development*, 132(20):4521–4531.
- Vince-Prue, D., Guttridge, C. G., and Buck, M. W. 1976. Photocontrol of petiole elongation in light-grown strawberry plants. *Planta*, 131:109–114.
- Wagner, G. P., Kin, K., and Lynch, V. J. 2012. Measurement of mRNA abundance using RNA-seq data: RPKM measure is inconsistent among samples. *Theory in Biosciences*, 131:281–285.
- Wagner, U., Edwards, R., Dixon, D. P., and Mauch, F. 2002. Probing the diversity of the Arabidopsis glutathione S-transferase gene family. *Plant Molecular Biology*, 49:515–532.
- Walker, J. C. and Key, J. L. 1982. Isolation of cloned cDNAs to auxin-responsive poly(A)⁺RNAs of elongating soybean hypocotyl. *Proceedings of the National Academy of Sciences of the United States of America*, 79:7185–7189.
- Waltz, A. L., Martin, A. R., Roeth, F. W., and Lindquist, J. L. 2004. Glyphosate efficacy on velvetleaf varies with application time of day. *Weed Technology*, 18(4): 931–939.
- Wang, D., Weaver, N., Kesarwani, M., and Dong, X. 2005. Induction of protein secretory pathway is required for systemic acquired. *Science*, 308:1036–1041.
- Wang, H.-Z., Yang, K.-Z., Zou, J.-J., Zhu, L.-L., Xie, Z. D., Morita, M. T., Tasaka, M., Friml, J., Grotewold, E., Beeckman, T., Vanneste, S., Sack, F., and Le, J. 2015. Transcriptional regulation of *PIN* genes by FOUR LIPS and MYB88 during Arabidopsis root gravitropism. *Nature Communications*, 6(8822).
- Wang, L., Kim, J., and Somers, D. E. 2013. Transcriptional corepressor TOPLESS complexes with pseudoresponse regulator proteins and histone deacetylases to reg-

- ulate circadian transcription. *Proceedings of the National Academy of Sciences of the United States of America*, 110(2):761–766.
- Wang, S., Wang, X., He, Q., Liu, X., Xu, W., Li, L., Gao, J., and Wang, F. 2012. Transcriptome analysis of the roots at early and late seedling stages using Illumina paired-end sequencing and development of EST-SSR markers in radish. *Plant Cell Reports*, 31:1437–1447.
- Wang, W., Barnaby, J. Y., Tada, Y., Li, H., Tör, M., Caldelari, D., Lee, D. U., Fu, X. D., and Dong, X. 2011. Timing of plant immune responses by a central circadian regulator. *Nature*, 470(7332):110–115.
- Wang, Z., Fang, B., Chen, J., Zhang, X., Luo, Z., Huang, L., Chen, X., and Li, Y. 2010. De novo assembly and characterization of root transcriptome using Illumina paired-end sequencing and development of cSSR markers in sweetpotato (*Ipomoea batatas*). *BMC Genomics*, 11(726).
- Wang, Z.-Y. and Tobin, E. M. 1998. Constitutive expression of the *CIRCADIAN CLOCK ASSOCIATED 1 (CCA1)* gene disrupts circadian rhythms and suppresses its own expression. *Cell*, 93:1207–1217.
- Watanabe, S., Xia, Z., Hideshima, R., Tsubokura, Y., Sato, S., Yamanaka, N., Takahashi, R., Anai, T., Tabata, S., Kitamura, K., and Harada, K. 2011. A map-based cloning strategy employing a residual heterozygous line reveals that the *GIGANTEA* gene is involved in soybean maturity and flowering. *Genetics*, 188:395–407.
- Wax, L. M. and Behrens, R. 1965. Absorption and translocation of atrazine in quackgrass. *Weeds*, 13(2):107–109.
- Weaver, L. M. and Herrmann, K. M. 1997. Dynamics of the shikimate pathway in plants. *Trends in Plant Science*, 2(9):346–351.
- Webb, A. A., Seki, M., Satake, A., and Caldana, C. 2019. Continuous dynamic adjustment of the plant circadian oscillator. *Nature Communications*, 10(550).
- Weber, A. P. 2015. Discovering new biology through sequencing of RNA. *Plant Physiology*, 169:1524–1531.
- Wehtje, G. 2008. Synergism of dicamba with diflufenzopyr with respect to turfgrass weed control. *Weed Technology*, 22:679–684.
- Weis, B. L., Kovacevic, J., Missbach, S., and Schleiff, E. 2015. Plant-specific features of ribosome biogenesis. *Trends in Plant Science*, 20(11):729–740.
- Wells, B. *Effects of lactofen herbicide on cellular uptake of glyphosate herbicide in Malva parviflora L.* PhD thesis, Oregon State University, 1989.
- Welsch, R., Beyer, P., Huguency, P., Kleinig, H., and von Lintig, J. 2000. Regulation and activation of phytoene synthase, a key enzyme in carotenoid biosynthesis, during photomorphogenesis. *Planta*, 211:846–854.
- Welsh, D. K., Imaizumi, T., and Kay, S. A. 2005. Real-time reporting of circadian-regulated gene expression by luciferase imaging in plants and mammalian cells. *Methods in Enzymology*, 393:269–288.

- Westwood, J. H. and Weller, S. C. 1997. Cellular mechanisms influence differential glyphosate sensitivity in field bindweed (*Convolvulus arvensis*) biotypes. *Weed Science*, 45(1):2–11.
- Whitlow, T. H., Bassuk, N. L., Ranney, T. G., and Reichert, D. L. 1992. An improved method for using electrolyte leakage to assess membrane competence in plant tissues. *Plant Physiology*, 98:198–205.
- WHO. Terbutylazine (TBA) in drinking-water. Technical report, 2003.
- Wiese, A., Elzinga, N., Wobbes, B., and Smeekens, S. 2004. A conserved upstream open reading frame mediates sucrose-induced repression of translation. *The Plant Cell*, 16:1717–1729.
- Wilkins, O., Bräutigam, K., and Campbell, M. M. 2010. Time of day shapes Arabidopsis drought transcriptomes. *The Plant Journal*, 63:715–727.
- Winter, D., Vinegar, B., Nahal, H., Ammar, R., Wilson, G. V., and Provart, N. J. 2007. An "electronic fluorescent pictograph" browser for exploring and analyzing large-scale biological data sets. *PLoS ONE*, 2(8).
- Xie, Q., Wang, P., Liu, X., Yuan, L., Wang, L., Zhang, C., Li, Y., Xing, H., Zhi, L., Yue, Z., Zhao, C., McClung, C. R., and Xu, X. 2014. LNK1 and LNK2 are transcriptional coactivators in the Arabidopsis circadian oscillator. *The Plant Cell*, 26(7):2843–2857.
- Xing, H., Wang, P., Cui, X., Zhang, C., Wang, L., Liu, X., Yuan, L., Li, Y., Xie, Q., and Xu, X. 2015. LNK1 and LNK2 recruitment to the evening element require morning expressed circadian related MYB-like transcription factors. *Plant Signaling and Behavior*, 10(3):10–12.
- Xu, F., He, S., Zhang, J., Mao, Z., Wang, W., Li, T., Hua, J., Du, S., Xu, P., Li, L., Lian, H., and Yang, H. Q. 2018. Photoactivated CRY1 and phyB interact directly with AUX/IAA proteins to inhibit auxin signaling in Arabidopsis. *Molecular Plant*, 11:523–541.
- Yamashita, Y., Takamatsu, S., Glasbrenner, M., Becker, T., Naito, S., and Beckmann, R. 2017. Sucrose sensing through nascent peptide-mediated ribosome stalling at the stop codon of Arabidopsis *bZIP11* uORF2. *FEBS Letters*, 591:1266–1277.
- Yan, Q., Xia, X., Sun, Z., and Fang, Y. 2017. Depletion of Arabidopsis SC35 and SC35-like serine/arginine-rich proteins affects the transcription and splicing of a subset of genes. *PLoS Genetics*, 13(3).
- Yang, P., Wang, J., Huang, F. Y., Yang, S., and Wu, K. 2018. The plant circadian clock and chromatin modifications. *Genes*, 9(11):1–11.
- Yang, X., Beres, Z. T., Jin, L., Parrish, J. T., Zhao, W., Mackey, D., and Snow, A. A. 2017. Effects of over-expressing a native gene encoding 5-enolpyruvylshikimate-3-phosphate synthase (EPSPS) on glyphosate resistance in *Arabidopsis thaliana*. *PLoS ONE*, 12(4).
- Yannicari, M., Tambussi, E., Istilart, C., and Castro, A. M. 2012. Glyphosate effects on gas exchange and chlorophyll fluorescence responses of two *Lolium perenne* L.

- biotypes with differential herbicide sensitivity. *Plant Physiology and Biochemistry*, 57:210–217.
- Zenoni, S., Ferrarini, A., Giacomelli, E., Xumerle, L., Fasoli, M., Malerba, G., Bellin, D., Pezzotti, M., and Delledonne, M. 2010. Characterization of transcriptional complexity during berry development in *Vitis vinifera* using RNA-seq. *Plant Physiology*, 152:1787–1795.
- Zhang, B., Aken, O. V., Thatcher, L., Clercq, I. D., Duncan, O., Law, S. R., Murcha, M. W., van der Merwe, M., Seifi, H. S., Carrie, C., Cazzonelli, C., Radomiljac, J., Höfte, M., Singh, K. B., Breusegem, F. V., and Whelan, J. 2014a. The mitochondrial outer membrane AAA ATPase AtOM66 affects cell death and pathogen resistance in *Arabidopsis thaliana*. *The Plant Journal*, 80:709–727.
- Zhang, J. J., Zhou, Z. S., Song, J. B., Liu, Z. P., and Yang, H. 2012. Molecular dissection of atrazine-responsive transcriptome and gene networks in rice by high-throughput sequencing. *Journal of Hazardous Materials*, 219-220:57–68.
- Zhang, R., Lahens, N. F., Ballance, H. I., Hughes, M. E., and Hogenesch, J. B. 2014b. A circadian gene expression atlas in mammals: Implications for biology and medicine. *Proceedings of the National Academy of Sciences of the United States of America*, 111(45):16219–16224.
- Zhang, R., Wang, B., Ouyang, J., Li, J., and Wang, Y. 2008. Arabidopsis indole synthase, a homolog of tryptophan synthase alpha, is an enzyme involved in the Trp-independent indole-containing metabolite biosynthesis. *Journal of Integrative Plant Biology*, 50(9):1070–1077.
- Zhang, R., Calixto, C. P., Marquez, Y., Venhuizen, P., Tzioutziou, N. A., Guo, W., Spensley, M., Entizne, J. C., Lewandowska, D., Have, S. T., Frey, N. F., Hirt, H., James, A. B., Nimmo, H. G., Barta, A., Kalyna, M., and Brown, J. W. 2017. A high quality Arabidopsis transcriptome for accurate transcript-level analysis of alternative splicing. *Nucleic Acids Research*, 45(9):5061–5073.
- Zhao, Y. 2010. Auxin biosynthesis and its role in plant development. *Annual Review of Plant Biology*, 61:49–64.
- Zhao, Y. 2012. Auxin biosynthesis: A simple two-step pathway converts tryptophan to indole-3-Acetic acid in plants. *Molecular Plant*, 5(2):334–338.
- Zhu, J.-Y., Oh, E., Wang, T., and Wang, Z.-Y. 2016. TOC1–PIF4 interaction mediates the circadian gating of thermoresponsive growth in Arabidopsis. *Nature Communications*, 7(13692).
- Zhu, J., Patzoldt, W. L., Radwan, O., Tranel, P. J., and Clough, S. J. 2009. Effects of photosystem-II-interfering herbicides atrazine and bentazon on the soybean transcriptome. *The Plant Genome Journal*, 2(2):191–205.
- Zhu, Q. H., Stephen, S., Kazan, K., Jin, G., Fan, L., Taylor, J., Dennis, E. S., Helliwell, C. A., and Wang, M. B. 2013. Characterization of the defense transcriptome responsive to *Fusarium oxysporum*-infection in Arabidopsis using RNA-seq. *Gene*, 512:259–266.
- Zielinski, T., Moore, A. M., Troup, E., Halliday, K. J., and Millar, A. J. 2014.

Strengths and limitations of period estimation methods for circadian data. *PLoS ONE*, 9(5).

Zimdahl, R. L. 2013. *Fundamentals of Weed Science*. Third edition.

Zobiolo, L. H. S., Kremer, R. J., Oliveira, R. S., and Constantin, J. 2011. Glyphosate affects chlorophyll, nodulation and nutrient accumulation of "second generation" glyphosate-resistant soybean (*Glycine max* L.). *Pesticide Biochemistry and Physiology*, 99:53–60.

Zulet, A., Gil-Monreal, M., Villamor, J. G., Zabalza, A., van der Hoorn, R. A. L., and Royuela, M. 2013. Proteolytic pathways induced by herbicides that inhibit amino acid biosynthesis. *PLoS ONE*, 8(9).